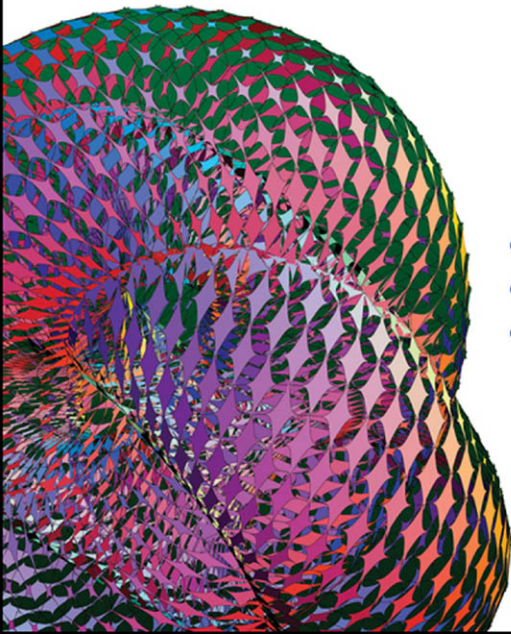


SIXTH EDITION

Principles of Modern Chemistry



OXTOBY

GILLIS

CAMPION

PERIODIC TABLE OF THE ELEMENTS

I																	VIII			
1 1.0079 H <small>Hydrogen</small>																	2 4.0026 He <small>Helium</small>			
	II	Transition elements												III	IV	V	VI	VII		
	3 6.941 Li <small>Lithium</small>	4 9.0122 Be <small>Beryllium</small>													5 10.811 B <small>Boron</small>	6 12.0107 C <small>Carbon</small>	7 14.0067 N <small>Nitrogen</small>	8 15.9994 O <small>Oxygen</small>	9 18.9984 F <small>Fluorine</small>	10 20.1797 Ne <small>Neon</small>
	11 22.9898 Na <small>Sodium</small>	12 24.3050 Mg <small>Magnesium</small>													13 26.9815 Al <small>Aluminum</small>	14 28.0855 Si <small>Silicon</small>	15 30.9738 P <small>Phosphorus</small>	16 32.065 S <small>Sulfur</small>	17 35.453 Cl <small>Chlorine</small>	18 39.948 Ar <small>Argon</small>
	19 39.0983 K <small>Potassium</small>	20 40.078 Ca <small>Calcium</small>	21 44.9559 Sc <small>Scandium</small>	22 47.867 Ti <small>Titanium</small>	23 50.9415 V <small>Vanadium</small>	24 51.9961 Cr <small>Chromium</small>	25 54.9380 Mn <small>Manganese</small>	26 55.845 Fe <small>Iron</small>	27 58.9332 Co <small>Cobalt</small>	28 58.6934 Ni <small>Nickel</small>	29 63.546 Cu <small>Copper</small>	30 65.409 Zn <small>Zinc</small>	31 69.723 Ga <small>Gallium</small>	32 72.64 Ge <small>Germanium</small>	33 74.9216 As <small>Arsenic</small>	34 78.96 Se <small>Selenium</small>	35 79.904 Br <small>Bromine</small>	36 83.798 Kr <small>Krypton</small>		
	37 85.4678 Rb <small>Rubidium</small>	38 87.62 Sr <small>Strontium</small>	39 88.9058 Y <small>Yttrium</small>	40 91.224 Zr <small>Zirconium</small>	41 92.9064 Nb <small>Niobium</small>	42 95.94 Mo <small>Molybdenum</small>	43 (98) Tc <small>Technetium</small>	44 101.07 Ru <small>Ruthenium</small>	45 102.9055 Rh <small>Rhodium</small>	46 106.42 Pd <small>Palladium</small>	47 107.8682 Ag <small>Silver</small>	48 112.411 Cd <small>Cadmium</small>	49 114.818 In <small>Indium</small>	50 118.710 Sn <small>Tin</small>	51 121.760 Sb <small>Antimony</small>	52 127.60 Te <small>Tellurium</small>	53 126.9045 I <small>Iodine</small>	54 131.293 Xe <small>Xenon</small>		
	55 132.9055 Cs <small>Cesium</small>	56 137.327 Ba <small>Barium</small>	71 174.967 Lu <small>Lutetium</small>	72 178.49 Hf <small>Hafnium</small>	73 180.9479 Ta <small>Tantalum</small>	74 183.84 W <small>Tungsten</small>	75 186.207 Re <small>Rhenium</small>	76 190.23 Os <small>Osmium</small>	77 192.217 Ir <small>Iridium</small>	78 195.084 Pt <small>Platinum</small>	79 196.9666 Au <small>Gold</small>	80 200.59 Hg <small>Mercury</small>	81 204.3833 Tl <small>Thallium</small>	82 207.2 Pb <small>Lead</small>	83 208.9804 Bi <small>Bismuth</small>	84 (209) Po <small>Polonium</small>	85 (210) At <small>Astatine</small>	86 (222) Rn <small>Radon</small>		
	87 (223) Fr <small>Francium</small>	88 (226) Ra <small>Radium</small>	103 (262) Lr <small>Lawrencium</small>	104 (261) Rf <small>Rutherfordium</small>	105 (262) Db <small>Dubnium</small>	106 (266) Sg <small>Seaborgium</small>	107 (264) Bh <small>Bohrium</small>	108 (277) Hs <small>Hassium</small>	109 (268) Mt <small>Meitnerium</small>	110 (281) Ds <small>Darmstadtium</small>	111 (272) Rg <small>Roentgenium</small>	112 (285) Uub <small>Ununbium</small>	113 (284) Uut <small>Ununtrium</small>	114 (289) Uuq <small>Ununquadium</small>	115 (288) Uup <small>Ununpentium</small>	116 (293) Uuh <small>Ununhexium</small>		118 (294) Uuo <small>Ununoctium</small>		

Lanthanide series

57 138.9053 La <small>Lanthanum</small>	58 140.116 Ce <small>Cerium</small>	59 140.9076 Pr <small>Praseodymium</small>	60 144.242 Nd <small>Neodymium</small>	61 (145) Pm <small>Promethium</small>	62 150.36 Sm <small>Samarium</small>	63 151.964 Eu <small>Europium</small>	64 157.25 Gd <small>Gadolinium</small>	65 158.9254 Tb <small>Terbium</small>	66 162.500 Dy <small>Dysprosium</small>	67 164.9303 Ho <small>Holmium</small>	68 167.259 Er <small>Erbium</small>	69 168.9342 Tm <small>Thulium</small>	70 173.04 Yb <small>Ytterbium</small>
---	---	--	--	---	--	---	--	---	---	---	---	---	---

Actinide series

89 (227) Ac <small>Actinium</small>	90 232.0381 Th <small>Thorium</small>	91 231.0359 Pa <small>Protactinium</small>	92 238.0289 U <small>Uranium</small>	93 (237) Np <small>Neptunium</small>	94 (244) Pu <small>Plutonium</small>	95 (243) Am <small>Americium</small>	96 (247) Cm <small>Curium</small>	97 (247) Bk <small>Berkelium</small>	98 (251) Cf <small>Californium</small>	99 (252) Es <small>Einsteinium</small>	100 (257) Fm <small>Fermium</small>	101 (258) Md <small>Mendelevium</small>	102 (259) No <small>Nobelium</small>
---	---	--	--	--	--	--	---	--	--	--	---	---	--

Physical Constants

Avogadro's number	$N_A = 6.0221415 \times 10^{23} \text{ mol}^{-1}$
Bohr radius	$a_0 = 0.5291772108 \text{ \AA} = 5.291772108 \times 10^{-11} \text{ m}$
Boltzmann's constant	$k_B = 1.3806505 \times 10^{-23} \text{ J K}^{-1}$
Electron charge	$e = 1.60217653 \times 10^{-19} \text{ C}$
Faraday constant	$\mathcal{F} = 96,485.3383 \text{ C mol}^{-1}$
Masses of fundamental particles:	
Electron	$m_e = 9.1093826 \times 10^{-31} \text{ kg}$
Proton	$m_p = 1.67262171 \times 10^{-27} \text{ kg}$
Neutron	$m_n = 1.67492728 \times 10^{-27} \text{ kg}$
Permittivity of vacuum	$\epsilon_0 = 8.854187817 \times 10^{-12} \text{ C}^2 \text{ J}^{-1} \text{ m}^{-1}$
Planck's constant	$h = 6.62606893 \times 10^{-34} \text{ J s}$
Ratio of proton mass to electron mass	$m_p/m_e = 1836.15267261$
Speed of light in a vacuum	$c = 2.99792458 \times 10^8 \text{ m s}^{-1}$ (exactly)
Standard acceleration of terrestrial gravity	$g = 9.80665 \text{ m s}^{-2}$ (exactly)
Universal gas constant	$R = 8.314472 \text{ J mol}^{-1} \text{ K}^{-1}$ $= 0.0820574 \text{ L atm mol}^{-1} \text{ K}^{-1}$

Values are taken from the 2002 CODATA recommended values, as listed by the National Institute of Standards and Technology.

Conversion Factors

Ångström	$1 \text{ \AA} = 10^{-10} \text{ m}$
Atomic mass unit	$1 \text{ u} = 1.66053886 \times 10^{-27} \text{ kg}$ $1 \text{ u} = 1.49241790 \times 10^{-10} \text{ J} = 931.494043 \text{ MeV}$ (energy equivalent from $E = mc^2$)
Calorie	$1 \text{ cal} = 4.184 \text{ J}$ (exactly)
Electron volt	$1 \text{ eV} = 1.60217653 \times 10^{-19} \text{ J}$ $= 96.485335 \text{ kJ mol}^{-1}$
Foot	$1 \text{ ft} = 12 \text{ in} = 0.3048 \text{ m}$ (exactly)
Gallon (U.S.)	$1 \text{ gallon} = 4 \text{ quarts} = 3.78541 \text{ L}$ (exactly)
Liter	$1 \text{ L} = 10^{-3} \text{ m}^3 = 10^3 \text{ cm}^3$ (exactly)
Liter-atmosphere	$1 \text{ L atm} = 101.325 \text{ J}$ (exactly)
Metric ton	$1 \text{ t} = 1000 \text{ kg}$ (exactly)
Pound	$1 \text{ lb} = 16 \text{ oz} = 0.4539237 \text{ kg}$ (exactly)
Rydberg	$1 \text{ Ry} = 2.17987209 \times 10^{-18} \text{ J}$ $= 1312.7136 \text{ kJ mol}^{-1}$ $= 13.6056923 \text{ eV}$
Standard atmosphere	$1 \text{ atm} = 1.01325 \times 10^5 \text{ Pa}$ $= 1.01325 \times 10^5 \text{ kg m}^{-1} \text{ s}^{-2}$ (exactly)
Torr	$1 \text{ torr} = 133.3224 \text{ Pa}$

SIXTH EDITION

Principles of Modern Chemistry

This page intentionally left blank

SIXTH EDITION

Principles of Modern Chemistry

DAVID W. OXTOBY

Pomona College

H.P. GILLIS

University of California–Los Angeles

ALAN CAMPION

The University of Texas at Austin

Images of orbitals in Chapters 4, 5, 6 and 8 contributed by

HATEM H. HELAL

California Institute of Technology

KELLY P. GAITHER

The University of Texas at Austin

THOMSON

BROOKS/COLE™

Australia • Brazil • Canada • Mexico • Singapore • Spain
United Kingdom • United States



Principles of Modern Chemistry, Sixth Edition

David W. Oxtoby, H.P. Gillis, Alan Campion

Acquisitions Editor: *Lisa Lockwood*
Development Editor: *Jay Campbell*
Assistant Editor: *Sylvia Krick*
Editorial Assistant: *Toriana Holmes*
Technology Project Manager: *Lisa Weber*
Marketing Manager: *Amee Mosley*
Marketing Communications Manager: *Brian Vann*
Content Project Manager, Editorial Production: *Teresa Trego*
Creative Director: *Rob Hugel*
Art Director: *John Walker*
Print Buyer: *Doreen Suruki*
Permissions Editor: *Roberta Broyer*

Photo Researcher: *Dena Digilio Betz*
Production Service: *Graphic World Inc.*
Text Designer: *Carolyn Deacy*
Illustrator: *Greg Gambino, 2064design*
OWL Producers: *Stephen Battisti, Cindy Stein, David Hart*
(*Center for Educational Software Development, University of Massachusetts, Amherst*)
Cover Designer: *Andrew Ogus*
Cover Image: *Eric Heller*
Cover Printer: *Courier-Kendallville*
Compositor: *Graphic World Inc.*
Printer: *Courier-Kendallville*

© 2008 Thomson Brooks/Cole, a part of The Thomson Corporation. Thomson, the Star logo, and Brooks/Cole are trademarks used herein under license.

Thomson Higher Education
10 Davis Drive
Belmont, CA 94002-3098
USA

ALL RIGHTS RESERVED. No part of this work covered by the copyright hereon may be reproduced or used in any form or by any means—graphic, electronic, or mechanical, including photocopying, recording, taping, Web distribution, information storage and retrieval systems, or in any other manner—without the written permission of the publisher.

Printed in the United States of America
1 2 3 4 5 6 7 11 10 09 08 07

ExamView® and *ExamView Pro*® are registered trademarks of FSCreations, Inc. Windows is a registered trademark of the Microsoft Corporation used herein under license. Macintosh and Power Macintosh are registered trademarks of Apple Computer, Inc. Used herein under license.

© 2008 Thomson Learning, Inc. All Rights Reserved. Thomson Learning WebTutor™ is a trademark of Thomson Learning, Inc.

Library of Congress Control Number 2006941020
Student Edition:
ISBN-13: 978-0-534-49366-0
ISBN-10: 0-534-49366-1

Asia
Thomson Learning
5 Shenton Way
#01-01 UIC Building
Singapore 068808

Canada
Thomson Nelson
1120 Birchmount Road
Toronto, Ontario M1K 5G4
Canada

Latin America
Thomson Learning
Seneca, 53
Colonia Polanco
11560 Mexico D.F.
Mexico

Australia/New Zealand
Thomson Learning Australia
102 Dodds Street
Southbank, Victoria 3006
Australia

UK/Europe/Middle East/Africa
Thomson Learning
High Holborn House
50/51 Bedford Row
London WC1R 4LR
United Kingdom

Spain/Portugal
Thomson Paraninfo
Calle Magallanes, 25
28015 Madrid, Spain

For more information about our products, contact us at:
Thomson Learning Academic Resource Center
1-800-423-0563

For permission to use material from this text or product, submit a request online at <http://www.thomsonrights.com>. Any additional questions about permissions can be submitted by e-mail to thomsonrights@thomson.com.

IN APPRECIATION OF

*Harry B. Gray, Bruce H. Mahan[†], and George C. Pimentel[†]
for the legacy of their textbooks and lectures*

*The search for truth is in one way hard and in another easy,
for it is evident that no one can master it fully or miss it completely.
But each adds a little to our knowledge of nature, and from all
the facts assembled there arises a certain grandeur.*

(Greek inscription, taken from Aristotle, on the facade of the
National Academy of Sciences building in Washington, D.C.)

This page intentionally left blank

Brief Contents

UNIT I

Introduction to the Study of Modern Chemistry 1

- 1 The Atom in Modern Chemistry 2
- 2 Chemical Formulas, Chemical Equations, and Reaction Yields 29

UNIT II

Chemical Bonding and Molecular Structure 52

- 3 Chemical Bonding: The Classical Description 54
- 4 Introduction to Quantum Mechanics 114
- 5 Quantum Mechanics and Atomic Structure 169
- 6 Quantum Mechanics and Molecular Structure 211
- 7 Bonding in Organic Molecules 275
- 8 Bonding in Transition Metal Compounds and Coordination Complexes 313

UNIT III

Kinetic Molecular Description of the States of Matter 362

- 9 The Gaseous State 364
- 10 Solids, Liquids, and Phase Transitions 409
- 11 Solutions 441

UNIT IV

Equilibrium in Chemical Reactions 484

- 12 Thermodynamic Processes and Thermochemistry 486
- 13 Spontaneous Processes and Thermodynamic Equilibrium 529
- 14 Chemical Equilibrium 569
- 15 Acid–Base Equilibria 625
- 16 Solubility and Precipitation Equilibria 677
- 17 Electrochemistry 705

UNIT V

Rates of Chemical and Physical Processes 748

- 18** Chemical Kinetics 750
- 19** Nuclear Chemistry 793
- 20** Interaction of Molecules with Light 825

UNIT VI

Materials 862

- 21** Structure and Bonding in Solids 864
- 22** Inorganic Materials 895
- 23** Polymeric Materials and Soft Condensed Matter 929

APPENDICES

- A** Scientific Notation and Experimental Error A.2
- B** SI Units, Unit Conversions, Physics for General Chemistry A.9
- C** Mathematics for General Chemistry A.21
- D** Standard Chemical Thermodynamic Properties A.37
- E** Standard Reaction Potentials at 25°C A.45
- F** Physical Properties of the Elements A.47
- G** Solutions to the Odd-Numbered Problems A.57

Index ■ Glossary I.1

Preface

When the first edition of *Principles of Modern Chemistry* appeared in 1986, the standard sequence of topics in honors and high-level mainstream general chemistry courses began with macroscopic descriptions of chemical phenomena and proceeded to interpret these in terms of molecular structure. This traditional “macro-to-micro” approach has shifted in recent years, and today the central topics in these courses are chemical bonding and molecular structure. The relation of molecular structure to function and properties requires the introduction of molecular structure early in the course and the use of structural arguments in presenting the remaining topics.

In preparing the sixth edition, we have revised the textbook extensively to meet these present-day needs. In particular, we believe that the most logical sequence of topics begins with the physical properties and structure of atoms; is followed by structure, bonding, and properties of molecules; proceeds to describe macroscopic collections of atoms and molecules; continues with a discussion of chemical properties and reactions under equilibrium conditions; and finishes with dynamics and kinetics.

Significant Changes in This Edition

- ***New Treatment and Placement of Structure and Bonding*** Chemical bonding and molecular structure are now at the beginning of the book. We describe the classical elements of bonding theory—ionic, covalent, and polar bonds; dipole moments; Lewis electron diagrams; and Valence Shell Electron Pair Repulsion (VSEPR) theory. We present a unified and thorough treatment of quantum bonding theory, presenting the molecular orbital (MO) and valence bond (VB) models on equal footing and at the same intellectual and conceptual level. We provide detailed comparisons of these two models and show how either one can be the starting point for the development of computational quantum chemistry and molecular simulation programs that our students will encounter soon in subsequent chemistry courses.
- ***New Molecular Art*** Molecular shapes are rendered with quantitative accuracy and in modern graphical style. All illustrations of atomic and molecular orbitals, charge density, and electrostatic potential energy maps were generated from accurate quantum chemistry calculations carried out at the California Institute of Technology. For this edition, the orbitals were plotted using state-of-the-art software at the Texas Advanced Computing Center at the University of Texas at Austin. The colors, lighting effects, and viewing angles were chosen to display three-dimensional objects with maximum clarity and to provide chemical insight.

- **Revised Writing Style without Loss of Rigor** The language is more modern and less formal. We have introduced a more conversational writing style, designed to engage our students as active participants in developing the presentation. We have examined every sentence in the book to simplify and lighten the language without compromising intellectual integrity.
- **Greater Flexibility in Topic Coverage** In response to user and reviewer comments, greater modularity and flexibility have been built into the text to make it compatible with alternative sequences of topics. While moving the discussion of bonding and structure to the beginning of the book, we have been careful to maintain the option to follow the “macro-to-micro” approach used in previous editions. Selecting alternative approaches is facilitated by the Unit structure of the book; we offer several suggestions in the **Teaching Options** section.
- **New End-of-Chapter Student Aids** In response to suggestions by users and reviewers, we provide a *Chapter Summary*, *Chapter Review*, and list of *Key Equations* (with citations to the sections in which they appear) at the end of each chapter. These are integrated with the *Cumulative Exercises* and *Concepts & Skills* from previous editions to provide a comprehensive set of tools for reviewing and studying the contents of each chapter.
- **New Problems** Approximately 85 new problems have been added, mostly in Unit II on bonding and structure. These follow the tradition established in previous editions that problems are based on real data for real chemical systems. We intend the problems to guide our students to develop intuition for chemical results and the magnitudes of chemical quantities, as well as facility in manipulating the equations in the problems.
- **OWL Online Homework System** Homework management is now included in the text’s instructional package. Approximately 15 problems from each chapter are available for assignment in the OWL program. See the section on Supporting Materials for a description of OWL.

Major Changes in Content and Organization

Chapter 1: The Atom in Modern Chemistry

This chapter has been reorganized to place greater emphasis on the physical structure of the atom, as determined from the classic experiments of Thomson, Millikan, and Rutherford. The chapter ends with direct scanning tunneling microscopy images of individual atoms in chemical reactions. Section 1.6 in *Principles of Modern Chemistry*, fifth edition (mole, density, molecular volume), has been moved to Chapter 2, which now gives a comprehensive treatment of formulas, stoichiometry, and chemical equations.

Chapter 3: Chemical Bonding: The Classical Description

This chapter provides a substantial introduction to molecular structure by coupling experimental observation with interpretation through simple classical models. Today, the tools of classical bonding theory—covalent bonds, ionic bonds, polar covalent bonds, electronegativity, Lewis electron dot diagrams, and VSEPR Theory—have all been explained by quantum mechanics. It is a matter of taste whether to present the classical theory first and then gain deeper insight from the

quantum explanations, or to cover the quantum theory first and then see the classical theory as a limiting case. We have found that presenting the classical description first enables our students to bring considerably greater sophistication to their first encounter with quantum mechanics and therefore to develop a deeper appreciation for that subject. In our classroom experience, we have seen that this approach offers definitive pedagogical advantages by enabling students to

- learn the language and vocabulary of the chemical bond starting from familiar physical concepts
- become familiar with the properties of a broad array of real molecules *before* attempting to explain these results using quantum mechanics
- develop experience in using physical concepts and equations to describe the behavior of atoms and molecules

We have revised this chapter to more effectively meet these goals. Changes include the following:

- Section 3.2 is completely new. It illustrates the Coulomb potential with several quantitative applications and introduces the screened potential in many-electron atoms.
- In Section 3.4 the description of electron affinity has been extended and clarified, and the Pauling and Mulliken descriptions of electronegativity are discussed together.
- Section 3.5 describing forces and potential energy in molecules is completely new. We identify the driving force for the formation of chemical bonds between atoms as a reduction of the total energy of the system. We introduce the virial theorem to analyze the separate contributions of potential and kinetic energy to this total energy reduction in various bonding models.
- The role of Coulomb stabilization in ionic bonding has been substantially simplified and clarified.

Chapter 4: Introduction to Quantum Mechanics

This chapter is the revision of Sections 15.1–15.5 in *Principles of Modern Chemistry*, fifth edition. It presents a significant introduction to the concepts and vocabulary of quantum mechanics through very careful choice of language, illustrations with experimental data, interpretation with aid of simple models, and extensive use of graphical presentations. We highlight five features of this new chapter:

- We present quantitative, computer-generated plots of the solutions to the particle-in-a-box models in two and three dimensions and use these examples to introduce contour plots and three-dimensional isosurfaces as tools for visual representation of wave functions. We show our students how to obtain physical insight into quantum behavior from these plots without relying on equations. In the succeeding chapters we expect them to use this skill repeatedly to interpret quantitative plots for more complex cases.
- The discussion of Planck's analysis of blackbody radiation has been greatly simplified and clarified.
- The description of the wavelike behavior of electrons has been extended and clarified, based on a careful description of an electron diffraction experiment.
- The explanation of uncertainty and indeterminacy has been extended and clarified.
- Section 4.7 introduces the quantum harmonic oscillator and provides the groundwork for subsequent discussions of vibrational spectroscopy. This section is completely new.

Chapter 5: Quantum Mechanics and Atomic Structure

This chapter is the revision of Sections 15.7–15.9 in *Principles of Modern Chemistry*, fifth edition. Three features are new:

- The very long Section 15.8 has been broken into three parts (Sec. 5.2–5.4) for greater ease of presentation.
- Photoelectron spectroscopy has been moved into Section 5.4, where it fits logically with the discussion of the shell structure of the atom and the periodic table.
- All atomic orbitals have been re-calculated and rendered in modern style.

Chapter 6: Quantum Mechanics and Molecular Structure

This revision has the same logical structure as Chapter 16 of *Principles of Modern Chemistry*, fifth edition. It achieves more uniform coverage and proper depth, and it adds several important new features. The mathematical level is uniform throughout the chapter. Notable features of the present version include:

- An expanded treatment of H_2^+ as the starting point for describing molecular quantum mechanics and for motivating the development of the linear combination of atomic orbitals (LCAO) approximation. This expanded treatment includes:
 - A simplified and more thorough description of the Born–Oppenheimer approximation.
 - New graphical representations of the exact molecular orbitals for H_2^+ that make it easier to visualize these orbitals and interpret their meanings. These images provide a foundation for developing MO theory for the first- and second-period diatomic molecules.
 - Careful attention has been paid to the description and analysis of potential energy curves, zero-point energy, and total energy.
 - “A Deeper Look” section shows how the H_2^+ molecular orbitals correlate with sums and differences of hydrogen atomic orbitals at large internuclear separations. This correlation provides a very clear motivation for developing the LCAO approximation to exact molecular orbitals.
- Application of the virial theorem to reveal the interplay between kinetic and potential energy in the mechanism of bond formation described by MO theory.
- Application of the LCAO approximation to small polyatomic molecules to demonstrate the generality of the method.
- Molecular photoelectron spectroscopy to connect molecular orbital energy levels to experimental measurements.
- Much more thorough treatment of the VB method than in the fifth edition; it is now on equal footing with that for LCAO.
- Detailed comparison between LCAO and VB methods, including ways to improve both, showing how each is the starting point for high-level computational quantum chemistry.

Throughout this revision we have simplified notation to the maximum extent possible without sacrificing clarity, and we have devoted considerable attention to graphical explanations of the concepts.

Chapter 7: Bonding in Organic Molecules

This chapter represents a significant reorganization and extension of Chapter 20 and Section 16.4 in the fifth edition. We describe the bonding and nomenclature

in alkanes, alkenes, alkynes, aromatics, and conjugated hydrocarbons and in the major functional groups. Our main goal is to illustrate the bonding theories from Chapter 6 with examples from organic chemistry that can be used in conjunction with Chapter 6. Our secondary goal is to provide sufficient material for a brief introduction to systematic organic chemistry. These goals are developed in these contexts:

- Petroleum refining as the source of starting materials for organic processes organizes a survey of organic structures and reactions.
- Organic synthesis organizes a survey of organic functional groups and reaction types.
- Pesticides and pharmaceuticals introduce a variety of organic compounds and structures in familiar contexts.

Chapter 8: Bonding in Transition Metal Compounds and Coordination Complexes

We have presented a comprehensive introduction to bonding in transition metal compounds and coordination complexes using MO and VB theory as developed in Chapter 6. Our goal was to demonstrate that MO theory is not limited to the first- and second-period diatomic molecules and that it provides the most satisfactory method for describing bonding in coordination complexes. The material covered in this chapter now provides a self-contained introduction to structure and bonding in inorganic chemistry that should provide sound preparation for an advanced inorganic chemistry course.

Chapter 9: The Gaseous State

A new “Deeper Look” section introduces the Boltzmann energy distribution and applies it to determine the relative populations of molecular energy states.

Chapter 10: Solids, Liquids, and Phase Transitions

Section 10.2 on Intermolecular Forces includes an introduction to electrostatic potential energy maps. We define these surfaces very carefully to provide a solid foundation for our students when they encounter these representations in their organic chemistry courses.

Chapter 14: Chemical Equilibrium

The language of this chapter has been completely revised, but the contents are essentially the same as in Chapter 9 of the fifth edition. To provide flexibility for instructors, this chapter was written to allow thermodynamics to be taught either before or after equilibrium. Each topic is introduced first from the empirical point of view then followed immediately with the thermodynamic treatment of the same topic. Instructors who prefer to treat thermodynamics first can use the chapter as written, whereas those who prefer the empirical approach can skip appropriate sections, then come back and pick up the thermo-based equilibrium sections after they cover basic thermodynamics. “Signposts” are provided in each section to guide these two groups of readers; the options are clearly marked. Specific examples of this flexible approach are:

- Section 14.2 provides a thorough discussion of procedures for writing the empirical law of mass action for gas-phase, solution, and heterogeneous reactions, with specific examples for each.

- Section 14.3 follows with the thermodynamic prescription for calculating the equilibrium constant from tabulated Gibbs free energy values for gas-phase, solution, and heterogeneous reactions, with specific examples for each.
- Sections 14.4 and 14.5 present a variety of equilibrium calculations based on the empirical law of mass action.
- Section 14.6 discusses direction of change in terms of the empirical reaction quotient Q , with illustrations in gas-phase, solution, and heterogeneous reactions.
- Section 14.7 discusses direction of change from the point of view of thermodynamics, relating Q to the Gibbs free energy change and the equilibrium constant.

Chapter 22: Inorganic Materials

Chapters 22 and 23 in the fifth edition have been combined, reorganized, and revised to provide a systematic introduction to ceramics, electronic materials, and optical materials. Structural, electrical, and optical properties are related to the nature of the chemical bonds in each class of materials.

Teaching Options

The text is structured and written to give instructors significant flexibility in choosing the order in which topics are presented. We suggest several such possibilities here. In all cases we recommend starting with Chapter 1 to provide a contemporary introduction to the structure and properties of the atom, followed by Chapter 2 to establish a secure foundation in “chemical accounting methods” that is necessary for studying all the remaining chapters. Particularly well-prepared students can skip Chapter 2, especially if diagnostics are available to ascertain satisfactory background.

Classical Bonding before Introduction to Quantum Theory

Chapters 1, 2, 3, 4, 5, 6; selections from Chapter 7 and Chapter 8; Chapters 9–23

This is the sequence we have found most effective because it enables our students to bring substantially greater maturity to their first exposure to quantum theory. This leads to deeper and quicker mastery of quantum theory and its applications to atomic and molecular structure. Instructors who wish to introduce molecular spectroscopy earlier can easily cover Sections 20.1–20.4 immediately after Chapter 6.

Introduction to Quantum Theory before Bonding

Chapters 1, 2, 4, 5, 3, 6; selections from Chapter 7 and Chapter 8; Chapters 9–23

Chapters 1, 2, 4, 5, 6, 3; selections from Chapter 7 and Chapter 8; Chapters 9–23

These sequences are appropriate for instructors who prefer to establish background in quantum theory before discussing ionic and covalent bonding, Lewis diagrams, and VSEPR theory. Instructors who prefer to cover these classical bonding topics after quantum mechanics but before MO and VB theory would cover

Chapter 3 before Chapter 6. Those who want to present the full quantum story first and then present the classical description as the limiting case would cover Chapter 3 after Chapter 6. We recommend that both of these sequences cover Section 3.2 (force and potential energy in atoms) before Chapter 4 to give a good physical feeling for Rutherford's planetary model of the atom in preparation for the quantum theory. Instructors who wish to introduce molecular spectroscopy earlier can easily cover Sections 20.1–20.4 immediately after Chapter 6.

Traditional “Macro-to-Micro” Approach

Chapters 1, 2, 9–19, 3–8, 20–23

This sequence covers fully the macroscopic descriptions of chemical phenomena and then begins to interpret them in terms of molecular structure. Instructors could choose either of the two bonding approaches suggested earlier for the specific order of Chapters 3–6 late in this course. This sequence represents a rather pure form of the “macro-to-micro” approach that was followed in the first three editions. Alternatively, they could cover Chapter 3 between Chapter 2 and Chapter 9, as was done in the fourth and fifth editions. This approach has the advantage of building a substantial foundation in structure—and a complete discussion of chemical nomenclature—as the basis for the macroscopic descriptions, while leaving the quantum theory of bonding to come later in the course.

Thermodynamics before Chemical Equilibrium

Chapters 12, 13, 14, 15, 16, 17

This is the sequence we have found to be the most effective. If our students first have a good understanding for the physical basis of equilibrium, then the facts and trends of chemical equilibrium quickly begin to form patterns around molecular structure. Changes in entropy and bond energy immediately organize chemical equilibrium.

Empirical Chemical Equilibrium before Thermodynamics

Chapter 14 (omit Sections 14.3, 14.7); Chapters 15, 16, 12, 13; Sections 14.3, 14.7; Chapter 17

Perhaps to provide background for quantitative laboratory work, others may wish to present chemical equilibrium earlier in the course in a more empirical fashion, before the presentation of thermodynamics. Chapter 14 is clearly marked with “signposts” to facilitate this sequence.

General Aspects of Flexibility

Certain topics may be omitted without loss of continuity. For example, a principles-oriented course might cover the first 20 chapters thoroughly and then select one or two specific topics in the last chapters for close attention. A course with a more descriptive orientation might omit the sections entitled “A Deeper Look,” which are more advanced conceptually and mathematically than the sections in the main part of the book, and cover the last three chapters more systematically. Additional suggestions are given in the *Instructor's Manual* that accompanies the book.

Features

Mathematical Level

This book presupposes a solid high school background in algebra and coordinate geometry. The concepts of slope and area are introduced in the physical and chemical contexts in which they arise, and differential and integral notation is used only when necessary. The book is designed to be fully self-contained in its use of mathematical methods. In this context, Appendix C should prove particularly useful to the student and the instructor.

Key equations in the text are highlighted in color and numbered on the right side of the text column. Students should practice using them for chemical calculations. These key equations appear again in a special section at the end of each chapter. Other equations, such as intermediate steps in mathematical derivations, are less central to the overall line of reasoning in the book.

Updated Design and New Illustrations and Photographs

This sixth edition features a modern design, whose elements have been carefully arranged for maximum clarity and whose aesthetics should engage today's visually oriented students. We have selected photographs and illustrations to amplify and illuminate concepts in the narrative text. All illustrations of atomic and molecular orbitals, charge density, and electrostatic potential energy maps were generated expressly for this textbook. The orbitals and charge densities were calculated by Mr. Hatem Helal in the Materials Simulation Center at the California Institute of Technology, directed by Professor William A. Goddard III. Dr. Kelly Gaither plotted the images using state-of-the-art software at the Scientific Visualization Laboratory at The University of Texas at Austin. The colors, lighting effects, and viewing angles were chosen to display three-dimensional objects with maximum clarity and chemical insight. In many cases quantitative contour plots accompany the three-dimensional isosurfaces representing orbitals to help our students understand how the appearances of isosurfaces depend on choices made by scientists and that these isosurfaces are neither unique nor definitive.

Worked Examples

This textbook includes worked examples that demonstrate the methods of reasoning applied in solving chemical problems. The examples are inserted immediately after the presentation of the corresponding principles, and cross-references are made to related problems appearing at the end of the chapter.

A Deeper Look

Sections entitled “A Deeper Look” provide students with a discussion of the physical origins of chemical behavior. The material that they present is sometimes more advanced mathematically than that in the main parts of the book. The material provided in these sections allows instructors to more easily tailor the breadth and depth of their courses to meet their specific objectives.

Key Terms

Key terms appear in boldface where they are first introduced. Definitions for most key terms are also included in the Index/Glossary for ready reference.

NEW Chapter Summary

Immediately at the end of each chapter is a summary that ties together the main themes of the chapter in a retrospective manner. This complements the introductory passage at the beginning of the chapter in a manner that conveys the importance of the chapter. The summary is the first in a set of six end-of-chapter features that constitute a comprehensive set of tools for organizing, studying, and evaluating mastery of the chapter.

Cumulative Exercise

At the end of each of Chapters 2 through 21 is a cumulative exercise that focuses on a problem of chemical interest and draws on material from the entire chapter for its solution. Working through a chapter's cumulative exercise provides a useful review of material in the chapter, helps students put principles into practice, and prepares them to solve the problems that follow.

NEW Chapter Review

The chapter review is a concise summary of the main ideas of the chapter. It provides a checklist for students to review their mastery of these topics and return to specific points that need further study.

Concepts & Skills

Each chapter concludes with a list of concepts and skills for review by our students. Included in this list are cross-references to the section in which the topic was covered and to problems that help test mastery of the particular skill involved. This feature is helpful for self-testing and review of material.

NEW Key Equations

All the equations that are highlighted in color in the chapter text are collected here, with references to the section in which they appeared. This list guides our students to greater familiarity with these important equations and enables quick location of additional information related to each equation.

Problems

Problems are grouped into three categories. Answers to odd-numbered “paired problems” are provided in Appendix G; they enable students to check the answer to the first problem in a pair before tackling the second problem. The *Additional Problems*, which are unpaired, illustrate further applications of the principles developed in the chapter. The *Cumulative Problems* integrate material from the chapter with topics presented earlier in the book. We integrate more challenging problems throughout the problems sets and identify them with asterisks.

Appendices

Appendices A, B, and C are important pedagogically. Appendix A discusses experimental error and scientific notation. Appendix B introduces the SI system of units used throughout the book and describes the methods used for converting units. Appendix B also provides a brief review of some fundamental principles in physics,

which may be particularly helpful to students in understanding topics covered in Chapters 3, 4, 5, 6, 9, 10, 12, and 13. Appendix C provides a review of mathematics for general chemistry. Appendices D, E, and F are compilations of thermodynamic, electrochemical, and physical data, respectively.

Index/Glossary

The Index/Glossary at the back of the book provides brief definitions of key terms, as well as cross-references to the pages on which the terms appear.

Supporting Materials

Student Resources

Student Solutions Manual (ISBN: 0-495-11226-7)

The *Student Solutions Manual*, written by Wade A. Freeman of the University of Illinois at Chicago, presents detailed solutions to all of the odd-numbered problems in this book.

OWL: Online Web-based Learning

Written by Roberta Day and Beatrice Botch of the University of Massachusetts, Amherst, and William Vining of the State University of New York at Oneonta. Used by more than 300 institutions and proven reliable for tens of thousands of students, OWL offers unsurpassed ease of use, reliability, and dedicated training and service. OWL makes homework management a breeze and helps students improve their problem-solving skills and visualize concepts, providing instant analysis and feedback on a variety of homework problems, including tutors, simulations, and chemically and/or numerically parameterized short-answer questions and questions that employ graphic rendering programs such as Jmol. OWL is the only system specifically designed to support mastery learning, where students work as long as they need to master each chemical concept and skill. *Approximately 15 problems from each chapter are available for assignment in OWL.*

NEW *A Complete e-Book!*

The **Oxtoby e-Book in OWL** includes the complete textbook as an assignable resource that is fully linked to OWL homework content, including the Oxtoby problems mentioned earlier. This new **e-Book in OWL** is an exclusive option that will be available to all your students if you choose it. The e-Book in OWL can be packaged with the text and/or ordered as a text replacement. Please consult your Thomson Brooks/Cole representative for pricing details.

To learn more about OWL, visit <http://owl.thomsonlearning.com> or contact your Thomson Brooks/Cole representative. OWL is only available for use by adopters in North America.

Instructor Resources

eBank Instructor's Manual

The *Instructor's Manual*, written by Wade A. Freeman of the University of Illinois at Chicago, contains solutions to the even-numbered problems, as well as suggestions for ways to use this textbook in courses with different sequences of topics. *Contact your Thomson Brooks/Cole representative to download your copy.*

NEW *eBank Testbank*

The test bank includes problems and questions representing every chapter in the text. *Contact your Thomson Brooks/Cole representative to download your copy.*

NEW ExamView (Windows/Macintosh)

This easy-to-use software allows professors to create, print, and customize exams. The test bank includes problems and questions representing every chapter in the text. Answers are provided on a separate grading key, making it easy to use the questions for tests, quizzes, or homework assignments. *ExamView* is packaged as a hybrid CD for both Windows' and Macintosh formats.

OWL: *Online Web-based Learning and e-Book in OWL*
See description under Student Resources.

Presentation Tools

Online Images for Oxtoby/Gillis/Campion's
Principles of Modern Chemistry, Sixth Edition

This digital library of artwork from the text is available in PowerPoint® format on the book's website. Download at www.thomsonedu.com/chemistry/oxtoby.

Laboratory Resources

Customize your own lab manual for your general chemistry course using the wide range of high-quality experiments available from CER, Outernet, and Brooks/Cole. Work with your Brooks/Cole or Thomson Custom Publishing representative and/or visit www.textchoice.com/chemistry to select the specific experiments you want, collate in any order, and combine them with materials of your own for a lab manual that is perfectly suited to your particular course needs. The full-service website allows you to search by course and experiment and view each lab in its entirety—including new labs as they are developed—before selecting. Add your own material—course notes, lecture outlines, articles, and more at the beginning and end of any experiment—online in minutes. It's easy! Your custom lab manual can be packaged with any Brooks/Cole text for even greater value and convenience. Visit www.textchoice.com/chemistry.

Acknowledgments

In preparing the sixth edition, we have benefited greatly from the comments of students who used the first five editions over the years. We would also like to acknowledge the many helpful suggestions of colleagues at Pomona College, The University of Chicago, the University of California–Los Angeles, the University of Texas at Austin and other colleges and universities who have taught from this book. We are particularly grateful to Professor Samir Anz of California Polytechnic State University, Pomona, and to Professor Andrew Pounds of Mercer University for their comments and advice. Professors Eric Anslyn, Ray Davis, Brad Holliday, Brent Iverson, Richard Jones, Peter Rossky, Jason Shear, John Stanton, David Vanden Bout, Grant Willson, and Robert Wyatt of The University of Texas at Austin were unfailingly generous with their time and advice.

We extend special thanks to the following professors who offered comments on the fifth edition or reviewed manuscript for the sixth edition:

Joseph J. Belbruno, Dartmouth College

Laurie J. Butler, The University of Chicago

Patricia D. Christie, Massachusetts Institute of Technology

Regina F. Frey, Washington University, Saint Louis
Roberto A. Garza, Pomona College
Graeme C. Gerrans, University of Virginia
Henry C. Griffin, University of Michigan, Ann Arbor
Jeffrey Krause, University of Florida
Adam List, Vanderbilt University
Andrew J. Pounds, Mercer University
George C. Schatz, Northwestern University
John E. Straub, Boston University
Michael R. Topp, University of Pennsylvania
John Weare, University of California–San Diego
Peter M. Weber, Brown University
John S. Winn, Dartmouth College

We are grateful to Dr. Justin Fermann for his very careful attention to detail as accuracy reviewer of the sixth edition.

We are much indebted to our longtime friend Professor Eric J. Heller of Harvard University for the beautiful and striking image that graces the cover of our book. Professor Heller's work demonstrates that images of great beauty can arise from scientific research and that artistic renderings effectively convey the meaning of scientific results. We are certain this image will entice readers to peek between the covers of our book, and we hope they find scientific beauty on the inside as well as on the cover!

We are particularly grateful to friends and colleagues who provided original scientific illustrations for the book. They are Professor Wilson Ho (University of California–Irvine), Dr. Gilberto Medeiros-Ribeiro and Dr. R. Stanley Williams (Hewlett-Packard Research Laboratories), Professor Leonard Fine (Columbia University), Professor Andrew J. Pounds (Mercer University) and Dr. Mark Iken (Scientific Visualization Laboratory, Georgia Institute of Technology), Dr. Stuart Watson and Professor Emily Carter (Princeton University), Professor Nathan Lewis (California Institute of Technology), Dr. Don Eigler (IBM Almaden Research Center), Dr. Gerard Parkinsen and Mr. William Gerace (OMICRON Vakuumphysik), Dr. Richard P. Muller and Professor W.A. Goddard III (California Institute of Technology), Professor Mounqi Bawendi and Ms. Felice Frankel (Massachusetts Institute of Technology), Professor Graham Fleming (University of California–Berkeley), Professor Donald Levy (The University of Chicago), Professor W.E. Moerner (Stanford University), Dr. Jane Strouse (University of California–Los Angeles), Professor James Speck and Professor Stephen Den Baars (University of California–Santa Barbara), and Professor John Baldeschwieler (California Institute of Technology).

We are especially grateful to Mr. Hatem H. Helal (California Institute of Technology) who carried out all the quantum chemistry calculations for the orbital illustrations in Chapters 4, 5, 6, and 8 and to Dr. Kelly P. Gaither (Texas Advanced Computing Center, The University of Texas at Austin) who generated these illustrations from the results of the calculations. Our longtime friend and colleague Professor William A. Goddard III (California Institute of Technology) very generously made his computational facilities available for these calculations and provided much good advice as we selected and prepared these illustrations. Sarah Chandler (The University of Texas–Austin) was very helpful in generating a number of graphs and two-dimensional surfaces.

We are also indebted to Professor Charles M. Knobler of the University of California–Los Angeles, Professor Jurg Waser formerly of the California Institute of Technology, and Mrs. Jean T. Trueblood (widow of the late Professor Kenneth N.

Trueblood of the University of California–Los Angeles) for permission to incorporate selected problems from their distinguished textbook *ChemOne*, Second Edition, McGraw-Hill, New York (1980).

On a personal note, it gives us genuine pleasure to dedicate this sixth edition of our textbook to Professor Harry Gray and to the memory of Professors Bruce Mahan and George Pimentel. We have enjoyed and been inspired by their textbooks, lectures, research papers, and seminars since our student days in the 1970s. Our own education owes much to their pioneering explanations of the role of quantum mechanics in chemical bonding.

The staff members at Brooks/Cole have been most helpful in preparing this sixth edition. In particular, we acknowledge the key role of our Acquisitions Editor Lisa Lockwood and our Developmental Editor Jay Campbell for guiding us toward revisions in this edition. Assistant Editor Sylvia Krick and Editorial Assistant Toriana Holmes coordinated production of the ancillary materials. Technology Project Manager Lisa Weber handled the media products. Senior Content Project Manager Teresa L. Trego of Brooks/Cole and Production Editor Alison Trulock of Graphic World Publishing Services kept the schedule moving smoothly. We acknowledge the contributions of Art Director Rob Hugel, who shepherded the new illustrations through the production process in this edition, and of Photo Researcher Dena Digilio Betz, who assisted in obtaining key photographs. Jim Smith, color consultant, made important contributions to the development of the color palette for the book. We are grateful to Marketing Manager Ameer Mosley for helping us obtain valuable comments from users and reviewers. We gratefully acknowledge the continuing support of Publisher David Harris.

Finally, Alan Champion would like to acknowledge his parents, Alice and Harold Champion, for their support and encouragement during the course of his education and career. And special thanks go to his wife, Ellen, and daughters, Blair and Ali, for putting up with him for the past 18 months with more patience and grace than he deserves.

David W. Oxtoby
Pomona College

H.P. Gillis
University of California–Los Angeles

Alan Champion
The University of Texas at Austin

November 2006

This page intentionally left blank

Contents

UNIT I

Introduction to the Study of Modern Chemistry 1

CHAPTER 1

The Atom in Modern Chemistry 2

- 1.1 The Nature of Modern Chemistry 2
- 1.2 Macroscopic Methods for Classifying Matter 5
- 1.3 Indirect Evidence for the Existence of Atoms: Laws of Chemical Combination 8
- 1.4 The Physical Structure of Atoms 14
- 1.5 Imaging Atoms, Molecules, and Chemical Reactions 22

CHAPTER 2

Chemical Formulas, Chemical Equations, and Reaction Yields 29

- 2.1 The Mole: Weighing and Counting Molecules 30
- 2.2 Empirical and Molecular Formulas 34
- 2.3 Chemical Formula and Percentage Composition 35
- 2.4 Writing Balanced Chemical Equations 37
- 2.5 Mass Relationships in Chemical Reactions 39
- 2.6 Limiting Reactant and Percentage Yield 41

UNIT II

Chemical Bonding and Molecular
Structure 52

CHAPTER 3

Chemical Bonding: The Classical Description 54

- 3.1 The Periodic Table 56
- 3.2 Forces and Potential Energy in Atoms 59
- 3.3 Ionization Energies and the Shell Model of the Atom 63
- 3.4 Electronegativity: The Tendency of Atoms to Attract Electrons 69
- 3.5 Forces and Potential Energy in Molecules: Formation of Chemical Bonds 72
- 3.6 Ionic Bonding 75
- 3.7 Covalent and Polar Covalent Bonding 78
- 3.8 Lewis Diagrams for Molecules 85
- 3.9 The Shapes of Molecules: Valence Shell Electron-Pair Repulsion Theory 92
- 3.10 Oxidation Numbers 97
- 3.11 Inorganic Nomenclature 100

CHAPTER 4

Introduction to Quantum Mechanics 114

- 4.1 Preliminaries: Wave Motion and Light 116
- 4.2 Evidence for Energy Quantization in Atoms 119
- 4.3 The Bohr Model: Predicting Discrete Energy Levels 127
- 4.4 Evidence for Wave-Particle Duality 131
- 4.5 The Schrödinger Equation 141
- 4.6 Quantum Mechanics of Particle-in-a-Box Models 145
- 4.7 Quantum Harmonic Oscillator 155

CHAPTER 5

Quantum Mechanics and Atomic Structure 169

- 5.1 The Hydrogen Atom 171
- 5.2 Shell Model for Many-Electron Atoms 184
- 5.3 Aufbau Principle and Electron Configurations 189
- 5.4 Shells and the Periodic Table: Photoelectron Spectroscopy 194
- 5.5 Periodic Properties and Electronic Structure 198

CHAPTER 6**Quantum Mechanics and Molecular Structure 211**

- 6.1 Quantum Picture of the Chemical Bond 213
- 6.1.6 A Deeper Look** *Nature of the Chemical Bond in H_2^+* 222
- 6.2 De-localized Bonds: Molecular Orbital Theory and the Linear Combination of Atomic 223
- 6.2.5 A Deeper Look** *Potential Energy and Bond Formation in the LCAO Approximation* 242
- 6.2.6 A Deeper Look** *Small Polyatomic Molecules* 245
- 6.3 Photoelectron Spectroscopy for Molecules 247
- 6.4 Localized Bonds: The Valence Bond Model 252
- 6.5 Comparison of Linear Combination of Atomic Orbitals and Valence Bond Methods 261

CHAPTER 7**Bonding in Organic Molecules 275**

- 7.1 Petroleum Refining and the Hydrocarbons 276
- 7.2 The Alkanes 277
- 7.3 The Alkenes and Alkynes 282
- 7.4 Aromatic Hydrocarbons 288
- 7.5 Fullerenes 290
- 7.6 Functional Groups and Organic Reactions 292
- 7.7 Pesticides and Pharmaceuticals 300

CHAPTER 8**Bonding in Transition Metal Compounds and Coordination Complexes 313**

- 8.1 Chemistry of the Transition Metals 314
- 8.2 Bonding in Simple Molecules That Contain Transition Metals 318
- 8.3 Introduction to Coordination Chemistry 328
- 8.4 Structures of Coordination Complexes 334
- 8.5 Crystal Field Theory: Optical and Magnetic Properties 339
- 8.6 Optical Properties and the Spectrochemical Series 345
- 8.7 Bonding in Coordination Complexes 348

UNIT III

Kinetic Molecular Description of the States of Matter 362

CHAPTER 9

The Gaseous State 364

- 9.1 The Chemistry of Gases 365
- 9.2 Pressure and Temperature of Gases 367
- 9.3 The Ideal Gas Law 374
- 9.4 Mixtures of Gases 377
- 9.5 The Kinetic Theory of Gases 379
- 9.6 **A Deeper Look** *Distribution of Energy among Molecules* 386
- 9.7 Real Gases: Intermolecular Forces 388
- 9.8 **A Deeper Look** *Molecular Collisions and Rate Processes* 393

CHAPTER 10

Solids, Liquids, and Phase Transitions 409

- 10.1 Bulk Properties of Gases, Liquids, and Solids: Molecular Interpretation 410
- 10.2 Intermolecular Forces: Origins in Molecular Structure 415
- 10.3 Intermolecular Forces in Liquids 423
- 10.4 Phase Equilibrium 426
- 10.5 Phase Transitions 428
- 10.6 Phase Diagrams 430

CHAPTER 11

Solutions 441

- 11.1 Composition of Solutions 442
- 11.2 Nature of Dissolved Species 446
- 11.3 Reaction Stoichiometry in Solutions: Acid–Base Titrations 449
- 11.4 Reaction Stoichiometry in Solutions: Oxidation–Reduction Titrations 452
- 11.5 Phase Equilibrium in Solutions: Nonvolatile Solutes 458
- 11.6 Phase Equilibrium in Solutions: Volatile Solutes 467
- 11.7 Colloidal Suspensions 471

UNIT IV

Equilibrium in Chemical Reactions 484

CHAPTER 12

Thermodynamic Processes
and Thermochemistry 486

- 12.1 Systems, States, and Processes 488
- 12.2 The First Law of Thermodynamics: Internal Energy, Work, and Heat 491
- 12.3 Heat Capacity, Enthalpy, and Calorimetry 497
- 12.4 Illustrations of the First Law of Thermodynamics in Ideal Gas Processes 500
- 12.5 Thermochemistry 503
- 12.6 Reversible Processes in Ideal Gases 512

CHAPTER 13

Spontaneous Processes and Thermodynamic
Equilibrium 529

- 13.1 The Nature of Spontaneous Processes 530
- 13.2 Entropy and Spontaneity: A Molecular Statistical Interpretation 533
- 13.3 Entropy and Heat: Experimental Basis of the Second Law of Thermodynamics 537
- 13.4 A Deeper Look** *Carnot Cycles, Efficiency, and Entropy* 540
- 13.5 Entropy Changes and Spontaneity 543
- 13.6 The Third Law of Thermodynamics 550
- 13.7 The Gibbs Free Energy 552

CHAPTER 14

Chemical Equilibrium 569

- 14.1 The Nature of Chemical Equilibrium 570
- 14.2 The Empirical Law of Mass Action 574
- 14.3 Thermodynamic Description of the Equilibrium State 580
- 14.4 The Law of Mass Action for Related and Simultaneous Equilibria 587
- 14.5 Equilibrium Calculations for Gas-Phase and Heterogeneous Reactions 591
- 14.6 The Direction of Change in Chemical Reactions: Empirical Description 597

- 14.7 The Direction of Change in Chemical Reactions: Thermodynamic Explanation 603
- 14.8 Distribution of a Single Species between Immiscible Phases: Extraction and Separation Processes 606

CHAPTER 15

Acid–Base Equilibria 625

- 15.1 Classifications of Acids and Bases 626
- 15.2 Properties of Acids and Bases in Aqueous Solutions: The Brønsted–Lowry Scheme 629
- 15.3 Acid and Base Strength 633
- 15.4 Equilibria Involving Weak Acids and Bases 639
- 15.5 Buffer Solutions 645
- 15.6 Acid–Base Titration Curves 649
- 15.7 Polyprotic Acids 654
- 15.8 A Deeper Look** *Exact Treatment of Acid–Base Equilibria* 658
- 15.9 Organic Acids and Bases: Structure and Reactivity 660

CHAPTER 16

Solubility and Precipitation Equilibria 677

- 16.1 The Nature of Solubility Equilibria 678
- 16.2 Ionic Equilibria between Solids and Solutions 681
- 16.3 Precipitation and the Solubility Product 684
- 16.4 The Effects of pH on Solubility 688
- 16.5 A Deeper Look** *Selective Precipitation of Ions* 690
- 16.6 Complex Ions and Solubility 692

CHAPTER 17

Electrochemistry 705

- 17.1 Electrochemical Cells 706
- 17.2 The Gibbs Free Energy and Cell Voltage 710
- 17.3 Concentration Effects and the Nernst Equation 718
- 17.4 Batteries and Fuel Cells 723
- 17.5 Corrosion and Its Prevention 728
- 17.6 Electrometallurgy 730
- 17.7 A Deeper Look** *Electrolysis of Water and Aqueous Solutions* 735

UNIT V

Rates of Chemical and Physical Processes 748

CHAPTER 18

Chemical Kinetics 750

- 18.1 Rates of Chemical Reactions 751
- 18.2 Rate Laws 754
- 18.3 Reaction Mechanisms 761
- 18.4 Reaction Mechanisms and Rate 765
- 18.5 Effect of Temperature on Reaction Rates 770
- 18.6 **A Deeper Look** *Reaction Dynamics* 773
- 18.7 Kinetics of Catalysis 775

CHAPTER 19

Nuclear Chemistry 793

- 19.1 Mass–Energy Relationships in Nuclei 794
- 19.2 Nuclear Decay Processes 798
- 19.3 Kinetics of Radioactive Decay 803
- 19.4 Radiation in Biology and Medicine 807
- 19.5 Nuclear Fission 809
- 19.6 Nuclear Fusion and Nucleosynthesis 813

CHAPTER 20

Interaction of Molecules with Light 825

- 20.1 General Aspects of Molecular Spectroscopy 826
- 20.2 Vibrations and Rotations of Molecules: Infrared and Microwave Spectroscopy 829
- 20.3 Excited Electronic States: Electronic Spectroscopy of Molecules 835
- 20.4 Nuclear Magnetic Resonance Spectroscopy 842
- 20.5 Introduction to Atmospheric Photochemistry 845
- 20.6 Photosynthesis 851

UNIT VI

Materials 862

CHAPTER 21

Structure and Bonding in Solids 864

- 21.1 Crystal Symmetry and the Unit Cell 865
- 21.2 Crystal Structure 871
- 21.3 Cohesion in Solids 875
- 21.4 **A Deeper Look** *Lattice Energies of Crystals* 882
- 21.5 Defects and Amorphous Solids 884

CHAPTER 22

Inorganic Materials 895

- 22.1 Minerals: Naturally Occurring Inorganic Minerals 896
- 22.2 Properties of Ceramics 901
- 22.3 Silicate Ceramics 903
- 22.4 Nonsilicate Ceramics 908
- 22.5 Electrical Conduction in Materials 913
- 22.6 Band Theory of Conduction 917
- 22.7 Semiconductors 919
- 22.8 Pigments and Phosphors: Optical Displays 922

CHAPTER 23

Polymeric Materials and Soft Condensed Matter 929

- 23.1 Polymerization Reactions for Synthetic Polymers 930
- 23.2 Applications for Synthetic Polymers 934
- 23.3 Liquid Crystals 940
- 23.4 Natural Polymers 943

Appendices A.1

- A Scientific Notation and Experimental Error A.2
- B SI Units, Unit Conversions, Physics for General Chemistry A.9
- C Mathematics for General Chemistry A.21
- D Standard Chemical Thermodynamic Properties A.37
- E Standard Reaction Potentials at 25°C A.45
- F Physical Properties of the Elements A.47
- G Solutions to the Odd-Numbered Problems A.57



About the Authors

David W. Oxtoby

David W. Oxtoby is a physical chemist who studies the statistical mechanics of liquids, including nucleation, phase transitions, and liquid-state reaction and relaxation. He received his B.A. (Chemistry and Physics) from Harvard University and his Ph.D. (Chemistry) from the University of California at Berkeley. After a postdoctoral position at the University of Paris, he joined the faculty at The University of Chicago, where he taught general chemistry, thermodynamics, and statistical mechanics and served as Dean of Physical Sciences. Since 2003 he has been President and Professor of Chemistry at Pomona College in Claremont, California.

H.P. Gillis

H.P. Gillis is an experimental physical chemist who studies the surface chemistry of electronic and optical materials, including fabrication and characterization of nanostructures. He received his B.S. (Chemistry and Physics) at Louisiana State University and his Ph.D. (Chemical Physics) at The University of Chicago. After postdoctoral research at the University of California–Los Angeles and 10 years on the technical staff at Hughes Research Laboratories in Malibu, California, he joined the faculty of Georgia Institute of Technology, and now serves as Adjunct Professor of Materials Science and Engineering at the University of California–Los Angeles. He has taught general chemistry, physical chemistry, quantum mechanics, surface science, and materials science at Georgia Tech and at UCLA.

Alan Campion

Alan Campion is an experimental physical chemist who develops and applies novel methods of molecular spectroscopy to study the physical and chemical properties of solid surfaces, thin films, adsorbed molecules, and nanostructured materials. He received his B.A. (Chemistry) from New College of Florida and his Ph.D. (Chemical Physics) from the University of California–Los Angeles. After a postdoctoral position at the University of California at Berkeley, he joined the faculty of The University of Texas at Austin where he is Dow Chemical Company Professor of Chemistry and University Distinguished Teaching Professor. He teaches the honors general chemistry course, chemistry in context for students not majoring in science or engineering, physical chemistry, and advanced topics graduate courses in molecular spectroscopy.

Introduction to the Study of Modern Chemistry

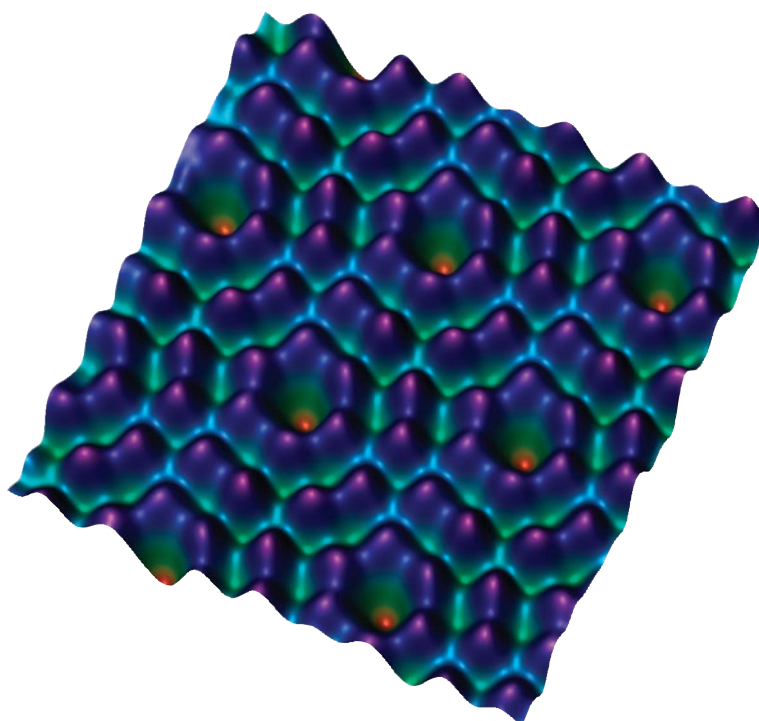


Photo courtesy of Wilson Ho, University of California, Irvine. Reprinted by permission of *Physical Review Letters*, 79, 4397–4400 (1997).

The surface of a silicon crystal imaged using a scanning tunneling microscope. Individual silicon atoms appear as purple protrusions above the background. The surface was cleaned in ultrahigh vacuum to remove all impurity atoms and the image was taken at very low temperatures (-220°C) to obtain the high resolution shown here. There are two kinds of surface silicon atoms shown in this image: "corner" silicon atoms that form hexagonal rings around a hole in the surface layer and "center" silicon atoms that appear as pairs arranged around the hexagonal rings.

Modern chemistry explores the world of atoms and molecules, seeking to explain not only their bonding, structures, and properties but also how these very structures are transformed in chemical reactions. The search for atoms and molecules began with the speculations of ancient philosophers and—stimulated by the classic experiments of the 18th- and 19th-centuries—led to John Dalton’s famed atomic hypothesis in 1808. The quest continues. Thanks to the invention of the scanning tunneling microscope (STM) in the 1980s, today’s scientists can detect and manipulate individual atoms and molecules.

UNIT CHAPTERS

CHAPTER 1

The Atom in Modern Chemistry

CHAPTER 2

Chemical Formulas, Chemical Equations, and Reaction Yields

UNIT GOALS

- To describe the key experiments, and the underlying physical models, that justify the central role of the atom in modern chemistry
 - Indirect (chemical) evidence for the existence of atoms and molecules
 - Direct (physical) evidence for the existence of atoms and molecules
 - The modern, planetary model of the atom
- To convey the established quantitative procedures for describing chemical reactions as rearrangements of atoms from reactants to products
 - The mole concept that connects weighing and counting molecules and atoms
 - Balanced chemical equations that connect moles of reactants to moles of products

The Atom in Modern Chemistry

- 1.1 The Nature of Modern Chemistry
- 1.2 Macroscopic Methods for Classifying Matter
- 1.3 Indirect Evidence for the Existence of Atoms: Laws of Chemical Combination
- 1.4 The Physical Structure of Atoms
- 1.5 Imaging Atoms, Molecules, and Chemical Reactions

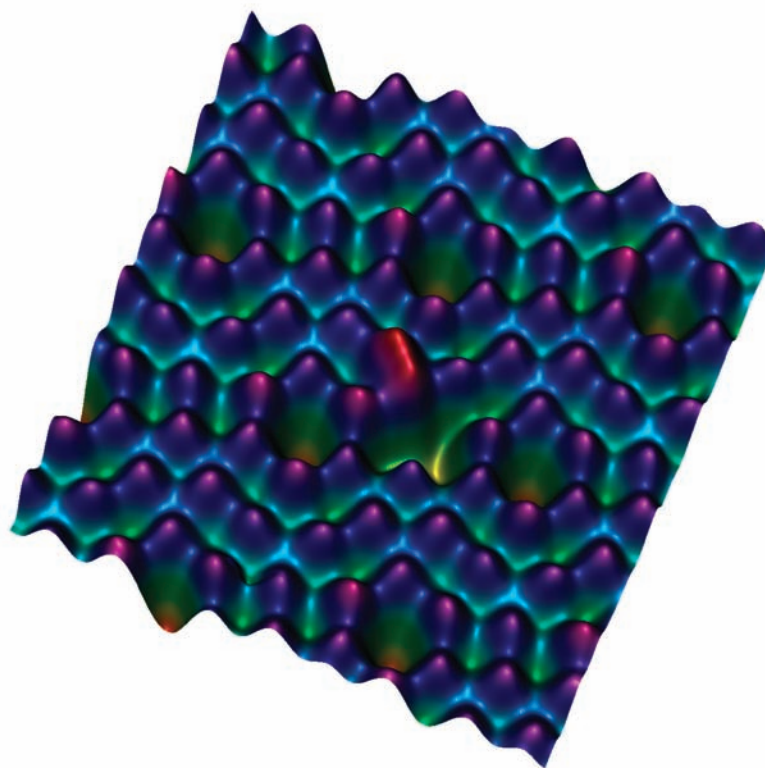


Photo courtesy of Wilson Ho, University of California, Irvine. Reprinted by permission of *Physical Review Letters*, 79, 4397–4400, (1997).

Reversible single atom transfer using the scanning tunneling microscope. This image was taken under the same conditions as the one shown opposite page 1. One of the “center” silicon atoms (imaged in red) has been transferred halfway to another center atom site by the scanning tunneling microscope tip. The atom is stable in this position at low temperatures but returns to its home site as the temperature is raised above -100°C .

1.1 The Nature of Modern Chemistry

Chemists study the properties of substances, their aim being to understand that reactions can transform substances into still other substances. Chemistry thus provides ways to tailor the properties of existing substances to meet a particular need—and even to create entirely new materials designed to have specific properties. This is how chemistry has improved agricultural production, helped prevent and cure many diseases, increased the efficiency of energy production, and reduced environmental pollution, to cite just a few advances. A particularly exciting challenge for modern chemical research is to understand the molecular dynamics of



Painting *The Alchemist* by Hendrick Heerschop, 1671; Courtesy of Dr. Alfred Bader

FIGURE 1.1 Alchemists searched in vain for procedures that would turn base metals into gold. Their apparatus foreshadowed equipment in modern chemical laboratories.

these chemical transformations, for they govern phenomena as diverse as the evolution of small carbon-containing molecules in interstellar space, changes in terrestrial atmospheric and climatic patterns caused by pollutants, and the unfolding of life processes in living organisms. Perhaps no other science covers as broad a range of topics as does chemistry; it influences disciplines from solid-state physics to molecular biology. Within a single modern chemistry department, you're apt to find chemists studying high-temperature superconductors, detecting and identifying single molecules, tailoring the properties of catalytic antibodies, and developing highly selective integrated sensors for a variety of applications in science and technology. Despite the diversity of these areas of scientific inquiry, they are all unified by a single set of fundamental scientific principles, which we will introduce to you in this textbook.

Chemistry is a relatively young science and its foundations weren't established until the last quarter of the 18th century. Before that, most chemists were known as *alchemists*—early entrepreneurs who sought to transform the properties of materials for economic gain (Fig. 1.1). For many centuries their obsession was to transform “base” metals, such as lead, into gold. They boldly assumed that the properties of one material could somehow be extracted from that material and transferred to another. If the essential properties—such as yellow color, softness, and ductility—could be assembled from various inexpensive sources, then gold could be created at great profit.

The alchemists persisted in their efforts for more than a thousand years. Although they collected many useful, empirical results that have since been incorporated into modern chemistry, they never transformed base metals into gold. Toward the middle of the 17th century, a number of individuals began to challenge the validity of the basic assumptions of the alchemists. These doubts culminated in publication of *The Sceptical Chymist* by Robert Boyle in England in the 1660s, which is one of the pivotal events that began the evolution of modern chemistry. Another century was required to complete the conceptual foundations of modern chemistry, which then flourished throughout the 19th and 20th centuries.

To observers in the early 21st century, the mistake of the alchemists is immediately clear: They did not follow the scientific method. In the scientific method, a new idea is accepted only temporarily, in the form of a **hypothesis**. It is then subjected to rigorous testing, in carefully controlled experiments. Only by surviving many such tests is a hypothesis elevated to become a **scientific law**. In addition to having explained the results of numerous experiments, a scientific law must be predictive; failure to accurately predict the results of a new experiment is sufficient to invalidate a scientific law. Concepts or ideas that have earned the status of scientific laws by direct and repeated testing then can be applied with confidence in new environments. Had a proper set of tests been made in separate, independent experiments, the alchemists would have recognized that the properties of a material are, in fact, intrinsic, inherent characteristics of that material and cannot be separated from it.

The history of the alchemists shows the origin of a certain duality in the nature of modern chemistry, which persists to the present. Because chemistry contributes to the foundations of numerous professions and industries, we see the urge to apply established chemical knowledge for profit. But we also see the urge to create new chemical knowledge, driven by both intellectual curiosity and by the desire to have reliable information for applications. Both aspects involve numerous scientists and engineers in addition to professional chemists. No matter what the specific context, the second aspect requires scrupulous adherence to the scientific method, in which new knowledge is subjected to rigorous scrutiny before it earns the confidence of the scientific community.

During their professional careers, most students who learn chemistry will be more concerned with applying chemistry than with generating new chemical knowledge. Still, a useful strategy for learning to think like an experienced chemist is to assume that you are personally responsible for establishing the scientific

foundations of chemistry for the very first time. Upon encountering a new topic, try this: imagine that you are the first person ever to see the laboratory results on which it is based. Imagine that you must construct the new concepts and explanations to interpret these results, and that you will present and defend your conclusions before the scientific community. Be suspicious. Cross check everything. Demand independent confirmations. Always remain, with Boyle, the “skeptical chemist.” Follow the scientific method in your acquisition of knowledge, even from textbooks. In this way, you will make the science of chemistry your own, and you will experience the intellectual joys of discovery and interpretation. Most important, you will recognize that chemistry is hardly a closed set of facts and formulas. Quite the contrary, it is a living, growing method for investigating all aspects of human experience that depend on the changes in the composition of substances.

Conservation of Matter and Energy

The science of chemistry rests on two well-established principles: the conservation of matter and the conservation of energy. What this means with respect to matter is absolute: The total amount of matter involved in any chemical reaction is *conserved*—that is, it remains constant throughout the reaction. Matter is neither created nor destroyed in chemical reactions; its components are simply *rearranged* to transform one substance into another.

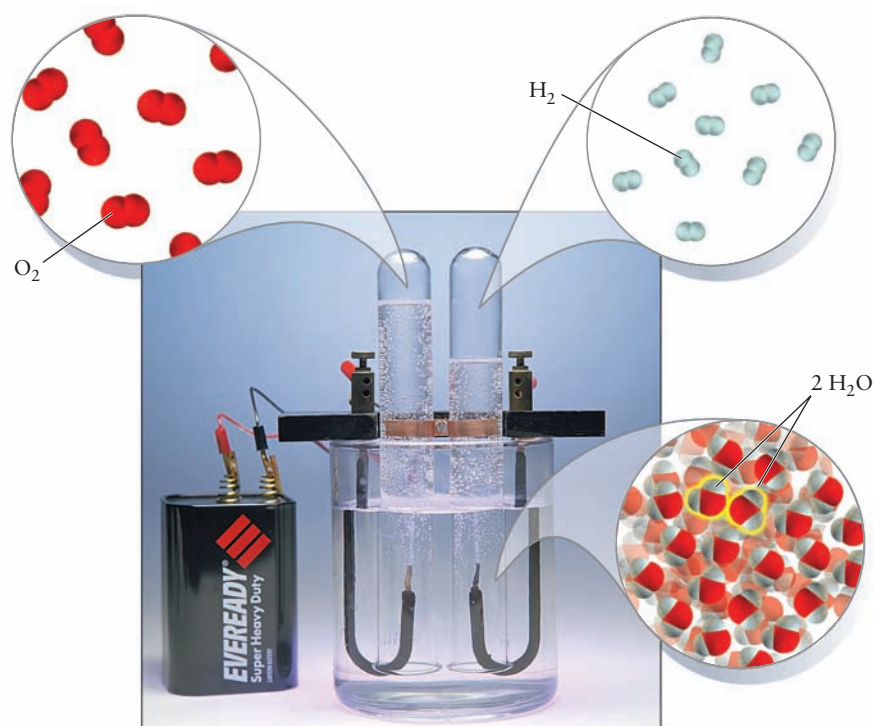
These rearrangements are inevitably accompanied by changes in energy, which brings us to the second principle. The amounts of chemical energy stored in the molecules of two different substances are intrinsically different, and chemical energy may be converted into thermal, electrical, or mechanical energy during reactions. Energy may also flow in the opposite direction. But energy is neither created nor destroyed during chemical reactions. The total amount of energy involved in a chemical reaction has always been found to be conserved.

These two core principles must be modified slightly for nuclear reactions, which occur at energies so high that matter and energy can be converted into one another through Einstein’s relation, $E = mc^2$. The *sum* of mass and energy is conserved in nuclear reactions.

Macroscopic Methods and Nanoscopic Models

Chemical reasoning, both in applications and in basic research, resembles a detective story in which tangible clues lead to a mental picture of events never directly witnessed by the detective. Chemical experiments are conducted in laboratories equipped with beakers, flasks, analytical balances, pipettes, optical spectrophotometers, lasers, vacuum pumps, pressure gauges, mass spectrometers, centrifuges, and other apparatus. Each of these devices exists on the *macroscopic* scale—that is, it is perceptible to ordinary human senses. Macroscopic sizes reach from 1 meter (m) down to 1 millimeter (mm), which is 1×10^{-3} m. But the actual chemical transformation events occur in the *nanoscopic* world of atoms and molecules—objects far too small to be detected by the naked eye, even with the aid of a first-class microscope. One nanometer (nm) is 1×10^{-9} m. So our modern laboratory instruments are the bridge between these worlds, giving us the means not only to influence the actions of the atoms and molecules but also to measure their response. Figure 1.2 shows both worlds simultaneously. In illustrating the chemical decomposition of water into gaseous hydrogen and oxygen by electrolysis, it shows the relation between events on the macroscale and the nanoscale. Chemists *think* in the highly visual nanoscopic world of atoms and molecules, but they *work* in the tangible world of macroscopic laboratory apparatus. These two aspects of chemical science cannot be divorced, and we will emphasize their interplay throughout this textbook. Students of chemistry must master not only the fascinating concepts of chemistry, which describe the nanoscopic world of atoms and molecules, but also the macroscopic procedures of chemistry on which those concepts are founded.

FIGURE 1.2 As electric current passes through water containing dissolved sulfuric acid, gaseous hydrogen and oxygen form as bubbles at the electrodes, producing the two gases in the 2:1 ratio by volume. The chemical transformation, induced by the macroscopic apparatus, proceeds by rearrangement of atoms at the nanoscale.



© Thomson Learning/Charles D. Winters

1.2 Macroscopic Methods for Classifying Matter

Chemists study how one set of pure substances will transform into another set of pure substances in a chemical reaction. This study involves two traditions—**analysis** (taking things apart) and **synthesis** (putting things together)—that go back to early Greek philosophers, who sought to analyze the constituents of all matter for four elements: air, earth, fire, and water. Contemporary chemists classify matter using a very different set of fundamental building blocks, but the analysis and synthesis steps are basically unchanged.

Substances and Mixtures

Investigating chemical reactions can be greatly complicated and often obscured by the presence of extraneous materials. So, the first step, therefore, is to learn how to analyze and classify materials to be sure you are working with *pure* substances before commencing with reactions (Fig. 1.3). Suppose you take a sample of a material—some gas, liquid, or solid—and examine its various properties or distinguishing characteristics, such as its color, odor, or density. How uniform are those properties? Different regions of a piece of wood, for example, have different properties, such as variations in color. Wood, then, is said to be **heterogeneous**. Other materials, such as air or a mixture of salt and water, are classified as **homogeneous** because their properties do not vary throughout the sample. We cannot call them pure substances, however. We still have to call them **mixtures**, because it is possible to separate them into components by ordinary physical means such as melting, freezing, boiling, or dissolving in solvents (Fig. 1.4). These operations provide ways of separating materials from one another by their properties, such as freezing point, boiling point, and solubility. For example, air is a mixture of several components—oxygen, nitrogen, argon, and various other gases. If air is liquefied and then warmed slowly, the gases with the lowest boiling points will evaporate first, leaving behind in the liquid those with higher boiling points. Such a separation would not be perfect, but the processes of liquefaction and evaporation could

FIGURE 1.3 Outline of the steps in the analysis of matter.

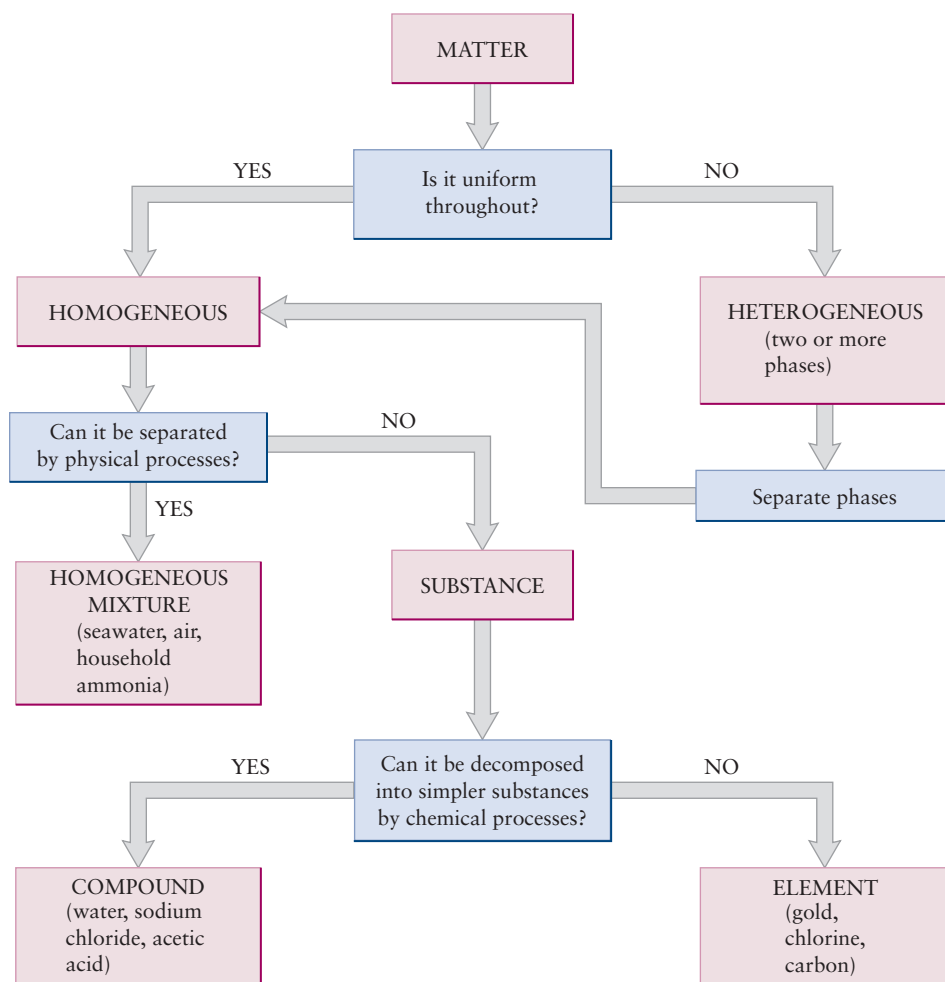
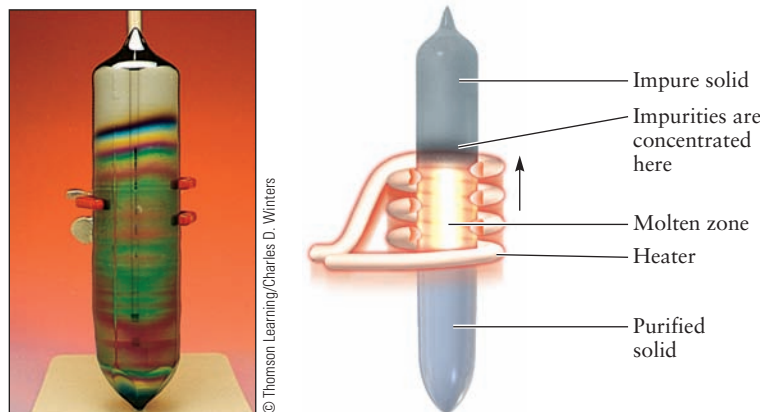


FIGURE 1.4 (a) A solid mixture of blue $\text{Cu}(\text{NO}_3)_2 \cdot 6\text{H}_2\text{O}$ and yellow CdS is added to water. (b) Although the $\text{Cu}(\text{NO}_3)_2 \cdot 6\text{H}_2\text{O}$ dissolves readily and passes through the filter, the CdS remains largely undissolved and is held on the filter. (c) Evaporation of the solution leaves nearly pure crystals of $\text{Cu}(\text{NO}_3)_2 \cdot 6\text{H}_2\text{O}$.

be repeated to improve the resolution of air into its component gases to any required degree of purity.

If all these physical procedures (and many more) fail to separate matter into portions that have different properties, the material is said to be a **substance**. What about the common material sodium chloride, which we call table salt? Is it a substance? The answer is yes if we use the term *sodium chloride*, but no if we use the

FIGURE 1.5 Nearly pure elemental silicon is produced by pulling a 10-inch-long solid cylinder (called a boule) out of the melt, leaving most of the impurities behind.



term *table salt*. Table salt is a mixture of sodium chloride with small additives of sodium iodide (needed by the thyroid gland) and magnesium carbonate (needed to prevent the salt from caking). Even if these two components were not added, table salt would contain other impurities that had not been removed in its preparation, so to that extent, table salt is a mixture. In contrast, when we refer to sodium chloride, we imply that all other materials are absent, so it qualifies as a substance.

In practice, nothing is absolutely pure, so the word *substance* is an idealization. Among the purest materials ever prepared are silicon (Fig. 1.5) and germanium. These elements are used in electronic devices and solar cells, and their electronic properties require either high purity or else precisely controlled concentrations of deliberately added impurities. Meticulous chemical and physical methods have enabled scientists to prepare germanium and silicon with concentrations less than one part per billion of impurities. Anything more would alter their electrical properties.

Elements

Literally millions of substances have so far been either discovered or synthesized and formally identified. Are these the fundamental building blocks of matter? Happily not, for their classification alone would pose an insurmountable task. In fact, all these substances are merely combinations of much smaller numbers of building blocks called **elements**. Elements are substances that cannot be decomposed into two or more simpler substances by ordinary physical or chemical means. The word *ordinary* excludes the processes of radioactive decay, whether natural or artificial, and high-energy nuclear reactions that *do* transform one element into another. When a substance contains two or more chemical elements, we call it a **compound**. For example, hydrogen and oxygen are elements because no further chemical separation is possible, whereas water is a compound because it can be separated into hydrogen and oxygen by passing an electric current through it (see Fig. 1.2). *Binary* compounds are substances, such as water, that contain two elements, *ternary* compounds contain three elements, *quaternary* compounds contain four elements, and so on.

At present, scientists have identified some 112 chemical elements. A few have been known since before recorded history, principally because they occur in nature as elements rather than in combination with one another in compounds. Gold, silver, lead, copper, and sulfur are chief among them. Gold is found in streams in the form of little granules (placer gold) or nuggets in loosely consolidated rock. Sulfur is associated with volcanoes, and copper often can be found in its native state in shallow mines. Iron occurs in its elemental state only rarely (in meteorites); it usually is combined with oxygen or other elements. In the second millennium B.C., ancient metallurgists somehow learned to reduce iron oxide to iron with charcoal in forced-draft fires, and the Iron Age was born.

The names of the chemical elements and the symbols that designate them have a fascinating history. Many elements have Latin roots that describe physical or chemical properties, such as gold (*aurum*, symbol Au), copper (*cuprum*, Cu), iron (*ferrum*, Fe), and mercury (*hydrargyrum*, Hg). Hydrogen (H) means “water former.” Potassium (*kalium*, K) takes its common name from potash (potassium carbonate), a useful chemical obtained in early times by leaching the ashes of wood fires with water. Many elements take their names from Greek and Roman mythology: cerium (Ce) from Ceres, goddess of plenty; tantalum (Ta) from Tantalus, who was condemned in the afterlife to an eternity of hunger and thirst while close to water and fruit that were always tantalizingly just out of reach; and niobium (Nb) from Niobe, daughter of Tantalus. Some elements are named for continents: europium (Eu) and americium (Am). Other elements are named after countries: germanium (Ge), francium (Fr), and polonium (Po). Cities provide the names of other elements: holmium (Stockholm, Ho), ytterbium (Ytterby, Yb), and berkelium (Berkeley, Bk). Still more elements are named for the planets: uranium (U), plutonium (Pu), and neptunium (Np). Other elements take their names from colors: praseodymium (green, Pr), rubidium (red, Rb), and cesium (sky blue, Cs). Still others honor great scientists: curium (Marie Curie, Cm), mendelevium (Dmitri Mendeleev, Md), fermium (Enrico Fermi, Fm), einsteinium (Albert Einstein, Es), and seaborgium (Glenn Seaborg, Sg).

1.3 Indirect Evidence for the Existence of Atoms: Laws of Chemical Combination

How did we acquire the chemical evidence for the existence of atoms and the scale of relative atomic masses? It is an instructive story, both in its own right and as an illustration of how science progresses.

We may know the elements to be the most fundamental substances, and we may know they can be combined chemically to form compound substances, but that knowledge provides us no information on the nanoscopic structure of matter or how that nanoscopic structure controls and is revealed by chemical reactions. Ancient philosophers dealt with these fascinating questions by proposing assumptions, or *postulates*, about the structure of matter. The Greek philosopher Democritus (c. 460–370 B.C.) postulated the existence of unchangeable *atoms* of the elements, which he imagined to undergo continuous random motion in the vacuum, a remarkably modern point of view. It follows from this postulate that matter is not divisible without limit; there is a lower limit to which a compound can be divided before it becomes separated into atoms of the elements from which it is made. Lacking both experimental capabilities and the essentially modern scientific view that theories must be tested and refined by experiment, the Greek philosophers were content to leave their views in the form of assertions.

More than 2000 years passed before a group of European chemists demonstrated experimentally that elements combine only in masses with definite ratios when forming compounds, and that compounds react with each other only in masses with definite ratios. These results could be interpreted only by inferring that smallest indivisible units of the elements (atoms) combined to form smallest indivisible units of the compounds (molecules). The definite mass ratios involved in reactions were interpreted as a convenient means for counting the number of atoms of each element participating in the reaction. These results, summarized as the **laws of chemical combination**, provided overwhelming, if indirect, evidence for the existence of atoms and molecules.

For more than a century, we have become so accustomed to speaking of atoms that we rarely stop to consider the experimental evidence for their existence collected in the 18th and 19th centuries. Twentieth-century science developed a



© Richard Megna/Fundamental Photographs, NYC

FIGURE 1.6 When the red solid mercury(II) oxide is heated, it decomposes to mercury and oxygen. Note the drops of liquid mercury condensing on the side of the test tube.

number of sophisticated techniques to measure the properties of single atoms, and powerful microscopes even allow us to observe them (see Section 1.5). But long before single atoms were detected, chemists could speak with confidence about their existence and the ways in which they combine to form molecules. Moreover, although the absolute masses of single atoms of oxygen and hydrogen were not measured until the early 20th century, chemists could assert (correctly) some 50 years earlier that the *ratio* of the two masses was close to 16:1.

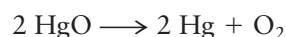
Law of Conservation of Mass

The first key steps toward formulating the laws of chemical composition were taken during the 18th century in the course of studies of heat and combustion. It had been observed that an organic material, such as wood, left a solid residue of ash when burned; similarly, a metal heated in air was transformed into a “calx,” which we now call an oxide. The popular explanation for these phenomena in the early 18th century was that a property called *phlogiston* was driven out of wood or metal by the heat of a fire. From the modern perspective, this seems absurd, because the ash weighs less than the original wood, whereas the calx weighs more than the metal. But at the time, the principle of conservation of mass had not yet been established, and people saw no reason why the mass of a material should not change on heating.

Further progress could be made only by carefully measuring the changes in mass¹ that occur in chemical reactions. The balance had been known since antiquity, but it had been used principally as an assayer’s tool and for verifying the masses of coins or commodities in commerce. The analytical balance developed in the 18th century, however, was accurate to perhaps 1 part in 10,000, enabling much more accurate measurements of mass changes accompanying chemical reactions than had been possible previously. French chemist Antoine Lavoisier used the analytical balance (See the photo on page 29 to demonstrate that the sum of the masses of the products of a chemical reaction equals the sum of the masses of the reactants to the high degree of accuracy provided by the instrument. Lavoisier heated mercury in a sealed flask that contained air. After several days, a red substance, mercury(II) oxide, was produced. The gas remaining in the flask was reduced in mass and could no longer support life or combustion; a candle was extinguished by it, and animals suffocated when forced to breathe it. We now know that this residual gas was nitrogen, and that the oxygen in the air had reacted with the mercury. Lavoisier then took a carefully weighed amount of the red oxide of mercury and heated it strongly (Fig. 1.6). He weighed both the mercury and the gas that were produced and showed that their combined mass was the same as that of the mercury(II) oxide with which he had started. After further experiments, Lavoisier was able to state the **law of conservation of mass**:

In every chemical operation an equal quantity of matter exists before and after the operation.

Lavoisier was the first to observe that a chemical reaction is analogous to an algebraic equation. We would write his second reaction as



although during Lavoisier’s lifetime, the identity of the gas (oxygen) was not known.

¹Chemists sometimes use the term *weight* in place of *mass*. Strictly speaking, weight and mass are not the same. The mass of a body is an invariant quantity, but its weight is the force exerted on it by gravitational attraction (usually by the Earth). Newton’s second law relates the two ($w = m \times g$, where g is the acceleration due to gravity). As g varies from place to place on the Earth’s surface, so does the weight of a body. In chemistry, we deal mostly with ratios, which are the same for masses and weights. In this textbook we use the term *mass* exclusively, but *weight* is still in colloquial chemical use.

Law of Definite Proportions

Rapid progress ensued as chemists began to make accurate determinations of the masses of reactants and products. A controversy arose between two schools of thought, led by a pair of French chemists, Claude Berthollet and Joseph Proust. Berthollet believed that the proportions (by mass) of the elements in a particular compound were not fixed, but could actually vary over a certain range. Water, for example, rather than containing 11.1% by mass of hydrogen, might have somewhat less or more than this mass percentage. Proust disagreed, arguing that any apparent variation was due to impurities and experimental errors. He also stressed the difference between homogeneous mixtures and chemical compounds. In 1794, Proust published the fundamental **law of definite proportions**:

In a given chemical compound, the proportions by mass of the elements that compose it are fixed, independent of the origin of the compound or its mode of preparation.

Pure sodium chloride contains 60.66% chlorine by mass, whether we obtain it from salt mines, crystallize it from waters of the oceans or inland salt seas, or synthesize it from its elements, sodium and chlorine.²

The law of definite proportions was a crucial step in the development of modern chemistry, and by 1808, Proust's conclusions had become widely accepted. We now recognize that this law is not strictly true in all cases. Although all gaseous compounds obey Proust's law, certain solids exist with a small range of compositions and are called **nonstoichiometric compounds**. An example is wüstite, which has the nominal chemical formula FeO (with 77.73% iron by mass), but the composition of which, in fact, ranges continuously from Fe_{0.95}O (with 76.8% iron) down to Fe_{0.85}O (74.8% iron), depending on the method of preparation. Such compounds are called **berthollides**, in honor of Berthollet. We now know, on the atomic level, why they are nonstoichiometric (see the discussion in Section 21.6).

This account illustrates a common pattern of scientific progress: Experimental observation of parallel behavior leads to the establishment of a law, or principle. More accurate studies may then demonstrate exceptions to the general principle. The following explanation of the exceptions leads to deeper understanding.

Dalton's Atomic Theory

English scientist John Dalton was by no means the first person to propose the existence of atoms; as we have seen, speculations about them date back to Greek times (the word *atom* is derived from Greek *a-* ["not"] plus *tomos* ["cut"], meaning "not divisible"). Dalton's major contribution to chemistry was to marshal the evidence for the existence of atoms. He showed that the mass relationships found by Lavoisier and Proust could be interpreted most simply by postulating the existence of atoms of the various elements.

In 1808, Dalton published *A New System of Chemical Philosophy*, in which the following five postulates comprise the **atomic theory of matter**:

1. Matter consists of indivisible atoms.
2. All the atoms of a given chemical element are identical in mass and in all other properties.
3. Different chemical elements have different kinds of atoms; in particular, their atoms have different masses.

²This statement needs some qualification. As explained in the next section, many elements have several *isotopes*, which are species whose atoms have almost identical chemical properties but different masses. Natural variation in isotope abundance leads to small variations in the mass proportions of elements in a compound, and larger variations can be induced by artificial isotopic enrichment.

4. Atoms are indestructible and retain their identities in chemical reactions.
5. A compound forms from its elements through the combination of atoms of unlike elements in small whole-number ratios.

Dalton's fourth postulate clearly is related to the law of conservation of mass. The fifth aims to explain the law of definite proportions. Perhaps Dalton's reasoning went something like this: Suppose you reject the atomic theory and believe instead that compounds are subdivisible without limit. What, then, ensures the constancy of composition of a substance such as sodium chloride? Nothing! But if each sodium atom in sodium chloride is matched by one chlorine atom, then the constancy of composition can be understood. So in this argument for the law of definite proportions, it does not matter how small the atoms of sodium and chlorine are. It is important merely that there be some lower bound to the subdivisibility of matter, because the moment we put in such a lower bound, arithmetic steps in. Matter becomes countable, and the units of counting are simply atoms. Believing in the law of definite proportions as an established experimental fact, Dalton *postulated* the existence of the atom.

Law of Multiple Proportions

The composition of a compound is shown by its **chemical formula**. The symbol H_2O for water indicates that the substance water contains two atoms of hydrogen for each atom of oxygen. It is now known that in water the atoms in each group of three (two H and one O) are linked by attractive forces strong enough to keep the group together for a reasonable period. Such a group is called a **molecule**. In the absence of knowledge about a compound's molecules, the numerical subscripts in the chemical formula simply give the relative proportions of the elements in the compound. How do we know that these are the true proportions? The determination of chemical formulas (and the accompanying determination of relative atomic masses), building on the atomic hypothesis of Dalton, was a major accomplishment of 19th-century chemistry.

In the simplest type of compound, two elements combine, contributing equal numbers of atoms to the union to form **diatomic molecules**, which consist of two atoms each. Eighteenth- and 19th-century chemists knew, however, that two elements will often combine in different proportions, thus forming more than one compound.

For example, carbon (C) and oxygen (O) combine under different conditions to form two different compounds, which we will call A and B. Analysis shows that A contains 1.333 grams (g) of oxygen per 1.000 g of carbon, and B contains 2.667 g of oxygen per 1.000 g of carbon. Although at this point we know nothing about the chemical formulas of the two oxides of carbon, we can say immediately that molecules of compound A contain half as many oxygen atoms per carbon atom as do molecules of compound B. The evidence for this is that the ratio of the masses of oxygen in A and B, for a fixed mass of carbon in each, is 1.333:2.667, or 1:2. If the formula of compound A were CO , then the formula of compound B would have to be CO_2 , C_2O_4 , C_3O_6 , or some other multiple of CO_2 . If compound A were CO_2 , then compound B would be CO_4 or C_2O_8 , and so on. From these data, we cannot say which of these (or an infinite number of other possibilities) are the true formulas of the molecules of compounds A and B, but we do know this: The number of oxygen atoms per carbon atom in the two compounds is the *quotient of integers*.

Consider another example. Arsenic (As) and sulfur (S) combine to form two sulfides, A and B, in which the masses of sulfur per 1.000 g of arsenic are 0.428 and 0.642 g, respectively. The ratio of these sulfur masses is $0.428:0.642 = 2:3$. We conclude that *if* the formula of compound A is a multiple of AsS , then the formula of compound B must be a multiple of As_2S_3 .

These two examples illustrate the **law of multiple proportions**:

When two elements form a series of compounds, the masses of one element that combine with a fixed mass of the other element are in the ratio of small integers to each other.

In the first example, the ratio of the masses of oxygen in the two compounds, for a given mass of carbon, was 1:2. In the second example, the ratio of the masses of sulfur in the two compounds, for a given mass of arsenic, was 2:3. Today, we know that the carbon oxides are CO (carbon monoxide) and CO₂ (carbon dioxide), and the arsenic sulfides are As₄S₄ and As₂S₃. Dalton could not have known this, however, because he had no information from which to decide how many atoms of carbon and oxygen are in one molecule of the carbon–oxygen compounds or how many atoms of arsenic and sulfur are in the arsenic–sulfur compounds.

EXAMPLE 1.1

Chlorine (Cl) and oxygen form four different binary compounds. Analysis gives the following results:

Compound	Mass of O Combined with 1.0000 g Cl
A	0.22564 g
B	0.90255 g
C	1.3539 g
D	1.5795 g

- (a) Show that the law of multiple proportions holds for these compounds.
 (b) If the formula of compound A is a multiple of Cl₂O, then determine the formulas of compounds B, C, and D.

SOLUTION

- (a) Form ratios by dividing each mass of oxygen by the smallest, which is 0.22564 g:

$$0.22564 \text{ g} : 0.22564 \text{ g} = 1.0000 \text{ for compound A}$$

$$0.90255 \text{ g} : 0.22564 \text{ g} = 4.0000 \text{ for compound B}$$

$$1.3539 \text{ g} : 0.22564 \text{ g} = 6.0003 \text{ for compound C}$$

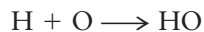
$$1.5795 \text{ g} : 0.22564 \text{ g} = 7.0001 \text{ for compound D}$$

The ratios are whole numbers to a high degree of precision, and the law of multiple proportions is satisfied. Ratios of whole numbers also would have satisfied that law.

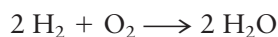
- (b) If compound A has a formula that is some multiple of Cl₂O, then compound B is Cl₂O₄ (or ClO₂, or Cl₃O₆, and so forth) because it is four times richer in oxygen than is compound A. Similarly, compound C, which is six times richer in oxygen than compound A, is Cl₂O₆ (or ClO₃, or Cl₃O₉, and so forth), and compound D, which is seven times richer in oxygen than compound A, is Cl₂O₇ (or a multiple thereof).

Related Problems: 7, 8, 9, 10

Dalton made a sixth assumption to resolve the dilemma of the absolute number of atoms present in a molecule; he called it the “rule of greatest simplicity.” It states that if two elements form only a single compound, its molecules will have the simplest possible formula: AB. Thus, he assumed that when hydrogen and oxygen combine to form water, the reaction is



However, Dalton was wrong, as we now know, and the correct reaction is



Law of Combining Volumes

At this time, French chemist Joseph Gay-Lussac conducted some important experiments on the volumes of gases that react with one another to form new gases. He discovered the **law of combining volumes**:

The volumes of two reacting gases (at the same temperature and pressure) are in the ratio of simple integers. Moreover, the ratio of the volume of each product gas to the volume of either reacting gas is the ratio of simple integers.

Here are three examples:

2 volumes of hydrogen + 1 volume of oxygen \longrightarrow 2 volumes of water vapor

1 volume of nitrogen + 1 volume of oxygen \longrightarrow 2 volumes of nitrogen oxide

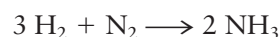
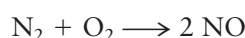
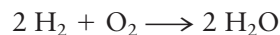
3 volumes of hydrogen + 1 volume of nitrogen \longrightarrow 2 volumes of ammonia

Avogadro's Hypothesis

Gay-Lussac did not theorize on his experimental findings, but in 1811 shortly after their publication the Italian chemist Amedeo Avogadro used them to formulate an important postulate since known as **Avogadro's hypothesis**:

Equal volumes of different gases at the same temperature and pressure contain equal numbers of particles.

The question immediately arose; Are “particles” of the elements the same as Dalton's atoms? Avogadro believed that they were not; rather, he proposed that elements could exist as diatomic molecules. Avogadro's hypothesis could explain Gay-Lussac's law of combining volumes (Fig. 1.7). Thus, the reactions we wrote out in words become



The coefficients of the above reactions are proportional to the volumes of the reactant and product gases in Gay-Lussac's experiments, and the chemical formulas

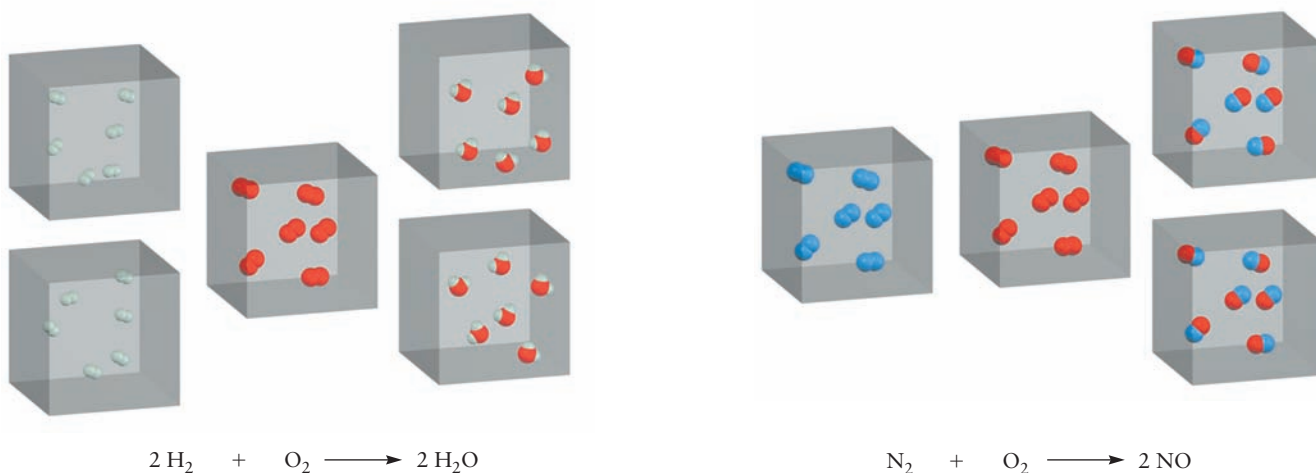
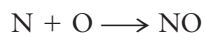
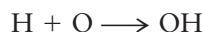


FIGURE 1.7 Each cube represents a container of equal volume under the same conditions. If each cube contains the same number of molecules (Avogadro's hypothesis), and if hydrogen, oxygen, and nitrogen exist as diatomic molecules, then the combining volumes that Gay-Lussac observed in the two reactions can be understood.

of the reactions agree with modern results. Dalton, on the other hand, would have written



The coefficients of the previous reactions disagree with Gay-Lussac's observations of their relative volumes.

Besides predicting correct molecular formulas, Avogadro's hypothesis gives correct results for the relative atomic masses of the elements. Analysis by chemists during the 18th century had demonstrated that 1 g of hydrogen reacts completely with 8 g of oxygen to produce 9 g of water. If Dalton's formula for water, HO, were correct, then an atom of oxygen would have to weigh 8 times as much as an atom of hydrogen; that is, Dalton's assumption requires the **relative atomic mass** of oxygen to be 8 on a scale where the relative atomic mass of hydrogen is set at 1. Avogadro's hypothesis predicted, however, that each water molecule has twice as many atoms of hydrogen as oxygen; therefore, to explain the observed experimental mass relation, the relative mass for oxygen must be 16, a result consistent with modern measurements.

We might expect that Dalton would have welcomed Avogadro's brilliant hypothesis, but he did not. Dalton and others insisted that elements could not exist as diatomic molecules. One reason for their belief was the then-popular idea that a force called *affinity* held molecules together. Affinity expressed the attraction of opposites, just as we think of the attraction between positive and negative electric charges. If the affinity theory were true, why should two *like* atoms be held together in a molecule? Moreover, if like atoms somehow did hold together in pairs, why should they not aggregate further to form molecules with three, four, or six atoms, and so forth? With so many chemists accepting the affinity theory, Avogadro's reasoning did not attract the attention it deserved. Because different chemists adopted different chemical formulas for molecules, confusion reigned. A textbook published by the German chemist August Kekulé in 1861 gave 19 different chemical formulas for acetic acid!

In 1860, 50 years after Avogadro's work, Italian chemist Stanislao Cannizzaro presented a paper at the First International Chemical Congress in Karlsruhe, Germany, that convinced others to accept Avogadro's approach. Cannizzaro had analyzed many gaseous compounds and was able to show that their chemical formulas could be established with a consistent scheme that used Avogadro's hypothesis and avoided any extra assumptions about molecular formulas. Gaseous hydrogen, oxygen, and nitrogen (as well as fluorine, chlorine, bromine, and iodine), indeed, turn out to consist of diatomic molecules under ordinary conditions.

1.4 The Physical Structure of Atoms

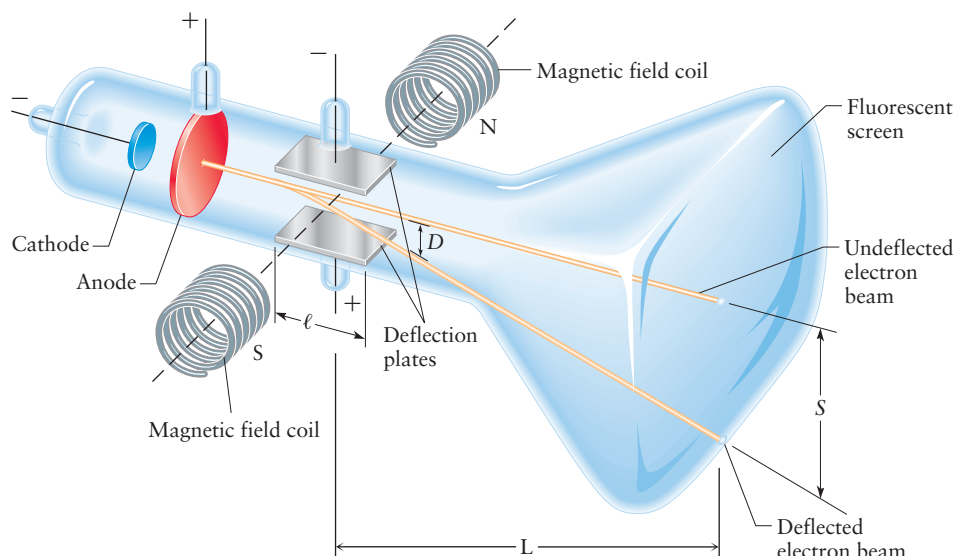
In the original Greek conception, carried over into Dalton's time and reenforced by the laws of chemical combination, the atom was considered the ultimate and indivisible building block of matter. But by the end of the 19th century, this notion began to be replaced by the view that atoms were themselves composed of smaller, *elementary* particles. Scientists had carried the process of analysis (see Section 1.2) down to the subatomic level. Because many of the experiments described in the following paragraphs require an elementary understanding of electricity and magnetism, we suggest that you review the relevant sections of Appendix B before continuing.

Electrons

One key piece of evidence for the existence of subatomic particles came from studies of the effects of large electric fields on atoms and molecules. In these experiments, a gas was enclosed in a glass tube that had two conducting plates inside. When a large electrical potential difference (voltage) was established between the plates, current passed through the gas. The magnitude of this current could be measured in the external circuit connecting the two metal plates. This result suggested that the electric field had broken down the atoms into new species that carry charge. (The same effect occurs when an electrical discharge from a lightning bolt passes through air.) The magnitude of the current was proportional to the amount of gas in the tube. But when the gas was nearly all removed, the current did not go to zero; this suggested that the current originated from one of the metal plates. The mysterious invisible current carriers appeared to travel in straight lines from the cathode (the plate at negative potential) and produced a luminous spot where they impinged on the glass tube near the anode (the plate at positive potential). These current carriers were called **cathode rays**, or **beta rays**. After several decades of research, experimenters learned that cathode rays could be deflected by both magnetic and electric fields and could heat a piece of metal foil in the tube until it glowed. Influenced by Maxwell's electromagnetic theory of light, one school of physicists believed the cathode rays to be a strange form of invisible light, whereas another group considered them to be a stream of negatively charged particles.

In 1897, British physicist J. J. Thomson performed a series of experiments that resolved the controversy. He proved that cathode rays are negatively charged particles; these particles were subsequently named **electrons**. Thomson's key experiment is depicted schematically in Figure 1.8. A beam of cathode rays was produced by a cathode and anode in the usual way in a highly evacuated tube. A hole in the anode allowed some of the rays to pass between a second pair of plates that could be charged positively and negatively to establish an electric field oriented perpendicular to the cathode ray trajectory. For the arrangement shown in Figure 1.8, the cathode rays were deflected downward (indicating that they carried a negative charge), and the deviation could be measured accurately from the displacement of the luminous spot on a screen at the end of the tube. The only sensible explanation of these results was to view the cathode rays as material particles with negative charge and unknown mass. Thomson calculated e/m_e (the charge-to-mass ratio of the electron) by relating the net deflection to the forces applied to the particle, through Newton's second law of motion. Thomson's method is explained in the next few paragraphs.

FIGURE 1.8 Thomson's apparatus to measure the electron charge-to-mass ratio, e/m_e . Electrons (cathode rays) stream across the tube from left to right. The electric field alone deflects the beam down, and the magnetic field alone deflects it up. By adjusting the two field strengths, Thomson could achieve a condition of zero net deflection. (ℓ indicates the length of the deflection plates.)



As soon as the electron flies into the space between the plates, it begins to experience a constant downward force, given by

$$F_E = eE \quad [1.1]$$

where E is the electric field between the plates. By the time the electron flies out of the space between the plates, it has experienced a downward deflection, D , given by Newton's second law as

$$D = \frac{1}{2} at^2 \quad [1.2]$$

where t is the time required to travel the distance ℓ , the length of the plates. The value of t can be determined from the velocity of the electron because $v = \ell/t$, and a can be determined from Newton's second law:

$$F_E = m_e a = eE \quad [1.3]$$

The net downward deflection of the electron by the time it escapes from the plates is then

$$D = \frac{1}{2} at^2 = \frac{1}{2} \left(\frac{e}{m_e} \right) \left(\frac{\ell}{v} \right)^2 E \quad [1.4]$$

After the electron escapes from the plates, it experiences no further forces, so it continues in straight-line motion toward the fluorescent screen. This motion carries the electron farther from the undeflected path and "magnifies" the displacement by the factor $2L/\ell$, where L is the distance from the center of the plates to the screen. When the electron arrives at the screen, the net displacement will be

$$S = 2 \frac{L}{\ell} D = \left(\frac{e}{m_e} \right) \left(\frac{\ell}{v} \right)^2 \left(\frac{L}{\ell} \right) E \quad [1.5]$$

All of these quantities could be read off the apparatus except for the velocity of the electron, which was hard to measure directly.

So Thomson took one additional ingenious experimental step to determine e/m_e . He established a magnetic field in the same region as the electric deflection plates by passing an electric current through a pair of coils, located to make the magnetic field direction perpendicular to that of the electric field and to the flight path of the electrons. The magnetic field deflected the electrons in the direction opposite to that caused by the electric field. By varying the strengths of the two fields, Thomson could pass the electron beam through the tube without deflection. Under these conditions, the beam experienced two equal but opposing forces; from this force balance, Thomson determined the velocity of the electrons in the beam. The force due to the electric field E was

$$F_E = eE \quad [1.6]$$

and the force due to the magnetic field H was

$$F_H = evH \quad [1.7]$$

The velocity of the electrons was therefore

$$v = \frac{E}{H} \quad [1.8]$$

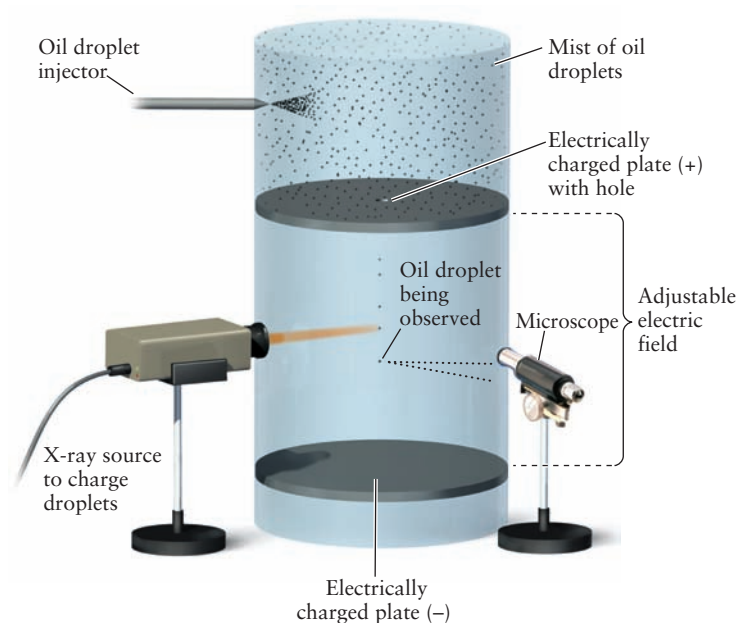
Substituting for the velocity in Equation 1.5 gives the net deflection as

$$S = \left(\frac{e}{m_e} \right) \left(\frac{\ell H}{E} \right) \left(\frac{L}{\ell} \right) E \quad [1.9]$$

which can be solved to give

$$\frac{e}{m_e} = \frac{SE}{\ell LH^2} \quad [1.10]$$

FIGURE 1.9 Millikan's apparatus to measure the charge on an electron, e . By adjusting the electric field strength between the charged plates, Millikan could halt the fall of negatively charged oil drops and determine their net charge.



From Equation 1.10 the charge-to-mass ratio for the electron could be determined from quantities read directly off Thomson's apparatus. The currently accepted value is $e/m_e = 1.7588202 \times 10^{11} \text{ C kg}^{-1}$, where charge is measured in coulombs and mass in kilograms. (See Appendix B for a full discussion of units of measure.)

Thomson's apparatus is the forerunner of the modern cathode ray tube (crt) display widely used as a video monitor. Electrons emitted from the cathode are steered by rapidly varying electric and magnetic fields to "write" the video image on light-emitting materials deposited on the inside wall of the tube. The image is viewed through the glass wall at the end of the tube.

Thomson's experiment determined only the *ratio* of the charge to the mass of the electron. The actual value of the electric charge was measured in 1906 by American physicist Robert Millikan with his student H. A. Fletcher. In Millikan and Fletcher's elegant experiment (Fig. 1.9), tiny drops of oil were charged by a source of ionizing radiation. A charged oil drop (with charge Q and mass M) situated in an electric field between two plates was subject to two forces: the force of gravity $-Mg$, causing it to fall, and a force QE from the electric field, causing it to rise. By adjusting the electric field to balance the two forces and independently determining the masses, M , of the drops from their falling speeds in the absence of an electric field, Millikan showed that the charge Q was always an integral multiple of the same basic charge, $1.59 \times 10^{-19} \text{ C}$. He suggested that the different oil drops carried integral numbers of a fundamental charge, which he took to be the charge of a single electron. More accurate modern measurements led to the value $e = 1.60217646 \times 10^{-19} \text{ C}$. Combining this result with the e/m_e ratio found by Thomson gives $m_e = 9.1093819 \times 10^{-31} \text{ kg}$ for the electron mass.

The Nucleus

It had been known as early as 1886 that light was emitted in gas discharge tubes, devices constructed much like the one Thomson used to study cathode rays. The chief difference between the cathode ray tube and gas discharge tubes was the pressure of the gases contained in the tube. Gas discharge tubes contained gases at moderate-to-low pressure, whereas the cathode ray tube operated under high vacuum (extremely low pressure). The electric field applied between the cathode and anode of a discharge tube caused "electrical breakdown" of the gas to form a *glow*

discharge that emitted light. This phenomenon created great excitement among physicists and stimulated intense research projects to explain the nature of the glow and the origin of the light.

One approach was to determine the identity and properties of electrically charged particles within the glow. Imagine the following experiment, conducted in an apparatus similar to that shown in Figure 1.8, but with two modifications: (1) the voltages are reversed so that the anode (the plate with the hole) becomes the cathode, and (2) provisions are made to add different gases at different pressures. Under these conditions, a glow discharge was observed between the anode and the cathode, some of which leaked through the hole in the cathode and formed rays aimed toward the end of the tube. These came to be known as **canal rays** because they passed through the canal in the cathode. A contemporary of Thomson, the German physicist Wilhelm Wien, carefully studied the properties of these rays and drew three important conclusions:

1. The particles that emerged from the glow discharge to form canal rays were accelerated toward the cathode, so they must be positively charged.
2. Much larger electric and magnetic fields were required to deflect these particles than those used in Thomson's experiments, implying that they were much more massive than the electron.
3. If different gases were leaked into the apparatus, the magnitude of the fields required to displace canal rays of a different gas by the same amount differed, implying that the charged particles associated with each gas had different masses.

Wien's experiments suggested the existence of massive, positively charged particles in the glow discharge.

As an aside, studies of the glow discharge led to significant developments in physics and chemistry which continue to this day. Research on canal rays formed the basis for the mass spectrometer, our most accurate tool for measuring relative masses of atomic and molecular species. The physics and chemistry of **plasmas**—gases that contain charged particles—grew from understanding the structure of the glow itself. Plasma science is active in the 21st century, with fundamental and applied studies ranging from the nature of radiation in deep space to fabrication of nanometer-sized electronic and optical devices for computation and communication.

As exemplified in the results of the experiments of Thomson and Wien, physicists had discovered two quite different types of particles in matter: a light particle that was negatively charged, and a number of much heavier positively charged particles, particles whose relative masses depended on the element from which they were produced. Although it was generally agreed that these particles were the building blocks of atoms, it was not at all clear how they were assembled. That piece of the puzzle remained unsolved until Rutherford's pivotal discovery.

New Zealander Ernest Rutherford and his students at the University of Manchester made a startling discovery in 1911. They had been studying radioactive decay for a number of years and turned their attention to investigating the properties of alpha particles emitted from radium, an element that had been recently isolated by Marie and Pierre Curie. In the Rutherford experiment, a collimated beam of alpha particles irradiated an extremely thin (600 nm) piece of gold foil, and their deflections after colliding with the foil were measured by observing the scintillations they produced on a fluorescent ZnS screen (Fig. 1.10). Almost all of the alpha particles passed straight through the foil, but a few were deflected through large angles. Rarely, a particle was found to have been scattered backward! Rutherford was astounded, because the alpha particles were relatively massive and fast moving. In his words, "It was almost as incredible as if you fired a 15-inch shell at a piece of tissue paper and it came back and hit you." He and his students studied the frequency with which such large deflections occurred. They concluded

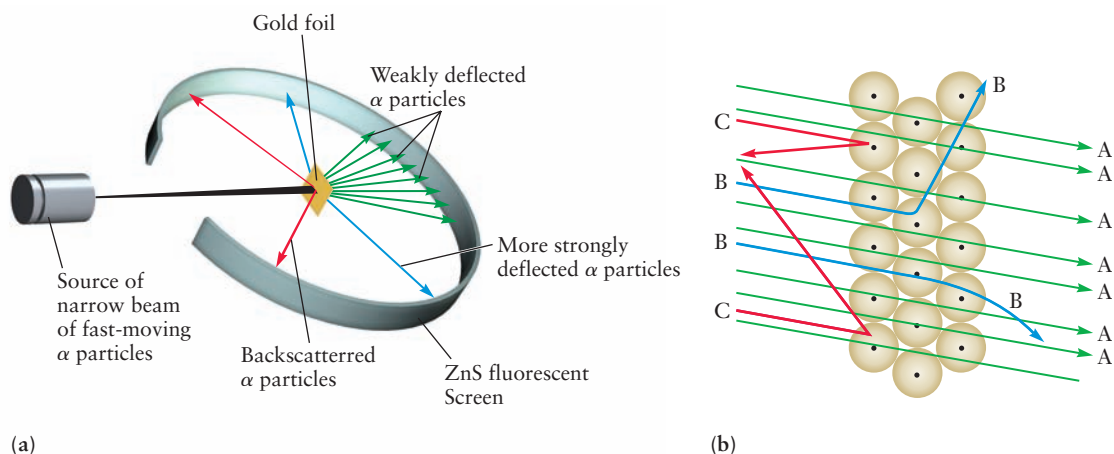


FIGURE 1.10 (a) Flashes of light mark the arrival of alpha particles at the detector screen. In the Rutherford experiment, the rate of hits on the screen varied from about 20 per minute at high angles to nearly 132,000 per minute at low angles. (b) Interpretation of the Rutherford experiment. Most of the alpha particles pass through the space between nuclei and undergo only small deflections (A). A few pass close to a nucleus and are more strongly deflected (B). Some are even scattered backward (C). The nucleus is far smaller proportionately than the dots suggest.

that most of the mass in the gold foil was concentrated in dense, extremely small, positively charged particles that they called **nuclei**. By analyzing the trajectories of the particles scattered by the foil, they estimated the radius of the gold nucleus to be less than 10^{-14} m and the positive charge on each nucleus to be approximately $+100e$ (the actual value is $+79e$).

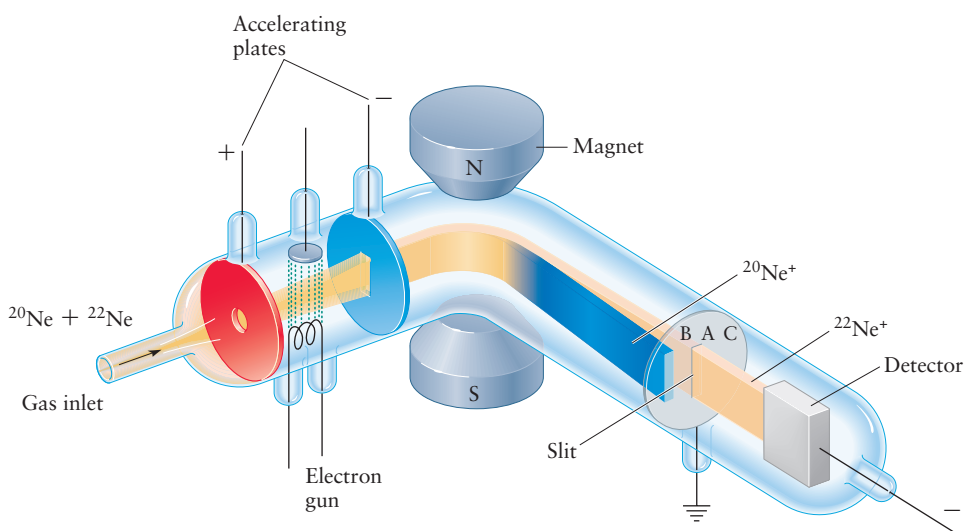
Rutherford proposed a model of the atom in which the charge on the nucleus was $+Ze$, with Z electrons surrounding the nucleus out to a distance of about 10^{-10} m (0.1 nm). The Rutherford model for a gold atom has 79 electrons (each with a charge of $-1e$) arranged about a nucleus of charge $+79e$. The electrons occupy nearly the entire volume of the atom, whereas nearly all its mass is concentrated in the nucleus; this model is often called the “planetary model.”

The Rutherford model has become the universally accepted picture of the structure of the atom. The properties of a given chemical element arise from the charge $+Ze$ on its nucleus and the presence of Z electrons around the nucleus. This integer Z is called the **atomic number** of the element. Atomic numbers are given on the inside back cover of this book.

Mass Spectrometry and the Measurement of Relative Masses

Mass spectrometry, besides being the chemist’s most accurate method for determining relative atomic masses, also led to the discovery of other subatomic particles in addition to electrons and nuclei. In a mass spectrometer (Fig. 1.11), one or more electrons are removed from each such atom, usually by collision with a high-energy electron beam. The resulting positively charged species, called **ions**, are accelerated by an electric field and then passed through a magnetic field. The extent of curvature of the particle trajectories depends on the ratio of their charges to their masses, just as in Thomson’s experiments on cathode rays (electrons) described earlier in this section. This technique allows species of different masses to be separated and detected. Early experiments in mass spectrometry demonstrated, for example, a mass ratio of 16:1 for oxygen relative to hydrogen, confirming by *physical* techniques a relationship deduced originally on *chemical* grounds. Although we focus here on the use of mass spectrometry to establish the relative

FIGURE 1.11 A simplified representation of a modern mass spectrometer. A gas mixture containing the isotopes ^{20}Ne and ^{22}Ne is introduced through the gas inlet. Some of these atoms are ionized by collisions with electrons as they pass through the electron gun. The resulting ions are accelerated to a particular kinetic energy by the electric field between the accelerating plates. The ion beam passes into a magnetic field, where it is separated into components, each containing ions with a characteristic charge-to-mass ratio. Here, the spectrometer has been adjusted to detect the less strongly deflected $^{22}\text{Ne}^+$ in the inlet mixture. By changing the magnitude of the electric or magnetic field, one can move the beam of $^{22}\text{Ne}^+$ from A to C, and the beam of $^{20}\text{Ne}^+$ from B to A, so that $^{20}\text{Ne}^+$ can be detected.



masses of atoms, it has become one of the chemist's most powerful tools for determining the masses and structures of molecules as well.

When a pure elemental gas, such as neon, was analyzed by a mass spectrometer, multiple peaks (two in the case of neon) were observed (see Fig. 1.11). Apparently, several kinds of atoms of the same element exist, differing only by their relative masses. Experiments on radioactive decay showed no differences in the *chemical* properties of these different forms of each element, so they all occupy the same place in the periodic table of the elements (see Chapter 3). Thus the different forms were named **isotopes**. Isotopes are identified by the chemical symbol for the element with a numerical superscript on the left side to specify the measured relative mass, for example ^{20}Ne and ^{22}Ne . Although the existence of isotopes of the elements had been inferred from studies of the radioactive decay paths of uranium and other heavy elements, mass spectrometry provided confirmation of their existence and their physical characterization. Later, we discuss the properties of the elementary particles that account for the mass differences of isotopes. Here, we discuss mass spectrometry as a tool for measuring atomic and molecular masses and the development of the modern atomic mass scale.

Because many elements have more than one naturally occurring isotope, the relationship between the chemist's and the physicist's relative atomic mass scales was not always simple. The atomic mass of chlorine determined by chemical means was 35.45 (relative to an oxygen atomic mass of 16), but instead of showing a single peak in the mass spectrum corresponding to a relative atomic mass of 35.45, chlorine showed 2 peaks, with relative masses near 35 and 37. Approximately three fourths of all chlorine atoms appear to have relative atomic mass 35 (the ^{35}Cl atoms), and one fourth have relative atomic mass 37 (the ^{37}Cl atoms). Naturally occurring chlorine is thus a mixture of two isotopes with different masses but nearly identical chemical properties. Elements in nature usually are mixtures, after all. Dalton's second assumption, that all atoms of a given element are identical in mass, thus is shown to be wrong in most cases.

Until 1900, chemists worked with a scale of relative atomic masses in which the average relative atomic mass of hydrogen was set at 1. At about that time, they changed to a scale in which the average relative atomic mass of naturally occurring oxygen (a mixture of ^{16}O , ^{17}O , and ^{18}O) was set at 16. In 1961, by international agreement, the atomic mass scale was revised further, with the adoption of exactly 12 as the relative atomic mass of ^{12}C . There are two stable isotopes of carbon: ^{12}C and ^{13}C (^{14}C and other isotopes of carbon are unstable and of very low terrestrial abundance). Natural carbon contains 98.892% ^{12}C and 1.108% ^{13}C by mass. The relative atomic masses of the elements as found in nature can be obtained as averages over the masses of the isotopes of each element, weighted by

their observed fractional abundances. If an element consists of n isotopes, of which the i th isotope has a mass A_i and a fractional abundance p_i , then the average relative atomic mass of the element in nature (its chemical relative atomic mass) will be

$$A = A_1p_1 + A_2p_2 + \cdots + A_np_n \equiv \sum_{i=1}^n A_i p_i \quad [1.11]$$

The relative atomic mass of a nuclide is close to (except for ^{12}C) but not exactly equal to its mass number.

EXAMPLE 1.2

Calculate the relative atomic mass of carbon, taking the relative atomic mass of ^{13}C to be 13.003354 on the ^{12}C scale.

SOLUTION

Set up the following table:

Isotope	Isotopic Mass \times Abundance
^{12}C	$12.000000 \times 0.98892 = 11.867$
^{13}C	$13.003354 \times 0.01108 = 0.144$

Chemical relative atomic mass = 12.011

Related Problems: 15, 16, 17, 18

The number of significant figures in a table of chemical or natural relative atomic masses (see the inside back cover of this book) is limited not only by the accuracy of the mass spectrometric data but also by any variability in the natural abundances of the isotopes. If lead from one mine has a relative atomic mass of 207.18 and lead from another has a mass of 207.23, there is no way a result more precise than 207.2 can be obtained. In fact, geochemists are now able to use small variations in the ^{16}O : ^{18}O isotopic abundance ratio as a “thermometer” to deduce the temperatures at which different oxygen-containing rocks were formed in the Earth’s crust over geological time scales. They also find anomalies in the oxygen isotopic compositions of certain meteorites, implying that their origins may lie outside our solar system.

Relative atomic masses have no units because they are ratios of two masses measured in whatever units we choose (grams, kilograms, pounds, and so forth). The **relative molecular mass** of a compound is the sum of the relative atomic masses of the elements that constitute it, each one multiplied by the number of atoms of that element in a molecule. For example, the formula of water is H_2O , so its relative molecular mass is

$$2 \text{ (relative atomic mass of H)} + 1 \text{ (relative atomic mass of O)} = 2(1.0079) + 1(15.9994) = 18.0152$$

Protons, Neutrons, and Isotopes

The experiments described earlier led to the identification of the elementary particles that make up the atom. We discuss their properties in this section. The smallest and simplest nucleus is that of the hydrogen atom—the **proton**. It has a positive unit charge of exactly the same magnitude as the negative unit charge of the

electron, but its mass is 1.67262×10^{-27} kg, which is 1836 times greater than the electron mass. Nuclei of other elements contain Z times the charge on the proton, but their masses are greater than Z times the proton mass. For example, the atomic number for helium is $Z = 2$, but its mass is approximately four times the mass of the proton. In 1920, Rutherford suggested the existence of an uncharged particle in nuclei, the **neutron**, with a mass close to that of the proton. In his model, the nucleus consists of Z protons and N neutrons. The **mass number** A is defined as $Z + N$.

A nuclear species (**nuclide**) is characterized by its atomic number Z (that is, the nuclear charge in units of e , or the number of protons in the nucleus) and its mass number A (the sum of the number of protons plus the number of neutrons in the nucleus). We denote an atom that contains such a nuclide with the symbol A_ZX , where X is the chemical symbol for the element. The atomic number Z is sometimes omitted because it is implied by the chemical symbol for the element. Thus, ${}^1_1\text{H}$ (or ${}^1\text{H}$) is a hydrogen atom and ${}^{12}_6\text{C}$ (or ${}^{12}\text{C}$) is a carbon atom with a nucleus that contains six protons and six neutrons. Isotopes are nuclides of the same chemical species (that is, they have the same Z), but with different mass numbers A , and therefore different numbers of neutrons in the nucleus. The nuclear species of hydrogen, deuterium, and tritium, represented by ${}^1_1\text{H}$, ${}^2_1\text{H}$, and ${}^3_1\text{H}$, respectively, are all members of the family of isotopes that belong to the element hydrogen.

EXAMPLE 1.3

Radon-222 (${}^{222}\text{Rn}$) has recently received publicity because its presence in basements may increase the number of cancer cases in the general population, especially among smokers. State the number of electrons, protons, and neutrons that make up an atom of ${}^{222}\text{Rn}$.

SOLUTION

From the table on the inside back cover of the book, the atomic number of radon is 86; thus, the nucleus contains 86 protons and $222 - 86 = 136$ neutrons. The atom has 86 electrons to balance the positive charge on the nucleus.

Related Problems: 19, 20, 21, 22

1.5 Imaging Atoms, Molecules, and Chemical Reactions

The laws of chemical combination provided indirect evidence for the existence of atoms. The experiments of Thomson, Wien, and Rutherford provided direct physical evidence for the existence of the elementary particles that make up the atom. We conclude this chapter by describing an experimental method that allows us not only to image individual atoms and molecules but also to observe and control a chemical reaction at the single molecule level—a feat only dreamed of as recently as the mid-1980s.

Scanning Tunneling Microscopy Imaging of Atoms

Microscopy began with the fabrication of simple magnifying glasses and had evolved by the late 17th century to create the first optical microscopes through which single biological cells could be observed. By the 1930s, the electron microscope had been developed to detect objects too small to be seen in optical microscopes. The electron microscope showed single atoms, but at the cost of

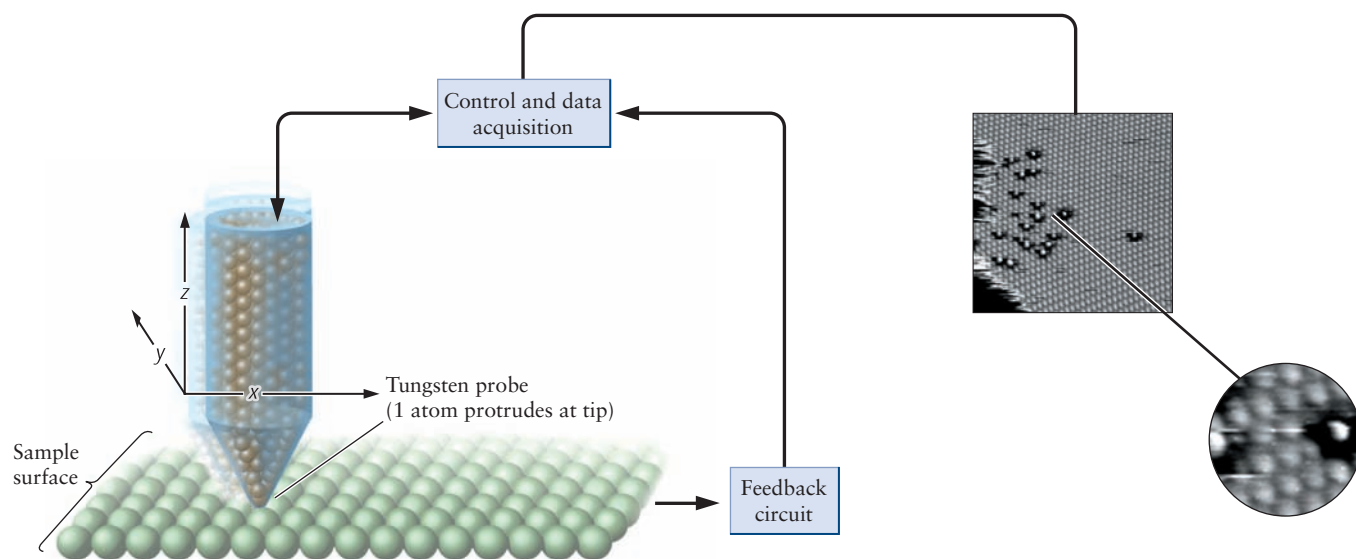


FIGURE 1.12 In a scanning tunneling microscope (STM), an electric current passes through a single atom or a small group of atoms in the probe tip, and then into the surface of the sample being examined. As the probe moves over the surface, its distance is adjusted to keep the current constant, allowing a tracing out of the shapes of the atoms or molecules on the surface.

Institut Für Allgemeine Physik, Technical University, Vienna, Austria; b: courtesy of Dr. Don Eigler/IBM Almaden Research Center, San Jose, CA

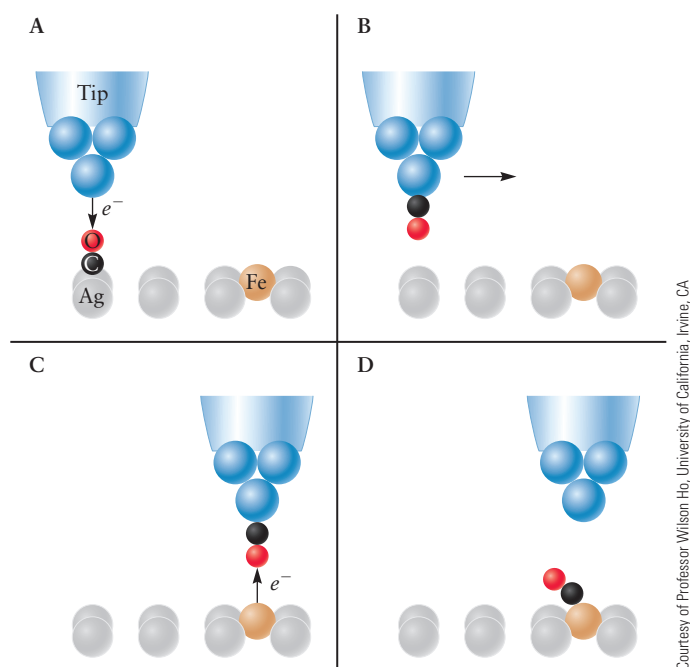
damage inflicted to the sample by the high-energy beam of electrons required to resolve such small objects. In the 1980s in Switzerland, Gerd Binnig and Heinrich Rohrer developed the scanning tunneling microscope (STM), which images atoms using low-energy electrons. For this accomplishment they received the 1986 Nobel Prize in Physics. Their device uses a sharp, electrically conducting tip that is passed over the surface of the sample being examined (Fig. 1.12a). When the tip approaches atoms of the sample, a small electrical current called the *tunneling current* can pass from the sample to the probe. The magnitude of this current is extremely sensitive to the distance of the probe from the surface, decreasing by a factor of 1000 as the probe moves away from the surface by a distance as small as 0.1 nm. Feedback circuitry holds the current constant while the probe is swept laterally across the surface, moving up and down as it passes over structural features in the surface. The vertical position of the tip is monitored, and that information is stored in a computer. By sweeping the probe tip along each of a series of closely spaced parallel tracks, one can construct and display a three-dimensional image of the surface (see the figure opposite page 1 and the figure on page 2).

Scanning tunneling microscope images visually confirm many features, such as size of atoms and the distances between them, which are already known from other techniques. But, much new information has been obtained as well. The STM images have shown the positions and shapes of molecules undergoing chemical reactions on surfaces, which helps guide the search for new ways of carrying out such reactions. They have also revealed the shape of the surface of the molecules of the nucleic acid DNA, which plays a central role in genetics.

Imaging and Controlling Reactions at the Single Molecule Level Using the Scanning Tunneling Microscope

The STM has been used to image the surfaces of materials since the mid-1980s, but only recently has it been used to image single molecules and initiate chemical reactions at the single molecule level, as we illustrate with the following

FIGURE 1.13 Schematic diagram showing the different steps in the formation of a single chemical bond using the scanning tunneling microscope (STM). (a) The tip is positioned over a single carbon monoxide (CO) molecule, ready to pluck it from the silver (Ag) surface. (b) CO is adsorbed onto the tip, bonded via the carbon (C) atom, and is translated across the surface to a region near an iron (Fe) atom. (c) CO is transferred to the surface where it will bond to the Fe atom. (d) The tip is withdrawn and the product molecule, FeCO, is bound to the Ag surface.

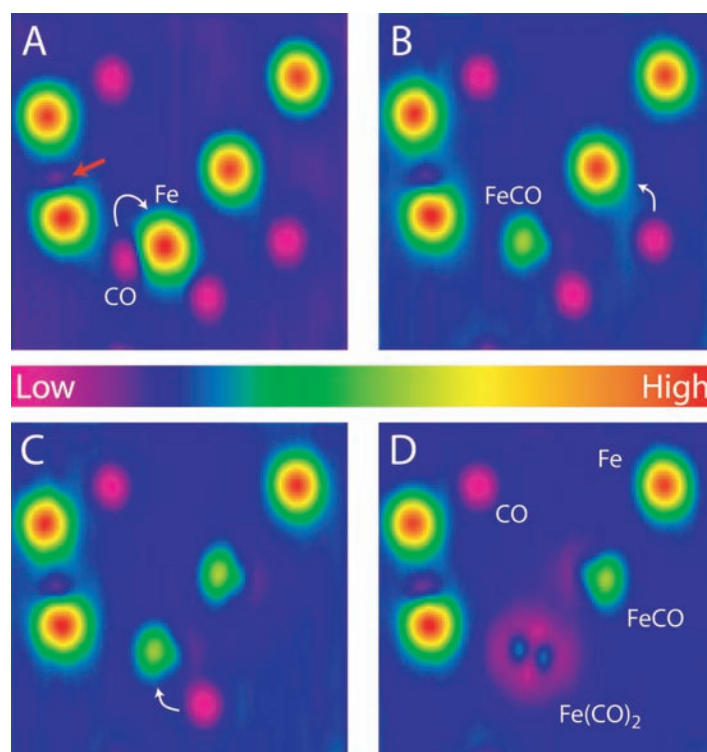


Courtesy of Professor Wilson Ho, University of California, Irvine, CA

example. Although the STM can be used to image objects in air, the experiments described here were conducted in ultrahigh vacuum (ultralow pressure) to ensure that only the reactants of interest were present on the surface. Figure 1.13, a schematic of an STM probe hovering over a silver (Ag) surface on which an iron (Fe) atom and a carbon monoxide (CO) molecule have been chemically bonded (adsorbed), illustrates the steps leading to the formation of the product molecule Fe(CO). Figure 1.13a shows the tip approaching the CO molecule with the voltage and current adjusted so that the tip can pluck the molecule from the surface and attach it to the tip (see Fig. 1.13b). Note that the CO molecule has flipped and is bound to the tip via the carbon atom. In response to the voltage change (see Fig. 1.13c), the CO molecule inverts once again and is placed in position to bind to the Fe atom via the carbon atom, forming the molecule FeCO (see Fig. 1.13d).

The schematic in Figure 1.13 serves as a guide to the eye for interpreting the real STM images shown in Figure 1.14. Each image represents an area of the surface that is 6.3×6.3 nm. The false color scale reflects the height of the object above the plane of the silver surface atoms; the red end of the scale represents protrusions, whereas the purple end represents depressions. The identity of each chemical species was established by the nature of the image and also by the way in which the current varied with the applied voltage. That variation provides a chemical signature. In Figure 1.14a, five Fe atoms and five CO molecules are clearly seen; the red arrow identifies one Fe atom that is a bit difficult to see otherwise. The curved white arrow shows a CO molecule in close proximity to an Fe atom; Figure 1.14b shows the FeCO molecule formed as a result of the transfer of that CO molecule to the Fe atom by the tip, as well as another potentially reactive pair identified by the white curved arrow. From the shape of the resulting image in Figure 1.14c, we can see that another FeCO molecule has been formed. The white curved arrow suggests the possibility of adding an additional CO molecule to the first FeCO synthesized to form Fe(CO)₂, which, indeed, occurs as shown in Figure 1.14d. This remarkable sequence of images shows clearly the synthesis of a pair of distinct Fe(CO) molecules, as well as an Fe(CO)₂ molecule, from the reactants Fe and CO adsorbed onto a silver surface. These syntheses were accomplished by manipulating single CO molecules to place them sufficiently close to Fe atoms to initiate a chemical reaction, demonstrating our ability to observe and control chemical reactions at the single molecule level.

FIGURE 1.14 Scanning tunneling microscope (STM) images of chemical bond formation. Each image is 6.3×6.3 nm. The species are identified by their height above or below the surface silver (Ag) atoms and by the shapes of their current-voltage curves. (a) Five iron (Fe) atoms (concentric red-green circles) and five carbon monoxide (CO) molecules (purple) are observed in this region. The red arrow points to one CO molecule that is a little hard to see, and the white arrow shows a CO molecule about to react with an Fe atom. (b) Formation of the first FeCO molecule (green) and identification of another reactive Fe/CO pair (curved white arrow). (c) Formation of the second FeCO molecule (green) and identification of a second possible reaction to form $\text{Fe}(\text{CO})_2$ (curved white arrow). (d) Image of individual $\text{Fe}(\text{CO})_2$ and $\text{Fe}(\text{CO})$ molecules synthesized on a surface by the STM.



CHAPTER SUMMARY

We have come a long way since the attempts of the alchemists to turn base metals into gold, to transmute one element into another. Through the early chemical experiments of Dalton, Gay-Lussac, and Avogadro, we have learned that matter is ultimately indivisible, at least as far as its physical and chemical properties are concerned. The experiments of Thomson, Wien, and Rutherford confirmed, from the results of physical measurements, the existence of the atom. These experiments also identified and characterized the elementary particles from which the atom is made, and this led to the modern model of the atom as an object with a small, dense nucleus surrounded by a much larger volume occupied by the electrons. Physicists in the 21st century have developed tools of unprecedented power with which to analyze and synthesize single molecules, an achievement that has already led to exciting new applications in almost every area of modern science and engineering.

CHAPTER REVIEW

- Matter can be classified systematically by its uniformity and its response to a variety of separation processes; compounds and elements are the basic chemical building blocks.
- The existence of atoms was inferred from several lines of indirect evidence that all pointed to the conclusion that there was a fundamental limit below which no further division was possible.
- The existence of atoms was confirmed and the modern model of the atom developed from physical measurements that determined the properties of the electron and the nucleus and demonstrated the existence of isotopes.
- Individual atoms and molecules can be imaged and manipulated directly using the STM.

CONCEPTS & SKILLS

After studying this chapter and working the problems that follow, you should be able to:

1. Describe in operational terms how to distinguish among mixtures, compounds, and elements (Section 1.2).
2. Outline Dalton's atomic theory of matter and describe its experimental basis (Section 1.3).
3. Describe the reasoning that permits chemical formulas to be determined by purely chemical means (Section 1.3, Problems 7–10).
4. Describe the experiments that led to the discovery of the electron and the measurement of its mass and charge, and describe those that demonstrated the nature of the nucleus (Section 1.4).
5. Given the atomic masses and natural abundances of the isotopes of an element, calculate its chemical atomic mass (Section 1.4, Problems 15–18).
6. State the numbers of protons, neutrons, and electrons in particular atoms (Section 1.4, Problems 19–22).

KEY EQUATIONS

$$\frac{e}{m_e} = \frac{SE}{\ell LH^2} \quad \text{Section 1.4}$$

$$A = A_1p_1 + A_2p_2 + \cdots + A_np_n \equiv \sum_{i=1}^n A_i p_i \quad \text{Section 1.4}$$

PROBLEMS

Answers to problems whose numbers are boldface appear in Appendix G. Problems that are more challenging are indicated with asterisks.

Macroscopic Methods for Classifying Matter

1. Classify the following materials as substances or mixtures: table salt, wood, mercury, air, water, seawater, sodium chloride, and mayonnaise. If they are mixtures, subclassify them as homogeneous or heterogeneous; if they are substances, subclassify them as compounds or elements.
2. Classify the following materials as substances or mixtures: absolute (pure) alcohol, milk (as purchased in a store), copper wire, rust, barium bromide, concrete, baking soda, and baking powder. If they are mixtures, subclassify them as homogeneous or heterogeneous; if they are substances, subclassify them as compounds or elements.
3. A 17th-century chemist wrote of the “simple bodies which enter originally into the composition of mixtures and into which these mixtures resolve themselves or may be finally resolved.” What is being discussed?
4. Since 1800, almost 200 sincere but erroneous reports of the discovery of new chemical elements have been made. Why have mistaken reports of new elements been so numerous?

Why is it relatively easy to prove that a material is not a chemical element, but difficult to prove absolutely that a material is an element?

Indirect Evidence for the Existence of Atoms: Laws of Chemical Combination

5. A sample of ascorbic acid (vitamin C) is synthesized in the laboratory. It contains 30.0 g carbon and 40.0 g oxygen. Another sample of ascorbic acid, isolated from lemons (an excellent source of the vitamin), contains 12.7 g carbon. Compute the mass of oxygen (in grams) in the second sample.
6. A sample of a compound synthesized and purified in the laboratory contains 25.0 g hafnium and 31.5 g tellurium. The identical compound is discovered in a rock formation. A sample from the rock formation contains 0.125 g hafnium. Determine how much tellurium is in the sample from the rock formation.
7. Nitrogen (N) and silicon (Si) form two binary compounds with the following compositions:

Compound	Mass % N	Mass % Si
1	33.28	66.72
2	39.94	60.06

- (a) Compute the mass of silicon that combines with 1.0000 g of nitrogen in each case.
- (b) Show that these compounds satisfy the law of multiple proportions. If the second compound has the formula Si_3N_4 , what is the formula of the first compound?
8. Iodine (I) and fluorine (F) form a series of binary compounds with the following compositions:

Compound	Mass % I	Mass % F
1	86.979	13.021
2	69.007	30.993
3	57.191	42.809
4	48.829	51.171

- (a) Compute in each case the mass of fluorine that combines with 1.0000 g iodine.
- (b) By figuring out small whole-number ratios among the four answers in part (a), show that these compounds satisfy the law of multiple proportions.
9. Vanadium (V) and oxygen (O) form a series of compounds with the following compositions:

Mass % V	Mass % O
76.10	23.90
67.98	32.02
61.42	38.58
56.02	43.98

What are the relative numbers of atoms of oxygen in the compounds for a given mass of vanadium?

10. Tungsten (W) and chlorine (Cl) form a series of compounds with the following compositions:

Mass % W	Mass % Cl
72.17	27.83
56.45	43.55
50.91	49.09
46.36	53.64

If a molecule of each compound contains only one tungsten atom, what are the formulas for the four compounds?

11. A liquid compound containing only hydrogen and oxygen is placed in a flask. Two electrodes are dipped into the liquid, and an electric current is passed between them. Gaseous hydrogen forms at one electrode and gaseous oxygen at the other. After a time, 14.4 mL hydrogen has evolved at the negative terminal, and 14.4 mL oxygen has evolved at the positive terminal.
- (a) Assign a chemical formula to the compound in the cell.
- (b) Explain why more than one formula is possible as the answer to part (a).
12. A sample of liquid N_2H_4 is decomposed to give gaseous N_2 and gaseous H_2 . The two gases are separated, and the nitrogen occupies 13.7 mL at room conditions of pressure and temperature. Determine the volume of the hydrogen under the same conditions.
13. Pure nitrogen dioxide (NO_2) forms when dinitrogen oxide (N_2O) and oxygen (O_2) are mixed in the presence of a

certain catalyst. What volumes of N_2O and oxygen are needed to produce 4.0 L NO_2 if all gases are held at the same conditions of temperature and pressure?

14. Gaseous methanol (CH_3OH) reacts with oxygen (O_2) to produce water vapor and carbon dioxide. What volumes of water vapor and carbon dioxide will be produced from 2.0 L methanol if all gases are held at the same temperature and pressure conditions?

Physical Structure of Atoms

15. The natural abundances and isotopic masses of the element silicon (Si) relative to $^{12}\text{C} = 12.00000$ are

Isotope	% Abundance	Isotopic Mass
^{28}Si	92.21	27.97693
^{29}Si	4.70	28.97649
^{30}Si	3.09	29.97376

Calculate the atomic mass of naturally occurring silicon.

16. The natural abundances and isotopic masses of the element neon (Ne) are

Isotope	% Abundance	Isotopic Mass
^{20}Ne	90.00	19.99212
^{21}Ne	0.27	20.99316
^{22}Ne	9.73	21.99132

Calculate the atomic mass of naturally occurring neon.

17. Only two isotopes of boron (B) occur in nature; their atomic masses and abundances are given in the following table. Complete the table by computing the relative atomic mass of ^{11}B to four significant figures, taking the tabulated relative atomic mass of natural boron as 10.811.

Isotope	% Abundance	Atomic Mass
^{10}B	19.61	10.013
^{11}B	80.39	?

18. More than half of all the atoms in naturally occurring zirconium are ^{90}Zr . The other four stable isotopes of zirconium have the following relative atomic masses and abundances:

Isotope	% Abundance	Atomic Mass
^{91}Zr	11.27	90.9056
^{92}Zr	17.17	91.9050
^{94}Zr	17.33	93.9063
^{96}Zr	2.78	95.9083

Compute the relative atomic mass of ^{90}Zr to four significant digits, using the tabulated relative atomic mass 91.224 for natural zirconium.

19. The isotope of plutonium used for nuclear fission is ^{239}Pu . Determine (a) the ratio of the number of neutrons in a ^{239}Pu nucleus to the number of protons, and (b) the number of electrons in a single plutonium atom.
20. The last “missing” element from the first six periods was promethium, which was finally discovered in 1947 among

the fission products of uranium. Determine (a) the ratio of the number of neutrons in a ^{145}Pm nucleus to the number of protons, and (b) the number of electrons in a single promethium atom.

21. The americium isotope ^{241}Am is used in smoke detectors. Describe the composition of a neutral atom of this isotope for protons, neutrons, and electrons.
22. In 1982, the production of a single atom of $^{266}_{109}\text{Mt}$ (meitnerium-266) was reported. Describe the composition of a neutral atom of this isotope for protons, neutrons, and electrons.

ADDITIONAL PROBLEMS

23. Soft wood chips weighing 17.2 kg are placed in an iron vessel and mixed with 150.1 kg water and 22.43 kg sodium hydroxide. A steel lid seals the vessel, which is then placed in an oven at 250°C for 6 hours. Much of the wood fiber decomposes under these conditions; the vessel and lid do not react.
- (a) Classify each of the materials mentioned as a substance or mixture. Subclassify the substances as elements or compounds.
- (b) Determine the mass of the contents of the iron vessel after the reaction.
- * 24. In a reproduction of the Millikan oil-drop experiment, a student obtains the following values for the charges on nine different oil droplets.

$6.563 \times 10^{-19} \text{ C}$	$13.13 \times 10^{-19} \text{ C}$	$19.71 \times 10^{-19} \text{ C}$
$8.204 \times 10^{-19} \text{ C}$	$16.48 \times 10^{-19} \text{ C}$	$22.89 \times 10^{-19} \text{ C}$
$11.50 \times 10^{-19} \text{ C}$	$18.08 \times 10^{-19} \text{ C}$	$26.18 \times 10^{-19} \text{ C}$

- (a) Based on these data alone, what is your best estimate of the number of electrons on each of the above droplets?

(Hint: Begin by considering differences in charges between adjacent data points, and see into what groups these are categorized.)

- (b) Based on these data alone, what is your best estimate of the charge on the electron?
- (c) Is it conceivable that the actual charge is half the charge you calculated in (b)? What evidence would help you decide one way or the other?
25. A rough estimate of the radius of a nucleus is provided by the formula $r = kA^{1/3}$, where k is approximately $1.3 \times 10^{-13} \text{ cm}$ and A is the mass number of the nucleus. Estimate the density of the nucleus of ^{127}I (which has a nuclear mass of $2.1 \times 10^{-22} \text{ g}$) in grams per cubic centimeter. Compare with the density of solid iodine, 4.93 g cm^{-3} .
26. In a neutron star, gravity causes the electrons to combine with protons to form neutrons. A typical neutron star has a mass half that of the sun, compressed into a sphere of radius 20 km. If such a neutron star contains 6.0×10^{56} neutrons, calculate its density in grams per cubic centimeter. Compare this with the density inside a ^{232}Th nucleus, in which 142 neutrons and 90 protons occupy a sphere of radius $9.1 \times 10^{-13} \text{ cm}$. Take the mass of a neutron to be $1.675 \times 10^{-24} \text{ g}$ and that of a proton to be $1.673 \times 10^{-24} \text{ g}$.
27. Dalton's 1808 version of the atomic theory of matter included five general statements (see Section 1.3). According to modern understanding, four of those statements require amendment or extension. List the modifications that have been made to four of the five original postulates.
28. Naturally occurring rubidium (Rb) consists of two isotopes: ^{85}Rb (atomic mass 84.9117) and ^{87}Rb (atomic mass 86.9092). The atomic mass of the isotope mixture found in nature is 85.4678. Calculate the percentage abundances of the two isotopes in rubidium.

Chemical Formulas, Chemical Equations, and Reaction Yields

- 2.1 The Mole: Weighing and Counting Molecules
- 2.2 Empirical and Molecular Formulas
- 2.3 Chemical Formula and Percentage Composition
- 2.4 Writing Balanced Chemical Equations
- 2.5 Mass Relationships in Chemical Reactions
- 2.6 Limiting Reactant and Percentage Yield



© Thomson Learning/ Charles D. Winters. Balance courtesy of the Chandler Museum at Columbia University, New York, NY.

An “assay balance of careful construction” of the type used by Lavoisier before 1788. This balance became the production model that served as a general, all-purpose balance for approximately 40 years. Users of this type of balance included Sir Humphrey Davy and his young assistant Michael Faraday.

Chapter 1 explained how chemical and physical methods are used to establish chemical formulas and relative atomic and molecular masses. This chapter begins our study of chemical reactions. We start by developing the concept of the mole, which allows us to count molecules by weighing macroscopic quantities of matter. We examine the balanced chemical equations that summarize these reactions and show how to relate the masses of substances consumed to the masses of substances produced. This is an immensely practical and important subject. The questions how much of a substance will react with a given amount of another substance and how much product will be generated are central to all chemical processes, whether industrial, geological, or biological.

2.1 The Mole: Weighing and Counting Molecules

The laws of chemical combination assert that chemical reactions occur in such a way that the number of atoms of a given type are conserved in every chemical reaction, except nuclear reactions. How do we weigh out a sample containing exactly the number of atoms or molecules needed for a particular chemical reaction? What is the mass of an atom or a molecule? These questions must be answered indirectly, because atoms and molecules are far too small to be weighed individually.

In the process of developing the laws of chemical combination, chemists had determined indirectly the relative masses of atoms of different elements; for example, 19th-century chemists concluded that oxygen atoms weigh 16 times as much as hydrogen atoms. In the early 20th century, relative atomic and molecular masses were determined much more accurately through the work of J. J. Thomson, F. W. Aston, and others using mass spectrometry. These relative masses on the atomic scale must be related to absolute masses on the gram scale by a conversion factor. Once this conversion factor is determined, we simply weigh out a sample with the mass required to provide the desired number of atoms or molecules of a substance for a particular reaction. These concepts and methods are developed in this section.

Relation between Atomic and Macroscopic Masses: Avogadro's Number

What are the actual masses (in grams) of individual atoms and molecules? To answer this question, we must establish a connection between the absolute macroscopic scale for mass used in the laboratory and the relative microscopic scale established for the masses of individual atoms and molecules. The link between the two is provided by **Avogadro's number** (N_A), defined as the number of atoms in exactly 12 g of ^{12}C . We consider below some of the many experimental methods devised to determine the numerical value of N_A . Its currently accepted value is

$$N_A = 6.0221420 \times 10^{23}$$

The mass of a single ^{12}C atom is then found by dividing exactly 12 g carbon (C) by N_A :

$$\text{Mass of a } ^{12}\text{C} \text{ atom} = \frac{12.00000 \text{ g}}{6.0221420 \times 10^{23}} = 1.9926465 \times 10^{-23} \text{ g}$$

This is truly a small mass, reflecting the large number of atoms in a 12-g sample of carbon.

Avogadro's number is defined relative to the ^{12}C atom because that isotope has been chosen by international agreement to form the basis for the modern scale of relative atomic masses. We can apply it to other substances as well in a particularly simple fashion. Consider sodium, which has a relative atomic mass of 22.98977. A sodium atom is 22.98977/12 times as heavy as a ^{12}C atom. If the mass of N_A atoms of ^{12}C is 12 g, then the mass of N_A atoms of sodium must be

$$\frac{22.98977}{12} (12 \text{ g}) = 22.98977 \text{ g}$$

The mass (in grams) of N_A atoms of *any* element is numerically equal to the relative atomic mass of that element. The same conclusion applies to molecules. From the relative molecular mass of water calculated earlier, the mass of N_A molecules of water is 18.0152 g.

EXAMPLE 2.1

One of the heaviest atoms found in nature is ^{238}U . Its relative atomic mass is 238.0508 on a scale in which 12 is the atomic mass of ^{12}C . Calculate the mass (in grams) of one ^{238}U atom.

SOLUTION

Because the mass of N_{A} atoms of ^{238}U is 238.0508 g and N_{A} is 6.0221420×10^{23} , the mass of one ^{238}U atom must be

$$\frac{238.0508 \text{ g}}{6.0221420 \times 10^{23}} = 3.952926 \times 10^{-22} \text{ g}$$

Related Problems: 1, 2

The Mole

Because the masses of atoms and molecules are so small, laboratory scale chemical reactions must involve large numbers of atoms and molecules. It is convenient to group atoms or molecules in counting units of $N_{\text{A}} = 6.0221420 \times 10^{23}$ to measure the **number of moles** of a substance. One of these counting units is called a **mole** (abbreviated mol; derived from Latin *moles*, meaning “heap” or “pile”). One mole of a substance is the amount that contains Avogadro’s number of atoms, molecules, or other entities. That is, 1 mol of ^{12}C contains N_{A} ^{12}C atoms, 1 mol of water contains N_{A} water molecules, and so forth. We must be careful in some cases, because a phrase such as “1 mol of oxygen” is ambiguous. We should refer instead to “1 mol of O_2 ” if there are N_{A} oxygen *molecules*, and “1 mol of O” if there are N_{A} oxygen *atoms*. Henceforth, for *any* species we use “number of moles of a particular species” to describe the number of moles in a sample of that species.

The mass of one mole of atoms of an element—the **molar mass**, with units of grams per mole—is numerically equal to the dimensionless relative atomic mass of that element, and the same relationship holds between the molar mass of a compound and its relative molecular mass. Thus, the relative molecular mass of water is 18.0152, and its molar mass is $18.0152 \text{ g mol}^{-1}$.

To determine the number of moles of a given substance, we use the chemist’s most powerful tool, the laboratory balance. If a sample of iron weighs 8.232 g, then

$$\begin{aligned} \text{moles of iron} &= \frac{\text{number of grams of iron}}{\text{molar mass of iron}} \\ &= \frac{8.232 \text{ g Fe}}{55.847 \text{ g mol}^{-1}} \\ &= 0.1474 \text{ mol Fe} \end{aligned}$$

where the molar mass of iron was obtained from the periodic table of the elements or a table of relative atomic masses (see the inside front and back covers of this book). The calculation can be turned around as well. Suppose a certain amount, for example, 0.2000 mol, of water is needed in a chemical reaction. We have

$$\begin{aligned} (\text{moles of water}) \times (\text{molar mass of water}) &= \text{mass of water} \\ (0.2000 \text{ mol H}_2\text{O}) \times (18.015 \text{ g mol}^{-1}) &= 3.603 \text{ g H}_2\text{O} \end{aligned}$$

We simply weigh 3.603 g water to get the 0.2000 mol needed for the reaction. In both cases, the molar mass is the conversion factor between the mass of the substance and the number of moles of the substance.

Although the number of moles in a sample is frequently determined by weighing, it is still preferable to think of a mole as a fixed number of particles (Avogadro's number) rather than as a fixed mass. The term *mole* is thus analogous to a term such as *dozen*: one dozen pennies weighs 26 g, which is substantially less than the mass of one dozen nickels, 60 g; but each group contains 12 coins. Figure 2.1 shows mole quantities of several substances.

EXAMPLE 2.2

Nitrogen dioxide (NO_2) is a major component of urban air pollution. For a sample containing 4.000 g NO_2 , calculate (a) the number of moles of NO_2 and (b) the number of molecules of NO_2 .

SOLUTION

(a) From the tabulated molar masses of nitrogen ($14.007 \text{ g mol}^{-1}$) and oxygen ($15.999 \text{ g mol}^{-1}$), the molar mass of NO_2 is

$$14.007 \text{ g mol}^{-1} + (2 \times 15.999 \text{ g mol}^{-1}) = 46.005 \text{ g mol}^{-1}$$

The number of moles of NO_2 is then

$$\text{mol of NO}_2 = \frac{4.000 \text{ g NO}_2}{46.005 \text{ g mol}^{-1}} = 0.08695 \text{ mol NO}_2$$

(b) To convert from moles to number of molecules, multiply by Avogadro's number:

$$\begin{aligned} \text{Molecules of NO}_2 &= (0.08695 \text{ mol NO}_2) \times 6.0221 \times 10^{23} \text{ mol}^{-1} \\ &= 5.236 \times 10^{22} \text{ molecules NO}_2 \end{aligned}$$

Related Problems: 7, 8

The fact that N_A is the ratio of the molar volume to the atomic volume of any element provides a route to measuring its value, and several methods have been used to determine this ratio. A new method to refine the value currently is under development. Nearly perfectly smooth spheres of highly crystalline silicon (Si) can be prepared and characterized. The surface roughness of these spheres (which affects the determination of their volume) is ± 1 silicon atom. The molar volume is determined by carefully measuring the mass and volume of the sphere, and the atomic volume is determined by measuring the interatomic distances directly using x-ray diffraction. (X-ray diffraction from solids is described in Chapter 21.) Avogadro's number is the ratio of these two quantities.

Density and Molecular Size

The **density** of a sample is the ratio of its mass to its volume:

$$\text{density} = \frac{\text{mass}}{\text{volume}} \quad [2.1]$$

The base unit of mass in the International System of Units (SI; see discussion in Appendix B) is the kilogram (kg), but it is inconveniently large for most practical purposes in chemistry. The gram often is used instead; moreover, it is the standard unit for molar masses. Several units for volume are in frequent use. The base SI unit of the cubic meter (m^3) is also unwieldy for laboratory purposes (1 m^3 water weighs 1000 kg, or 1 metric ton). We will, therefore, use the liter (1 L = 10^{-3} m^3) and the cubic centimeter, which is identical to the milliliter

FIGURE 2.1 One-mole quantities of several substances. (Clockwise from top) Graphite (C), potassium permanganate (KMnO₄), copper sulfate pentahydrate (CuSO₄ · 5 H₂O), copper (Cu), sodium chloride (NaCl), and potassium dichromate (K₂Cr₂O₇). Antimony (Sb) is at the center.



© Thomson Learning/Leon Lewandowski

($1 \text{ cm}^3 = 1 \text{ mL} = 10^{-3} \text{ L} = 10^{-6} \text{ m}^3$), for volume. Table 2.1 lists the densities of some substances in units of grams per cubic centimeter.

The density of a substance is not a fixed, invariant property of the substance; its value depends on the pressure and temperature at the time of measurement. For some substances (especially gases and liquids), the volume may be more convenient to measure than the mass, and when the density is known, it provides the conversion factor between volume and mass. For example, near room temperature, the density of liquid benzene (C₆H₆) is 0.8765 g cm^{-3} . Suppose that 0.2124 L benzene is measured into a container. The mass of benzene is then the product of the volume and the density:

$$m = \rho V$$

where m is the mass, ρ is the density, and V is the volume. Therefore, the value of the mass of benzene is

$$m = 0.2124 \text{ L} \times (1 \times 10^3 \text{ cm}^3 \text{ L}^{-1}) \times (0.8765 \text{ g cm}^{-3}) = 186.2 \text{ g}$$

TABLE 2.1 Densities of Some Substances

Substance	Density (g cm ⁻³)
Hydrogen	0.000082
Oxygen	0.00130
Water	1.00
Magnesium	1.74
Sodium chloride	2.16
Quartz	2.65
Aluminum	2.70
Iron	7.86
Copper	8.96
Silver	10.5
Lead	11.4
Mercury	13.5
Gold	19.3
Platinum	21.4

These densities were measured at room temperature and at average atmospheric pressure near sea level.

Dividing the above amount by the molar mass of benzene ($78.114 \text{ g mol}^{-1}$) gives the corresponding number of moles, 2.384 mol.

Knowing the density and molar mass of a substance, we can readily compute its **molar volume**, that is, the volume occupied by one mole of a substance:

$$V_m = \frac{\text{molar mass (g mol}^{-1}\text{)}}{\text{density (g cm}^{-3}\text{)}} = \text{molar volume (cm}^3 \text{ mol}^{-1}\text{)}$$

For example, near 0°C , ice has a density of 0.92 g cm^{-3} ; thus, the molar volume of solid water under these conditions is

$$V_m = \frac{18.0 \text{ g mol}^{-1}}{0.92 \text{ g cm}^{-3}} = 20 \text{ cm}^3 \text{ mol}^{-1}$$

The molar volume of a gas is much larger than that of either a liquid or a solid. For O_2 under room conditions, the data in Table 2.1 give a molar volume of $24,600 \text{ cm}^3 \text{ mol}^{-1} = 24.6 \text{ L mol}^{-1}$, which is more than 1000 times larger than the molar volume just computed for ice under the same conditions of temperature and pressure. How can we interpret this fact on a microscopic level? We also note that the volumes of liquids and solids do not shift much with changes in temperature or pressure, but that the volumes of gases are quite sensitive to these changes. One hypothesis that would explain these observations is that the molecules in liquids and solids are close enough to touch one another, but that they are separated by large distances in gases. If this hypothesis is correct (as has been well established by further study), then the sizes of the molecules themselves can be estimated from the volume occupied per molecule in the liquid or solid state. The volume per molecule is the molar volume divided by Avogadro's number; for ice, this gives

$$\text{Volume per H}_2\text{O molecule} = \frac{20 \text{ cm}^3 \text{ mol}^{-1}}{6.02 \times 10^{23} \text{ mol}^{-1}} = 3.3 \times 10^{-23} \text{ cm}^3$$

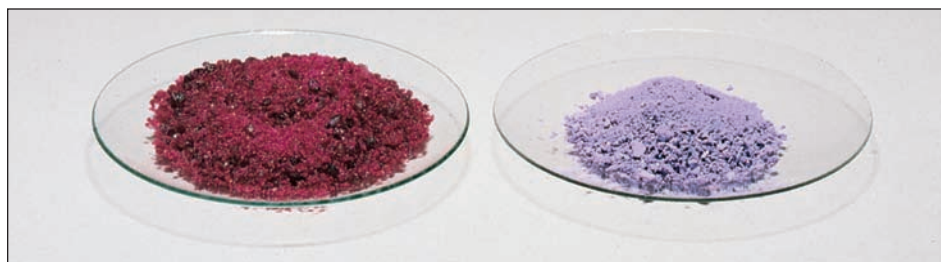
This volume corresponds to that of a cube with edges about $3.2 \times 10^{-8} \text{ cm}$ (0.32 nm) on a side. We conclude from this and other density measurements that the characteristic size of atoms and small molecules is about 10^{-8} cm , or about 0.1 nm. Avogadro's number provides the link between the length and mass scales of laboratory measurements and the masses and volumes of single atoms and molecules.

2.2 Empirical and Molecular Formulas

According to the laws of chemical combination, each substance may be described by a chemical formula that specifies the relative numbers of atoms of the elements in that substance. We now distinguish between two types of formulas: the molecular formula and the empirical formula. The **molecular formula** of a substance specifies the number of atoms of each element in one molecule of that substance. Thus, the molecular formula of carbon dioxide is CO_2 ; each molecule of carbon dioxide contains 1 atom of carbon and 2 atoms of oxygen. The molecular formula of glucose is $\text{C}_6\text{H}_{12}\text{O}_6$; each glucose molecule contains 6 atoms of carbon, 6 of oxygen, and 12 of hydrogen. Molecular formulas can be defined for all gaseous substances and for those liquids or solids that, like glucose, possess well-defined molecular structures.

In contrast, the **empirical formula** of a compound is the simplest formula that gives the correct relative numbers of atoms of each kind in a compound. For example, the empirical formula of glucose is CH_2O , indicating that the numbers of atoms of carbon, hydrogen, and oxygen are in a ratio of 1:2:1. When a molecular formula is known, it is clearly preferable because it conveys more information. In some solids and liquids, however, distinct small molecules do not exist, and the

FIGURE 2.2 When cobalt(II) chloride crystallizes from solution, it brings with it six water molecules per formula unit, giving a red solid with the empirical formula $\text{CoCl}_2 \cdot 6 \text{H}_2\text{O}$. This solid melts at 86°C ; at greater than about 110°C , it loses some water and forms a lavender solid with the empirical formula $\text{CoCl}_2 \cdot 2 \text{H}_2\text{O}$.



© Thomson Learning/Leon Lewandowski

only meaningful chemical formula is an empirical one. Solid cobalt(II) chloride, which has the empirical formula CoCl_2 , is an example. There are strong attractive forces between a cobalt atom and two adjoining chlorine (Cl) atoms in solid cobalt(II) chloride, but it is impossible to distinguish the forces *within* such a “molecule” of CoCl_2 from those operating *between* it and a neighbor; the latter are equally strong. The solid is, in effect, a single giant molecule. Consequently, cobalt(II) chloride is represented with an empirical formula and referred to by a **formula unit** of CoCl_2 , rather than by “a molecule of CoCl_2 .” Many solids can be represented only by their formula units because it is not possible to identify a molecular unit in a unique way; other examples include sodium chloride (NaCl), the major component in table salt, and silicon dioxide (SiO_2), the major component of sand. In some cases, small molecules are incorporated into a solid structure, and the chemical formula is written to show this fact explicitly. Thus, cobalt and chlorine form not only the anhydrous salt CoCl_2 mentioned earlier but also the hexahydrate $\text{CoCl}_2 \cdot 6 \text{H}_2\text{O}$, in which six water molecules are incorporated per CoCl_2 formula unit (Fig. 2.2). The dot in this formula is used to set off a well-defined molecular component of the solid, such as water.

2.3 Chemical Formula and Percentage Composition

The empirical formula H_2O specifies that for every atom of oxygen in water, there are two atoms of hydrogen. Equivalently, one mole of H_2O contains two moles of hydrogen atoms and one mole of oxygen atoms. The number of atoms and the number of moles of each element are present in the same ratio, namely, 2:1. The empirical formula for a substance is clearly related to the percentage composition by mass of that substance. This connection can be used in various ways.

Empirical Formula and Percentage Composition

The empirical formula of a compound can be simply related to the mass percentage of its constituent elements using the mole concept. For example, the empirical formula for ethylene (molecular formula C_2H_4) is CH_2 . Its composition by mass is calculated from the masses of carbon and hydrogen in 1 mol of CH_2 formula units:

$$\text{Mass of C} = 1 \text{ mol C} \times (12.011 \text{ g mol}^{-1}) = 12.011 \text{ g}$$

$$\text{Mass of H} = 2 \text{ mol H} \times (1.00794 \text{ g mol}^{-1}) = 2.0159 \text{ g}$$

Adding these masses together gives a total mass of 14.027 g. The mass percentages of carbon and hydrogen in the compound are then found by dividing each of their masses by this total mass and multiplying by 100%, giving 85.628% C and 14.372% H by weight, respectively.

Determination of Empirical Formula from Measured Mass Composition

We can reverse the procedure just described and determine the empirical formula from the elemental analysis of a compound, as illustrated by Example 2.3.

EXAMPLE 2.3

A 60.00-g sample of a dry-cleaning fluid was analyzed and found to contain 10.80 g carbon, 1.36 g hydrogen, and 47.84 g chlorine. Determine the empirical formula of the compound using a table of atomic masses.

SOLUTION

The amounts of each element in the sample are

$$\text{carbon: } \frac{10.80 \text{ g C}}{12.011 \text{ g mol}^{-1}} = 0.8992 \text{ mol C}$$

$$\text{hydrogen: } \frac{1.36 \text{ g H}}{1.008 \text{ g mol}^{-1}} = 1.35 \text{ mol H}$$

$$\text{chlorine: } \frac{47.84 \text{ g Cl}}{35.453 \text{ g mol}^{-1}} = 1.349 \text{ mol Cl}$$

The ratio of the amount of carbon to that of chlorine (or hydrogen) is $0.8992:1.349 = 0.6666$, which is close to $2:3$. The numbers of moles form the ratio $2:3:3$; therefore, the empirical formula is $\text{C}_2\text{H}_3\text{Cl}_3$. Additional measurements would be necessary to find the actual molecular mass and the correct *molecular* formula from among $\text{C}_2\text{H}_3\text{Cl}_3$, $\text{C}_4\text{H}_6\text{Cl}_6$, or any higher multiples $(\text{C}_2\text{H}_3\text{Cl}_3)_n$.

Related Problems: 19, 20, 21, 22, 23, 24

Empirical Formula Determined from Elemental Analysis by Combustion

A **hydrocarbon** is a compound that contains only carbon and hydrogen. Its empirical formula can be determined by using the combustion train shown in Figure 2.3. In this device, a known mass of the hydrocarbon is burned completely in oxygen,

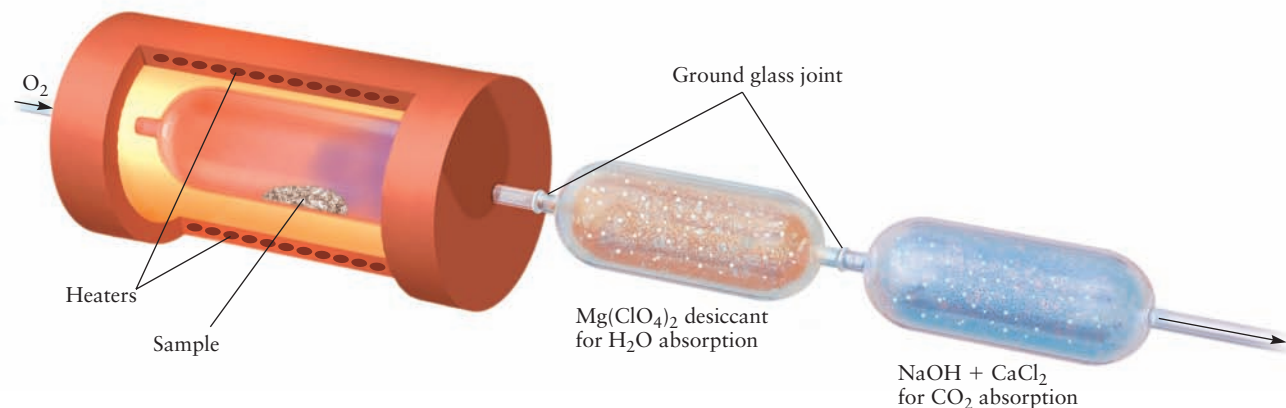


FIGURE 2.3 A combustion train to determine amounts of carbon and hydrogen in hydrocarbons. A weighed sample is burned in a flow of oxygen to form water and carbon dioxide. These products of combustion pass over a desiccant such as magnesium perchlorate, $\text{Mg}(\text{ClO}_4)_2$, which absorbs the water. In a second stage, the carbon dioxide passes over and is absorbed on finely divided particles of sodium hydroxide, NaOH , mixed with calcium chloride, CaCl_2 . The changes in mass of the two absorbers give the amounts of water and carbon dioxide produced.

yielding carbon dioxide and water. The masses of water and carbon dioxide that result can then be determined, and from these data the empirical formula calculated, as illustrated in Example 2.4.

EXAMPLE 2.4

A certain compound, used as a welding fuel, contains only carbon and hydrogen. Burning a small sample of this fuel completely in oxygen produces 3.38 g CO₂, 0.692 g water, and no other products. What is the empirical formula of the compound?

SOLUTION

We first compute the amounts of CO₂ and H₂O. Because all the carbon has been converted to CO₂ and all the hydrogen to water, the amounts of C and H in the unburned gas can be determined:

$$\text{mol of C} = \text{mol of CO}_2 = \frac{3.38 \text{ g}}{44.01 \text{ g mol}^{-1}} = 0.0768 \text{ mol}$$

$$\text{mol of H} = 2(\text{mol of H}_2\text{O}) = \left(\frac{0.692 \text{ g}}{18.02 \text{ g mol}^{-1}} \right) = 0.0768 \text{ mol}$$

Because each water molecule contains two hydrogen atoms, it is necessary to multiply the number of moles of water by 2 to find the number of moles of hydrogen atoms. Having found that the compound contains equal numbers of moles of carbon and hydrogen, we have determined that its empirical formula is CH. Its molecular formula may be CH, C₂H₂, C₃H₃, and so on.

Related Problems: 25, 26

Connection between the Empirical Formula and the Molecular Formula

The molecular formula is some whole-number multiple of the empirical formula. To determine the molecular formula, you must know the approximate molar mass of the compound under study. From Avogadro's hypothesis, the ratio of molar masses of two gaseous compounds is the same as the ratio of their densities, provided that those densities are measured at the same temperature and pressure. (This is true because a given volume contains the same number of molecules of the two gases.) The density of the welding gas from Example 2.4 is 1.06 g L⁻¹ at 25°C and atmospheric pressure. Under the same conditions, the density of gaseous oxygen (which exists as diatomic O₂ molecules with molar mass of 32.0 g mol⁻¹) is 1.31 g L⁻¹. The approximate molar mass of the welding gas is, therefore,

$$\text{Molar mass of welding gas} = \frac{1.06 \text{ g L}^{-1}}{1.31 \text{ g L}^{-1}} (32.0 \text{ g mol}^{-1}) = 25.9 \text{ g mol}^{-1}$$

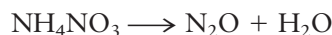
The molar mass corresponding to the *empirical* formula CH is 13.0 g mol⁻¹. Because 25.9 g mol⁻¹ is approximately twice this value, there must be two CH units per molecule; therefore, the molecular formula is C₂H₂. The gas is acetylene.

2.4 Writing Balanced Chemical Equations

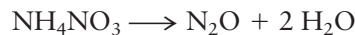
Chemical reactions combine elements into compounds, decompose compounds back into elements, and transform existing compounds into new compounds. Because atoms are indestructible in chemical reactions, the same number of atoms (or moles of atoms) of each element must be present before and after any ordinary (as opposed to nuclear) chemical reaction. The conservation of matter in a chemical

change is represented in a balanced chemical equation for that process. The study of the relationships between the numbers of reactant and product molecules is called **stoichiometry** (derived from the Greek *stoicheion*, meaning “element,” and *metron*, meaning “measure”). Stoichiometry is fundamental to all aspects of chemistry.

An equation can be balanced using stepwise reasoning. Consider the decomposition of ammonium nitrate (NH_4NO_3) on gentle heating to produce dinitrogen oxide (N_2O) and water. The *unbalanced* equation for this process is

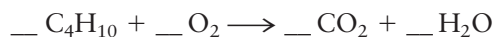


The formulas on the left side of the arrow denote **reactants**, and those on the right side denote **products**. This equation is unbalanced because there are 3 mol of oxygen atoms on the left side of the equation (and 4 of hydrogen), but only 2 mol of oxygen atoms and 2 mol of hydrogen atoms on the right side. To balance the equation, begin by assigning 1 as the coefficient of one species, usually the species that contains the most elements—in this case, NH_4NO_3 . Next, seek out the elements that appear in only one other place in the equation and assign coefficients to balance the numbers of their atoms. Here, nitrogen appears in only one other place (N_2O), and a coefficient of 1 for the N_2O ensures that there are 2 mol of nitrogen atoms on each side of the equation. Hydrogen appears in H_2O ; thus, its coefficient is 2 to balance the 4 mol of hydrogen atoms on the left side. This gives

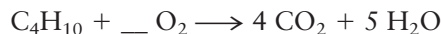


Finally, verify that the last element, oxygen, is also balanced by noting that there are 3 mol of oxygen atoms on each side. The coefficients of 1 in front of the NH_4NO_3 and N_2O are omitted by convention.

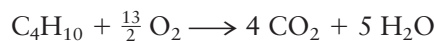
As a second example, consider the reaction in which butane (C_4H_{10}) is burned in oxygen to form carbon dioxide and water:



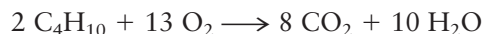
Spaces have been left for the coefficients that specify the number of moles of each reactant and product. Begin with 1 mol of butane, C_4H_{10} . It contains 4 mol of carbon atoms and must produce 4 mol of carbon dioxide molecules to conserve the number of carbon atoms in the reaction. Therefore, the coefficient for CO_2 is 4. In the same way, the 10 mol of hydrogen *atoms* must form 5 mol of water *molecules*, because each water molecule contains 2 hydrogen atoms; thus, the coefficient for the H_2O is 5:



Four moles of CO_2 contain 8 mol of oxygen atoms, and 5 mol of H_2O contain 5 mol of oxygen atoms, resulting in a total of 13 mol of oxygen atoms. Thirteen moles of oxygen atoms are equivalent to $\frac{13}{2}$ moles of oxygen molecules; therefore, the coefficient for O_2 is $\frac{13}{2}$. The balanced equation is



There is nothing wrong with fractions such as $\frac{13}{2}$ in a balanced equation, because fractions of moles are perfectly meaningful. It is often customary, however, to eliminate such fractions. In this case, multiplying all coefficients in the equation by 2 gives



A summary of the steps in balancing a chemical equation is as follows:

1. Assign 1 as the coefficient of one species. The best choice is the most complicated species; that is, the species with the largest number of elements.
2. Identify, in sequence, elements that appear in only one chemical species, the coefficient of which has not yet been determined. Choose that coefficient to balance the number of moles of atoms of that element. Continue until all coefficients have been identified.
3. If desired, multiply the whole equation by the smallest integer that will eliminate any fractions.

This method of balancing equations “by inspection” works in many, but not all, cases. Section 11.4 presents techniques for balancing certain more complex chemical equations.

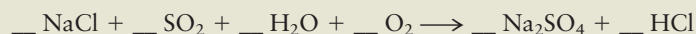
Once the reactants and products are known, balancing chemical equations is a routine, mechanical process of accounting. The difficult part (and the part where chemistry comes in) is to know which substances will react with each other and to determine which products are formed. We return to this question many times throughout this book.

EXAMPLE 2.5

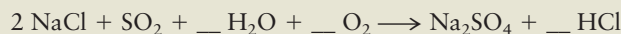
Hargreaves process is an industrial procedure for making sodium sulfate (Na_2SO_4) for use in papermaking. The starting materials are sodium chloride (NaCl), sulfur dioxide (SO_2), water, and oxygen. Hydrogen chloride (HCl) is generated as a by-product. Write a balanced chemical equation for this process.

SOLUTION

The unbalanced equation is



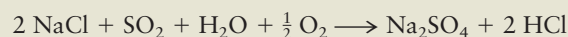
Begin by assigning a coefficient of 1 to Na_2SO_4 because it is the most complex species, composed of 3 different elements. There are 2 mol of sodium atoms on the right; therefore, the coefficient for NaCl must be 2. Following the same argument, the coefficient for SO_2 must be 1 to balance the 1 mol of sulfur on the right. This gives



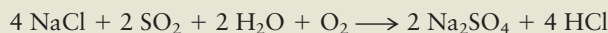
Next, we note that there are 2 mol of Cl atoms on the left (reactant) side; therefore, the coefficient for HCl must be 2. Hydrogen is the next element to balance, with 2 mol on the right side, and therefore a coefficient of 1 for the H_2O :



Finally, the oxygen atoms must be balanced. There are 4 mol of oxygen atoms on the right side, but there are 2 mol from SO_2 and 1 mol from H_2O on the left side; therefore, 1 mol of oxygen *atoms* must come from O_2 . Therefore, the coefficient for O_2 is $\frac{1}{2}$:



Multiplying all coefficients in the equation by 2 gives

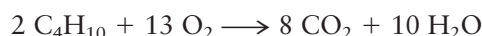


In balancing this equation, oxygen was considered last because it appears in several places on the left side of the equation.

Related Problems: 31, 32

2.5 Mass Relationships in Chemical Reactions

A balanced chemical equation makes a quantitative statement about the relative masses of the reacting substances. The chemical equation for the combustion of butane,



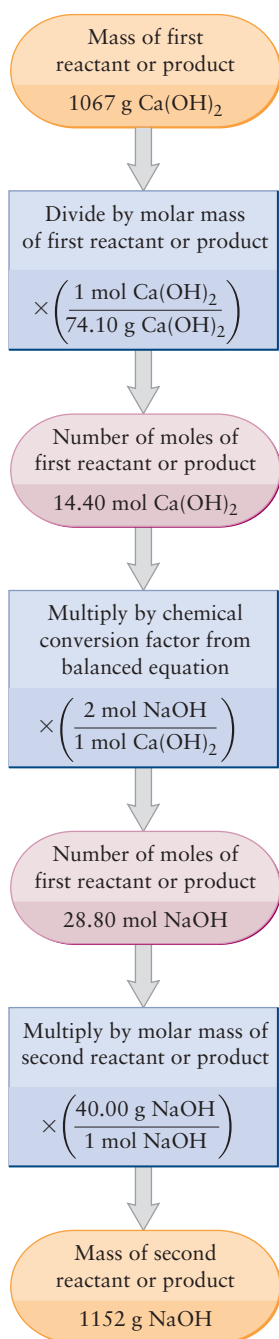
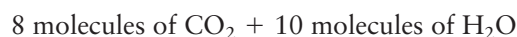
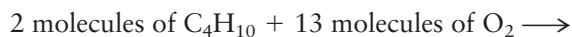
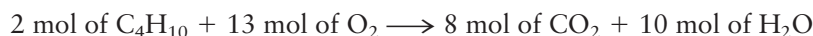


FIGURE 2.4 The steps in a stoichiometric calculation. In a typical calculation, the mass of one reactant or product is known and the masses of one or more other reactants or products are to be calculated using the balanced chemical equation and a table of relative atomic masses.

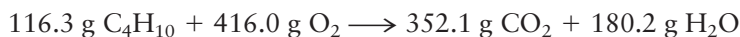
can be interpreted as either



or



Multiplying the molar mass of each substance in the reaction by the number of moles represented in the balanced equation gives



The coefficients in a balanced chemical equation give “chemical conversion factors” between the amounts of substances consumed in or produced by a chemical reaction. If 6.16 mol butane reacts according to the preceding equation, the amounts of O_2 consumed and CO_2 generated are

$$\text{mol O}_2 = 6.16 \text{ mol C}_4\text{H}_{10} \times \left(\frac{13 \text{ mol O}_2}{2 \text{ mol C}_4\text{H}_{10}} \right) = 40.0 \text{ mol O}_2$$

$$\text{mol CO}_2 = 6.16 \text{ mol C}_4\text{H}_{10} \times \left(\frac{8 \text{ mol CO}_2}{2 \text{ mol C}_4\text{H}_{10}} \right) = 24.6 \text{ CO}_2$$

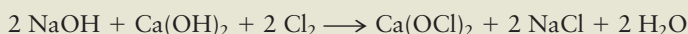
For most practical purposes we are interested in the *masses* of reactants and products, because those are the quantities that are directly measured. In this case, the molar masses (calculated from a table of atomic masses) are used to convert the number of moles of a substance (in moles) to its mass (in grams), as illustrated by Example 2.6. Sometimes, however, we are also interested in knowing the number of molecules in a sample. The mole allows us to convert easily from mass to numbers of molecules as follows:

$$\overset{\text{molar mass}}{\text{mass}} \longleftrightarrow \overset{N_A}{\text{moles}} \longleftrightarrow \text{number of molecules}$$

Mass and moles are related by the molar mass; Avogadro’s number N_A relates number and moles. You should practice using these relationships to calculate any desired quantity from any given quantity. You can use dimensional analysis to help figure out whether to divide or multiply in any given problem.

EXAMPLE 2.6

Calcium hypochlorite, Ca(OCl)_2 , is used as a bleaching agent. It is produced from sodium hydroxide, calcium hydroxide, and chlorine according to the following overall equation:



How many grams of chlorine and sodium hydroxide react with 1067 g Ca(OH)_2 , and how many grams of calcium hypochlorite are produced?

SOLUTION

The amount of Ca(OH)_2 consumed is

$$\frac{1067 \text{ g Ca(OH)}_2}{74.09 \text{ g mol}^{-1}} = 14.40 \text{ mol Ca(OH)}_2$$

where the molar mass of Ca(OH)_2 has been obtained from the molar masses of calcium, oxygen, and hydrogen as

$$40.08 + 2(15.999) + 2(1.0079) = 74.09 \text{ g mol}^{-1}$$

According to the balanced equation, 1 mol $\text{Ca}(\text{OH})_2$ reacts with 2 mol NaOH and 2 mol Cl_2 to produce 1 mol $\text{Ca}(\text{OCl})_2$. If 14.40 mol of $\text{Ca}(\text{OH})_2$ reacts completely, then

$$\begin{aligned}\text{mol NaOH} &= 14.40 \text{ mol Ca}(\text{OH})_2 \left(\frac{2 \text{ mol NaOH}}{1 \text{ mol Ca}(\text{OH})_2} \right) \\ &= 28.80 \text{ mol NaOH}\end{aligned}$$

$$\begin{aligned}\text{mol Cl}_2 &= 14.40 \text{ mol Ca}(\text{OH})_2 \left(\frac{2 \text{ mol Cl}_2}{1 \text{ mol Ca}(\text{OH})_2} \right) \\ &= 28.80 \text{ mol Cl}_2\end{aligned}$$

$$\begin{aligned}\text{mol Ca}(\text{OCl})_2 &= 14.40 \text{ mol Ca}(\text{OH})_2 \left(\frac{1 \text{ mol Ca}(\text{OCl})_2}{1 \text{ mol Ca}(\text{OH})_2} \right) \\ &= 14.40 \text{ mol Ca}(\text{OCl})_2\end{aligned}$$

From the number of moles and molar masses of reactants and products, the following desired masses are found:

$$\text{Mass NaOH reacting} = (28.80 \text{ mol})(40.00 \text{ g mol}^{-1}) = 1152 \text{ g}$$

$$\text{Mass Cl}_2 \text{ reacting} = (28.80 \text{ mol})(70.91 \text{ g mol}^{-1}) = 2042 \text{ g}$$

$$\text{Mass Ca}(\text{OCl})_2 \text{ produced} = (14.40 \text{ mol})(142.98 \text{ g mol}^{-1}) = 2059 \text{ g}$$

Related Problems: 33, 34, 35, 36

In calculations such as the one illustrated in Example 2.6, we are given a known mass of one substance and are asked to calculate the masses of one or more of the other reactants or products. Figure 2.4 summarizes the three-step process used. With experience, it is possible to write down the answers in a shorthand form so that all three conversions are conducted at the same time. The amount of NaOH reacting in the preceding example can be written as

$$\left(\frac{1067 \text{ g Ca}(\text{OH})_2}{74.10 \text{ g mol}^{-1}} \right) \times \left(\frac{2 \text{ mol NaOH}}{1 \text{ mol Ca}(\text{OH})_2} \right) \times 40.00 \text{ g mol}^{-1} = 1152 \text{ g NaOH}$$

At first, however, it is better to follow a stepwise procedure for such calculations.

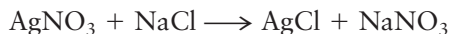
2.6 Limiting Reactant and Percentage Yield

In the cases we have considered so far, the reactants were present in the exact ratios necessary for them all to be completely consumed in forming products. This is not the usual case, however. It is necessary to have methods for describing cases in which one of the reactants may not be present in sufficient amount and in which conversion to products is less than complete.

Limiting Reactant

Suppose arbitrary amounts of reactants are mixed and allowed to react. The one that is used up first is called the **limiting reactant**; some quantity of the other reactants remains after the reaction has gone to completion. These other reactants are present **in excess**. An increase in the amount of the limiting reactant leads to an increase in the amount of product formed. This is not true of the other reactants. In an industrial process, the limiting reactant is often the most expensive one, to

ensure that none of it is wasted. For instance, the silver nitrate used in preparing silver chloride for photographic film by the reaction



is far more expensive than the sodium chloride (ordinary salt). Thus, it makes sense to perform the reaction with an excess of sodium chloride to ensure that as much of the silver nitrate as possible reacts to form products.

There is a systematic method to find the limiting reactant and determine the maximum possible amounts of products. Take each reactant in turn, assume that it is used up completely in the reaction, and calculate the mass of one of the products that will be formed. Whichever reactant gives the *smallest* mass of this product is the limiting reactant. Once it has reacted fully, no further product can be formed.

EXAMPLE 2.7

Sulfuric acid (H_2SO_4) forms in the chemical reaction



Suppose 400 g SO_2 , 175 g O_2 , and 125 g H_2O are mixed and the reaction proceeds until one of the reactants is used up. Which is the limiting reactant? What mass of H_2SO_4 is produced, and what masses of the other reactants remain?

SOLUTION

The number of moles of each reactant originally present is calculated by dividing each mass by the corresponding molar mass:

$$\frac{400 \text{ g SO}_2}{64.06 \text{ g mol}^{-1}} = 6.24 \text{ mol SO}_2$$

$$\frac{175 \text{ g O}_2}{32.00 \text{ g mol}^{-1}} = 5.47 \text{ mol O}_2$$

$$\frac{125 \text{ g H}_2\text{O}}{18.02 \text{ g mol}^{-1}} = 6.94 \text{ mol H}_2\text{O}$$

If all the SO_2 reacted, it would give

$$6.24 \text{ mol SO}_2 \times \left(\frac{2 \text{ mol H}_2\text{SO}_4}{2 \text{ mol SO}_2} \right) = 6.24 \text{ mol H}_2\text{SO}_4$$

If all the O_2 reacted, it would give

$$5.47 \text{ mol O}_2 \times \left(\frac{2 \text{ mol H}_2\text{SO}_4}{1 \text{ mol O}_2} \right) = 10.94 \text{ mol H}_2\text{SO}_4$$

Finally, if all the water reacted, it would give

$$6.94 \text{ mol H}_2\text{O} \times \left(\frac{2 \text{ mol H}_2\text{SO}_4}{2 \text{ mol H}_2\text{O}} \right) = 6.94 \text{ mol H}_2\text{SO}_4$$

In this case, SO_2 is the limiting reactant because the computation based on its amount produces the smallest amount of product (6.24 mol H_2SO_4). Oxygen and water are present in excess. After reaction, the amount of each reactant that remains is the original amount minus the amount reacted:

$$\begin{aligned} \text{mol O}_2 &= 5.47 \text{ mol O}_2 - \left(6.24 \text{ mol SO}_2 \times \frac{1 \text{ mol O}_2}{2 \text{ mol SO}_2} \right) \\ &= 5.47 - 3.12 \text{ mol O}_2 = 2.35 \text{ mol O}_2 \end{aligned}$$

$$\begin{aligned} \text{mol H}_2\text{O} &= 6.94 \text{ mol H}_2\text{O} - \left(6.24 \text{ mol SO}_2 \times \frac{2 \text{ mol H}_2\text{O}}{2 \text{ mol SO}_2} \right) \\ &= 6.94 - 6.24 \text{ mol H}_2\text{O} = 0.70 \text{ mol H}_2\text{O} \end{aligned}$$

The masses of reactants and products after the reaction are

$$\text{Mass H}_2\text{SO}_4 \text{ produced} = (6.24 \text{ mol})(98.07 \text{ g mol}^{-1}) = 612 \text{ g}$$

$$\text{Mass O}_2 \text{ remaining} = (2.35 \text{ mol})(32.00 \text{ g mol}^{-1}) = 75 \text{ g}$$

$$\text{Mass H}_2\text{O remaining} = (0.70 \text{ mol})(18.02 \text{ g mol}^{-1}) = 13 \text{ g}$$

The total mass at the end is $612 \text{ g} + 13 \text{ g} + 75 \text{ g} = 700 \text{ g}$, which is, of course, equal to the total mass originally present, $400 \text{ g} + 175 \text{ g} + 125 \text{ g} = 700 \text{ g}$, as required by the law of conservation of mass.

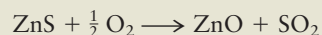
Related Problems: 47, 48

Percentage Yield

The amounts of products calculated so far have been **theoretical yields**, determined by assuming that the reaction goes cleanly and completely. The **actual yield** of a product (that is, the amount present after separating it from other products and reactants and purifying it) is less than the theoretical yield. There are several possible reasons for this. The reaction may stop short of completion, so reactants remain unreacted. There may be competing reactions that give other products, and therefore reduce the yield of the desired one. Finally, in the process of separation and purification, some of the product is invariably lost, although that amount can be reduced by careful experimental techniques. The ratio of the actual yield to the theoretical yield (multiplied by 100%) gives the **percentage yield** for that product in the reaction.

EXAMPLE 2.8

The sulfide ore of zinc (ZnS) is reduced to elemental zinc by “roasting” it (heating it in air) to give ZnO, and then heating the ZnO with carbon monoxide. The two reactions can be written as



Suppose 5.32 kg ZnS is treated in this way and 3.30 kg pure Zn is obtained. Calculate the theoretical yield of zinc and its actual percentage yield.

SOLUTION

From the molar mass of ZnS (97.46 g mol^{-1}), the number of moles of ZnS initially present is

$$\frac{5320 \text{ g ZnS}}{97.46 \text{ g mol}^{-1}} = 54.6 \text{ mol ZnS}$$

Because each mole of ZnS gives 1 mol of ZnO in the first chemical equation, and each mole of ZnO then gives 1 mol of Zn, the theoretical yield of zinc is 54.6 mol. In grams, this is

$$54.6 \text{ mol Zn} \times 65.39 \text{ g mol}^{-1} = 3570 \text{ g Zn}$$

The ratio of actual yield to theoretical yield, multiplied by 100%, gives the percentage yield of zinc:

$$\% \text{ yield} = \left(\frac{3.30 \text{ kg}}{3.57 \text{ kg}} \right) \times 100\% = 92.4\%$$

Related Problems: 49, 50

It is clearly desirable to achieve the highest percentage yield of product possible to reduce the consumption of raw materials. In some synthetic reactions (especially in organic chemistry), the final product is the result of many successive reactions. In such processes, the yields in the individual steps must be quite high if the synthetic method is to be a practical success. Suppose, for example, that ten consecutive reactions must be performed to reach the product, and that each has a percentage yield of only 50% (a fractional yield of 0.5). The overall yield is the product of the fractional yields of the steps:

$$(0.5) \times (0.5) \times \dots \times (0.5) = (0.5)^{10} = 0.001$$

10 terms

This overall percentage yield of 0.1% makes the process useless for synthetic purposes. If all the individual percentage yields could be increased to 90%, however, the overall yield would then be $(0.9)^{10} = 0.35$, or 35%. This is a much more reasonable result, and one that might make the process worth considering.

CHAPTER SUMMARY

We have shown you how chemists count molecules by weighing macroscopic quantities of substances. Avogadro's number connects the nanoscopic world of atoms and molecules to the macroscopic scale of the laboratory—1 mol = 6.02×10^{23} atoms or molecules. The relative number of atoms in a molecule or solid is given by its empirical or its molecular formula, and we have shown how these formulas are determined experimentally. The principle of conservation of mass has been sharpened a bit in our discussion of balancing chemical reactions. Not only is the total mass conserved in ordinary (as opposed to nuclear) chemical reactions but the total number of atoms of every element also is conserved. Balancing a chemical reaction requires nothing more than assuring that the same numbers of atoms (or moles of atoms) of each element appear on each side of the balanced equation. Because chemists weigh macroscopic quantities of reactants and products, it is important to understand how mass ratios relate to mole ratios in chemical reactions. Finally, we point out that not every reactant is completely consumed in a chemical reaction, and that the limiting reactant determines the maximum theoretical yield; the actual percentage yield may be somewhat less.

CUMULATIVE EXERCISE

Titanium

Metallic titanium and its alloys (especially those with aluminum and vanadium) combine the advantages of high strength and light weight and are therefore used widely in the aerospace industry for the bodies and engines of airplanes. The major natural source for titanium is the ore rutile, which contains titanium dioxide (TiO_2).

- (a) An intermediate in the preparation of elemental titanium from TiO_2 is a volatile chloride of titanium (boiling point 136°C) that contains 25.24% titanium by mass. Determine the empirical formula of this compound.
- (b) At 136°C and atmospheric pressure, the density of this gaseous chloride is 5.6 g L^{-1} . Under the same conditions, the density of gaseous nitrogen (N_2 , molar mass 28.0 g mol^{-1}) is 0.83 g L^{-1} . Determine the molecular formula of this compound.



© Wolfgang Kumm/dpa/CORBIS

A jet engine fan blade made of a single crystal titanium alloy.

- (c) The titanium chloride dealt with in parts (a) and (b) is produced by the reaction of chlorine with a hot mixture of titanium dioxide and coke (carbon), with carbon dioxide generated as a by-product. Write a balanced chemical equation for this reaction.
- (d) What mass of chlorine is needed to produce 79.2 g of the titanium chloride?
- (e) The titanium chloride then reacts with liquid magnesium at 900°C to give titanium and magnesium chloride (MgCl₂). Write a balanced chemical equation for this step in the refining of titanium.
- (f) Suppose the reaction chamber for part (e) contains 351 g of the titanium chloride and 63.2 g liquid magnesium. Which is the limiting reactant? What maximum mass of titanium could result?
- (g) Isotopic analysis of the titanium from a particular ore gave the following results:

Isotope	Relative Mass	Abundance (%)
⁴⁶ Ti	45.952633	7.93
⁴⁷ Ti	46.95176	7.28
⁴⁸ Ti	47.947948	73.94
⁴⁹ Ti	48.947867	5.51
⁵⁰ Ti	49.944789	5.34

Calculate the mass of a single ⁴⁸Ti atom and the *average* mass of the titanium atoms in this ore sample.

Answers

- (a) TiCl₄
- (b) TiCl₄
- (c) $\text{TiO}_2 + \text{C} + 2 \text{Cl}_2 \longrightarrow \text{TiCl}_4 + \text{CO}_2$
- (d) 59.2 g
- (e) $\text{TiCl}_4 + 2 \text{Mg} \longrightarrow \text{Ti} + 2 \text{MgCl}_2$
- (f) Mg; 62.3 g
- (g) 7.961949×10^{-23} g; 7.950×10^{-23} g

CHAPTER REVIEW

- A mole is Avogadro's number of anything: $N_A = 6.022 \times 10^{23}$. It allows us to count molecules by weighing. N_A is the number of molecules in exactly 12 g ¹²C, by international agreement.
- The molar mass is the mass of one mole of a substance.
- Mass, moles, and the number of molecules are related as follows:

$$\text{mass} \xleftrightarrow{\text{molar mass}} \text{moles} \xleftrightarrow{N_A} \text{number of molecules}$$

- The density of a substance is its mass divided by its volume; in chemistry, the units are generally grams per cubic centimeter (g cm⁻³). The density of gases is typically 10⁻³ g cm⁻³, whereas that of liquids and solids is generally in the range 1 to 20 g cm⁻³.
- The molar volume, V_m , is the volume occupied by one mole of a substance; it is typically about a few tens of cubic centimeters for liquids and solids and about 25 L mol⁻¹ for gases at room temperature and atmospheric pressure.

- The empirical formula for a substance is the simplest ratio of the number of atoms or moles of each element. The molecular formula gives the exact number of each atom or moles of atoms in a molecule, whereas the formula unit is the empirical formula for a solid for which no discrete molecules exist.
- Chemical equations are balanced by inspection, ensuring that the same number of atoms of each element appears on both sides of the equation.
- The limiting reagent is the one that is completely consumed first; it determines the degree to which the reaction goes to completion.
- The percentage yield determined by the limiting reagent is the theoretical yield; other losses may occur, resulting in a lower actual yield.

CONCEPTS & SKILLS

After studying this chapter and working the problems that follow, you should be able to:

1. Interconvert mass, number of moles, number of molecules, and (using density) the molar volume of a substance (Section 2.1, Problems 1–12).
2. Given the percentages by mass of the elements in a compound, determine its empirical formula and vice versa (Section 2.3, Problems 13–24).
3. Use ratios of gas densities to estimate molecular mass and determine molecular formulas (Section 2.3, Problems 27–30).
4. Balance simple chemical equations (Section 2.4, Problems 31 and 32).
5. Given the mass of a reactant or product in a chemical reaction, use a balanced chemical equation to calculate the masses of other reactants consumed and other products formed (Section 2.4, Problems 33–46).
6. Given a set of initial masses of reactants and a balanced chemical equation, determine the limiting reactant and calculate the masses of reactants and products after the reaction has gone to completion (Section 2.6, Problems 47 and 48).
7. Determine the percentage yield of a reaction from its calculated theoretical yield and its measured actual yield (Section 2.6, Problems 49 and 50).

PROBLEMS

Answers to problems whose numbers are boldface appear in Appendix G. Problems that are more challenging are indicated with asterisks.

The Mole: Weighing and Counting Molecules

1. Compute the mass (in grams) of a single iodine atom if the relative atomic mass of iodine is 126.90447 on the accepted scale of atomic masses (based on 12 as the relative atomic mass of ^{12}C).
2. Determine the mass (in grams) of exactly 100 million atoms of fluorine if the relative atomic mass of fluorine is 18.998403 on a scale on which exactly 12 is the relative atomic mass of ^{12}C .
3. Compute the relative molecular masses of the following compounds on the ^{12}C scale:

(a) P_4O_{10}	(b) BrCl
(c) $\text{Ca}(\text{NO}_3)_2$	(d) KMnO_4
(e) $(\text{NH}_4)_2\text{SO}_4$	
4. Compute the relative molecular masses of the following compounds on the ^{12}C scale:

(a) $[\text{Ag}(\text{NH}_3)_2]\text{Cl}$	(b) $\text{Ca}_3[\text{Co}(\text{CO}_3)_3]_2$
(c) OsO_4	(d) H_2SO_4
(e) $\text{Ca}_3\text{Al}_2(\text{SiO}_4)_3$	
5. Suppose that a person counts out gold atoms at the rate of one each second for the entire span of an 80-year life. Has the person counted enough atoms to be detected with an ordinary balance? Explain.

- A gold atom has a diameter of 2.88×10^{-10} m. Suppose the atoms in 1.00 mol of gold atoms are arranged just touching their neighbors in a single straight line. Determine the length of the line.
- The vitamin A molecule has the formula $C_{20}H_{30}O$, and a molecule of vitamin A_2 has the formula $C_{20}H_{28}O$. Determine how many moles of vitamin A_2 contain the same number of atoms as 1.000 mol vitamin A.
- Arrange the following in order of increasing mass: 1.06 mol SF_4 ; 117 g CH_4 ; 8.7×10^{23} molecules of Cl_2O_7 ; and 417×10^{23} atoms of argon (Ar).
- Mercury is traded by the “flask,” a unit that has a mass of 34.5 kg. Determine the volume of a flask of mercury if the density of mercury is 13.6 g cm^{-3} .
- Gold costs \$400 per troy ounce, and 1 troy ounce = 31.1035 g. Determine the cost of 10.0 cm^3 gold if the density of gold is 19.32 g cm^{-3} at room conditions.
- Aluminum oxide (Al_2O_3) occurs in nature as a mineral called corundum, which is noted for its hardness and resistance to attack by acids. Its density is 3.97 g cm^{-3} . Calculate the number of atoms of aluminum in 15.0 cm^3 corundum.
- Calculate the number of atoms of silicon (Si) in 415 cm^3 of the colorless gas disilane at 0°C and atmospheric pressure, where its density is $0.00278 \text{ g cm}^{-3}$. The molecular formula of disilane is Si_2H_6 .
- Bromoform is 94.85% bromine, 0.40% hydrogen, and 4.75% carbon by mass. Determine its empirical formula.
- Fulgurites are the products of the melting that occurs when lightning strikes the earth. Microscopic examination of a sand fulgurite shows that it is a globule with variable composition that contains some grains of the definite chemical composition Fe 46.01%, Si 53.99%. Determine the empirical formula of these grains.
- A sample of a “suboxide” of cesium gives up 1.6907% of its mass as gaseous oxygen when gently heated, leaving pure cesium behind. Determine the empirical formula of this binary compound.
- Barium and nitrogen form two binary compounds containing 90.745% and 93.634% barium, respectively. Determine the empirical formulas of these two compounds.
- Carbon and oxygen form no fewer than five different binary compounds. The mass percentages of carbon in the five compounds are as follows: A, 27.29; B, 42.88; C, 50.02; D, 52.97; and E, 65.24. Determine the empirical formulas of the five compounds.
- A sample of 1.000 g of a compound containing carbon and hydrogen reacts with oxygen at elevated temperature to yield 0.692 g H_2O and 3.381 g CO_2 .
 - Calculate the masses of C and H in the sample.
 - Does the compound contain any other elements?
 - What are the mass percentages of C and H in the compound?
 - What is the empirical formula of the compound?

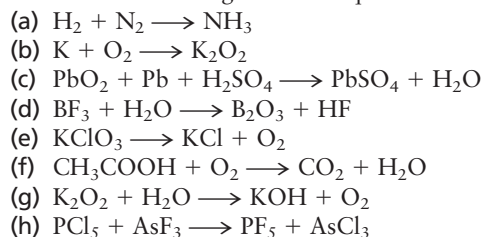
Chemical Formula and Percentage Composition

- A newly synthesized compound has the molecular formula $ClF_2O_2PtF_6$. Compute, to four significant figures, the mass percentage of each of the four elements in this compound.
- Acetaminophen is the generic name of the pain reliever in Tylenol and some other headache remedies. The compound has the molecular formula $C_8H_9NO_2$. Compute, to four significant figures, the mass percentage of each of the four elements in acetaminophen.
- Arrange the following compounds from left to right in order of increasing percentage by mass of hydrogen: H_2O , $C_{12}H_{26}$, N_4H_6 , LiH .
- Arrange the following compounds from left to right in order of increasing percentage by mass of fluorine: HF , C_6HF_5 , BrF , UF_6 .
- “Q-gas” is a mixture of 98.70% helium and 1.30% butane (C_4H_{10}) by mass. It is used as a filling for gas-flow Geiger counters. Compute the mass percentage of hydrogen in Q-gas.
- A pharmacist prepares an antiulcer medicine by mixing 286 g Na_2CO_3 with water, adding 150 g glycine ($C_2H_5NO_2$), and stirring continuously at 40°C until a firm mass results. The pharmacist heats the mass gently until all the water has been driven away. No other chemical changes occur in this step. Compute the mass percentage of carbon in the resulting white crystalline medicine.
- Zinc phosphate is used as a dental cement. A 50.00-mg sample is broken down into its constituent elements and gives 16.58 mg oxygen, 8.02 mg phosphorus, and 25.40 mg zinc. Determine the empirical formula of zinc phosphate.
- Burning a compound of calcium, carbon, and nitrogen in oxygen in a combustion train generates calcium oxide (CaO), carbon dioxide (CO_2), nitrogen dioxide (NO_2), and no other substances. A small sample gives 2.389 g CaO , 1.876 g CO_2 , and 3.921 g NO_2 . Determine the empirical formula of the compound.
- The empirical formula of a gaseous fluorocarbon is CF_2 . At a certain temperature and pressure, a 1-L volume holds 8.93 g of this fluorocarbon, whereas under the same conditions, the 1-L volume holds only 1.70 g gaseous fluorine (F_2). Determine the molecular formula of this compound.
- At its boiling point (280°C) and at atmospheric pressure, phosphorus has a gas density of 2.7 g L^{-1} . Under the same conditions, nitrogen has a gas density of 0.62 g L^{-1} . How many atoms of phosphorus are there in one phosphorus molecule under these conditions?
- A gaseous binary compound has a vapor density that is 1.94 times that of oxygen at the same temperature and pressure. When 1.39 g of the gas is burned in an excess of oxygen, 1.21 g water is formed, removing all the hydrogen originally present.
 - Estimate the molecular mass of the gaseous compound.
 - How many hydrogen atoms are there in a molecule of the compound?
 - What is the maximum possible value of the atomic mass of the second element in the compound?
 - Are other values possible for the atomic mass of the second element? Use a table of atomic masses to identify the element that best fits the data.
 - What is the molecular formula of the compound?

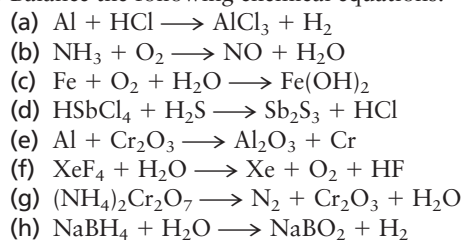
30. A gaseous binary compound has a vapor density that is 2.53 times that of nitrogen at 100°C and atmospheric pressure. When 8.21 g of the gas reacts with AlCl₃ at 100°C, 1.62 g gaseous nitrogen is produced, removing all of the nitrogen originally present.
- Estimate the molecular mass of the gaseous compound.
 - How many nitrogen atoms are there in a molecule of the compound?
 - What is the maximum possible value of the atomic mass of the second element?
 - Are other values possible for the atomic mass of the second element? Use a table of atomic masses to identify the element that best fits the data.
 - What is the molecular formula of the compound?

Writing Balanced Chemical Equations

31. Balance the following chemical equations:

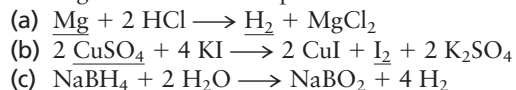


32. Balance the following chemical equations:

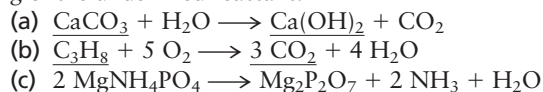


Mass Relationships in Chemical Reactions

33. For each of the following chemical reactions, calculate the mass of the underlined reactant that is required to produce 1.000 g of the underlined product.



34. For each of the following chemical reactions, calculate the mass of the underlined product that is produced from 1.000 g of the underlined reactant.



35. An 18.6-g sample of K₂CO₃ was treated in such a way that all of its carbon was captured in the compound K₂Zn₃[Fe(CN)₆]₂. Compute the mass (in grams) of this product.

36. A chemist dissolves 1.406 g pure platinum (Pt) in an excess of a mixture of hydrochloric and nitric acids and then, after a series of subsequent steps involving several other chemicals, isolates a compound of molecular formula Pt₂C₁₀H₁₈N₂S₂O₆. Determine the maximum possible yield of this compound.

37. Disilane (Si₂H₆) is a gas that reacts with oxygen to give silica (SiO₂) and water. Calculate the mass of silica that would form if 25.0 cm³ disilane (with a density of 2.78 × 10⁻³ g cm⁻³) reacted with excess oxygen.

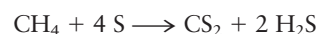
38. Tetrasilane (Si₄H₁₀) is a liquid with a density of 0.825 g cm⁻³. It reacts with oxygen to give silica (SiO₂) and water. Calculate the mass of silica that would form if 25.0 cm³ tetrasilane reacted completely with excess oxygen.

39. Cryolite (Na₃AlF₆) is used in the production of aluminum from its ores. It is made by the reaction



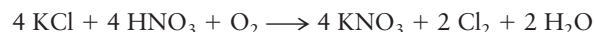
Calculate the mass of cryolite that can be prepared by the complete reaction of 287 g Al₂O₃.

40. Carbon disulfide (CS₂) is a liquid that is used in the production of rayon and cellophane. It is manufactured from methane and elemental sulfur via the reaction



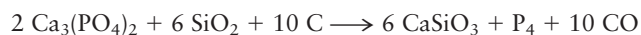
Calculate the mass of CS₂ that can be prepared by the complete reaction of 67.2 g sulfur.

41. Potassium nitrate (KNO₃) is used as a fertilizer for certain crops. It is produced through the reaction



Calculate the minimum mass of KCl required to produce 567 g KNO₃. What mass of Cl₂ will be generated as well?

42. Elemental phosphorus can be prepared from calcium phosphate via the overall reaction



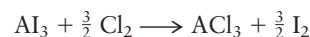
Calculate the minimum mass of Ca₃(PO₄)₂ required to produce 69.8 g P₄. What mass of CaSiO₃ is generated as a by-product?

43. An element X has a dibromide with the empirical formula XBr₂ and a dichloride with the empirical formula XCl₂. The dibromide is completely converted to the dichloride when it is heated in a stream of chlorine according to the reaction



When 1.500 g XBr₂ is treated, 0.890 g XCl₂ results.

- Calculate the atomic mass of the element X.
 - By reference to a list of the atomic masses of the elements, identify the element X.
- * 44. An element A has a triiodide with the formula AI₃ and a trichloride with the formula ACl₃. The triiodide is quantitatively converted to the trichloride when it is heated in a stream of chlorine, according to the reaction

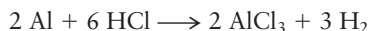


If 0.8000 g AI₃ is treated, 0.3776 g ACl₃ is obtained.

- Calculate the atomic mass of the element A.
 - Identify the element A.
- * 45. A mixture consisting of only sodium chloride (NaCl) and potassium chloride (KCl) weighs 1.0000 g. When the mixture is dissolved in water and an excess of silver nitrate is added, all the chloride ions associated with the original

mixture are precipitated as insoluble silver chloride (AgCl). The mass of the silver chloride is found to be 2.1476 g. Calculate the mass percentages of sodium chloride and potassium chloride in the original mixture.

- * 46. A mixture of aluminum and iron weighing 9.62 g reacts with hydrogen chloride in aqueous solution according to the parallel reactions



A 0.738-g quantity of hydrogen is evolved when the metals react completely. Calculate the mass of iron in the original mixture.

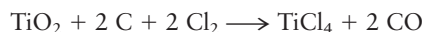
Limiting Reactant and Percentage Yield

47. When ammonia is mixed with hydrogen chloride (HCl), the white solid ammonium chloride (NH_4Cl) is produced. Suppose 10.0 g ammonia is mixed with the same mass of hydrogen chloride. What substances will be present after the reaction has gone to completion, and what will their masses be?
48. The poisonous gas hydrogen cyanide (HCN) is produced by the high-temperature reaction of ammonia with methane (CH_4). Hydrogen is also produced in this reaction.
- Write a balanced chemical equation for the reaction that occurs.
 - Suppose 500.0 g methane is mixed with 200.0 g ammonia. Calculate the masses of the substances present after the reaction is allowed to proceed to completion.
49. The iron oxide Fe_2O_3 reacts with carbon monoxide (CO) to give iron and carbon dioxide:



The reaction of 433.2 g Fe_2O_3 with excess CO yields 254.3 g iron. Calculate the theoretical yield of iron (assuming complete reaction) and its percentage yield.

50. Titanium dioxide, TiO_2 , reacts with carbon and chlorine to give gaseous TiCl_4 :

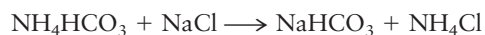
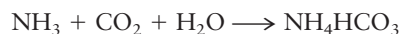


The reaction of 7.39 kg titanium dioxide with excess C and Cl_2 gives 14.24 kg titanium tetrachloride. Calculate the theoretical yield of TiCl_4 (assuming complete reaction) and its percentage yield.

ADDITIONAL PROBLEMS

51. Human parathormone has the impressive molecular formula $\text{C}_{691}\text{H}_{898}\text{N}_{125}\text{O}_{164}\text{S}_{11}$. Compute the mass percentages of all the elements in this compound.
52. A white oxide of tungsten is 79.2976% tungsten by mass. A blue tungsten oxide also contains exclusively tungsten and oxygen, but it is 80.8473% tungsten by mass. Determine the empirical formulas of white tungsten oxide and blue tungsten oxide.
53. A dark brown binary compound contains oxygen and a metal. It is 13.38% oxygen by mass. Heating it moderately drives off some of the oxygen and gives a red binary compound that is 9.334% oxygen by mass. Strong heating drives off more oxygen and gives still another binary compound, which is only 7.168% oxygen by mass.
- Compute the mass of oxygen that is combined with 1.000 g of the metal in each of these three oxides.
 - Assume that the empirical formula of the first compound is MO_2 (where M represents the metal). Give the empirical formulas of the second and third compounds.
 - Name the metal.
54. A binary compound of nickel and oxygen contains 78.06% nickel by mass. Is this a stoichiometric or a nonstoichiometric compound? Explain.
55. Two binary oxides of the element manganese contain, respectively, 30.40% and 36.81% oxygen by mass. Calculate the empirical formulas of the two oxides.
- * 56. A sample of a gaseous binary compound of boron and chlorine weighing 2.842 g occupies 0.153 L. This sample is decomposed to give 0.664 g solid boron and enough gaseous chlorine (Cl_2) to occupy 0.688 L at the same temperature and pressure. Determine the molecular formula of the compound.
57. A possible practical way to eliminate oxides of nitrogen (such as NO_2) from automobile exhaust gases uses cyanuric acid, $\text{C}_3\text{N}_3(\text{OH})_3$. When heated to the relatively low temperature of 625°F, cyanuric acid converts to gaseous isocyanic acid (HNCO). Isocyanic acid reacts with NO_2 in the exhaust to form nitrogen, carbon dioxide, and water, all of which are normal constituents of the air.
- Write balanced equations for these two reactions.
 - If the process described earlier became practical, how much cyanuric acid (in kilograms) would be required to absorb the 1.7×10^{10} kg NO_2 generated annually in auto exhaust in the United States?
58. Aspartame (molecular formula $\text{C}_{14}\text{H}_{18}\text{N}_2\text{O}_5$) is a sugar substitute in soft drinks. Under certain conditions, 1 mol of aspartame reacts with 2 mol of water to give 1 mol of aspartic acid (molecular formula $\text{C}_4\text{H}_7\text{NO}_4$), 1 mol of methanol (molecular formula CH_3OH), and 1 mol of phenylalanine. Determine the molecular formula of phenylalanine.
59. 3'-Methylphthalanilic acid is used commercially as a "fruit set" to prevent premature drop of apples, pears, cherries, and peaches from the tree. It is 70.58% carbon, 5.13% hydrogen, 5.49% nitrogen, and 18.80% oxygen. If eaten, the fruit set reacts with water in the body to produce an innocuous product, which contains carbon, hydrogen, and oxygen only, and *m*-toluidine ($\text{NH}_2\text{C}_6\text{H}_4\text{CH}_3$), which causes anemia and kidney damage. Compute the mass of the fruit set that would produce 5.23 g *m*-toluidine.
60. Aluminum carbide (Al_4C_3) reacts with water to produce gaseous methane (CH_4). Calculate the mass of methane formed from 63.2 g Al_4C_3 .
61. Citric acid ($\text{C}_6\text{H}_8\text{O}_7$) is made by fermentation of sugars such as sucrose ($\text{C}_{12}\text{H}_{22}\text{O}_{11}$) in air. Oxygen is consumed and water generated as a by-product.
- Write a balanced equation for the overall reaction that occurs in the manufacture of citric acid from sucrose.
 - What mass of citric acid is made from 15.0 kg sucrose?

62. A sample that contains only SrCO_3 and BaCO_3 weighs 0.800 g. When it is dissolved in excess acid, 0.211 g carbon dioxide is liberated. What percentage of SrCO_3 did the sample contain? Assume all the carbon originally present is converted to carbon dioxide.
63. A sample of a substance with the empirical formula XBr_2 weighs 0.5000 g. When it is dissolved in water and all its bromine is converted to insoluble AgBr by addition of an excess of silver nitrate, the mass of the resulting AgBr is found to be 1.0198 g. The chemical reaction is
- $$\text{XBr}_2 + 2 \text{AgNO}_3 \longrightarrow 2 \text{AgBr} + \text{X}(\text{NO}_3)_2$$
- (a) Calculate the molecular mass (that is, formula mass) of XBr_2 .
- (b) Calculate the atomic mass of X and give its name and symbol.
64. A newspaper article about the danger of global warming from the accumulation of greenhouse gases such as carbon dioxide states that “reducing driving your car by 20 miles a week would prevent release of over 1000 pounds of CO_2 per year into the atmosphere.” Is this a reasonable statement? Assume that gasoline is octane (molecular formula C_8H_{18}) and that it is burned completely to CO_2 and H_2O in the engine of your car. Facts (or reasonable guesses) about your car’s gas mileage, the density of octane, and other factors will also be needed.
65. In the Solvay process for producing sodium carbonate (Na_2CO_3), the following reactions occur in sequence:



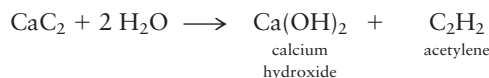
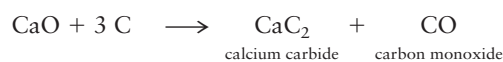
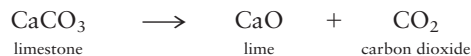
How many metric tons of sodium carbonate would be produced per metric ton of NH_3 if the process were 100% efficient (1 metric ton = 1000 kg)?

66. A yield of 3.00 g KClO_4 is obtained from the (unbalanced) reaction



when 4.00 g of the reactant is used. What is the percentage yield of the reaction?

67. An industrial-scale process for making acetylene consists of the following sequence of operations:

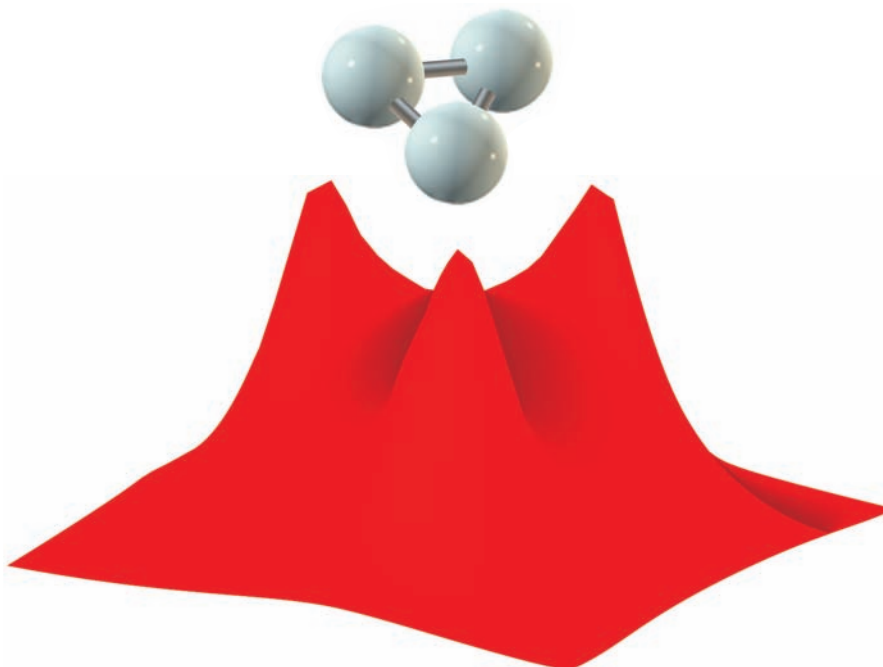


What is the percentage yield of the overall process if 2.32 metric tons C_2H_2 is produced from 10.0 metric tons limestone (1 metric ton = 1000 kg)?

68. Silicon nitride (Si_3N_4), a valuable ceramic, is made by the direct combination of silicon and nitrogen at high temperature. How much silicon must react with excess nitrogen to prepare 125 g silicon nitride if the yield of the reaction is 95.0%?

This page intentionally left blank

Chemical Bonding and Molecular Structure



The electron density in a delocalized three-center bond for H_3^+ calculated by quantum mechanics.

Courtesy of Dr. Richard P. Muller and Professor William A. Goddard III, California Institute of Technology.

How do atoms bond together to form molecules, three-dimensional objects with unique structures? Rutherford's planetary model of atomic structure described in Section 1.4 (Z electrons moving around a dense nucleus of charge $+Ze$) suggests that the chemical bond involves the gain, loss, or sharing of electrons by atoms. This idea leads to the classical description of bonding, used daily by chemists worldwide. This classical description is neither quantitative nor complete. The existence of the chemical bond was fully explained only when a new theory called quantum mechanics replaced Newtonian mechanics for describing the nanoscopic world of molecules, atoms, and fundamental particles. Quantum mechanics explains the chemical bond as the distribution of electron density around the nuclei for which the energy of the molecule is lower than the energy of the separated atoms.

UNIT CHAPTERS

CHAPTER 3

Chemical Bonding: The Classical Description

CHAPTER 4

Introduction to Quantum Mechanics

CHAPTER 5

Quantum Mechanics and Atomic Structure

CHAPTER 6

Quantum Mechanics and Molecular Structure

CHAPTER 7

Bonding in Organic Molecules

CHAPTER 8

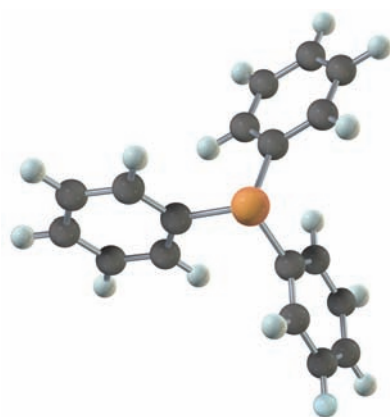
Bonding in Transition Metals
and Coordination Complexes

UNIT GOALS

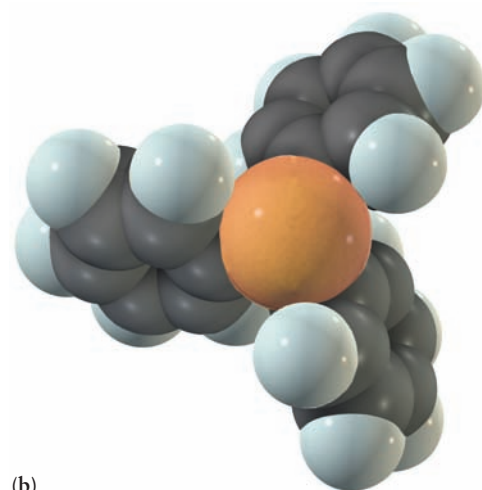
- To introduce the classical description of chemical bonding as a tool for describing and understanding the structures and shapes of molecules
- To convey the basic concepts and methods of quantum mechanics that describe the discrete energy levels and the statistical behavior of microscopic systems
- To develop an intuition for the behavior of quantum systems and an appreciation for the magnitudes of the relevant physical quantities
- To use quantum mechanics to:
 - Describe the allowed energies and electron densities in atoms
 - Explain the structure of the periodic table and periodic trends in the properties of atoms
 - Describe covalent bond formation and the structures of diatomic and small polyatomic molecules
 - Describe covalent bond formation and the structures of organic molecules
 - Describe bonding in more complex structures that include transition metal complexes

Chemical Bonding: The Classical Description

- 3.1 The Periodic Table
- 3.2 Forces and Potential Energy in Atoms
- 3.3 Ionization Energies and the Shell Model of the Atom
- 3.4 Electronegativity: The Tendency of Atoms to Attract Electrons
- 3.5 Forces and Potential Energy in Molecules: Formation of Chemical Bonds
- 3.6 Ionic Bonding
- 3.7 Covalent and Polar Covalent Bonding
- 3.8 Lewis Diagrams for Molecules
- 3.9 The Shapes of Molecules: Valence Shell Electron-Pair Repulsion Theory
- 3.10 Oxidation Numbers
- 3.11 Inorganic Nomenclature



(a)



(b)

(a) The shape of the molecule triphenyl-phosphine, $(C_6H_5)_3P$, is determined by locating the valence shell electron pairs in those positions that minimize the overall energy of the molecule. (b) The space-filling representation aids the analysis and understanding of the steric environment responsible for the specific molecular geometry observed.

The previous chapters showed how the laws of conservation of mass and conservation of atomic identity, together with the concept of the mole, determine quantitative mass relationships in chemical reactions. That discussion assumed prior knowledge of the chemical formulas of the reactants and products in each equation. The far more open-ended questions of which compounds are found in nature (or which can be made in the laboratory) and what types of reactions they undergo now arise. Why are some elements and compounds violently reactive and others inert? Why are there compounds with chemical formulas H_2O and $NaCl$, but never H_3O or $NaCl_2$? Why are helium and the other noble gases monatomic, but molecules of hydrogen and chlorine diatomic? All of these questions can be answered by examining the formation of chemical bonds between atoms.

When two atoms come sufficiently close together, the electrons of each atom experience the additional attractive force of the other nucleus, the electrons repel

each other, and the positively charged nuclei experience a mutually repulsive force. A stable chemical bond between two atoms in the gas phase is formed only when the total energy of the resulting molecule is lower than that of the two isolated atoms. A quantitative description of chemical bonding depends on the detailed arrangement of electrons in each atom and requires quantum mechanics for its explanation. **Quantum mechanics**—the fundamental branch of physics that describes the properties, interactions, and motions of atomic and subatomic particles—was established in 1926, and scientists immediately sought to explain chemical bond formation using its principles. More than 50 years of intense research were required to develop a comprehensive and useful quantum explanation of chemical bonding.

During that period, however, chemists developed a powerful suite of concepts and tools—covalent bonds, ionic bonds, polar covalent bonds, electronegativity, Lewis electron dot diagrams, and valence shell electron-pair repulsion (VSEPR) theory—that rationalized a great deal of information about the structure of molecules and patterns of chemical reactivity. This suite constitutes the *classical description of the chemical bond*, and it is part of the daily vocabulary of every working chemist, especially in organic and biological chemistry. These tools are the foundation of chemical intuition, by which we mean the ability to explain and even predict chemical phenomena. Intuition is judgment informed by experience. To guide the development of your own chemical intuition using these tools, we provide you with a comprehensive discussion of their conceptual basis and give you extensive practice in applying them to interpret factual information.

Today, all the tools of classical bonding theory have been explained by quantum mechanics. It is largely a matter of taste whether you first learn the classical theory and then gain deeper insight from the quantum explanations, or you first learn the quantum theory and then see the classical theory as a limiting case. We prefer to present the classical description first, and this chapter is devoted to that subject. That way, we establish the language and vocabulary of the chemical bond and allow you to become familiar with the properties of a broad array of real molecules *before* attempting to explain these results using quantum mechanics in Chapters 4, 5, and 6. Your instructor may prefer the opposite sequence, in which case you will read Chapters 4 and 5 before this chapter. This book was written to accommodate either approach.

The classical theory of chemical bonding and molecular shapes starts with conceptual models of the chemical bond. Much of structure and bonding can be understood on the basis of simple electrostatics. The distributions of electrons in atoms, molecules, and solids determine nearly all of their physical and chemical properties, with structure and reactivity being those of greatest interest to the chemist. Chemical bonds form by sharing or transferring electrons between atoms. The degree to which electrons are shared or transferred varies considerably in different chemical bonds, but chemists generally identify two extreme cases. In a **covalent** bond, the electrons are shared more or less equally between the two atoms comprising the bond. In an **ionic** bond, one or more electrons is essentially completely transferred from one atom to the other, and the dominant contribution to the strength of the bond is the electrostatic interaction between the resulting ions. Although many real chemical bonds are well described by these idealized models, most bonds are neither completely ionic nor completely covalent and are best described as having a mixture of ionic and covalent character. In **polar covalent** bonds, a partial transfer of charge from one atom to the other occurs. **Electronegativity**, the tendency of an atom in a molecule to draw electrons toward itself, explains whether a given pair of atoms form ionic, covalent, or polar covalent bonds.

Two simple tools, developed in the first half of the 20th century, are used to implement the classical theory of bonding and structure. The first tool is the

Lewis electron dot diagram, a schematic that shows the number of **valence** (outermost) electrons associated with each atom and whether they are bonding (shared) or nonbonding. These diagrams are useful in predicting connectivity—that is, which atoms are bonded to each other in polyatomic molecules. They do not, however, provide information about the three-dimensional shapes of molecules. The second tool, the **VSEPR theory**, is a simple, yet powerful, method to predict molecular shapes, based on the simple electrostatic argument that electron pairs in a molecule will arrange themselves to be as far apart as possible. These two physical tools allow for the organization of vast amounts of chemical information in a rational and systematic way.

We begin by describing the **periodic table**, a list of the elements arranged to display at a glance patterns of their physical properties and chemical reactivity. Relating bond formation to the positions of atoms in the periodic table reveals trends that build up chemical intuition. Next, we invoke Rutherford’s planetary model of the atom and show how electrical forces control the gain or loss of electrons by the atom. We then examine the electrical forces within molecules and show how they lead to the ionic and covalent models of the chemical bond. The use of Lewis diagrams to describe bond formation and the VSEPR theory to describe molecular shapes completes the classical theory of bonding. We conclude with a brief survey of the procedures for assigning proper names to chemical compounds.

We urge you to keep Rutherford’s planetary model of the atom (Section 1.4) in mind while reading this chapter. That model, with its consideration of the electrical forces within atoms and molecules, provides the foundation of the entire subject of chemical bonding and molecular structure.

3.1 The Periodic Table

The number of known chemical compounds is already huge and it continues to increase rapidly as the result of significant investments in chemical research. An unlimited number of chemical reactions is available among these compounds. The resultant body of chemical knowledge, viewed as a collection of facts, is overwhelming in its size, range, and complexity. It has been made manageable by the observation that the properties of the elements naturally display certain regularities. These regularities enable the classification of the elements into families whose members have similar chemical and physical properties. When the elements are arranged in order of increasing atomic number, Z , remarkable patterns emerge. Families of elements with similar chemical properties are easily identified by their locations in this arrangement. This discovery is summarized concisely by **the periodic law**:

The chemical properties of the elements are periodic functions of the atomic number Z .

Consequently, the elements listed in order of increasing Z can be arranged in a chart called the periodic table, which displays, at a glance, the patterns of chemical similarity. The periodic table then permits systematic classification, interpretation, and prediction of all chemical information.

The modern periodic table (Fig. 3.1 and the inside front cover of this book) places elements in **groups** (arranged vertically) and **periods** (arranged horizontally).

There are eight groups of **representative elements**, or “main-group” elements. In addition to the representative elements, there are ten groups (and three periods) of **transition-metal elements**, a period of elements with atomic numbers 57 through 71 called the rare-earth or **lanthanide elements**, and a period of elements from atomic numbers 89 through 103 called the **actinides**, all of which are unstable and

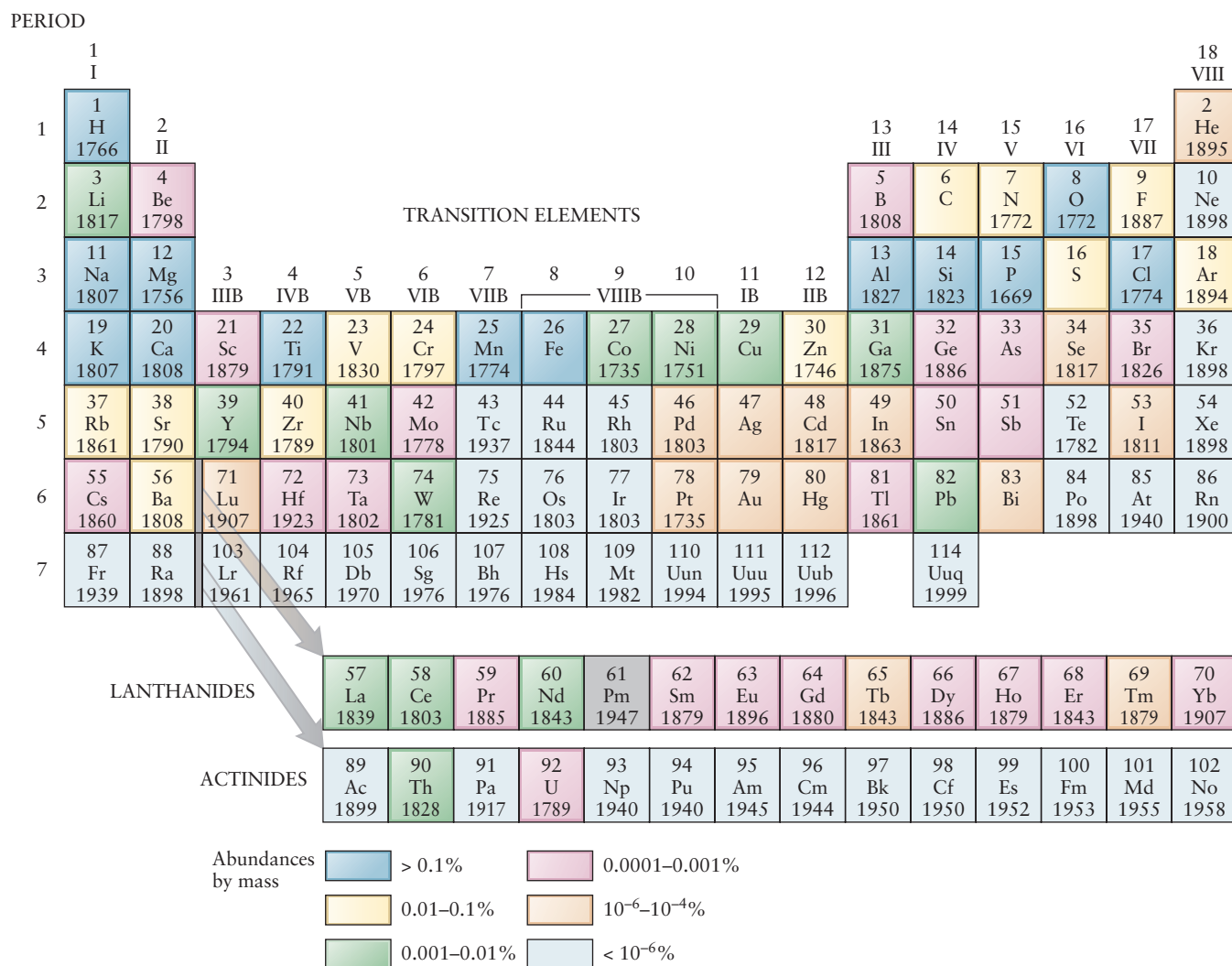


FIGURE 3.1 The modern periodic table of the elements. Below each symbol is the year in which that element was discovered; elements with no dates have been known since ancient times. Above each symbol is the atomic number. The color coding indicates the relative abundance by mass of the elements in the world (the atmosphere, oceans and fresh water bodies, and the Earth's crust to a depth of 40 km). Oxygen alone comprises almost 50% of the mass, and silicon comprises more than 25%.

most of which must be produced artificially. The lanthanide and actinide elements are usually placed below the rest of the table to conserve space. The groups of representative elements are numbered (using Roman numerals) from I to VIII, with the letter *A* sometimes added to differentiate them from the transition-metal groups, which are labeled from IB to VIIIB. This book uses group numbers exclusively for the representative elements (dropping the *A*) and refers to the transition-metal elements by the first element in the corresponding group. For example, the elements in the carbon group (C, Si, Ge, Sn, Pb) are designated as Group IV, and the elements chromium (Cr), molybdenum (Mo), and tungsten (W) as the chromium group.¹

¹Recently, several international organizations recommended a new system of group designation in which the main-group elements make up Groups 1, 2, and 13 through 18, and the transition-metal elements fill Groups 3 through 12.

Survey of Physical and Chemical Properties: The Representative Elements

Lothar Meyer and Dmitri Mendeleev independently and simultaneously organized the elements into tables based on their atomic weights. Meyer was more interested in the periodic variation in the physical properties of the elements, whereas Mendeleev was more interested in patterns of chemical reactivity. Therefore, most chemists consider Mendeleev to be responsible for the creation of the modern periodic table.

The elements have been classified empirically based on similarities in their physical or chemical properties. **Metals** and **nonmetals** are distinguished by the presence (or absence) of a characteristic metallic luster, good (or poor) ability to conduct electricity and heat, and malleability (or brittleness). Certain elements (boron, silicon, germanium, arsenic, antimony, and tellurium) resemble metals in some respects and nonmetals in others, and are therefore called **semimetals** or **metalloids**. Their ability to conduct electricity, for example, is much worse than metals, but is not essentially zero like the nonmetals.

The empirical formulas of the binary compounds formed by the elements with chlorine (their *chlorides*), with oxygen (their *oxides*), and with hydrogen (their *hydrides*) show distinct periodic trends.

Group I, the **alkali metals** (lithium, sodium, potassium, rubidium, and cesium), are all relatively soft metals with low melting points that form 1:1 compounds with chlorine, with chemical formulas such as NaCl and RbCl. The alkali metals react with water to liberate hydrogen; potassium, rubidium, and cesium liberate enough heat upon reaction to ignite the hydrogen. Group II, the **alkaline-earth metals** (beryllium, magnesium, calcium, strontium, barium, and radium), react in a 1:2 atomic ratio with chlorine, producing compounds such as MgCl₂ and CaCl₂.

Of the nonmetallic elements, Group VI, the **chalcogens** (oxygen, sulfur, selenium, and tellurium), forms 1:1 compounds with the alkaline-earth metals (such as CaO and BaS) but 2:1 compounds with the alkali metals (such as Li₂O and Na₂S). Members of Group VII, the **halogens** (fluorine, chlorine, bromine, and iodine), differ significantly in their physical properties (fluorine and chlorine are gases at room temperature, bromine is a liquid, and iodine a solid), but their chemical properties are similar. Any alkali metal will combine with any halogen in 1:1 proportion to form a compound such as LiF or RbI, which is called an **alkali halide**.

The remaining elements fall into three additional groups whose chemical and physical properties are somewhat less clearly delineated than those already discussed. Group III includes a semimetal (boron) and four metals (aluminum, gallium, indium, and thallium). All metals form 1:3 chlorides (such as GaCl₃) and 2:3 oxides (such as Al₂O₃). Group IV comprises the elements carbon, silicon, germanium, tin, and lead. All of these elements form 1:4 chlorides (such as SiCl₄), 1:4 hydrides (such as GeH₄), and 1:2 oxides (such as SnO₂). Tin and lead are metals with low melting points, and silicon and germanium are **semiconductors**. Although we classified silicon and germanium as semimetals earlier, their electrical properties can be finely tuned by incorporating small amounts of impurities. These two elements form the basis for the modern semiconductor industry, which manufactures computer chips and other solid-state devices. Several different allotropes of elemental carbon exist (for example, graphite, diamond, and the recently discovered fullerenes). **Allotropes** are modifications of an element with differing atomic arrangements that lead to different physical and chemical properties. For example, ozone (O₃) and ordinary diatomic oxygen (O₂) are also allotropes. Group V includes nitrogen, phosphorus, arsenic, antimony, and bismuth. These elements form binary compounds with hydrogen and oxygen that have empirical formulas such as PH₃ and N₂O₅. The hydrides become increasingly unstable as their molar masses increase, and BiH₃ is stable only below

-45°C . A similar trend exists for the oxides, and Bi_2O_5 has never been obtained in pure form. The lighter members of this group are clearly nonmetals (nitrogen and phosphorus), bismuth is clearly a metal, and arsenic and antimony are classified as semimetals.

Group VIII, the **noble gases** (helium, neon, argon, krypton, xenon, and radon), are sometimes called the **inert gases** because of their relative inertness toward chemical combination. They are all monatomic, in contrast with the other elements that exist as gases at room temperature and atmospheric pressure (hydrogen, oxygen, nitrogen, fluorine, chlorine), which are diatomic molecules.

Systematic trends in both the physical and chemical properties of the elements give important clues as to the structure of the atom. In addition to the properties that distinguish metals from nonmetals (electrical and thermal conductivity, malleability, luster, and ductility), there are a number of other physical properties that show clear periodic trends; these properties include melting and boiling points, densities, atomic sizes, and the energy changes that occur when an electron is added to or removed from a neutral atom. Numerical values for most of these properties are tabulated in Appendix F. In general, the elements on the left side of the table (especially in the later periods) are metallic solids and good conductors of electricity. On the right side (especially in earlier periods), they are poor electrical conductors of electricity and are generally gases at room temperature and atmospheric pressure. In between, the semimetals separate the metals from the nonmetals by a diagonal zigzag line (see the inside front cover of this book).

Patterns in chemical reactivity of the elements correlate with patterns in the physical structure of the atom; they are both periodic functions of Z . Reading across the periodic table (horizontally) shows that each main-group element (Groups I–VIII) in Period 3 has exactly 8 more electrons than the element immediately above it in Period 2. Similarly, each main-group element in Periods 4 and 5 has exactly 18 more electrons than the corresponding element in the period above. The sequence of numbers, 8, 8, 18, 18, and so forth, that organize the periodic table into groups (columns), whose elements have similar physical and chemical properties, arises from the quantum theory of atomic structure (see discussion in Chapter 5).

3.2 Forces and Potential Energy in Atoms

The atom arose in the domain of chemistry, its existence inferred indirectly from the laws of chemical combination. With the work of Thomson and Rutherford, the atom also became the province of physics, which sought to explain its structure and behavior as consequences of the electrical forces between the electrons and the nucleus. Modern chemistry combines these themes and uses the forces inside the atom to explain chemical behavior. The purpose of this section is to give you, a student of chemistry, a good appreciation for the nature of these forces, and the potential energy associated with them, in preparation for your studies of chemical bond formation. It is essential that you understand and learn to use potential energy diagrams for atoms. We suggest you review the background material on force, work, potential energy, potential energy diagrams, and electricity and magnetism in Appendix B2.

Rutherford's planetary model of the atom assumes that an atom of atomic number Z comprises a dense, central nucleus of positive charge $+Ze$ surrounded by a total of Z electrons moving around the nucleus. The attractive forces between each electron and the nucleus, and the repulsive forces between the electrons, are described by Coulomb's law. We first discuss Coulomb's law in general terms, and then apply it to the planetary atom.

According to Coulomb's law, the force of interaction between two charges, q_1 and q_2 , separated by a distance, r , is

$$F(r) = \frac{q_1 q_2}{4\pi\epsilon_0 r^2} \quad [3.1]$$

where ϵ_0 , called the *permittivity of the vacuum*, is a proportionality constant with a numerical value of $8.854 \times 10^{-12} \text{ C}^2 \text{ J}^{-1} \text{ m}^{-1}$.

In the International System of Units (SI), charge is expressed in coulombs (C), distance in meters (m), and force in newtons (N). In Equation 3.1 and related equations, the symbol q for each charge represents both the magnitude and the sign of the charge. The position of one of the particles is chosen as the origin of coordinates, and the displacement, r , runs outward to locate the second particle. Throughout physics, the sign convention for the direction of the force is chosen to be positive if the force is in the same direction as the displacement, and negative if the force is opposite to the displacement. If the particles have the same charge, their mutual repulsion pushes them apart in the same direction as r increases; thus, the repulsive force between them is assigned the positive sign. If they have opposite charges, their mutual attraction pulls them together in the direction *opposite* to the direction in which r increases. Thus, the attractive force between them is given the negative sign.

To determine how a particle responds to a force exerted on it, we normally solve Newton's second law, $F = ma$, to predict the new location of the particle after the force has been applied. Another approach, which is often easier, is to examine the *potential energy function* associated with the force. For example, if you compress a spring and hold it in position, you know it has the capability to push back on your hand as soon as you release it. The potential energy stored in the compressed spring measures how much force the spring can exert when it is released. We determine the amount of potential energy by measuring or calculating the amount of work done against the spring to compress it from its relaxed length to the particular length of interest.

The potential energy can be calculated from Coulomb's force law, and the result is

$$V(r) = \frac{q_1 q_2}{4\pi\epsilon_0 r} \quad [3.2]$$

for the potential energy of two charges, q_1 and q_2 , separated by a distance r . In SI units, energy is expressed in joules (J), charge in coulombs (C), and distance in meters (m), as noted earlier. By convention, $V(r) \rightarrow 0$ as $r \rightarrow \infty$. This is a logical choice for the zero of potential energy because there is no interaction between the particles at such large distances. It is also consistent with our definition that the change in potential energy is the work done on or by the two charges. The sign of the potential energy, like the force, depends on the signs of the charges. If the charges have the same sign, the potential energy, as expressed by Equation 3.2, is positive. This makes physical sense, because to increase the potential energy, we would have to push q_2 in from infinity against the repulsive force exerted by q_1 . Work done *against* the force is positive, so the results agree with our physical intuition. If the charges have opposite signs, the expression in Equation 3.2 is negative. Again, the results agree with our physical intuition. When we start with q_2 at infinity, we have to rush madly after it and hold it back as the attractive force tries to pull it right up to q_1 . This time, work is done *by* the force and is negative in sign.

Let's apply these insights to the planetary atom. Associated with each electron (of charge $-e$) and the nucleus (of charge $+Ze$) there is potential energy:

$$V(r) = -\frac{Ze^2}{4\pi\epsilon_0 r} \quad [3.3]$$

The minus sign indicates an attractive interaction; the potential energy becomes lower as the particles get closer together. We will see in Chapter 5 that the typical proton-electron distance in a hydrogen atom is about 10^{-10} m. This is an extremely small distance, and it appears throughout atomic and molecular physics. To avoid the inconvenience of always expressing powers of ten, this length has been given the special name angstrom ($1 \text{ \AA} = 10^{-10}$ m). The potential energy of the hydrogen atom when the proton and electron are separated by a distance of 1 \AA is

$$\begin{aligned} V(1 \text{ \AA}) &= -\frac{(1.602 \times 10^{-19} \text{ C})^2}{4\pi(8.854 \times 10^{-12} \text{ C}^2 \text{ J}^{-1} \text{ m}^{-1})(1 \times 10^{-10} \text{ m})} \\ &= -\frac{(8.988 \times 10^9)(1.602 \times 10^{-19})^2}{(1 \times 10^{-10})} \text{ J} \\ V(1 \text{ \AA}) &= -2.307 \times 10^{-18} \text{ J} \end{aligned} \quad [3.4]$$

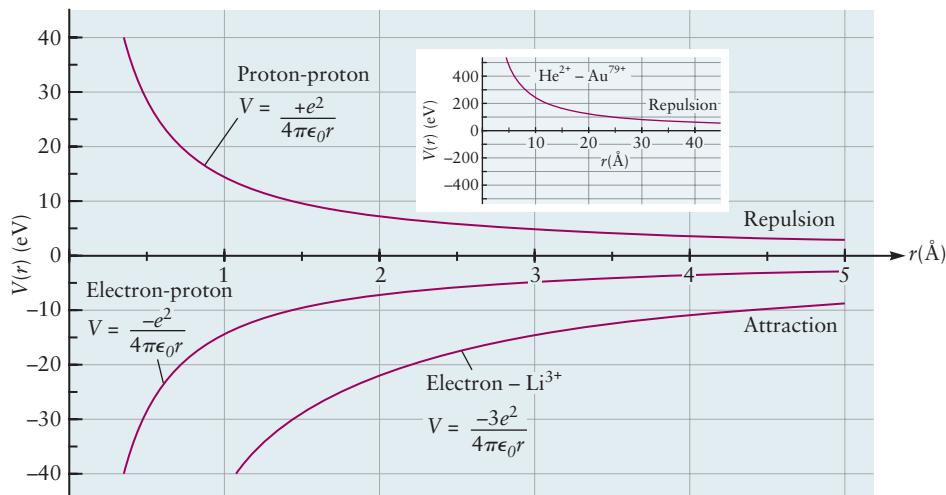
On the scale of ordinary human experience, this is an extremely small amount of energy. In comparison, one food calorie equals 4.184×10^3 J, so the amount of energy in one hydrogen atom is very small indeed. Energy values in this range appear regularly in atomic and molecular physics because of the small electrical charges involved, so it is appropriate to define a special energy unit for these applications. An electron accelerated through a potential difference of 1 V gains kinetic energy in the amount $\mathcal{E} = eV = (1.60217646 \times 10^{-19} \text{ C})(1 \text{ V}) = 1.60217646 \times 10^{-19}$ J. Therefore, it is convenient to define a unit of energy called the **electron volt (eV)**, such that $1 \text{ eV} = 1.60217646 \times 10^{-19}$ J.

Thus, the potential energy between the proton and electron separated by 1 \AA is

$$V(1 \text{ \AA}) = -\frac{2.307 \times 10^{-18} \text{ J}}{1.602 \times 10^{-19} \text{ J(eV)}^{-1}} = -14.40 \text{ eV} \quad [3.5]$$

Figure 3.2 plots the potential energy (in eV) versus distance (in \AA) for proton-electron, proton-proton, electron-lithium nucleus, and helium nucleus-gold

FIGURE 3.2 Potential energy curves for pairs of charged particles interacting according to Coulomb's law.



nucleus interactions. (The last pair was studied experimentally in Rutherford’s experiment described in Section 1.4.) These plots summarize a great deal of physical information, and you should become skilled at interpreting them. The potential energy scale is defined to have the value zero when the particles are infinitely far apart and do not interact. At shorter separations, the sign of the potential energy depends on the signs of the charges, as explained earlier (see Fig. 3.2).

Once the potential energy curve is known, we can use it to predict the motions of the particles. The force between a pair of particles is the negative of the derivative of their potential energy (see Appendix B2). Therefore, regions in which the slope of the potential energy is *negative* are regions in which the force on the particle is *positive*. The particles will be pushed apart in these regions. Wherever the slope of the potential energy is *positive*, the force in that region is *negative*, and the particles will be attracted to one another. Let’s illustrate this conclusion for the proton–electron interaction, for which the slope of the potential energy curve is positive everywhere:

$$F_{\text{coul}} = -\frac{d}{dr} \left(-\frac{Ze^2}{4\pi\epsilon_0 r} \right) = \frac{d}{dr} \left(\frac{Ze^2}{4\pi\epsilon_0 r} \right) = -\frac{Ze^2}{4\pi\epsilon_0 r^2} \quad [3.6]$$

Equation 3.6 shows that the force is always attractive (as indicated by the negative sign) and decreases with increasing r . You should run through a similar analysis for each of the curves shown in Figure 3.2 to be sure that you understand how to interpret these diagrams. We make extensive use of potential energy curves to predict the motions of particles in many areas of chemistry discussed throughout this book.

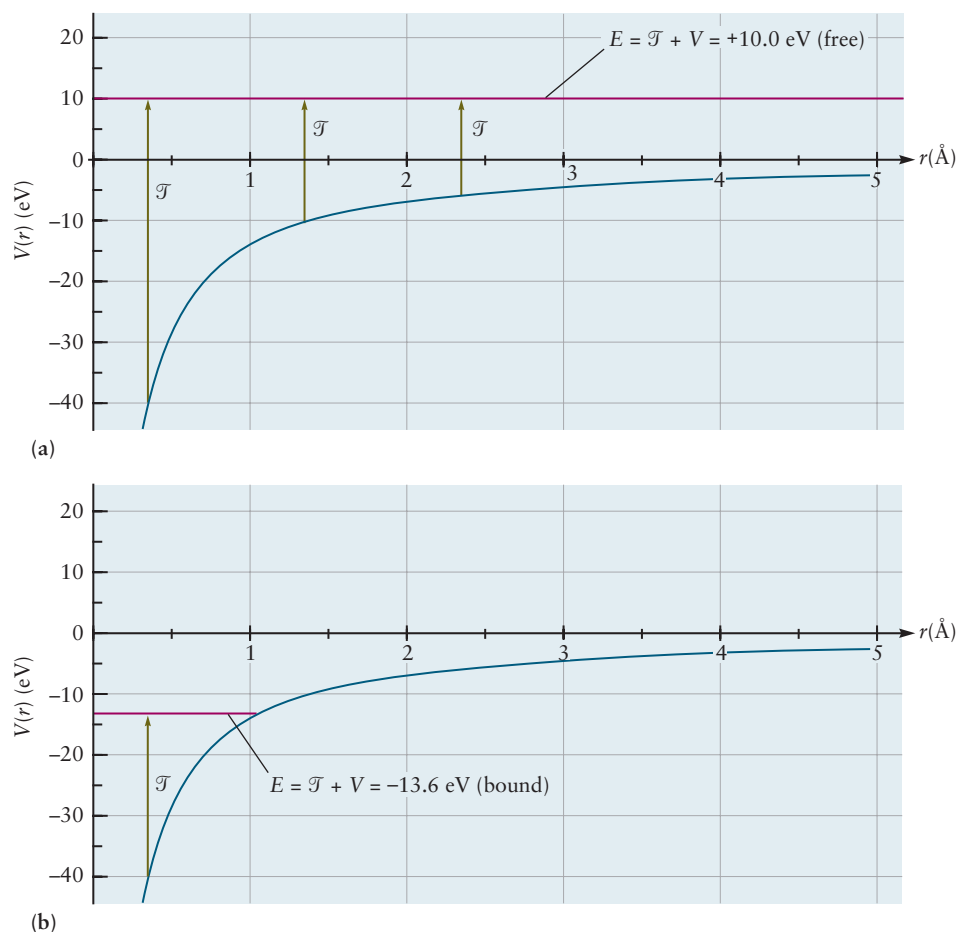
Let’s examine the motion of the electron in the hydrogen atom, which has only one proton and one electron. The total energy (kinetic and potential) of the electron in the atom is

$$E = \frac{1}{2} m_e v^2 - \frac{Ze^2}{4\pi\epsilon_0 r} \quad [3.7]$$

Suppose the atom has a fixed total energy E . It is informative to represent this situation by a straight line on the potential energy curve and show the kinetic energy value \mathcal{T} at each point as a vertical arrow connecting V to E . (See Appendix B2 for background.)

Figure 3.3a shows the total energy set to +10.0 eV. The graph shows that the electron has significant kinetic energy everywhere, so the case of positive E corresponds to *unbound motion* in which the electron approaches the proton but passes by without becoming trapped or attached. Imagine a helicopter flying above a canyon represented by the potential energy well; its motion is not affected by the presence of the canyon at all. Figure 3.3b shows the total energy set to –13.6 eV. The kinetic energy is large at small values of r and decreases to zero at the point where this line intersects V (the *turning point* of the electron’s motion). For values of r larger than the turning point, the kinetic energy would be negative, which is not allowed in Newtonian mechanics. Therefore, the case of negative total energy describes *bound motion* in which the electron is said to be “trapped within a potential well around the proton,” and its motions are limited to the range between zero and the turning point. In this case, we can imagine the helicopter being free to explore all of the regions of the canyon at the altitude of the red line until it approaches the canyon wall, at which point the pilot will turn around and head back! Some of these points will be refined by the quantum mechanical treatment of Chapter 5, where we will see that only certain specific values of the bound state energy are allowed, one of which is –13.6 eV.

FIGURE 3.3 Potential energy, total energy, and kinetic energy for interaction of an electron with a proton. When the total energy is fixed, the kinetic energy at each point is represented by a vertical arrow from the potential energy curve to the value of the total energy. (a) Total energy $E > 0$ corresponds to unbound motion, characterized by significant kinetic energy at all positions. (b) Total energy $E < 0$ corresponds to bound motion where the electron is confined to distances smaller than the “turning point,” at which the potential and total energy are equal, and the kinetic energy is 0.



The key point to keep in mind here is that the electron is bound within the atom whenever the total energy is less than zero. To remove the electron from the atom, it is necessary to add enough energy to make the total energy greater than zero. Thus, for the bound state of the hydrogen atom mentioned earlier, adding 13.6 eV of energy will set the electron free, but just barely. Adding 23.6 eV of energy to the atom would enable the electron to depart the atom with 10.0 eV of kinetic energy.

3.3 Ionization Energies and the Shell Model of the Atom

Electron distributions change during the course of all chemical reactions. The simplest possible chemical reactions are those in which an electron is either removed from or added to a neutral atom to form a positively charged **cation** or negatively charged **anion**, respectively. Although these might be considered to be physical processes, the reactants and products in both cases have different chemical properties, so these are clearly chemical changes. This section focuses on the process that creates positively charged ions, and Section 3.4 discusses the complementary process. The energy changes associated with each of these processes show clear periodic trends that correlate with the trends in chemical reactivity discussed in

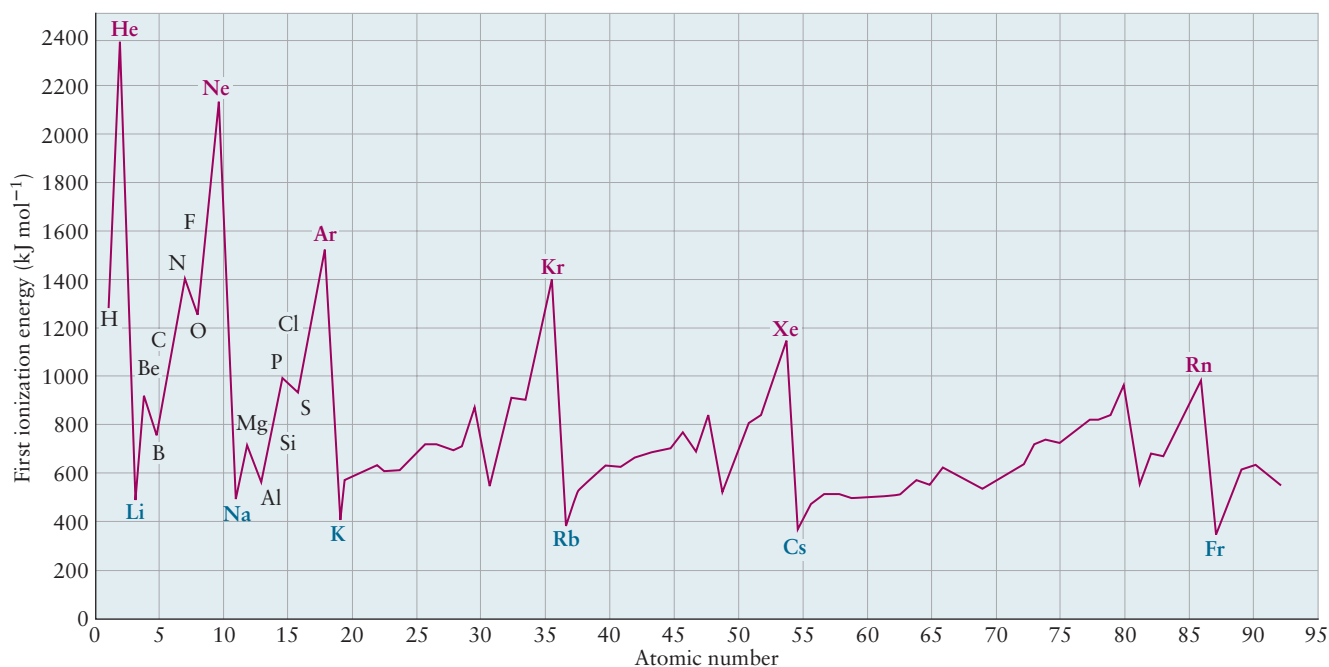
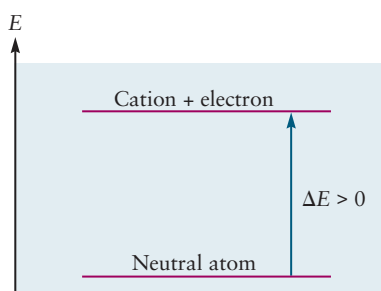


FIGURE 3.4 First ionization energy plotted versus atomic number shows periodic behavior. Symbols for the noble gases are shown in red; those for alkali metals are shown in blue.

Section 3.1. This correlation suggests that a qualitative explanation of chemical bonding may begin by understanding the factors that control the loss or gain of electrons by atoms.

The **ionization energy**, IE_1 , of an atom (also referred to as the first ionization energy, or in some texts, the ionization potential) is the minimum energy necessary to detach an electron from the neutral gaseous atom and form a positively charged gaseous ion. It is the change in energy, ΔE , for the process



Ionization requires sufficient energy to enable the electron to escape from the potential energy well of the atom.

The Greek letter capital delta, Δ , is widely used to symbolize the difference in value of a property caused by a process or change carried out in the laboratory. Here, $\Delta E = [\text{energy of reaction products}] - [\text{energy of reactants}]$. Thus, ΔE is positive when energy must be provided for the process to occur, and ΔE is negative if the process liberates energy. To achieve the ionization of $X(g)$ to the products $X^+(g) + e^-$ in the previous reaction, it is necessary to add energy to the neutral atom $X(g)$ to liberate the electron. This energy enables the electron to escape from the potential energy well that holds it in the atom. Therefore, the energy of the final state [free electron and ion $X^+(g)$] is greater than that of the initial state (neutral atom).

ΔE for ionization reactions is always positive. The ionization energy is a measure of the stability of the free atom. Those atoms with larger ionization energies are more stable than those with smaller ionization energies because their electrons must be removed from deeper potential energy wells.

Figure 3.4 shows the measured ionization energies of the elements plotted against their atomic numbers. Note that these ionization energies are reported in kJ per *mole* of atoms; following the discussion of Section 3.2, 1 eV per *atom* equals 96.48 kJ per mole.

The values generally increase moving across a period (from left to right), becoming large for each noble gas atom, and then fall abruptly for the alkali atom

at the beginning of the next period. The large values for the noble gas atoms demonstrate that their electron configurations are extremely stable, and that considerable energy is required to liberate their electrons. Moreover, the electron configurations of the noble gas atoms are more stable than those of the atoms immediately before and after them in the periodic table.

Ionization energy is thus a periodic property of elemental atoms (see Section 3.1). The general trend of this periodicity in IE_1 correlates with the fact that each main-group element (Groups I–VIII) in Period 3 (through element 20, Ca) contains exactly 8 more electrons than the element immediately above it, and each main-group element in Periods 4 and 5 (from element 31, Ga, through element 56, Ba) contains exactly 18 more electrons than the element immediately above it. The small local increases and decreases observed across a period will be explained in detail by the quantum description of atomic structure in Chapter 5. Our primary objective here is to show that removing the first electron, as a simple model chemical reaction, is periodic in the atomic number Z . For this purpose, it is not necessary to consider the small local variations.

The *second* ionization energy, IE_2 , is the minimum energy required to remove a second electron, or ΔE for the process



The third, fourth, and higher ionization energies are defined in analogous fashion. Successive ionization energies always increase due to the greater electrostatic attraction of the electron to the product ions, which have increasingly greater positive charges.

Examination of successive ionization energies suggests that the electrons in an atom are organized in a very interesting structure. This pattern is revealed in Table 3.1, which shows the first ten ionization energies for the elements H through Ar. Note that in Table 3.1 the values of ionization energy are expressed in MJ mol^{-1} , rather than kJ mol^{-1} , as in Figure 3.4, to make it easier to display them in tabular form.

Let's first consider He. IE_1 for He is 2.37, which is much greater than that of H (1.31) or Li (0.52). The electronic structure of He is thus much more stable than that of either H or Li. Further disruption of the stable He structure by removing a second electron requires $IE_2 = 5.25$.

Next, let's consider Li. IE_1 for Li is 0.52, whereas IE_2 is 7.30, far greater than the difference between IE_1 and IE_2 for He. Note that the difference $IE_3 - IE_2$ for Li is comparable with the difference $IE_2 - IE_1$ for He. These results show that one electron is removed easily from Li to form Li^+ , which has two electrons and is much more stable than the He atom.

As we proceed across Period 2, an interesting pattern develops. The ionization energies for Be show a large jump between IE_2 and IE_3 , demonstrating that it easily loses two electrons to form Be^{2+} , which has two electrons and heliumlike stability. Boron ionization energies display a large jump between IE_3 and IE_4 , showing that three electrons are easily removed, and C has a large jump between IE_4 and IE_5 , showing that four electrons are easily removed. The pattern continues, showing that F has seven electrons that can be removed more easily than the last two, whereas Ne has eight. This pattern is shown in Table 3.1 through highlighting of the ionization energies for the more easily removed electrons in each atom. These results suggest that electrons in the atoms of Period 2 are arranged as a stable heliumlike *inner core*, surrounded by less tightly bound electrons. The number of less tightly bound electrons increases from one to eight as the atomic number increases from three to ten.

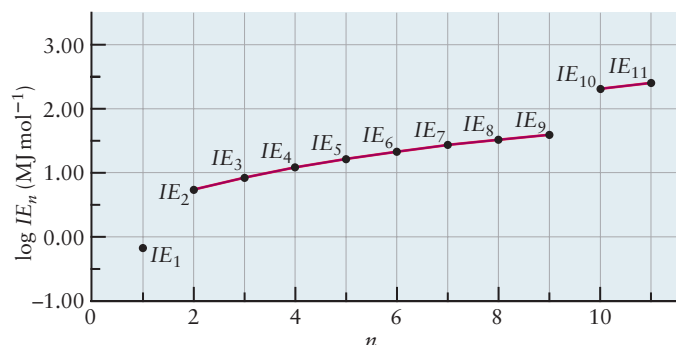
Examination of the atoms in Period 3, Na through Ar, reveals a similar pattern of relatively more easily removed electrons outside a stable core, which resembles the Ne atom. This is shown in Table 3.1 through highlighting of the ionization

TABLE 3.1 Successive Ionization Energies of the Elements Hydrogen through Argon

		Ionization Energy (MJ mol ⁻¹)									
Z	Element	IE ₁	IE ₂	IE ₃	IE ₄	IE ₅	IE ₆	IE ₇	IE ₈	IE ₉	IE ₁₀
1	H	1.31									
2	He	2.37	5.25								
3	Li	0.52	7.30	11.81							
4	Be	0.90	1.76	14.85	21.01						
5	B	0.80	2.42	3.66	25.02	32.82					
6	C	1.09	2.35	4.62	6.22	37.83	47.28				
7	N	1.40	2.86	4.58	7.48	9.44	53.27	64.36			
8	O	1.31	3.39	5.30	7.47	10.98	13.33	71.33	84.08		
9	F	1.68	3.37	6.05	8.41	11.02	15.16	17.87	92.04	106.43	
10	Ne	2.08	3.95	6.12	9.37	12.18	15.24	20.00	23.07	115.38	131.43
11	Na	0.50	4.56	6.91	9.54	13.35	16.61	20.11	25.49	28.93	141.37
12	Mg	0.74	1.45	7.73	10.54	13.62	17.99	21.70	25.66	31.64	35.46
13	Al	0.58	1.82	2.74	11.58	14.83	18.38	23.30	27.46	31.86	38.46
14	Si	0.79	1.58	3.23	4.36	16.09	19.78	23.79	29.25	33.87	38.73
15	P	1.06	1.90	2.91	4.96	6.27	21.27	25.40	29.85	35.87	40.96
16	S	1.00	2.25	3.36	4.56	7.01	8.49	27.11	31.67	36.58	43.14
17	Cl	1.26	2.30	3.82	5.16	6.54	9.36	11.02	33.60	38.60	43.96
18	Ar	1.52	2.67	3.93	5.77	7.24	8.78	11.99	13.84	40.76	46.19
19	K	0.42	3.05	4.40	5.87	7.96	9.63	11.32
20	Ca	0.59	1.14	4.90	6.46	8.13	10.48	12.30
21	Sc	0.63	1.23	2.38	7.08	8.82	10.70	13.29

energy values for the more easily removed electrons in each atom. (The ionization energy values highlighted show the beginning of this pattern for Period 4.) Na appears to have a single weakly bound electron outside a neonlike core. Further insight into this arrangement is obtained by plotting the successive ionization energies of Na versus n , the total number of electrons that have been removed at each step. It is convenient to plot the logarithm of ionization energy versus n to compress the vertical scale. The result for Na (Fig. 3.5) suggests that the electrons of the Na atom are arranged in three *shells*. The first electron is easily removed to produce Na⁺, which has neonlike stability as indicated by the large jump between IE₁ and IE₂. Electrons 2 through 9 occupy the second shell, and all of them are more tightly bound than the first electron. A big jump between IE₉ and IE₁₀ suggests that the last two electrons occupy a third shell, the electrons of which are the most tightly bound of all.

FIGURE 3.5 Logarithm of successive ionization energies for Na versus number of electrons removed suggests a three-shell electronic structure.



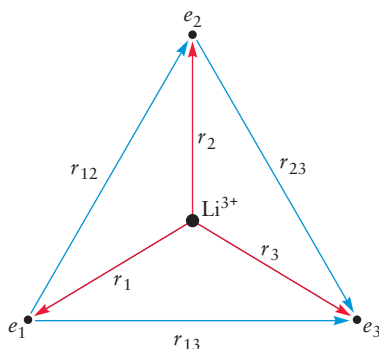
The Shell Model of the Atom

Examining the ionization process as a prototype simple chemical reaction leads us to conclude that electrons occupy a set of shells that surround the nucleus. This is a remarkable experimental result. All of the electrons in an atom are identical, and they all interact with the same nucleus. Why should they be arranged in shells, and what determines the number of electrons that can occupy a given shell?

We begin by considering the forces that act within and the potential energy functions for many-electron atoms. Consider Li, for which $Z = 3$.

Each of the electrons is attracted to the nucleus and repelled by the other electrons via the Coulomb interaction. The electrons are located relative to the nucleus by coordinates r_1, r_2, r_3 , and the distances between the pairs of electrons are given by $r_{12} = r_1 - r_2$, $r_{13} = r_1 - r_3$ and $r_{23} = r_2 - r_3$. The potential energy is then given by

$$V = \frac{Ze^2}{4\pi\epsilon_0} \left(-\frac{1}{r_1} - \frac{1}{r_2} - \frac{1}{r_3} + \frac{1}{r_{12}} + \frac{1}{r_{13}} + \frac{1}{r_{23}} \right) \quad [3.8]$$



Li atom with three electrons.

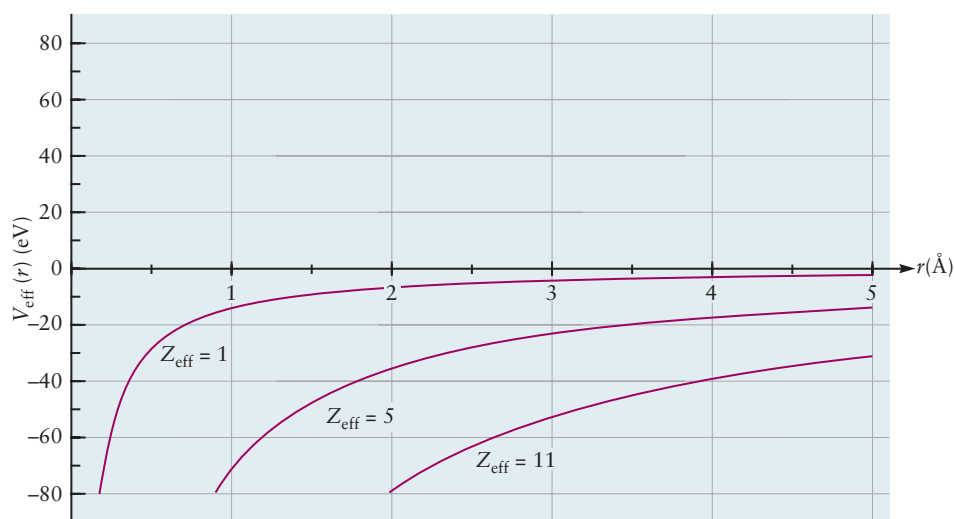
We can calculate the potential energy for any configuration of the atom, for example, with the electrons at the vertices of an equilateral triangle with specific side lengths and the nucleus at the center. But unlike the case of the hydrogen atom, there is no simple way to relate this potential energy to the bound motion of the electrons in the atom and to describe how each electron is held inside the atom. There is no way to describe exactly the motions of more than two interacting particles, either in Newtonian mechanics or quantum mechanics. So we develop an approximate description in which we examine the behavior of one electron at the time. We imagine that (for example) electron 1 is fixed at r_1 , whereas the other electrons move all around the atom. Their motion, in effect, averages all the terms in the potential energy except the first. The combination of this average and the first term gives an *effective potential energy* that governs the motion of electron 1. One way to generate this effective potential is to recognize that when the other electrons come between electron 1 and the nucleus, they *screen* or *shield* electron 1 from the full strength of the nuclear attraction. It is useful to think of the Coulomb interaction as strictly “line of sight,” so intrusion by another electron will reduce its strength. In effect, the charge of the nucleus, as seen by electron 1, has been reduced by the presence of the other electrons. We can then take the effective potential energy to be the Coulomb potential energy with an *effective charge* Z_{eff} on the nucleus:

$$V_{\text{eff}}(r) = -\frac{Z_{\text{eff}}e^2}{4\pi\epsilon_0 r} \quad [3.9]$$

Our approximate description of many-electron atoms thus relies on considering each electron to be bound within the atom by an effective potential well, where an appropriate value for Z_{eff} must be determined for each electron. In Chapter 5 we will see how to generate values for Z_{eff} systematically, and that they range from 1 to the full value of the nonscreened Z for the atom. Here, it is sufficient to get a sense of how much V_{eff} changes within a given atom. Consider Na, for which $Z = 11$. Figure 3.6 shows plots of V_{eff} curves for $Z_{\text{eff}} = 1, 5, 11$. Clearly, those electrons that experience the lower values of Z_{eff} are more weakly bound than those with higher values of Z_{eff} .

Our simple model for V_{eff} shows that the trend in successive ionization energies in a single atom arises naturally from screening and shielding. The key idea here is that the higher the value of Z_{eff} , the more energy is required to remove an electron from the atom. In Chapter 5 we combine this simple physical model with principles of quantum mechanics to understand why the electrons are organized in

FIGURE 3.6 Curves for the effective potential energy $V_{\text{eff}}(r)$ for electrons in Na ($Z = 11$) when $Z_{\text{eff}} = 1, 5, 11$. An electron at any location is more strongly bound in the atom as the value of Z_{eff} increases.



shells of 2, 8, and 18 electrons. Here, we consider the shell model to be justified by studies of successive ionization energies, and we use it to explain periodic trends in bond formation.

Electrons in the inner shells (called **core** electrons) do not participate significantly in chemical reactions. The outermost, partially filled shell (called the **valence shell**) contains the electrons involved in chemical bonding, the **valence electrons**. Progressing through the elements in order of increasing atomic number along a period, we see that stability increases from left to right, as indicated by increasing values of the ionization potential. The period ends in a filled shell, which is the stable configuration of the noble gases helium, neon, argon, and so on. Atoms with filled shells are extremely stable chemically, as shown by the large values of their ionization energies. The increase in stability observed when moving from left to right along a period (row) is easily explained classically. If the electrons in each shell are located at roughly the same distance from the nucleus, then the attractive electrostatic forces increase nearly monotonically as one unit of positive charge is added to the nucleus and one valence electron is added. The large decrease in ionization energy that occurs between a noble gas and the element whose valence electron occupies a new shell also is explained easily. If we envision these shells as a concentric series, each of which has a fixed radius that is larger than its predecessor, then it is clear why the electron-nuclear attraction decreases abruptly as an electron is added to the first empty shell outside a filled shell. This simple classical argument explains the major periodic trends in ionization energies; the small dips observed in going from left to right across a period require quantum mechanics for their explanation.

The number of valence electrons in a neutral atom of a main-group element (those in Groups I–VIII) of the second and third periods is equal to the group number of the element in the periodic table. However, the main-group elements that follow a series of transition-metal elements require some special attention. Atoms of bromine, for example, have 17 more electrons than atoms of argon, the preceding noble gas, but only 7 are considered to be valence electrons. This is true for two reasons. First, in the fourth, fifth, and sixth rows, the 10 electrons added to complete the transition metal series (although they are important for the bonding of those elements) have become *core* electrons by the time the end of the transition-metal series is reached. They are closer to the nucleus, on average, than the electrons that fill the rest of the shells of those periods, and it might be useful to visualize them as occupying a subshell. Second, and more importantly, the chemical properties of the main group elements in this part of the periodic table are characteristic of the group to which they belong. The bonding properties of an element such as bromine, for example, resemble those of the lighter elements in its group.

3.4 Electronegativity: The Tendency of Atoms to Attract Electrons

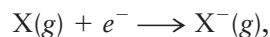
The type of bond formed between a pair of atoms is determined by the degree to which electrons are attracted to each nucleus. The ability of a free, isolated atom to lose an electron is measured by its ionization energy, whereas its ability to gain an electron is measured by its electron affinity, EA . The relative tendency of atoms to either gain or lose electrons is expressed succinctly by a new quantity called electronegativity. The most intuitively appealing definition of electronegativity for isolated atoms is simply the average of the ionization energy and the electron affinity. Atoms that are hard to ionize and have large electron affinities will tend to attract electrons; those that are easily ionized and have low electron affinities will tend to donate electrons. A comparison of the electronegativities of two atoms will suggest whether they will most likely form an ionic, covalent, or polar covalent bond.

This section defines electron affinity and two different electronegativity scales. Although the two electronegativity scales were developed using different physical models, they are essentially proportional to one another. Electronegativity, not surprisingly, is also a periodic property, and much can be learned about the nature of a particular bond simply by comparing the locations of its constituent elements in the periodic table. The remaining sections of this chapter apply this concept to describe systemically ionic, covalent, and polar covalent bonds.

Electron Affinity

Ionization energy, which measures the difficulty with which an atom gives up an electron to form a cation, is defined in Section 3.3. The energy change of the opposite reaction, in which an atom accepts an extra electron to form an anion, is the electron affinity of the atom.

An anion is formed by the electron attachment reaction,

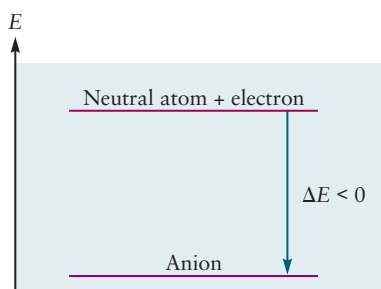
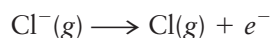


for which the energy change ΔE (see definition in Section 3.3) is called the **electron attachment energy**. This energy change is readily shown on a potential energy diagram where $X(g)$ and the electron are initially separated by large distances and do not interact, then approach to form the anion $X^{-}(g)$, whose energy is lower than that of the separated particles.

Because the energy of the products is lower than the energy of the reactants, ΔE is negative, energy is released in the reaction, and the anion is stable. This means that the neutral atom can accommodate an extra electron to form the anion in which the electron is strongly bound by the effective potential V_{eff} . The energy change, ΔE , for the reverse reaction, in which the electron is removed from $X^{-}(g)$ to give the neutral atom $X(g)$, is positive because energy must be supplied to overcome V_{eff} in the anion.

For historical reasons, **electron affinity** has been defined as the amount of energy *released* when an electron is attached to a neutral atom, but it is always expressed as a positive number. This is a time-honored, if frustrating, exception to the otherwise universal convention adopted by chemists and physicists that energy liberated in a process is assigned a negative number, an exception that must simply be remembered.

It is difficult to measure the electron attachment energy directly, and to obtain the electron affinity from $EA = -\Delta E$ (electron attachment). It is easier to obtain EA from another measurement that determines the stability of the gaseous anion in the same way that ionization energies are measured. The reaction



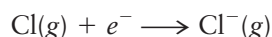
When an electron attaches to an atom to form a stable anion, the electron becomes trapped in the potential well of the atom, the energy of the products is lower than the energy of the reactants, and $\Delta E < 0$.

TABLE 3.2 Electron Affinity of Selected Atoms (in kJ mol^{-1})

H						
73						
Li	Be	B	C	N	O	F
60	*	27	122	*	141	328
Na	Mg	Al	Si	P	S	Cl
53	*	42	134	72	200	349
K	Ca	Ga	Ge	As	Se	Br
48	2	41	119	79	195	325
Rb	Sr	In	Sn	Sb	Te	I
47	5	29	107	101	190	295
Cs	Ba	Tl	Pb	Bi	Po	At
46	14	19	35	91	183	270

*No stable anion A^- exists for this element in the gas phase.

which is the reverse of the electron attachment reaction, has positive ΔE because energy must be supplied to overcome V_{eff} in the anion. By measuring the energy required to remove the electron from the ion, we can obtain the electron affinity for the atom as $EA = \Delta E$ (electron detachment). Removal of the electron from Cl^- requires $\Delta E = +349 \text{ kJ mol}^{-1}$ of energy, which shows that the Cl^- anion is stable. Thus, EA for Cl, defined as the energy released in the reaction



is 349 kJ mol^{-1} . We do not explicitly include the plus sign when using electron affinities to help you remember that they are always positive by convention. Values of electron affinity for selected elements are shown in Table 3.2. We choose not to consider “negative” electron affinities, which you might see tabulated in other texts or reference materials. An atom with a negative electron affinity would require energy be expended to hold the electron on the atom. Such an “anion” would be unstable with respect to dissociation; thus, the concept is not particularly useful in our view.

The periodic trends in electron affinity largely parallel those in ionization energy, increasing across a period to become large and positive for the halogens, then decreasing abruptly to essentially zero for the noble gases. A notable difference between the trends in ionization energy and electron affinity is that the dramatic changes in electron affinities occur between atoms whose atomic numbers are one lower than the corresponding breaks in the trends in ionization energy. The following examples illustrate and explain this point. Attaching an electron to F gives F^- , which has the same electron arrangement as Ne, and is therefore very stable. (Recall the discussion of ionization energy in Section 3.3 as a measure of stability.) Similarly, the noble gases have essentially zero electron affinities for the same reason that the alkali metals have small ionization energies; the outermost electron in Ne^- or Xe^- would reside in a new shell, and the resulting ion would be less stable than the neutral parent atom. Therefore, Ne^- is less stable than Ne for precisely the same reason that Na is less stable than Ne. Fluorine has the highest electron affinity, and that of Ne is nearly zero.

No gaseous atom has a positive electron affinity for a *second* electron, because a gaseous ion with a net charge of $-2e$ is always unstable with respect to ionization. Attaching a second electron means bringing it close to a species that is already negatively charged. The two repel each other, and the potential energy between them increases. In crystalline environments, however, doubly negative ions such as O^{2-} can be stabilized by electrostatic interactions with neighboring positive ions.

Mulliken’s and Pauling’s Electronegativity Scales

The values of IE_1 and EA determine how readily an atom might form a positive or a negative ion. To combine these propensities into a single quantity with predictive value, in 1934, the American physicist Robert Mulliken defined electronegativity

as a measure of the relative tendency of atoms to attract electrons to one another in a chemical bond. Mulliken observed that elements located in the lower left corner of the periodic table have low ionization energies and small electron affinities. This means that they give up electrons readily (to form positive ions) but do not readily accept electrons (to form negative ions). They tend to act as electron *donors* in interactions with other elements. In contrast, elements in the upper right corner of the periodic table have large ionization energies and also (except for the noble gases) large electron affinities. As a result, these elements accept electrons easily but give them up only reluctantly; they act as electron *acceptors*.

Mulliken simply *defined* electronegativity as a quantity that is proportional to the average of the ionization energy and the electron affinity:

$$\text{EN (Mulliken)} \propto \frac{1}{2}(IE_1 + EA) \quad [3.10]$$

Electron acceptors (such as the halogens) have both large ionization energies and large electron affinities; they are highly **electronegative**. Electron donors (such as the alkali metals) have small ionization energies and small electron affinities, and therefore low electronegativities; they are **electropositive**. The noble gases rarely participate in chemical bonding. Their large ionization energies and essentially zero electron affinities mean that they are reluctant either to give up or to accept electrons. Electronegativities, therefore, are not generally assigned to the noble gases.

Two years before Mulliken's publication, the American chemist Linus Pauling proposed a different electronegativity scale, based on a comparison of the bond energies of a large number of heteronuclear bond pairs with those of homonuclear diatomics comprising the same elements (for example, HF, HCl and HBr compared with H₂, F₂, Cl₂ and Br₂). Pauling observed that bonds formed between elements from opposite sides of the periodic table were stronger than those between identical elements or even those located in close proximity to one another. He suggested that this extra stability was provided by an *ionic* contribution to the bond strength and constructed an empirical formula for his electronegativity scale that explicitly took these contributions into account.

Pauling's argument goes as follows. Suppose the dissociation energy of an A—A bond is ΔE_{AA} , and that of a B—B bond is ΔE_{BB} ; both bonds are covalent because the atoms in them are identical. Then an estimate of the *covalent* contribution to the dissociation energy of an A—B bond is the (geometric) mean of these two energies, $\sqrt{\Delta E_{AA}\Delta E_{BB}}$. (The postulate of the geometric mean was inspired by elementary quantum mechanical arguments but was retained only because it gave better fits than did the arithmetic mean.) The actual A—B bond, however, must include some ionic character because some charge transfer occurs between the atoms. The ionic character tends to strengthen the bond and to increase its value of ΔE_{AB} . Pauling suggested that the difference between the actual and covalent bond energies,

$$\Delta = \Delta E_{AB} - \sqrt{\Delta E_{AA}\Delta E_{BB}} \quad [3.11]$$

called the **excess bond energy**, is a measure of the ionic contribution to the bond strength and should arise from the electronegativity difference between the two atoms A and B. He defined this electronegativity difference as

$$\chi_A - \chi_B = 0.102\Delta^{1/2} \quad [3.12]$$

where χ_A and χ_B (Greek letter small chi) are the electronegativities of A and B, respectively. The coefficient 0.102 arises when Δ is measured in kilojoules per mole (kJ mol^{-1}). The atom that more readily accepts an electron (and thus tends to carry a partial negative charge) has the larger χ value. Note that Pauling's formula provides a recipe for calculating only differences in electronegativities, not their absolute values. Pauling himself, after proposing a number of absolute values, arbitrarily assigned the value 4.0 to fluorine. The modern Pauling table (Fig. 3.7) is the result of slight modifications made as better thermochemical data became available.



FIGURE 3.7 Average electronegativity of atoms, computed with the method that Linus Pauling developed. Electronegativity values have no units.

Let's compare Mulliken's and Pauling's approaches to the development of their respective electronegativity scales. Mulliken's approach was based on a simple physical model that focused on the properties of individual elements, which, although intuitively appealing, could not take into account any differences in the covalent contributions to the bond. In contrast, Pauling provided a model that explicitly separated the ionic and covalent contributions to the character of the bond, thus providing the framework for our contemporary understanding of the nature of the chemical bond. The other important contribution of his approach is that it averaged, in some sense, the electronegativity of a particular element when it is bonded to a variety of other elements. Despite the differences discussed earlier, Mulliken's and Pauling's scales produce values that are nearly proportional, and it has simply become customary to use the latter.

The periodic trends in electronegativity (Pauling; see Fig. 3.7) are quite interesting. Electronegativity increases across a period from left to right and decreases down a group from top to bottom. The latter trend is more pronounced for the representative elements. These trends can be rationalized semiclassically as before. Moving from left to right across a period, the increasing nuclear charge makes it energetically more difficult to remove an electron and also energetically more favorable to accommodate an additional electron. The trends observed moving down a group are much less dramatic (except for the differences between the second and third periods, in general, and the halogens) and less easy to rationalize. It is important to continue to emphasize, however, the predictive power of this remarkably simple concept, as we shall demonstrate in the sections that follow.

The essential points of this section can be summarized as follows: The tendency of an atom to donate or accept electrons in a chemical bond is expressed by its electronegativity. Highly electronegative atoms, on the right side of the periodic table, readily accept electrons to form negative ions. Highly electropositive atoms, on the left side of the table, readily donate electrons to form positive ions. Bonds formed by the complete transfer of an electron from one atom to another to form a pair of ions bound largely by electrostatic attraction are called ionic (see discussion in Section 3.5).

3.5 Forces and Potential Energy in Molecules: Formation of Chemical Bonds

What determines the stability of a chemical bond? Why is the H_2 molecule more stable than a pair of separated hydrogen atoms in the gas phase at normal temperatures and pressures? But what is the meaning of "more stable?" And how do bonds form spontaneously once the atoms are close enough together?

Experience shows that systems move spontaneously toward configurations that reduce their potential energy. A car rolls downhill, converting its gravitational potential energy into kinetic energy. We have already learned in Section 3.2 that microscopic charged particles move to reduce their electrostatic (Coulomb) potential energy. However, formation of a chemical bond is more subtle than ordinary motion of charged particles under Coulomb's force law, because it involves a special event. Two atoms flying toward each other have a certain total energy that includes contributions from their internal structure, their potential energy relative to each other, and their kinetic energy. To enter into what the distinguished chemist and author George C. Pimentel has characterized as “the blissful state of bondedness” in which the atoms fly together as a bonded pair forever after, they must give up some of their total energy. A diatomic molecule is more stable than the separated atoms from which it was formed because its *total energy* is less than that of the two atoms. You can reach the same conclusion by examining the reverse process; dissociation of a diatomic molecule requires energy. The formation of a chemical bond from a pair of atoms occurs spontaneously in the gas phase only if the reaction is **exothermic**—that is, one that releases heat into the surroundings. With the introduction of the second law of thermodynamics in Chapter 13, we show a deep connection between release of heat and spontaneity. But for this chapter, it is adequate to recognize that a reduction of the total energy of the system is the key to bond formation.

Let us interpret this fact in terms of the potential energy changes in formation of the molecule, illustrated with the specific example of H_2 shown in Figure 3.8. (We could equally well illustrate this with the atomic pairs Cl-Cl and Na-Cl, but the details would be more complicated.) The nuclei are labeled A and B, and the electrons are labeled 1 and 2. The distance between each electron and each proton (r_{1A} , r_{1B} , r_{2A} , r_{2B}) is shown in blue in Figure 3.8, while the distance between the two electrons (r_{12}) and the distance between the two protons (R_{AB}) are shown in red. The potential energy of the molecule is most conveniently expressed in terms of these distances.

$$V = -\frac{e^2}{4\pi\epsilon_0} \left(\frac{1}{r_{1A}} + \frac{1}{r_{2A}} + \frac{1}{r_{1B}} + \frac{1}{r_{2B}} \right) + \frac{e^2}{4\pi\epsilon_0} \left(\frac{1}{r_{12}} \right) + \frac{e^2}{4\pi\epsilon_0} \left(\frac{1}{R_{AB}} \right)$$

$$V = V_{en} + V_{ee} + V_{nn} \quad [3.13]$$

The first four terms in Equation 3.13 represent the attractions between the electrons and the nuclei, and all are negative. The last two terms represent the repulsions between the pair of electrons and the pair of protons, and both are positive. The value of V can be calculated for any configuration of the molecule. But just as in the case of the lithium atom in Section 3.3, this potential energy function does not give a simple pictorial explanation of the stability of the molecule, because there is no exact solution for the motions of four interacting particles.

Out of these building blocks we must construct some new approximate potential energy function, V_{eff} , that holds the molecule together. That means that V_{eff} must depend on R_{AB} , which tracks the transition from two separated atoms to a diatomic molecule. At large distances, $V_{\text{eff}} \rightarrow 0$ because the isolated atoms do not interact. As R_{AB} decreases, V_{eff} must become negative because the atoms begin to attract each other. At small distances, V_{eff} must become positive and large as $V_{\text{eff}} \rightarrow \infty$ due to the repulsion between the protons. Therefore, at some intermediate value of R_{AB} , the potential function must reach a minimum negative value and change its slope as it heads toward positive values. Figure 3.9 is a sketch of a generic V_{eff} that shows all these features.

As explained in Section 3.2, the force between the protons is the negative of the slope of V_{eff} , that is, the negative of its derivative with respect to R_{AB} . For values of R_{AB} larger than the minimum, the attractive forces tend to reduce R_{AB} ; for values of R_{AB} smaller than the minimum, the repulsive forces tend to increase R_{AB} . Thus, both the depth of the potential and the position of the minimum are

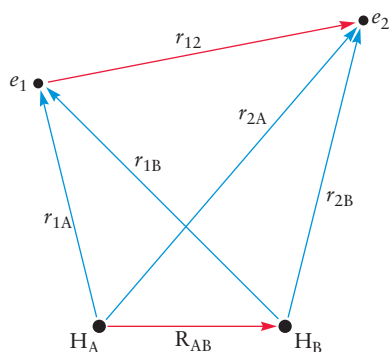
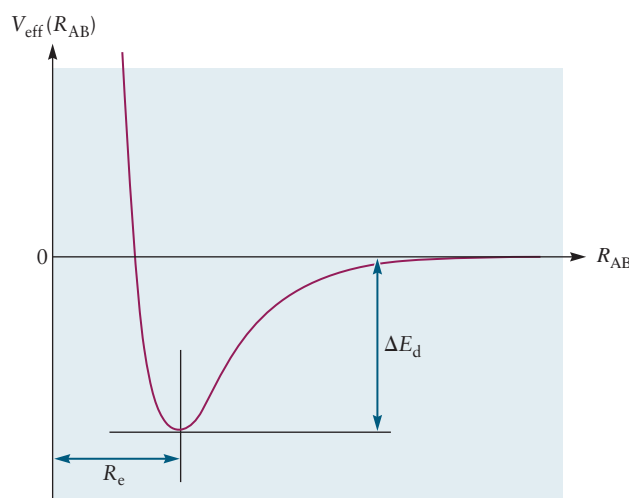


FIGURE 3.8 Coordinates for the hydrogen molecule. The nuclei are assumed stationary at fixed positions separated by the distance R_{AB} . The distance of electron 1 from nuclei A and B is given by r_{1A} , r_{1B} ; the distance of electron 2 from nuclei A and B is given by r_{2A} , r_{2B} ; the distance between the electrons is given by r_{12} .

FIGURE 3.9 Dependence of the effective potential energy V_{eff} for a diatomic on the internuclear distance R_{AB} . The location of the minimum corresponds to the equilibrium bond length. The depth of the well relative to the separated atoms is the energy required to dissociate the molecule to form the atoms, and it measures the stability of the molecule.



determined by the competition between the attractive and repulsive forces along the internuclear direction. Therefore, we identify the value of R_{AB} at the minimum as the *equilibrium bond length* of the molecule. The depth of the minimum relative to the separated atoms is identified as the **bond dissociation energy**, ΔE_d , which is a measure of the strength of the bond and the extent to which the molecule is more stable than the separated atoms.

Formation of the chemical bond is associated with a reduction of the electrostatic potential energy and a release of this energy in the form of heat. The actual shape of V_{eff} must be determined by analyzing the Coulomb terms in Equation 3.13. Different classical models of bond formation achieve this goal in different ways. We see how this is done for the two main models for ionic and covalent bonding in Sections 3.6 and 3.7.

The Virial Theorem

We have asserted that bond formation from gas-phase atoms *reduces* the total energy of the system, and we have illustrated how bond formation reduces the electrostatic potential energy. To complete the story, we must see how this reduction in the total energy is partitioned between the kinetic and potential energies of the particles in the system and also gather what we can learn about the driving force for bond formation. For this, we invoke, without proof, the virial theorem, a powerful and quite generally applicable theorem of both classical and quantum mechanics that connects the kinetic, potential, and total energies of a system together, regardless of the details that characterize a particular system of interest. The **virial theorem** states that the average kinetic and the average potential energy of a system of particles interacting only through *electrostatic* forces are related as follows:

$$\overline{\mathcal{T}} = -\frac{1}{2} \overline{V} \quad [3.14]$$

where $\overline{\mathcal{T}}$ and \overline{V} are the average kinetic and potential energies, respectively. The bar above each symbol identifies it as an average quantity. Now, because

$$\overline{E} = \overline{\mathcal{T}} + \overline{V} \quad [3.15]$$

we can state for any process that involves a change in the system that

$$\Delta \overline{E} = \Delta \overline{\mathcal{T}} + \Delta \overline{V} \quad [3.16]$$

Therefore,

$$\Delta\bar{E} = \frac{1}{2} \Delta\bar{V} \quad [3.17]$$

and

$$\Delta\bar{\mathcal{F}} = -\frac{1}{2} \Delta\bar{V} \quad [3.18]$$

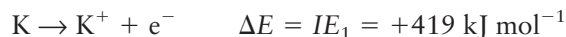
Several important conclusions can be drawn from Equations 3.17 and 3.18. First, Equation 3.17 shows clearly that the reduction in the total energy has the same sign as the reduction in the potential energy. In cases where potential energy makes the dominant contribution to the total bond energy (ionic bonds), the reduction in the potential energy can be thought of as the driving force for the formation of the bond. This is consistent with what you have been taught previously and with your own experience in the macroscopic world. Note, however, that Equation 3.18 requires the kinetic energy to increase, but only by half as much as the potential energy decreases. For bonds in which both the kinetic and potential energies play comparably important roles (covalent and polar covalent bonds), cause and effect become much more subtle, and their understanding requires some elementary notions from quantum mechanics. There is an interesting, delicate, and beautiful interplay between kinetic and potential energy during the formation of a covalent chemical bond (see Chapter 6 for a detailed discussion).

3.6 Ionic Bonding

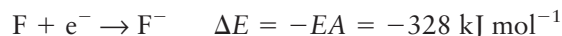
Ionic bonds form between atoms with large differences in electronegativity, such as sodium and fluorine. A practical definition of an ionic bond is one in which the dominant contribution to the strength of the bond is the electrostatic attraction between the ions. Conceptually, the formation of an ionic bond from neutral gas-phase atoms can be thought of as the result of two sequential processes. The more electropositive ion transfers an electron to the more electronegative atom, forming an ion pair that is then drawn together by the attractive electrostatic force. Although we focus our discussion on ionic bonding in a gaseous diatomic molecule where we can clearly identify the forces responsible, most ionic compounds are solids under normal conditions. In an ionic solid, ions of one charge are surrounded by an orderly array of ions of the opposite charge, resulting in extremely large Coulomb stabilization energies. They generally have high melting and boiling points (for example, NaCl melts at 801°C and boils at 1413°C) and can form large crystals. Solid ionic compounds usually conduct electricity poorly, but their melts (molten salts) conduct well.

The charges of the most common ionic forms of the representative elements are determined easily by observing how many electrons must be added or removed to achieve a noble gas configuration, that is, a filled octet. The alkali metals, therefore, form cations of +1 charge, the alkaline-earth metals form cations with +2 charge, and the halogens form anions with -1 charge, for example. The total charge on the compound must be zero, thus the stoichiometry is determined by charge balance. Elemental cations retain the name of the parent element, whereas the suffix *-ide* is added to the root name of the element that forms the anion. For example, Cl⁻ is chloride and, the compound it forms with Na⁺ is sodium chloride, the major ingredient in table salt. For this reason, ionic solids are often called salts. Simple, binary ionic compounds are easily named by inspection; if more than one ion is included in a compound, the Greek prefixes *mono-*, *di-*, *tri-*, and so forth are added for specificity. The preceding considerations allow us to write CaBr₂ as the molecular formula for calcium dibromide, for example. A more comprehensive discussion of inorganic nomenclature is presented in Section 3.11.

Let's consider the formation of an ionic bond from two neutral gas-phase atoms, potassium and fluorine to be specific. When the atoms are infinitely far apart, their interactions are negligible and we assign their potential energy of interaction as zero (see discussion in Section 3.5). Ionizing potassium requires energy, whereas attaching an electron to fluorine releases energy. The relevant reactions and their energy changes are



and



The total energy cost for the creation of this ion pair when the parent atoms are infinitely far apart, is

$$\Delta E_\infty = IE_1(\text{K}) - EA(\text{F}) = +91 \text{ kJ mol}^{-1}$$

Note that, even for this case, in which one element is highly electronegative and the other is highly electropositive, it still *costs* energy to transfer an electron from a potassium atom to a fluorine atom. This is always true. Because the smallest ionization energy of any element (Cs, 376 kJ mol^{-1}) is larger than the largest electron affinity of any element (Cl, 349 kJ mol^{-1}), creating an ion pair from neutral atoms always requires energy. Starting from an ion pair separated by a large distance, what interaction and which mechanism will lead to the reduction in the potential energy of the system required for the spontaneous formation of an ionic bond?

The ions are attracted to one another (because they have opposite charges) by the electrostatic force, and the potential energy of the system is described by Coulomb's law:

$$V(R_{12}) = \frac{q_1 q_2}{4\pi\epsilon_0 R_{12}} \text{ (J per ion pair)} \quad [3.19]$$

where q_1 and q_2 are the charges on the ions, R_{12} is the separation between the ions, and ϵ_0 is defined in Equation 3.1. This energy, expressed in joules per ion pair, can be converted to kJ mol^{-1} by multiplying by Avogadro's number, N_A , and dividing by 10^3 to get

$$V(R_{12}) = \frac{q_1 q_2}{4\pi\epsilon_0 R_{12}} \cdot \frac{N_A}{10^3} \text{ (kJ mol}^{-1}\text{)} \quad [3.20]$$

Consider the potential energy diagram shown in Figure 3.10. We have plotted the potential energy of the system as a function of the distance between the ions, choosing as our zero the potential energy of the neutral atoms when they are infinitely far apart, as before. We have plotted the function

$$V(R_{12}) = Ae^{-\alpha R_{12}} - B\left(\frac{(e)(-e)}{R_{12}}\right) + \Delta E_\infty \quad [3.21]$$

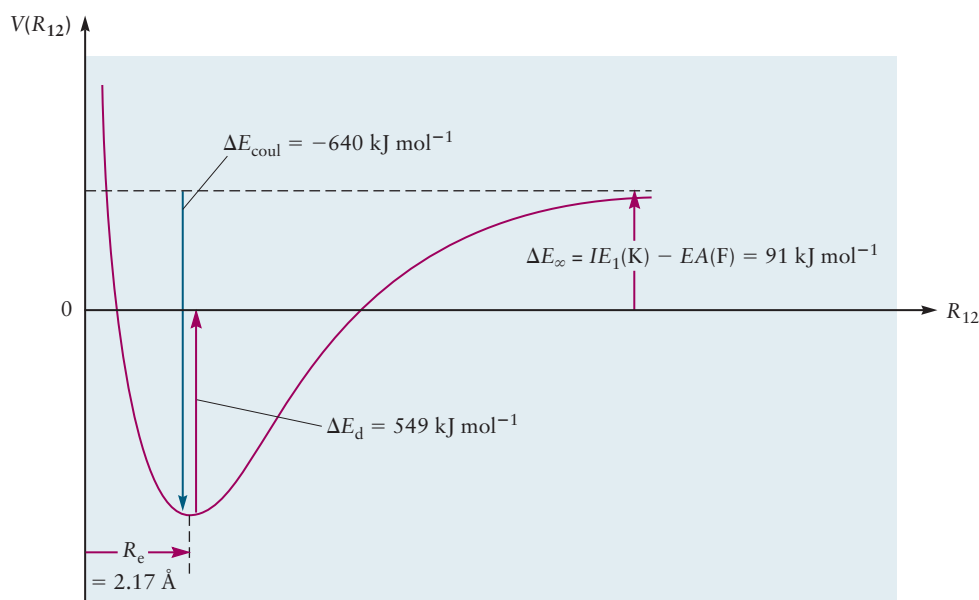
where the first term represents the repulsion between the ions as they get very close together, the second term is the attractive Coulomb potential, and the third term is the energy required to make the ions from their respective neutral atoms (see earlier). We have written the potential in this way for simplicity; the constants A and B reflect the relative contributions made by the attractive and repulsive terms, and they are usually obtained by fitting to experiment, as is the value for α , which tells us at what distance repulsion becomes important.

Starting at the right side of the curve in Figure 3.10, notice that the potential energy of the system (the pair of ions) is greater than that of the neutral atoms by

$$\Delta E_\infty = IE_1(\text{K}) - EA(\text{F}) = +91 \text{ kJ mol}^{-1}$$

Moving toward the left of Figure 3.10, the potential energy of the system decreases rapidly due to the attractive **Coulomb stabilization energy** (the second term in Eq. 3.21), reaching a minimum at the equilibrium bond length, $R_e = 2.17 \text{ \AA}$. If

FIGURE 3.10 The potential energy of the system K^+ and F^- as a function of their internuclear separation R_{12} .



we were to try to force the ions to move closer together, we would encounter the resistance depicted by the steep repulsive wall on the left side of the curve, which arises from the repulsive interactions between the electrons of the two ions and is accounted for by the first term in Equation 3.3. The equilibrium bond length, R_e , is determined by the balance between the attractive and repulsive forces.

At last, we can estimate the stabilization of an ionic bond such as KF relative to the neutral atoms. From Figure 3.10, this energy difference is

$$\Delta E_d \approx \frac{q_1 q_2}{4\pi\epsilon_0 R_e} \cdot \frac{N_A}{10^3} - \Delta E_\infty \quad [3.22]$$

where $\Delta E_\infty = IE_1(K) - EA(F)$. This stabilization energy measures the strength of the ionic bond and is approximately equal to the bond dissociation energy, which is the energy required to break the ionic bond and liberate neutral atoms.

EXAMPLE 3.1

Estimate the energy of dissociation to neutral atoms for KF, which has a bond length of 2.17×10^{-10} m. For KF, $\Delta E_\infty = IE_1(K) - EA(F) = 91 \text{ kJ mol}^{-1}$.

SOLUTION

$$\begin{aligned} \Delta E_d &\approx -\frac{q_1 q_2}{4\pi\epsilon_0 R_e} \cdot \frac{N_A}{10^3} - \Delta E_\infty \\ &= \frac{-(1.602 \times 10^{-19} \text{ C})^2 (6.022 \times 10^{23} \text{ mol}^{-1})}{(4)(3.1416)(8.854 \times 10^{-12} \text{ C}^2 \text{ J}^{-1} \text{ m}^{-1})(2.17 \times 10^{-10} \text{ m})(10^3 \text{ J kJ}^{-1})} \\ &\quad - 91 \text{ kJ mol}^{-1} \\ &= 640 \text{ kJ mol}^{-1} - 91 \text{ kJ mol}^{-1} \\ &= 549 \text{ kJ mol}^{-1} \end{aligned}$$

This estimate compares fairly well with the experimentally measured dissociation energy of 498 kJ mol^{-1} .

Related Problems: 25, 26

As shown in Example 3.1, our simple model for ionic bonding in KF predicts a bond dissociation energy ΔE_d (the energy required to dissociate the molecule into neutral atoms, starting from the equilibrium bond length R_e) of 549 kJ mol^{-1} , which agrees reasonably well with the experimental value of 498 kJ mol^{-1} . We can conclude that the bonding is predominantly ionic, and that the driving force for the formation of the bond is indeed the reduction of the potential energy of the system, relative to that of the separated atoms. The formation of the ions is a key intermediate step between the separated atoms and the stable ionic bond. There are several reasons why this simple model does not do a better job in calculating the bond energy. First, all bonds have some degree of covalent character, which involves electron sharing between the atoms. Second, we have assumed that each ion is a point charge. In reality, the distribution of electrons around the fluoride ion is distorted by presence of the sodium ion; this distortion is called **polarization**. The effect of the nonsymmetric shape of the charge distribution on the bond energy is accounted for in more detailed calculations.

The mechanism by which an ionic bond forms from gas-phase atoms is interesting. Unusually large reactivities are observed for collisions between alkali-metal atoms and the diatomic halogen molecules, reactivities that are much larger than could be explained using conventional theories of chemical reaction dynamics. Canadian Nobel Laureate John Polanyi proposed the following intriguing possibility. Electron transfer takes place at distances much greater than the distances at which most reactive molecular collisions occur. The strong coulombic attraction of the newly created ion pair then rapidly pulls the reactants together, where they form an ionic bond. The metal has sent its electron to “harpoon” the halogen, pulling it in with the “rope” of the Coulomb interaction. This **harpoon mechanism** has been studied extensively for a variety of systems and is generally agreed to provide a satisfactory semiquantitative description of the formation of gas-phase alkali halide molecules. You should keep in mind that although gas-phase molecules with predominantly ionic bonding can be prepared and are stable at high temperatures, most ionic bonds occur in ionic solids.

3.7 Covalent and Polar Covalent Bonding

We have discussed how ionic bonding results from electron transfer and Coulomb stabilization of the resulting ions and that the propensity of a pair of atoms to form an ionic bond is determined by the difference in their electronegativities. What kinds of bonds are formed between elements of identical or comparable electronegativities such as H_2 or CO , and what is the driving force for bond formation from separated atoms in the gas phase?

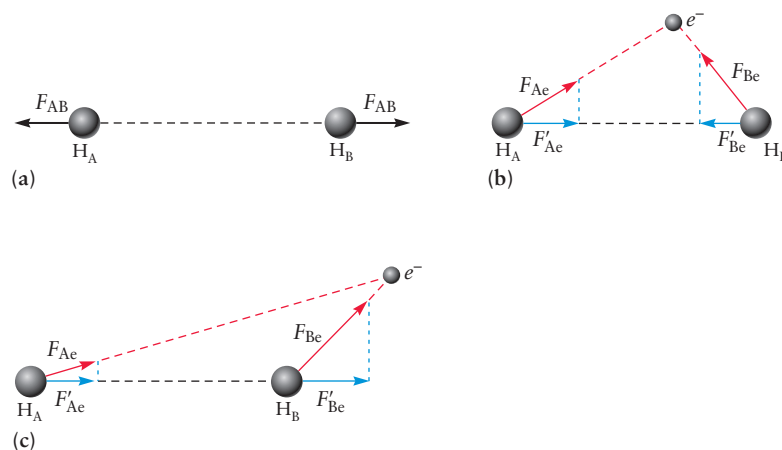
Section 3.5 provides a general argument for how a chemical bond forms from a pair of isolated atoms. We have used that argument to show that for ionic compounds the driving force is the Coulomb stabilization of the ion pair. We present below a plausibility argument to suggest why a covalent bond might form, by focusing on the *forces* acting on the nuclei due to the electrons.

Let's consider the simplest possible molecule, H_2^+ (the hydrogen molecule ion), which has only one electron. In Figure 3.11, H_A identifies the position of nucleus H_A , and H_B that of nucleus B. The distance between the two nuclei is R_{AB} . The distance between the electron and each nucleus is r_{Ae} and r_{Be} , respectively.

Consider the forces between the three particles. There is the internuclear repulsive force, $F_{AB} \propto (+Z_Ae)(+Z_Be)/R_{AB}^2$, and two electron–nuclear attractive forces, $F_{Ae} \propto (-e)(+Z_Ae)/r_{Ae}^2$ and $F_{Be} \propto (-e)(+Z_Be)/r_{Be}^2$. The internuclear repulsive

FIGURE 3.11 The forces between the particles in H_2^+ . (a) The internuclear repulsion always opposes bonding the nuclei together. (b) An electron positioned in a region that will tend to bond the nuclei together. (c) An electron positioned in a region that will tend to pull the nuclei apart.

(Adapted from G.C. Pimentel and R.D. Spratley, *Chemical Bonding Clarified through Quantum Mechanics*, Holden-Day Inc., San Francisco, 1969, Page 74.)

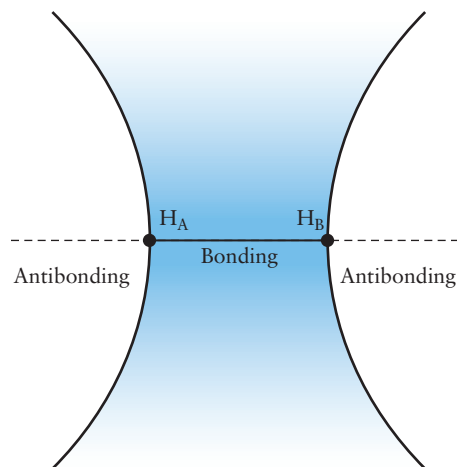


force always opposes formation of a chemical bond (Figure 3.11a), so we must identify some force that overcomes this repulsion. We need only consider the attractive forces and ask, “Over what region in space does the electron exert forces on the nuclei that will tend to pull them together?” Only the component of the attractive force directed along the internuclear axis is important. Clearly, for all positions of the electron “between” the nuclei (for example, see Fig. 3.11b), the forces F'_{Ae} and F'_{Be} will tend to pull the nuclei together. In contrast, however, when the electron is outside the internuclear region (for example, see Fig. 3.11c), it exerts a greater force on the nearer nucleus than the farther, pulling the nuclei apart. It is straightforward (for some chemists!) to calculate the net forces using Coulomb’s law and to identify a bonding and an antibonding region, the boundary of which is plotted in Figure 3.12. The curve that separates the bonding and antibonding regions approximates a hyperbola of revolution. Whenever the electron is found in the region between the two curves, the net force along the internuclear axis is attractive, encouraging bonding; when it is outside this region, the net force along the internuclear axis is repulsive, precluding bonding. This simple model is supported by experimental data for H_2^+ . Its equilibrium bond length R_e is 1.06 Å, and its bond dissociation energy ΔE_d is 255.5 kJ mol⁻¹, which is characteristic of a stable covalent bond.

This picture of covalent bonding in the H_2^+ molecular ion can be applied to other molecules. For example, the H_2 molecule is quite stable (its bond dissociation

FIGURE 3.12 Bonding and antibonding regions in a homonuclear diatomic molecule. An electron located within the bonding region will tend to pull the nuclei together, whereas an electron in the antibonding regions will tend to pull the nuclei apart.

(Adapted from G.C. Pimentel and R.D. Spratley, *Chemical Bonding Clarified through Quantum Mechanics*, Holden-Day Inc., San Francisco, 1969, Page 75.)



energy is 432 kJ mol^{-1}), yet it consists of two identical atoms. There is no possibility of a net charge transfer from one to the other to form an ionic bond. The stability of H_2 arises from the sharing of electrons between atoms in a covalent bond.

Any classical theory of chemical bond formation must explain certain properties of the chemical bond, explain trends observed in bonding, and most important, predict likely bonding properties of molecules not yet made. The most important classical descriptors of the chemical bond are the bond length, energy, order, and polarity.

Bond Lengths

For a diatomic molecule, the only relevant structural parameter is the bond length, that is, the distance between the nuclei of the two atoms. Table 3.3 lists the bond lengths of a number of diatomic molecules, expressed in units of angstroms ($1 \text{ \AA} = 10^{-10} \text{ m}$). Certain systematic trends are immediately obvious. Among the members of a group in the periodic table, bond lengths usually increase with increasing atomic number Z . The I_2 bond is longer than the F_2 bond, for example, and those of Cl_2 and Br_2 fall in line, as they should. A particularly significant result from experiment is that the length of a bond of the same type (see later) between a given pair of atoms changes little from one molecule to another. For example, C—H bond lengths in acetylsalicylic acid (aspirin, $\text{C}_9\text{H}_8\text{O}_4$) are about the same as they are in methane (CH_4), although the molecules have different structures and physical and chemical properties. Table 3.4 shows that the lengths of O—H, C—C, and C—H bonds in a number of molecules are constant to within a few percent.

Bond Energies

The stability of a molecule is determined by the energy required to dissociate the molecule into its constituent atoms. The greater the energy required, the more stable the molecule. The **bond energy**, also called the bond dissociation energy, is the

TABLE 3.3 Properties of Diatomic Molecules

Molecule	Bond Length (Å)	Bond Energy (kJ mol^{-1})
H_2	0.751	433
N_2	1.100	942
O_2	1.211	495
F_2	1.417	155
Cl_2	1.991	240
Br_2	2.286	190
I_2	2.669	148
HF	0.926	565
HCl	1.284	429
HBr	1.424	363
HI	1.620	295
ClF	1.632	252
BrF	1.759	282
BrCl	2.139	216
ICl	2.324	208
NO	1.154	629
CO	1.131	1073

T A B L E 3.4 Reproducibility of Bond Lengths

Bond	Molecule	Bond Length (Å)
O—H	H ₂ O	0.958
	H ₂ O ₂	0.960
	HCOOH	0.95
	CH ₃ OH	0.956
C—C	Diamond	1.5445
	C ₂ H ₆	1.536
	CH ₃ CHF ₂	1.540
	CH ₃ CHO	1.50
C—H	CH ₄	1.091
	C ₂ H ₆	1.107
	C ₂ H ₄	1.087
	C ₆ H ₆	1.084
	CH ₃ Cl	1.11
	CH ₂ O	1.06

energy required to break one mole of the particular bond under discussion (see Section 3.5). The bond energy is denoted by ΔE_d (“d” stands for *dissociation* here) and is measured directly in units of kJ mol^{-1} . Table 3.3 lists bond energies for selected diatomic molecules. Again, certain systematic trends with changes in atomic number are evident. Bonds generally grow weaker with increasing atomic number, as shown by the decrease in the bond energies of the hydrogen halides in the order $\text{HF} > \text{HCl} > \text{HBr} > \text{HI}$. Note, however, the unusual weakness of the bond in the fluorine molecule, F_2 . Its bond energy is significantly *smaller* than that of Cl_2 and comparable with that of I_2 . Bond strength decreases dramatically in the diatomic molecules from N_2 (942 kJ mol^{-1}) to O_2 (495 kJ mol^{-1}) to F_2 (155 kJ mol^{-1}). What accounts for this behavior? A successful theory of bonding must explain both the general trends and the reasons for particular exceptions.

Bond energies, like bond lengths, are fairly reproducible (within about 10%) from one compound to another. It is therefore possible to tabulate *average* bond energies from measurements on a series of compounds. The energy of any given bond in different compounds will deviate somewhat from those shown in Table 3.4, but in most cases, the deviations are small.

Bond Order

Sometimes, the length and energy of the bond between two specific kinds of atoms are *not* comparable among different compounds, but rather are sharply different. Table 3.5 shows the great differences in bond lengths and bond energies of carbon–carbon bonds in ethane (H_3CCH_3), ethylene (H_2CCH_2), and acetylene (HCCH). Carbon–carbon bonds from many other molecules all fit into one of the three classes given in the table (that is, some carbon–carbon bond lengths are close to 1.54 \AA , others are close to 1.34 \AA , and still others are close to 1.20 \AA). This observation confirms the existence of not one, but three types of carbon–carbon bonds. We classify these as single, double, and triple bonds, respectively, based on their bond lengths and bond dissociation energies. The longest and weakest (as in ethane) is a single bond represented by C—C; that of intermediate strength (as in ethylene) is a double bond, C=C; and the shortest and strongest (as in acetylene) is a triple bond, C≡C. In Section 3.8, the **bond order** is shown to be the number of shared electron pairs for these bonds: 1, 2, and 3, respectively.

TABLE 3.5 Three Types of Carbon–Carbon Bonds

Bond	Molecule	Bond Length (Å)	Bond Energy (kJ mol ⁻¹)
C–C	C ₂ H ₆ (or H ₃ CCH ₃)	1.536	345
C=C	C ₂ H ₄ (or H ₂ CCH ₂)	1.337	612
C≡C	C ₂ H ₂ (or HCCH)	1.204	809

Even these three types do not cover all the carbon–carbon bonds found in nature, however. In benzene (C₆H₆), the experimental carbon–carbon bond length is 1.397 Å, and its bond dissociation energy is 505 kJ mol⁻¹. This bond is intermediate between a single bond and a double bond (its bond order is 1½). In fact, the bonding in compounds such as benzene differs from that in many other compounds (see Chapter 7). Although many bonds have properties that depend primarily on the two atoms that form the bond (and thus are similar from one compound to another), bonding in benzene and related molecules, and a few other classes of compounds, depends on the nature of the whole molecule.

Multiple bonds occur between atoms other than carbon and even between unlike atoms. Some representative bond lengths are listed in Table 3.6.

Polar Covalent Bonding: Electronegativity and Dipole Moments

Laboratory measurements show that most real bonds are neither fully ionic nor fully covalent, but instead possess a mixture of ionic and covalent character. Bonds in which there is a partial transfer of charge are called **polar covalent**. This section provides an approximate description of the polar covalent bond based on the relative abilities of each atom to attract the electron pair toward its nucleus. This ability is estimated by comparing the electronegativity values for the two atoms.

On the Pauling scale (see Fig. 3.7 and Appendix F), electronegativities range from 3.98 (for fluorine) to 0.79 (for cesium). These numerical values are useful for exploring periodic trends and for making semiquantitative comparisons. They represent the average tendency of an atom to attract electrons within a molecule, based on the properties of the bond it makes in a large range of compounds.

The absolute value of the difference in electronegativity of two bonded atoms tells the degree of *polarity* in their bond. A large difference (greater than about 2.0) means that the bond is ionic and that an electron has been transferred completely or nearly completely to the more electronegative atom. A small difference (less than about 0.4) means that the bond is largely covalent, with electrons in the bond shared fairly evenly. Intermediate values of the difference signify a polar covalent bond with intermediate character. These suggested dividing points between bond types are not sharply defined (see later) and your instructor may suggest alternatives.

TABLE 3.6 Average Bond Lengths (in Å)

C–C	1.54	N–N	1.45	C–H	1.10
C=C	1.34	N=N	1.25	N–H	1.01
C≡C	1.20	N≡N	1.10	O–H	0.96
C–O	1.43	N–O	1.43	C–N	1.47
C=O	1.20	N=O	1.18	C≡N	1.16

EXAMPLE 3.2

Using Figure 3.7, arrange the following bonds in order of decreasing polarity: H—C, O—O, H—F, I—Cl, Cs—Au.

SOLUTION

The differences in electronegativity among the five pairs of atoms (without regard to sign) are 0.35, 0.00, 1.78, 0.50, and 1.75, respectively. The order of decreasing polarity is the order of decrease in this difference: H—F, Cs—Au, I—Cl, H—C, and O—O. The last bond in this listing is nonpolar.

Related Problems: 33, 34

Dipole Moments and Percent Ionic Character

A bond that is almost purely ionic, such as that of KF, can be thought of as arising from the nearly complete transfer of one electron from the electropositive to the electronegative species. KF can be described fairly accurately as K^+F^- , with charges $+e$ and $-e$ on the two ions. However, characterizing the charge distribution for a molecule such as HF, which has significant covalent character, is more complex. If we wish to approximate the bond by its ionic character, it is best described as $H^{\delta+}F^{\delta-}$, where some fraction, δ , of the full charge, e , is on each nucleus. A useful measure of the ionic character of a bond, arising from electronegativity differences, especially for diatomic molecules, is the dipole moment of the molecule. If two charges of equal magnitude and opposite sign, $+q$ and $-q$, are separated by a distance R , the **dipole moment** μ (Greek letter lowercase mu) of that charge distribution is

$$\mu = qR \quad [3.23]$$

In SI units, μ is measured in coulomb meters, an inconveniently large unit for discussing molecules. The unit most often used is the debye (D), which is related to SI units by

$$1 \text{ D} = 3.336 \times 10^{-30} \text{ C m}$$

(This apparently peculiar definition arises from the transition from electrostatic units to SI units). The debye can also be defined as the dipole moment of two charges $\pm e$ separated by 0.2082 Å. If δ is the fraction of a unit charge on each atom in a diatomic molecule ($q = e\delta$) and R is the equilibrium bond length, then

$$\mu(\text{D}) = [R(\text{Å})/0.2082 \text{ Å}] \delta \quad [3.24]$$

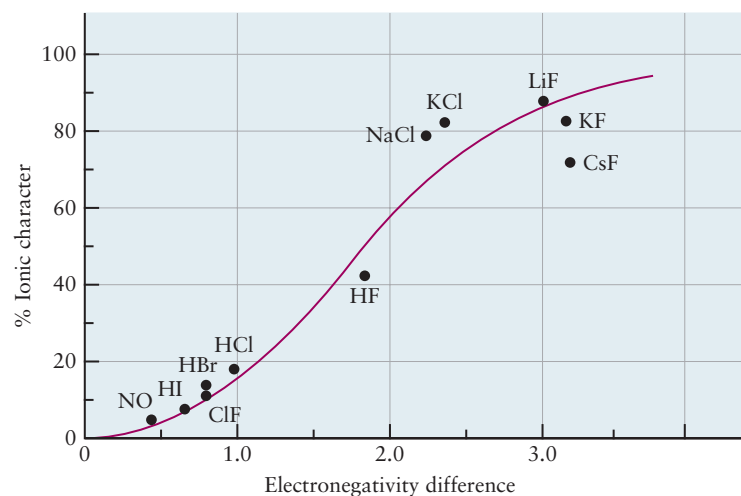
This equation can, of course, be inverted to determine the fraction ionic character from the experimental value of the dipole moment. Dipole moments are measured experimentally by electrical and spectroscopic methods and provide useful information about the nature of bonding. In HF, for example, the value of δ calculated from the dipole moment ($\mu = 1.82 \text{ D}$) and bond length ($R = 0.917 \text{ Å}$) is 0.41, substantially less than the value of 1 for a purely ionic bond. We convert δ to a “percent ionic character” by multiplying by 100% and say that the bond in HF is 41% ionic. Deviations from 100% ionic bonding occur for two reasons: (1) covalent contributions lead to electron sharing between atoms, and (2) the electronic charge distribution around one ion may be distorted by the electric field of the other ion (polarization). When polarization is extreme, regarding the ions as point charges is no longer a good approximation, and a more accurate description of the distribution of electric charge is necessary.

Table 3.7 provides a scale of ionic character for diatomic molecules, based on the definition of δ . The degree of ionic character inferred from the dipole moment is reasonably well correlated with the Pauling electronegativity differences (Fig. 3.13). A great deal of ionic character usually corresponds to a large electronegativity difference, with the more electropositive atom carrying the charge $+\delta$. There are exceptions to this general trend, however. Carbon is less electronegative than oxygen, so one would predict a charge distribution of $C^{\delta+}O^{\delta-}$ in the CO molecule. In fact, the measured dipole moment is quite small in magnitude and is oriented in the opposite direction: $C^{\delta-}O^{\delta+}$, with $\delta = 0.02$. The discrepancy arises because of the lone-pair electron density on the carbon atom (which is reflected in the formal charge of -1 carried by that atom, as discussed in Section 3.8).

TABLE 3.7 Dipole Moments of Diatomic Molecules

Molecule	Bond Length (Å)	Dipole Moment (D)	Percent Ionic Character (100δ)
H ₂	0.751	0	0
CO	1.131	0.112	2
NO	1.154	0.159	3
HI	1.620	0.448	6
ClF	1.632	0.888	11
HBr	1.424	0.828	12
HCl	1.284	1.109	18
HF	0.926	1.827	41
CsF	2.347	7.884	70
LiCl	2.027	7.129	73
LiH	1.604	5.882	76
KBr	2.824	10.628	78
NaCl	2.365	9.001	79
KCl	2.671	10.269	82
KF	2.176	8.593	82
LiF	1.570	6.327	84
NaF	1.931	8.156	88

FIGURE 3.13 Two measures of ionic character for diatomic molecules are the electronegativity difference (from Fig. 3.7) and the percent ionic character 100δ , calculated from the observed dipole moment and bond length. The curve shows that the two correlate approximately but that there are many exceptions.

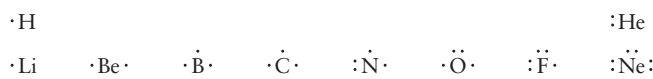


In summary, the properties of a chemical bond are often quite similar in a variety of compounds, but we must be alert for exceptions that may signal new types of chemical bonding.

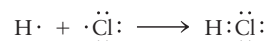
The Lewis model (see Section 3.8) represents covalent bonds as shared valence-electron pairs positioned between two nuclei, where they presumably are involved in net attractive interactions that pull the nuclei together and contribute to the strengthening of the bond. The mechanism cannot be explained by classical physics, and is examined through quantum mechanics in Chapter 6.

3.8 Lewis Diagrams for Molecules

The American chemist G. N. Lewis introduced a useful model that describes the electronic structure of the atom and provides a starting point for describing chemical bonds. The Lewis model represents the valence electrons as dots arranged around the chemical symbol for the atom; the core electrons are not shown. The first four dots are displayed singly around the four sides of the elemental symbol. If the atom has more than four valence electrons, their dots are then paired with those already present. The result is a **Lewis dot symbol** for that atom. The Lewis notation for the elements of the first two periods is



The Lewis model for covalent bonding starts with the recognition that electrons are not transferred from one atom to another in a nonionic compound, but rather are *shared* between atoms to form covalent bonds. Hydrogen and chlorine combine, for example, to form the **covalent compound** hydrogen chloride. This result can be indicated with a **Lewis diagram** for the molecule of the product, in which the valence electrons from each atom are redistributed so that one electron from the hydrogen atom and one from the chlorine atom are now shared by the two atoms. The two dots that represent this electron pair are placed between the symbols for the two elements:



The basic rule that governs Lewis diagrams is the **octet rule**: Whenever possible, the electrons in a covalent compound are distributed in such a way that each main-group element (except hydrogen) is surrounded by eight electrons (an *octet* of electrons). Hydrogen has two electrons in such a structure. When the octet rule is satisfied, the atom attains the special stability of a noble-gas shell. As a reminder, the special stability of the noble-gas configuration arises from the fact that electrons in a filled shell experience the maximum electron-nuclear attraction possible, because the number of protons (Z) is also the maximum allowed for a particular shell. In the structure for HCl shown earlier, the H nucleus has two valence electrons in its shell (like the noble gas, He), and Cl has eight (like Ar). Electrons that are shared between two atoms are counted as contributing to the filling of the valence shell of each atom.

A shared pair of electrons can also be represented by a short line (–):



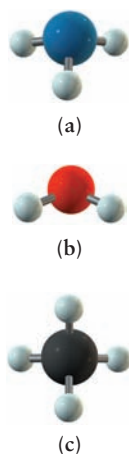
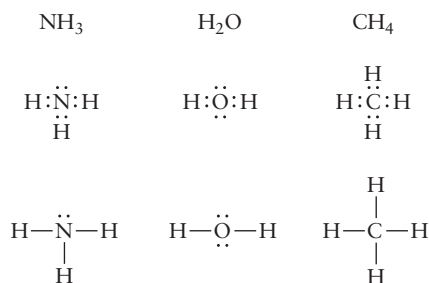


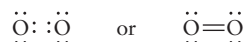
FIGURE 3.14 Molecules of three familiar substances, drawn in ball-and-stick fashion. The sizes of the balls have been reduced somewhat to show the bonds more clearly, but the relative sizes of the balls are correct. (a) Ammonia, NH₃. (b) Water, H₂O. (c) Methane, CH₄.

The unshared electron pairs around the chlorine atom in the Lewis diagram are called **lone pairs**, and they make no contribution to the bond between the atoms. Lewis diagrams of some simple covalent compounds are

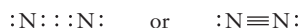


Lewis diagrams show how bonds connect the atoms in a molecule, but they do not show the spatial geometry of the molecule. The ammonia molecule is not planar, but pyramidal, for example, with the nitrogen atom at the apex. The water molecule is bent rather than straight. Three-dimensional geometries can be represented by ball-and-stick models (such as those shown in Fig. 3.14).

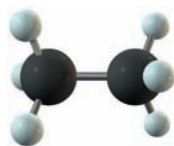
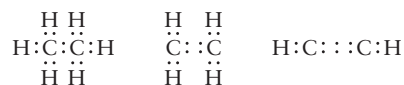
More than one pair of electrons may be shared by two atoms in a bond. For example, in the oxygen molecule, each atom has six valence electrons. Thus, for each to achieve an octet configuration, *two* pairs of electrons must be shared, making a **double bond** between the atoms:



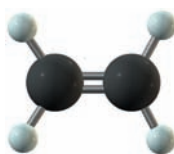
Similarly, the N₂ molecule has a **triple bond**, involving three shared electron pairs:



In contrast, the F₂ molecule has only a single bond. The number of shared electron pairs in a bond determines the order of the bond, which has already been connected with bond energy and bond length in Section 3.7. The decrease in bond order from 3 to 2 to 1 explains the dramatic reduction in the bond energies of the sequence of diatomic molecules N₂, O₂, and F₂ pointed out in Section 3.7. A carbon-carbon bond can involve the sharing of one, two, or three electron pairs. A progression from single to triple bonding is found in the hydrocarbons ethane (C₂H₆), ethylene (C₂H₄), and acetylene (C₂H₂):



Ethane, C₂H₆, can be burned in oxygen as a fuel, and if strongly heated, it reacts to form hydrogen and ethylene.



Ethylene, C₂H₄, is the largest volume organic (carbon-containing) chemical produced.

This progression corresponds to the three types of carbon-carbon bonds with properties that are related to bond order in Section 3.7 and are summarized in Tables 3.4 and 3.5.

Multiple bonding to attain an octet most frequently involves the elements carbon, nitrogen, oxygen, and to a lesser degree, sulfur. Double and triple bonds are shorter than a single bond between the same pair of atoms (see illustrative examples in Table 3.5).

Formal Charges

In **homonuclear** diatomic molecules (in which both atoms are the same, as in H₂ and Cl₂), the electrons are shared equally between the two atoms, and the covalency is nearly ideal for such molecules.

Consider, however, a molecule of carbon monoxide (CO). Its Lewis diagram has a triple bond



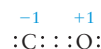


Acetylene, C_2H_2 , has a triple bond that makes it highly reactive.



Carbon monoxide, CO , is a colorless, odorless, and toxic gas produced by the incomplete burning of hydrocarbons in air. It is used in the production of elemental metals from their oxide ores.

that uses the ten valence electrons (four from the C and six from the O) and gives each atom an octet. If the six bonding electrons were shared equally, the carbon atom would own five valence electrons (one *more* than its group number) and the oxygen atom would own five electrons (one *less* than its group number). Equal sharing implies that, formally, the carbon atom must gain an electron and the oxygen atom must lose an electron. This situation is described by assigning a **formal charge** to each atom, defined as the charge an atom in a molecule would have if the electrons in its Lewis diagram were divided equally among the atoms that share them. Thus, in CO , C has a formal charge of -1 and O has a formal charge of $+1$:



Carbon monoxide is a covalent compound, and the assignment of formal charges does not make it ionic.

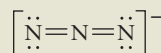
We emphasize that the equal sharing of electrons in the bonds of such **heteronuclear** diatomic molecules is without experimental basis and is simply a postulate. It has a useful purpose in cases in which two or more Lewis diagrams are possible for the same molecule. When this happens, the diagram with the smallest formal charges is the preferred one, and it generally gives the best description of bonding in the molecule. This is yet another example where simple electrostatic arguments can provide great chemical insight.

The formal charge on an atom in a Lewis diagram is simple to calculate. If the valence electrons were removed from an atom, it would have a positive charge equal to its group number in the periodic table (elements in Group VI, the chalcogens, have six valence electrons, and therefore a charge of $+6$ when those electrons are removed). From this positive charge, subtract the number of lone-pair valence electrons possessed by the atom in the Lewis diagram, and then subtract half of the number of bonding electrons it shares with other atoms:

$$\begin{aligned} \text{formal charge} &= \text{number of valence electrons} - \text{number of electrons in lone pairs} \\ &\quad - \frac{1}{2} (\text{number of electrons in bonding pairs}) \end{aligned}$$

EXAMPLE 3.3

Compute the formal charges on the atoms in the following Lewis diagram, which represents the azide ion (N_3^-):



SOLUTION

Nitrogen is in Group V. Hence, each N atom contributes 5 valence electrons to the bonding, and the negative charge on the ion contributes one more electron. The Lewis diagram correctly represents 16 electrons.

Each of the terminal nitrogen atoms has four electrons in lone pairs and four bonding electrons (which comprise a double bond) associated with it. Therefore,

$$\text{formal charge}_{(\text{terminal N})} = 5 - 4 - \frac{1}{2}(4) = -1$$

The nitrogen atom in the center of the structure has no electrons in lone pairs. Its entire octet comprises the eight bonding electrons:

$$\text{formal charge}_{(\text{central N})} = 5 - 0 - \frac{1}{2}(8) = +1$$

The sum of the three formal charges is -1 , which is the true overall charge on this polyatomic ion. Failure of this check indicates an error either in the Lewis diagram or in the arithmetic.

Related Problems: 39, 40

Drawing Lewis Diagrams

When drawing Lewis diagrams, we shall assume that the molecular “skeleton” (that is, a plan of the bonding of specific atoms to other atoms) is known. In this respect, it helps to know that hydrogen and fluorine only bond to one other atom and are always terminal atoms in Lewis diagrams. A systematic procedure for drawing Lewis diagrams can then be used, as expressed by the following rules:

1. Count the total number of valence electrons available by first using the group numbers to add the valence electrons from all the atoms present. If the species is a negative ion, *add* additional electrons to achieve the total charge. If it is a positive ion, *subtract* enough electrons to result in the total charge.
2. Calculate the total number of electrons that would be needed if each atom had its *own* noble-gas shell of electrons around it (two for hydrogen, eight for carbon and heavier elements).
3. Subtract the number in step 1 from the number in step 2. This is the number of shared (or bonding) electrons present.
4. Assign two bonding electrons (one pair) to each bond in the molecule or ion.
5. If bonding electrons remain, assign them in pairs by making some double or triple bonds. In some cases, there may be more than one way to do this. In general, double bonds form only between atoms of the elements C, N, O, and S. Triple bonds are usually restricted to C, N, or O.
6. Assign the remaining electrons as lone pairs to the atoms, giving octets to all atoms except hydrogen.
7. Determine the formal charge on each atom and write it next to that atom. Check that the formal charges add up to the correct total charge on the molecule or polyatomic ion. If more than one diagram is possible, choose the one with the smallest number of formal charges. This rule not only guides you to the best structure, it also provides a check for inadvertent errors (such as the wrong number of dots).

The use of these rules is illustrated by Example 3.4.

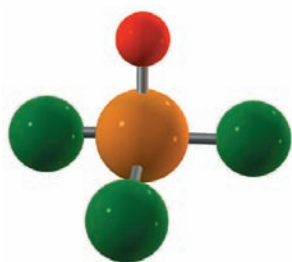


FIGURE 3.15 Phosphoryl chloride, POCl_3 , is a reactive compound used to introduce phosphorus into organic molecules in synthesis reactions. Experimental studies show that the $\text{P}=\text{O}$ bond is more like a double bond than a single bond. Lewis diagrams rationalizing the existence of the $\text{P}=\text{O}$ double bond can be constructed as an example of valence shell expansion. See the discussion on p. 90.

EXAMPLE 3.4

Write a Lewis electron dot diagram for phosphoryl chloride, POCl_3 (Fig. 3.15). Assign formal charges to all the atoms.

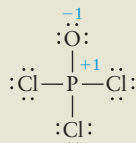
SOLUTION

The first step is to calculate the total number of valence electrons available in the molecule. For POCl_3 , it is

$$5 \text{ (from P)} + 6 \text{ (from O)} + [3 \times 7 \text{ (from Cl)}] = 32$$

Next, calculate how many electrons would be necessary if each atom were to have its own noble-gas shell of electrons around it. Because there are 5 atoms in the present case (none of them hydrogen), 40 electrons would be required. From the difference of these numbers ($40 - 32 = 8$), each atom can achieve an octet only if 8 electrons are shared between pairs of atoms. Eight electrons correspond to 4 electron pairs, so each of the four linkages in POCl_3 must be a single bond. (If the number of shared electron pairs were *larger* than the number of bonds, double or triple bonds would be present.)

The other 24 valence electrons are assigned as lone pairs to the atoms in such a way that each achieves an octet configuration. The resulting Lewis diagram is



The two singly bonded oxygen atoms carry formal charges of -1 , and the charge of the nitrogen atom is $+1$. The bond lengths should all be equal and should lie between the values given in Table 3.5 for $\text{N}-\text{O}$ (1.43 \AA) and $\text{N}=\text{O}$ (1.18 \AA). The experimentally measured value is 1.24 \AA .

Related Problems: 51, 52, 53, 54, 55, 56

Breakdown of the Octet Rule

Lewis diagrams and the octet rule are useful tools for predicting the types of molecules that will be stable under ordinary conditions of temperature and pressure. For example, we can write a simple Lewis diagram for water (H_2O),



in which each atom has a noble-gas configuration. It is impossible to do this for OH or for H_3O , which suggests that these species are either unstable or highly reactive.

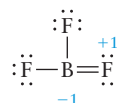
There are several situations in which the octet rule is *not* satisfied.

CASE 1: ODD-ELECTRON MOLECULES The electrons in a Lewis diagram that satisfies the octet rule must occur in pairs—bonding pairs or lone pairs. Any molecule that has an odd number of electrons cannot satisfy the octet rule. Most stable molecules have even numbers of electrons, but a few have odd numbers. An example is nitrogen oxide (NO), a stable (although reactive) molecule that is an important factor in air pollution. Nitrogen oxide has 11 electrons, and the best electron dot diagram for it is



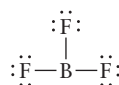
in which only the oxygen atom has a noble-gas configuration. The stability of NO contradicts the octet rule.

CASE 2: OCTET-DEFICIENT MOLECULES Some molecules are stable even though they have too few electrons to achieve an octet. For example, the standard rules for BF_3 would lead to the Lewis diagram



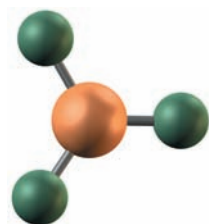
but experimental evidence strongly suggests there are no double bonds in BF_3 (fluorine never forms double bonds).

Moreover, the placement of a positive formal charge on fluorine is never correct. The following diagram avoids both problems:

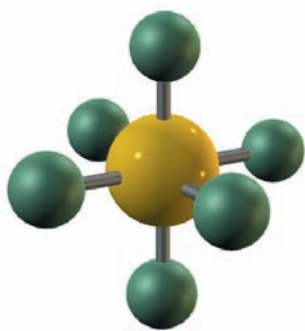


Although this Lewis diagram denies an octet to the boron atom, it does at least assign zero formal charges to all atoms.

CASE 3: VALENCE SHELL EXPANSION Lewis diagrams become more complex in compounds formed from elements in the third and subsequent periods. For example, sulfur forms some compounds that are readily described by Lewis diagrams that give closed shells to all atoms. An example is hydrogen sulfide (H_2S),



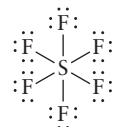
Boron trifluoride, BF_3 , is a highly reactive gas that condenses to a liquid at -100°C . Its major use is in speeding up a large class of reactions that involve carbon compounds.



Sulfur hexafluoride, SF_6 , is an extremely stable, dense, and unreactive gas. It is used as an insulator in high-voltage generators and switches.

which is analogous to water in its Lewis diagram. In sulfur hexafluoride (SF_6), however, the central sulfur is bonded to six fluorine atoms.

This molecule cannot be described by a Lewis diagram unless more than eight electrons are allowed around the sulfur atom, a process called **valence shell expansion**. The resulting Lewis diagram is



The fluorine atoms have octets, but the central sulfur atom shares a total of 12 electrons.

In the standard procedure for writing Lewis diagrams, the need for valence shell expansion is signaled when the number of shared electrons is not sufficient to place a bonding pair between each pair of atoms that are supposed to be bonded. In SF_6 , for example, 48 electrons are available, but 56 are needed to form separate octets on 7 atoms. This means that $56 - 48 = 8$ electrons would be shared. Four electron pairs are not sufficient to make even single bonds between the central S atom and the 6 terminal F atoms. In this case, we still follow rule 4 (assign one bonding pair to each bond in the molecule or ion; see earlier), even though it requires that we use more than 8 electrons. Rule 5 becomes irrelevant because there are no extra shared electrons. Rule 6 is now replaced with a new rule:

Rule 6': Assign lone pairs to the terminal atoms to give them octets. If any electrons still remain, assign them to the central atoms as lone pairs.

The effect of rule 6' is to abandon the octet rule for the central atom but preserve it for the terminal atoms.

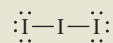
EXAMPLE 3.6

Write a Lewis diagram for the linear I_3^- (tri-iodide) ion.

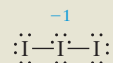
SOLUTION

There are 7 valence electrons from each iodine atom plus 1 from the overall ion charge, giving a total of 22. Because $3 \times 8 = 24$ electrons would be needed in separate octets, $24 - 22 = 2$ are shared according to the original rules. Two electrons are not sufficient to make two different bonds, however, so valence expansion is necessary.

A pair of electrons is placed in each of the two bonds, and rule 6' is used to complete the octets of the two terminal I atoms. This leaves



At this stage, 16 valence electrons have been used. The remaining 6 are placed as lone pairs on the central I atom. A formal charge of -1 then resides on this atom:



Note the valence expansion on the central atom: It shares or owns a total of 10 electrons, rather than the 8 required by adherence to the octet rule.

Related Problems: 57, 58

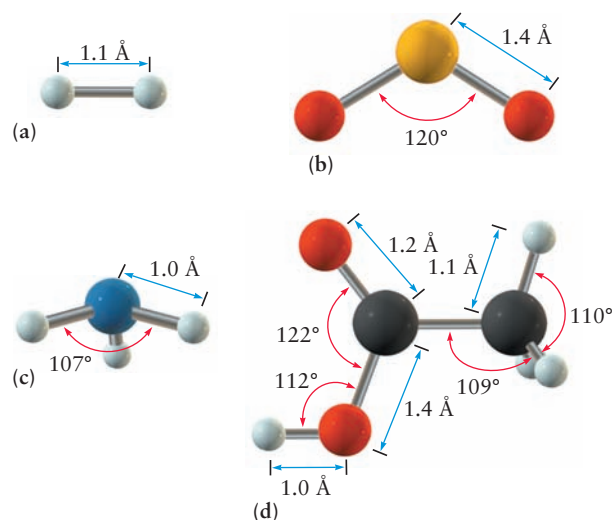
3.9 The Shapes of Molecules: Valence Shell Electron-Pair Repulsion Theory

When two molecules approach one another to begin a chemical reaction, the probability of a successful encounter can depend critically on the three-dimensional shapes and the relative orientation of the molecules, as well as on their chemical identities. Shape is especially important in biological and biochemical reactions, in which molecules must fit precisely onto specific sites on membranes and templates; drug and enzyme activity are important examples. Characterization of molecular shape is therefore an essential part of the study of molecular structure.

The structure of a stable molecule is defined by the three-dimensional arrangement of its constituent atoms. Pictorial representations of molecular structure—for example, the familiar “ball-and-stick” models and sketches—show the positions of the nuclei of the constituent atoms, but not the positions of their electrons. The electrons are responsible for the chemical bonds that hold the atomic nuclei together as the molecule. Several properties characterize the three-dimensional structure of molecules (Fig. 3.17). The bond length measures the distance between the atomic nuclei in a particular bond; summing bond lengths projected along the three Cartesian axes provides a measure of the size and shape of the molecule. Bond angles, defined as the angle between the axes of adjacent bonds, provide a more detailed view of the three-dimensional structures of molecules. Finally, the relationships between planes defined by three atoms having one atom in common (the angle between these planes is the *dihedral angle*) provide additional insights into the topology of simple molecules. However, molecules are not rigid entities, with structures that are precisely defined by the coordinates of their nuclei. Their atoms vibrate about their equilibrium positions, albeit with relatively small displacements. Average bond lengths and angles are measured by spectroscopic techniques (see Chapter 21) and x-ray diffraction (see Section 22.1).

Molecular shape or geometry is governed by energetics; a molecule assumes the geometry that gives it the lowest potential energy. Sophisticated quantum mechanical calculations consider numerous possible geometrical arrangements for a molecule, calculate the total potential energy of the molecule for each arrangement, and identify the arrangement that gives the lowest potential energy. This procedure can be mimicked within the approximate classical model described in

FIGURE 3.17 Three-dimensional molecular structures of (a) H_2 , (b) SO_2 , (c) NH_3 , and (d) $\text{C}_2\text{H}_4\text{O}_2$, showing bond lengths and angles. (Courtesy of Prof. Andrew J. Pounds, Mercer University, Macon, GA, and Dr. Mark A. Iken, Scientific Visualization Laboratory, Georgia Institute of Technology, Atlanta, GA.)



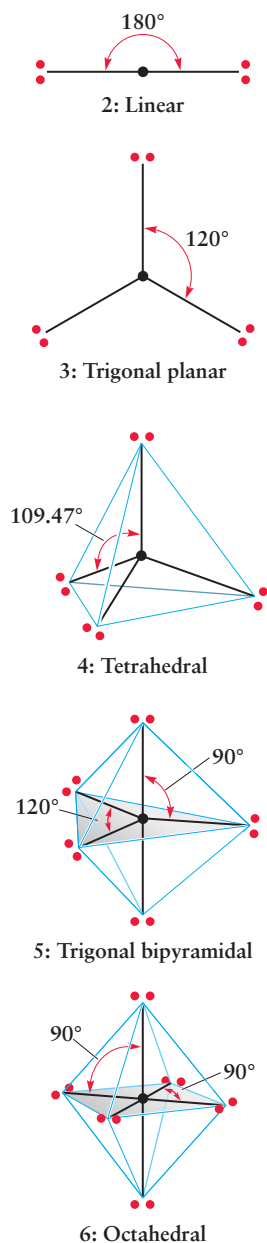


FIGURE 3.18 The positions of minimum energy for electron pairs on a sphere centered on the nucleus of an atom. The angles between the electron pairs are indicated. For two, three, and four electron pairs they are 180°, 120°, and 109.47°, respectively.

this chapter by considering numerous possible arrangements of bond angles and then identifying the one that corresponds to the lowest potential energy of the molecule. Because a covalent bond is formed by the sharing of a pair of electrons between two atoms (as described by the Lewis model in Section 3.8), changes in bond angles change the relative positions of the electron pairs around a given central atom. Electrons tend to repel each other through the electrostatic (Coulomb) repulsion between like charges and through quantum mechanical effects. Consequently, it is desirable in terms of energy for electrons to avoid each other. The VSEPR theory provides procedures for predicting molecular geometry by minimizing the potential energy due to electron-pair repulsions.

The Valence Shell Electron-Pair Repulsion Theory

The VSEPR theory starts with the fundamental idea that electron pairs in the valence shell of an atom repel each other. These include both lone pairs, which are localized on the atom and are not involved in bonding, and bonding pairs, which are shared covalently with other atoms. The electron pairs position themselves as far apart as possible to minimize their repulsions. The molecular geometry, which is defined by the positions of the *nuclei*, is then traced from the relative locations of the electron pairs.

The arrangement that minimizes repulsions naturally depends on the number of electron pairs. Figure 3.18 shows the minimum energy configuration for two to six electron pairs located around a central atom. Two electron pairs place themselves on opposite sides of the atom in a linear arrangement, three pairs form a trigonal planar structure, four arrange themselves at the corners of a tetrahedron, five define a trigonal bipyramid, and six define an octahedron. To find which geometry applies, we determine the **steric number**, SN , of the central atom, which is defined as

$$SN = \left(\begin{array}{c} \text{number of atoms} \\ \text{bonded to central atom} \end{array} \right) + \left(\begin{array}{c} \text{number of lone pairs} \\ \text{on central atom} \end{array} \right)$$

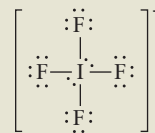
The steric number of an atom in a molecule can be determined by inspection from the Lewis diagram of the molecule.

EXAMPLE 3.7

Calculate steric numbers for iodine in IF_4^- and for bromine in BrO_4^- . These molecular ions have central I or Br surrounded by the other four atoms.

SOLUTION

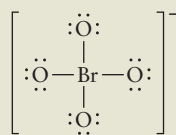
The central I^- atom has eight valence electrons.



Each F atom has seven valence electrons of its own and needs to share one of the electrons from I^- to achieve a noble-gas configuration. Thus, four of the I^- valence electrons take part in covalent bonds, leaving the remaining four to form two lone pairs. The steric number is given by

$$SN = 4 \text{ (bonded atoms)} + 2 \text{ (lone pairs)} = 6$$

In BrO_4^- , each oxygen atom needs to share two of the electrons from Br^- to achieve a noble-gas configuration.



Because this assignment accounts for all eight of the Br^- valence electrons, there are no lone pairs on the central atom and

$$SN = 4 \text{ (bonded atoms)} + 0 \text{ (lone pairs)} = 4$$

Double-bonded or triple-bonded atoms count the same as single-bonded atoms in determining the steric number. In CO_2 , for example, two double-bonded oxygen atoms are attached to the central carbon and there are no lone pairs on that atom, so $SN = 2$.

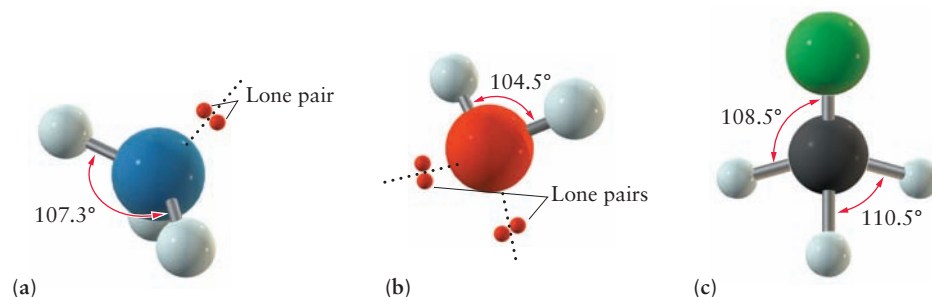
The steric number is used to predict molecular geometries. In molecules XY_n , in which there are no lone pairs on the central atom X (the simplest case),

$$SN = \text{number of bonded atoms} = n$$

The n bonding electron pairs (and therefore the outer atoms) position themselves (see Fig. 3.18) to minimize electron-pair repulsion. Thus, CO_2 is predicted (and found experimentally) to be linear, BF_3 is trigonal planar, CH_4 is tetrahedral, PF_5 is trigonal bipyramidal, and SF_6 is octahedral.

When lone pairs are present, the situation changes slightly. There can now be three different types of repulsions: (1) bonding pair against bonding pair, (2) bonding pair against lone pair, and (3) lone pair against lone pair. Consider the ammonia molecule (NH_3), which has three bonding electron pairs and one lone pair (Fig. 3.19a). The steric number is 4, and the electron pairs arrange themselves into an approximately tetrahedral structure. The lone pair is not identical to the three bonding pairs, however, so there is no reason for the electron-pair structure to be *exactly* tetrahedral. It is found that lone pairs tend to occupy more space than bonding pairs (because the bonding pairs are held closer to the central atom), so the angles of bonds opposite to them are reduced. The geometry of the *molecule*, as distinct from that of the electron pairs, is named for the sites occupied by actual atoms. The description of the molecular geometry makes no reference to lone pairs that may be present on the central atom, even though their presence affects that geometry. The structure of the ammonia molecule is thus predicted to be a trigonal pyramid in which the H—N—H bond angle is smaller than the tetrahedral angle of 109.5° . The observed structure has an H—N—H bond angle of 107.3° . The H—O—H bond angle in water, which has two lone pairs and two bonding pairs, is still smaller at 104.5° (see Fig. 3.19b).

FIGURE 3.19 (a) Ammonia (NH_3) has a pyramidal structure in which the bond angles are less than 109.5° . (b) Water (H_2O) has a bent structure with a bond angle less than 109.5° and smaller than that of NH_3 . (c) CH_3Cl has a distorted tetrahedral structure.



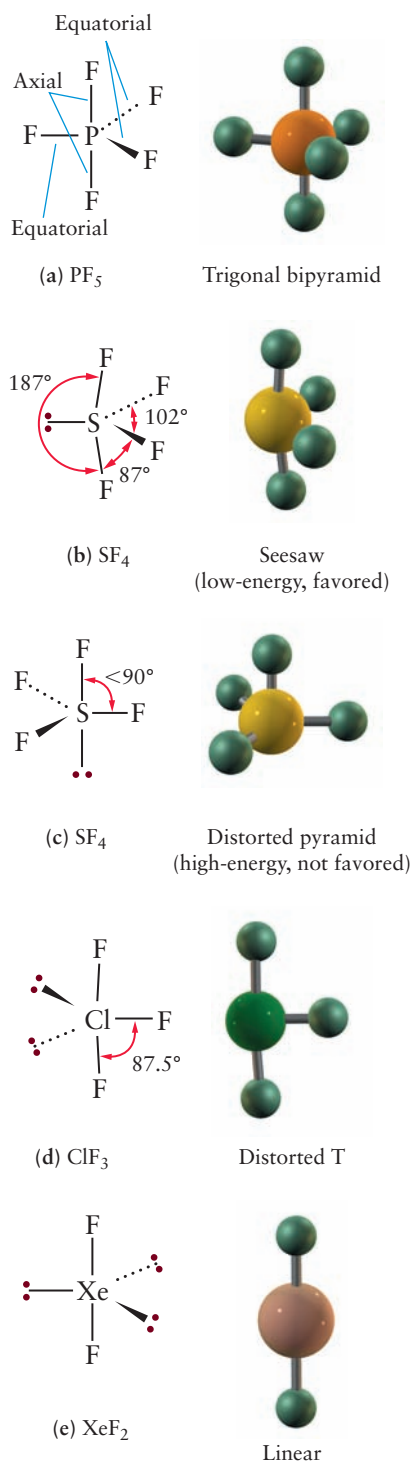


FIGURE 3.20 Molecules with steric number 5. The molecular geometry is named for the sites occupied by the *atoms*, not the underlying trigonal-bipyramidal structure of electron pairs.

A similar distortion takes place when two types of outer atoms are present. In CH_3Cl , the bonding electron pair in the $\text{C}-\text{Cl}$ bond is not the same as those in the $\text{C}-\text{H}$ bonds, so the structure is a distorted tetrahedron (see Fig. 3.19c). Because Cl is more electronegative than H , it tends to attract electrons away from the central atom, reducing the electron-pair repulsion. This allows the $\text{Cl}-\text{C}-\text{H}$ bond angles to become 108.5° , which is smaller than tetrahedral, whereas the $\text{H}-\text{C}-\text{H}$ angles become 110.5° , which is larger than tetrahedral. In effect, electropositive substituents repel other substituents more strongly than do electronegative substituents.

The fluorides PF_5 , SF_4 , ClF_3 , and XeF_2 all have steric number 5 but have different numbers of lone pairs (0, 1, 2, and 3, respectively). What shapes do their molecules have? We have already mentioned that PF_5 is trigonal bipyramidal. Two of the fluorine atoms occupy **axial** sites (See Fig. 3.20a), and the other three occupy **equatorial** sites. Because the two kinds of sites are not equivalent, there is no reason for all of the $\text{P}-\text{F}$ bond lengths to be equal. Experiment shows that the equatorial $\text{P}-\text{F}$ bond length is 1.534 \AA , which is shorter than the 1.577 \AA axial $\text{P}-\text{F}$ lengths.

SF_4 has four bonded atoms and one lone pair. Does the lone pair occupy an axial or an equatorial site? In the VSEPR theory, when electron pairs form a 90° angle to the central atom, they repel each other much more strongly than when the angle is larger. A single lone pair therefore finds a position that minimizes the number of 90° repulsions it has with bonding electron pairs. It occupies an equatorial position with two 90° repulsions (see Fig. 3.20b), rather than an axial position with three 90° repulsions (see Fig. 3.20c). The axial $\text{S}-\text{F}$ bonds are bent slightly away from the lone pair; consequently, the molecular structure of SF_4 is a distorted seesaw. A second lone pair (in ClF_3 , for example) also takes an equatorial position, leading to a distorted T-shaped molecular structure (see Fig. 3.20d). A third lone pair (in XeF_2 or I_3^- , for example) occupies the third equatorial position, and the molecular geometry is linear (see Fig. 3.20e). Table 3.8 summarizes the molecular shapes predicted by VSEPR and provides examples of each.

EXAMPLE 3.8

Predict the geometry of the following molecules and ions: (a) ClO_3^+ , (b) ClO_2^+ , (c) SiH_4 , (d) IF_5 .

SOLUTION

- The central Cl atom has all of its valence electrons (six, because the ion has a net positive charge) involved in bonds to the surrounding three oxygen atoms and has no lone pairs. Its steric number is 3. In the molecular ion, the central Cl should be surrounded by the three O atoms arranged in a trigonal planar structure.
- The central Cl atom in this ion also has a steric number of 3, comprising two bonded atoms and a single lone pair. The predicted molecular geometry is a bent molecule with an angle somewhat less than 120° .
- The central Si atom has a steric number of 4 and no lone pairs. The molecular geometry should consist of the Si atom surrounded by a regular tetrahedron of H atoms.
- Iodine has seven valence electrons, of which five are shared in bonding pairs with F atoms. This leaves two electrons to form a lone pair, so the steric number is 5 (bonded atoms) + 1 (lone pair) = 6. The structure will be based on the octahedron of electron pairs from Figure 3.18, with five F atoms and one lone pair. The lone pair can be placed on any one of the six equivalent sites and will cause the four F atoms to bend away from it toward the fifth F atom, giving the distorted structure shown in Figure 3.21.

Related Problems: 59, 60, 61, 62

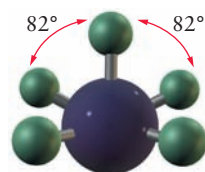


FIGURE 3.21 The structure of IF_5 . Note the distortions of $\text{F}-\text{I}-\text{F}$ bond angles from 90° because of the lone pair at the bottom (not shown).

TABLE 3.8 Molecular Shapes Predicted by the Valence Shell Electron-Pair Repulsion Theory

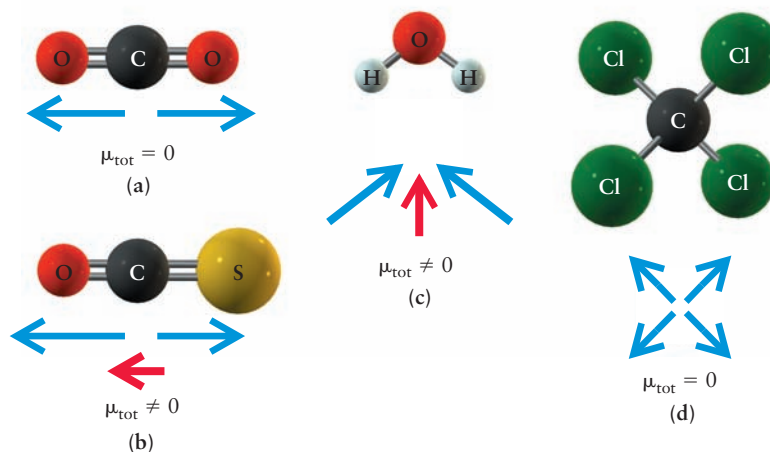
Molecule	Steric Number	Predicted Geometry	Example
AX_2	2	Linear	180° CO_2
AX_3	3	Trigonal planar	120° BF_3
AX_4	4	Tetrahedral	109.5° CF_4
AX_5	5	Trigonal bipyramidal	120° , 90° PF_5
AX_6	6	Octahedral	90° SF_6

The VSEPR theory is a simple but remarkably powerful model for predicting the geometries and approximate bond angles of molecules that have a central atom. Its success is even more remarkable when we realize that the VSEPR theory is based purely on empirical arguments, not theoretical calculations. However, it has its limitations. The VSEPR theory does not account for the fact that observed bond angles in the Group V and VI hydrides H_2S (92°), H_2Se (91°), PH_3 (93°), and AsH_3 (92°) are so far from tetrahedral (109.5°) and so close to right angles (90°).

Dipole Moments of Polyatomic Molecules

Polyatomic molecules, like the diatomic molecules considered in the previous section, may have dipole moments. Often, a good approximation is to assign a dipole moment (which is now a vector, shown as an arrow pointing from the positive charge to the negative charge) to each bond, and then obtain the total dipole moment by carrying out a vector sum of the bond dipoles. In CO_2 , for example, each $\text{C}-\text{O}$ has a bond dipole (Fig. 3.22a). However, because the dipoles are equal in magnitude and point in opposite directions, the total molecular dipole moment vanishes. In OCS , which is also linear with a central carbon atom, the $\text{C}-\text{O}$ and $\text{C}-\text{S}$ bond dipole moments have different magnitudes, leaving a net non-zero dipole moment (see Fig. 3.22b). In the water molecule (Fig. 3.22c), the two bond dipoles add vectorially to give a net molecular dipole moment. The more symmetric molecule CCl_4 , on the other hand, has no net dipole moment (see Fig. 3.22d). Even though each of the four $\text{C}-\text{Cl}$ bonds (pointing from the four corners of a tetrahedron) has

FIGURE 3.22 The total dipole moment of a molecule is obtained by vector addition of its bond dipoles. This operation is performed by adding the arrows when they lie pointing in the same direction, and subtracting the arrows if they lie pointing in different directions. (a) CO_2 . (b) OCS . (c) H_2O . (d) CCl_4 .



a dipole moment, their vector sum is zero. Molecules such as H_2O and OCS , with nonzero dipole moments, are **polar**; those such as CO_2 and CCl_4 , with no net dipole moment, are **nonpolar**, even though they contain polar bonds. Intermolecular forces differ between polar and nonpolar molecules (see discussion in Chapter 10), a fact that significantly affects their physical and chemical properties.

EXAMPLE 3.9

Predict whether the molecules NH_3 and SF_6 will have dipole moments.

SOLUTION

The NH_3 molecule has a dipole moment because the three N-H bond dipoles add to give a net dipole pointing upward to the N atom from the base of the pyramid that defines the NH_3 structure. The SF_6 molecule has no dipole moment because each S-F bond dipole is balanced by one of equal magnitude pointing in the opposite direction on the other side of the molecule.

Related Problems: 65, 66

3.10 Oxidation Numbers

The terms *ionic* and *covalent* have been used in this chapter as though they represent the complete transfer of one or more electrons from one atom to another or the equal sharing of pairs of electrons between atoms in a molecule. In reality, both types of bonding are idealizations that rarely apply exactly. To account for the transfer of electrons from one molecule or ion to another in oxidation–reduction reactions and to name different binary compounds of the same elements, it is not necessary to have detailed knowledge of the exact electron distributions in molecules, whether they are chiefly ionic or covalent. Instead, we can assign convenient fictitious charges to the atoms in a molecule and call them **oxidation numbers**, making certain that the law of charge conservation is strictly observed. Oxidation numbers are chosen so that in ionic compounds the oxidation number coincides with the charge on the ion. The following simple conventions are useful:

1. The oxidation numbers of the atoms in a neutral molecule must add up to zero, and those in an ion must add up to the charge on the ion.
2. Alkali-metal atoms are assigned the oxidation number +1, and the alkaline-earth atoms +2, in their compounds.

- Fluorine is always assigned oxidation number -1 in its compounds. The other halogens are generally assigned oxidation number -1 in their compounds, except those containing oxygen and other halogens in which the halogen can have a positive oxidation number.
- Hydrogen is assigned oxidation number $+1$ in its compounds, except in metal hydrides such as LiH , where convention 2 takes precedence and the oxidation number of hydrogen is -1 .
- Oxygen is assigned oxidation number -2 in nearly all compounds. However, there are two exceptions: In compounds with fluorine, convention 3 takes precedence, and in compounds that contain $\text{O}-\text{O}$ bonds, conventions 2 and 4 take precedence. Thus, the oxidation number for oxygen in OF_2 is $+2$; in peroxides (such as H_2O_2 and Na_2O_2), it is -1 . In superoxides (such as KO_2), the oxidation number of oxygen is $-\frac{1}{2}$.

Convention 1 is fundamental because it guarantees charge conservation: The total number of electrons must remain constant in chemical reactions. This rule also makes the oxidation numbers of the neutral atoms of all elements zero. Conventions 2 to 5 are based on the principle that in ionic compounds the oxidation number should equal the charge on the ion. Note that fractional oxidation numbers, although uncommon, are allowed and, in fact, are necessary to be consistent with this set of conventions.

With the preceding conventions in hand, chemists can assign oxidation numbers to the atoms in most compounds. Apply conventions 2 through 5 as listed previously, noting the exceptions given, and then assign oxidation numbers to the other elements in such a way that convention 1 is always obeyed. Note that convention 1 applies not only to free ions, but also to the components that make up ionic solids. Chlorine has oxidation number -1 not only as a free Cl^- ion, but in the ionic solid AgCl and in covalent CH_3Cl . It is important to recognize common ionic species (especially molecular ions) and to know the total charges they carry. Table 3.9 lists the names and formulas of many common anions. Inspection of the table reveals that several elements exhibit different oxidation numbers in different compounds. In Ag_2S , sulfur appears as the sulfide ion and has oxidation number -2 , but in Ag_2SO_4 , it appears as part of a sulfate (SO_4^{2-}) ion. In this case,

(oxidation number of S) + $[4 \times (\text{oxidation number of O})]$ = total charge on ion

$$x + [4(-2)] = -2$$

$$\text{oxidation number of S} = x = +6$$

TABLE 3.9 Formulas and Names of Some Common Anions

F^-	Fluoride	CO_3^{2-}	Carbonate
Cl^-	Chloride	HCO_3^-	Hydrogen carbonate
Br^-	Bromide	NO_2^-	Nitrite
I^-	Iodide	NO_3^-	Nitrate
H^-	Hydride	SiO_4^{4-}	Silicate
O^{2-}	Oxide	PO_4^{3-}	Phosphate
S^{2-}	Sulfide	HPO_4^{2-}	Hydrogen phosphate
O_2^{2-}	Peroxide	H_2PO_4^-	Dihydrogen phosphate
O_2^-	Superoxide	SO_3^{2-}	Sulfite
OH^-	Hydroxide	SO_4^{2-}	Sulfate
CN^-	Cyanide	HSO_4^-	Hydrogen sulfate
CNO^-	Cyanate	ClO^-	Hypochlorite
SCN^-	Thiocyanate	ClO_2^-	Chlorite
MnO_4^-	Permanganate	ClO_3^-	Chlorate
CrO_4^{2-}	Chromate	ClO_4^-	Perchlorate
$\text{Cr}_2\text{O}_7^{2-}$	Dichromate		



FIGURE 3.23 Several oxides of manganese. They are arranged in order of increasing oxidation number of the Mn, counterclockwise from the bottom left: MnO, Mn₃O₄, Mn₂O₃ and MnO₂. A compound of still higher oxidation state, Mn₂O₇, is a dark red liquid that explodes easily.

A convenient way to indicate the oxidation number of an atom is to write it directly above the corresponding symbol in the formula of the compound:



EXAMPLE 3.10

Assign oxidation numbers to the atoms in the following chemical compounds and ions: NaCl, ClO⁻, Fe₂(SO₄)₃, SO₂, I₂, KMnO₄, CaH₂.

SOLUTION

⁺¹ Na ⁻¹ Cl	From conventions 2 and 3.
⁺¹ Cl ⁻² O ⁻	From conventions 1 and 5.
⁺³ Fe ₂ ⁺⁶ (⁻² SO ₄) ₃	From conventions 1 and 5. This is solved by recognizing the presence of sulfate (SO ₄ ²⁻) groups.
⁺⁴ S ⁻² O ₂	From conventions 1 and 5.
⁰ I ₂	From convention 1. I ₂ is an element.
⁺¹ K ⁺⁷ Mn ⁻² O ₄	From conventions 1, 2, and 5.
⁺² Ca ⁻¹ H ₂	From conventions 1 and 2 (metal hydride case).

Related Problems: 71, 72

Oxidation numbers must not be confused with the formal charges on Lewis dot diagrams (see Section 3.8). They resemble formal charges to the extent that both are assigned, by arbitrary conventions, to symbols in formulas for specific purposes. The purposes differ, however. Formal charges are used solely to identify preferred Lewis diagrams. Oxidation numbers are used in nomenclature, in

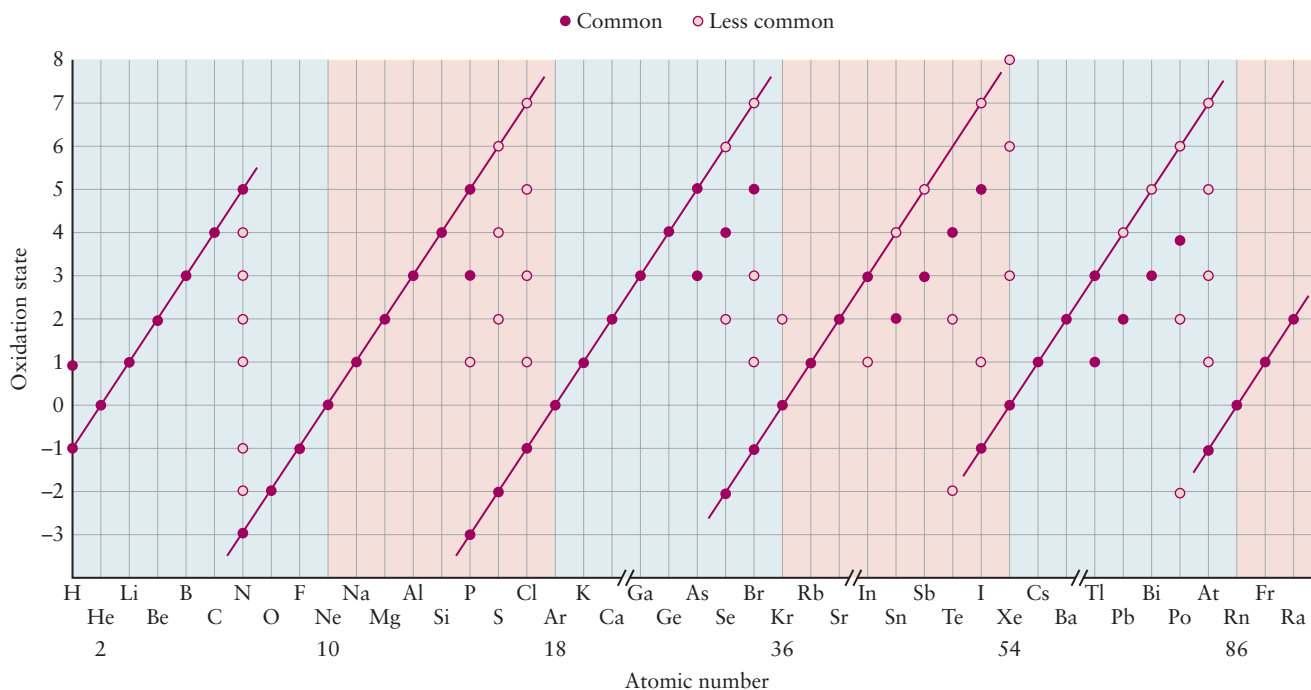


FIGURE 3.24 Important oxidation states of the main-group elements.

identifying oxidation–reduction reactions, and in exploring trends in chemical reactivity across the periodic table. Oxidation numbers are often not the same as the true charges on atoms. In KMnO_4 or Mn_2O_7 , for example, Mn has the oxidation number +7, but the actual net charge on the atom is much less than +7. A high oxidation state usually indicates significant covalent character in the bonding of that compound. The oxides of manganese with lower oxidation states (Fig. 3.23) have more ionic character.

Figure 3.24 shows the most common oxidation states of the elements of the main groups. The strong diagonal lines for these elements reflect the stability of closed electron octets. For example, the oxidation states +6 and –2 for sulfur would correspond to losing or gaining enough electrons to attain a noble gas configuration, in this case that of Ar. The octet-based Lewis model is not useful for compounds of the transition elements (see Chapter 8 for further discussion).

3.11 Inorganic Nomenclature

Sections 3.6 and 3.7 used the periodic table and the Lewis model to describe the transfer and sharing of electrons in chemical compounds. We conclude this chapter by discussing the systematic nomenclature of inorganic compounds. The definitive source for the naming of inorganic compounds is *Nomenclature of Inorganic Chemistry-IUPAC Recommendations 2005* (N. G. Connelly and T. Damhus, Sr., Eds. Royal Society of Chemistry, 2005). Of the wide variety of inorganic compounds, we discuss only simple covalent and ionic compounds and emphasize current usage.

Names and Formulas of Ionic Compounds

Ionic compounds are made from ions, bound by electrostatic forces such that the total charge of the compound is zero. The stoichiometry of an ionic compound is determined by inspection, to satisfy charge neutrality. As mentioned earlier, gas-phase ionic compounds exist, but most ionic compounds are solids in which each ion is strongly bound to a number of the nearest neighbor ions of the opposite sign. An ionic compound is named by listing the name of the cation followed by that of the anion. Ions can either be monatomic or polyatomic; the latter are also referred to as molecular ions.

A monatomic cation bears the name of the parent element. We have already encountered the sodium ion (Na^+) and the calcium ion (Ca^{2+}); ions of the other elements in Groups I and II are named in the same way. The transition metals and the metallic elements of Groups III, IV, and V differ from the Group I and II metals in that they often form several stable ions in compounds and in solution. Although calcium compounds never contain Ca^{3+} (always Ca^{2+}), the element iron forms both Fe^{2+} and Fe^{3+} , and thallium forms both Tl^+ and Tl^{3+} . When a metal forms ions of more than one charge, we distinguish them by placing a Roman numeral in parentheses after the name of the metal, indicating the charge on the ion:

Cu^+	copper(I) ion	Fe^{2+}	iron(II) ion	Sn^{2+}	tin(II) ion
Cu^{2+}	copper(II) ion	Fe^{3+}	iron(III) ion	Sn^{4+}	tin(IV) ion

An earlier method for distinguishing between such pairs of ions used the suffixes *-ous* and *-ic* added to the root of the (usually Latin) name of the metal to indicate the ions of lower and higher charge, respectively. Thus, Fe^{2+} was called the ferrous ion and Fe^{3+} the ferric ion. This method, although still used occasionally, is not recommended for systematic nomenclature and is not used in this book.

A few polyatomic cations are important in inorganic chemistry. These include the ammonium ion, NH_4^+ (obtained by adding H^+ to ammonia); the hydronium ion, H_3O^+ (obtained by adding H^+ to water); and the particularly interesting molecular ion formed by mercury, Hg_2^{2+} , the mercury(I) ion. This species must be carefully distinguished from Hg^{2+} , the mercury(II) ion. The Roman numeral I in parentheses means, in this case, that the average charge on each of the two mercury atoms is +1. Compounds with the empirical formulas HgCl and HgBr have molecular formulas Hg_2Cl_2 and Hg_2Br_2 , respectively.

A monatomic anion is named by adding the suffix *-ide* to the first portion of the name of the element. Thus, *chlorine* becomes the *chloride* ion, and *oxygen* becomes the *oxide* ion. The other monatomic anions of Groups V, VI, and VII are named similarly. Many polyatomic anions exist, and the naming of these species is more complex. The names of the oxoanions (each contains oxygen in combination with a second element) are derived by adding the suffix *-ate* to the stem of the name of the second element. Some elements form two oxoanions. The *-ate* ending is then used for the oxoanion with the larger number of oxygen atoms (such as NO_3^- , *nitrate*), and the ending *-ite* is added for the name of the anion with the smaller number (such as NO_2^- , *nitrite*). For elements such as chlorine, which form more than two oxoanions, we use the additional prefixes *per-* (largest number of oxygen atoms) and *hypo-* (smallest number of oxygen atoms). An oxoanion that contains hydrogen as a third element includes that word in its name. For example, the HCO_3^- oxoanion is called the hydrogen carbonate ion in preference to its common (nonsystematic) name, “bicarbonate ion,” and HSO_4^- , often called “bisulfate ion,” is better designated as the hydrogen sulfate ion. Table 3.9 lists some of the most important anions. It is important to be able to recognize and name the ions from that table, bearing in mind that the electric charge is an essential part of the formula.

It is customary (and recommended) to name ionic compounds (salts) using the Roman numeral notation, based on group numbers or oxidation states. CuSO_4 is copper(I) sulfate, $\text{Fe}(\text{NO}_3)_2$ is iron(II) nitrate and KMnO_4 is potassium permanganate, the Roman numeral being omitted in the last example because potassium cations always carry only +1 charge.

The composition of an ionic compound is determined by overall charge neutrality. The total positive charge on the cations must exactly balance the total negative charge on the anions. The following names and formulas of ionic compounds illustrate this point:

Tin(II) bromide	One 2+ cation, two 1− anions	SnBr_2
Potassium permanganate	One 1+ cation, one 1− anion	KMnO_4
Ammonium sulfate	Two 1+ cations, one 2− anion	$(\text{NH}_4)_2\text{SO}_4$
Iron(II) dihydrogen phosphate	One 2+ cation, two 1− anions	$\text{Fe}(\text{H}_2\text{PO}_4)_2$

EXAMPLE 3.11

Give the chemical formulas of (a) calcium cyanide and (b) copper(II) phosphate.

SOLUTION

- (a) Calcium cyanide is composed of Ca^{2+} and CN^- . For the overall charge to be 0, there must be two CN^- for each Ca^{2+} . Thus, the chemical formula of calcium cyanide is $\text{Ca}(\text{CN})_2$.
- (b) The ions present in copper(II) phosphate are Cu^{2+} and PO_4^{3-} . To ensure charge neutrality, there must be three Cu^{2+} (total charge +6) and two PO_4^{3-} (total charge −6) per formula unit. Thus, the chemical formula of copper(II) phosphate is $\text{Cu}_3(\text{PO}_4)_2$.

Related Problems: 77, 78

TABLE 3.10
Prefixes Used for Naming
Binary Covalent Compounds

Number	Prefix
1	<i>mono-</i>
2	<i>di-</i>
3	<i>tri-</i>
4	<i>tetra-</i>
5	<i>penta-</i>
6	<i>hexa-</i>
7	<i>hepta-</i>
8	<i>octa-</i>
9	<i>nona-</i>
10	<i>deca-</i>

Naming Binary Covalent Compounds

How do we name nonionic (covalent) compounds? If a pair of elements forms only one compound, begin with the name of the element that appears first in the chemical formula, followed by the second element, with the suffix *-ide* added to its root. This is analogous to the naming of ionic compounds. Just as NaBr is sodium bromide, so the following names designate typical covalent compounds:

HBr	hydrogen bromide
BeCl ₂	beryllium chloride
H ₂ S	hydrogen sulfide
BN	boron nitride

Many well-established nonsystematic names continue to be used (even the strictest chemist does not call water “hydrogen oxide”!) They include:

H ₂ O	water
NH ₃	ammonia
N ₂ H ₄	hydrazine
PH ₃	phosphine
AsH ₃	arsine
COCl ₂	phosgene

If a pair of elements forms more than one compound, two methods can be used to distinguish between them:

1. Use Greek prefixes (Table 3.10) to specify the number of atoms of each element in the molecular formula of the compound (*di-* for two, *tri-* for three, and so forth). If the compound is a solid without well-defined molecules, name the empirical formula in this way. The prefix for one (*mono-*) is omitted, except in the case of carbon monoxide.
2. Write the oxidation number of the first-named element in Roman numerals and place it in parentheses after the name of that element.

Applying the two methods to the oxides of nitrogen gives

N ₂ O	dinitrogen oxide	nitrogen(I) oxide
NO	nitrogen oxide	nitrogen(II) oxide
N ₂ O ₃	dinitrogen trioxide	nitrogen(III) oxide
NO ₂	nitrogen dioxide	nitrogen(IV) oxide
N ₂ O ₄	dinitrogen tetraoxide	nitrogen(IV) oxide
N ₂ O ₅	dinitrogen pentaoxide	nitrogen(V) oxide

The first method has some advantages over the second and is recommended. It distinguishes between NO₂ (nitrogen dioxide) and N₂O₄ (dinitrogen tetraoxide), two distinct compounds that would both be called nitrogen(IV) oxide under the second system of nomenclature. Two of these oxides have common (nonsystematic) names that may be encountered elsewhere: N₂O is often called nitrous oxide, and NO is called nitric oxide.

CHAPTER SUMMARY

The classical description of chemical bonding provides the conceptual framework and language used by all chemists in their daily work. The classical description is based largely on simple electrostatics. We can understand a great deal about the nature of the chemical bond by examining the forces and potential energy of interaction between the electrons and the nuclei, which are governed by Coulomb’s

law. Potential energy diagrams will help you understand the interactions between and among electrons and nuclei that determine a wide variety of properties of atoms and molecules. We encourage you to learn to interpret and use these diagrams, because they will appear over and over again in this text and in subsequent chemistry courses.

The periodic table organizes the elements in a way that shows similar physical and chemical properties of groups and the variations of these properties across periods. Examination of periodic trends in ionization energies suggests that the electrons in an atom are organized in a series of concentric shells around the nucleus. These trends can be explained by the decreased electron–nuclear attraction in successive shells, as well as the screening or shielding of the outer electrons from the full nuclear charge by the inner electrons. Electron affinity is a measure of the tendency of an atom to form a stable anion. Periodic trends in electron affinities are explained in the same way as those observed for ionization energies.

Chemical bonds are generally classified according to the amount of charge separation in the bond. The character of a particular chemical bond—ionic, covalent, or polar covalent—can be predicted by comparing the electronegativities of the atoms involved. The electronegativity of an element is a measure of its relative propensity to attract electrons in a chemical bond. Elements with large ionization energies and large electron affinities tend to attract electrons, whereas those with small ionization energies and small electron affinities tend to donate electrons. Bonds formed between two atoms with large electronegativity differences tend to be ionic, whereas those formed between those atoms with nearly the same electronegativities tend to be covalent. Most bonds are somewhere in between—that is, they are polar covalent.

The arrangements of atoms in a molecule and the three-dimensional shape of a molecule can be rationalized or predicted using the Lewis dot model and the VSEPR theory, respectively. The Lewis model predicts the most likely arrangement of atoms in a molecule, the existence of multiple bonds, and charge distributions using the idea of formal charges. It is based on the idea that the representative elements (except hydrogen) are most stable with a filled octet of valence electrons (hydrogen only needs two). This stability can be understood from the empirical fact that eight electrons is the maximum each valence shell can hold, and that each electron added to a shell decreases the energy of the atom via the Coulomb interaction with the nucleus. Each element is represented by its chemical symbol, with its valence electrons arranged as dots. The atoms are combined in a way that creates the maximum number of filled octets around each representative element and a pair of electrons around each hydrogen atom. The VSEPR theory predicts the three-dimensional structures of molecules by arranging electron pairs to minimize their mutual repulsion.

Oxidation numbers are used to track the gain and loss of electrons in chemical reactions and are used in the systematic naming of inorganic compounds.

The concepts introduced in this chapter provide a sound basis for understanding a great deal of chemistry. A firm understanding of these concepts is essential for you to conduct and interpret experiments, read the chemical literature, and develop a deeper understanding based on quantum mechanics, which we develop in Chapters 4–6.

CUMULATIVE EXERCISE

Oxides and Peroxides

Consider the three compounds KO_2 , BaO_2 , and TiO_2 . Each contains two oxygen atoms per metal atom, but the oxygen occurs in different forms in the three compounds.

- (a) The oxygen in TiO_2 occurs as O^{2-} ions. What is the Lewis dot symbol for this ion? How many valence electrons does this ion have? What is the chemical name for TiO_2 ?

- (b) Recall that Group II elements form stable $2+$ ions. Using Table 3.9, identify the oxygen-containing ion in BaO_2 and give the name of the compound. Draw a Lewis diagram for the oxygen-containing ion, showing formal charge. Is the bond in this ion a single or a double bond?
- (c) Recall that Group I elements form stable $1+$ ions. Using Table 3.9, identify the oxygen-containing ion in KO_2 and give the name of the compound. Show that the oxygen-containing ion is an odd-electron species. Draw the best Lewis diagram you can for it.

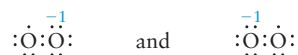
Answers

- (a) The ion $:\ddot{\text{O}}:^{2-}$ has eight valence electrons (an octet). TiO_2 is titanium(IV) oxide.
- (b) The ion in BaO_2 must be the peroxide ion (O_2^{2-}), and the compound is barium peroxide. The Lewis diagram for the peroxide ion is



and the O—O bond is a single bond.

- (c) The ion in KO_2 must be the superoxide ion (O_2^-), and the compound is potassium superoxide. The superoxide ion has 13 valence electrons. The best Lewis diagram is a pair of resonance diagrams



in which only one of the oxygen atoms attains an octet electron configuration.

CHAPTER REVIEW

- The periodic table organizes the elements into groups with similar physical and chemical properties.
- The physical structure of the atom, as determined by experiments, is summarized in the planetary model. In an atom with atomic number Z , there are Z electrons moving around a dense nucleus, which has positive charge $+Ze$.
- The physical structure of the atom can be understood using Coulomb's law, which describes the forces between each electron and the nucleus and between the electrons in many-electron atoms.
- Ionization energy is the minimum energy required to remove an electron from an atom and place it infinitely far away with zero kinetic energy.
- Periodic trends in ionization energies suggested the shell model of the atom in which electrons occupy concentric shells located at increasing distances from the nuclei.
- Electron affinity is the energy released when an electron attaches to an atom to form a stable anion; by convention, it is reported as a positive quantity.
- Ionization energies and electron affinities can be understood in terms of the effective potential energy of interaction between each electron and the nucleus, derived from Coulomb's law.
- Electronegativity is the relative tendency of atoms in a chemical bond to attract electrons. Mulliken's scale is based on a simple physical model for a gas-phase atom that averages the ionization energy and the electron affinity; Pauling's scale averages this tendency over a variety of bonding partners.
- Chemists generally distinguish among three types of chemical bonds based on the electronegativity differences between the atoms: covalent (nearly identical electronegativities), ionic (greatly different electronegativities), and polar

covalent (anything in between these extremes). The percent ionic character can be determined by measuring experimentally the dipole moments of molecules.

- The driving force for the formation of a chemical bond from a pair of atoms in the gas phase is the reduction in the total energy of the system. Bond formation is accompanied by a reduction in potential energy, relative to the free atoms. For ionic bonds, this is calculated easily using Coulomb's law.
- The formation of a covalent chemical bond can be understood classically by examining the forces between the electrons and the nuclei to discover bonding and antibonding regions in the locations of the electrons.
- The virial theorem relates the changes in average total energy in the formation of both ionic and covalent chemical bonds to the changes in the average potential energy and average kinetic energy.
- Important properties of the chemical bond include its length, dissociation energy, order, and dipole moment.
- Bond lengths and bond energies of the same type (for example, CH *single* bonds) are remarkably similar in all compounds in which they appear. Bond lengths decrease and bond dissociation energies increase for double and triple bonds formed between the same pairs of atoms.
- Lewis dot diagrams are a tool for predicting the most likely connectivity, or arrangement of bonds between atoms, in a molecule. They are also useful for predicting the existence of multiple bonds and for determining qualitatively the distribution of charges in a molecule.
- The VSEPR theory predicts the three-dimensional shapes of molecules. It is based on simple electrostatics—electron pairs in a molecule will arrange themselves in such a way as to minimize their mutual repulsion. The steric number determines the geometry of the electron pairs (linear, trigonal pyramidal, tetrahedral, and so forth), whereas the molecular geometry is determined by the arrangement of the nuclei and may be less symmetric than the geometry of the electron pairs.
- Oxidation numbers are assigned to elements to name inorganic compounds, to keep track of electrons in electron transfer (oxidation-reduction) reactions, and to explore trends in chemical reactivity across the periodic table.

CONCEPTS & SKILLS

After studying this chapter and working the problems that follow, you should be able to:

1. Describe the structure of the periodic table, and predict chemical and physical properties of an element based on those of others in its group and period (Section 3.1, Problems 1–4).
2. Calculate the force and potential energy between a pair of charged particles, and predict the direction of relative motion of the particles (Section 3.2, Problems 5–8).
3. Describe the trends in ionization energy across the periodic table (Section 3.3, Problems 9 and 10).
4. Describe the shell structure of the atom, and represent valence shell electrons of an atom by its Lewis electron dot symbol (Section 3.3, Problems 11 and 12).
5. Describe the trends in electron affinity and electronegativity across the periodic table (Section 3.4, Problems 13–16).
6. Correlate the shape of the effective potential energy function between the nuclei with trends in the bond length and bond energies of diatomic molecules (Section 3.5, Problems 17–20).

- Use the principle of charge balance and Lewis diagrams to write chemical formulas for ionic compounds (Section 3.6, Problems 21–24).
- Calculate the energy of dissociation of gaseous diatomic ionic compounds into neutral atoms and ions (Section 3.6, Problems 25 and 26).
- Describe the relations among bond order, length, and energy (Section 3.7, Problems 27–32).
- Estimate the percent ionic character of a bond from its dipole moment (Section 3.7, Problems 33–38).
- Given a molecular formula, draw a Lewis diagram for the molecule and assign formal charge (Section 3.8, Problems 39–50).
- Assign formal charges and identify resonance diagrams for a given Lewis diagram (Section 3.8, Problems 51–58).
- Predict the geometries of molecules by use of the VSEPR model (Section 3.9, Problems 59–64).
- Determine whether a polyatomic molecule is polar or nonpolar (Section 3.9, Problems 65–70).
- Assign oxidation numbers to atoms in compounds (Section 3.10, Problems 71 and 72).
- Name inorganic compounds, given their chemical formulas, and write chemical formulas for inorganic compounds (Section 3.11, Problems 73–84).

KEY EQUATIONS

Coulomb's law is the conceptual basis of this chapter. All the key equations are devoted to stating this law and using it to describe the physical structure of atoms (their ionization energies, electron affinities, and electronegativities) and the stabilization of chemical bonds.

$$F(r) = \frac{q_1 q_2}{4\pi\epsilon_0 r^2} \quad \text{Section 3.2}$$

$$V(r) = \frac{q_1 q_2}{4\pi\epsilon_0 r} \quad \text{Section 3.2}$$

$$V(r) = -\frac{Ze^2}{4\pi\epsilon_0 r} \quad \text{Section 3.2}$$

$$F_{\text{coul}} = -\frac{d}{dr} \left(-\frac{Ze^2}{4\pi\epsilon_0 r} \right) = \frac{d}{dr} \left(\frac{Ze^2}{4\pi\epsilon_0 r} \right) = -\frac{Ze^2}{4\pi\epsilon_0 r^2} \quad \text{Section 3.2}$$

$$E = \frac{1}{2} m_e v^2 - \frac{Ze^2}{4\pi\epsilon_0 r} \quad \text{Section 3.2}$$

$$V_{\text{eff}}(r) = -\frac{Z_{\text{eff}} e^2}{4\pi\epsilon_0 r} \quad \text{Section 3.3}$$

$$\text{EN (Mulliken)} \propto \frac{1}{2} (IE_1 + EA) \quad \text{Section 3.4}$$

$$\chi_A - \chi_B = 0.102\Delta^{1/2} \quad \text{Section 3.4}$$

$$V(R_{12}) = Ae^{-\alpha R_{12}} - B \left(\frac{(e)(-e)}{R_{12}} \right) + \Delta E_\infty \quad \text{Section 3.6}$$

$$\Delta E_d \approx \frac{q_1 q_2}{4\pi\epsilon_0 R_c} \cdot \frac{N_A}{10^3} - \Delta E_\infty \quad \text{Section 3.6}$$

PROBLEMS

Answers to problems whose numbers are boldface appear in Appendix G. Problems that are more challenging are indicated with asterisks.

The Periodic Table

1. Before the element scandium was discovered in 1879, it was known as “eka-boron.” Predict the properties of scandium from averages of the corresponding properties of its neighboring elements in the periodic table. Compare your predictions with the observed values in Appendix F.

Element	Symbol	Melting Point (°C)	Boiling Point (°C)	Density (g cm ⁻³)
Calcium	Ca	839	1484	1.55
Titanium	Ti	1660	3287	4.50
Scandium	Sc	?	?	?

2. The element technetium (Tc) is not found in nature but has been produced artificially through nuclear reactions. Use the data for several neighboring elements in the table below to estimate the melting point, boiling point, and density of technetium. Compare your predictions with the observed values in Appendix F.

Element	Symbol	Melting Point (°C)	Boiling Point (°C)	Density (g cm ⁻³)
Manganese	Mn	1244	1962	7.2
Molybdenum	Mo	2610	5560	10.2
Rhenium	Re	3180	5627	20.5
Ruthenium	Ru	2310	3900	12.3

3. Use the group structure of the periodic table to predict the empirical formulas for the binary compounds that hydrogen forms with the elements antimony, bromine, tin, and selenium.
4. Use the group structure of the periodic table to predict the empirical formulas for the binary compounds that hydrogen forms with the elements germanium, fluorine, tellurium, and bismuth.

Forces and Potential Energy in Atoms

5. An electron is located at the origin of the coordinates, and a second electron is brought to a position 2 Å from the origin.
- Calculate the force between the two electrons.
 - Calculate the potential energy of the two electrons.
6. A gold nucleus is located at the origin of coordinates, and an electron is brought to a position 2 Å from the origin.
- Calculate the force between the gold nucleus and the electron.
 - Calculate the potential energy of the gold nucleus and the electron.

7. The electron in a hydrogen atom is initially at a distance 1 Å from the proton, and then moves to a distance 0.5 Å from the proton.
- Calculate the change in the force between the proton and the electron.
 - Calculate the change in the potential energy between the proton and the electron.
 - Calculate the change in the velocity of the electron.
8. A gold nucleus is located at the origin of coordinates, and a helium nucleus initially 2 Å from the origin is moved to a position 1 Å from the origin.
- Calculate the change in the force between the two nuclei.
 - Calculate the change in the potential energy of the two nuclei.
 - Calculate the change in the velocity of the helium nucleus.

Ionization Energies and the Shell Model of the Atom

9. For each of the following pairs of atoms, state which you expect to have the higher first ionization energy: (a) Rb or Sr; (b) Po or Rn; (c) Xe or Cs; (d) Ba or Sr.
10. For each of the following pairs of atoms, state which you expect to have the higher first ionization energy: (a) Bi or Xe; (b) Se or Te; (c) Rb or Y; (d) K or Ne.
11. Use the data in Table 3.1 to plot the logarithm of ionization energy versus the number of electrons removed for Be. Describe the electronic structure of the Be atom.
12. Use the data in Table 3.1 to plot the logarithm of ionization energy versus the number of electrons removed for Ne. Describe the electronic structure of the Ne atom.

Electronegativity: The Tendency of Atoms to Attract Electrons

13. For each of the following pairs of atoms, state which you expect to have the greater electron affinity: (a) Xe or Cs; (b) Pm or F; (c) Ca or K; (d) Po or At.
14. For each of the following pairs of atoms, state which you expect to have the higher electron affinity: (a) Rb or Sr; (b) I or Rn; (c) Ba or Te; (d) Bi or Cl.
15. Ignoring tables of electronegativity values and guided only by the periodic table, arrange these atoms in order of increasing electronegativity: O, F, S, Si, K. Briefly explain your reasoning.
16. Ignoring tables of electronegativity values and guided only by the periodic table, arrange these atoms in order of increasing electronegativity: S, Cl, Sb, Se, In. Briefly explain your reasoning.

Forces and Potential Energy in Molecules: Formation of Chemical Bonds

17. We will see later that H₂ has equilibrium bond length of 0.751 Å and bond dissociation energy of 433 kJ mol⁻¹, whereas F₂ has equilibrium bond length of 1.417 Å and

bond dissociation energy of 155 kJ mol^{-1} . On the same graph show qualitative sketches of the effective potential energy curve V_{eff} for H_2 and F_2 . (*Hint:* Convert the bond energy to electron volts (eV) before preparing your graphs.)

18. We will see later that N_2 has equilibrium bond length of 1.100 \AA and bond dissociation energy of 942 kJ mol^{-1} , whereas O_2 has equilibrium bond length of 1.211 \AA and bond dissociation energy of 495 kJ mol^{-1} . On the same graph show qualitative sketches of the effective potential energy curve V_{eff} for N_2 and O_2 . (*Hint:* Convert the bond energy to electron volts (eV) before preparing your graphs.)
19. We will see later that HF has equilibrium bond length of 0.926 \AA and bond dissociation energy of 565 kJ mol^{-1} . Compare the effective potential curve for HF with those for H_2 and F_2 in Problem 17.
20. We will see later that NO has equilibrium bond length of 1.154 \AA and bond dissociation energy of 629 kJ mol^{-1} . Compare the effective potential curve for NO with those for N_2 and O_2 in Problem 18.

Ionic Bonding

21. For each of the following atoms or ions, state the total number of electrons, the number of valence electrons, and the number of core electrons.
(a) Rn (b) Sr^+ (c) Se^{2-} (d) Sb^-
22. For each of the following atoms or ions, state the total number of electrons, the number of valence electrons, and the number of core electrons.
(a) Ra^{2+} (b) Br (c) Bi^{2-} (d) Ga^+
23. Use the data in Figure 3.4 and Table 3.2 to calculate the energy changes (ΔE) for the following pairs of reactions:
(a) $\text{K}(g) + \text{Cl}(g) \longrightarrow \text{K}^+(g) + \text{Cl}^-(g)$
 $\text{K}(g) + \text{Cl}(g) \longrightarrow \text{K}^-(g) + \text{Cl}^+(g)$
(b) $\text{Na}(g) + \text{Cl}(g) \longrightarrow \text{Na}^+(g) + \text{Cl}^-(g)$
 $\text{Na}(g) + \text{Cl}(g) \longrightarrow \text{Na}^-(g) + \text{Cl}^+(g)$
Explain why K^+Cl^- and Na^+Cl^- form in preference to K^-Cl^+ and Na^-Cl^+ .
24. Use the data in Figure 3.4 and Table 3.2 to calculate the energy changes (ΔE) for the following pairs of reactions:
(a) $\text{Na}(g) + \text{I}(g) \longrightarrow \text{Na}^+(g) + \text{I}^-(g)$
 $\text{Na}(g) + \text{I}(g) \longrightarrow \text{Na}^-(g) + \text{I}^+(g)$
(b) $\text{Rb}(g) + \text{Br}(g) \longrightarrow \text{Rb}^+(g) + \text{Br}^-(g)$
 $\text{Rb}(g) + \text{Br}(g) \longrightarrow \text{Rb}^-(g) + \text{Br}^+(g)$
Explain why Na^+I^- and Rb^+Br^- form in preference to Na^-I^+ and Rb^-Br^+ .
25. In a gaseous KCl molecule, the internuclear distance is $2.67 \times 10^{-10} \text{ m}$. Using data from Appendix F and neglecting the small, short-range repulsion between the ion cores of K^+ and Cl^- , estimate the dissociation energy of gaseous KCl into K and Cl atoms (in kJ mol^{-1}).
26. In a gaseous RbF molecule, the bond length is $2.274 \times 10^{-10} \text{ m}$. Using data from Appendix F and neglecting the small, short-range repulsion between the ion cores of Rb^+ and F^- , estimate the dissociation energy of gaseous RbF into Rb and F atoms (in kJ mol^{-1}).

Covalent and Polar Covalent Bonding

27. The bond lengths of the X–H bonds in NH_3 , PH_3 , and SbH_3 are 1.02 , 1.42 , and 1.71 \AA , respectively. Estimate the length of the As–H bond in AsH_3 , the gaseous compound that decomposes on a heated glass surface in Marsh's test for arsenic. Which of these four hydrides has the weakest X–H bond?
28. Arrange the following covalent diatomic molecules in order of the lengths of the bonds: BrCl, ClF, IBr. Which of the three has the weakest bond (the smallest bond energy)?
29. The bond length in H–I (1.62 \AA) is close to the sum of the atomic radii of H (0.37 \AA) and I (1.33 \AA). What does this fact indicate about the polarity of the bond?
30. The bond length in F_2 is 1.417 \AA , instead of twice the atomic radius of F, which is 1.28 \AA . What can account for the unexpected length of the F–F bond?
31. Use electronegativity values to arrange the following bonds in order of decreasing polarity: N–O, N–N, N–P, and C–N.
32. Use electronegativity values to rank the bonds in the following compounds from least ionic to most ionic in character: IF, ICl, ClF, BrCl, and Cl_2 .
33. Ionic compounds tend to have higher melting and boiling points and to be less volatile (that is, have lower vapor pressures) than covalent compounds. For each of the following pairs, use electronegativity differences to predict which compound has the higher vapor pressure at room temperature.
(a) Cl_4 or KI
(b) BaF_2 or OF_2
(c) SiH_4 or NaH
34. For each of the following pairs, use electronegativity differences to predict which compound has the higher boiling point.
(a) MgBr_2 or PBr_3
(b) OsO_4 or SrO
(c) Cl_2O or Al_2O_3
35. Estimate the percent ionic character of the bond in each of the following diatomic molecules, based on the dipole moment.

	Bond Length (Å)	Dipole Moment (D)
ClO	1.573	1.239
KI	3.051	10.82
TiCl	2.488	4.543
InCl	2.404	3.79

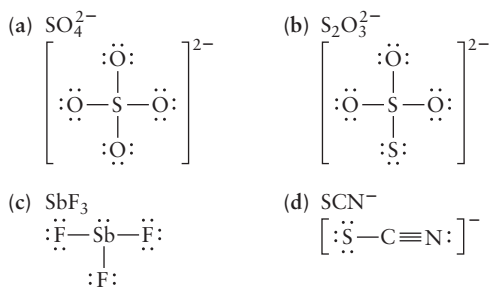
36. Estimate the percent ionic character of the bond in each of the following species. All the species are unstable or reactive under ordinary laboratory conditions, but they can be observed in interstellar space.

	Bond Length (Å)	Dipole Moment (D)
OH	0.980	1.66
CH	1.131	1.46
CN	1.175	1.45
C_2	1.246	0

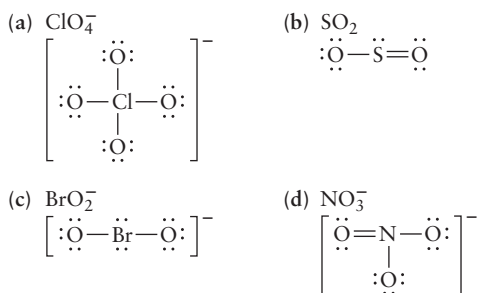
37. The percent ionic character of a bond can be approximated by the formula $16\Delta + 3.5\Delta^2$, where Δ is the magnitude of the difference in the electronegativities of the atoms (see Fig. 3.7). Calculate the percent ionic character of HF, HCl, HBr, HI, and CsF, and compare the results with those in Table 3.7.
38. The percent ionic character of the bonds in several interhalogen molecules (as estimated from their measured dipole moments and bond lengths) are ClF (11%), BrF (15%), BrCl (5.6%), ICl (5.8%), and IBr (10%). Estimate the percent ionic characters for each of these molecules, using the equation in Problem 37, and compare them with the given values.

Lewis Diagrams for Molecules

39. Assign formal charges to all atoms in the following Lewis diagrams.



40. Assign formal charges to all atoms in the following Lewis diagrams.

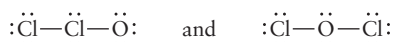


41. Determine the formal charges on all the atoms in the following Lewis diagrams.



Which one would best represent bonding in the molecule HNO?

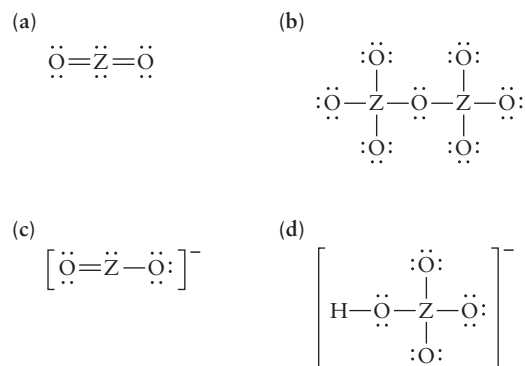
42. Determine the formal charges on all the atoms in the following Lewis diagrams.



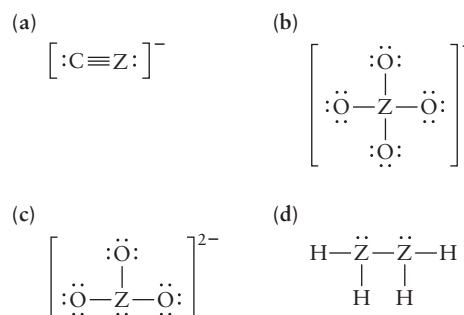
Which one would best represent bonding in the molecule Cl_2O ?

43. In each of the following Lewis diagrams, Z represents a main-group element. Name the group to which Z belongs in

each case and give an example of such a compound or ion that actually exists.



44. In each of the following Lewis diagrams, Z represents a main-group element. Name the group to which Z belongs in each case and give an example of such a compound or ion that actually exists.



45. Draw Lewis electron dot diagrams for the following species: (a) AsH_3 ; (b) HOCl ; (c) KrF^- ; (d) PO_2Cl_2^- (central P atom).

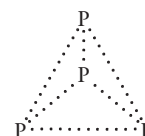
46. Draw Lewis electron dot diagrams for the following species: (a) methane; (b) carbon dioxide; (c) phosphorus trichloride; (d) perchlorate ion.

47. Urea is an important chemical fertilizer with the chemical formula $(\text{H}_2\text{N})\text{CO}(\text{NH}_2)$. The carbon atom is bonded to both nitrogen atoms and the oxygen atom. Draw a Lewis diagram for urea and use Table 3.6 to estimate its bond lengths.

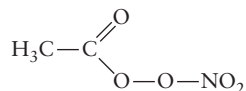
48. Acetic acid is the active ingredient of vinegar. Its chemical formula is CH_3COOH , and the second carbon atom is bonded to the first carbon atom and to both oxygen atoms. Draw a Lewis diagram for acetic acid and use Table 3.6 to estimate its bond lengths.

49. Under certain conditions, the stable form of sulfur consists of rings of eight sulfur atoms. Draw the Lewis diagram for such a ring.

50. White phosphorus (P_4) consists of four phosphorus atoms arranged at the corners of a tetrahedron. Draw the valence electrons on this structure to give a Lewis diagram that satisfies the octet rule.



51. Draw Lewis electron dot diagrams for the following species, indicating formal charges and resonance diagrams where applicable.
- H_3NBF_3
 - CH_3COO^- (acetate ion)
 - HCO_3^- (hydrogen carbonate ion)
52. Draw Lewis electron dot diagrams for the following species, indicating formal charges and resonance diagrams where applicable.
- HNC (central N atom)
 - SCN^- (thiocyanate ion)
 - H_2CNN (the first N atom is bonded to the carbon and the second N)
53. Draw Lewis diagrams for the two resonance forms of the nitrite ion, NO_2^- . In what range do you expect the nitrogen–oxygen bond length to fall? (*Hint*: Use Table 3.6.)
54. Draw Lewis diagrams for the three resonance forms of the carbonate ion, CO_3^{2-} . In what range do you expect the carbon–oxygen bond length to fall? (*Hint*: Use Table 3.6.)
55. Methyl isocyanate, which was involved in the disaster in Bhopal, India, in 1984, has the chemical formula CH_3NCO . Draw its Lewis diagram, including resonance forms. (**Note**: The N atom is bonded to the two C atoms.)
56. Peroxyacetyl nitrate (PAN) is one of the prime irritants in photochemical smog. It has the formula $\text{CH}_3\text{COOONO}_2$, with the following structure:



Draw its Lewis diagram, including resonance forms.

57. Draw Lewis diagrams for the following compounds. In the formula the symbol of the central atom is given first. (*Hint*: The valence octet may be expanded for the central atom.)
- PF_5
 - SF_4
 - XeO_2F_2
58. Draw Lewis diagrams for the following ions. In the formula the symbol of the central atom is given first. (*Hint*: The valence octet may be expanded for the central atom.)
- BrO_4^-
 - PCl_6^-
 - XeF_6^+

The Shapes of Molecules: Valence Shell Electron-Pair Repulsion Theory

59. For each of the following molecules, give the steric number and sketch and name the approximate molecular geometry. In each case, the central atom is listed first and the other atoms are all bonded directly to it.
- CBr_4
 - SO_3
 - SeF_6
 - SOCl_2
 - ICl_3
60. For each of the following molecules or molecular ions, give the steric number and sketch and name the approximate molecular geometry. In each case, the central atom is listed first and the other atoms are all bonded directly to it.
- PF_3
 - SO_2Cl_2
 - PF_6^-
 - ClO_2^-
 - GeH_4
61. For each of the following molecules or molecular ions, give the steric number, sketch and name the approximate molecular geometry, and describe the directions of any *distortions* from the approximate geometry due to lone pairs. In each case, the central atom is listed first and the other atoms are all bonded directly to it.
- ICl_4^-
 - OF_2
 - BrO_3^-
 - CS_2
62. For each of the following molecules or molecular ions, give the steric number, sketch and name the approximate molecular geometry, and describe the direction of any *distortions* from the approximate geometry due to lone pairs. In each case, the central atom is listed first and the other atoms are all bonded directly to it.
- TeH_2
 - AsF_3
 - PCl_4^+
 - XeF_5^+
63. Give an example of a molecule or ion having a formula of each of the following types and structures.
- B_3 (planar)
 - AB_3 (pyramidal)
 - AB_5 (bent)
 - AB_3^{2-} (planar)
64. Give an example of a molecule or ion having a formula of each of the following types and structures.
- AB_4 (tetrahedral)
 - AB_2 (linear)
 - AB_6 (octahedral)
 - AB_5 (pyramidal)
65. For each of the answers in Problem 59, state whether the species is polar or nonpolar.
66. For each of the answers in Problem 60, state whether the species is polar or nonpolar.
67. The molecules of a certain compound contain one atom each of nitrogen, fluorine, and oxygen. Two possible structures are NOF (O as central atom) and ONF (N as central atom). Does the information that the molecule is bent limit the choice to one of these two possibilities? Explain.
68. Mixing SbCl_3 and GaCl_3 in a 1 : 1 molar ratio (using liquid sulfur dioxide as a solvent) gives a solid ionic compound of empirical formula GaSbCl_6 . A controversy arises over whether this compound is $(\text{SbCl}_2^+)(\text{GaCl}_4^-)$ or $(\text{GaCl}_2^+)(\text{SbCl}_4^-)$.
- Predict the molecular structures of the two anions.
 - It is learned that the cation in the compound has a bent structure. Based on this fact, which formulation is more likely to be correct?
69. (a) Use the VSEPR theory to predict the structure of the NNO molecule.
- (b) The substance NNO has a small dipole moment. Which end of the molecule is more likely to be the positive end, based only on electronegativity?
70. Ozone (O_3) has a nonzero dipole moment. In the molecule of O_3 , one of the oxygen atoms is directly bonded to the other two, which are not bonded to each other.
- Based on this information, state which of the following structures are possible for the ozone molecule: symmetric linear, nonsymmetric linear (for example, different O–O bond lengths), and bent. (**Note**: Even an O–O bond can have a bond dipole if the two oxygen atoms are bonded to different atoms or if only one of the oxygen atoms is bonded to a third atom.)
 - Use the VSEPR theory to predict which of the structures of part (a) is observed.

Oxidation Numbers

71. Assign oxidation numbers to the atoms in each of the following species: SrBr_2 , $\text{Zn}(\text{OH})_4^{2-}$, SiH_4 , CaSiO_3 , CrO_7^{2-} , $\text{Ca}_5(\text{PO}_4)_3\text{F}$, KO_2 , C_6H_6 .
72. Assign oxidation numbers to the atoms in each of the following species: NH_4NO_3 , CaMgSiO_4 , $\text{Fe}(\text{CN})_6^{4-}$, B_2H_6 , BaH_2 , PbCl_2 , $\text{Cu}_2\text{O}(\text{SO}_4)$, $\text{S}_4\text{O}_6^{2-}$.

Inorganic Nomenclature

73. Give the name and formula of an ionic compound involving only the elements in each pair that follows. Write Lewis symbols for the elements both before and after chemical combination.
- (a) Chlorine and cesium (b) Calcium and astatine
(c) Aluminum and sulfur (d) Potassium and tellurium
74. Give the name and formula of an ionic compound involving only the elements in each pair that follows. Write Lewis symbols for the elements both before and after chemical combination.
- (a) Gallium and bromine (b) Strontium and polonium
(c) Magnesium and iodine (d) Lithium and selenium
75. Give systematic names to the following compounds:
- (a) Al_2O_3 (b) Rb_2Se
(c) $(\text{NH}_4)_2\text{S}$ (d) $\text{Ca}(\text{NO}_3)_2$
(e) Cs_2SO_4 (f) KHCO_3
76. Give systematic names to the following compounds:
- (a) KNO_2 (b) $\text{Sr}(\text{MnO}_4)_2$
(c) MgCr_2O_7 (d) NaH_2PO_4
(e) BaCl_2 (f) NaClO_3
77. Write the chemical formulas for the following compounds:
- (a) Silver cyanide
(b) Calcium hypochlorite
(c) Potassium chromate
(d) Gallium oxide
(e) Potassium superoxide
(f) Barium hydrogen carbonate
78. Write the chemical formulas for the following compounds:
- (a) Cesium sulfite
(b) Strontium thiocyanate
(c) Lithium hydride
(d) Sodium peroxide
(e) Ammonium dichromate
(f) Rubidium hydrogen sulfate
79. Trisodium phosphate (TSP) is a heavy-duty cleaning agent. Write its chemical formula. What would be the systematic name for this ionic compound?
80. Monoammonium phosphate is the common name for a compound made up of NH_4^+ and H_2PO_4^- ; it is used as a flame retardant. (Its use for this purpose was first suggested by Gay-Lussac in 1821.) Write its chemical formula. What is the systematic chemical name of this compound?
81. Write the chemical formula for each of the following compounds:
- (a) Silicon dioxide
(b) Ammonium carbonate
(c) Lead(IV) oxide
(d) Diphosphorus pentoxide
(e) Calcium iodide
(f) Iron(III) nitrate

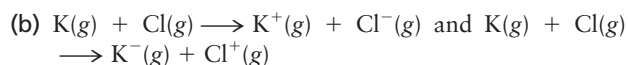
82. Write the chemical formula for each of the following compounds:
- (a) Lanthanum(III) sulfide
(b) Cesium sulfate
(c) Dinitrogen trioxide
(d) Iodine pentafluoride
(e) Chromium(III) sulfate
(f) Potassium permanganate
83. Give the systematic name for each of the following compounds:
- (a) Cu_2S and CuS (b) Na_2SO_4
(c) As_4O_6 (d) ZrCl_4
(e) Cl_2O_7 (f) Ga_2O
84. Give the systematic name for each of the following compounds:
- (a) Mg_2SiO_4 (b) $\text{Fe}(\text{OH})_2$ and $\text{Fe}(\text{OH})_3$
(c) As_2O_5 (d) $(\text{NH}_4)_2\text{HPO}_4$
(e) SeF_6 (f) Hg_2SO_4

Additional Problems

85. Refer to Figure 3.7 and compute the difference in electronegativity between the atoms in LiCl and those in HF . Based on their physical properties (see below), are the two similar or different in terms of bonding?

	LiCl	HF
Melting point	605°C	83.1°C
Boiling point	1350°C	19.5°C

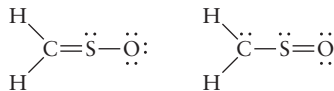
86. Ordinarily, two metals, when mixed, form alloys that show metallic character. If the two metals differ sufficiently in electronegativity, they can form compounds with significant ionic character. Consider the solid produced by mixing equal chemical amounts of Cs and Rb, compared with that produced by mixing Cs and Au. Compute the electronegativity difference in each case, and determine whether either mixture has significant ionic character. If either compound is ionic or partially ionic, which atom carries the net negative charge? Are there alkali halides with similar or smaller electronegativity differences?
- * 87. At large interatomic separations, an alkali halide molecule MX has a lower energy as two neutral atoms, $\text{M} + \text{X}$; at short separations, the ionic form $(\text{M}^+)(\text{X}^-)$ has a lower energy. At a certain distance, R_c , the energies of the two forms become equal, and it is near this distance that the electron will jump from the metal to the halogen atom during a collision. Because the forces between neutral atoms are weak at large distances, a reasonably good approximation can be made by ignoring any variation in potential $V(R)$ for the neutral atoms between R_c and $R = \infty$. For the ions in this distance range, $V(R)$ is dominated by their Coulomb attraction.
- (a) Express R_c for the first ionization energy of the metal M and the electron affinity of the halogen X .
(b) Calculate R_c for LiF , KBr , and NaCl using data from Appendix F.
88. Use the data in Appendix F to compute the energy changes (ΔE) of the following pairs of reactions:
- (a) $\text{Na}(g) + \text{I}(g) \longrightarrow \text{Na}^+(g) + \text{I}^-(g)$ and $\text{Na}(g) + \text{I}(g) \longrightarrow \text{Na}^-(g) + \text{I}^+(g)$



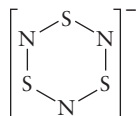
Explain why Na^+I^- and K^+Cl^- form in preference to Na^-I^+ and K^-Cl^+ .

89. The carbon–carbon bond length in C_2H_2 is 1.20 Å, that in C_2H_4 is 1.34 Å, and that in C_2H_6 is 1.53 Å. Near which of these values would you predict the bond length of C_2 to lie? Is the experimentally observed value, 1.31 Å, consistent with your prediction?

90. Two possible Lewis diagrams for sulfine (H_2CSO) are



- (a) Compute the formal charges on all atoms.
 (b) Draw a Lewis diagram for which all the atoms in sulfine have formal charges of zero.
91. There is persuasive evidence for the brief existence of the unstable molecule OPCl .
- (a) Draw a Lewis diagram for this molecule in which the octet rule is satisfied on all atoms and the formal charges on all atoms are zero.
 (b) The compound OPCl reacts with oxygen to give O_2PCl . Draw a Lewis diagram of O_2PCl for which all formal charges are equal to zero. Draw a Lewis diagram in which the octet rule is satisfied on all atoms.
92. The compound SF_3N has been synthesized.
- (a) Draw the Lewis diagram of this molecule, supposing that the three fluoride atoms and the nitrogen atom surround the sulfur atom. Indicate the formal charges. Repeat, but assume that the three fluorine atoms and the sulfur atom surround the nitrogen atom.
 (b) From the results in part (a), speculate about which arrangement is more likely to correspond to the actual molecular structure.
93. In nitryl chloride (NO_2Cl), the chlorine atom and the two oxygen atoms are bonded to a central nitrogen atom, and all the atoms lie in a plane. Draw the two electron dot resonance forms that satisfy the octet rule and that together are consistent with the fact that the two nitrogen–oxygen bonds are equivalent.
94. The molecular ion S_3N_3^- has the cyclic structure



All S–N bonds are equivalent.

- (a) Give six equivalent resonance hybrid Lewis diagrams for this molecular ion.
 (b) Compute the formal charges on all atoms in the molecular ion in each of the six Lewis diagrams.
 (c) Determine the charge on each atom in the polyatomic ion, assuming that the true distribution of electrons is the *average* of the six Lewis diagrams arrived at in parts (a) and (b).
 (d) An advanced calculation suggests that the actual charge resident on each N atom is -0.375 and on each S atom is $+0.041$. Show that this result is consistent with the overall $+1$ charge on the molecular ion.

- * 95. The two compounds nitrogen dioxide and dinitrogen tetraoxide are introduced in Section 3.11.

- (a) NO_2 is an odd-electron compound. Draw the best Lewis diagrams possible for it, recognizing that one atom cannot achieve an octet configuration. Use formal charges to decide whether that should be the (central) nitrogen atom or one of the oxygen atoms.
 (b) Draw resonance forms for N_2O_4 that obey the octet rule. The two N atoms are bonded in this molecule.

96. Although magnesium and the alkaline-earth metals situated below it in the periodic table form ionic chlorides, beryllium chloride (BeCl_2) is a covalent compound.

- (a) Follow the usual rules to write a Lewis diagram for BeCl_2 in which each atom attains an octet configuration. Indicate formal charges.
 (b) The Lewis diagram that results from part (a) is an extremely unlikely one because of the double bonds and formal charges it shows. By relaxing the requirement of placing an octet on the beryllium atom, show how a Lewis diagram without formal charges can be written.

97. (a) The first noble-gas compound, prepared by Neil Bartlett in 1962, was an orange-yellow ionic solid that consisted of XeF^+ and PtF_6^- . Draw a Lewis diagram for XeF^+ .

- (b) Shortly after the preparation of the ionic compound discussed in part (a), it was found that the irradiation of mixtures of xenon and fluorine with sunlight produced white crystalline XeF_2 . Draw a Lewis diagram for this molecule, allowing valence expansion on the central xenon atom.

- * 98. Represent the bonding in SF_2 ($\text{F}-\text{S}-\text{F}$) with Lewis diagrams. Include the formal charges on all atoms. The dimer of this compound has the formula S_2F_4 . It was isolated in 1980 and shown to have the structure $\text{F}_3\text{S}-\text{SF}$. Draw a possible Lewis diagram to represent the bonding in the dimer, indicating the formal charges on all atoms. Is it possible to draw a Lewis diagram for S_2F_4 in which all atoms have valence octets? Explain why or why not.

- * 99. A stable triatomic molecule can be formed that contains one atom each of nitrogen, sulfur, and fluorine. Three bonding structures are possible, depending on which is the central atom: NSF , SNE , and SFN .

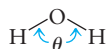
- (a) Write a Lewis diagram for each of these molecules, indicating the formal charge on each atom.
 (b) Often, the structure with the least separation of formal charge is the most stable. Is this statement consistent with the observed structure for this molecule—namely, NSF , which has a central sulfur atom?
 (c) Does consideration of the electronegativities of N, S, and F from Figure 3.7 help rationalize this observed structure? Explain.

100. The gaseous potassium chloride molecule has a measured dipole moment of 10.3 D, which indicates that it is a very polar molecule. The separation between the nuclei in this molecule is 2.67 Å. What would the dipole moment of a KCl molecule be if there were opposite charges of one fundamental unit (1.60×10^{-19} C) at the nuclei?

101. (a) Predict the geometry of the SbCl_5^{2-} ion, using the VSEPR method.
 (b) The ion SbCl_6^{3-} is prepared from SbCl_5^{2-} by treatment with Cl^- . Determine the steric number of the central

antimony atom in this ion, and discuss the extension of the VSEPR theory that would be needed for the prediction of its molecular geometry.

102. The element xenon (Xe) is by no means chemically inert; it forms a number of chemical compounds with electronegative elements such as fluorine and oxygen. The reaction of xenon with varying amounts of fluorine produces XeF_2 and XeF_4 . Subsequent reaction of one or the other of these compounds with water produces (depending on conditions) XeO_3 , XeO_4 , and H_4XeO_6 , as well as mixed compounds such as XeOF_4 . Predict the structures of these six xenon compounds, using the VSEPR theory.
103. Predict the arrangement of the atoms about the sulfur atom in F_4SPO , assuming that double-bonded atoms require more space than single-bonded atoms.
104. Draw Lewis diagrams and predict the geometries of the following molecules. State which are polar and which are nonpolar.
- (a) ONCl (b) O_2NCl
 (c) XeF_2 (d) SCl_4
 (e) CHF_3
- *105. Suppose that any given kind of bond, such as $\text{O}-\text{H}$, has a characteristic electric dipole. That is, suppose that electric dipole moments can be assigned to bonds just as bond energies can be. Both are usefully accurate approximations. Consider the water molecule



Show that if μ_{OH} is the dipole moment of the OH bond, then the dipole moment of water is $\mu(\text{H}_2\text{O}) = 2\mu_{\text{OH}} \cos(\theta/2)$. What is the dipole moment μ_{OH} if $\mu(\text{H}_2\text{O})$ is 1.86 D?

106. A good method of preparing pure oxygen on a small scale is the decomposition of KMnO_4 in a vacuum above 215°C :



Assign an oxidation number to each atom and verify that the total number of electrons lost is equal to the total number gained.

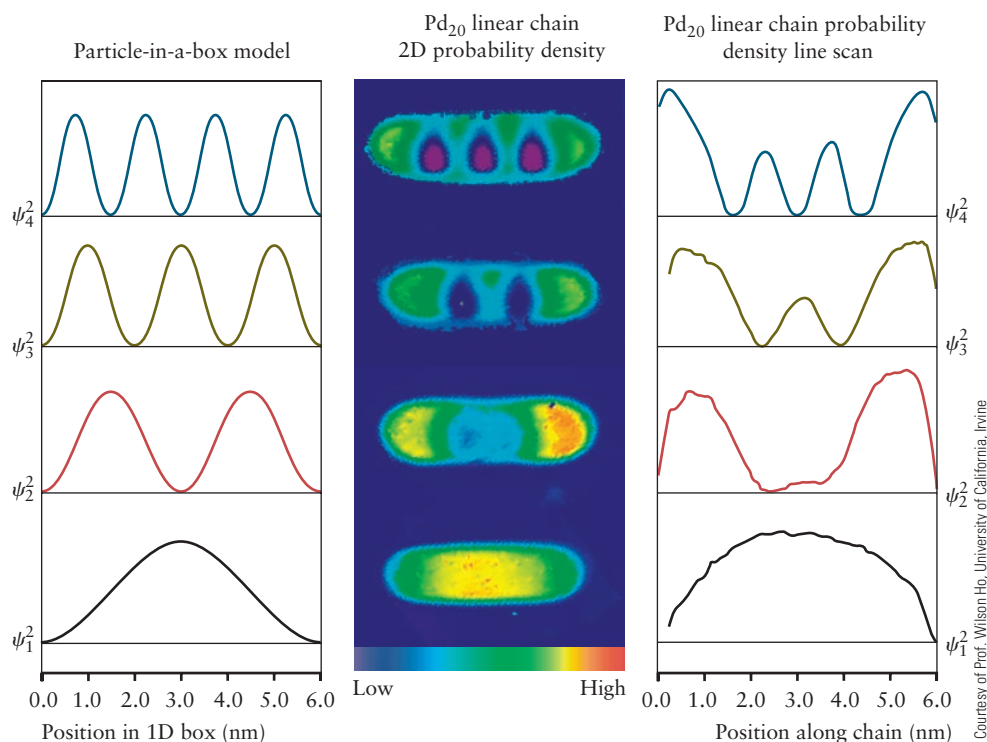
107. Bismuth forms an ion with the formula Bi_3^{3+} . Arsenic and fluorine form a complex ion $[\text{AsF}_6]^-$, with fluorine atoms arranged around a central arsenic atom. Assign oxidation numbers to each of the atoms in the bright yellow crystalline solid with the formula $\text{Bi}_3(\text{AsF}_6)_3 \cdot 2\text{SO}_2$.
108. In some forms of the periodic table, hydrogen is placed in Group I; in others, it is placed in Group VII. Give arguments in favor of each location.
- *109. (a) Determine the oxidation number of lead in each of the following oxides: PbO , PbO_2 , Pb_2O_3 , Pb_3O_4 .
 (b) The only known lead ions are Pb^{2+} and Pb^{4+} . How can you reconcile this statement with your answer to part (a)?
110. There have been some predictions that element 114 will be relatively stable in comparison with many other elements beyond uranium in the periodic table. Predict the maximum oxidation state of this element. Based on the trends in the oxidation states of other members of its group, is it likely that this oxidation state will be the dominant one?

CUMULATIVE PROBLEMS

111. A certain element, M, is a main-group metal that reacts with chlorine to give a compound with the chemical formula MCl_2 and with oxygen to give the compound MO .
- (a) To which group in the periodic table does element M belong?
 (b) The chloride contains 44.7% chlorine by mass. Name the element M.
- *112. An ionic compound used as a chemical fertilizer has the composition (by mass) 48.46% O, 23.45% P, 21.21% N, 6.87% H. Give the name and chemical formula of the compound and draw Lewis diagrams for the two types of ions that make it up.
113. A compound is being tested for use as a rocket propellant. Analysis shows that it contains 18.54% F, 34.61% Cl, and 46.85% O.
- (a) Determine the empirical formula for this compound.
 (b) Assuming that the molecular formula is the same as the empirical formula, draw a Lewis diagram for this molecule. Review examples elsewhere in this chapter to decide which atom is most likely to lie at the center.
- (c) Use the VSEPR theory to predict the structure of the molecule from part (b).
114. Many important fertilizers are ionic compounds that contain the elements nitrogen, phosphorus, and potassium because these are frequently the limiting plant-growth nutrients in soil.
- (a) Write the chemical formulas for the following chemical fertilizers: ammonium phosphate, potassium nitrate, ammonium sulfate.
 (b) Calculate the mass percentage of nitrogen, phosphorus, and potassium for each of the compounds in part (a).

Introduction to Quantum Mechanics

- 4.1 Preliminaries: Wave Motion and Light
- 4.2 Evidence for Energy Quantization in Atoms
- 4.3 The Bohr Model: Predicting Discrete Energy Levels
- 4.4 Evidence for Wave–Particle Duality
- 4.5 The Schrödinger Equation
- 4.6 Quantum Mechanics of Particle-in-a-Box Models
- 4.7 Quantum Harmonic Oscillator



Particle-in-a-box states for an electron in a 20 Pd atom linear chain assembled on a single crystal NiAl surface. The left set of curves shows the predictions of the one-dimensional particle-in-a-box model, the center set of images is the 2D probability density distribution, and the right of curves is a line scan of the probability density distribution taken along the center of the chain. The chain was assembled and the probability densities measured using a scanning tunneling microscope.

Science can advance in different ways. Usually, the slow and steady accumulation of experimental results supports and refines existing models, which leads to a more satisfactory description of natural phenomena. Occasionally, however, the results of new experiments directly contradict previously accepted theories. In this case, a period of uncertainty ensues; it is resolved only through the eventual emergence of a new and more complete theory that explains both the previously understood results and the new experiments. This process is called a *scientific revolution*. In the first 25 years of the 20th century, a revolution in

physics led to the development of the quantum theory, which also profoundly affected the science of chemistry.

One of the fundamental assumptions of early science was that nature is continuous; that is, nature does not make “jumps.” On a macroscopic scale, this appears to be true enough. We can measure out an amount of graphite (carbon) of mass 9, or 8.23, or 6.4257 kg, and it appears that the mass can have any value provided that our balance is sufficiently accurate. On an atomic scale, however, this apparently continuous behavior breaks down. An analogy may be useful here. A sand beach from a distance appears smooth and continuous, but a close look reveals that it is made up of individual grains of sand. This same “graininess” is found in matter observed on the atomic scale. The mass of carbon (^{12}C) comes in “packets,” each of which weighs 1.99265×10^{-26} kg. Although, in principle, two, three, or any integral number of such packets can be “weighed out,” we cannot obtain $1\frac{1}{2}$ packets. Carbon is not a continuous material, but comes in chunks, each containing the minimum measurable mass of carbon—that of an atom. Similarly, electric charge comes in packets of size e , as shown in Section 1.4, and fractional charges are never observed in chemical reactions.

The central idea of quantum theory is that energy, like matter, is not continuous but it exists only in discrete packets. Whereas discreteness of matter and charge on the microscopic scale seems entirely reasonable and familiar to us, based on the modern picture of the physical structure of the atom, the idea that energy also exists only in discrete chunks is contrary to our experience of the macroscopic world. The motions of a soccer ball rolling up and down the sides of a gully involve arbitrary amounts of kinetic and potential energy; nothing in ordinary human experience suggests that the energy of a system should change abruptly by “jumps.” Understanding quantum mechanics requires that we develop a new kind of physical intuition, based on the results of experiments that are impossible to understand using classical mechanics. These results are completely divorced from ordinary human experience in the macroscopic world around us, and our physical intuition from the macroscopic world cannot be transferred to the quantum domain. We must remain vigilant against the urge to interpret these quantum results in terms of ordinary experience.

To understand the far-reaching nature of the quantum revolution, you should consider the state of physics at the end of the 19th century. The 200 years that followed the seminal work of Isaac Newton were the classical period in the study of mechanics, the branch of physics that predicts the motions of particles and the collections of particles that make up working mechanisms. By the end of that period, about 1900, physicists had achieved a deep understanding that successfully dealt with problems ranging from the motions of the planets in their orbits to the design of a bicycle. These achievements make up the field now called **classical mechanics**.

Classical mechanics can predict the future positions of a group of particles from their present positions and velocities if the forces among them are known. At the end of the 19th century, it was naturally thought that the motion of elementary particles—such as the recently discovered electron—could be described by classical mechanics. Once the correct force laws had been discovered, the properties of atoms and molecules could be predicted to any desired accuracy by solving Newton’s equations of motion. It was believed that all the fundamental laws of physics had been discovered. At the dedication of the Ryerson Physics Laboratory at the University of Chicago in 1894, the American physicist A. A. Michelson said, “Our future discoveries must be looked for in the sixth decimal place.” Little did he imagine the revolutionary changes that would shake physics and chemistry during the following 30 years.

Central to those changes was not only the recognition that energy is quantized but also the discovery that all particles display wavelike properties in their motions. The effects of wavelike properties are most pronounced for small, low-mass

particles such as electrons in atoms. **Quantum mechanics** incorporated both the ideas of “wave–particle duality” and energy quantization into a single comprehensive theory that superseded classical mechanics to describe the properties of matter on the nanometer length scale. Quantum mechanics is one of the greatest intellectual achievements of the 20th century.

This chapter describes the origins of the quantum theory, summarizes its techniques, and demonstrates their application to simple model systems. Our goals are to help you become skilled and confident in using the language, concepts, and tools of quantum theory. With these skills, we will guide you to develop an intuitive understanding of the behavior of quantum systems—so foreign to our ordinary human experience—and the magnitudes of the observable quantities (energy, momentum, length) in the quantum domain. Chapter 5 shows how quantum mechanics explains the structure of atoms and the periodic table and Chapter 6 shows how the quantum theory explains the formation of chemical bonds.

4.1 Preliminaries: Wave Motion and Light

Many kinds of waves are studied in physics and chemistry. Familiar examples include water waves stirred up by the winds over the oceans, set off by a stone dropped into a quiet pool, or created for teaching demonstrations by a laboratory water-wave machine. Sound waves are periodic compressions of the air that move from a source to a detector such as the human ear. Light waves, as discussed later in this chapter, consist of oscillating electric and magnetic fields moving through space. Even some chemical reactions occur in such a way that waves of color pass through the sample as the reaction proceeds. Common to all these wave phenomena is the oscillatory variation of some property with time at a given fixed location in space (Table 4.1). All of these waves are described by the same equations.

TABLE 4.1 Kinds of Waves

Wave	Oscillating Quantity
Water	Height of water surface
Sound	Density of air
Light	Electric and magnetic fields
Chemical	Concentrations of chemical species

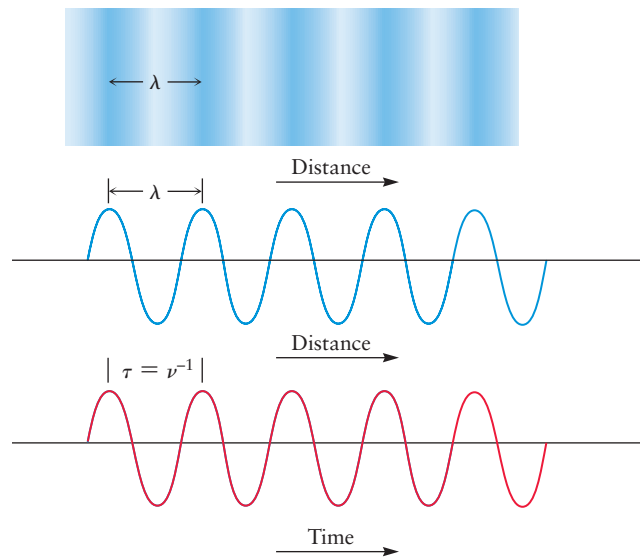
A snapshot of a water wave (Fig. 4.1) records the crests and troughs present at some instant in time. The **amplitude** of the wave is the height or the displacement of the water surface compared with the undisturbed level of the water; this undisturbed height is customarily chosen as the reference height and assigned the value zero. Positive amplitudes describe displacements that increase the level of the water, whereas negative amplitudes describe those that decrease the level of the water. We define the **maximum amplitude** as either the height of a crest or the depth of a trough, and it is always given as an absolute value.¹ The distance between two successive crests (or troughs) is called the **wavelength**, λ (Greek lambda), of the wave, provided that this distance is reproducible from peak to peak. The **frequency** of a water wave can be measured by counting the number of peaks or troughs observed moving past a fixed point in space per second. The frequency, ν (Greek nu), is measured in units of waves (or cycles) per second, or simply s^{-1} . The fundamental frequency unit one cycle per second has been named the **hertz (Hz)** in honor of the German physicist Heinrich Hertz. For example, if 12 water-wave peaks are observed to pass a certain point in 30 seconds, the frequency is

$$\text{frequency} = \nu = \frac{12}{30 \text{ s}} = 0.40 \text{ s}^{-1} = 0.40 \text{ Hz}$$

The wavelength and frequency of a wave are related through its speed—the rate at which a particular wave crest moves through the medium. In Figure 4.1, the crest at the left end of the horizontal black arrow will move forward exactly one wavelength in one cycle of the wave. By definition, the time required for the crest to

¹Most physics texts, especially older ones, define the amplitude as the quantity we call the maximum amplitude here. We have chosen the present definition to facilitate later discussions of the wave functions that describe atomic structure.

FIGURE 4.1 As a water wave moves across an otherwise calm tank, its maximum amplitude and wavelength can be determined. Its speed is found by dividing the travel distance of a particular wave crest by the time elapsed.



travel this distance is the reciprocal of the frequency, $\tau = \nu^{-1}$, so the speed (the distance traveled divided by the time elapsed) is given by

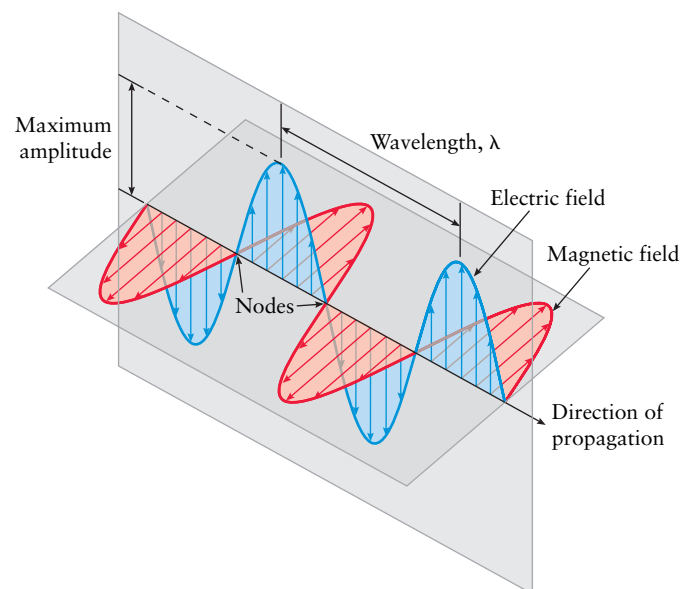
$$\text{speed} = \frac{\text{distance traveled}}{\text{time elapsed}} = \frac{\lambda}{\nu^{-1}} = \lambda\nu$$

The speed of a wave is the product of its wavelength and its frequency.

Electromagnetic Radiation

By the end of the 18th century, the behavior of light was well described by a wave model. The signature properties of light—diffraction, interference, and polarization—were understood as consequences of wave propagation. In 1865, the Scottish physicist James Clerk Maxwell proposed a theory that described visible light as a propagating wave of **electromagnetic radiation** that carries both energy and momentum. Unlike water and sound waves, electromagnetic waves are not sustained by some “propagating medium” such as water or air. Rather, a beam of light consists of oscillating *electric* and *magnetic fields* oriented perpendicular to one another and to the direction in which the light is propagating (Fig. 4.2). These

FIGURE 4.2 Light consists of waves of oscillating electric and magnetic fields that are perpendicular to each other and to the direction of propagation of the light.



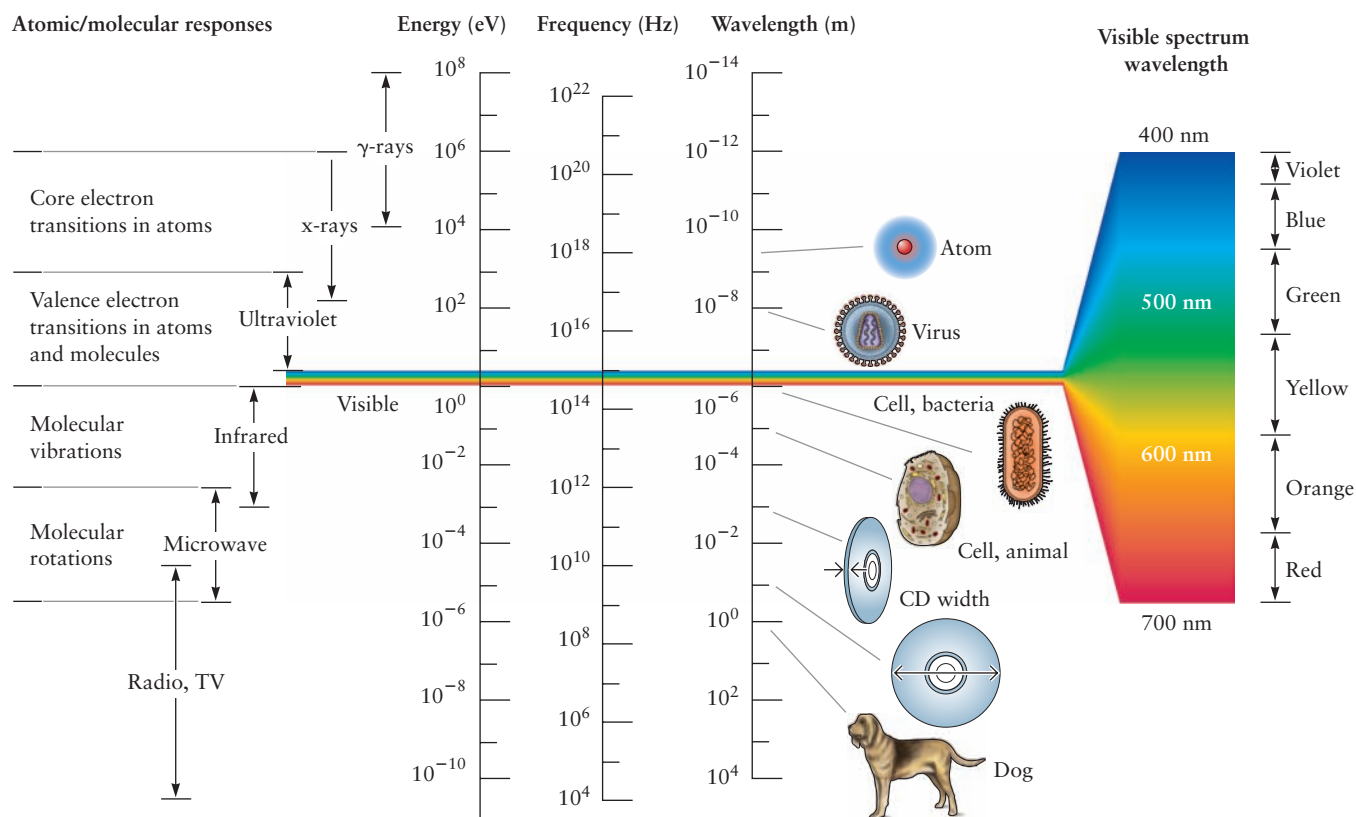
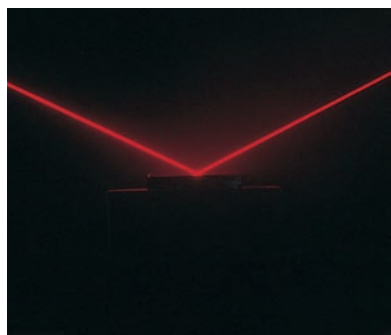


FIGURE 4.3 The electromagnetic spectrum. Note the small fraction that is visible to the human eye.

fields are produced by the motion of charged particles in the source of the light. These oscillating fields can transfer energy and momentum to other charged particles that intercept the beam in some location that is remote from the source. Electromagnetic waves carry information from a broadcast source to a remote receiver in wireless communication. Indeed, one of the early triumphs of Maxwell's theory was the development of radio, based largely on the experimental work of Heinrich Hertz. We will see that electromagnetic radiation is both emitted and absorbed by atoms and molecules. It is, therefore, one of our most effective tools for probing the nature of atoms and molecules.

Electromagnetic waves are described by the equations introduced earlier. The speed, c , of light passing through a vacuum is equal to the product $\lambda\nu$, and its value *by definition* is

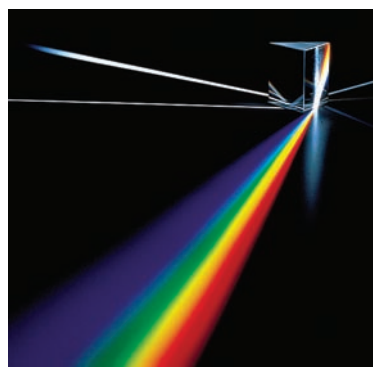
$$c = \lambda\nu = 2.99792458 \times 10^8 \text{ m s}^{-1} \quad [4.1]$$



Thomson Learning/Henry Leap and Jim Lehman

FIGURE 4.4 A laser emits a well-collimated beam of light with a narrow range of wavelengths. The direction of motion of a laser beam can be manipulated by inserting mirrors in the path of the beam.

The speed, c , is a universal constant; it is the same for all types of radiation in the electromagnetic spectrum (Fig. 4.3). Regions of the electromagnetic spectrum are characterized by different values of wavelength and frequency. The region visible to the eye, which is a small fraction of the entire spectrum, comprises bands of colored light that cover particular ranges of wavelength and frequency. The band of light we perceive as green is centered about 5.7×10^{14} Hz with wavelengths near 5.3×10^{-7} m (530 nm). Red light is characterized by a lower frequency and a longer wavelength than green light, and violet light is characterized by a higher frequency and shorter wavelength than green light. A laser, such as the one shown in Figure 4.4, emits nearly monochromatic light (light of a single frequency and wavelength). White light contains the full range of visible wavelengths; it can be resolved into its component wavelengths by passing it through a prism (Fig. 4.5).



©Alfred Pasierba/Peter Arnold, Inc.

FIGURE 4.5 When white light is passed through slits to produce a narrow beam and then refracted in a glass prism, the various colors blend smoothly into one another.

Electromagnetic radiation that lies outside the visible region is also familiar to us (see Fig. 4.3). The warmth radiated from a stone pulled from a fire is largely due to infrared radiation, whose wavelength is longer than that of visible light. Microwave ovens use radiation whose wavelength is longer than infrared wavelengths, and radio communication uses still longer wavelengths. Radio stations are identified by their broadcast frequencies. FM stations typically broadcast at frequencies of tens to hundreds of megahertz ($1 \text{ MHz} = 10^6 \text{ s}^{-1}$), whereas AM stations broadcast at lower frequencies, from hundreds to thousands of kilohertz ($1 \text{ kHz} = 10^3 \text{ s}^{-1}$). You might check the frequencies of some of your favorite radio stations; ours include a classical music station broadcasting at 90.5 MHz (FM) and a sports station broadcasting at 1300 kHz (AM). Radiation with wavelengths shorter than that of visible light includes ultraviolet light, x-rays, and gamma rays; radiation in these regions of the electromagnetic spectrum (with wavelengths shorter than about 340 nm) can cause ionization and damage in biological tissue and are often collectively called **ionizing radiation**.

EXAMPLE 4.1

Almost all commercially available microwave ovens use radiation with a frequency of $2.45 \times 10^9 \text{ Hz}$. Calculate the wavelength of this radiation.

SOLUTION

The wavelength is related to the frequency as follows:

$$\lambda = \frac{c}{\nu} = \frac{3.00 \times 10^8 \text{ s}^{-1}}{2.45 \times 10^9 \text{ s}^{-1}} = 0.122 \text{ m}$$

Thus, the wavelength is 12.2 cm.

Related Problems: 3, 4

4.2 Evidence for Energy Quantization in Atoms

Rutherford's planetary model of the atom was completely inconsistent with the laws of classical physics (see discussion in Section 3.2). According to Maxwell's electromagnetic theory, accelerated charges must emit electromagnetic radiation. An electron in orbit around the nucleus is accelerating because its direction is constantly changing. It must, therefore, emit electromagnetic radiation, lose energy, and eventually spiral into the nucleus. The very existence of stable atoms was perhaps the most fundamental conceptual challenge facing physicists in the early 1900s. The recognition that energy is quantized in atoms provided a path toward resolving the conceptual conflicts.

This section begins with a discussion of blackbody radiation, the experiment that introduced energy quantization into science. Two sets of experiments that demonstrated quantization of energy in free atoms in the gas phase then are described. We interpret these experiments using energy-level diagrams, which represent the discrete energy states of the atom. Our goal here is to introduce you to the relationship between the experimental evidence for energy quantization and the energy-level diagrams used to interpret these experiments. Later in the chapter, we use the quantum theory to explain how energy is quantized and to predict the allowed values of the energy for several model problems. We have organized our discussion to group key concepts together, for better coherence and to provide physical insight; it does not strictly follow the historical development of the field.

Blackbody Radiation and Planck's Hypothesis

We are about to discuss a monumental achievement in the development of modern science, which changed forever the way we look at the world. This was the recognition that objects cannot gain or lose energy in arbitrary or continuous amounts, but instead transfer energy only in discrete, discontinuous amounts that are multiples of some fundamental quantity of energy. The German physicist Max Planck achieved this insight in 1901 while trying to explain some puzzling new experimental measurements on the interaction of solid objects with radiant energy, which was known as **blackbody radiation**. You will shortly see that you are already familiar with blackbody radiation in various guises, and we relate the discussion closely to the experimental results so that you can always see the problem exactly as Planck saw it. We invite you to read and think along with Planck and to witness an important demonstration of how science advances. When experimental results do not agree with established scientific theories, the theories must be either modified or discarded and replaced with new ones, to account for both the new and the old experimental results. This process leads to the development of theories that provide a more fundamental understanding of a wider range of phenomena than their predecessors.

Every object emits energy from its surface in the form of thermal radiation. This energy is carried by electromagnetic waves; the distribution of the wavelengths of electromagnetic waves depends on the temperature of the object. At ordinary temperatures, thermal radiation falls within the infrared portion of the electromagnetic spectrum; imaging this radiation is used to map the surface of Earth from satellites in space and for tracking the movement of people in darkness using “night vision” detectors. As objects are heated to higher temperatures, the total intensity of radiation emitted over all frequencies increases, and the frequency distribution of the intensity also changes. The solid curves in Figure 4.6 show how the measured radiation intensity depends on frequency and temperature. There are two important features of these curves. First, the maximum in the radiation intensity distribution moves to higher frequency (shorter wavelength) as the temperature increases. This phenomenon is observed in familiar objects such as the heating element on an electric kitchen range or the filament in an incandescent lightbulb. As these objects are heated, they first glow red, then orange, then yellow, and finally, white. It also explains the differences in color among stars; the hottest stars appear to be nearly white, whereas the colors of cooler stars can range from red to yellow. Second—and this is a key result—the radiation intensity falls to zero at extremely high frequencies for objects heated to any temperature.

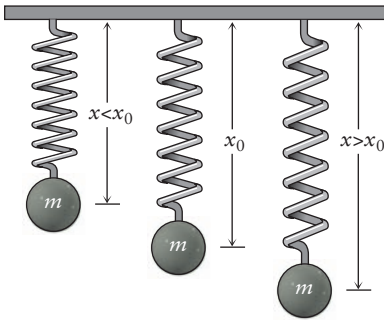
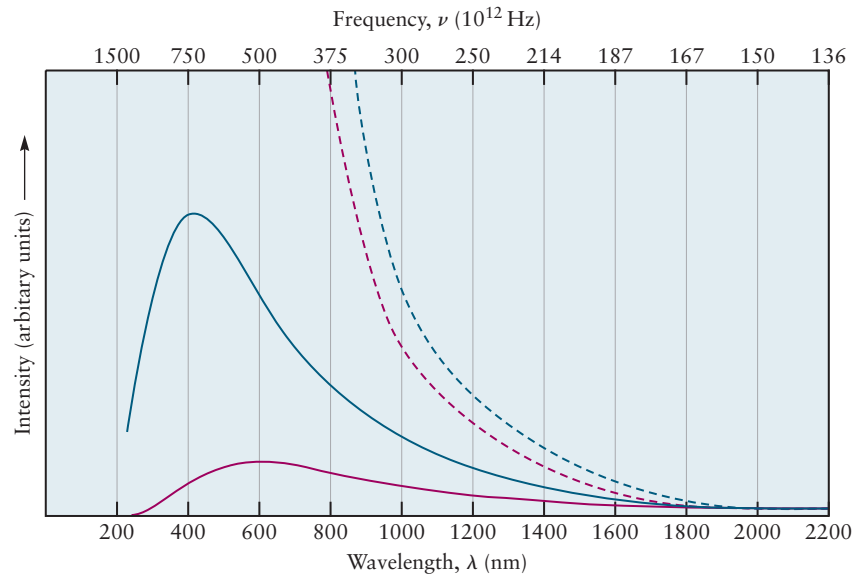
The sources of blackbody radiation, according to classical physics, are oscillating electrical charges in the surfaces of these objects that have been accelerated by ordinary thermal motion. Each motion persists for a certain period, producing radiation whose frequency is inversely related to that period. A number of scientists used different methods to calculate the radiation intensity curves using this simplified model and arrived at the following result:

$$\rho_T(\nu) = \frac{8\pi k_B T \nu^2}{c^3} \quad [4.2]$$

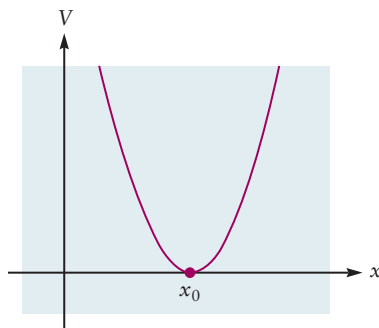
where $\rho_T(\nu)$ is the intensity of the radiation at the frequency ν ; k_B is a fundamental constant called the Boltzmann constant, which is discussed in Sections 9.5 and 9.6; T is the temperature in kelvins (K) and c is the speed of light.

These calculated results, shown for 5000 and 7000 K by the dashed curves in Figure 4.6, agree well with experiment at lower frequency. But the theory does not predict a maximum in the intensity distribution, and even worse, it disagrees badly with the experimental results at high frequencies. This feature of the result was called the “ultraviolet catastrophe” because it predicts an infinite intensity at very

FIGURE 4.6 The dependence of the intensity of blackbody radiation on wavelength for two temperatures: 5000 K (red curve) and 7000 K (blue curve). The sun has a blackbody temperature near 5780 K, and its light-intensity curve lies between the two shown. The classical theory (dashed curves) disagrees with observation at shorter wavelengths.



A charged particle of mass m bound to a solid surface by a spring is a model for the oscillatory motions of the surface atoms of a black body. The particle is shown at its rest position x_0 , at a position closer to the surface ($x < x_0$), and at one further from the surface ($x > x_0$).



The potential energy curve for an oscillator is a consequence of the “restoring force” that always drives the oscillator toward its equilibrium position.

short wavelengths, whereas the experimental intensities always remain finite and actually fall to zero at very short wavelengths (very high frequencies). The calculated result failed completely to explain the frequency distribution in blackbody radiation; yet, it is a direct consequence of the laws of classical physics. How could this conflict be resolved?

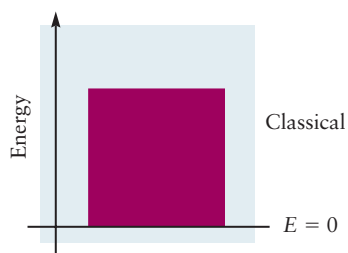
Blackbody radiation was explained by Max Planck in 1901, but only by overthrowing the very foundations of classical mechanics. Planck reasoned that the very high-frequency oscillators must not be excited by the thermal energy of the hot body to the same degree as the lower frequency oscillators. This was a challenge to explain because classical mechanics allows an oscillator to have any energy. Planck’s argument involved two steps, which are explained as follows.

For simplicity in following Planck’s hypothesis, let us focus on just one of the oscillating charged particles and visualize it as a ball of mass, m , held in place by a spring. As the particle moves in response to the thermal motion of the atoms in the hot body, the spring exerts a “restoring force,” F , which returns the particle to its equilibrium position, which we will call x_0 . As discussed in Appendix B for this same model problem, the restoring force is directly proportional to the displacement, and the force law is $F = -k(x - x_0)$, where the constant k measures the “stiffness” of the spring. The displacement of the particle oscillates about x_0 in a periodic motion of frequency $\nu = (1/2\pi)\sqrt{k/m}$, and the associated potential energy of the particle is $V(x) = \frac{1}{2}k(x - x_0)^2$. This model is the simple harmonic oscillator described in Appendix B. Classical mechanics puts no restrictions on the value of the total energy, E . The total energy can be large or small, and it can be changed smoothly and continuously from one arbitrary value to another.

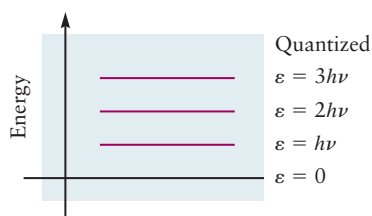
Planck’s first step was to pose a daring hypothesis: It is *not* possible to put an arbitrary amount of energy into an oscillator of frequency ν . Instead, he postulated that the oscillator must gain and lose energy in “packets,” or *quanta*, of magnitude $h\nu$, and that the total energy of an oscillator, ϵ_{osc} , can take only discrete values that are integral multiples of $h\nu$:

$$\epsilon_{\text{osc}} = nh\nu \quad n = 1, 2, 3, 4, \dots$$

[4.3]



An oscillator obeying classical mechanics has continuous values of energy and can gain or lose energy in arbitrary amounts.



An oscillator described by Planck's postulate has discrete energy levels. It can gain or lose energy only in amounts that correspond to the difference between two energy levels.

In Planck's hypothesis, h was a constant with physical units $\text{energy} \times \text{frequency}^{-1} = \text{energy} \times \text{time}$, but the value of which was yet to be determined.

You can easily visualize the consequences of Planck's hypothesis using the simple harmonic oscillator model. Replace the spring and ball with a rubber band stretched between your fingers. Experience shows that you can stretch the band to any arbitrary length by applying the right amount of energy (so long as you do not rupture the band). But under Planck's hypothesis, the band would accept only certain specific values of energy. The rubber band would behave as if it could be stretched only to certain specific positions. It simply would not respond to attempts to give it energy between these specific values. This fact is contrary to all ordinary human experience with tangible, macroscopic objects. And yet, this is how energy transfer operates in the microscopic world of atoms, electrons, and molecules.²

The dramatic contrast between the energy values allowed by classical mechanics and those that arise from Planck's postulate is illustrated using **energy-level diagrams**, in which a horizontal line represents an allowed energy value for a system. The height of each line above the zero of energy represents the total energy in that level. In macroscopic systems that are well described by classical mechanics, all energies are allowed; the upper energy level diagram in the margin represents the continuum of energies that the rubber band can accept up to the point where it breaks. For the quantum oscillators that Planck proposed, only those levels shown on the lower energy level diagram are allowed.

Planck's second step was to predict the radiation intensity curves by calculating the average energy in these quantized oscillators at each frequency as a function of temperature. The key idea is that the excitation of a particular oscillator is an all-or-nothing event; there is either enough thermal energy to cause it to oscillate or there is not. According to Planck, the falloff in the intensity with frequency at a given temperature of the blackbody radiation is due to a diminishing probability of exciting the high-frequency oscillators. Planck's intensity distribution is

$$\rho_T(\nu) = \frac{8\pi h\nu^3}{c^3} \frac{1}{e^{h\nu/k_B T} - 1} \quad [4.4]$$

All of the symbols in Equation 4.4 have been identified earlier in this chapter. The value of h was determined by finding the best fit between this theoretical expression and the experimental results. Figure 4.7 shows the fit for $T = 1646$ K, resulting in the value $h = 6.63 \times 10^{-34}$ J s. The value of h , a fundamental constant of nature, has been measured to very high precision over the years by a number of other techniques. It is referred to as **Planck's constant**, and the currently accepted value is

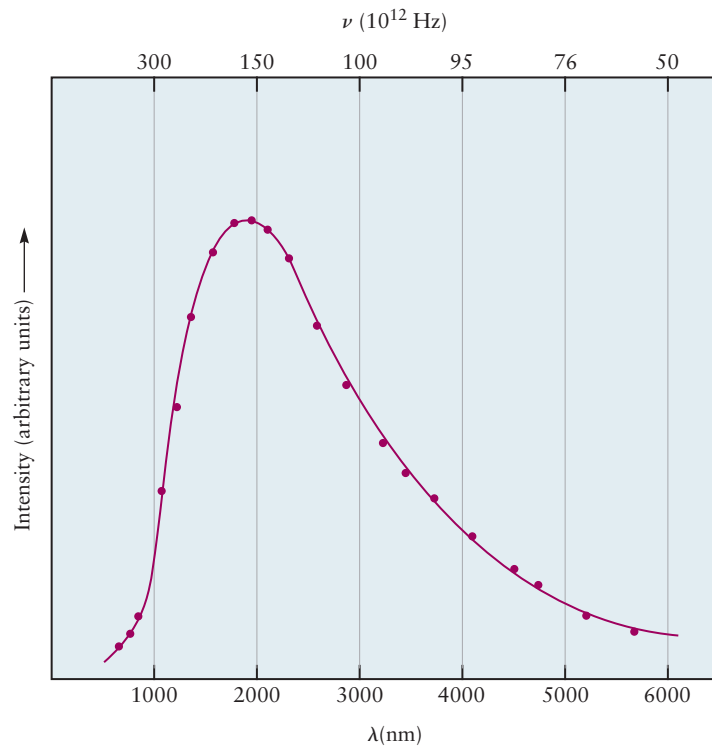
$$h = 6.62608 \times 10^{-34} \text{ J s}$$

We ask you to accept that the second fraction on the right-hand side of Equation 4.4 is the probability that an oscillator of frequency ν is activated at a given temperature T . Chapter 9 presents the origin of this probability in the famous Maxwell–Boltzmann distribution, but in this chapter we want to use the result to demonstrate some additional consequences of Planck's hypothesis.

Before proceeding to explore the implications of the Planck distribution, we need to check whether it reduces to the classical expression under the appropriate conditions. It is always important to check whether new concepts can be

²We will see later that energy transfer into macroscopic objects is also quantized. However, the discrete values are so closely spaced that they appear continuous.

FIGURE 4.7 Experimental test of Planck's distribution for blackbody radiation. The dots represent experimental data acquired at $T = 1646$ K. The continuous curve represents Planck's predicted distribution, with the parameter $h = 6.63 \times 10^{-34}$ J s. Agreement between experiment and theory is spectacular, demonstrating the validity of Planck's theory and also determining the value of the previously unknown parameter h .



matched with old concepts under appropriate conditions; this demonstrates that the new concepts represent an orderly advance in knowledge. We can imagine that all of the oscillators would be excited at sufficiently high temperatures, in which case, the system should behave according to the laws of classical physics. We express this condition mathematically by setting $h\nu/k_B T \ll 1$, a ratio that is nearly zero. You will soon learn in calculus that most functions can be represented by simpler forms as the argument of the function approaches zero. For the exponential function, $\exp(x) \approx 1 + x$ when x is nearly zero. Using this approximation, we obtain the high temperature limit of Planck's distribution

$$\rho_T(\nu) = \frac{8\pi h\nu^3}{c^3} \frac{1}{e^{h\nu/k_B T} - 1} \approx \frac{8\pi h\nu^3}{c^3} \frac{1}{([1 + h\nu/k_B T] - 1)} = \frac{8\pi k_B T \nu^2}{c^3} \quad [4.5]$$

which is valid as $T \rightarrow \infty$. This is indeed the classical result quoted in Equation 4.2.

Behind all the mathematics, Planck's dramatic explanation of blackbody radiation includes three fundamentally new ideas:

1. The energy of a system can take only discrete values, which are represented on its energy-level diagram.
2. A quantized oscillator can gain or lose energy only in discrete amounts $\Delta\varepsilon$, which are related to its frequency by $\Delta\varepsilon = h\nu$.
3. To emit energy from higher energy states, the temperature of a quantized system must be sufficiently high to excite those states.

These three ideas have permeated all areas of science and technology. They are the basis for our understanding that energy (like matter) is discrete, not continuous, and that it can be transferred only in discrete chunks and not by arbitrary amounts. Every system has its own energy-level diagram that describes the allowed energy values and the possible values of energy transfers.

Atomic Spectra and Transitions between Energy States

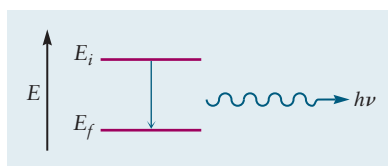
Light that contains a number of different wavelengths (Fig. 4.8) can be resolved into its components by passing it through a prism, because each wavelength is refracted through a different angle. One instrument used to separate light into its component wavelengths is called a **spectrograph** (Figs. 4.9a, b). The spectrograph is enclosed in a boxlike container to exclude stray light. The light to be analyzed enters through a narrow slit in the walls. The light passes to the prism, where it is dispersed into its components, and then falls on a photographic plate or other detector. The detector records the position and intensity of an image of the slit formed by each component wavelength. The recorded array of images is called the *spectrum* of the incoming light. If the light contains all frequencies, the spectrum is a continuous band (see Fig. 4.3). Early experiments showed that light emitted from gaseous atoms excited in flames or in electrical discharges gave discrete spectra, that is, a series of parallel lines. Each line was an image of the slit at a specific wavelength (see Fig. 4.9a). If white light is passed through a sample of gaseous atoms and the transmitted light then is sent into the spectrograph, the absorption spectrum that results consists of dark slit images superimposed on the continuous spectrum of white light (see Fig. 4.9b). These experiments show that atoms emit and absorb light at a discrete set of frequencies characteristic of a particular element (Fig. 4.10). For example, in 1885, J. J. Balmer discovered that hydrogen atoms emit a series of lines in the visible region, with frequencies given by the following simple formula:

$$\nu = \left[\frac{1}{4} - \frac{1}{n^2} \right] \times 3.29 \times 10^{15} \text{ s}^{-1} \quad n = 3, 4, 5, \dots \quad [4.6]$$

The hydrogen atom lines shown in Figure 4.10 fit this equation, with $n = 3, 4, 5,$ and 6 going from red to blue. Trying to understand the existence of discrete line spectra and the various empirical equations that relate the frequencies of the lines challenged physicists for more than three decades.

The first explanation for these surprising experimental results was provided in 1913 by the Danish physicist Niels Bohr. He proposed a model of the hydrogen atom that allowed only discrete energy states to exist. He also proposed that light absorption resulted from a *transition* of the atoms between two of these states. The frequency of the light absorbed is connected to the energy of the initial and final states by the expression

$$\nu = \frac{E_f - E_i}{h} \quad \text{or} \quad \Delta E = h\nu \quad [4.7]$$



An atom makes a transition from state E_i to E_f and emits a photon of frequency $\nu = [E_i - E_f]/h$.

where h is Planck's constant. In absorption, the energy of the final state, E_f , is greater than that of the initial state so the signs work out correctly; ν is a positive number as it must be. For emission, however, $E_f < E_i$, and Equation 4.7 would predict a negative frequency, which is, of course, impossible. To account for both absorption and emission processes using the convention universally adopted by chemists that $\Delta E = E_f - E_i$, we use the more general expression that $|\Delta E| = h\nu$ and that $\Delta E > 0$ for absorption, whereas $\Delta E < 0$ for emission. The Bohr model also accounts for the values of the discrete energy levels in the hydrogen atom (see Section 4.3).

The atoms of every element can be represented by an energy-level diagram in which the energy difference between two levels is related by Equation 4.7 to the frequency of a specific line in the experimental spectrum of the atom. Except for the simplest case of hydrogen, however, constructing the energy-level diagram from the experimental spectrum is difficult because numerous transitions are involved. Nonetheless, spectroscopists have assigned the atomic spectra of most of the elements in the periodic table, and extensive tabulations of the results are readily available.

FIGURE 4.8 When a gas is excited in an electrical discharge, it glows as it emits light. The colors of the light emitted by three gases are shown: (a) neon, (b) argon, and (c) mercury. Each emission consists of several wave-lengths of light, and the perceived color depends on which wavelength predominates.

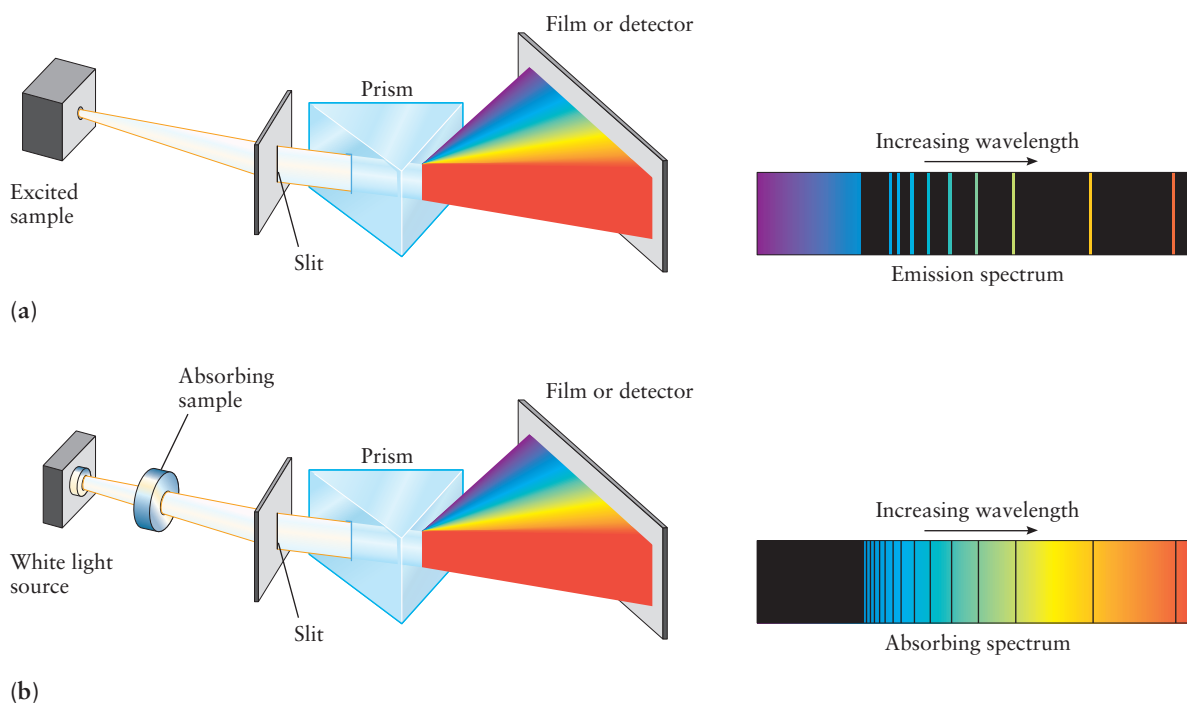
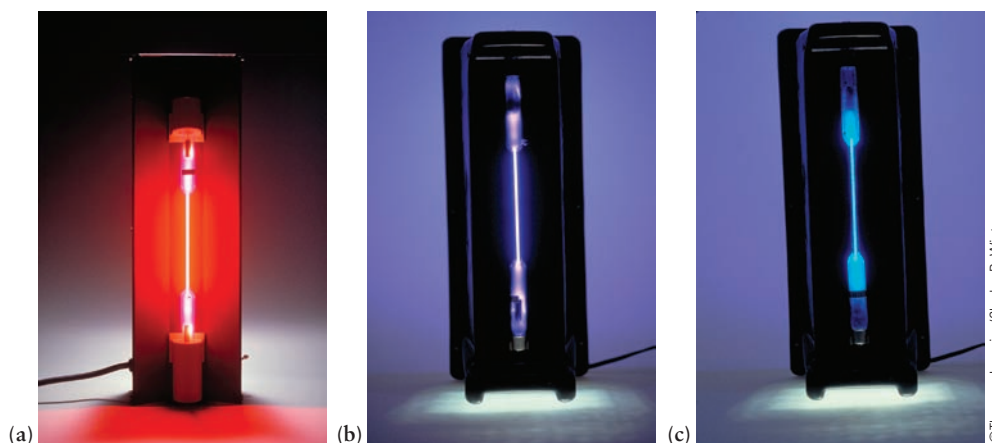


FIGURE 4.9 (a) The emission spectrum of atoms or molecules is measured by passing the light emitted from an excited sample through a prism to separate it according to wavelength, then recording the image on photographic film or with another detector. (b) In absorption spectroscopy, white light from a source passes through the unexcited sample, which absorbs certain discrete wavelengths of light. Dark lines appear on a bright background.

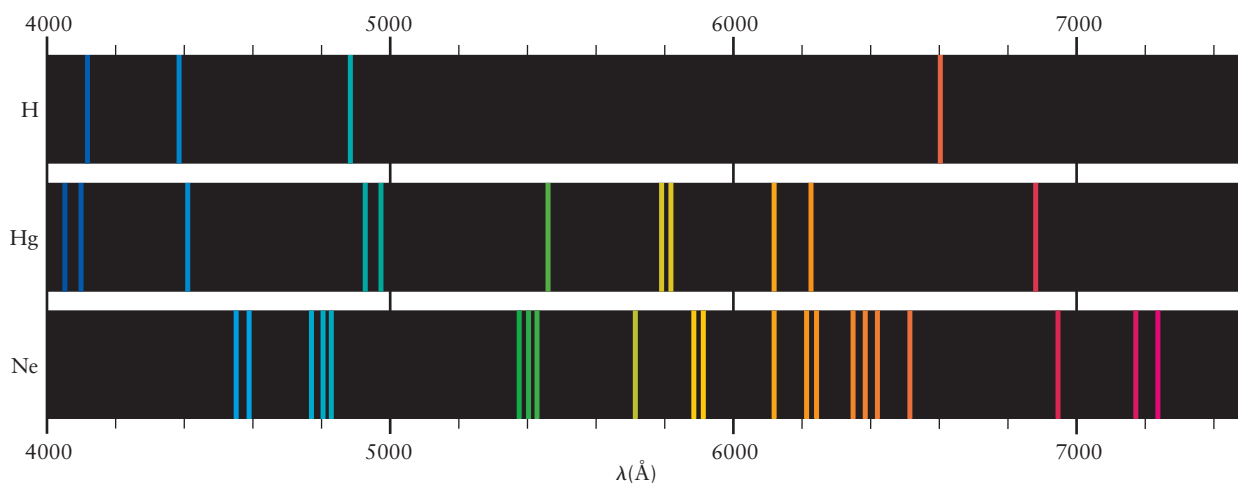


FIGURE 4.10 Atoms of hydrogen, mercury, and neon emit light at discrete wavelengths. The pattern seen is characteristic of the element under study. $1 \text{ \AA} = 10^{-10} \text{ m}$.

The Franck–Hertz Experiment and the Energy Levels of Atoms

In 1914, the German physicists James Franck and Gustav Hertz (nephew of Heinrich Hertz) conducted an experiment to test Bohr's hypothesis that the energy of atoms is quantized by measuring the energy transferred to an atom in collisions with electrons. In their apparatus (Fig. 4.11), electrons of known energy collided with gaseous atoms, and the energy lost from the electrons was measured. Electrons were emitted from the heated cathode C and accelerated toward the anode A. Holes in the anode allowed electrons to pass toward the collector plate P with known kinetic energy controlled by the accelerating voltage between C and A. The apparatus was filled to a low pressure with the gas to be studied. The current arriving at P was studied as a function of the kinetic energy of the electrons by varying the accelerating voltage.

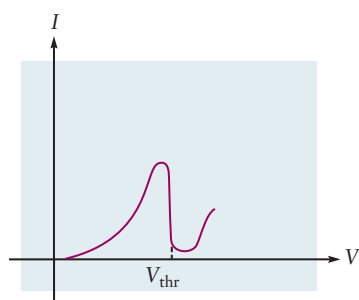
The experiment was started using a very low accelerating voltage, and the current was found to increase steadily as the accelerating voltage was increased. At a certain voltage, V_{thr} , the current dropped sharply, going nearly to zero. This observation implied that most of the electrons had lost their kinetic energy in collisions with the gas atoms and were unable to reach the collector. As the voltage was increased above V_{thr} , the current rose again. This result indicated that electrons were reaccelerated after collisions and gained sufficient energy to reach the collector.

The abrupt fall in the plot of current versus voltage at V_{thr} suggested that the kinetic energy of the electrons must reach a threshold eV_{thr} to transfer energy to the gas atoms, suggesting that the energy of the atoms must be quantized in discrete states. The **first excited state** must lie above the **ground state** (the state with lowest energy) by the amount eV_{thr} . Continuing the experiment with higher values of accelerating voltage revealed additional energy thresholds corresponding to excited states with higher energies.

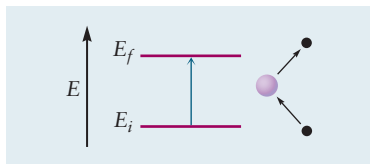
To confirm their interpretation, Franck and Hertz used a spectrograph to analyze light that was emitted by the excited atoms. When the accelerating voltage was below V_{thr} , no light was observed. When the accelerating voltage was slightly above V_{thr} , a single emission line was observed whose frequency was very nearly equal to

$$\nu = \frac{\Delta E}{h} = \frac{eV_{\text{thr}}}{h} \quad [4.8]$$

At higher accelerating voltages, additional spectral emission lines appeared as each additional excitation energy threshold was reached.

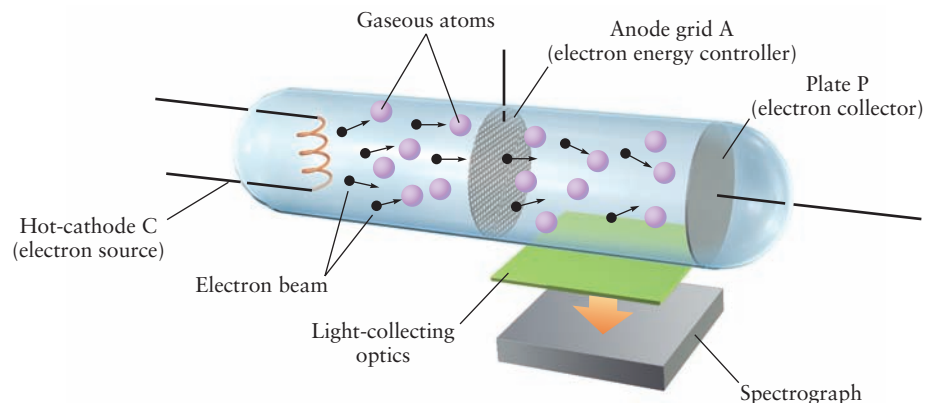


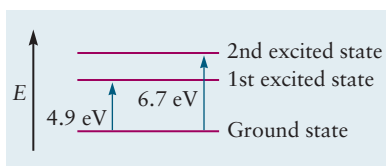
The current in the Franck–Hertz experiment shows a sharp change at a particular value of the accelerating voltage, corresponding to the threshold energy transfer from the electron to a gaseous atom.



The Franck–Hertz experiment measures directly the separation between energy levels of the atom by measuring the energy lost by an electron colliding with the atom.

FIGURE 4.11 Apparatus of Franck and Hertz that demonstrates the quantization of energy in atoms. Gaseous atoms collide with electrons and gain energy by collisions only when the energy of the electron exceeds a certain threshold. The excited atom then emits a photon whose frequency is determined by the energy transferred to the atom during the collision.





Simplified energy-level diagram for mercury.

EXAMPLE 4.2

The first two excitation voltage thresholds in the Franck–Hertz study of mercury vapor were found at 4.9 and 6.7 V. Calculate the wavelength of light emitted by mercury atoms after excitation past each of these thresholds.

SOLUTION

The emitted wavelength at a particular value of V_{thr} is given by the following equation:

$$\begin{aligned}\lambda &= \frac{hc}{\Delta E} = \frac{hc}{eV_{\text{thr}}} = \frac{(6.6261 \times 10^{-34} \text{ J s})(2.9979 \times 10^8 \text{ ms}^{-1})}{(1.6022 \times 10^{-19} \text{ C})(V_{\text{thr}}[\text{V}])} \\ &= \frac{1239.8 \text{ nm}}{V_{\text{thr}}[\text{V}]}\end{aligned}$$

The value of each emission wavelength is calculated by substituting in a particular value of V_{thr} expressed in units of volts (V).

At $V_{\text{thr}} = 4.9 \text{ V}$, the calculated wavelength is $\lambda = 250 \text{ nm}$. The wavelength actually observed above this threshold was 253.7 nm.

At $V_{\text{thr}} = 6.7 \text{ V}$, the calculated wavelength is $\lambda = 180 \text{ nm}$. The wavelength actually observed above this threshold was 184.9 nm.

Energy differences measured by the Franck–Hertz method and by optical emission spectroscopy agree quite closely. The optical measurements are more precise. These results enable us to begin to construct the energy diagram for mercury, showing the location of the first two excited states relative to the ground state.

Related Problems: 17, 18

The significance of the Franck–Hertz experiment in the development of atomic physics cannot be exaggerated. It demonstrated that atoms absorb energy in collisions with electrons only in discrete, quantized amounts. The energy is then released only in discrete, quantized amounts by light emission. The Franck–Hertz experiment provided dramatic confirmation of Bohr’s hypothesis that the energy of atoms is quantized in discrete states. It also provided a direct mechanical method for measuring the energy differences between these states and for constructing the energy-level diagram starting with the ground state. The technique continues to be used today to construct energy-level diagrams for molecules in the methods called “electron impact spectroscopy” or “electron energy loss spectroscopy.”

4.3 The Bohr Model: Predicting Discrete Energy Levels

Atomic spectra and Franck–Hertz experiments measure the differences between energy levels, which can be calculated from the experimental data using Equations 4.7 and 4.8. In 1913, Niels Bohr developed the first theoretical model to predict the energy levels of the hydrogen atom and one-electron ions such as He^+ , Li^{2+} , and Be^{3+} . The Bohr theory started from Rutherford’s *planetary model* of the atom. (You should review Section 3.2 before continuing further in this chapter.) Pay careful attention to the definition of an absolute energy scale for atoms by choosing a reference state whose energy we set as zero. The logical choice, as discussed in Section 3.2, is the electron at rest located infinitely far from the nucleus.

Bohr supplemented Rutherford’s planetary model of the atom with the assumption that an electron of mass m_e moves in a circular orbit of radius r about a

fixed nucleus. The total energy of the hydrogen atom, kinetic plus potential, is given by Equation 3.7, which we reproduce and renumber here as Equation 4.9 for convenience:

$$E = \frac{1}{2} m_e v^2 - \frac{Ze^2}{4\pi\epsilon_0 r} \quad [4.9]$$

The Coulomb force that attracts the electron to the nucleus, F_{coul} , is the negative derivative of the potential energy with respect to the separation r : $F_{\text{coul}} = -Ze^2/4\pi\epsilon_0 r^2$. Newton's second law relating force and acceleration is $F = m_e a$, and for uniform circular motion, the acceleration, a , of the electron is v^2/r . Combining these results gives the following relation for the *magnitude* of the force:

$$|F_{\text{Coulomb}}| = |m_e a| \quad [4.10a]$$

$$\frac{Ze^2}{4\pi\epsilon_0 r^2} = m_e \frac{v^2}{r} \quad [4.10b]$$

As mentioned earlier, classical physics requires that an accelerated electron emit electromagnetic radiation, thereby losing energy and eventually spiraling into the nucleus. Bohr avoided this conflict by simply *postulating* that only certain discrete orbits (characterized by radius r_n and energy E_n) are allowed, and that light is emitted or absorbed only when the electron “jumps” from one stable orbit to another. This bold assertion was Bohr's attempt to explain the existence of stable atoms, a well-established experimental fact. Faced with the contradiction between the experimental results and the requirements of classical electrodynamics, he simply discarded the latter in the formulation of his model.

The next step in the development of the Bohr model was his assertion that the angular momentum of the electron is quantized. This was an ad hoc assumption designed to produce stable orbits for the electron; it had no basis in either classical theory or experimental evidence. The **linear momentum** of an electron is the product of its mass and its velocity, $m_e v$. The **angular momentum**, L , is a different quantity that describes rotational motion about an axis. An introduction to angular momentum is provided in Appendix B. For the circular paths of the Bohr model, the angular momentum of the electron is the product of its mass, its velocity, and the radius of the orbit ($L = m_e v r$). Bohr postulated that the angular momentum is quantized in integral multiples of $h/2\pi$, where h is Planck's constant:

$$L = m_e v r = n \frac{h}{2\pi} \quad n = 1, 2, 3, \dots \quad [4.11]$$

The existence of discrete orbits and quantized energies follows directly as a consequence of the quantization of angular momentum.

We can determine the properties of these discrete orbits as follows. Equations 4.9 and 4.10 contain two unknowns, v and r . Solving Equation 4.11 for v ($= nh/2\pi m_e r$), inserting it into Equation 4.10, and solving for r gives the allowed values for radius of the orbits:

$$r_n = \frac{\epsilon_0 n^2 h^2}{\pi Z e^2 m_e} = \frac{n^2}{Z} a_0 \quad [4.12]$$

where a_0 , the **Bohr radius**, has the numerical value $5.29 \times 10^{-11} \text{ m} = 0.529 \text{ \AA}$. (The Bohr radius ($a_0 = \epsilon_0 h^2 / \pi e^2 m_e$) is a convenient, fundamental unit of length in

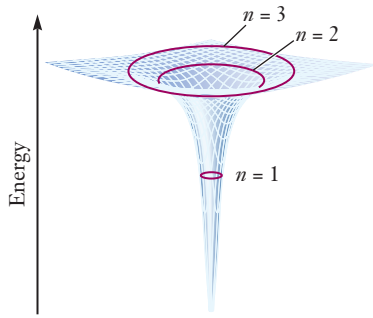


FIGURE 4.12 The potential energy of the electron and nucleus in the hydrogen atom has its lowest (most negative) value when the electron is closest to the nucleus. (Compare with the one-dimensional plot in Figure 3.2.) The electron moving away from the nucleus can be seen as moving up the sides of a steep potential energy well. In the Bohr theory, it can “catch” and stick on the sides only at certain allowed values of r , the radius, and E , the energy. The first three of these are shown by rings.

atomic physics that relieves us from the burden of carrying along all of the constants in Eq. 4.12.) This first prediction of the Bohr model is the existence of a series of orbits whose distances from the nucleus increase dramatically with increasing n . Substituting r_n from Equation 4.12 into Equation 4.11 allows us to calculate the velocity v_n corresponding to the orbit with radius r_n .

$$v_n = \frac{nh}{2\pi m_e r_n} = \frac{Ze^2}{2\epsilon_0 nh} \quad [4.13]$$

The results obtained for r_n and v_n can now be substituted into Equation 4.9 to give us the allowed values of the energy:

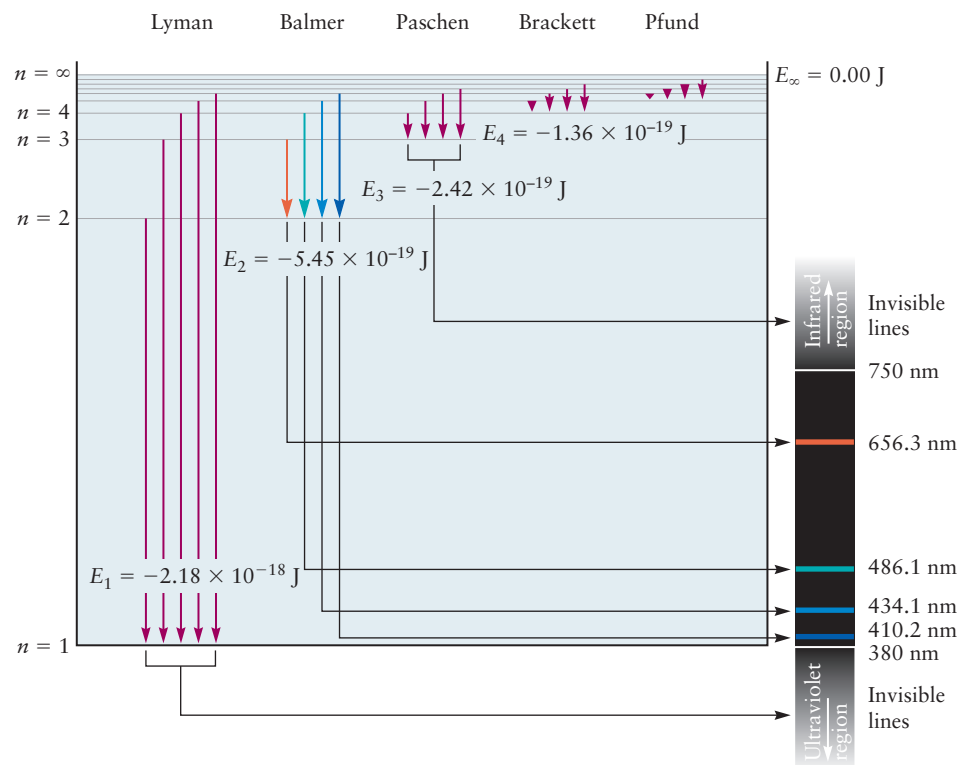
$$E_n = \frac{-Z^2 e^4 m_e}{8\epsilon_0^2 n^2 h^2} = -(2.18 \times 10^{-18} \text{ J}) \frac{Z^2}{n^2} \quad n = 1, 2, 3, \dots \quad [4.14a]$$

That these energies are negative is a consequence of our choice for the zero of energy, as discussed in Section 3.2 and shown in Figure 3.2. For the same reason that we introduced the Bohr radius, it is convenient to express atomic energy levels in units of **rydbergs**, where 1 rydberg = 2.18×10^{-18} J. The energy level expression then becomes

$$E_n = -\frac{Z^2}{n^2} \quad (\text{rydberg}) \quad n = 1, 2, 3, \dots \quad [4.14b]$$

The Bohr model thus predicts a discrete energy-level diagram for the one-electron atom (Figs. 4.12 and 4.13). The ground state is identified by $n = 1$, and the excited states have higher values of n (see Fig. 4.12).

FIGURE 4.13 In energy levels of the hydrogen atom, the separated electron and proton are arbitrarily assigned zero energy, and all other energies are more negative than that. Atoms emit light as they fall from higher to lower energy levels (blue arrows). Each series of related transitions is named after the person who discovered it.



The **ionization energy** is the minimum energy required to remove an electron from an atom (see Section 3.3). In the Bohr model, ionization involves a transition from the $n = 1$ state to the $n = \infty$ state, in which $E_n = 0$. The associated energy change is

$$\Delta E = E_{\text{final}} - E_{\text{initial}} = 0 - (-2.18 \times 10^{-18} \text{ J}) = 2.18 \times 10^{-18} \text{ J}$$

Multiplying this result by Avogadro's number gives the ionization energy, IE , per mole of atoms:

$$IE = (6.022 \times 10^{23} \text{ atoms mol}^{-1})(2.18 \times 10^{-18} \text{ J atom}^{-1}) = 1.31 \times 10^6 \text{ J mol}^{-1} = 1310 \text{ kJ mol}^{-1}$$

This prediction agrees with the experimentally observed ionization energy of hydrogen atoms and provides confidence in the validity of the Bohr model. The discussion in Section 3.3 related measured ionization energies qualitatively to the effective potential energy binding electrons inside atoms. The Bohr model was the first physical theory that could predict ionization energies with remarkable accuracy.

EXAMPLE 4.3

Consider the $n = 2$ state of Li^{2+} . Using the Bohr model, calculate the radius of the electron orbit, the electron velocity, and the energy of the ion relative to that of the nucleus and electron separated by an infinite distance.

SOLUTION

Because $Z = 3$ for Li^{2+} (the nuclear charge is $+3e$) and $n = 2$, the radius is

$$r_2 = \frac{n^2}{Z} a_0 = \frac{4}{3} a_0 = \frac{4}{3} (0.529 \text{ \AA}) = 0.705 \text{ \AA}$$

The velocity is

$$v_2 = \frac{nh}{2\pi m_e r_2} = \frac{2(6.626 \times 10^{-34} \text{ J s})}{2\pi(9.11 \times 10^{-31} \text{ kg})(0.705 \times 10^{-10} \text{ m})} = 3.28 \times 10^6 \text{ m s}^{-1}$$

The energy is

$$E_2 = -\frac{(3)^2}{(2)^2} (2.18 \times 10^{-18} \text{ J}) = -4.90 \times 10^{-18} \text{ J}$$

Typically, atomic sizes fall in the range of angstroms, and atomic excitation energies in the range of 10^{-18} J. This is consistent with the calculations of coulomb potential energies in electron volts and dimensions in angstroms in Section 3.2.

Related Problems: 19, 20

Atomic Spectra: Interpretation by the Bohr Model

When a one-electron atom or ion undergoes a transition from a state characterized by quantum number n_i to a state lower in energy with quantum number n_f ($n_i > n_f$), light is emitted to carry off the energy $h\nu$ lost by the atom. By conservation of energy, $E_i = E_f + h\nu$; thus,

$$h\nu = \frac{Z^2 e^4 m_e}{8\epsilon_0^2 h^2} \left[\frac{1}{n_f^2} - \frac{1}{n_i^2} \right] \quad (\text{emission}) \quad [4.15]$$

As n_i and n_f take on a succession of integral values, lines are seen in the emission spectrum (see Fig. 4.13) with frequencies

$$\nu = \frac{Z^2 e^4 m_e}{8 \epsilon_0^2 h^3} \left(\frac{1}{n_f^2} - \frac{1}{n_i^2} \right) = (3.29 \times 10^{15} \text{ s}^{-1}) Z^2 \left(\frac{1}{n_f^2} - \frac{1}{n_i^2} \right) \quad [4.16]$$

$$n_i > n_f = 1, 2, 3, \dots \text{ (emission)}$$

Conversely, an atom can *absorb* energy $h\nu$ from a photon as it undergoes a transition to a *higher* energy state ($n_f > n_i$). In this case, conservation of energy requires $E_i + h\nu = E_f$; thus, the absorption spectrum shows a series of lines at frequencies

$$\nu = (3.29 \times 10^{15} \text{ s}^{-1}) Z^2 \left(\frac{1}{n_i^2} - \frac{1}{n_f^2} \right) \quad [4.17]$$

$$n_f > n_i = 1, 2, 3, \dots \text{ (absorption)}$$

For hydrogen, which has an atomic number of $Z = 1$, the predicted emission spectrum with $n_f = 2$ corresponds to the series of lines in the visible region measured by Balmer and shown in Figure 4.13. A series of lines at higher frequencies (in the ultraviolet region) is predicted for $n_f = 1$ (the Lyman series), and other series are predicted at lower frequencies (in the infrared region) for $n_f = 3, 4, \dots$. In fact, the predicted and observed spectra of hydrogen and one-electron ions are in excellent agreement—a major triumph of the Bohr theory.

Despite these successes, the Bohr theory has a number of shortcomings. Most important, it cannot predict the energy levels and spectra of atoms and ions with more than one electron. Also, more fundamentally, it was an uncomfortable hybrid of classical and nonclassical concepts. The postulate of quantized angular momentum—which led to the circular orbits—had no fundamental basis and was simply grafted onto classical physics to force the predictions of classical physics to agree with the experimental results. In 1926, the Bohr theory was replaced by modern quantum mechanics in which the quantization of energy and angular momentum arise as natural consequences of the basic postulates and require no additional assumptions. The circular orbits of the Bohr theory do not appear in quantum mechanics. The Bohr theory provided the conceptual bridge from classical theoretical physics to the new quantum mechanics. Its historical and intellectual importance cannot be exaggerated.

4.4 Evidence for Wave–Particle Duality

The Bohr theory provided a prescription for calculating the discrete energy levels of a one-electron atom or ion, but it did not explain the origin of energy quantization. A key step toward the development of modern quantum mechanics was the concept of **wave–particle duality**—the idea that particles sometimes behave as waves, and vice versa. Experiments were forcing physicists to recognize that physical systems could display either particle or wave characteristics, depending on the experimental conditions to which they were subjected. German physicist Albert Einstein introduced wave–particle duality to explain the photoelectric effect, in which light acted as a particle. French physicist Louis de Broglie suggested that particles could exhibit wavelike properties, and the stage was set for the new quantum mechanics to synthesize wave–particle duality and energy quantization into a comprehensive new theory.

The Photoelectric Effect

In addition to the conceptual problems with the planetary model of the atom and the difficulties with blackbody radiation, another conflict between experiment and classical theory arose from the observation of the **photoelectric effect**. A beam of light shining onto a metal surface (called the *photocathode*) can eject electrons (called *photoelectrons*) and cause an electric current (called a *photocurrent*) to flow (Fig. 4.14). The photocurrent shows an extremely interesting dependence on the frequency and intensity of the incident light (Fig. 4.15). Regardless of the light intensity, no photocurrent flows until the frequency exceeds a particular threshold value ν_0 , which is unique for each metal. Low-frequency (long wavelength; for example, red) light apparently cannot provide enough energy to eject the electrons, no matter how intense it is. When the frequency of the light is increased through the threshold value (corresponding, perhaps, to green or blue light), electrons are emitted and the photocurrent is directly proportional to the light intensity. The frequency of the light apparently is the key to delivering enough energy to eject the electrons; no electrons are emitted when the surface is excited by light whose frequency is below the threshold frequency, but electrons are readily emitted for

FIGURE 4.14 In a photoelectric cell (photocell), light strikes a metal surface in an evacuated space and ejects electrons. The electrons are attracted to a positively charged collector, and a current flows through the cell.

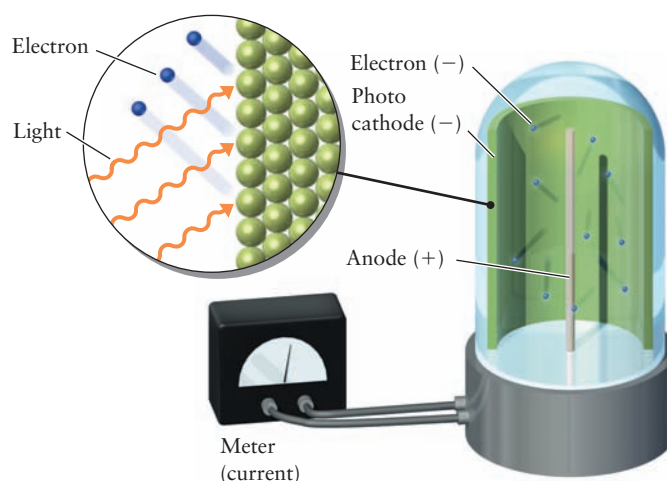
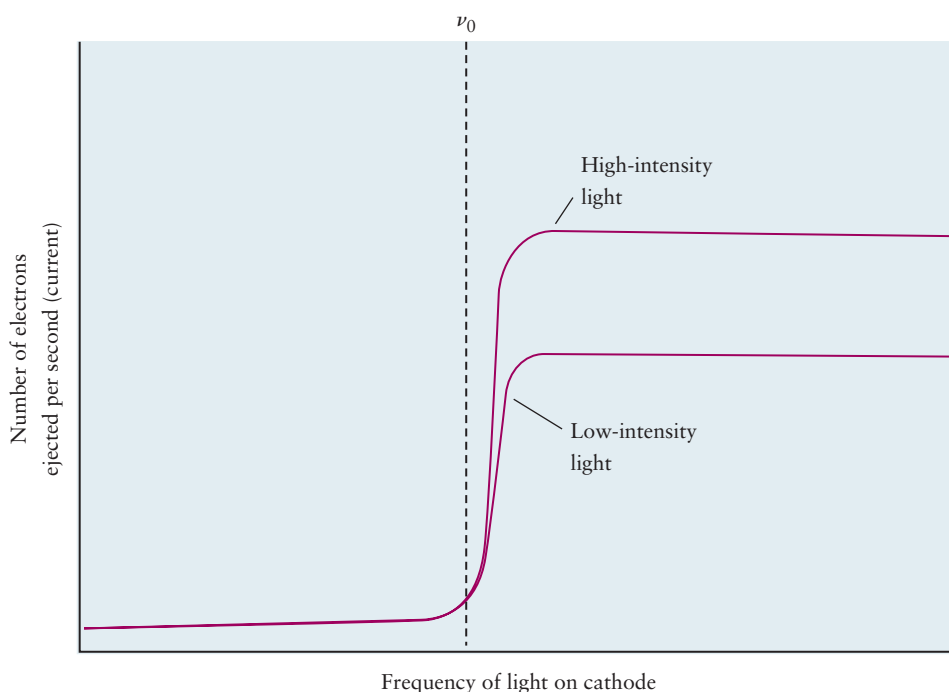


FIGURE 4.15 Frequency and intensity dependence of the photoelectric effect. Only light above the threshold frequency can eject photoelectrons from the surface. Once the frequency threshold has been passed, the total current of photoelectrons emitted depends on the intensity of the light, not on its frequency.



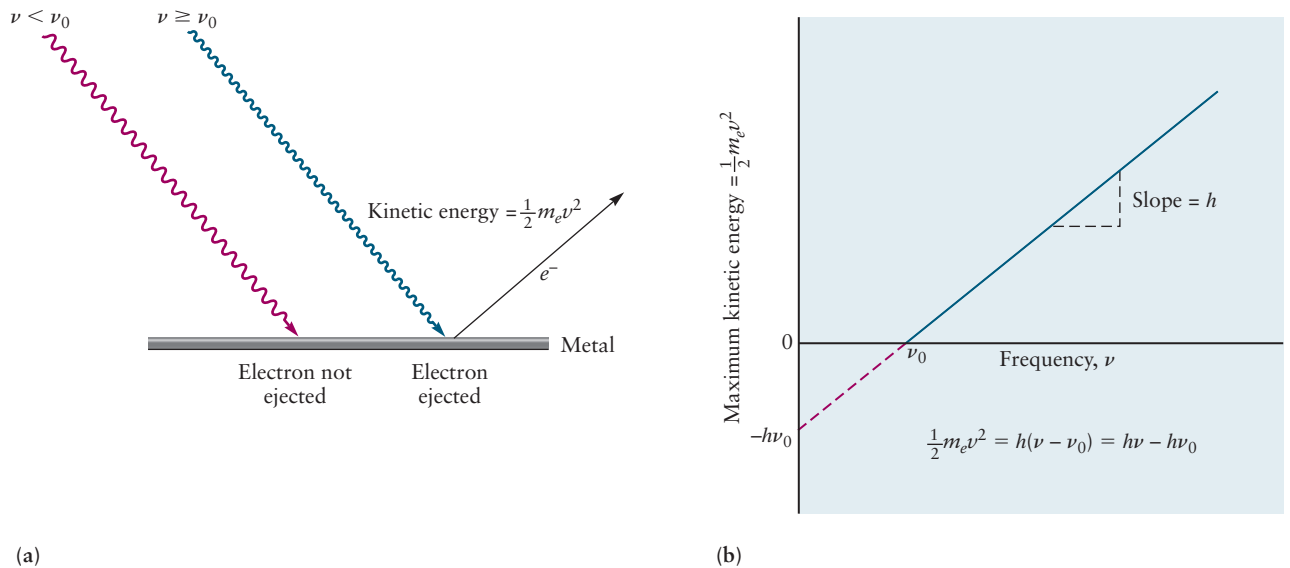
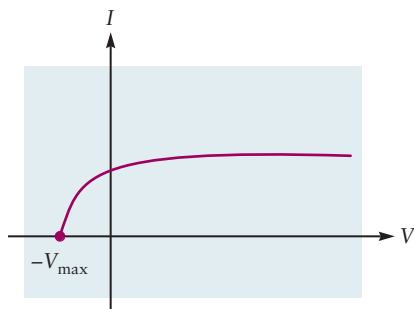


FIGURE 4.16 (a) Two key aspects of the photoelectric effect. Blue light is effective in ejecting electrons from the surface of this metal, but red light is not. (b) The maximum kinetic energy of the ejected electrons varies linearly with the frequency of light used.

all frequencies above the threshold frequency. These results could not be explained by classical physics. According to classical electromagnetic theory, the energy associated with electromagnetic radiation depends on only the intensity of the radiation, not on its frequency. Why, then, could a low-intensity (dim) beam of blue light (high frequency) eject electrons from sodium when a high-intensity (bright) beam of red light (low frequency) had no effect at all (Fig. 4.16a)? The key to the explanation is to relate the energy imparted by the light at ν_0 to the energy with which the photoelectrons are emitted from atoms in the metal.

The photoelectrons leaving the metal surface and traveling toward the detector have a range of kinetic energies. Let's assume that those photoelectrons arriving at the collector with E_{\max} were emitted from atoms at the surface of the metal. Assume those arriving with lower kinetic energy were emitted deeper in the metal but lost some kinetic energy through collisions with other metal atoms before escaping from the surface. Then, the value of E_{\max} should be directly related to the energy acquired by the photoelectron during the ejection process. We determine this maximum kinetic energy as follows. When the frequency and intensity of the beam are held constant, the magnitude of the photocurrent depends on the electrical potential (voltage) of the collector relative to the photocathode. At sufficiently positive potentials, all of the photoelectrons are attracted to the collector and the current–voltage curve becomes flat, or saturated. As the potential of the collector is made more negative, photoelectrons arriving with kinetic energies less than the maximum are repelled and the photocurrent decreases. Only those photoelectrons with sufficient kinetic energy to overcome this repulsion reach the collector. As the collector is made still more negative, the photocurrent drops sharply to zero at $-V_{\max}$, identifying the maximum in the kinetic energy of the photoelectrons: $E_{\max} = eV_{\max}$. The potential required to stop all of the electrons from arriving at the collector is thus a direct measure of their maximum kinetic energy, expressed in units of electron volts (eV) (see Section 3.2). But what was the connection between ν_0 and E_{\max} ?

In 1905, Einstein used Planck's quantum hypothesis to explain the photoelectric effect. First, he suggested that a light wave of frequency ν consists of quanta of energy (later called **photons** by G. N. Lewis), each of which carries energy, $E_{\text{photon}} = h\nu$. Second, Einstein assumed that, in the photoelectric effect, an electron in the metal absorbs a photon of light and thereby gains the energy required to escape from the metal. A photoelectron emitted from beneath the



The current in a photocell depends on the potential between cathode and collector.

surface will lose energy E' in collisions with other atoms and Φ in escaping through the surface, after which it travels through the vacuum to the detector with kinetic energy E . Conservation of energy leads to the relation $h\nu = E' + \Phi + E_k$ for the process. Electrons with the maximum kinetic energy are emitted at the surface, so for them $E' = 0$. Therefore, Einstein's theory predicts that the maximum kinetic energy of photoelectrons emitted by light of frequency ν is given by

$$E_{\max} = \frac{1}{2}mv_e^2 = h\nu - \Phi \quad [4.18]$$

where $\Phi = h\nu_0$ is a constant characteristic of the metal. The key idea of Einstein's explanation is that the interaction of a photon with an electron is a single event and the result is all or nothing; either the photon does or does not have enough energy to overcome the forces that bind the electron to the solid.

Einstein's theory predicts that the maximum kinetic energy is a linear function of the frequency, which provides a means for testing the validity of the theory. Experiments conducted at several frequencies demonstrated that the relation between E_{\max} and frequency is indeed linear (see Fig. 4.16b). The slope of the experimental data determined the numerical value of h to be identical to the value that Planck found by fitting the experimental data to his theoretical blackbody radiation intensity distribution. Einstein's interpretation also provided a means to obtain the value of the quantity Φ from the experimental data as the "energy intercept" of the linear graph. Φ , called the **work function** of the metal, represents the binding energy, or energy barrier, that electrons must overcome to escape from the metal surface after they have absorbed a photon inside the metal. Φ governs the extraction of electrons from metal surfaces by heat and by electric fields, as well as by the photoelectric effect, and it is an essential parameter in the design of numerous electronic devices.

EXAMPLE 4.4

Light with a wavelength of 400 nm strikes the surface of cesium in a photocell, and the maximum kinetic energy of the electrons ejected is 1.54×10^{-19} J. Calculate the work function of cesium and the longest wavelength of light that is capable of ejecting electrons from that metal.

SOLUTION

The frequency of the light is

$$\nu = \frac{c}{\lambda} = \frac{3.00 \times 10^8 \text{ m s}^{-1}}{4.00 \times 10^{-7} \text{ m}} = 7.50 \times 10^{14} \text{ s}^{-1}$$

The binding energy $h\nu_0$ can be calculated from Einstein's formula:

$$\begin{aligned} E_{\max} &= h\nu - h\nu_0 \\ 1.54 \times 10^{-19} \text{ J} &= (6.626 \times 10^{-34} \text{ J s})(7.50 \times 10^{14} \text{ s}^{-1}) - h\nu_0 \\ &= 4.97 \times 10^{-19} \text{ J} - h\nu_0 \\ \Phi = h\nu_0 &= (4.97 - 1.54) \times 10^{-19} \text{ J} = 3.43 \times 10^{-19} \text{ J} \end{aligned}$$

The minimum frequency ν_0 for the light to eject electrons is then

$$\nu_0 = \frac{3.43 \times 10^{-19} \text{ J}}{6.626 \times 10^{-34}} = 5.18 \times 10^{14} \text{ s}^{-1}$$

From this, the maximum wavelength λ_0 is

$$\lambda_0 = \frac{c}{\nu_0} = \frac{3.00 \times 10^8 \text{ m s}^{-1}}{5.18 \times 10^{14} \text{ s}^{-1}} = 5.79 \times 10^{-7} \text{ m} = 579 \text{ nm}$$

Related Problems: 27, 28

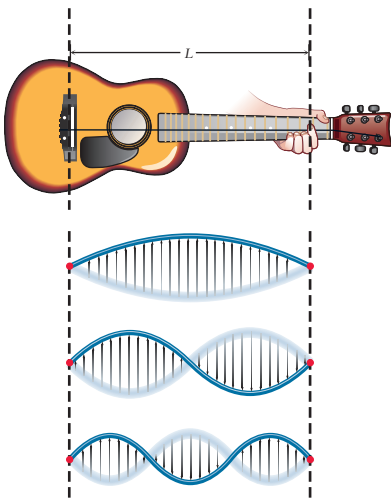


FIGURE 4.17 A guitar string of length L with fixed ends can vibrate in only a restricted set of ways. The positions of largest amplitude for the first three harmonics are shown here. In standing waves such as these, the whole string is in motion except at its end and at the nodes.

That two independent experiments involving two totally different phenomena gave the same value of h inspired great confidence in the validity of the quantum hypotheses that Planck and Einstein proposed, despite their unsettling implications. Einstein's bold assertion that light consisted of a stream of bundles of energy that appeared to transfer their energy through collisions like those of material particles was completely at odds with the classical wave representation of light, which had already been amply confirmed by experimental studies. How could light be both a wave and a particle?

By 1930, these paradoxes had been resolved by quantum mechanics, which superseded Newtonian mechanics. The classical wave description of light is adequate to explain phenomena such as interference and diffraction, but the emission of light from matter and the absorption of light by matter are described by the particlelike photon picture. A hallmark of quantum, as opposed to classical, thinking is not to ask “What is light?” but instead “How does light behave under particular experimental conditions?” Thus, wave–particle duality is not a contradiction, but rather part of the fundamental nature of light and also of matter.

De Broglie Waves

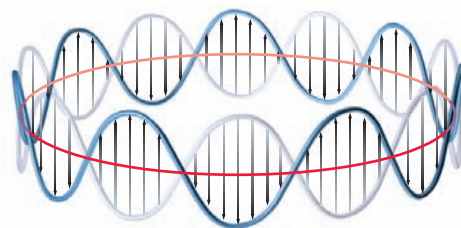
Thus far, this chapter has considered only one type of wave, a **traveling wave**. Electromagnetic radiation (light, x-rays, and gamma rays) is described by such a traveling wave moving through space at speed c . Another type of wave is a **standing wave**, of which a simple example is a guitar string with fixed ends (an example of a physical *boundary condition*). A plucked string vibrates, but only certain oscillations of the string are possible. Because the ends are fixed, the only oscillations that can persist are those in which an integral number of half-wavelengths fits into the length of string, L (Fig. 4.17). The condition on the allowed wavelengths is

$$n \frac{\lambda}{2} = L \quad n = 1, 2, 3, \dots \quad [4.19]$$

It is impossible to create a wave with any other value of λ if the ends of the string are fixed. The oscillation with $n = 1$ is called the **fundamental** or first harmonic, and higher values of n correspond to higher harmonics. At certain points on the standing wave, the amplitude of oscillation is zero; these points are called **nodes**. (The fixed ends are not counted as nodes.) The higher the number of the harmonic n , the more numerous the nodes, the shorter the wavelength, the higher the frequency, and the higher the energy of the standing wave.

De Broglie realized that such standing waves are examples of quantization: Only certain discrete vibrational modes, characterized by the “quantum number” n , are allowed for the vibrating string. He suggested that the quantization of energy in a one-electron atom might have the same origin, and that the electron might be associated with a standing wave, in this case, a *circular* standing wave oscillating about the nucleus of the atom (Fig. 4.18). For the amplitude of the wave to be well defined (single valued and smooth), an integral number of

FIGURE 4.18 A circular standing wave on a closed loop. The state shown has $n = 7$, with seven full wavelengths around the circle.



wavelengths must fit into the circumference of the circle ($2\pi r$). The condition on the allowed wavelengths for standing circular waves is

$$n\lambda = 2\pi r \quad n = 1, 2, 3, \dots \quad [4.20]$$

Bohr's assumption about quantization of the angular momentum of the electron was

$$m_e v r = n \frac{h}{2\pi} \quad [4.21]$$

which can be rewritten as

$$2\pi r = n \left[\frac{h}{m_e v} \right] \quad [4.22]$$

Comparison of de Broglie's equation (see Eq. 4.20) with Bohr's equation (see Eq. 4.22) shows that the wavelength of the standing wave is related to the linear momentum, p , of the electron by the following simple formula:

$$\lambda = \frac{h}{m_e v} = \frac{h}{p} \quad [4.23]$$

De Broglie used the theory of relativity to show that exactly the same relationship holds between the wavelength and momentum of a *photon*. De Broglie therefore proposed as a generalization that any particle—no matter how large or small—moving with linear momentum p has wavelike properties and a wavelength of $\lambda = h/p$ associated with its motion.

EXAMPLE 4.5

Calculate the de Broglie wavelengths of (a) an electron moving with velocity $1.0 \times 10^6 \text{ m s}^{-1}$ and (b) a baseball of mass 0.145 kg , thrown with a velocity of 30 m s^{-1} .

SOLUTION

$$\begin{aligned} \text{(a)} \quad \lambda &= \frac{h}{p} = \frac{h}{m_e v} = \frac{6.626 \times 10^{-34} \text{ J s}}{(9.11 \times 10^{-31} \text{ kg})(1.0 \times 10^6 \text{ m s}^{-1})} \\ &= 7.3 \times 10^{-10} \text{ m} = 7.3 \text{ \AA} \end{aligned}$$

$$\begin{aligned} \text{(b)} \quad \lambda &= \frac{h}{mv} = \frac{6.626 \times 10^{-34} \text{ J s}}{(0.145 \text{ kg})(30 \text{ m s}^{-1})} \\ &= 1.5 \times 10^{-34} \text{ m} = 1.5 \times 10^{-24} \text{ \AA} \end{aligned}$$

The latter wavelength is far too small to be observed. For this reason, we do not recognize the wavelike properties of baseballs or other macroscopic objects, even though they are always present. However, on a microscopic level, electrons moving in atoms show wavelike properties that are essential for explaining atomic structure.

Related Problems: 31, 32

Electron Diffraction

Under what circumstances does the wavelike nature of particles become apparent? When waves from two sources pass through the same region of space, they *interfere* with each other. Consider water waves as an example. When two crests meet,

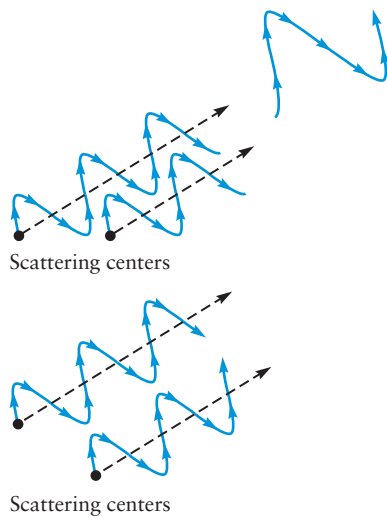


FIGURE 4.19 A beam of x-rays (not shown) is striking two scattering centers that emit scattered radiation. The difference in the lengths of the paths followed by the scattered waves determines whether they interfere (a) constructively or (b) destructively.

constructive interference occurs and a higher crest (greater amplitude) appears; where a crest of one wave meets a trough of the other, *destructive* interference (smaller or even zero amplitude) occurs (Fig. 4.19).

As discussed in more detail in Chapter 21, it was known by 1914 that x-rays diffract from the lattice planes of a single crystal, because the spacing between the planes is comparable with the wavelength of the x-rays used in the experiment. Figure 4.20 shows the construction used to derive the scattering law. Clearly, waves scattered by planes located farther from the surface must travel a greater distance to reach the detector than those scattered from the surface plane. The condition for *constructive* interference is given by Bragg's law:

$$n\lambda = 2d \sin \theta \quad [4.24]$$

which is derived in Chapter 21. The integer n tells which planes are responsible, λ is the x-ray wavelength, d is the spacing between the planes, and θ is the angle of incidence the impinging x-ray makes with the surface plane. If the x-ray source and detector are fixed in space and the sample is rotated about an axis that changes the angle θ , then a series of peaks appears whenever the diffraction condition is satisfied, allowing the lattice spacing d to be determined. X-ray diffraction was (and still is) among our most powerful tools for determining the three-dimensional structures of crystals.

If the de Broglie hypothesis was correct, then particles whose de Broglie wavelengths were comparable with lattice spacings should also diffract. This was indeed demonstrated to be the case in 1927 by the American physicists C. Davisson and L. H. Germer. In their experiment, a beam of low-energy electrons was directed toward a single crystal nickel sample in vacuum. The kinetic energy of the electrons could be varied continuously, and the sample could be rotated in space to change the angle θ . They conducted two experiments (the results of these experiments are shown in Fig. 4.21). They measured the angular dependence of the scattered electron current at fixed incident energy, and they measured the energy dependence of the scattered electron current at fixed θ . Let's see whether the de Broglie wavelength of the electrons used in this experiment is comparable with atomic lattice spacings, as required for the electrons to diffract from the planes of atoms in the solid.

The kinetic energy of an electron accelerated from rest to a final voltage V is $\mathcal{T} = eV$, where e is the charge on the electron. Recalling that $p = mv$ and

FIGURE 4.20 Constructive interference of x-rays scattered by atoms in lattice planes. Three beams of x-rays, scattered by atoms in three successive layers of a crystal are shown. Note that the phases of the waves are the same along the line CH, indicating constructive interference at this scattering angle 2θ .

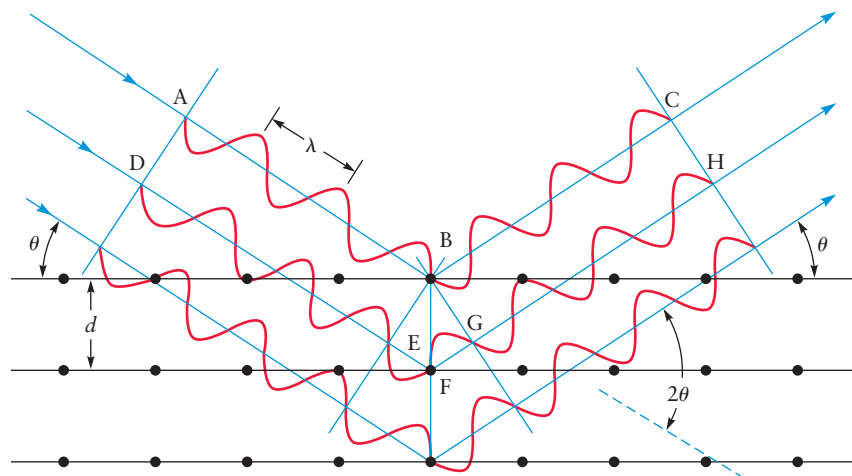
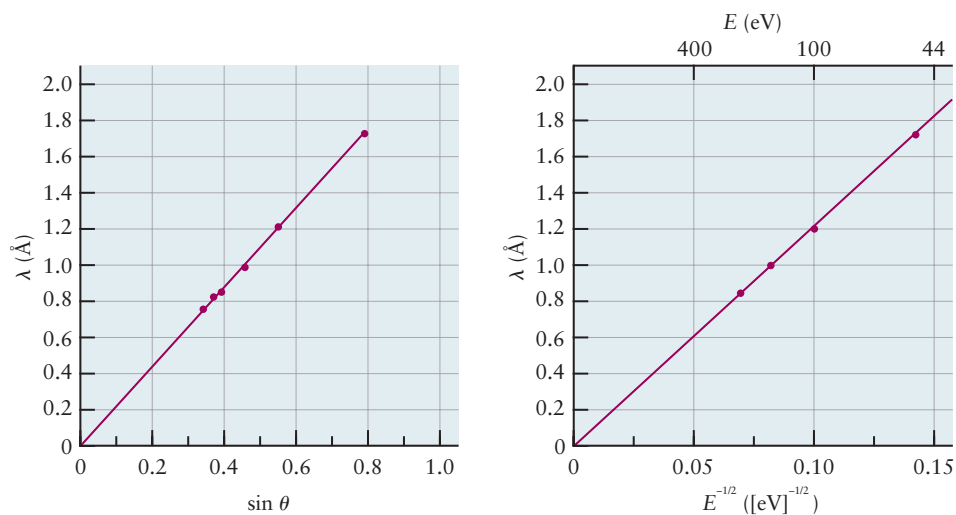


FIGURE 4.21 Results of the Davisson–Germer experiment showing (a) the $\sin \theta$ dependence predicted by Bragg’s law and (b) the dependence of the scattered intensity on the square root of the incident electron energy.



$\mathcal{T} = \frac{1}{2} mv^2$, we can set $\mathcal{T} = p^2/2m_e$ and solve for the momentum of the electron to get $p = \sqrt{2m_e eV}$. Calculations using these formulas must express the kinetic energy of the electron in joules ($1 \text{ eV} = 1.6 \times 10^{-19} \text{ J}$) in order to obtain the proper units for momentum and wave length. The de Broglie wavelength of the electron is therefore $\lambda = h/\sqrt{2m_e eV}$. An electron accelerated through a voltage of 50 V (typical of the Davisson–Germer experiment) has a de Broglie wavelength of 1.73 \AA , which is comparable to the spacing between atomic planes in metals. Davisson and Germer showed that, at a fixed angle, the scattered electron current depended on the square root of the incident energy and, at fixed energy, showed the expected $\sin \theta$ dependence as the sample was rotated. These experiments demonstrated electron diffraction, and thereby provided a striking confirmation of de Broglie’s hypothesis about the wavelike nature of matter. These experiments led to the development of a technique called low-energy electron diffraction (LEED) that now is used widely to study the atomic structure of solid surfaces (Fig. 4.22). It should be clear to you by now that “waves” and “particles” are idealized models that describe objects found in nature. Photons, electrons, and even helium atoms all have both wave and particle character; which aspect they display depends strongly on the conditions under which they are observed.

Indeterminacy and Uncertainty: The Heisenberg Principle

An inevitable consequence of de Broglie's standing-wave description of an electron in an orbit around the nucleus is that the position and momentum of a particle cannot both be known precisely and simultaneously. The momentum of the circular standing wave shown in Figure 4.18 is given exactly by $p = h/\lambda$, but because the wave is spread uniformly around the circle, we cannot specify the angular position of the electron on the circle at all. We say the angular position is **indeterminate** because it has no definite value. This conclusion is in stark contrast with the principles of classical physics in which the positions and momenta are all known precisely and the trajectories of particles are well defined. How was this paradox resolved?

In 1927, the German physicist Werner Heisenberg proposed that **indeterminacy** is a general feature of quantum systems. Indeterminacy presents a fundamental limit to the “knowability” of the properties of these systems that is intrinsic and not just a limitation of our ability to make more precise measurements. In particular, it influences which combinations of properties can be measured together. Heisenberg identified pairs of properties that *cannot* be measured together with complete precision, and estimated the best precision we can hope to obtain when we do measure them. For example, we cannot measure position and momentum simultaneously and obtain sharp, definite values for each. The same is true for energy and time. Notice that the combination of dimensions *length* \times *momentum* is the same as the combination *energy* \times *time*. (You should verify this by simple dimensional analysis.) Either combination is called **action**, and it has the same dimensions as Planck's constant. The **Heisenberg indeterminacy principle** states that when we measure two properties, A and B , the product of which has dimensions of action, we will obtain a spread in results for each identified by ΔA and ΔB that will satisfy the following condition:

$$(\Delta A)(\Delta B) \geq h/4\pi \quad [4.25]$$

If we try to measure A precisely and make ΔA nearly zero, then the spread in ΔB will have to increase to satisfy this condition. Trying to determine the angular position of the orbiting electron described by the de Broglie wave discussed earlier is a perfect illustration. Indeterminacy is intrinsic to the quantum description of matter and applies to all particles no matter how large or small.

The practical consequence of indeterminacy for the outcome of measurements is best seen by applying the Heisenberg principle in specific cases. How are the position and momentum of a macroscopic object such as a baseball in motion determined? The simplest way is to take a series of snapshots at different times, with each picture recording the light (photons) scattered by the baseball. This is true for imaging any object; we must scatter something (like a photon) from the object and then record the positions of the scattered waves or particles (Fig. 4.23). Scattering a photon from a baseball does not change the trajectory of the baseball appreciably (see Fig. 4.23a) because the momentum of the photon is negligible compared with that of the baseball, as shown in Example 4.6. Scattering photons from an electron, however, is another thing altogether. To locate the *position* of any object, we must use light with a wavelength that is comparable with or shorter than the size of the object. Thus, to measure the position of an electron in an atom to a precision of, say, 1% of the size of the atom, we would need a probe with a wavelength of order 10^{-12} m. The momentum of such a wave, given by the de Broglie relation, is 6.625×10^{-22} kg m s⁻¹. Using the virial theorem introduced in Chapter 3, we know that the kinetic energy, \mathcal{T} , of an electron in the ground state of the hydrogen atom is half the total energy or -1.14×10^{-18} J, corresponding to a momentum ($p = \sqrt{2m_e\mathcal{T}}$) of 1.44×10^{-24} kg m s⁻¹. Trying to measure the position of an electron to a precision of 10^{-12} m with a photon of sufficiently short wavelength turns out to be roughly equivalent to trying to

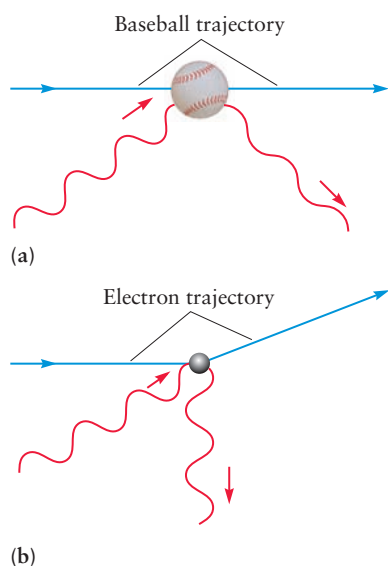


FIGURE 4.23 A photon, which has a negligible effect on the trajectory of a baseball (a), significantly perturbs the trajectory of the far less massive electron (b).

measure the position of a marble using a bowling ball as a probe! So on the length and mass scale of elementary particles, it is clear that we cannot measure simultaneously, to arbitrary precision, the values of the momentum and the position of a particle.

To make a rough estimate of the precision allowed by the indeterminacy principle, let us take as our spread of values in the position, Δx , the wavelength of our probe λ . This choice means that we can locate the particle somewhere between two crests of the wave. Let us take as our estimate of the spread in the momentum, Δp , the value of the momentum itself, p ; that is, we know p to within $\pm p$. Their product is therefore $\Delta x \Delta p = h$, but because we have asserted that this is the *best* we can do, we write $\Delta x \Delta p \geq h$. A better choice for the spread in both variables is one standard deviation or the root mean square deviation from a series of measurements. For this choice, the result becomes

$$(\Delta x)(\Delta p) \geq h/4\pi \quad [4.26]$$

which is in agreement with the Heisenberg principle.

At last, we can resolve the paradox between de Broglie waves and classical orbits, which started our discussion of indeterminacy. The indeterminacy principle places a *fundamental limit* on the precision with which the position and momentum of a particle can be known simultaneously. It has profound significance for how we think about the motion of particles. According to classical physics, the position and momentum are fully known simultaneously; indeed, we must know both to describe the classical trajectory of a particle. The indeterminacy principle forces us to abandon the classical concepts of trajectory and orbit. The most detailed information we can possibly know is the statistical spread in position and momentum allowed by the indeterminacy principle. In quantum mechanics, we think not about particle trajectories, but rather about the probability distribution for finding the particle at a specific location.

EXAMPLE 4.6

Suppose photons of green light (wavelength 5.3×10^{-7} m) are used to locate the position of the baseball from Example 4.5 with precision of one wavelength. Calculate the minimum spread in the *speed* of the baseball.

SOLUTION

The Heisenberg relation,

$$(\Delta x)(\Delta p) \geq h/4\pi$$

gives

$$\Delta p \geq \frac{h}{4\pi\Delta x} = \frac{6.626 \times 10^{-34} \text{ J s}}{4\pi(5.3 \times 10^{-7} \text{ m})} = 9.9 \times 10^{-29} \text{ kg m s}^{-1}$$

Because the momentum is just the mass (a constant) times the speed, the spread in the speed is

$$\Delta v = \frac{\Delta p}{m} \geq \frac{9.9 \times 10^{-29} \text{ kg m s}^{-1}}{(0.145 \text{ kg})} = 6.8 \times 10^{-28} \text{ m s}^{-1}$$

This is such a tiny fraction of the speed of the baseball (30 m s^{-1}) that indeterminacy plays a negligible role in the measurement of the baseball's motion. Such is the case for all macroscopic objects.

Related Problems: 35, 36

Describing the indeterminacy principle presents certain challenges to language. Clearly, when a property of the system is indeterminate, measurements will produce a statistical spread of values for that property. In a colloquial sense, there will be *uncertainty* in the measurement, because its outcome is not precisely predictable, just as there is uncertainty in the outcome of playing a game of chance. In almost all English-language books on quantum mechanics, the spread in value of a property ΔA is called the *uncertainty in A*, and the relation in Equation 4.25 is called the *Heisenberg uncertainty principle*. A property is indeterminate if it has no definite value, whereas it is uncertain if it does have a definite value, but that value is not known to the experimenter. We prefer the phrase *indeterminacy principle* because it more accurately conveys that a fundamental limitation on measurements is being described, whereas *uncertainty principle* allows the suspicion to exist that more carefully designed experiments will make the problem disappear.

4.5 The Schrödinger Equation

de Broglie's work attributed wavelike properties to electrons in atoms, which inspired the Austrian physicist Erwin Schrödinger to think about how to describe electrons as waves. Schrödinger, a recognized authority on the theory of vibrations and the associated "quantization" of standing waves, reasoned that an electron (or any other particle with wavelike properties) might well be described by a wave function. A **wave function** maps out the amplitude of a wave in three dimensions; it may also be a function of time. Ocean waves have amplitudes that vary in both space and time, as do electromagnetic waves. Schrödinger's wave function, symbolized by the Greek letter psi (ψ), is the amplitude of the wave associated with the motion of a particle, at a position located by the coordinates x , y , z at time t . It is important to emphasize that the amplitude of a wave function (just like the amplitude of ordinary waves discussed at the beginning of this chapter) may be positive, negative, or zero. The sign of a wave function tells the direction of the displacement. If we assign zero as the amplitude of the undisturbed medium (or the value of the fields for electromagnetic radiation), then positive amplitude means that the wave is displaced "upward" (a crest), whereas negative amplitude means that the wave is displaced "downward" (a trough). Points or regions in space where the wave function goes through zero as it changes sign are called **nodes**. We cannot overemphasize the importance of both the magnitude and the sign of quantum mechanical wave functions, because they determine the extent to which two wave functions interfere. As discussed later, interference is an essential feature of the quantum description of atoms and molecules.

Schrödinger discovered the equation that bears his name in 1926, and it has provided the foundation for the wave-mechanical formulation of quantum mechanics. Heisenberg had independently, and somewhat earlier, proposed a matrix formulation of the problem, which Schrödinger later showed was an equivalent alternative to his approach. We choose to present Schrödinger's version because its physical interpretation is much easier to understand.

Origins of the Schrödinger Equation

Although it is beyond the scope of this text to explain the origins of the **Schrödinger equation**, it is nevertheless worthwhile to work through the logic that might have stimulated Schrödinger's thinking and, more importantly, to explore some of the properties of the mathematical form of the Schrödinger equation. Having been trained in the classical theory of waves and inspired by de Broglie's hypothesis, it

was natural for Schrödinger to seek a wave equation that described the properties of matter on the atomic scale. Classical wave equations relate the second derivatives of the amplitude with respect to distance to the second derivatives with respect to time; for simplicity, we shall see if we can find a wave equation that relates the second derivative of a function with respect to displacement to the function itself, leaving the time dependence for more advanced work.

We begin by considering a particle moving freely in one dimension with classical momentum, p . Such a particle is associated with a wave of wavelength $\lambda = h/p$. Two “wave functions” that describe such a wave are

$$\psi(x) = A \sin \frac{2\pi x}{\lambda} \quad \text{and} \quad \psi(x) = B \cos \frac{2\pi x}{\lambda} \quad [4.27]$$

where A and B are constants. Choosing the sine function, for example, let's see what its second derivative with respect to x looks like. From differential calculus, the derivative (or slope) of $\psi(x)$ is

$$\frac{d\psi(x)}{dx} = A \frac{2\pi}{\lambda} \cos \frac{2\pi x}{\lambda}$$

The slope of *this* function is given by the second derivative of ψ , written $\frac{d^2\psi(x)}{dx^2}$, which is equal to

$$\frac{d^2\psi(x)}{dx^2} = -A \left(\frac{2\pi}{\lambda} \right)^2 \sin \frac{2\pi x}{\lambda}$$

This is just a constant, $-(2\pi/\lambda)^2$, multiplied by the original wave function $\psi(x)$:

$$\frac{d^2\psi(x)}{dx^2} = - \left(\frac{2\pi}{\lambda} \right)^2 \psi(x)$$

This is an equation (called a *differential equation*) that is satisfied by the function $\psi(x) = A \sin (2\pi x/\lambda)$. It is easy to verify that this equation is also satisfied by the function $\psi(x) = B \cos (2\pi x/\lambda)$.

Let's now replace the wavelength λ with the momentum p from the de Broglie relation:

$$\frac{d^2\psi(x)}{dx^2} = - \left(\frac{2\pi}{h} p \right)^2 \psi(x) \quad [4.28]$$

We can rearrange this equation into a suggestive form by multiplying both sides by $-h^2/8\pi^2m$, giving

$$-\frac{h^2}{8\pi^2m} \frac{d^2\psi(x)}{dx^2} = \frac{p^2}{2m} \psi(x) = \mathcal{T}\psi(x)$$

where $\mathcal{T} = p^2/2m$ is the kinetic energy of the particle. This form of the equation suggests that there is a fundamental relationship between the second derivative of the wave function (also called its *curvature*) and the kinetic energy, \mathcal{T} .

If external forces are present, a potential energy term $V(x)$ (due to the presence of walls enclosing the particle or to the presence of fixed charges, for example) must be included. Writing the total energy as $E = \mathcal{T} + V(x)$ and substituting the result in the previous equation gives

$$-\frac{h^2}{8\pi^2m} \frac{d^2\psi(x)}{dx^2} + V(x)\psi(x) = E\psi(x) \quad [4.29]$$

This is the Schrödinger equation for a particle moving in one dimension. The development provided here is not a derivation of this central equation of quantum mechanics; rather, it is a plausibility argument based on the idea that the motions of particles can be described by a wave function with the wavelength of the particle being given by the de Broglie relation.

The Validity of the Schrödinger Equation

The validity of any scientific theory must be tested by extensive comparisons of its predictions with a large body of experimental data. Although we have presented a plausibility argument that suggests how Schrödinger might have initially developed his equation, understanding the source of his inspiration is not nearly as important as evaluating the accuracy of the theory. It is the same for all great scientific discoveries; the story of Newton and the apple is not nearly as important as the fact that classical mechanics has been shown to describe the behavior of macroscopic systems to astonishingly high accuracy. Quantum mechanics superseded Newtonian mechanics because the latter failed to account for the properties of atoms and molecules. We believe that quantum mechanics is correct because its predictions agree with experiment to better than $10^{-10}\%$. It is generally considered to be among the most accurate theories of nature because of this astonishingly good agreement. But even quantum mechanics began to fail as scientists were able to make more accurate measurements than those made in the early part of the 20th century. Relativistic corrections to Schrödinger's equations improved the situation dramatically, but only with the development of **quantum electrodynamics**—in which matter and radiation are treated completely equivalently—did complete agreement between theory and experiment occur. Quantum electrodynamics is an extremely active field of research today, and it continues to ask questions such as, “How does the system know that it is being measured?” and “How can we use quantum mechanics to make computers of unprecedented power?” The fundamental ideas of quantum mechanics—energy quantization and wave-particle duality—appear to be universally true in science. These properties of nature are less evident in the macroscopic world, however, and the predictions of quantum mechanics agree well with those of classical mechanics on the relevant length and mass scales for macroscopic systems.

Interpretation of the Energy in the Schrödinger Equation

The Schrödinger equation can be solved exactly for any number of model problems and for a few real problems, notably the hydrogen atom. What do the solutions of this equation tell us about the energies and other properties of quantum systems? Or, to phrase the question slightly differently, how do we interpret ψ , and what information does it contain?

Let's focus initially on the energy. For all systems confined in space, solutions of the Schrödinger equation that are independent of time can be found only for certain discrete values of the energy; energy quantization is a natural consequence of the Schrödinger equation. States described by these time-independent wave functions are called **stationary states**. For a given system, there may be many states with different energies characterized by different wave functions. The solution that corresponds to the lowest energy is called the ground state (just as in the Bohr model), and higher energy solutions are called excited states.

Interpretation of the Wave Function in the Schrödinger Equation

What is the physical meaning of the wave function ψ ? We have no way of measuring ψ directly, just as in classical wave optics we have no direct way of measuring the amplitudes of the electric and magnetic fields that constitute the light wave (see Fig. 4.2). What *can* be measured in the latter case is the intensity of the light wave, which, according to the classical theory of electromagnetism, is proportional to the square of the amplitude of the electric field:

$$\text{intensity} \propto (E_{\text{max}})^2$$

However, if we view electromagnetic radiation as a collection of *particles* (photons), then the intensity is simply proportional to the density of photons in a region of space. Connecting the wave and particle views of the electromagnetic field suggests that the *probability* of finding a photon is given by the square of the amplitude of the electric field.

By analogy, we interpret the square of the wave function ψ^2 for a particle as a probability density for that particle. That is, $[\psi(x, y, z)]^2 dV$ is the probability that the particle will be found in a small volume $dV = dx dy dz$ centered at the point (x, y, z) . This probabilistic interpretation of the wave function, proposed by the German physicist Max Born, is now generally accepted because it provides a consistent picture of particle motion on a microscopic scale.

The probabilistic interpretation requires that any function must meet three mathematical conditions before it can be used as a wave function. The next section illustrates how these conditions are extremely helpful in solving the Schrödinger equation. To keep the equations simple, we will state these conditions for systems moving in only one dimension. All the conditions extend immediately to three dimensions when proper coordinates and notation are used. (You should read Appendix A6, which reviews probability concepts and language, before proceeding further with this chapter.)

When the possible outcomes of a probability experiment are continuous (for example, the position of a particle along the x -axis) as opposed to discrete (for example, flipping a coin), the distribution of results is given by the probability density function $P(x)$. The product $P(x)dx$ gives the probability that the result falls in the interval of width dx centered about the value x . The first condition, that the probability density must be **normalized**, ensures that probability density is properly defined (see Appendix A6), and that all possible outcomes are included. This condition is expressed mathematically as

$$\int_{-\infty}^{+\infty} P(x)dx = \int_{-\infty}^{+\infty} [\psi(x)]^2 dx = 1 \quad [4.30]$$

The second and third conditions are subsidiary to the first, in that they must be satisfied to enable the first one to be satisfied. The second condition is that $P(x)$ must be continuous at each point x . At some specific point, call it x_a , the form of the probability density may change for physical reasons, but its value at x_a must be the same regardless of whether x_a is approached from the left or from the right. This translates into the condition that $\psi(x)$ and its first derivative $\psi'(x)$ are continuous at each point x . The third condition is that $\psi(x)$ must be bounded at large values of x . This is stated mathematically as

$$\psi \longrightarrow 0 \quad \text{as} \quad x \longrightarrow \pm \infty \quad [4.31]$$

The second and third conditions are examples of **boundary conditions**, which are restrictions that must be satisfied by the solutions to differential equations such as the Schrödinger equation. A differential equation does not completely define a physical problem until the equation is supplemented with boundary conditions. These conditions invariably arise from physical analysis, and they help to select from the long list of possible solutions to the differential equation those that apply specifically to the problem being studied.

We must acknowledge that our information about the location of a particle is limited, and that it is statistical in nature. So not only are we restricted by the uncertainty principle as to what we can measure, but we must also come to grips with the fact that fundamental properties of quantum systems are unknowable, except in a statistical sense. If this notion troubles you, you are in good company. Many of the best minds of the 20th century, notably Einstein, never became comfortable with this central conclusion of the quantum theory.

Procedures for Solving the Schrödinger Equation

The application of quantum mechanics to solve for the properties of any particular system is straightforward in principle. You need only substitute the appropriate potential energy term for that system into the Schrödinger equation and solve the equation to obtain two principal results: the allowed energy values and the corresponding wave functions. You will find that solutions only exist for specific, discrete energy values. Energy quantization arises as a direct consequence of the boundary conditions imposed on the Schrödinger equation (see later discussion) with no need for extra assumptions to be grafted on. Each energy value corresponds to one or more wave functions; these wave functions describe the distribution of particles when the system has a specific energy value.

We illustrate this procedure in detail for a simplified model in the next section so that you will see how energy levels and wave functions are obtained. We also use the model problem to illustrate important general features of quantum mechanics including restrictions imposed on the form of the wave function by the Schrödinger equation and its physical interpretation.

4.6 Quantum Mechanics of Particle-in-a-Box Models

We are about to show you how to solve the Schrödinger equation for a simple but important model for which we can carry out every step of the complete solution using only simple mathematics. We will convert the equations into graphical form and use the graphs to provide physical interpretations of the solutions. The key point is for you to learn how to achieve a physical understanding from the graphical forms of the solution. Later in this textbook we present the solutions for more complex applications only in graphical form, and you will rely on the skills you develop here to see the physical interpretation for a host of important chemical applications of quantum mechanics. This section is, therefore, one of the most important sections in the entire textbook.

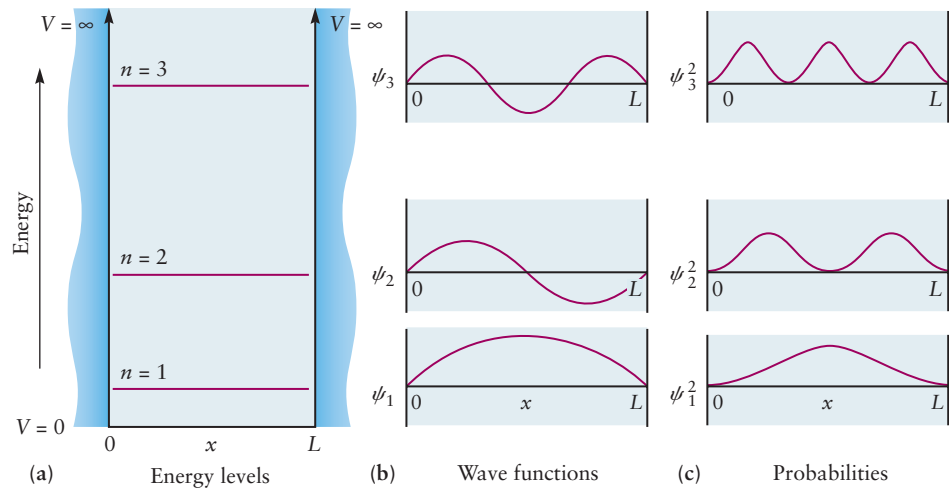
One-Dimensional Boxes

The simplest model problem for which the Schrödinger equation can be solved, and in which energy quantization appears, is the so-called particle in a box. It consists of a particle confined by potential energy barriers to a certain region of space (the “box”). In one dimension, the model is visualized easily as a bead sliding along a wire between barriers at the ends of the wire. The particle is located on the x -axis in the interval between 0 and L , where L is the length of the box (Fig. 4.24a). If the particle is to be completely confined in the box, the potential energy $V(x)$ must rise abruptly to an infinite value at the two end walls to prevent even fast-moving particles from escaping. Conversely, inside the box, the motion of the particle is free, so $V(x) = 0$ everywhere inside the box. This means that the total energy, $E = \mathcal{T} + V$, must be positive at each point inside the box. We will determine the possible values of E by solving the Schrödinger equation. The solution for this model illustrates the general methods used for other more difficult potential energy functions.

A quick inspection of the potential energy function tells us the general nature of the solution. Wherever the potential energy V is infinite, the probability of finding the particle must be zero. Hence, $\psi(x)$ and $\psi^2(x)$ must be zero in these regions:

$$\psi(x) = 0 \text{ for } x \leq 0 \text{ and } x \geq L \quad [4.32]$$

FIGURE 4.24 (a) The potential energy for a particle in a box of length L , with the first three energy levels marked. (b) Wave functions showing the ground state ψ_1 and the first two excited states. The more numerous the nodes, the higher the energy of the state. (c) The squares of the wave functions from (b), equal to the probability density for finding the particle at a particular point in the box.



Inside the box, where $V = 0$, the Schrödinger equation has the following form:

$$-\frac{\hbar^2}{8\pi^2m} \frac{d^2\psi(x)}{dx^2} = E\psi(x)$$

or equivalently,

$$\frac{d^2\psi(x)}{dx^2} = -\frac{8\pi^2mE}{\hbar^2} \psi(x)$$

As shown earlier, the sine and cosine functions are two possible solutions to this equation, because the second derivative of each function is the function itself multiplied by a (negative) constant.

Now let us apply the conditions defined in Section 4.5 to select the allowed solutions from these possibilities. The boundary conditions require that $\psi(x) = 0$ at $x = 0$ and $x = L$. An acceptable wave function must be continuous at both these points. The cosine function can be eliminated because it cannot satisfy the condition that $\psi(x)$ must be 0 at $x = 0$. The sine function does, however, satisfy this boundary condition since $\sin(0) = 0$ so

$$\psi(x) = A \sin kx \quad [4.33]$$

is a potentially acceptable wave function.

If the wave function is also to be continuous at $x = L$, then we must have

$$\psi(L) = 0 \quad [4.34]$$

or

$$\psi(L) = A \sin kL = 0$$

This can be true only if

$$kL = n\pi \quad n = 1, 2, 3, \dots$$

because $\sin(n\pi) = 0$. Thus, the combination of the boundary conditions and continuity requirement gives the allowed solutions as

$$\psi(x) = A \sin\left(\frac{n\pi x}{L}\right) \quad n = 1, 2, 3, \dots \quad [4.35]$$

where the constant A is still to be determined. The restriction of the solutions to this form in which n is an integer quantizes the energy and the wave functions.

As explained in Section 4.5, the wave function must be normalized. This condition is not always satisfied by solutions to the Schrödinger equation; thus, we must see how we can enforce it. To normalize the wave function just obtained we set

$$A^2 \int_0^L \sin^2\left(\frac{n\pi x}{L}\right) dx = 1$$

and solve for A . Evaluating the definite integral gives $L/2$, so

$$A^2 \left(\frac{L}{2} \right) = 1$$

and

$$A = \sqrt{\frac{2}{L}}$$

The normalized wave function for the one-dimensional particle in a box is

$$\psi_n(x) = \sqrt{\frac{2}{L}} \sin\left(\frac{n\pi x}{L}\right) \quad n = 1, 2, 3, \dots \quad [4.36]$$

where n labels a particular allowed solution of the Schrödinger equation.

To find the energy E_n for a particle described by the wave function ψ_n , we calculate the second derivative:

$$\begin{aligned} \frac{d^2\psi_n(x)}{dx^2} &= \frac{d^2}{dx^2} \left[\sqrt{\frac{2}{L}} \sin\left(\frac{n\pi x}{L}\right) \right] \\ &= -\left(\frac{n\pi}{L}\right)^2 \left[\sqrt{\frac{2}{L}} \sin\left(\frac{n\pi x}{L}\right) \right] \\ &= -\left(\frac{n\pi}{L}\right)^2 \psi_n(x) \end{aligned}$$

This must be equal to $-\frac{8\pi^2 m E_n}{h^2} \psi_n(x)$. Setting the coefficients equal to one another gives

$$\frac{8\pi^2 m E_n}{h^2} = \frac{n^2 \pi^2}{L^2} \quad \text{or}$$

$$E_n = \frac{n^2 h^2}{8mL^2} \quad n = 1, 2, 3, \dots \quad [4.37]$$

This solution of the Schrödinger equation demonstrates that the energy of a particle in the box is quantized. The energy, E_n , and wave function $\psi_n(x)$ are unique functions of the quantum number n , which must be a positive integer. These are the only allowed stationary states of the particle in a box. The allowed energy levels are plotted together with the potential energy function in Figure 4.24a. A system described by the particle-in-a-box model will have an emission or absorption spectrum that consists of a series of frequencies given by

$$h\nu = |E_n - E_{n'}| \quad [4.38]$$

where n and n' are positive integers, and the E_n values are given by Equation 4.37.

The wave functions $\psi_n(x)$ plotted in Figure 4.24b for the quantum states n are the standing waves of Figure 4.17. The guitar string and the particle in the box are physically analogous. The boundary condition that the amplitude of the wave function ψ must be zero at each end of the guitar string or at each wall of the box is responsible for the quantization of energy and the restriction on the motions allowed.

Following Born's interpretation that the probability of finding the particle at a particular position is the square of its wave function evaluated at that position, we can study the probability distributions for the particle in a box in various quantum

states. Figure 4.24c shows the probability distributions for the first three states of the particle in a box. For the ground state ($n = 1$), we see that the most likely place to find the particle is in the middle of the box, with a small chance of finding it near either wall. In the first excited state ($n = 2$), the probability is a maximum when it is near $L/4$ and $3L/4$ and zero near 0 , $L/2$, and L . And for the $n = 3$ state, the maxima are located at $L/6$, $3L/6$, and $5L/6$, with nodes located at $L/3$ and $2L/3$. Wherever there is a node in the wave function, the probability is zero that the particle will be found at that location.

The number of nodes in the wave function is important not only for helping us understand probability distributions but also because it provides an important, and perfectly general, criterion for ordering the energy levels in any quantum system. The wave function ψ_n has $n - 1$ nodes, and it is clear from Figure 4.24c that the number of nodes increases with the energy of each state. This is a general feature in quantum mechanics: For a given system, the relative ordering of the energy levels can be determined simply by counting the number of nodes.

Can a particle in a box have zero energy? Setting $n = 0$ and solving for E using the equation $E_n = n^2 h^2 / 8mL^2$ gives $E_0 = 0$. But this is not possible. Setting n equal to zero in $\psi_n(x) = A \sin(n\pi x/L)$ makes $\psi_0(x)$ zero everywhere. In this case, $\psi_0^2(x)$ would be zero everywhere in the box, and thus there would be no particle in the box. The same conclusion comes from the indeterminacy principle. If the energy of the lowest state could be zero, the momentum of the particle would also be zero. Moreover, the uncertainty or spread in the particle momentum, Δp_x , would also be zero, requiring that Δx be infinite, which contradicts our assertion that the particle is confined to a box of length L . Even at the absolute zero of temperature, where classical kinetic theory would suggest that all motion ceases, a finite quantity of energy remains for a bound system. It is required by the indeterminacy principle and is called the **zero-point energy**.

The wave functions for a particle in a box illustrate another important principle of quantum mechanics: the correspondence principle. We have already stated earlier (and will often repeat) that all successful physical theories must reproduce the explanations and predictions of the theories that preceded them on the length and mass scales for which they were developed. Figure 4.25 shows the probability density for the $n = 5$, 10 , and 20 states of the particle in a box. Notice how the probability becomes essentially uniform across the box, and at $n = 20$ there is little evidence of quantization. The **correspondence principle** requires that the results of quantum mechanics reduce to those of classical mechanics for large values of the quantum numbers, in this case, n .

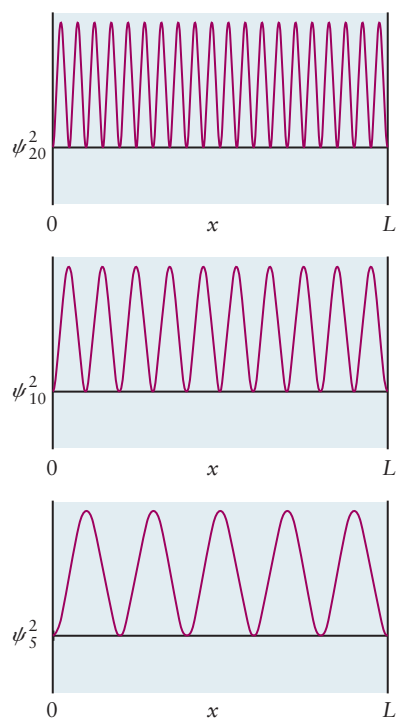


FIGURE 4.25 The probability distribution for a particle in a box of length L in the quantum states $n = 5$, 10 , and 20 . Compare these results with those shown in Figure 4.24c.

Energy Levels for Particles in Two- and Three-Dimensional Boxes

The Schrödinger equation is readily generalized to describe a particle in a box of two or three dimensions. A particle in a two-dimensional box can be visualized as a marble moving in the x - y plane at the bottom of a deep elevator shaft, with infinite potential walls confining its motion in the x and y directions. A particle in a three-dimensional rectangular box has infinite potential walls confining its motion in the x , y , and z directions. In both cases, the potential energy function is zero throughout the interior of the box. The wave function ψ and potential V now depend on as many as three coordinates (x , y , z), and derivatives with respect to each coordinate appear in the Schrödinger equation. Because the potential energy is constant in all directions inside the box, the motions in the x direction are independent of the motions in the y and z directions, and vice versa. For potential functions of this type, the Schrödinger equation can be solved by the method of *separation of variables*, and the results are quite interesting. The wave function is the product of the wave functions for independent motion in

each direction, and the energy is the sum of the energies for independent motion in each direction. Therefore, we can immediately apply the results for the one-dimensional motions developed earlier to discuss, in turn, the energies and wave functions for multidimensional boxes.

The allowed energies for a particle in a three-dimensional rectangular box are

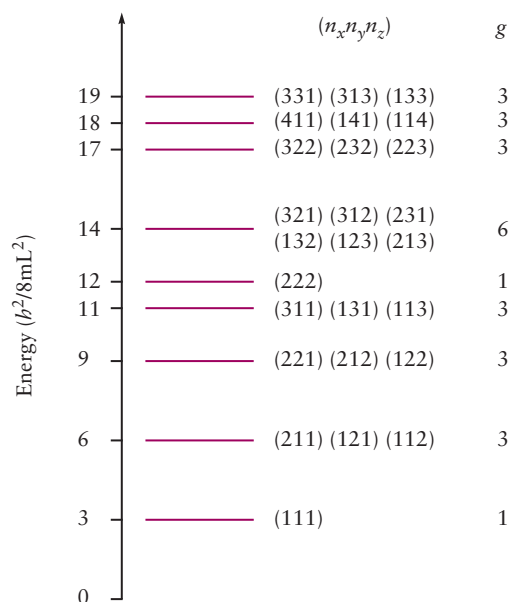
$$E_{n_x n_y n_z} = \frac{h^2}{8m} \left[\frac{n_x^2}{L_x^2} + \frac{n_y^2}{L_y^2} + \frac{n_z^2}{L_z^2} \right] \quad \begin{cases} n_x = 1, 2, 3, \dots \\ n_y = 1, 2, 3, \dots \\ n_z = 1, 2, 3, \dots \end{cases} \quad [4.39]$$

where L_x , L_y , and L_z are the side lengths of the box. Here the state is designated by a set of three quantum numbers, (n_x, n_y, n_z) . Each quantum number ranges independently over the positive integers. We can obtain the energy levels for a particle in a two-dimensional box in the x - y plane from Equation 4.39 by setting $n_z = 0$ and restrict the box to be a square by setting $L_x = L_y = L$. Similarly, we can specialize Equation 4.39 to a cubic box by setting $L_x = L_y = L_z = L$.

$$E_{n_x n_y n_z} = \frac{h^2}{8mL^2} [n_x^2 + n_y^2 + n_z^2] \quad \begin{cases} n_x = 1, 2, 3, \dots \\ n_y = 1, 2, 3, \dots \\ n_z = 1, 2, 3, \dots \end{cases} \quad [4.40]$$

Figure 4.26 plots the first few energy levels from Equation 4.40. We see that certain energy values appear more than once because the squares of different sets of quantum numbers can add up to give the same total. Such energy levels, which correspond to more than one quantum state, are called **degenerate**. Degenerate energy levels appear only in systems with potential energy functions that have symmetric features. (You should convince yourself that none of the energy levels in Eq. 4.39 is degenerate.) In Chapters 5 and 6, we encounter many examples of degenerate energy levels in atomic and molecular systems, as consequences of symmetry. As an exercise, we suggest that you apply Equation 4.40 to determine the energy levels in a square box and examine their degeneracy. You should master the concept of degeneracy in these simple examples because it is used in all branches of science to describe the absorption and emission of electromagnetic radiation by atoms and molecules.

FIGURE 4.26 The energy levels for a particle in a cubic box. The quantum numbers identifying the quantum states and the degeneracy values are given for each energy level.



EXAMPLE 4.7

Consider the following two systems: (a) an electron in a one-dimensional box of length 1.0 Å and (b) a helium atom in a cube 30 cm on an edge. Calculate the energy difference between ground state and first excited state, expressing your answer in kJ mol^{-1} .

SOLUTION

(a) For a one-dimensional box,

$$E_{\text{ground state}} = \frac{h^2}{8mL^2} (1^2)$$

$$E_{\text{first excited state}} = \frac{h^2}{8mL^2} (2^2)$$

Then, for one electron in the box,

$$\begin{aligned} \Delta E &= \frac{3h^2}{8mL^2} \\ &= \frac{3(6.626 \times 10^{-34} \text{ J s})^2}{8(9.11 \times 10^{-31} \text{ kg})(1.0 \times 10^{-10} \text{ m})^2} \\ &= 1.8 \times 10^{-17} \text{ J} \end{aligned}$$

Multiplying this result by $10^{-3} \text{ kJ J}^{-1}$ and by $N_A = 6.022 \times 10^{23} \text{ mol}^{-1}$ gives

$$\Delta E = 11,000 \text{ kJ mol}^{-1}$$

(b) For a three-dimensional cube, $L_x = L_y = L_z = L$, and

$$E_{\text{ground state}} = \frac{h^2}{8mL^2} (1^2 + 1^2 + 1^2)$$

$$E_{\text{first excited state}} = \frac{h^2}{8mL^2} (2^2 + 1^2 + 1^2)$$

In this case, the three states (2, 1, 1), (1, 2, 1), and (1, 1, 2) have the same energy.

$$\begin{aligned} \Delta E &= \frac{3h^2}{8mL^2} \\ &= \frac{3(6.626 \times 10^{-34} \text{ J s})^2}{8(6.64 \times 10^{-27} \text{ kg})(0.30 \text{ m})^2} \\ &= 2.8 \times 10^{-40} \text{ J} \\ &= 1.7 \times 10^{-19} \text{ kJ mol}^{-1} \end{aligned}$$

The energy levels are so close together in the latter case (due to the much larger dimensions of the box) that they appear continuous, and quantum effects play no role. The properties are almost those of a classical particle.

Related Problems: 37, 38

Wave Functions for Particles in Square Boxes

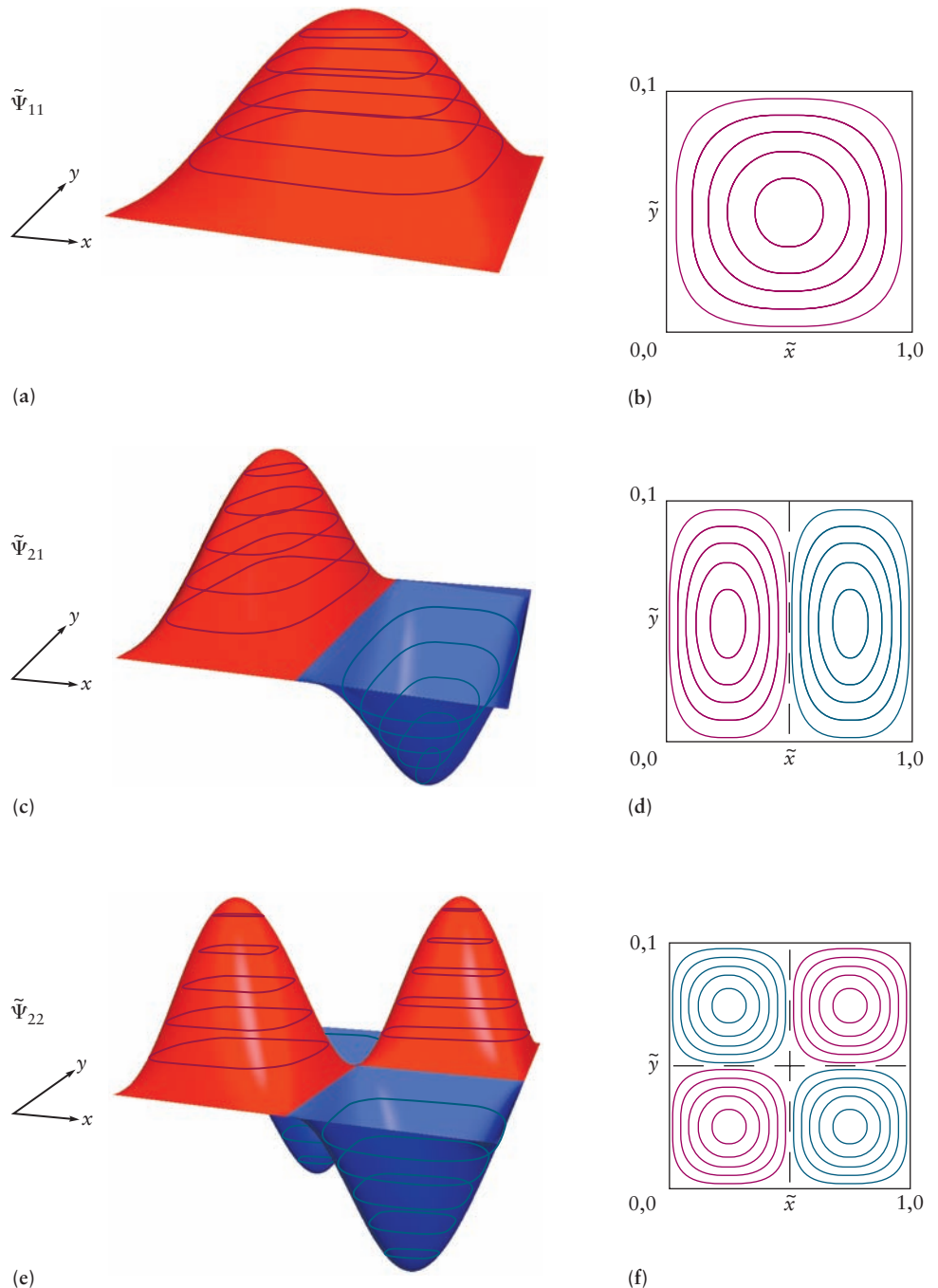
The wave function for a particle in a square box of length L on each side in the x - y plane, which we denote as Ψ , is given by

$$\Psi_{n_x n_y}(x, y) = \psi_{n_x}(x)\psi_{n_y}(y) = \frac{2}{L} \sin\left(\frac{n_x \pi x}{L}\right) \sin\left(\frac{n_y \pi y}{L}\right) \quad [4.41]$$

as explained earlier. To generate a graphical representation, we calculate the value of Ψ at each point (x, y) in the plane and plot this value as a third dimension above the x - y plane. To make our graphs apply to square boxes of any size, we show them for dimensionless variables $\tilde{x} = x/L$ and $\tilde{y} = y/L$, which range from 0 to 1. We also plot the value of the wave function as a dimensionless variable $\tilde{\Psi}$, defined as the ratio of the value of Ψ to its maximum value, $\tilde{\Psi}(\tilde{x}, \tilde{y}) = \Psi(\tilde{x}, \tilde{y})/\Psi_{\max}$. The value of $\tilde{\Psi}$ ranges from 0 to ± 1 . We show three examples in Figure 4.27.

The wave function for the ground state $\tilde{\Psi}_{11}(\tilde{x}, \tilde{y})$ (see Fig. 4.27a) has no nodes and has its maximum at the center of the box, as you would expect from the one-dimensional results in Figure 4.24 from which $\tilde{\Psi}_{11}(\tilde{x}, \tilde{y})$ is constructed. Figure 4.27b shows $\tilde{\Psi}_{11}(\tilde{x}, \tilde{y})$ as a contour plot in the x - y plane, generated by choosing

FIGURE 4.27 Wave function for a particle in a square box in selected quantum states. Dimensionless variables are used. (a) Three-dimensional plot for the ground state $\tilde{\Psi}_{11}(\tilde{x}, \tilde{y})$. (b) Contour plot for $\tilde{\Psi}_{11}(\tilde{x}, \tilde{y})$. (c) Three-dimensional plot for the first excited state $\tilde{\Psi}_{21}(\tilde{x}, \tilde{y})$. (d) Contour plot for $\tilde{\Psi}_{21}(\tilde{x}, \tilde{y})$. (e) Three-dimensional plot for the second excited state $\tilde{\Psi}_{22}(\tilde{x}, \tilde{y})$. (f) Contour plot for $\tilde{\Psi}_{22}(\tilde{x}, \tilde{y})$.



a particular value of the wave function in Figure 4.27a, “slicing” its three-dimensional image at that value, and projecting each point on the edge of that slice down to the x - y plane to form a closed contour in that plane. The contour then defines all points in the x - y plane for which $\tilde{\Psi}_{11}(\tilde{x}, \tilde{y})$ has the particular value selected. The process is continued by selecting other values of $\tilde{\Psi}_{11}(\tilde{x}, \tilde{y})$ until the entire three-dimensional image has been collapsed into a set of concentric contours in the two-dimensional x - y plane. Mountain climbers throughout the world use this method to generate contour maps of mountain ranges. The outermost contour identifies points at which the wave function has 10% of its maximum value. The second contour identifies points with 30% of the maximum value, and so on to the innermost contour that identifies points with 90% of the maximum value. Note that these contours, which correspond to uniform increases in amplitude, become much closer together as we approach the maximum. This indicates the value of the wave function is increasing rapidly as we approach the maximum. Notice in Figure 4.27b that the contours are circular at the large values of $\tilde{\Psi}_{11}(\tilde{x}, \tilde{y})$, but at lower values, they become squarish and approach perfect squares as $\tilde{\Psi}_{11}(\tilde{x}, \tilde{y}) \rightarrow 0$, as required by the boundary conditions imposed by the square box.

The wave function for the first excited state $\tilde{\Psi}_{21}(\tilde{x}, \tilde{y})$ is shown in Figure 4.27c. It has a maximum (positive) at $\tilde{x} = 0.25$, $\tilde{y} = 0.50$ and a minimum (negative) at $\tilde{x} = 0.75$, $\tilde{y} = 0.50$. The wave function changes sign as it moves along \tilde{x} for any value of \tilde{y} . There is a **nodal line** that lies along $\tilde{x} = 0.5$. The wave function does not change sign as it moves along \tilde{y} for any value of \tilde{x} . Make sure you see how these characteristics trace back to the one-dimensional solutions in Figure 4.24. Be especially mindful that nodal points in one dimension have become nodal lines in two dimensions. Figure 4.27d shows the contour plot for $\tilde{\Psi}_{21}(\tilde{x}, \tilde{y})$. Note that the contours are nearly circular near the maximum and minimum values, and they become ellipsoidal at smaller values of the wave function. This asymmetry in shape occurs because the motion in the x dimension occurs at a higher level of excitation than that in the y direction. At still lower values of the wave function, the contours begin to resemble rectangles. They approach perfect rectangles as $\tilde{\Psi}_{21}(\tilde{x}, \tilde{y}) \rightarrow 0$ to match the nodal line along $\tilde{x} = 0.5$ and the boundary conditions enforced by the box. To build up your expertise, we suggest that you construct and examine the wave function $\tilde{\Psi}_{12}(\tilde{x}, \tilde{y})$. Convince yourself it is degenerate with $\tilde{\Psi}_{21}(\tilde{x}, \tilde{y})$, and that its plots are the same as those of $\tilde{\Psi}_{21}(\tilde{x}, \tilde{y})$ rotated by 90 degrees in the x - y plane. Give a physical explanation why the two sets of plots are related in this way.

Finally, we plot the wave function for the second excited state $\tilde{\Psi}_{22}(\tilde{x}, \tilde{y})$ (see Fig. 4.27e). It has two maxima (positive) and two minima (negative) located at the values 0.25 and 0.75 for \tilde{x} and \tilde{y} . There are two nodal lines, along $\tilde{x} = 0.5$ and $\tilde{y} = 0.5$. They divide the x - y plane into quadrants, each of which contains a single maximum (positive) or minimum (negative) value. Make sure that you see how these characteristics trace back to the one-dimensional solutions in Figure 4.24. Figure 4.27f shows the contour plots for $\tilde{\Psi}_{22}(\tilde{x}, \tilde{y})$. As the magnitude (absolute value) of $\tilde{\Psi}_{22}(\tilde{x}, \tilde{y})$ decreases, the contours distort from circles to squares to match the nodal lines and boundary conditions of the box.

The pattern is now clearly apparent. You can easily produce hand sketches, in three dimensions and as contour plots, for any wave function for a particle in a square box. You need only pay attention to the magnitude of the quantum numbers n_x and n_y , track the number of nodes that must appear along the x and y axes, and convert these into nodal lines in the x - y plane.

The probability of locating the particle in a small element of area of size $d\tilde{x}d\tilde{y}$ centered on the point (\tilde{x}, \tilde{y}) is given by $[\tilde{\Psi}_{n_x n_y}(\tilde{x}, \tilde{y})]^2 d\tilde{x}d\tilde{y}$ when the system is in the quantum state described by n_x and n_y . For the wave functions shown in Figures 4.27a, c, and e, $\tilde{\Psi}^2$ will show 1, 2, and 4 peaks above the x - y plane, respectively. You should make hand sketches of these probability functions and also of their contour plots in the x - y plane. The physical interpretation is straightforward. In the ground state, the probability has a global maximum at the center of the

box. In progressively higher excited states, the probability spreads out from the center into a series of local maxima, just as the one-dimensional case in Figure 4.24. These local maxima are arranged in a pattern determined by the quantum numbers in the x and y directions. If $n_x = n_y$, the local maxima will form a highly symmetric arrangement with pairs separated by nodal lines. If $n_x \neq n_y$, the pattern will not be symmetric. As n_x and n_y take on larger values, the probability becomes more nearly uniform through the box, and the motion becomes more like that predicted by classical mechanics (see the one-dimensional case in Fig. 4.26). As an exercise, we suggest that you determine the number of nodal lines and the number of local probability maxima for the highly excited state $\tilde{\Psi}_{20,20}(\tilde{x}, \tilde{y})$ and predict the nature of the motion of the particle.

Wave Functions for Particles in Cubic Boxes

The wave function for a particle in a cubic box of length L on each side, with one corner located at the origin of coordinates, is given by

$$\Psi_{n_x, n_y, n_z}(x, y, z) = \left(\frac{2}{L}\right)^{3/2} \sin\left(\frac{n_x \pi x}{L}\right) \sin\left(\frac{n_y \pi y}{L}\right) \sin\left(\frac{n_z \pi z}{L}\right) \quad [4.42]$$

where each of the quantum numbers n_x , n_y , and n_z can be any of the positive integers. Graphical representation of these wave functions requires some care. Equation 4.42 tells us simply to go to the point (x, y, z) , evaluate the wave function there, and draw a graph showing the results of visiting many such points. However, all three spatial dimensions have already been used up to define the location; thus, we would need a fourth dimension to display the value of the wave function. Alternatively, we could set up a table of numbers giving the value of the wave function at each point (x, y, z) , but it would be difficult to develop any intuition about shapes and structures from this table. We will get around these problems by slicing up three-dimensional space into various two- and one-dimensional regions, evaluating the wave function from Equation 4.42 at each point in these restricted regions, and generating graphical representations over these restricted regions. From the behavior of the wave function in these regions, we draw inferences about its overall behavior, even though we cannot graphically display its overall behavior in complete detail. For example, we could evaluate Equation 4.42 only at points in the x - y plane, and thereby generate contour maps of these wave functions in the x - y plane similar to those for the two-dimensional case shown in Figures 4.27b, d, and f. We could repeat this operation at several other “cut planes” through the box, and the resulting series of contour plots would provide considerable insight into the characteristics of the wave function.

In Figure 4.28, we examine the behavior of $\tilde{\Psi}_{123}(\tilde{x}, \tilde{y}, \tilde{z})$ using dimensionless variables defined earlier. Figure 4.28a shows a contour plot generated in a cut plane parallel to the x - y axis at $\tilde{z} = 0.5$. It demonstrates two sets of ellipses separated by one nodal line, arising because $n_x = 1$, $n_y = 2$. Figure 4.28b shows a contour plot generated in a cut plane at $\tilde{y} = 0.25$ or 0.75 parallel to the x - z plane. It shows three sets of ellipses separated by two nodal lines, as a consequence of $n_x = 1$, $n_z = 3$. Figure 4.28c shows a contour plot in the cut plane at $\tilde{x} = 0.5$. It shows six circles and three nodal lines, due to $n_y = 2$, $n_z = 3$. All of this suggests that $\tilde{\Psi}_{123}(\tilde{x}, \tilde{y}, \tilde{z})$ is an interesting object indeed!

How can we get some sense of the three-dimensional shape of a wave function? In Figure 4.28a, it is not necessary to have the cut plane $\tilde{z} = 0.5$ oriented parallel to the x - y axis. Let us imagine rotating this plane through a full 360-degree circle, always keeping the center of the plane anchored at $\tilde{z} = 0.5$, and let us generate contour plots at each of the angular orientations of the cut plane. The result will be that the ellipsoidal contours in Figure 4.28a generate a set of concentric

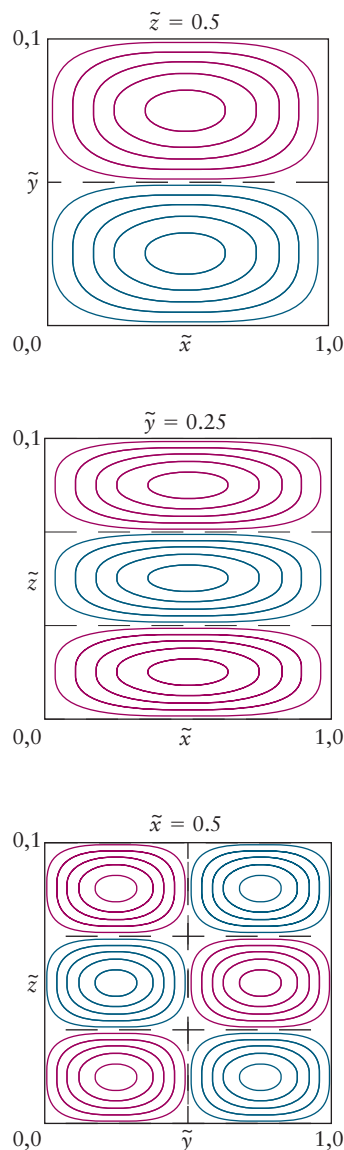
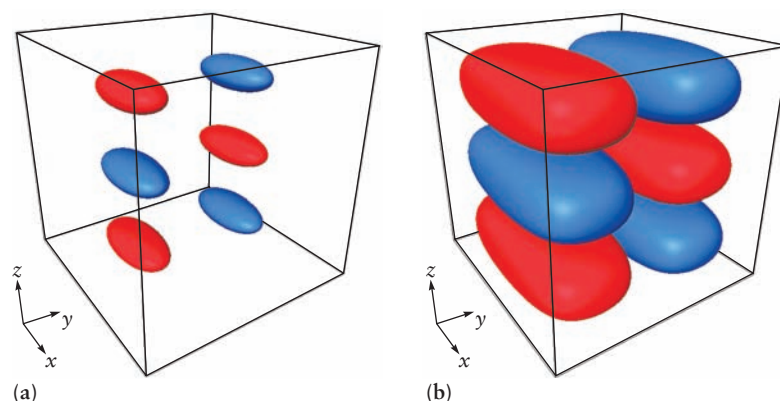


FIGURE 4.28 Contour plots for $\tilde{\Psi}_{123}(\tilde{x}, \tilde{y}, \tilde{z})$ for a particle in a cubic box. (a) Contours generated in a cut at $\tilde{z} = 0.5$. (b) Contours generated in a cut at $\tilde{y} = 0.25$. (c) Contours generated in a cut at $\tilde{x} = 0.5$. The location of nodal lines and shapes of the contours are explained in the text.

FIGURE 4.29 Isosurfaces for $\tilde{\Psi}_{123}(\tilde{x}, \tilde{y}, \tilde{z})$ for a particle in a cubic box. (a) Isosurfaces for wave function value $\tilde{\Psi}_{123} = \pm 0.8$. (b) Isosurfaces for wave function value $\tilde{\Psi}_{123} = \pm 0.2$. Each isosurface is shown in the same color as the corresponding contour in Figure 4.28.



“blimp-shaped” surfaces in three dimensions. Each of them identifies a surface of points (x, y, z) at every one of which $\tilde{\Psi}_{123}(\tilde{x}, \tilde{y}, \tilde{z})$ has the same value. These surfaces are called *isosurfaces* because the wave function has constant value at each point on them. In fact, we generate the isosurfaces in a more systematic way by evaluating $\tilde{\Psi}_{123}(\tilde{x}, \tilde{y}, \tilde{z})$ at every point in the cubic box and tracking in the computer all points that have, for example, the value $\tilde{\Psi} = \pm 0.9$. Then the computer plots the resulting isosurfaces in three dimensions. Figure 4.29 shows the isosurfaces for $\tilde{\Psi}_{123}(\tilde{x}, \tilde{y}, \tilde{z})$ at the values $\tilde{\Psi} = \pm 0.8, \pm 0.2$.

Figure 4.30 briefly summarizes key images for $\tilde{\Psi}_{222}(\tilde{x}, \tilde{y}, \tilde{z})$ for a particle in a cubic box. Figure 4.30a shows a contour plot in a cut plane at $\tilde{z} = 0.75$. Convince yourself that the contour plot in a cut at $\tilde{z} = 0.25$ would have the same pattern but each positive peak would become negative, and vice versa. Why should we not take a cut at $\tilde{z} = 0.5$? Be sure you understand the same concerns for cut planes perpendicular to \tilde{x} and \tilde{y} . Figure 4.30bc shows the isosurfaces for the maxima and minima of $\tilde{\Psi}_{222}(\tilde{x}, \tilde{y}, \tilde{z})$ at the values $\tilde{\Psi} = \pm 0.9, \pm 0.3$.

Notice how in Figures 4.29 and 4.30 the shape depends on the value selected for the isosurface. This demonstrates an important point about plots of wave functions for a particle moving in three dimensions: It is not possible to show the shape of the wave function in three dimensions. You should be mindful that precisely because the wave function is a four-dimensional object, its appearance in three-dimensional representations depends strongly on choices made by the illustrator.

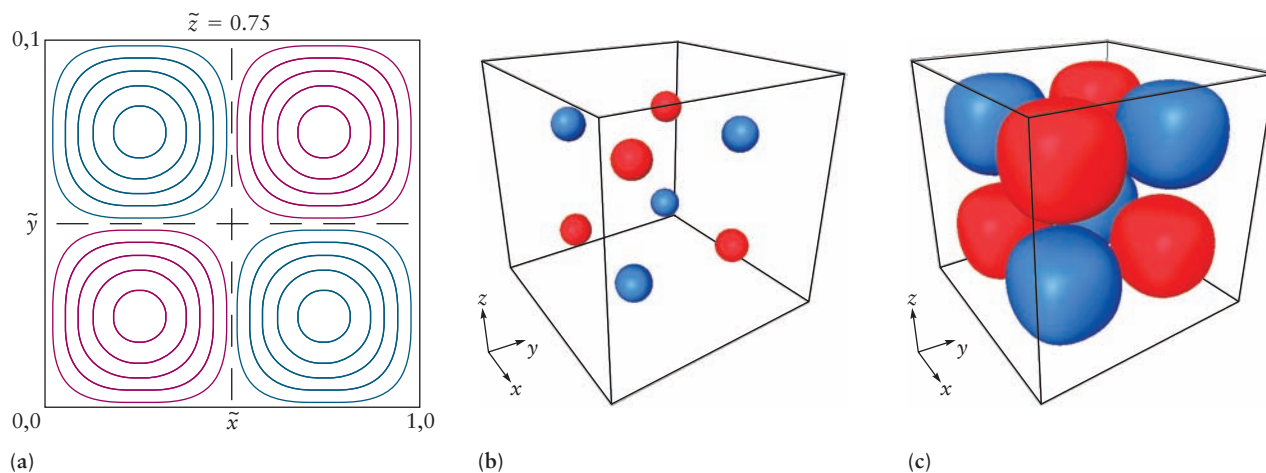


FIGURE 4.30 Representations of $\tilde{\Psi}_{222}(\tilde{x}, \tilde{y}, \tilde{z})$ for a particle in a cubic box. (a) Contour plots for a cut taken at $\tilde{z} = 0.75$. (b) Isosurfaces for wave function value $\tilde{\Psi}_{222} = \pm 0.9$. (c) Isosurfaces for wave function value $\tilde{\Psi}_{222} = \pm 0.3$. Each isosurface is shown in the same color as the corresponding contour in (a).

Be certain you understand these choices in each image you examine (or create!). These same issues appear in Chapter 5 when we discuss the wave functions for electrons in atoms, called *atomic orbitals*. Throughout this book, we have taken great care to generate accurate contour plots and isosurfaces for them from computer calculations to guide your thinking about the distribution of electrons in atoms and molecules.

4.7 Quantum Harmonic Oscillator

The quantum mechanical harmonic oscillator model system is used to describe the oscillators that are the sources of blackbody radiation previously discussed and also to describe the vibrational motions of molecules and solids. Moreover, it is the simplest model problem that illustrates the important but highly non-intuitive quantum process of tunneling. In classical mechanics, objects (cars, balls, particles, and so on) can make it up and over a hill only if they have enough kinetic energy to overcome the potential energy barrier imposed by the hill. But in the quantum world particles can **tunnel** through the hill; that is, they can go right through instead of over. This phenomenon is a consequence of the wave nature of matter, and it is one of the most difficult aspects of quantum mechanics to grasp. Because quantum mechanical tunneling is important in chemical kinetics, especially for reactions involving light particles such as electrons, protons, and hydrogen atoms, we want you to develop some familiarity with the concept here.

You have already encountered the classical version of the harmonic oscillator in our discussion of blackbody radiation in Section 4.2. The equations for the force and the potential energy of the harmonic oscillator are:

$$F(x) = -k(x - x_0)$$

and

$$V(x) = \frac{1}{2} k(x - x_0)^2$$

where k is the force constant that represents the “stiffness” of the spring, and $x - x_0$ is the displacement of the mass from its equilibrium position x_0 , as defined in Section 4.2. If we choose the origin of our coordinate system by setting $x_0 = 0$, the potential energy of the harmonic oscillator (plotted on page 122) is a simple parabola centered at the origin. The vibrational frequency of a harmonic oscillator is given by

$$\nu = \frac{1}{2\pi} \sqrt{\frac{k}{m}}$$

where k is the force constant, and m is the mass.

To obtain the quantum version, we substitute the potential energy function for the harmonic oscillator into the Schrödinger equation to get

$$-(\hbar^2/8\pi^2m)d^2\psi(x)/dx^2 + \frac{1}{2} kx^2\psi(x) = E\psi(x)$$

We simply list the solutions, which you can verify by substituting them into the Schrödinger equation. The first four wave functions for the quantum harmonic oscillator are listed in Table 4.2 and plotted in Figure 4.31. The energy levels of the harmonic oscillator are given by

$$E_n = \left(n + \frac{1}{2}\right) h\nu \quad n = 0, 1, 2, 3, \dots \quad [4.43]$$

TABLE 4.2 The First Four Harmonic Oscillator Wave Functions

$$\begin{aligned} \alpha &= \frac{2\pi}{h} (k\mu)^{1/2} & \psi_2(x) &= \left(\frac{\alpha}{4\pi}\right)^{1/4} (2\alpha x^2 - 1)e^{-\alpha x^2/2} \\ \psi_0(x) &= \left(\frac{\alpha}{\pi}\right)^{1/4} e^{-\alpha x^2/2} & \psi_3(x) &= \left(\frac{\alpha^3}{9\pi}\right)^{1/4} (2\alpha x^3 - 3x)e^{-\alpha x^2/2} \\ \psi_1(x) &= \left(\frac{4\alpha^3}{\pi}\right)^{1/4} x e^{-\alpha x^2/2} \end{aligned}$$

Note that, unlike the particle in a box, $n = 0$ is perfectly acceptable because the term $\frac{1}{2} h\nu$ ensures that the energy of the oscillator never goes to zero, which would violate the indeterminacy principle. The frequency of the harmonic oscillator is given by

$$\nu = \frac{1}{2\pi} \sqrt{\frac{k}{m}} \quad [4.44]$$

where m is the mass of the particle, and k (the force constant) represents the stiffness of the spring. The energy levels of a quantum harmonic oscillator are equally spaced; adjacent levels are separated by $\Delta E = h\nu$.

Potential energy diagrams for diatomic molecules were introduced in Section 3.5, and you can see that they are not parabolic over the entire region $0 < r < \infty$ (for example, see Fig. 3.9). Near the equilibrium internuclear separation the potential appears to be well approximated by a parabola. This similarity suggests that the harmonic oscillator should be a good model to describe the vibrations of diatomic molecules. The dependence of the vibrational frequency ν on the force constant k and the mass has the same form as Equation 4.44, but now the mass is the reduced mass μ of the two nuclei

$$\nu = \frac{1}{2\pi} \sqrt{\frac{k}{\mu}} \quad [4.45a]$$

$$\mu = \frac{m_1 m_2}{m_1 + m_2} \quad [4.45b]$$

(Vibrational frequencies are measured either by infrared or Raman spectroscopy, as discussed in Chapter 20.) The vibrational frequency is proportional to the square root of the force constant, a measure of the bond stiffness. Molecules with stiffer bonds are characterized by larger force constants (larger values of k) and greater vibrational frequencies. The vibrational frequencies of carbon–carbon single, double, and triple bonds are approximately 3×10^{13} Hz, 4.8×10^{13} Hz, and 6.6×10^{13} Hz respectively. This trend illustrates that stiffness of the bond correlates with bond order. For a given bond stiffness, the vibrational frequencies decrease as the masses of the atoms in the bond increase. To illustrate the mass dependence, compare the vibrational frequencies of two molecules with comparable bond stiffness, F_2 (2.7×10^{13} Hz) and I_2 (6.5×10^{12} Hz). Vibrational spectra of molecules, interpreted using the quantum harmonic oscillator model, are among our most powerful probes of molecular structure and dynamics.

Let's return to the characteristics of the harmonic oscillator wave functions (see Fig. 4.31). There are a number of interesting features to point out.

First, in contrast with the classical harmonic oscillator, the quantum harmonic oscillator in its ground state is most likely to be found at its equilibrium position. A classical harmonic oscillator spends most of its time at the classical turning points, the positions where it slows down, stops, and reverses directions. (It might

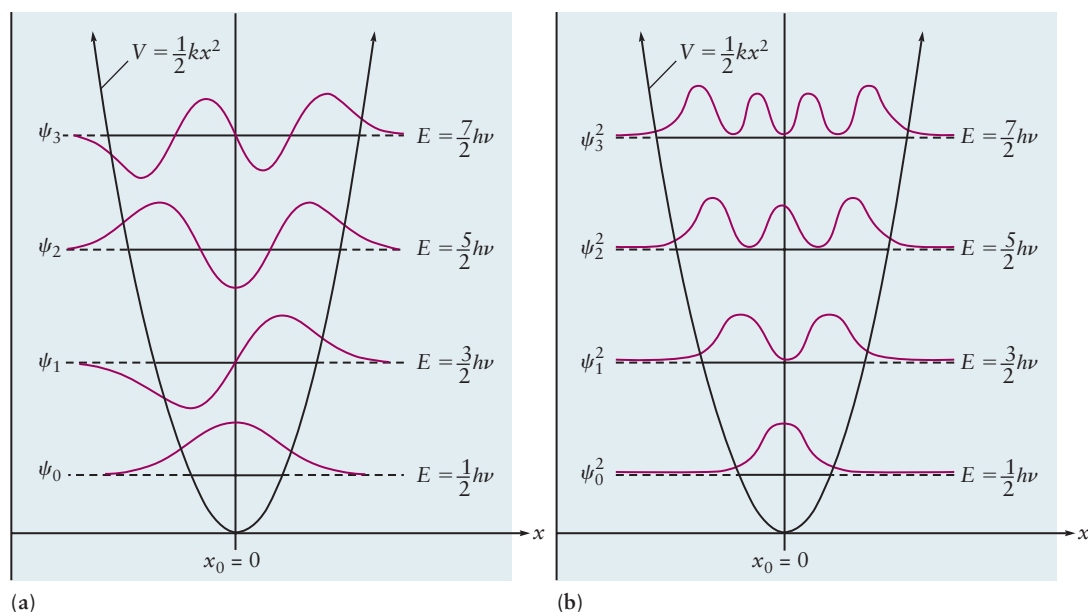


FIGURE 4.31 Solutions for the quantum harmonic oscillator. (a) The first four wave functions. (b) Probability densities corresponding to the first four wave functions.

be helpful to visualize the motions of a pendulum, which are described by the same equation.) The probability distribution function for the ground state quantum harmonic oscillator is different from its classical counterpart, just as that for the particle in a box differs dramatically from the classical prediction. Notice in Figure 4.31b how the probability density begins to accumulate near the classical turning points as the quantum number n increases. At higher energies, quantum systems begin to behave like their classical analogs.

Next, let's examine the energy of the quantum harmonic oscillator at the classical turning points. The horizontal line represents the total energy and the parabola represents the potential energy; at the classical turning point, the total energy equals the potential energy, which means that the kinetic energy is zero. This makes perfect sense classically. The oscillator must stop at some point while it changes direction, so its kinetic energy at that point goes to zero. The probability of the classical oscillator being outside that region is zero.

But it is clear from the figure that the amplitudes of the quantum harmonic oscillator wave functions do not go to zero past the classical turning point; thus, there is a finite probability of finding the particle in the classically forbidden regions. This “leaking out” of the probability is quantum mechanical tunneling, and it exists for every system that is not confined by an infinitely steep potential wall. If this concept is hard to grasp (which it is likely to be), focusing on the wavelike character of the oscillator might help. Just as light is partially reflected and partially transmitted through glass, quantum mechanical waves are partially transmitted through potential surfaces, like the parabolic well of the harmonic oscillator.

CHAPTER SUMMARY

We have introduced you to the concepts and methods of quantum mechanics; this branch of physics was developed to explain the behavior of matter on the nanometer length scale. The results of a number of key experiments demanded the creation of a new physical theory; classical mechanics and electrodynamics failed completely to account for these new observations. The pivotal experiments and observations included the spectrum and temperature dependence of blackbody radiation, the very existence of stable atoms and their discrete line spectra, the

photoelectric effect, and electron diffraction. Taken together, these experiments demonstrated unequivocally quantization of energy (blackbody radiation and atomic spectra) and wave–particle duality (photoelectric effect and electron diffraction), which would become the central concepts of quantum mechanics.

The quantum explanations of each of the experiments listed earlier required scientists to abandon or even discard long held truths from classical physics to make progress. Particularly striking were Planck’s explanation of blackbody radiation and the Bohr model of the hydrogen atom. Both scientists started fresh and made whatever assumptions were necessary to fit the experimental results, ignoring any conflicts with classical physics. Only after their models agreed so well with experiment did they begin to consider the radical philosophical implications of quantum mechanics and develop a new way of thinking about nature on the nanometer length scale. This was undoubtedly one of the most significant paradigm shifts in the history of science.

The key new ideas of quantum mechanics include the quantization of energy, a probabilistic description of particle motion, wave–particle duality, and indeterminacy. These ideas appear foreign to us because they are inconsistent with our experience of the macroscopic world. We have accepted them because they have provided the most comprehensive account of the behavior of matter and radiation and because the agreement between theory and the results of all experiments conducted to date has been astonishingly accurate.

Energy quantization arises for all systems that are confined by a potential. The one-dimensional particle-in-a-box model shows why quantization only becomes apparent on the atomic scale. Because the energy level spacing is inversely proportional to the mass and to the square of the length of the box, quantum effects become too small to observe for systems that contain more than a few hundred atoms or so.

Wave–particle duality accounts for the probabilistic nature of quantum mechanics and for indeterminacy. Once we accept that particles can behave as waves, then we can apply the results of classical electromagnetic theory to particles. By analogy, the probability is the square of the amplitude. Zero-point energy is a consequence of the Heisenberg uncertainty relation; all particles bound in potential wells have finite energy even at the absolute zero of temperature.

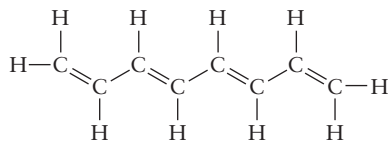
Particle-in-a-box models and the quantum harmonic oscillator illustrate a number of important features of quantum mechanics. The energy level structure depends on the nature of the potential; in the particle in a box, $E_n \propto n^2$, whereas for the harmonic oscillator, $E_n \propto n$. The probability distributions in both cases are different than for the classical analogs. The most probable location for the particle-in-a-box model in its ground state is the center of the box, rather than uniform over the box as predicted by classical mechanics. The most probable position for the quantum harmonic oscillator in the ground state is at its equilibrium position, whereas the classical harmonic oscillator is most likely to be found at the two classical turning points. Normalization ensures that the probabilities of finding the particle or the oscillator at all positions add up to one. Finally, for large values of n , the probability distribution looks much more classical, in accordance with the correspondence principle.

The concepts and principles we have discussed apply to any system of interest. In the next two chapters, we use quantum mechanics to explain atomic and molecular structure, respectively. In particular, it is important for you to have a firm grasp of these principles because they form the basis for our comprehensive discussion of chemical bonding in Chapter 6.

CUMULATIVE EXERCISE

An interesting class of carbon-containing molecules called *conjugated molecules* have structures that consist of a sequence of alternating single and double bonds. These chainlike molecules are represented as zigzag structures in which the angle

between adjacent segments is determined by the geometry of the C—C double bond. Various properties to be explored in later chapters indicate that the electrons forming the double bonds are “de-localized” over the entire chain. Such molecules absorb light in the visible and ultraviolet regions of the electromagnetic spectrum. Many dyestuffs and molecules with biological significance have these structures. The properties of these molecules can be described approximately by the particle-in-a-box model in which we assume there is no interaction between the electrons, the potential energy is constant along the chain, and the potential energy is infinite at the ends of the chain. Assume the length of the potential well is Nd , where N is the number of carbon atoms in the chain, and d is half the sum of the lengths of a C—C single bond and a C—C double bond. In a molecule of N atoms, there will be N electrons involved in the double bonds.



- Write the equation for the energy levels of an electron in this potential well.
- Write the equation for the wave function of an electron in this potential well. To describe the placement of N electrons in the energy levels, we anticipate a principle to be developed in Chapter 5 that requires that no more than two electrons can occupy a level. Therefore, levels will be occupied from the ground state up to level $n = N/2$. Absorption of light can cause one electron to move the next level $n = (N + 1)/2$.
- Write the equation for the frequency of light that will cause this transition.
- The molecule butadiene has four carbon atoms with conjugated structure; thus, $N = 4$. Calculate the wavelength of light in the first transition of butadiene.
- The molecular structure of vitamin A is conjugated with $N = 10$. Calculate the wavelength of light in the first transition of vitamin A.
- The molecule β -carotene has $N = 22$. Calculate the wavelength of light in the first transition of β -carotene.

We see in part (c) that the frequency of light absorbed should be inversely proportional to the length of the chain. Short-chain conjugated molecules absorb in the ultraviolet, whereas longer chain molecules absorb in the visible. This qualitative trend is predicted by the simple particle-in-a-box model. Later chapters detail how these results can be improved.

Answers

- $E_n = \frac{n^2 h^2}{8mN^2 d^2}$
- $\psi_n(x) = A \sin\left(\frac{n\pi x}{Nd}\right)$
- $h\nu = E_{N/2+1} - E_{N/2} = \frac{h^2(N+1)}{8md^2N^2} \approx \frac{h^2}{8md^2N}$
- $\lambda = 2050 \text{ \AA}$
- $\lambda = 3150 \text{ \AA}$
- $\lambda = 4410 \text{ \AA}$

CHAPTER REVIEW

- Waves are disturbances in space and time. Electromagnetic waves are characterized by their amplitude, wavelength, and frequency; the latter are related by the equation $c = \lambda\nu$, where c is the speed of light ($3 \times 10^8 \text{ m s}^{-1}$) and λ and ν are the wavelength and frequency, respectively.
- Blackbody radiation emitted from hot sources has a characteristic frequency distribution that is temperature dependent. The spectrum of cooler objects has

a comparatively narrow band that peaks near the red end of the visible spectrum, whereas that of hotter objects has a much broader band that is shifted toward the blue.

- The peak observed in the frequency distribution of blackbody radiation is completely inconsistent with the predictions of classical electromagnetic theory. This failure of classical physics is called the ultraviolet catastrophe.
- The only way that Planck could fit the experimental spectrum was to postulate that the oscillating charges responsible for the radiation were restricted to discrete energies, that an oscillator was either excited or not, and that the probability of an oscillator being excited depends on the temperature.
- Line spectra of atoms: Atoms emit and absorb light in discrete amounts, photons. $\Delta E = h\nu$ is the energy difference between two quantum states, where ν is the frequency of the light absorbed or emitted.
- The Franck–Hertz experiment and atomic energy levels: Electrons can excite atoms from one quantum state to another by energy transferred during collisions. The threshold energy for excitation exactly matches the emission of light as the atom drops back down to the lower state, thus confirming the existence of quantized states and showing that they may be excited by either mechanical impact of electrons or absorption of photons.
- The Bohr model of one-electron atoms: Bohr *postulated* quantization of the angular momentum, $L = m_e v r = nh/2\pi$, substituted the result in the classical equations of motion, and correctly accounted for the spectrum of all one-electron atoms. $E = -Z^2/n^2$ (rydbergs). The model could not, however, account for the spectra of many-electron atoms.
- Wave–particle duality: de Broglie postulated that the motion of an electron in an atom could be described as a circular standing wave, which required an integral number of wavelengths to fit the circumference, $n\lambda = 2\pi r$. Combining this result with Bohr’s quantization of angular momentum led to the de Broglie relation $\lambda = h/p$, which relates the wavelength and the momentum of a wave or a particle.
- Photoelectric effect: The photoelectric effect demonstrated the particle nature of electromagnetic radiation (formerly described only as waves).
- In the photoelectric effect, light shines on a metal surface in vacuum. The kinetic energy and photocurrent (number of electrons per second) emitted is measured as a function of frequency and intensity of the light.
- Experimental results of the photoelectric effect
 - No electrons are emitted below a threshold frequency ν_0 , regardless of intensity.
 - Above threshold, the electron kinetic energy is $\frac{1}{2}mv^2 = h\nu - h\nu_0$, where h is a new constant, Planck’s constant $6.625 \times 10^{-34} \text{ J sec}^{-1}$. $h\nu_0 = \Phi$, the work function of the metal, which is the energy required to remove the electron from the metal. Φ is different for different metals.
 - Above threshold, the photocurrent is proportional to the light intensity.
- Interpretation of the photoelectric effect: Light behaves like a stream of particles called photons, each with an energy $E = h\nu$. A photon of a given energy either does or does not provide enough energy to overcome the work function; if it does, the excess energy goes into the kinetic energy of the photoelectron. Intensity is the number of photons passing a point per unit time, just like a current.
- Electron diffraction: Electron diffraction demonstrated the wave nature of particles.
- Heisenberg uncertainty relation: The Heisenberg uncertainty relation $(\Delta x)(\Delta p) \geq h/4\pi$ is a quantitative expression of indeterminacy—a fundamental limit on

our ability to know simultaneously the values of two properties of a particle (for example, position and momentum) with an arbitrarily high precision.

- The Schrödinger equation: This equation can be solved, in principle, for the energies and the wave functions for any quantum system of interest. The energy is quantized whenever a particle is confined by a potential. The square of the wave function gives the probability of finding the particle at a particular position in space. Normalization of the wave function by requiring that

$$\int_{\text{all space}} \psi^2 dV = 1 \text{ ensures that the particle will be found somewhere.}$$

- Particle-in-a-box problems: The energies of a particle in a one-dimensional box are given by $E = n^2 h^2 / 8mL^2$, and the normalized wave functions by $\psi(x) = (2/L)^{1/2} \sin(n\pi x/L)$.
- The quantum harmonic oscillator is a model system that describes chemical and physical systems in which the restoring force is proportional to the displacement from the equilibrium position x_0 and is opposite to the direction of the displacement. The restoring force is given by $F(x) = -k(x - x_0)$ and the resulting potential energy is given by $V(x) = \frac{1}{2} k(x - x_0)^2$ where k is the force constant.
- The Schrödinger equation for the quantum harmonic oscillator can be solved exactly. The energy levels are given by $E_n = \left(n + \frac{1}{2}\right) h\nu$ with $n = 0, 1, 2, 3, \dots$

The harmonic oscillator has zero point energy $E_0 = \frac{1}{2} h\nu$, which cannot be extracted from the oscillator, even at absolute zero temperature.

- The vibrational frequency of the quantum oscillator is given by $\nu = \left(\frac{1}{2\pi}\right) \sqrt{k/m}$.
- The quantum oscillator is a good model to describe the vibrations of a diatomic molecule. The frequency is given by the familiar equation but using the reduced mass of the two nuclei $\mu = (m_1 m_2) / (m_1 + m_2)$ in place of m .
- The harmonic oscillator model enables measurement of the bond force constant through vibrational spectroscopy as follows. The measured frequency of the radiation absorbed is the same as the vibrational frequency of the molecule. The reduced mass is calculated for the molecule, and the force constant is evaluated as $k = (2\pi)^2 \mu \nu^2$.
- The harmonic oscillator wave functions explain how a particle can tunnel through a potential barrier to arrive at regions forbidden by classical mechanics.

CONCEPTS & SKILLS

After studying this chapter and working the problems that follow, you should be able to:

1. Relate the frequency, wavelength, and speed of light waves. Do the same for other kinds of waves (Section 4.1, Problems 1–8).
2. Describe blackbody radiation, and discuss how related paradoxes of classical physics were resolved by quantum mechanics (Section 4.2, Problems 9 and 10).
3. Use experimental emission and absorption spectra to determine spacings between energy levels in atoms (Section 4.2, Problems 11–16).
4. Use the Franck–Hertz method to determine spacings between adjacent energy levels in atoms (Section 4.2, Problems 17 and 18).

- Use the Bohr model to calculate the energy levels of one-electron atoms and to find the frequencies and wavelengths of light emitted in transitions between energy levels (Section 4.3, Problems 19–22).
- Describe the photoelectric effect, and discuss how related paradoxes of classical physics were resolved by quantum mechanics (Section 4.4, Problems 23 and 24).
- Using the law of conservation of energy, relate the work function of a metal to the wavelength of light used to eject electrons in the photoelectric effect and the kinetic energy of those electrons (Section 4.4, Problems 25–28).
- Discuss the de Broglie relation and use it to calculate the wavelengths associated with particles in motion (Section 4.4, Problems 29–32).
- Describe interference between wave functions for an electron. Explain how constructive and destructive interference influence the probability for finding the electron at a particular location (Section 4.5, Problems 33 and 34).
- State the Heisenberg indeterminacy principle and use it to establish bounds within which the position and momentum of a particle can be known (Section 4.4, Problems 35 and 36).
- State the conditions that a function must satisfy in order to be a solution of the Schrödinger equation. Explain how these conditions provide the probability interpretation of the wave function (Section 4.5).
- Determine the energy levels for particles in rigid rectangular boxes (Section 4.6, Problems 37 and 38).
- Prepare hand-drawn sketches for contour diagrams and isosurfaces of the wave functions for particles in square and cubic boxes. Relate the number and locations of the nodes, maxima, and minima to the quantum numbers for the wave function (Section 4.6, Problems 39–42).
- Use the energy levels and the wave functions of the quantum harmonic oscillator model to describe the vibrational motions of diatomic molecules (Section 4.7, Problems 43 and 44).
- Describe how particles tunnel through potential barriers (Section 4.7, Problems 45 and 46).

KEY EQUATIONS

$$c = \lambda\nu = 2.99792458 \times 10^8 \text{ m s}^{-1} \quad (\text{Section 4.1})$$

$$E_{\text{osc}} = nh\nu \quad (n = 1, 2, 3, 4, \dots) \quad (\text{Section 4.2})$$

$$\nu = \left[\frac{1}{4} - \frac{1}{n^2} \right] \times 3.29 \times 10^{15} \text{ s}^{-1} \quad n = 3, 4, 5, \dots \quad (\text{Section 4.2})$$

$$\nu = \frac{E_f - E_i}{h} \quad \text{or} \quad \Delta E = h\nu \quad (\text{Section 4.2})$$

$$\nu = \frac{\Delta E}{h} = \frac{eV_{\text{thr}}}{h} \quad (\text{Section 4.2})$$

$$E = \frac{1}{2} m_e v^2 - \frac{Ze^2}{4\pi\epsilon_0 r} \quad (\text{Section 4.3})$$

$$|F_{\text{Coulomb}}| = |m_e a| \quad (\text{Section 4.3})$$

$$\frac{Ze^2}{4\pi\epsilon_0 r^2} = m_e \frac{v^2}{r} \quad (\text{Section 4.3})$$

$$L = m_e v r = n \frac{h}{2\pi} \quad n = 1, 2, 3, \dots \quad (\text{Section 4.3})$$

$$r_n = \frac{\epsilon_0 n^2 h^2}{\pi Z e^2 m_e} = \frac{n^2}{Z} a_0 \quad (\text{Section 4.3})$$

$$v_n = \frac{nh}{2\pi m_e r_n} = \frac{Ze^2}{2\epsilon_0 nh} \quad (\text{Section 4.3})$$

$$E_n = \frac{-Z^2 e^4 m_e}{8\epsilon_0^2 n^2 h^2} = -(2.18 \times 10^{-18} \text{ J}) \frac{Z^2}{n^2} \quad n = 1, 2, 3, \dots \quad (\text{Section 4.3})$$

$$E_n = -\frac{Z^2}{n^2} \quad (\text{rydberg}) \quad n = 1, 2, 3, \dots \quad (\text{Section 4.3})$$

$$\nu = \frac{Z^2 e^4 m_e}{8\epsilon_0^2 h^3} \left(\frac{1}{n_f^2} - \frac{1}{n_i^2} \right) = (3.29 \times 10^{15} \text{ s}^{-1}) Z^2 \left(\frac{1}{n_f^2} - \frac{1}{n_i^2} \right)$$

$$n_i > n_f = 1, 2, 3, \dots \quad (\text{emission}) \quad (\text{Section 4.3})$$

$$\nu = (3.29 \times 10^{15} \text{ s}^{-1}) Z^2 \left(\frac{1}{n_i^2} - \frac{1}{n_f^2} \right)$$

$$n_f > n_i = 1, 2, 3, \dots \quad (\text{absorption}) \quad (\text{Section 4.3})$$

$$E_{\text{max}} = \frac{1}{2} m v_e^2 = h\nu - \Phi \quad (\text{Section 4.4})$$

$$\lambda = \frac{h}{m_e v} = \frac{h}{p} \quad (\text{Section 4.4})$$

$$n\lambda = 2d \sin \theta \quad (\text{Section 4.4})$$

$$(\Delta x)(\Delta p) \geq h/4\pi \quad (\text{Section 4.4})$$

$$-\frac{\hbar^2}{8\pi^2 m} \frac{d^2\psi(x)}{dx^2} + V(x)\psi(x) = E\psi(x) \quad (\text{Section 4.5})$$

$$\int_{-\infty}^{+\infty} P(x) dx = \int_{-\infty}^{+\infty} [\psi(x)]^2 dx = 1 \quad (\text{Section 4.5})$$

$$\psi \longrightarrow 0 \text{ as } x \longrightarrow \pm \infty \quad (\text{Section 4.5})$$

$$\psi_n(x) = \sqrt{\frac{2}{L}} \sin\left(\frac{n\pi x}{L}\right) \quad (n = 1, 2, 3, \dots) \quad (\text{Section 4.6})$$

$$E_n = \frac{\hbar^2 n^2}{8mL^2} \quad (n = 1, 2, 3, \dots) \quad (\text{Section 4.6})$$

$$E_{n_x, n_y, n_z} = \frac{\hbar^2}{8mL^2} [n_x^2 + n_y^2 + n_z^2] \quad \begin{cases} n_x = 1, 2, 3, \dots \\ n_y = 1, 2, 3, \dots \\ n_z = 1, 2, 3, \dots \end{cases} \quad (\text{Section 4.6})$$

$$\Psi_{n_x, n_y}(x, y) = \psi_{n_x}(x)\psi_{n_y}(y) = \frac{2}{L} \sin\left(\frac{n_x \pi x}{L}\right) \sin\left(\frac{n_y \pi y}{L}\right) \quad (\text{Section 4.6})$$

$$\Psi_{n_x, n_y, n_z}(x, y, z) = \left(\frac{2}{L}\right)^{3/2} \sin\left(\frac{n_x \pi x}{L}\right) \sin\left(\frac{n_y \pi y}{L}\right) \sin\left(\frac{n_z \pi z}{L}\right) \quad (\text{Section 4.6})$$

$$E_n = \left(n + \frac{1}{2} \right) h\nu \quad n = 0, 1, 2, 3, \dots \quad (\text{Section 4.7})$$

$$\nu = \frac{1}{2\pi} \sqrt{\frac{k}{m}} \quad (\text{Section 4.7})$$

$$\nu = \frac{1}{2\pi} \sqrt{\frac{k}{\mu}} \quad (\text{Section 4.7})$$

$$\mu = \frac{m_1 m_2}{m_1 + m_2} \quad (\text{Section 4.7})$$

PROBLEMS

Answers to problems whose numbers are boldface appear in Appendix G. Problems that are more challenging are indicated with asterisks.

Preliminaries: Wave Motion and Light

- Some water waves reach the beach at a rate of one every 3.2 s, and the distance between their crests is 2.1 m. Calculate the speed of these waves.
- The spacing between bands of color in a chemical wave from an oscillating reaction is measured to be 1.2 cm, and a new wave appears every 42 s. Calculate the speed of propagation of the chemical waves.
- An FM radio station broadcasts at a frequency of $9.86 \times 10^7 \text{ s}^{-1}$ (98.6 MHz). Calculate the wavelength of the radio waves.
- The gamma rays emitted by ^{60}Co are used in radiation treatment of cancer. They have a frequency of $2.83 \times 10^{20} \text{ s}^{-1}$. Calculate their wavelength, expressing your answer in meters and in angstroms.
- Radio waves of wavelength $6.00 \times 10^2 \text{ m}$ can be used to communicate with spacecraft over large distances.
 - Calculate the frequency of these radio waves.
 - Suppose a radio message is sent home by astronauts in a spaceship approaching Mars at a distance of $8.0 \times 10^{10} \text{ m}$ from Earth. How long (in minutes) will it take for the message to travel from the spaceship to Earth?
- An argon ion laser emits light of wavelength of 488 nm.
 - Calculate the frequency of the light.
 - Suppose a pulse of light from this laser is sent from Earth, is reflected from a mirror on the moon, and returns to its starting point. Calculate the time elapsed for the round trip, taking the distance from Earth to the moon to be $3.8 \times 10^5 \text{ km}$.
- The speed of sound in dry air at 20°C is 343.5 m s^{-1} , and the frequency of the sound from the middle C note on a piano is 261.6 s^{-1} (according to the American standard pitch scale). Calculate the wavelength of this sound and the time it will take to travel 30.0 m across a concert hall.
- Ultrasonic waves have frequencies too high to be detected by the human ear, but they can be produced and detected by vibrating crystals. Calculate the wavelength of an ultrasonic wave of frequency $5.0 \times 10^4 \text{ s}^{-1}$ that is propagating through

a sample of water at a speed of $1.5 \times 10^3 \text{ m s}^{-1}$. Explain why ultrasound can be used to probe the size and position of the fetus inside the mother's abdomen. Could audible sound with a frequency of 8000 s^{-1} be used for this purpose?

Evidence for Energy Quantization in Atoms

- The maximum in the blackbody radiation intensity curve moves to shorter wavelength as temperature increases. The German physicist Wilhelm Wien demonstrated the relation to be $\lambda_{\text{max}} \propto 1/T$. Later, Planck's equation showed the maximum to be $\lambda_{\text{max}} = 0.20 hc/kT$. In 1965 scientists researching problems in telecommunication discovered "background radiation" with maximum wavelength 1.05 mm (microwave region of the EM spectrum) throughout space. Estimate the temperature of space.
- Use the data in Figure 4.6 to estimate the ratio of radiation intensity at $10,000 \text{ \AA}$ (infrared) to that at 5000 \AA (visible) from a blackbody at 5000 K. How will this ratio change with increasing temperature? Explain how this change occurs.
- Excited lithium atoms emit light strongly at a wavelength of 671 nm. This emission predominates when lithium atoms are excited in a flame. Predict the color of the flame.
- Excited mercury atoms emit light strongly at a wavelength of 454 nm. This emission predominates when mercury atoms are excited in a flame. Predict the color of the flame.
- Barium atoms in a flame emit light as they undergo transitions from one energy level to another that is $3.6 \times 10^{-19} \text{ J}$ lower in energy. Calculate the wavelength of light emitted and, by referring to Figure 4.3, predict the color visible in the flame.
- Potassium atoms in a flame emit light as they undergo transitions from one energy level to another that is $4.9 \times 10^{-19} \text{ J}$ lower in energy. Calculate the wavelength of light emitted and, by referring to Figure 4.3, predict the color visible in the flame.
- The sodium D-line is actually a pair of closely spaced spectroscopic lines seen in the emission spectrum of sodium atoms. The wavelengths are centered at 589.3 nm. The intensity of this emission makes it the major source of light (and causes the yellow color) in the sodium arc light.
 - Calculate the energy change per sodium atom emitting a photon at the D-line wavelength.
 - Calculate the energy change per mole of sodium atoms emitting photons at the D-line wavelength.

- (c) If a sodium arc light is to produce 1.000 kilowatt (1000 J s^{-1}) of radiant energy at this wavelength, how many moles of sodium atoms must emit photons per second?
16. The power output of a laser is measured by its wattage, that is, the number of joules of energy it radiates per second ($1 \text{ W} = 1 \text{ J s}^{-1}$). A 10-W laser produces a beam of green light with a wavelength of 520 nm ($5.2 \times 10^{-7} \text{ m}$).
- Calculate the energy carried by each photon.
 - Calculate the number of photons emitted by the laser per second.
17. In a Franck–Hertz experiment on sodium atoms, the first excitation threshold occurs at 2.103 eV. Calculate the wavelength of emitted light expected just above this threshold. (Note: Sodium vapor lamps used in street lighting emit spectral lines with wavelengths 5891.8 and 5889.9 Å.)
18. In a Franck–Hertz experiment on hydrogen atoms, the first two excitation thresholds occur at 10.1 and 11.9 eV. Three optical emission lines are associated with these levels. Sketch an energy-level diagram for hydrogen atoms based on this information. Identify the three transitions associated with these emission lines. Calculate the wavelength of each emitted line.

The Bohr Model: Predicting Discrete Energy Levels

19. Use the Bohr model to calculate the radius and the energy of the B^{4+} ion in the $n = 3$ state. How much energy would be required to remove the electrons from 1 mol of B^{4+} in this state? What frequency and wavelength of light would be emitted in a transition from the $n = 3$ to the $n = 2$ state of this ion? Express all results in SI units.
20. He^+ ions are observed in stellar atmospheres. Use the Bohr model to calculate the radius and the energy of He^+ in the $n = 5$ state. How much energy would be required to remove the electrons from 1 mol of He^+ in this state? What frequency and wavelength of light would be emitted in a transition from the $n = 5$ to the $n = 3$ state of this ion? Express all results in SI units.
21. The radiation emitted in the transition from $n = 3$ to $n = 2$ in a neutral hydrogen atom has a wavelength of 656.1 nm. What would be the wavelength of radiation emitted from a doubly ionized lithium atom (Li^{2+}) if a transition occurred from $n = 3$ to $n = 2$? In what region of the spectrum does this radiation lie?
22. Be^{3+} has a single electron. Calculate the frequencies and wavelengths of light in the emission spectrum of the ion for the first three lines of each of the series that are analogous to the Lyman and the Balmer series of neutral hydrogen. In what region of the spectrum does this radiation lie?

Evidence for Wave–Particle Duality

23. Both blue and green light eject electrons from the surface of potassium. In which case do the ejected electrons have the higher average kinetic energy?
24. When an intense beam of green light is directed onto a copper surface, no electrons are ejected. What will happen if the green light is replaced with red light?
25. Cesium frequently is used in photocells because its work function ($3.43 \times 10^{-19} \text{ J}$) is the lowest of all the elements. Such photocells are efficient because the broadest range of
- wavelengths of light can eject electrons. What colors of light will eject electrons from cesium? What colors of light will eject electrons from selenium, which has a work function of $9.5 \times 10^{-19} \text{ J}$?
26. Alarm systems use the photoelectric effect. A beam of light strikes a piece of metal in the photocell, ejecting electrons continuously and causing a small electric current to flow. When someone steps into the light beam, the current is interrupted and the alarm is triggered. What is the maximum wavelength of light that can be used in such an alarm system if the photocell metal is sodium, with a work function of $4.41 \times 10^{-19} \text{ J}$?
27. Light with a wavelength of $2.50 \times 10^{-7} \text{ m}$ falls on the surface of a piece of chromium in an evacuated glass tube. If the work function of chromium is $7.21 \times 10^{-19} \text{ J}$, determine (a) the maximum kinetic energy of the emitted photoelectrons and (b) the speed of photoelectrons that have this maximum kinetic energy.
28. Calculate the maximum wavelength of electromagnetic radiation if it is to cause detachment of electrons from the surface of metallic tungsten, which has a work function of $7.29 \times 10^{-19} \text{ J}$. If the maximum speed of the emitted photoelectrons is to be $2.00 \times 10^6 \text{ m s}^{-1}$, what should the wavelength of the radiation be?
29. A guitar string with fixed ends has a length of 50 cm.
- Calculate the wavelengths of its fundamental mode of vibration (that is, its first harmonic) and its third harmonic.
 - How many nodes does the third harmonic have?
30. Suppose we picture an electron in a chemical bond as being a wave with fixed ends. Take the length of the bond to be 1.0 Å.
- Calculate the wavelength of the electron wave in its ground state and in its first excited state.
 - How many nodes does the first excited state have?
31. Calculate the de Broglie wavelength of the following:
- an electron moving at a speed of $1.00 \times 10^3 \text{ m s}^{-1}$
 - a proton moving at a speed of $1.00 \times 10^3 \text{ m s}^{-1}$
 - a baseball with a mass of 145 g, moving at a speed of 75 km hr^{-1}
32. Calculate the de Broglie wavelength of the following:
- electrons that have been accelerated to a kinetic energy of $1.20 \times 10^7 \text{ J mol}^{-1}$
 - a helium atom moving at a speed of 353 m s^{-1} (the root-mean-square speed of helium atoms at 20 K)
 - a krypton atom moving at a speed of 299 m s^{-1} (the root-mean-square speed of krypton atoms at 300 K)
33. In a particular Low Energy Electron Diffraction (LEED) study of a solid surface, electrons at 45 eV were diffracted at $\phi = 53^\circ$.
- Calculate the crystal spacing d .
 - Calculate the diffraction angle for 90 eV electrons on this same surface.
34. What electron energy is required to obtain the diffraction pattern for a surface with crystal spacing of 4.0 Å ?
35. (a) The position of an electron is known to be within 10 Å ($1.0 \times 10^{-9} \text{ m}$). What is the minimum uncertainty in its velocity?
- (b) Repeat the calculation of part (a) for a helium atom.

36. No object can travel faster than the speed of light, so it would appear evident that the uncertainty in the speed of any object is at most $3 \times 10^8 \text{ m s}^{-1}$.
- What is the minimum uncertainty in the position of an electron, given that we know nothing about its speed except that it is slower than the speed of light?
 - Repeat the calculation of part (a) for the position of a helium atom.

Quantum Mechanics of Particle-in-a-Box Models

37. Chapter 3 introduced the concept of a double bond between carbon atoms, represented by $\text{C}=\text{C}$, with a length near 1.34 \AA . The motion of an electron in such a bond can be treated crudely as motion in a one-dimensional box. Calculate the energy of an electron in each of its three lowest allowed states if it is confined to move in a one-dimensional box of length 1.34 \AA . Calculate the wavelength of light necessary to excite the electron from its ground state to the first excited state.
38. When metallic sodium is dissolved in liquid sodium chloride, electrons are released into the liquid. These dissolved electrons absorb light with a wavelength near 800 nm . Suppose we treat the positive ions surrounding an electron crudely as defining a three-dimensional cubic box of edge L , and we assume that the absorbed light excites the electron from its ground state to the first excited state. Calculate the edge length L in this simple model.
39. Write the wave function $\tilde{\Psi}_{12}(\tilde{x}, \tilde{y})$ for a particle in a square box.
- Convince yourself it is degenerate with $\tilde{\Psi}_{21}(\tilde{x}, \tilde{y})$.
 - Convince yourself that its plots are the same as those of $\tilde{\Psi}_{21}(\tilde{x}, \tilde{y})$ rotated by 90 degrees in the x - y plane.
 - Give a physical explanation why the two sets of plots are related in this way.
40. Write the wave function for the highly excited state $\tilde{\Psi}_{100,100}(\tilde{x}, \tilde{y})$ for a particle in a square box.
- Determine the number of nodal lines and the number of local probability maxima for this state.
 - Describe the motion of the particle in this state.
41. Consider the wave function $\tilde{\Psi}_{222}(\tilde{x}, \tilde{y}, \tilde{z})$ for a particle in a cubic box. Figure 4.30a shows a contour plot in a cut plane at $\tilde{z} = 0.75$.
- Convince yourself that the contour plot in a cut at $\tilde{z} = 0.25$ would have the same pattern, but each positive peak would become negative, and vice versa.
 - Describe the shape of this wave function in a plane cut at $\tilde{z} = 0.5$.
42. Consider the wave function $\tilde{\Psi}_{222}(\tilde{x}, \tilde{y}, \tilde{z})$ for a particle in a cubic box. Figure 4.30a shows a contour plot in a cut plane at $\tilde{z} = 0.75$.
- Describe the shape of this wave function in a cut plane at $\tilde{x} = 0.5$.
 - Describe the shape of this wave function in a cut plane at $\tilde{y} = 0.5$.

Quantum Harmonic Oscillator

43. Calculate the natural frequency of vibration for a ball of mass 10 g attached to a spring with a force constant of 1 N m^{-1} .

44. Calculate the natural frequency of vibration for a system with two balls, one with mass 1 g and the other with mass 2 g , held together by a spring of length 10 cm and force constant 0.1 N m^{-1} .
45. Vibrational spectroscopic studies of HCl show that the radiation absorbed in a transition has frequency $8.63 \times 10^{13} \text{ Hz}$.
- Calculate the energy absorbed in the transition.
 - Calculate the vibrational frequency of the molecule in this transition.
 - Calculate the reduced mass for HCl .
 - Calculate the value of the force constant for HCl .
46. Assume the force constant for DCl is the same as that for HCl . Calculate the frequency of the infrared radiation that will be absorbed by DCl . Compare with the observed absorption frequency, $6.28 \times 10^{13} \text{ Hz}$. (This result illustrates a general rule that replacing H by D lowers the vibrational frequency of a bond by the factor $\sqrt{2}$.)

ADDITIONAL PROBLEMS

47. A piano tuner uses a tuning fork that emits sound with a frequency of 440 s^{-1} . Calculate the wavelength of the sound from this tuning fork and the time the sound takes to travel 10.0 m across a large room. Take the speed of sound in air to be 343 m s^{-1} .
48. The distant galaxy called Cygnus A is one of the strongest sources of radio waves reaching Earth. The distance of this galaxy from Earth is $3 \times 10^{24} \text{ m}$. How long (in years) does it take a radio wave of wavelength 10 m to reach Earth? What is the frequency of this radio wave?
49. Hot objects can emit blackbody radiation that appears red, orange, white, or bluish white, but never green. Explain.
50. Compare the energy (in joules) carried by an x-ray photon (wavelength $\lambda = 0.20 \text{ nm}$) with that carried by an AM radio wave photon ($\lambda = 200 \text{ m}$). Calculate the energy of 1.00 mol of each type of photon. What effect do you expect each type of radiation to have for inducing chemical reactions in the substances through which it passes?
51. The maximum in Planck's formula for the emission of blackbody radiation can be shown to occur at a wavelength $\lambda_{\text{max}} = 0.20 hc/kT$. The radiation from the surface of the sun approximates that of a blackbody with $\lambda_{\text{max}} = 465 \text{ nm}$. What is the approximate surface temperature of the sun?
52. Photons of wavelength 315 nm or less are needed to eject electrons from a surface of electrically neutral cadmium.
- What is the energy barrier that electrons must overcome to leave an uncharged piece of cadmium?
 - What is the maximum kinetic energy of electrons ejected from a piece of cadmium by photons of wavelength 200 nm ?
 - Suppose the electrons described in (b) were used in a diffraction experiment. What would be their wavelength?
53. When ultraviolet light of wavelength of 131 nm strikes a polished nickel surface, the maximum kinetic energy of ejected electrons is measured to be $7.04 \times 10^{-19} \text{ J}$. Calculate the work function of nickel.
54. Express the velocity of the electron in the Bohr model for fundamental constants (m_e , e , h , ϵ_0), the nuclear charge Z ,

and the quantum number n . Evaluate the velocity of an electron in the ground states of He^+ ion and U^{91+} . Compare these velocities with the speed of light c . As the velocity of an object approaches the speed of light, relativistic effects become important. In which kinds of atoms do you expect relativistic effects to be greatest?

55. Photons are emitted in the Lyman series as hydrogen atoms undergo transitions from various excited states to the ground state. If ground-state He^+ are present in the same gas (near stars, for example), can they absorb these photons? Explain.
- * 56. Name a transition in C^{5+} that will lead to the absorption of green light.
57. The energies of macroscopic objects, as well as those of microscopic objects, are quantized, but the effects of the quantization are not seen because the difference in energy between adjacent states is so small. Apply Bohr's quantization of angular momentum to the revolution of Earth (mass 6.0×10^{24} kg), which moves with a velocity of 3.0×10^4 m s⁻¹ in a circular orbit (radius 1.5×10^{11} m) about the sun. The sun can be treated as fixed. Calculate the value of the quantum number n for the present state of the Earth-sun system. What would be the effect of an increase in n by 1?
58. Sound waves, like light waves, can interfere with each other, giving maximum and minimum levels of sound. Suppose a listener standing directly between two loudspeakers hears the same tone being emitted from both. This listener observes that when one of the speakers is moved 0.16 m farther away, the perceived intensity of the tone decreases from a maximum to a minimum.
- (a) Calculate the wavelength of the sound.
 (b) Calculate its frequency, using 343 m s⁻¹ as the speed of sound.
59. (a) If the kinetic energy of an electron is known to lie between 1.59×10^{-19} J and 1.61×10^{-19} J, what is the smallest distance within which it can be known to lie?
 (b) Repeat the calculation of part (a) for a helium atom instead of an electron.
60. By analyzing how the energy of a system is measured, Heisenberg and Bohr discovered that the uncertainty in the energy, ΔE , is related to the time, Δt , required to make the measurement by the relation $(\Delta E)(\Delta t) \geq h/4\pi$. The excited state of an atom responsible for the emission of a photon typically has an average life of 10^{-10} s. What energy uncertainty corresponds to this value? What is the corresponding uncertainty in the frequency associated with the photon?
61. It has been suggested that spacecraft could be powered by the pressure exerted by sunlight striking a sail. The force exerted on a surface is the momentum p transferred to the surface per second. Assume that photons of 6000 Å light strike the sail perpendicularly. How many must be reflected per second by 1 cm² of surface to produce a pressure of 10^{-6} atm?
62. A single particle of mass 2.30×10^{-26} kg held by a spring with force constant 150 N m⁻¹ undergoes harmonic oscillations. Calculate the zero point energy of this oscillator.
63. A single particle of mass 1.30×10^{-26} kg undergoes harmonic oscillations, and the energy difference between adjacent levels is 4.82×10^{-21} J. Calculate the value of the force constant.
64. It is interesting to speculate on the properties of a universe with different values for the fundamental constants.
- (a) In a universe in which Planck's constant had the value $h = 1$ J s, what would be the de Broglie wavelength of a 145-g baseball moving at a speed of 20 m s⁻¹?
 (b) Suppose the velocity of the ball from part (a) is known to lie between 19 and 21 m s⁻¹. What is the smallest distance within which it can be known to lie?
 (c) Suppose that in this universe the mass of the electron is 1 g and the charge on the electron is 1 C. Calculate the Bohr radius of the hydrogen atom in this universe.
65. The normalized wave function for a particle in a one-dimensional box, in which the potential energy is zero, is $\psi(x) = \sqrt{2/L} \sin(n\pi x/L)$, where L is the length of the box. What is the probability that the particle will lie between $x = 0$ and $x = L/4$ if the particle is in its $n = 2$ state?
66. A particle of mass m is placed in a three-dimensional rectangular box with edge lengths $2L$, L , and L . Inside the box the potential energy is zero, and outside it is infinite; therefore, the wave function goes smoothly to zero at the sides of the box. Calculate the energies and give the quantum numbers of the ground state and the first five excited states (or sets of states of equal energy) for the particle in the box.

This page intentionally left blank

Quantum Mechanics and Atomic Structure

- 5.1 The Hydrogen Atom
- 5.2 Shell Model for Many-Electron Atoms
- 5.3 Aufbau Principle and Electron Configurations
- 5.4 Shells and the Periodic Table: Photoelectron Spectroscopy
- 5.5 Periodic Properties and Electronic Structure



Fireworks above Paris; La Grande Arche is in the foreground. Many of the colors in fireworks are produced from atomic emission: red from strontium, orange from calcium, yellow from sodium, green from barium, and blue from copper. The sharp lines observed in the emission spectra of atoms can only be explained using the quantum theory of atomic structure.

The atom is the most fundamental concept in the science of chemistry. A chemical reaction occurs by regrouping a set of atoms initially found in those molecules called reactants to form those molecules called products. Atoms are neither created nor destroyed in chemical reactions. Chemical bonds between atoms in the reactants are broken, and new bonds are formed between atoms in the products. We have traced the concept of the atom from the suppositions of the Greek philosophers to the physics experiments of Thomson and Rutherford and we have arrived at the planetary model of the atom. We have used the Coulomb force and potential energy laws describing the interactions among the nucleus and the electrons in the planetary atom to account for the gain and loss of electrons by atoms,

and the formation of chemical bonds between atoms. These descriptions, based on the planetary model, accurately account for large amounts of experimental data.

Now we have to confront an inconvenient truth lurking quietly but ominously in the background of all these successful discussions. According to the laws of physics under which it was discovered, *the planetary atom cannot exist*. Newtonian mechanics says that an electron orbiting around a nucleus will be constantly accelerated. Maxwell's electromagnetic theory requires an accelerated charged particle to emit radiation. Thus, the electron should spiral into the nucleus, and the planetary atom should collapse in a fraction of a second. Clearly, real atoms are stable and do not behave as these theories predict. Real experimental data show that the internal physical structure of the atom is well described by the planetary model. The problem comes with attempts to analyze the planetary model using the classical physics of Newton and Maxwell. The physical picture is correct, but the equations are wrong for atoms.

The incompatibility of Rutherford's planetary model, based soundly on experimental data, with the principles of classical physics was the most fundamental of the conceptual challenges facing physicists in the early 1900s. The Bohr model was a temporary fix, sufficient for the interpretation of hydrogen (H) atomic spectra as arising from transitions between stationary states of the atom. The stability of atoms and molecules finally could be explained only after quantum mechanics had been developed.

The goal of this chapter is to describe the structure and properties of atoms using quantum mechanics. We couple the physical insight into the atom developed in Sections 3.2, 3.3, and 3.4 with the quantum methods of Chapter 4 to develop a quantitative description of atomic structure.

We begin with the hydrogen atom, for which the Schrödinger equation can be solved exactly because it has only one electron. We obtain exact expressions for the energy levels and the wave functions. The exact wave functions are called **hydrogen atomic orbitals**. The square of a wave function gives the probability of locating the electron at a specific position in space, determined by the properties of that orbital. The sizes and shapes of hydrogen atomic orbitals hold special interest, because they are the starting points for approximate solutions to more complex problems.

There is no exact solution for any other atom, so we must develop approximate solutions. We treat each electron in a many-electron atom as if it were moving in an *effective force field* that results from averaging its interactions with all the other electrons and the nucleus. The effective field was introduced by purely physical arguments in Section 3.2. Here, we develop this concept systematically and from it obtain approximate one-electron wave functions called **Hartree atomic orbitals** (to honor the English physicist Douglas Hartree who pioneered the method), which account for the effect of all the other electrons in the atom. The shapes of the Hartree orbitals are similar to those of the hydrogen atomic orbitals, but their sizes and their energy level patterns are quite different. We use the Hartree orbitals to explain the shell model of the atom, the structure of the periodic table, and the periodic behavior of atomic properties. The result is a comprehensive, approximate quantum description of atomic structure, which serves as the starting point for the quantum description of the chemical bond in Chapter 6.

The method of solving the Schrödinger equation for the hydrogen atom is the same as that used for the particle-in-a-box models in Section 4.6. Because the mathematics is more complicated, we do not show the details here, and we present the solutions only in graphical form. Your primary objective in this chapter should be to understand the shapes and structures of the hydrogen atomic orbitals and the Hartree orbitals from these graphical representations. You should be able to predict how the probability distribution for the electrons depends on the properties of the orbitals, as specified by their quantum numbers. Always keep in mind the distinction between the hydrogen atomic orbitals and the Hartree orbitals. The former apply only to the hydrogen atom, and the latter only to many-electron atoms. Be aware of their differences, as well as their similarities.

5.1 The Hydrogen Atom

The hydrogen atom is the simplest example of a one-electron atom or ion; other examples are He^+ , Li^{2+} , and other ions in which all but one electron have been stripped off. They differ only in the charge $+Ze$ on the nucleus, and therefore in the attractive force experienced by the electron.

The potential energy for the one-electron atom, discussed in the context of the planetary model in Section 3.2 and of the Bohr model in Section 4.3, depends only on the distance of the electron from the nucleus; it does not depend on angular orientation (see Fig. 4.12). Solution of the Schrödinger equation is most easily carried out in coordinates that reflect the natural symmetry of the potential energy function. For an isolated one-electron atom or ion, spherical coordinates are more appropriate than the more familiar Cartesian coordinates. Spherical coordinates are defined in Figure 5.1: r is the distance of the electron at P from the nucleus at O, and the angles θ and ϕ are similar to those used to locate points on the surface of the globe; θ is related to the latitude, and ϕ is related to the longitude.

The Schrödinger equation can be written out just as in Section 4.5, except in spherical polar coordinates, and the potential energy can be written as in Equation 3.2. The resulting equation is impressively complicated, but it nonetheless can be solved as in Section 4.6. The solution must be continuous in all three coordinates, and the radial portion must satisfy the boundary condition: $\psi \rightarrow 0$ as $r \rightarrow \infty$. This procedure leads naturally to quantization of the energy and the associated wave functions. We describe these parts of the solution in turn in the remainder of this section.

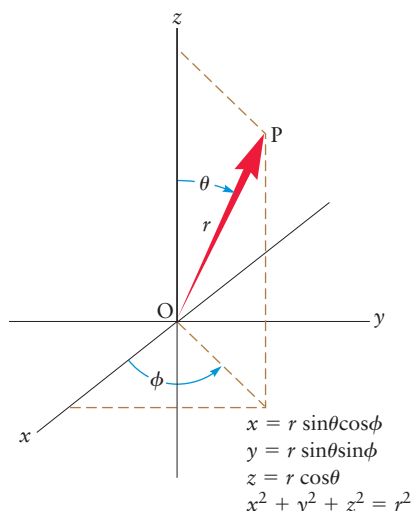


FIGURE 5.1 The relationship between spherical coordinates (r, θ, ϕ) and Cartesian coordinates (x, y, z). Here, θ is the angle with respect to the Cartesian z -axis, which ranges from 0 to π , and ϕ is the azimuthal angle (the angle between the x -axis and the projection onto the x - y plane of the arrow from the origin to P), which ranges from 0 to 2π . Here, r is the distance of the electron from the origin, and ranges from 0 to ∞ .

Energy Levels

Solutions of the Schrödinger equation for the one-electron atom exist only for particular values of the energy¹:

$$E = E_n = -\frac{Z^2 e^4 m_e}{8\epsilon_0^2 n^2 \hbar^2} \quad n = 1, 2, 3, \dots \quad [5.1a]$$

In energy units of rydbergs (1 rydberg = 2.18×10^{-18} J), this equation becomes (see Eq. 4.9b):

$$E_n = -\frac{Z^2}{n^2} \quad (\text{rydberg}) \quad n = 1, 2, 3, \dots \quad [5.1b]$$

The integer n , called the **principal quantum number**, indexes the individual energy levels. These are identical to the energy levels predicted by the Bohr theory. Here, however, quantization comes about naturally from the solution of the Schrödinger equation, rather than through an arbitrary assumption about the angular momentum.

The energy of a one-electron atom depends only on the principal quantum number n , because the potential energy depends only on the radial distance. The Schrödinger equation also quantizes L^2 , the square magnitude of the angular momentum, as well as L_z , the projection of the angular momentum along the z -axis. (A review of elementary aspects of angular momentum in Appendix B provides useful background for this discussion.) Quantization of the square of the angular momentum as well as its projection along the z -axis requires two additional

¹Strictly speaking, the electron mass m_e in the expressions for the energy levels of one-electron atoms should be replaced by the *reduced mass* μ , equal to $m_e m_N / (m_e + m_N)$, where m_N is the nuclear mass; μ differs from m_e by less than 0.1%.

quantum numbers. The **angular momentum quantum number** ℓ may take on any integral value from 0 to $n - 1$, and the angular momentum projection quantum number m may take on any integral value from $-\ell$ to ℓ . The quantum number m is referred to as the **magnetic quantum number** because its value governs the behavior of the atom in an external magnetic field. The allowed values of angular momentum L and its z projection are given by

$$L^2 = \ell(\ell + 1) \frac{h^2}{4\pi^2} \quad \ell = 0, 1, \dots, n - 1 \quad [5.2a]$$

$$L_z = m \frac{h}{2\pi} \quad m = -\ell, -\ell + 1, \dots, 0, \dots, \ell - 1, \ell \quad [5.2b]$$

For $n = 1$ (the ground state), the only allowed quantum numbers are ($\ell = 0$, $m = 0$). For $n = 2$, there are $n^2 = 4$ allowed sets of quantum numbers:

$$(\ell = 0, m = 0), (\ell = 1, m = 1), (\ell = 1, m = 0), (\ell = 1, m = -1)$$

The restrictions on ℓ and m give rise to n^2 sets of quantum numbers for every value of n . Each set (n, ℓ, m) identifies a specific **quantum state** of the atom in which the electron has energy equal to E_n , angular momentum equal to $\sqrt{\ell(\ell + 1)} h/2\pi$, and z -projection of angular momentum equal to $mh/2\pi$. When $n > 1$, a total of n^2 specific quantum states correspond to the single energy level E_n ; consequently, this set of states is said to be **degenerate**.

It is conventional to label specific states by replacing the angular momentum quantum number with a letter; we signify $\ell = 0$ with s , $\ell = 1$ with p , $\ell = 2$ with d , $\ell = 3$ with f , $\ell = 4$ with g , and on through the alphabet. Thus, a state with $n = 1$ and $\ell = 0$ is called a $1s$ state, one with $n = 3$ and $\ell = 1$ is a $3p$ state, one with $n = 4$ and $\ell = 3$ is a $4f$ state, and so forth. The letters s , p , d , and f derive from early (pre-quantum mechanics) spectroscopy, in which certain spectral lines were referred to as sharp, principal, diffuse, and fundamental. These terms are not used in modern spectroscopy, but the historical labels for the values of the quantum number ℓ are still followed. Table 5.1 summarizes the allowed combinations of quantum numbers.

The energy levels, including the degeneracy due to m and with states labeled by the spectroscopic notation, are conventionally displayed on a diagram as shown in Figure 5.2.

Wave Functions

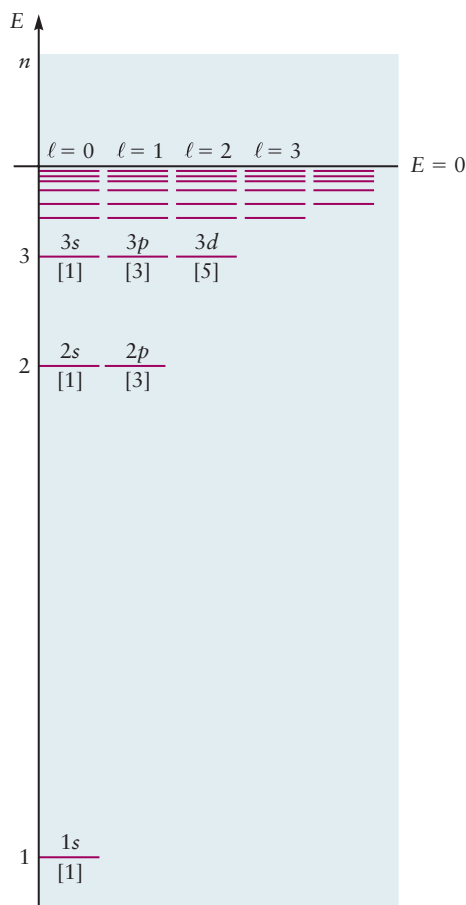
For each quantum state (n, ℓ, m) , solution of the Schrödinger equation provides a wave function of the form

$$\psi_{n\ell m}(r, \theta, \phi) = R_{n\ell}(r)Y_{\ell m}(\theta, \phi) \quad [5.3]$$

TABLE 5.1 Allowed Values of Quantum Numbers for One-Electron Atoms

n	1	2		3		
ℓ	0	0	1	0	1	2
m	0	0	-1, 0, +1	0	-1, 0, +1	-2, -1, 0, +1, +2
Number of degenerate states for each ℓ	1	1	3	1	3	5
Number of degenerate states for each n	1	4		9		

FIGURE 5.2 The energy-level diagram of the H atom predicted by quantum mechanics is arranged to show the degeneracy $(2\ell + 1)$ for each value of ℓ .



in which the total wave function is the product of a radial part, $R_{n\ell}(r)$, and an angular part, $Y_{\ell m}(\theta, \phi)$. This product form is a consequence of the spherically symmetric potential energy function, and it enables separate examination of the angular and radial contributions to the wave function. The functions $Y_{\ell m}(\theta, \phi)$ are called **spherical harmonics**. They appear in many physical problems with spherical symmetry and were already well known before the advent of the Schrödinger equation. The angular motions of the electron described by θ and ϕ influence the *shape* of the wave function through the angular factor $Y_{\ell m}$, even though they do not influence the energy.

The wave function itself is not measured. It is to be viewed as an intermediate step toward calculating the physically significant quantity ψ^2 , which is the probability density for locating the electron at a particular point in the atom. More precisely,

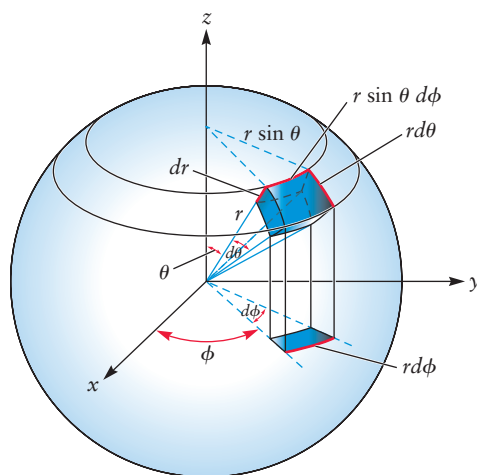
$$(\psi_{n\ell m})^2 dV = [R_{n\ell}(r)]^2 [Y_{\ell m}(\theta, \phi)]^2 dV \quad [5.4]$$

gives the probability of locating the electron within a small three-dimensional volume, dV , located at the position (r, θ, ϕ) when it is known that the atom is in the state n, ℓ, m . Specific examples are presented in succeeding paragraphs. The spherical volume element dV (Fig. 5.3) is defined as

$$dV = r^2 \sin \theta dr d\theta d\phi \quad [5.5]$$

A wave function $\psi_{n\ell m}(r, \theta, \phi)$ for a one-electron atom in the state (n, ℓ, m) is called an **orbital**. This term recalls the circular orbits of the Bohr atom, but there is

FIGURE 5.3 The differential volume element in spherical polar coordinates.



no real resemblance. An orbital is *not* a trajectory traced by an individual electron. When the one-electron atom is in state (n, ℓ, m) , it is conventional to say the electron is “in an (n, ℓ, m) orbital.” This phrase is merely a shorthand way of making the precise but cumbersome statement: “When an electron has energy, total angular momentum, and z component of angular momentum values corresponding to the quantum numbers n, ℓ, m , the probability density of finding the electron at the point (r, θ, ϕ) is given by $\psi_{n\ell m}^2(r, \theta, \phi)$.” Do not allow this verbal shorthand to mislead you into thinking an orbital is some sort of “region in space” inside which the electron is confined. The orbitals are labeled $1s, 2s, 2p, 3s, \dots$ by the spectroscopic notation previously introduced.

EXAMPLE 5.1

Give the names of all the orbitals with $n = 4$, and state how many m values correspond to each type of orbital.

SOLUTION

The quantum number ℓ may range from 0 to $n - 1$; thus, its allowed values in this case are 0, 1, 2, and 3. The labels for the groups of orbitals are then:

$\ell = 0$	4s	$\ell = 2$	4d
$\ell = 1$	4p	$\ell = 3$	4f

The quantum number m ranges from $-\ell$ to $+\ell$; thus, the number of m values is $2\ell + 1$. This gives one 4s orbital, three 4p orbitals, five 4d orbitals, and seven 4f orbitals for a total of $16 = 4^2 = n^2$ orbitals with $n = 4$. They all have the same energy, but they differ in shape.

Related Problems: 3, 4

Sizes and Shapes of Orbitals

The sizes and shapes of the hydrogen atom orbitals are important in chemistry because they provide the foundations for the quantum description of chemical bonding and the molecular shapes to which it leads. Sizes and shapes of the orbitals are revealed by graphical analysis of the wave functions, of which the first few are given in Table 5.2. Note that the radial functions are written in terms of the dimensionless variable σ , which is the ratio of Zr to a_0 . For $Z = 1$, $\sigma = 1$ at the radius of the first Bohr orbit of the hydrogen atom.

T A B L E 5.2 Angular and Radial Parts of Wave Functions for One-Electron Atoms

Angular Part $Y(\theta, \phi)$	Radial Part $R_{nl}(r)$
$\ell = 0 \left\{ Y_s = \left(\frac{1}{4\pi} \right)^{1/2} \right.$	$R_{1s} = 2 \left(\frac{Z}{a_0} \right)^{3/2} \exp(-\sigma)$
$\ell = 1 \left\{ \begin{array}{l} Y_{p_x} = \left(\frac{3}{4\pi} \right)^{1/2} \sin \theta \cos \phi \\ Y_{p_y} = \left(\frac{3}{4\pi} \right)^{1/2} \sin \theta \sin \phi \\ Y_{p_z} = \left(\frac{3}{4\pi} \right)^{1/2} \cos \theta \end{array} \right.$	$R_{2s} = \frac{1}{2\sqrt{2}} \left(\frac{Z}{a_0} \right)^{3/2} (2 - \sigma) \exp(-\sigma/2)$ $R_{3s} = \frac{2}{81\sqrt{3}} \left(\frac{Z}{a_0} \right)^{3/2} (27 - 18\sigma + 2\sigma^2) \exp(-\sigma/3)$ $R_{2p} = \frac{1}{2\sqrt{6}} \left(\frac{Z}{a_0} \right)^{3/2} \sigma \exp(-\sigma/2)$ $R_{3p} = \frac{4}{81\sqrt{6}} \left(\frac{Z}{a_0} \right)^{3/2} (6\sigma - \sigma^2) \exp(-\sigma/3)$
$\ell = 2 \left\{ \begin{array}{l} Y_{d_{z^2}} = \left(\frac{5}{16\pi} \right)^{1/2} (3 \cos^2 \theta - 1) \\ Y_{d_{xz}} = \left(\frac{15}{4\pi} \right)^{1/2} \sin \theta \cos \theta \cos \phi \\ Y_{d_{yz}} = \left(\frac{15}{4\pi} \right)^{1/2} \sin \theta \cos \theta \sin \phi \\ Y_{d_{xy}} = \left(\frac{15}{16\pi} \right)^{1/2} \sin^2 \theta \sin 2\phi \\ Y_{d_{x^2-y^2}} = \left(\frac{15}{16\pi} \right)^{1/2} \sin^2 \theta \cos 2\phi \end{array} \right.$	$R_{3d} = \frac{4}{81\sqrt{30}} \left(\frac{Z}{a_0} \right)^{3/2} \sigma^2 \exp(-\sigma/3)$
$\sigma = \frac{Zr}{a_0}$	$a_0 = \frac{\epsilon_0 h^2}{\pi e^2 m_e} = 0.529 \times 10^{-10} \text{ m}$

Graphical representation of the orbitals requires some care. Equation 5.3 tells us simply to go to the point (r, θ, ϕ) , evaluate the wave function there, and draw a graph showing the results of visiting many such points. But all three spatial dimensions have already been used to define the location; thus we would need a fourth dimension to display the value of the wave function at that point. Alternatively, we could create a table of numbers giving the value of the wave function at each point (r, θ, ϕ) , but it would be difficult to develop intuition about shapes and structures from this table. We get around these problems by slicing up three-dimensional space into various two- and one-dimensional regions and examining the wave function at each point in these regions. For example, suppose in Figure 5.1 we look only at points in the x - y plane and evaluate the wave function at each point. Then, just as we did for the three-dimensional particle in a box in Figure 4.28, we can generate a contour map that represents the shape of the hydrogen wave function at locations in the x - y plane. We can generate contour maps in any other “cut planes” in the same way. A second approach is to look only at the radial behavior. We start at the origin in Figure 5.1 and move out along the direction (r, θ, ϕ) , holding (θ, ϕ) constant, and plot the wave function at each value of r . We rely on contour plots to display the angular shapes of the wave function, and on two-dimensional graphs of the wave function versus r to display radial behavior. We use images that combine these angular and radial effects to display size and shape in three-dimensional space. We always state the conditions and limitations of such three-dimensional images. Because the wave function is a four-dimensional object, its appearance in three-dimensional representations depends strongly on choices made by the illustrator. Be certain you understand these choices in each image you examine (or create!).

s ORBITALS Let's begin with **s orbitals**, corresponding to $\psi_{n\ell m}$ with $\ell = 0$ (therefore, $m = 0$ as well). For all *s* orbitals, the angular part *Y* is a constant (see Table 5.2). Because ψ does not depend on either θ or ϕ , all *s* orbitals are spherically symmetric about the nucleus. This means that the amplitude of an *s* orbital (and therefore also the probability of finding the electron near some point in space) depends only on its distance, *r*, from the nucleus and not on its direction in space. There are several ways to visualize the radial variation of the *ns* orbitals with $n = 1, 2, 3, \dots$, and the probability density they describe.

One way (Fig. 5.4a) is to prepare a contour plot in the *x-y* plane. The contours are circles because the wave function does not depend on the angles. The outermost contour identifies points at which the amplitude of ψ is 5% of its maximum value. The second circle identifies points with ψ at 10% of the maximum, and so on in steps of 20% to the innermost contour, which identifies points with ψ at 90% of the maximum. Contours with positive phase (positive sign for the amplitude) are shown in red, whereas negative phase (negative sign for the amplitude) is represented in blue. Note that these contours, which identify uniform increases in magnitude, become much closer together as we approach the origin. This indicates the amplitude of the wave function increases rapidly as we approach the nucleus. The *x-y* plane corresponds to $\theta = \pi/2$ in Figure 5.1. Because the wave function does not depend on angles, this same contour plot could be obtained by tilting the *x-y* plane to any value of θ . It could also be obtained by starting with the *x-z* plane and the *y-z* plane and tilting either of them to any value of θ . Therefore, we can rotate the contour plot in Figure 5.4a to generate a set of concentric spheres in three dimensions. Each sphere identifies a surface of points in (r, θ, ϕ) at each of which the wave function has the same value. These spheres are called *isosurfaces* because the amplitude of the wave function has the same value at each point on them.

A second way to visualize wave functions (see Fig. 5.4b) is to plot their radial portions directly: $\psi_{n00} \propto R_{n0}(r)$. These plots give the amplitude of the wave function at a certain distance from the nucleus. For 2*s* and 3*s* orbitals, the wave function has lobes with positive and negative phases. The transition between positive and negative lobes is a node, at which the value of the wave function is zero.

A third way (see Fig. 5.4c) is to plot the **radial probability density** $r^2[R_{n0}(r)]^2$. This is the probability density of finding the electron at any point in space at a distance *r* from the nucleus for all angles θ and ϕ . More precisely, the product $r^2[R_{n0}(r)]^2 dr$ gives the probability of finding the electron anywhere within a thin spherical shell of thickness *dr*, located at distance *r* from the nucleus. This spherical shell is easily visualized with the aid of Figure 5.3. As the angle ϕ runs through its entire range from 0 to 2π , a circular annulus of width *dr* located between *r* and *r* + *dr* is traced out in the *x-y* plane. This annulus will become a spherical shell as the angle θ runs through its range from 0 to π . The factor r^2 in front accounts for the increasing volume of spherical shells at greater distances from the nucleus. The radial probability distribution is small near the nucleus, where the shell volume (proportional to r^2) is small, and reaches its maximum value at the distance where the electron is most likely to be found.

Finally, we want to plot the size of the orbital. What is meant by the *size* of an orbital? Strictly speaking, the wave function of an electron in an atom stretches out to infinity, so an atom has no clear boundary. We might define the size of an atom as the contour at which ψ^2 has fallen off to some particular numerical value, or as the extent of a “balloon skin” inside which some definite fraction (for example, 90% or 99%) of the probability density of the electron is contained. We have adopted the former practice in representing the size of orbitals. Figure 5.4d shows spheres generated from the contours at which the wave functions for the 1*s*, 2*s*, and 3*s* orbitals of hydrogen have fallen to 0.05 of their maximum amplitude. Figure 5.4d shows that the size of an orbital increases with increasing quantum number *n*. A 3*s* orbital is larger than a 2*s* orbital, which, in turn, is larger than a 1*s* orbital. This is the quantum analog of the increase in radius of the Bohr orbits with increasing *n*.

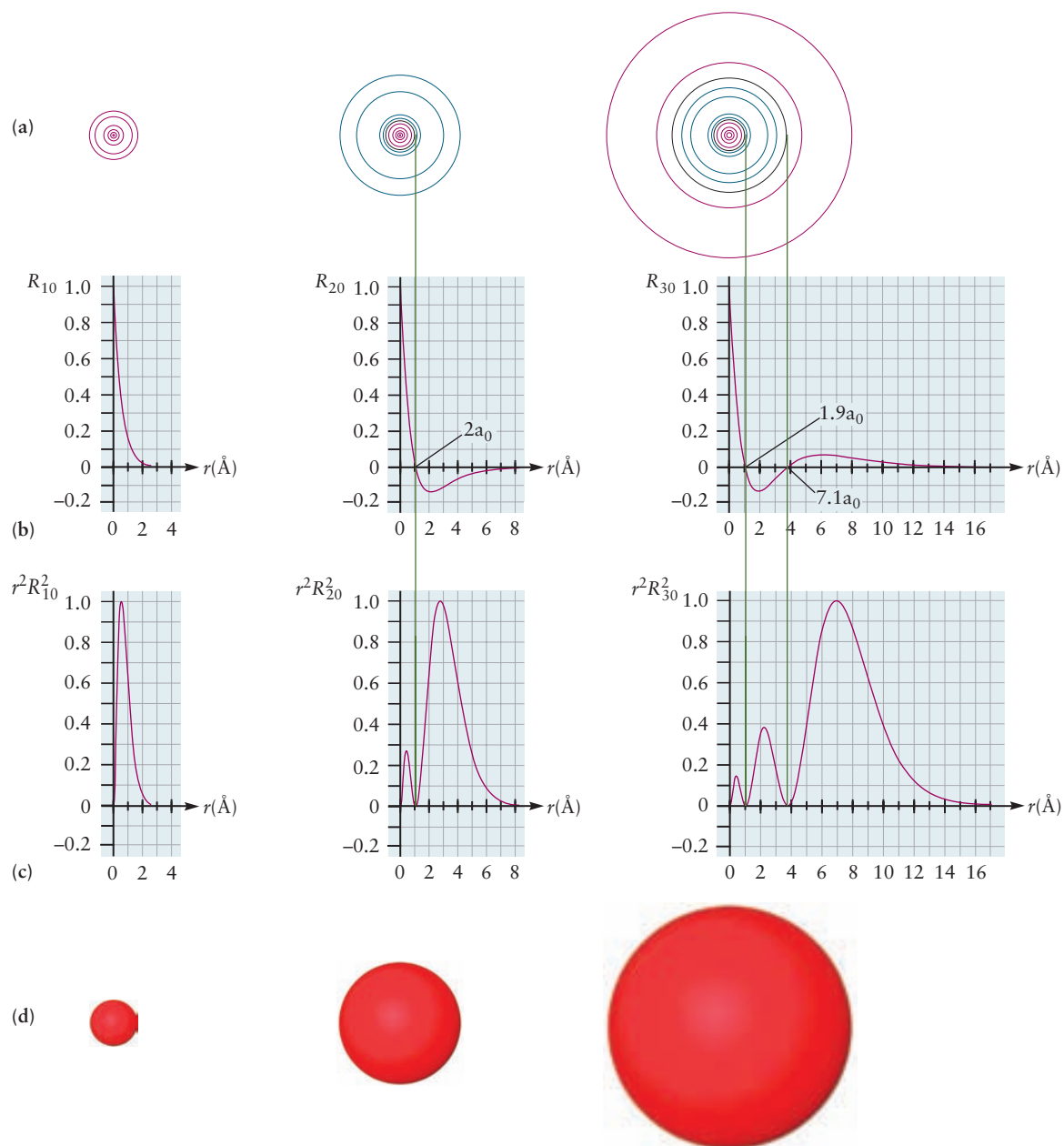


FIGURE 5.4 Four representations of hydrogen s orbitals. (a) A contour plot of the wave function amplitude for a hydrogen atom in its $1s$, $2s$, and $3s$ states. The contours identify points at which ψ takes on ± 0.05 , ± 0.1 , ± 0.3 , ± 0.5 , ± 0.7 , and ± 0.9 of its maximum value. Contours with positive phase are shown in red; those with negative phase are shown in blue. Nodal contours, where the amplitude of the wave function is zero, are shown in black. They are connected to the nodes in the lower plots by the vertical green lines. (b) The radial wave functions plotted against distance from the nucleus, r . (c) The radial probability density, equal to the square of the radial wave function multiplied by r^2 . (d) The “size” of the orbitals, as represented by spheres whose radius is the distance at which the probability falls to 0.05 of its maximum value.

Another measure of the size of an orbital is the most probable distance of the electron from the nucleus in that orbital. Figure 5.4c shows that the most probable location of the electron is progressively farther from the nucleus in ns orbitals for larger n . Nonetheless, there is a finite probability for finding the electron at the nucleus in both $2s$ and $3s$ orbitals. This happens because electrons in s orbitals have no angular momentum ($\ell = 0$), and thus can approach the nucleus along the radial direction. The ability of electrons in s orbitals to “penetrate” close to the nucleus has important consequences in the structure of many-electron atoms and molecules (see later).

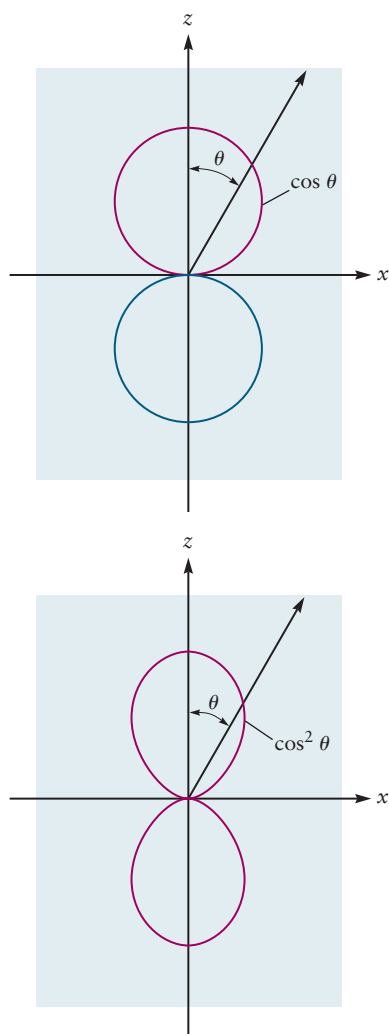


FIGURE 5.5 Two representations of hydrogen p orbitals. (a) The angular wave function for the p_z orbital. The p_x and p_y orbitals are the same, but are oriented along the x - and y -axis, respectively. (b) The square of the angular wave function for the p_z orbital. Results for the p_x and p_y orbitals are the same, but are oriented along the x - and y -axis, respectively.

Finally, note that an ns orbital has $n - 1$ **radial nodes**; a radial node is a spherical surface about the nucleus on which ψ and ψ^2 are 0. These spherical surfaces are the analogues of the nodal planes in the wave functions for a particle in a cubic box (Figure 4.28). The more numerous the nodes in an orbital, the higher the energy of the corresponding quantum state of the atom. Just as for the particle in a box, the energies of orbitals increase as the number of nodes increases.

p ORBITALS Orbitals with angular quantum numbers ℓ different from 0 are not spherically symmetric. Interesting angular effects arise from the quantization of angular momentum. The angular wave function $Y_{\ell m}(\theta, \phi)$ has separate lobes with positive and negative phase, with a node between them. Equation 5.2b specifies $2\ell + 1$ projections of these angular momentum values along the z -axis. The three angular wave functions with $\ell = 1$, for which the allowed m values are $-1, 0$, and $+1$, lead to three orbitals (the **p orbitals**) with the same shapes but different orientations in space.

The angular wave function $Y_{10}(\theta, \phi)$ with the combination $\ell = 1, m = 0$ is called the angular portion of the p_z orbital here because it is oriented along the z -axis. The wave function Y_{p_z} for the p_z orbital (see Table 5.2) is proportional to $\cos \theta$. From the relation between spherical and Cartesian coordinates illustrated in Figure 5.1, you can see that $\cos \theta \propto z$; thus, this orbital has its maximum amplitude along the z -axis (where $\theta = 0$ or π) and a node in the x - y plane (where $\theta = \pi/2$, so $\cos \theta = 0$) (Fig. 5.5a). The p_z orbital therefore points along the z -axis, with its positive phase (red in Fig. 5.5a) on the side of the x - y plane where the z -axis is positive and negative phase (blue in Fig. 5.5a) on the side where the z -axis is negative. The positive and negative lobes are circles tangent to one another at the x - y plane. An electron in a p_z orbital has the greatest probability of being found at significant values of z and has zero probability of being found in the x - y plane. This plane is a nodal plane or, more generally, an **angular node** across which the wave function changes sign.

The angular wave functions $Y_{11}(\theta, \phi)$ for $\ell = 1, m = 1$ and $Y_{1,-1}(\theta, \phi)$ for $\ell = 1, m = -1$ do not have a simple geometrical interpretation. However, their sum and their difference, which are also allowed solutions of the Schrödinger equation for the hydrogen atom, do have simple interpretations. Therefore, we form two new angular wave functions:

$$\begin{aligned} Y_{p_x} &= c_1(Y_{11} + Y_{1,-1}) \\ Y_{p_y} &= c_2(Y_{11} - Y_{1,-1}) \end{aligned} \quad [5.6]$$

where c_1 and c_2 are appropriate constants. The resulting expressions for Y_{p_x} and Y_{p_y} are given in Table 5.2. A comparison of these expressions with Figure 5.1 shows that Y_{p_x} lies along the x -axis and Y_{p_y} lies along the y -axis. The angular wave functions Y_{p_x} for the p_x orbital and Y_{p_y} for the p_y orbital thus have the same shape as Y_{p_z} , but point along the x - and y -axis, respectively. They have nodes at the y - z and x - z planes, respectively.

It is informative to examine the angular dependence of the probability density in the p orbitals, starting with p_z . The probability density for finding the electron at the position (θ, ϕ) with r constant is given by $Y_{p_z}^2$, the square of the angular wave function (see Fig. 5.5b). Notice that general shape is the same as Y_{p_z} , but the lobes are no longer circular. This happens because the values of $\cos \theta$, which are less than 1 except where $\theta = 0, \pi, -\pi$, become even smaller when squared and shrink the envelope away from the circular shape. The behavior of $Y_{p_x}^2$ and $Y_{p_y}^2$ are the same as $Y_{p_z}^2$. The radial parts of the np wave functions (represented by $R_{n\ell}$) are illustrated in Figure 5.6.

The p orbitals, like the s orbitals, may have radial nodes, at which the probability density vanishes at certain distances from the nucleus regardless of direction.

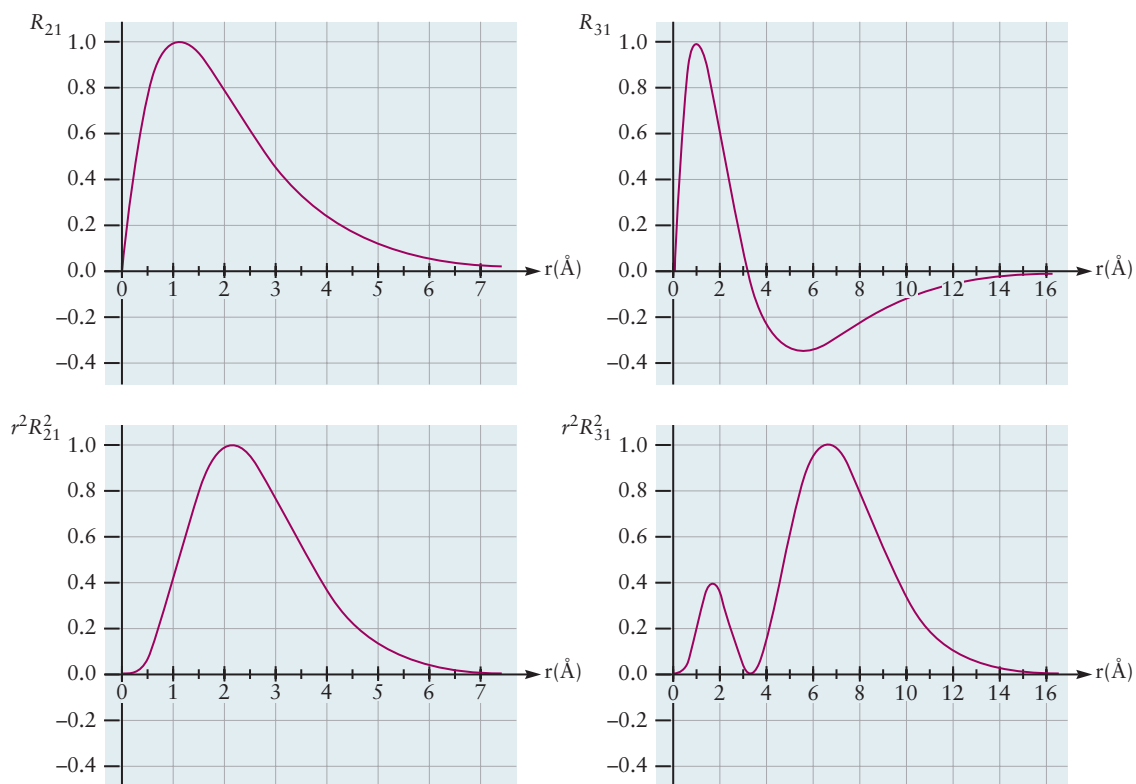


FIGURE 5.6 Radial wave functions $R_{n\ell}$ for np orbitals and the corresponding radial probability densities $r^2 R_{n\ell}^2$.

From Figure 5.6, the R_{21} wave function has no radial nodes, and the R_{31} function has one radial node; the R_{41} (not shown) function has two radial nodes. The $R_{n\ell}$ wave functions have $n - \ell - 1$ radial nodes. Because the angular part of the np wave function always has a nodal plane, the total wave function has $n - 1$ nodes ($n - 2$ radial and 1 angular), which is the same number as an s orbital with the same principal quantum number. The $R_{21}(r)$ function (that is, R_{2p}) in Table 5.2 contains the factor σ , which is proportional to r ($\sigma = Zr/a_0$) and causes it to vanish at the nucleus. This is true of all the radial wave functions except the ns functions, and it means that the probability is zero for the electron to be at the nucleus for all wave functions with $\ell > 0$ (p, d, f, \dots). Physically, electrons with angular momentum are moving around the nucleus, not toward it, and cannot “penetrate” toward the nucleus.

Finally, we combine the angular and radial dependence to get a sense of the shape of the complete orbital, $\psi_{n\ell m} = R_{n\ell} Y_{\ell m}$. Let’s examine the $2p_z$ orbital at points (r, θ, ϕ) confined to the x - z plane. At each point, we calculate the value of R_{21} (as in Fig. 5.6) and the value of Y_{2p_z} (as in Fig. 5.5a). Then we multiply these values together to obtain the value of ψ_{2p_z} at that point. We continue this process and generate a contour plot for ψ_{2p_z} in the x - z plane. The results are shown in Figure 5.7. Contours identify points at which ψ_{2p_z} takes on $\pm 0.1, \pm 0.3, \pm 0.5, \pm 0.7,$ and ± 0.9 of its maximum value. Contours with positive phase are shown in red; blue contours represent negative phase. The radial wave function from Figure 5.6 has dramatically changed the circular angular wave function from Figure 5.5a. The circles have been flattened, especially on the sides nearest the x - y plane. The contours are not concentric, but rather bunch together on the sides nearest the x - y plane. This reflects the rapid decrease in amplitude near the nucleus (see Fig. 5.6) and the much slower decrease in amplitude at longer distances beyond the maximum in the radial function.

Finally, we can represent the $2p_z$ orbital as a three-dimensional object by rotating Figure 5.7 about the z -axis. Each of the closed contours in Figure 5.7 will then trace out a three-dimensional isosurface on which all the points (r, θ, ϕ) have the

FIGURE 5.7 Contour plot for the amplitude in the p_z orbital for the hydrogen atom. This plot lies in the x - z plane. The z -axis (not shown) would be vertical in this figure, and the x -axis (not shown) would be horizontal. The lobe with positive phase is shown in red, and the lobe with negative phase in blue. The x - y nodal plane is shown as a dashed black line. Compare with Figure 5.5a.

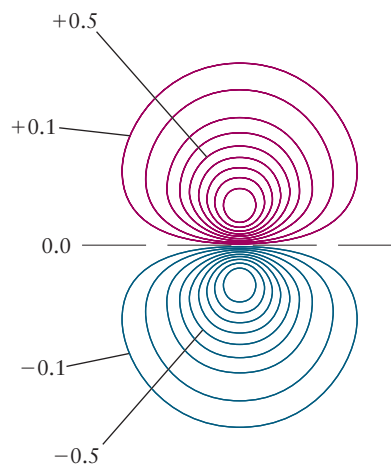
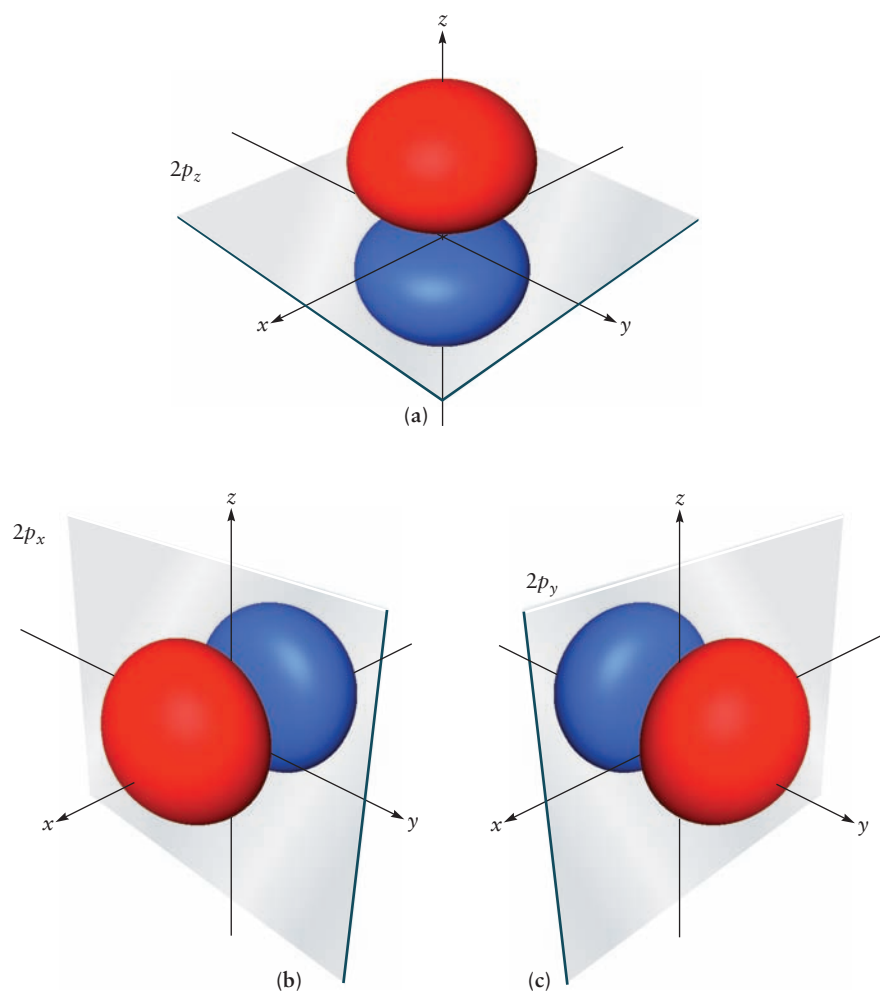


FIGURE 5.8 The shapes of the three $2p$ orbitals, with phases and nodal planes indicated. The isosurfaces in (a), (b), and (c) identify points where the amplitude of each wave function is ± 0.2 of its maximum amplitude. (a) $2p_z$ orbital. (b) $2p_x$ orbital. (c) $2p_y$ orbital.



same amplitude and phase of the wave function. The same analysis generates isosurfaces for $2p_x$ and $2p_y$. Figure 5.8abc shows plots of all three, with the phases and nodal planes indicated, as isosurfaces at ± 0.2 times the maximum amplitude.

Each $2p$ orbital appears, loosely speaking, as a pair of flattened and distorted hemispheres, with opposite phase, facing each other across their nodal plane. You can see how this shape would change dramatically if we selected for display isosurfaces with other values of amplitude. Sometimes you see the $2p$ orbitals

represented (in a manner similar to Fig. 5.8) with no explanation of how the images were obtained. Although such pictures reliably indicate the gross shape and extent of the orbitals, they obscure completely all the rich structure *inside* this skin, in particular the location—even the existence—of the maximum. We encourage you to develop your intuition for orbitals by looking at detailed contour plots for angular information, and then visualizing three-dimensional isosurfaces at whatever value of amplitude is most appropriate for the problem you are investigating at the moment.

***d* ORBITALS** When $\ell = 2$ Equation 5.2b specifies five projections of the angular momentum along the z -axis. As with the p orbitals, we take linear combinations of the angular wave functions to obtain orbitals with specific orientations relative to the Cartesian axes. The conventionally chosen linear combinations of the solutions with $m = -2, -1, +1, +2$ give four orbitals with the same shape but different orientations with respect to the Cartesian axes: d_{xy} , d_{yz} , d_{xz} , and $d_{x^2-y^2}$ (Fig. 5.9).

For example, a d_{xy} orbital has four lobes, two with positive phase and two with negative phase; the maximum amplitude is at 45° to the x - and y -axes. The $d_{x^2-y^2}$ orbital has maximum amplitude along the x - and y -axes. The “down-axis” view of these four d orbitals, illustrated for one of them (d_{xy}) in Figure 5.9, shows that they all have the same shape when viewed down the appropriate axis. The fifth orbital, d_{z^2} , which corresponds to $m = 0$, has a different shape from the rest, with maximum amplitude along the z -axis and a little “doughnut” in the x - y plane. Each d orbital has two angular nodes (for example, the d_{xy} orbital has the x - z and y - z planes as its nodal surfaces). The radial functions, $R_{n2}(r)$, have $n - 3$ radial nodes, giving once again $n - 1$ total nodes.

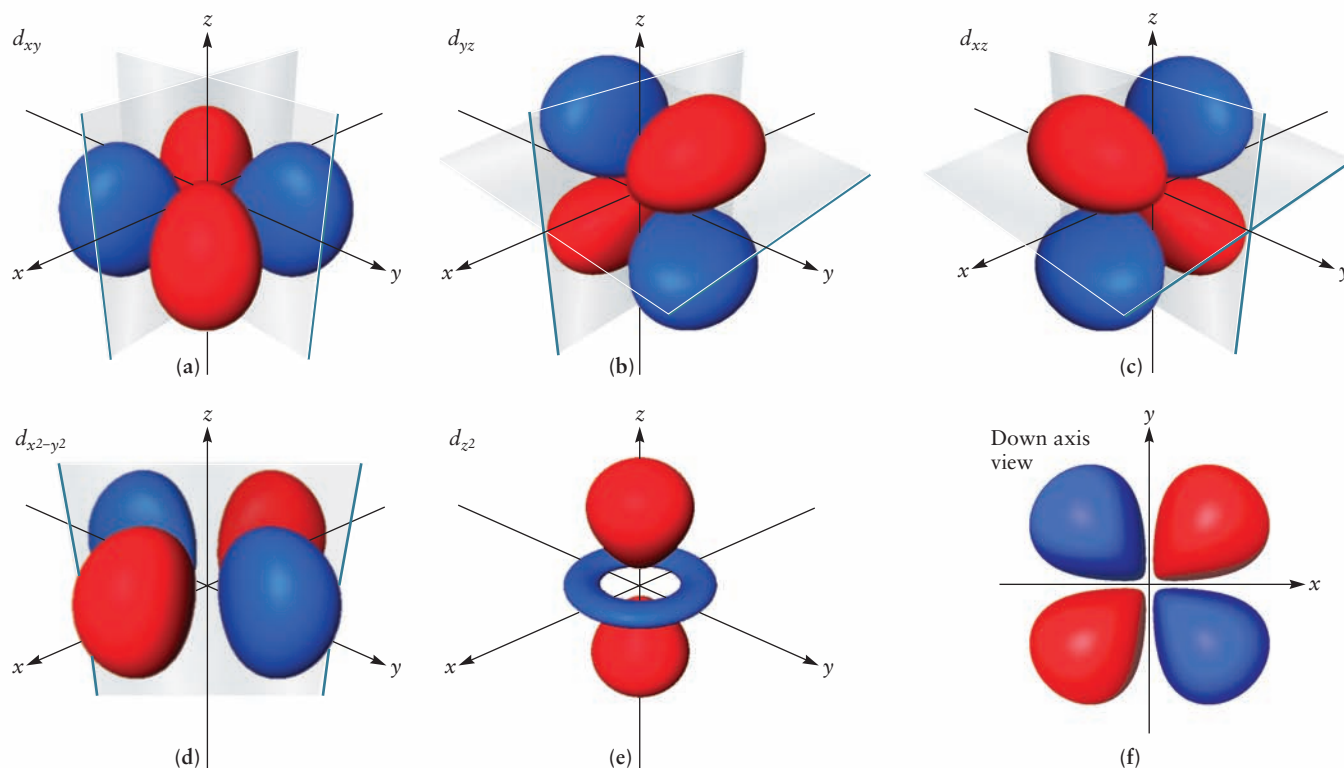


FIGURE 5.9 The shapes of the five $3d$ orbitals, with phases and nodal surfaces indicated. The “down-axis” view shows the shapes of the first four orbitals (a)–(d) when viewed down the appropriate axis; the specific example shown here is the d_{xy} orbital viewed down the z -axis.

The wave functions for f orbitals and orbitals of higher ℓ can be calculated, but they play a smaller role in chemistry than do the s , p , and d orbitals.

We summarize the important features of orbital shapes and sizes as follows:

1. For a given value of ℓ , an increase in n leads to an increase in the average distance of the electron from the nucleus, and therefore in the size of the orbital (see Figs. 5.4 and 5.6).
2. An orbital with quantum numbers n and ℓ has ℓ angular nodes and $n - \ell - 1$ radial nodes, giving a total of $n - 1$ nodes. An angular node is defined by a plane. A radial node is defined by a spherical surface. For a one-electron atom or ion, the energy depends only on the number of nodes—that is, on n but not on ℓ or m . The energy increases as the number of nodes increases.
3. As r approaches 0, $\psi(r, \theta, \phi)$ vanishes for all orbitals except s orbitals; thus, only an electron in an s orbital can “penetrate to the nucleus,” that is, have a finite probability of being found right at the nucleus.

The next section shows that these general statements are important for determining the electronic structure of many-electron atoms even though they are deduced from the one-electron case.

The characteristics of the orbitals of a one-electron atom (or ion) are especially well displayed by a quantitative plot showing s , p , and d orbitals all on the same scale (Fig. 5.10). The best quantitative measure of the size of an orbital is $\bar{r}_{n\ell}$, the average value of the distance of the electron from the nucleus in that orbital. Quantum mechanics calculates $\bar{r}_{n\ell}$ as

$$\bar{r}_{n\ell} = \frac{n^2 a_0}{Z} \left\{ 1 + \frac{1}{2} \left[1 - \frac{\ell(\ell + 1)}{n^2} \right] \right\} \quad [5.7]$$

The leading term of this expression is the radius of the n th Bohr orbit (see Eq. 4.12). In Figure 5.10, the small arrow on each curve locates the value of $\bar{r}_{n\ell}$ for that orbital.

EXAMPLE 5.2

Compare the $3p$ and $4d$ orbitals of a hydrogen atom with respect to the (a) number of radial and angular nodes and (b) energy of the corresponding atom.

SOLUTION

- (a) The $3p$ orbital has a total of $n - 1 = 3 - 1 = 2$ nodes. Of these, one is angular ($\ell = 1$) and one is radial. The $4d$ orbital has $4 - 1 = 3$ nodes. Of these, two are angular ($\ell = 2$) and one is radial.
- (b) The energy of a one-electron atom depends only on n . The energy of an atom with an electron in a $4d$ orbital is higher than that of an atom with an electron in a $3p$ orbital, because $4 > 3$.

Related Problems: 5, 6

Electron Spin

If a beam of hydrogen atoms in their ground state (with $n = 1$, $\ell = 0$, $m = 0$) is sent through a magnetic field whose intensity increases in the plane perpendicular to the flight of the beam, it splits into two beams, each containing half of the atoms (Fig. 5.11). The pioneering experiment of this type is called the Stern–Gerlach experiment after the German physicists who performed it, Otto Stern and Walther Gerlach.

FIGURE 5.10 Dependence of radial probability densities on distance from the nucleus for one-electron orbitals with $n = 1, 2, 3$. The small arrow below each curve locates the value of $\bar{r}_{n\ell}$ for that orbital. The distance axis is expressed in the same dimensionless variable introduced in Table 5.1. The value 1 on this axis is the first Bohr radius for the hydrogen atom. Because the radial probability density has dimensions $(\text{length})^{-1}$, the calculated values of $r^2[R_{n\ell}(r)]^2$ are divided by $(a_0)^{-1}$ to give a dimensionless variable for the probability density axis.

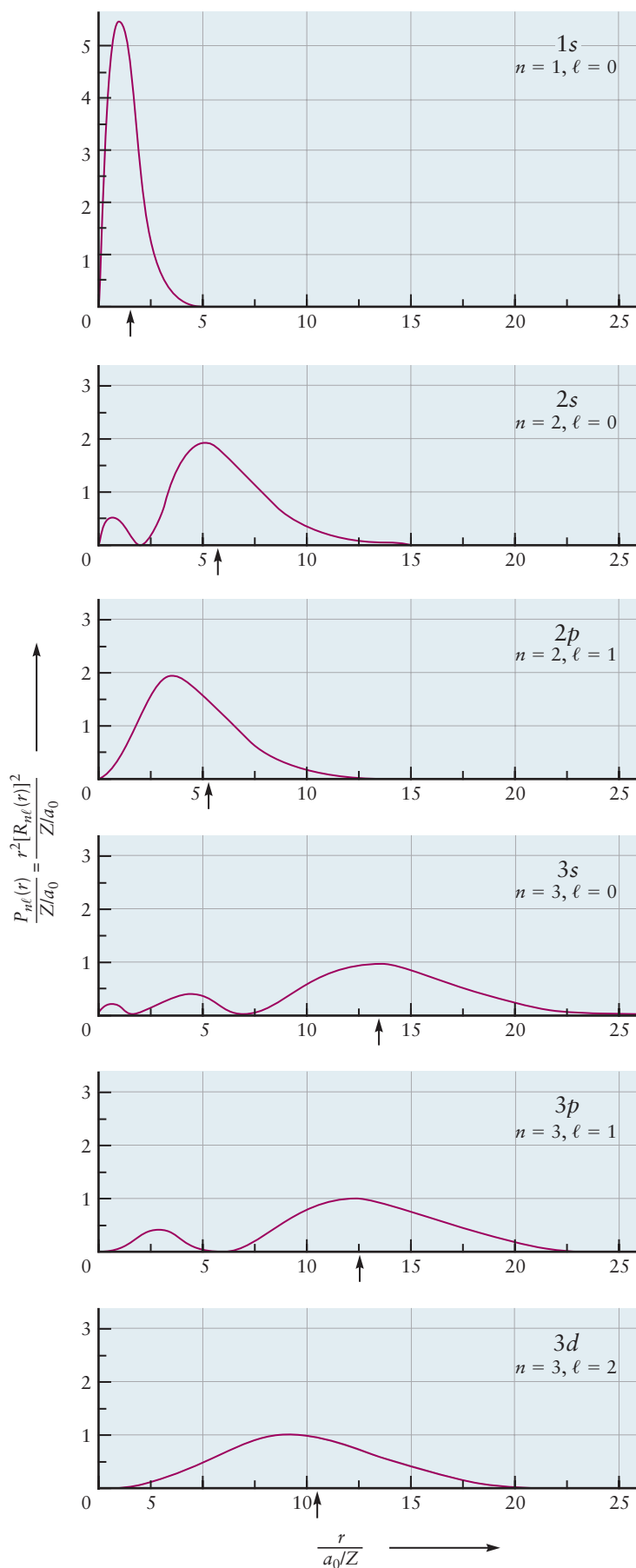
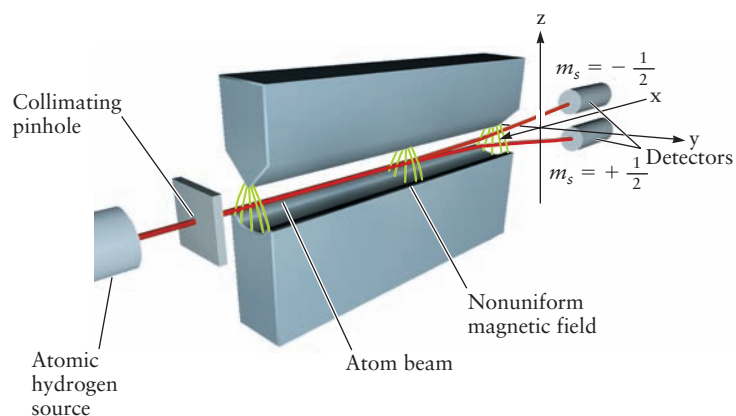


FIGURE 5.11 A beam of hydrogen atoms is split into two beams when it traverses a magnetic field, the value of which is not constant in the plane perpendicular to the path of the beam. The nonconstant field is created by the specially shaped cross section of the north and south poles of the magnet in the z - y plane. The green curved lines trace the pattern over which the field is varied. Regions where the green lines are closer together are regions of greater magnetic field. Atoms with spin quantum number $m_s = +\frac{1}{2}$ follow one trajectory, and those with $m_s = -\frac{1}{2}$ follow another.



Recall that a magnet, unlike a single electric charge, has two poles, and that a magnetic dipole moment can be used to describe the interactions of a magnet with a magnetic field in the same way that an electric dipole moment is used to describe the interaction of a pair of charges with an electric field. You may recall from classical physics (or your own experience) that a small bar magnet will rotate to orient itself in the presence of an external magnetic field. If the magnetic field changes strength along a particular direction, then a force will be exerted on the bar magnet that will cause it to *move* in the direction of the changing field, and not just rotate to a new direction. If the magnetic dipole moments of the hydrogen atoms were randomly oriented in space (as predicted by classical physics), then the beam would be smeared out at the detector to reflect all possible orientations of the magnetic moment. That the original beam is split into only two well-defined beams in this experiment demonstrates the unexpected fact that the *orientation* of the magnetic moment of the electron is quantized. The result of this experiment is explained by introducing a *fourth* quantum number, m_s , which can take on two values, conventionally chosen to be $+\frac{1}{2}$ and $-\frac{1}{2}$. For historical reasons, the fourth quantum number is referred to as the **spin quantum number**. When $m_s = +\frac{1}{2}$, the electron spin is said to be “up,” and when $m_s = -\frac{1}{2}$, the spin is “down.” The spin quantum number arises from relativistic effects that are not included in the Schrödinger equation. For most practical purposes in chemistry, it is sufficient simply to solve the ordinary Schrödinger equation, and then associate with each electron a spin quantum number $m_s = +\frac{1}{2}$ or $-\frac{1}{2}$ which does not affect the spatial probability distribution of the electron. Including the spin doubles the number of allowed quantum states with principal quantum number n , from n^2 to $2n^2$. This fact will assume considerable importance when considering the many-electron atoms in the next section.

5.2 Shell Model for Many-Electron Atoms

As we move from one-electron to many-electron atoms, both the Schrödinger equation and its solutions become increasingly complicated. The simplest many-electron atom, helium (He), has two electrons and a nuclear charge of $+2e$. The positions of the two electrons in a helium atom can be described using two sets of Cartesian coordinates, (x_1, y_1, z_1) and (x_2, y_2, z_2) , relative to the same origin. The wave function ψ depends on all six of these variables: $\psi = \psi(x_1, y_1, z_1, x_2, y_2, z_2)$. Its square, $\psi^2(x_1, y_1, z_1, x_2, y_2, z_2)$, is the probability density of finding the first electron at point (x_1, y_1, z_1) and, simultaneously, the second electron at (x_2, y_2, z_2) . The Schrödinger equation is now more complicated, and an explicit solution for helium is not possible. Nevertheless, modern computers have enabled us to solve this equation numerically with high accuracy, and the predicted properties of helium are in excellent agreement with experiment.

Although these numerical calculations demonstrate conclusively the usefulness of the Schrödinger equation for predicting atomic properties, they suffer from two defects. First, they are somewhat difficult to interpret physically, and second, they become increasingly difficult to solve, even numerically, as the number of electrons increases. As a result, approximate approaches to the many-electron Schrödinger equation have been developed.

Hartree Orbitals

The **self-consistent field (SCF) orbital approximation method** developed by Hartree is especially well suited for applications in chemistry. Hartree's method generates a set of approximate one-electron orbitals, φ_α , and associated energy levels, ε_α , reminiscent of those for the H atom. The subscript α represents the appropriate set of quantum numbers (see later in this chapter for a definition). The electronic structure of an atom with atomic number Z is then “built up” by placing Z electrons into these orbitals in accordance with certain rules (see later in this chapter for descriptions of these rules).

In this section, we introduce Hartree's method and use it to describe the electron arrangements and energy levels in many-electron atoms. Later sections detail how this approximate description rationalizes periodic trends in atomic properties and serves as a starting point for descriptions of chemical bond formation.

For any atom, Hartree's method begins with the exact Schrödinger equation in which each electron is attracted to the nucleus and repelled by all the other electrons in accordance with the Coulomb potential. The following three simplifying assumptions are made immediately:

1. Each electron moves in an *effective field* created by the nucleus and all the other electrons, and the effective field for electron i depends only on its position r_i .
2. The effective field for electron i is obtained by averaging its Coulomb potential interactions with each of the other electrons over all the positions of the other electrons so that r_i is the only coordinate in the description.
3. The effective field is spherically symmetric; that is, it has no angular dependence.

Under the first assumption, each electron moves as an independent particle and is described by a one-electron orbital similar to those of the hydrogen atom. The wave function for the atom then becomes a product of these one-electron orbitals, which we denote $\varphi_\alpha(r_i)$. For example, the wave function for lithium (Li) has the form $\psi_{\text{atom}} = \varphi_\alpha(r_1)\varphi_\beta(r_2)\varphi_\gamma(r_3)$. This product form is called **the orbital approximation for atoms**. The second and third assumptions in effect convert the exact Schrödinger equation for the atom into a set of simultaneous equations for the unknown effective field and the unknown one-electron orbitals. These equations must be solved by iteration until a self-consistent solution is obtained. (In spirit, this approach is identical to the solution of complicated algebraic equations by the method of iteration described in Appendix C.) Like any other method for solving the Schrödinger equation, Hartree's method produces two principal results: energy levels and orbitals.

These Hartree orbitals resemble the atomic orbitals of hydrogen in many ways. Their angular dependence is identical to that of the hydrogen orbitals, so quantum numbers ℓ and m are associated with each atomic orbital. The radial dependence of the orbitals in many-electron atoms differs from that of one-electron orbitals because the effective field differs from the Coulomb potential, but a principal quantum number n can still be defined. The lowest energy orbital is a $1s$ orbital and has no radial nodes, the next lowest s orbital is a $2s$ orbital and has one radial node, and so forth. Each electron in an atom has associated with it a set of four quantum numbers (n, ℓ, m, m_s). The first three quantum numbers describe its spatial distribution and the fourth specifies its spin state. The allowed quantum numbers follow the same pattern as those for the hydrogen atom. However, the number of states associated with each combination of (n, ℓ, m) is twice as large because of the two values for m_s .

Sizes and Shapes of Hartree Orbitals

The spatial properties of Hartree orbitals are best conveyed through a specific example. We present the results for argon (Ar), taken from Hartree's original work. The ground state of the argon atom has 18 electrons in the $1s$, $2s$, $2p$, $3s$, and $3p$ Hartree orbitals (see later). Figure 5.12 shows the radial probability density distributions for these five occupied orbitals as calculated by Hartree's method. The probability density distribution shown for the $2p$ level is the sum of the distributions for the $2p_x$, $2p_y$, and $2p_z$ orbitals; similarly, the $3p$ probability density distribution includes the $3p_x$, $3p_y$, and $3p_z$ orbitals. Comparing Figure 5.12 with Figure 5.10 shows that each Hartree orbital for argon is "smaller" than the corresponding orbital for hydrogen in the sense that the region of maximum probability density is closer to the nucleus. This difference occurs because the argon nucleus ($Z = 18$) exerts a much stronger attractive force on electrons than does the hydrogen nucleus ($Z = 1$). We develop a semiquantitative relation between orbital size and Z in the next subsection.

The fact that Hartree orbitals with the same value of n are large in the same narrow regions of space, despite their different values of ℓ , has interesting consequences. The total radial probability density function for a many-electron atom gives the probability of finding an electron at position r regardless of which orbital it occupies. We obtain this function by summing up the radial probability density functions of all the occupied orbitals. The resulting probability function is proportional to the *radial charge density distribution function* $\rho(r)$ for the atom. If the radial probability density functions in Figure 5.12 are all added together, the result reflects the contributions of electrons to the charge density $\rho(r)$ in a thin spherical shell of radius r , regardless of the orbital to which the electron belongs. A plot of $\rho(r)$ on the same scale as Figure 5.12 shows three peaks at r values of approximately 0.1, 0.3, and 1.2 in units of a_0 (Fig. 5.13) The total electron density

FIGURE 5.12 Dependence of radial probability densities on distance from the nucleus for Hartree orbitals in argon with $n = 1, 2, 3$. The results were obtained from self-consistent calculations using Hartree's method. Distance is plotted in the same dimensionless variable used in Figure 5.10 to facilitate comparison with the results for hydrogen. The fact that the radial probability density for all orbitals with the same value of n have maxima very near one another suggests that the electrons are arranged in "shells" described by these orbitals.

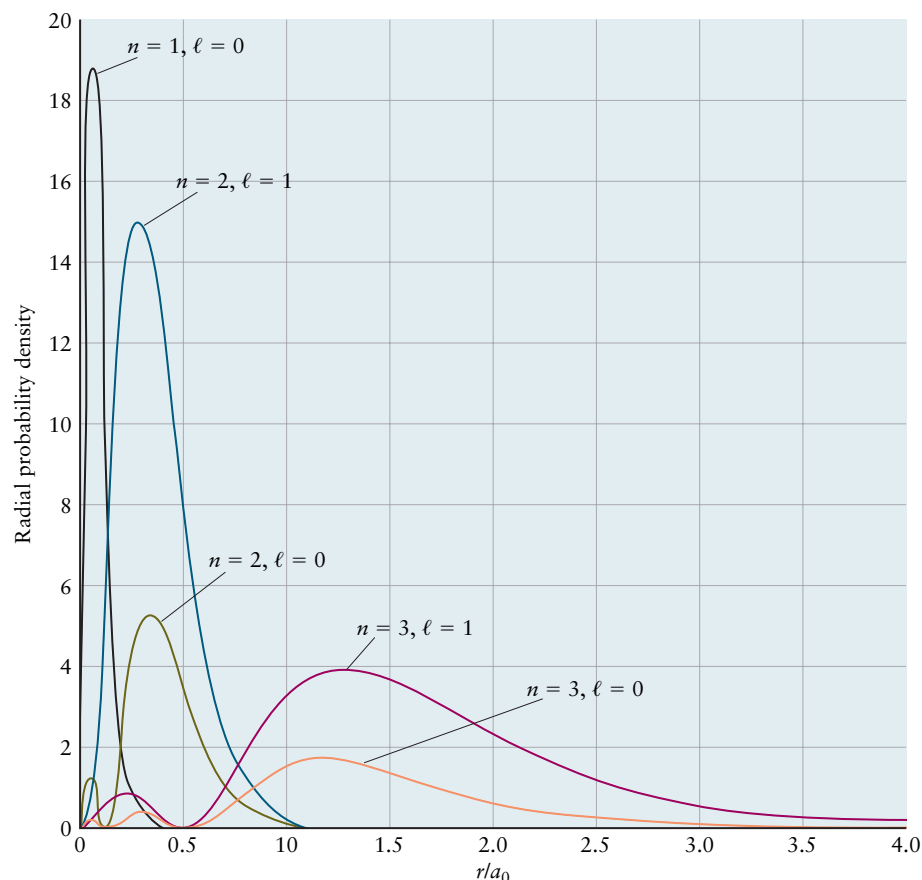
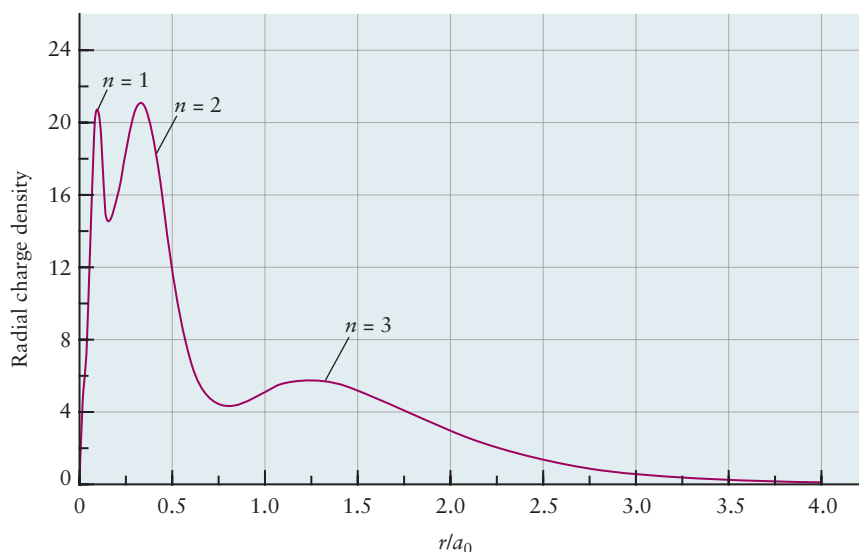


FIGURE 5.13 The radial charge density in the argon atom as calculated by Hartree's method. The charge is arrayed into three shells corresponding to the values 1, 2, and 3 for the principal quantum number n .



of the argon atom thus is concentrated in three concentric shells, where a **shell** is defined as all electrons with the same value of n . Each shell has a radius determined by the principal quantum number n . The shell model summarizes the coarse features of the electron density of an atom by averaging over all those local details not described by the principal quantum number n . Within each shell, a more detailed picture is provided by the **subshells**, defined as the set of orbitals with the same values of both n and ℓ .

The subshells (see Fig. 5.12) determine the structure of the periodic table and the formation of chemical bonds. In preparation for a discussion of these connections, it is necessary to describe the energy values for Hartree orbitals.

Shielding Effects: Energy Sequence of Hartree Orbitals

The energy-level diagrams calculated for many-electron atoms by Hartree's method resemble the diagram for the hydrogen atom (see Fig. 5.2), but differ in two important respects. First, the degeneracy of the p , d , and f orbitals is removed. Because the effective field in Hartree's method is different from the Coulomb field in the hydrogen atom, the energy levels of Hartree orbitals depend on both n and ℓ . Second, the energy values are distinctly shifted from the values of corresponding hydrogen orbitals because of the stronger attractive force exerted by nuclei with $Z > 1$.

These two effects can be explained qualitatively by a highly simplified one-electron model. Assume each of the electrons in shell n is moving in a Coulomb potential given approximately by

$$V_n^{\text{eff}}(r) \approx -\frac{Z_{\text{eff}}(n)e^2}{r} \quad [5.8]$$

where $Z_{\text{eff}}(n)$ is the **effective nuclear charge** in that shell. To understand the origin and magnitude of $Z_{\text{eff}}(n)$, consider a particular electron e_1 in an atom. Inner electrons near the nucleus *shield* e_1 from the full charge Z of the nucleus by effectively canceling some of the positive nuclear charge. $Z_{\text{eff}}(n)$ is thus the net reduced nuclear charge experienced by a particular electron, due to the presence of the other electrons. (See Section 3.2.) For a neutral atom, $Z_{\text{eff}}(n)$ can range from a maximum value of Z near the nucleus (no screening) to a minimum value of 1 far from the nucleus (complete screening by the other $Z - 1$ electrons). Detailed Hartree calculations for argon show that $Z_{\text{eff}}(1) \sim 16$, $Z_{\text{eff}}(2) \sim 8$, and $Z_{\text{eff}}(3) \sim 2.5$. The

effect of shielding on the energy and radius of a Hartree orbital is easily estimated in this simplified picture by using the hydrogen atom equations with Z replaced by $Z_{\text{eff}}(n)$. We use ϵ_n to distinguish a Hartree orbital energy from the H atom orbital E_n . Thus,

$$\epsilon_n \approx -\frac{[Z_{\text{eff}}(n)]^2}{n^2} \quad (\text{rydbergs}) \quad [5.9]$$

and

$$\bar{r}_{n\ell} \approx \frac{n^2 a_0}{Z_{\text{eff}}(n)} \left\{ 1 + \frac{1}{2} \left[1 - \frac{\ell(\ell + 1)}{n^2} \right] \right\} \quad [5.10]$$

Thus, electrons in inner shells (small n) are tightly bound to the nucleus, and their average position is quite near the nucleus because they are only slightly shielded from the full nuclear charge Z . Electrons in outer shells are only weakly attracted to the nucleus, and their average position is far from the nucleus because they are almost fully shielded from the nuclear charge Z .

EXAMPLE 5.3

Estimate the energy and the average value of r in the 1s orbital of argon. Compare the results with the corresponding values for hydrogen.

SOLUTION

Using Equation 5.9 and the value $Z_{\text{eff}}(1) \sim 16$ leads to $\epsilon_{1s} \sim -256$ rydbergs for argon. The Ar(1s) electron is more strongly bound than the H(1s) electron by a factor 256. (Compare Equation 5.1b for the hydrogen atom.)

Using Equation 5.10 and the value $Z_{\text{eff}}(1) \sim 16$ leads to $\bar{r}_{1s} = \frac{3a_0}{2 \cdot 16}$ for argon. This is smaller by a factor of 16 than \bar{r}_{1s} for hydrogen.

A comparison of Figure 5.12 with Figure 5.10 demonstrates that each Hartree orbital for argon is “smaller” than the corresponding orbital for hydrogen in the sense that the region of maximum probability is closer to the nucleus.

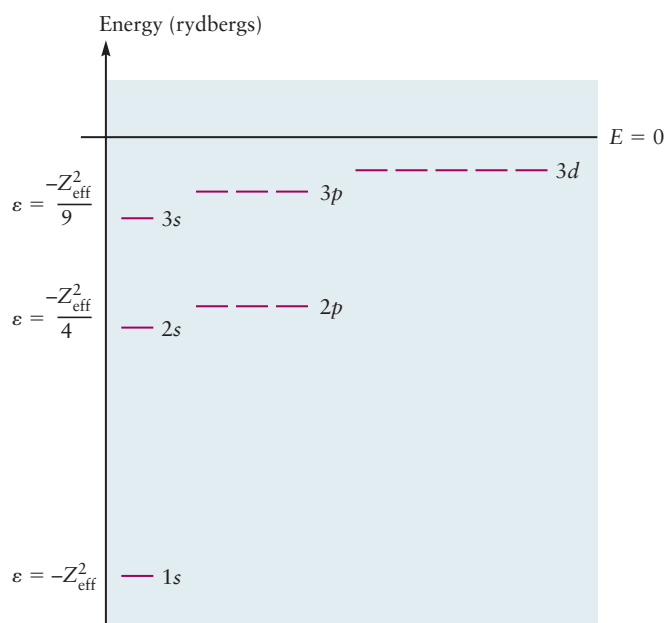
Related Problems: 9, 10, 11, 12, 13, 14

The dependence of the energy on ℓ in addition to n can be explained by comparing the extent of shielding in different subshells. Figures 5.4 through 5.10 show that only the s orbitals penetrate to the nucleus; both p and d orbitals have nodes at the nucleus. Consequently, the shielding will be smallest, and the electron most tightly bound, in s orbitals. Calculations show that

$$\epsilon_{ns} < \epsilon_{np} < \epsilon_{nd}$$

The approximate energy-level diagram for Hartree orbitals showing dependence on both n and ℓ is presented in Figure 5.14. Values of Z_{eff} are determined in advanced computer calculations of atomic structure, using a SCF approach based on Hartree’s method. Table 5.3 shows a representative sampling, and includes the actual Z value in parentheses after the symbol for the atom. Using these values and the method in Example 5.3, you can quickly generate an approximate energy-level diagram and estimate the size of the orbitals for any atom. How do we use these energy levels and orbitals to describe the electrons? The answer is the subject of the next section.

FIGURE 5.14 Approximate energy-level diagram for Hartree orbitals, estimated by incorporating values of Z_{eff} . Energy values are in units of rydbergs. The result of electron–electron repulsion is to remove the degeneracy of the hydrogen atom states with different ℓ values.



T A B L E 5.3 Z_{eff} for Selected Atoms

	H(1)							He(2)
1s	1.00							1.69
	Li(3)	Be(4)	B(5)	C(6)	N(7)	O(8)	F(9)	Ne(10)
1s	2.69	3.68	4.68	5.67	6.66	7.66	8.65	9.64
2s	1.28	1.91	2.58	3.22	3.85	4.49	5.13	5.76
2p			2.42	3.14	3.83	4.45	5.10	5.76

5.3 Aufbau Principle and Electron Configurations

The ground-state electronic configuration of an atom with atomic number Z is built up by arranging the Hartree atomic orbitals in order of increasing energy and adding one electron at a time, starting with the lowest energy orbital, until all Z electrons are in place. The following additional restrictions are imposed at each step:

1. The **Pauli exclusion principle** states that no two electrons in an atom can have the same set of four quantum numbers (n, ℓ, m, m_s). Another way of stating this principle is that each Hartree atomic orbital (characterized by a set of three quantum numbers, n, ℓ , and m) holds at most two electrons, one with spin up and the other with spin down.
2. **Hund's rules** state that when electrons are added to Hartree orbitals of equal energy, a single electron enters each orbital before a second one enters any orbital. In addition, the lowest energy configuration is the one with parallel spins (see later discussion).

The energy level diagram for Hartree orbitals is shown qualitatively in Figure 5.14. Energy levels for ns orbitals, and for $2p$ orbitals up through F, can be estimated by using values for Z_{eff} in Equation 5.9. Values of Z_{eff} for each element have been obtained in advanced computer calculations based on Hartree's method. Table 5.3 shows the results for atoms in the first two periods. Starting with Ne, the simplified picture in Equations 5.8 and 5.9 is no longer adequate to estimate the np and nd energies, and full Hartree calculations are necessary.

Building up from Helium to Argon

Let's see how the aufbau principle works for the atoms from helium (He) through neon (Ne). The lowest energy orbital is always the $1s$ orbital; therefore, helium has two electrons (with opposite spins) in that orbital. The ground-state electron configuration of the helium atom is symbolized as $1s^2$ and is conveniently illustrated by a diagram (for example, Fig. 5.15). The $1s$ orbital in the helium atom is somewhat larger than the $1s$ orbital in the helium ion (He^+). In the ion, the electron experiences the full nuclear charge $+2e$, but in the atom, each electron partially screens or shields the other electron from the nuclear charge. The orbital in the helium atom can be described by the approximate equations given previously with an "effective" nuclear charge Z_{eff} of 1.69, which lies between $+1$ (the value for complete shielding by the other electron) and $+2$ (no shielding).

A lithium (Li) atom has three electrons. The third electron does not join the first two in the $1s$ orbital. It occupies a different orbital because, by the Pauli principle, at most two electrons may occupy any one orbital. The third electron goes into the $2s$ orbital, which is the next lowest in energy. The ground state of the lithium atom is therefore $1s^2 2s^1$, and $1s^2 2p^1$ is an excited state.

The next two elements present no difficulties. Beryllium (Be) has the ground-state configuration $1s^2 2s^2$, and the $2s$ orbital is now filled. Boron (B), with five

FIGURE 5.15 The ground-state electron configurations of first- and second-period atoms. Each horizontal line represents a specific atomic orbital. Arrows pointing up represent electrons with spin quantum number $m_s = +\frac{1}{2}$ and arrows pointing down represent electrons with spin quantum number $m_s = -\frac{1}{2}$.

	1s	2s	2p _x	2p _y	2p _z
H: $1s^1$	<u>↑</u>	—	—	—	—
He: $1s^2$	<u>↑↓</u>	—	—	—	—
Li: $1s^2 2s^1$	<u>↑↓</u>	<u>↑</u>	—	—	—
Be: $1s^2 2s^2$	<u>↑↓</u>	<u>↑↓</u>	—	—	—
B: $1s^2 2s^2 2p_x^1$	<u>↑↓</u>	<u>↑↓</u>	<u>↑</u>	—	—
C: $1s^2 2s^2 2p_x^1 2p_y^1$	<u>↑↓</u>	<u>↑↓</u>	<u>↑</u>	<u>↑</u>	—
N: $1s^2 2s^2 2p_x^1 2p_y^1 2p_z^1$	<u>↑↓</u>	<u>↑↓</u>	<u>↑</u>	<u>↑</u>	<u>↑</u>
O: $1s^2 2s^2 2p_x^2 2p_y^1 2p_z^1$	<u>↑↓</u>	<u>↑↓</u>	<u>↑↓</u>	<u>↑</u>	<u>↑</u>
F: $1s^2 2s^2 2p_x^2 2p_y^2 2p_z^1$	<u>↑↓</u>	<u>↑↓</u>	<u>↑↓</u>	<u>↑↓</u>	<u>↑</u>
Ne: $1s^2 2s^2 2p_x^2 2p_y^2 2p_z^2$	<u>↑↓</u>	<u>↑↓</u>	<u>↑↓</u>	<u>↑↓</u>	<u>↑↓</u>

electrons, has the ground-state configuration $1s^2 2s^2 2p^1$. Because the three $2p$ orbitals of boron have the same energy, there is an equal chance for the electron to be in each one.

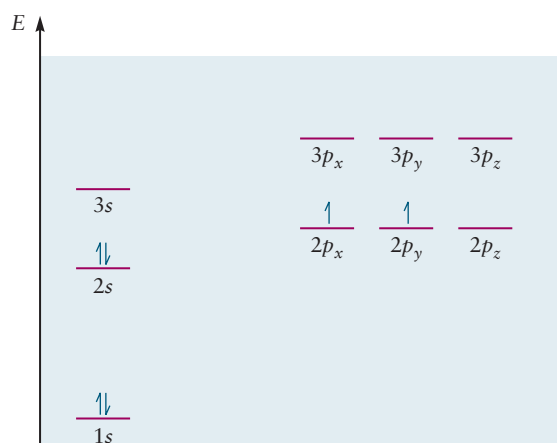
With carbon (C), the sixth element, a new question arises. Will the sixth electron go into the same orbital as the fifth (for example, both into a $2p_x$ orbital with opposite spins), or will it go into the $2p_y$ orbital, which has equal energy? The answer is found in the observation that two electrons that occupy the same atomic orbital experience stronger electron–electron repulsion than they would if they occupied orbitals in different regions of space. Thus, putting the last two electrons of carbon into two different p orbitals, such as $2p_x$ and $2p_y$, in accordance with Hund’s rule, leads to lower energy than putting them into the same p orbital. The electron configuration of carbon is then $1s^2 2s^2 2p_x^1 2p_y^1$, or more simply, $1s^2 2s^2 2p^2$. This configuration is shown in Figure 5.16.

The behavior of atoms in a magnetic field provides a test of their electron configuration. A substance is **paramagnetic** if it is attracted into a magnetic field. Any substance that has one or more unpaired electrons in the atoms, molecules, or ions that compose it is paramagnetic because a net magnetic moment arises from each of the unpaired electrons. (Recall the Stern–Gerlach experiment described in Section 5.1.) A substance in which all the electrons are paired is weakly **diamagnetic**: It is pushed *out* of a magnetic field, although the force it experiences is much smaller in magnitude than the force that pulls a typical paramagnetic substance into a magnetic field. Of the atoms discussed so far, hydrogen, lithium, boron, and carbon are known from experiments to be paramagnetic, whereas helium and beryllium are known to be diamagnetic. These results give us confidence in the validity of our description of atomic structure based on the orbital approximation and SCF calculations.

The electron configurations from nitrogen (N) through neon (Ne) follow from the stepwise filling of the $2p$ orbitals. The six elements from boron to neon are called **p-block** elements because their configurations involve filling of p orbitals in the building-up process. The four elements that precede them (hydrogen through beryllium) are called **s-block** elements.

The build-up of the third period, from sodium to argon, is an echo of what happened in the second; first the one $3s$ orbital is filled, and then the three $3p$ orbitals. As the number of electrons in an atom reaches 15 or 20, it is frequently the practice to explicitly include only those electrons added in the building up beyond the last preceding noble-gas element. The configuration of that noble gas is then represented by its chemical symbol enclosed in brackets. The ground-state configuration of silicon, for example, is written $[\text{Ne}]3s^2 3p^2$ using this system.

FIGURE 5.16 For a many-electron atom such as carbon, orbitals with different ℓ values (such as the $2s$ and $2p$ orbitals) have different energies (see Fig. 5.14). When two or more orbitals have the *same* energy (such as the three $2p$ orbitals here), electrons occupy different orbitals with parallel spins in the ground state.



EXAMPLE 5.4

Write the ground-state electron configurations for magnesium and sulfur. Are the gaseous atoms of these elements paramagnetic or diamagnetic?

SOLUTION

The noble-gas element preceding both elements is neon. Magnesium has two electrons beyond the neon core, which must be placed in the $3s$ orbital, the next higher in energy, to give the ground-state configuration $[\text{Ne}]3s^2$. A magnesium atom is diamagnetic because all of its electrons are paired in orbitals.

Sulfur has six electrons beyond the neon core; the first two of these are in the $3s$ orbital, and the next four are in the $3p$ orbitals. The ground-state configuration of sulfur is $[\text{Ne}]3s^23p^4$. When four electrons are put into three p orbitals, two electrons must occupy one of the orbitals, and the other two occupy different orbitals to reduce electron–electron repulsion. According to Hund’s rules, the electrons’ spins are parallel, and the sulfur atom is paramagnetic.

Related Problems: 15, 16, 17, 18

In summary, we remind you that the electron configuration for an atom is a concise, shorthand notation that represents a great deal of information about the structure and energy levels of the atom. Each configuration corresponds to an atomic wave function comprising a product of occupied Hartree orbitals. Each orbital has a well-defined energy (given by Equation 5.9 and shown in Figure 5.14) and average radius (given by Equation 5.10). The orbitals are grouped into subshells that are characterized by radial distribution functions (see Fig. 5.12). Chapter 6 describes the formation of chemical bonds by starting with the electron configurations of the participating atoms. We encourage you to become expert with atomic electronic configurations and all the information that they summarize.

EXAMPLE 5.5

The boron atom with $Z = 5$ has electron configuration $\text{B}: (1s)^2(2s)^2(2p_x)^1$.

- Write the atomic wave function for a B atom.
- Estimate the energy level diagram for a B atom.
- Estimate the radius of the $2s$ and $2p_x$ orbitals.

SOLUTION

- The atomic wave function for a B atom is

$$\psi_{\text{B}}(r_1, r_2, r_3, r_4, r_5) = [\varphi_{1s}(r_1)\varphi_{1s}(r_2)][\varphi_{2s}(r_3)\varphi_{2s}(r_4)][\varphi_{2p_x}(r_5)]$$

- Estimate the energy levels of a B atom.

$$\varepsilon_{1s} \approx -\frac{(4.68)^2}{1^2} = -21.90 \text{ Ry}$$

$$\varepsilon_{2s} \approx -\frac{(2.58)^2}{2^2} = -1.66 \text{ Ry}$$

$$\varepsilon_{2p} \approx -\frac{(2.42)^2}{2^2} = -1.46 \text{ Ry}$$

(c) Use Equation 5.10 and Z_{eff} values for boron from Table 5.3 to estimate orbital radii as follows:

$$\bar{r}_{2s} \approx \frac{2^2 a_0}{(2.58)} \left\{ 1 + \frac{1}{2} \left[1 - \frac{0(0+1)}{2^2} \right] \right\} = \frac{4a_0}{(2.58)} \left\{ \frac{3}{2} \right\} = 2.33a_0$$

$$\bar{r}_{2p} \approx \frac{2^2 a_0}{(2.42)} \left\{ 1 + \frac{1}{2} \left[1 - \frac{1(1+1)}{2^2} \right] \right\} = \frac{4a_0}{(2.42)} \left\{ \frac{5}{4} \right\} = 2.07a_0$$

Related Problems: 19, 20, 21, 22, 23, 24

Transition-Metal Elements and Beyond

After the $3p$ orbitals have been filled with six electrons, the natural next step is to continue the build-up process using the $3d$ subshell. Advanced calculations for elements 19 (K) through 30 (Zn) predict that ϵ_{3d} and ϵ_{4s} are very close, so the build-up process becomes rather subtle. For K and Ca, the calculations show that $\epsilon_{4s} < \epsilon_{3d}$. Optical spectroscopy confirms that the ground state of K is $[\text{Ar}]3d^0 4s^1$ and that of Ca is $[\text{Ar}]3d^0 4s^2$, as predicted by the sequence of calculated orbital energies. For Sc and the elements beyond, advanced calculations predict that $\epsilon_{3d} < \epsilon_{4s}$. Filling the $3d$ orbitals first would give the configurations $[\text{Ar}]3d^3 4s^0$ for Sc, $[\text{Ar}]3d^4 4s^0$ for Ti, and so on to $[\text{Ar}]3d^{10} 4s^0$ for Ni. These configurations are inconsistent with numerous optical, magnetic, and chemical properties of these elements, so some consideration besides the energies of the individual orbitals must also influence the build-up process. Let's consider the alternative configuration $[\text{Ar}]3d^1 4s^2$ for Sc and compare its total energy with that of the $[\text{Ar}]3d^3 4s^0$ configuration. This comparison must add the electrostatic repulsion energy between the electrons to the sum of the energies of the occupied one-electron orbitals to find the total energy of the atom. Because the $3d$ orbital is much more localized than the $4s$ orbital, the much greater repulsion energy of the two electrons in the $3d$ orbital outweighs the fact that $\epsilon_{3d} < \epsilon_{4s}$ and the configuration with two d electrons has higher energy. Thus, the configuration $[\text{Ar}]3d^1 4s^2$ has the lower energy and is the ground state for Sc. The same reasoning—minimizing the energy of the atom as a whole—predicts ground state electron configurations from $[\text{Ar}]3d^1 4s^2$ for Sc to $[\text{Ar}]3d^{10} 4s^2$ for Zn that agree with experimental results. The ten elements from scandium to zinc are called **d-block** elements because their configurations involve the filling of a d orbital in the building-up process.

Experimental evidence shows that chromium and copper do not fit this pattern. In its ground state, chromium has the configuration $[\text{Ar}]3d^5 4s^1$ rather than $[\text{Ar}]3d^4 4s^2$, and copper has the configuration $[\text{Ar}]3d^{10} 4s^1$ rather than $[\text{Ar}]3d^9 4s^2$. Similar anomalies occur in the fifth period, and others such as the ground-state configuration $[\text{Kr}]4d^7 5s^1$ that is observed for ruthenium in place of the expected $[\text{Kr}]4d^6 5s^2$.

In the sixth period, the filling of the $4f$ orbitals (and the generation of the **f-block** elements) begins as the rare-earth (lanthanide) elements from lanthanum to ytterbium are reached. The configurations determined from calculations and experiment can be recalled as needed by *assuming* that the orbitals are filled in the sequence $1s \rightarrow 2s \rightarrow 2p \rightarrow 3s \rightarrow 3p \rightarrow 4s \rightarrow 3d \rightarrow 4p \rightarrow 5s \rightarrow 4d \rightarrow 5p \rightarrow 6s \rightarrow 4f \rightarrow 5d \rightarrow 6p \rightarrow 7s \rightarrow 5f \rightarrow 6d$. The energies of the $4f$, $5d$, and $6s$ orbitals are comparable over much of the sixth period, and thus their order of filling is erratic.

The periodic table shown in Figure 5.17 classifies elements within periods according to the subshell that is being filled as the atomic number increases. Configurations are given explicitly for exceptions to this “standard” order of filling.

1s																		1s							
H																		He							
2s-filling																		2p-filling							
Li		Be																		B	C	N	O	F	Ne
3s-filling																		3p-filling							
Na		Mg																		Al	Si	P	S	Cl	Ar
4s-filling		3d-filling										4p-filling													
K	Ca	Sc	Ti	V	Cr	Mn	Fe	Co	Ni	Cu	Zn	Ga	Ge	As	Se	Br	Kr								
5s-filling		4d-filling										5p-filling													
Rb	Sr	Y	Zr	Nb	Mo	Tc	Ru	Rh	Pd	Ag	Cd	In	Sn	Sb	Te	I	Xe								
6s-filling		5d-filling										6p-filling													
Cs	Ba	Lu	Hf	Ta	W	Re	Os	Ir	Pt	Au	Hg	Tl	Pb	Bi	Po	At	Rn								
7s-filling		6d-filling																							
Fr	Ra	Lr	Rf	Ha	Sg	Ns	Hs	Mt	Uun	Uuu															

4f-filling													
La	Ce	Pr	Nd	Pm	Sm	Eu	Gd	Tb	Dy	Ho	Er	Tm	Yb
$5d^1 6s^2$	$4f^1 5d^1 6s^2$						$4f^7 5d^1 6s^2$						

5f-filling													
Ac	Th	Pa	U	Np	Pu	Am	Cm	Bk	Cf	Es	Fm	Md	No
$6d^1 7s^2$	$6d^2 7s^2$	$5f^1 6d^1 7s^2$	$5f^2 6d^1 7s^2$	$5f^4 6d^1 7s^2$			$5f^7 6d^1 7s^2$						

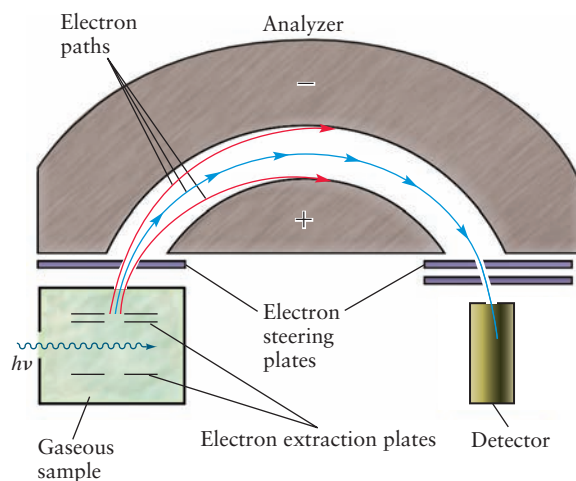
FIGURE 5.17 The filling of shells and the structure of the periodic table. Only the “anomalous” electron configurations are shown.

5.4 Shells and the Periodic Table: Photoelectron Spectroscopy

Our discussion of electronic structure began in Section 3.3 by analyzing patterns in the successive ionization energies of the atoms; these patterns suggested that the electrons are arranged in shells within the atom. In Section 5.2, we demonstrated that quantum theory *predicts* the shell structure of the atom. A shell is defined precisely as a set of orbitals that have the same principal quantum number, reflecting the fact that the average positions of the electrons in each of these shells are close to each other, but far from those of orbitals with different n values (see Fig. 5.12). Now, we can accurately interpret the results in Figure 3.5 as showing that Na has two electrons in the $n = 1$ shell, eight in the $n = 2$ shell, and one in the $n = 3$ shell.

The shell structure shows that two elements in the same group (column) of the periodic table have related valence electron configurations. For example, sodium (configuration $[\text{Ne}]3s^1$) and potassium (configuration $[\text{Ar}]4s^1$) each have a single valence electron in an s orbital outside a closed shell; consequently, the two elements closely resemble each other in their chemical properties. A major triumph of quantum mechanics is its ability to account for the periodic trends discovered by chemists many years earlier and organized empirically by Mendeleev and others in the periodic table (see Section 3.1). The ubiquitous octets in the Lewis electron dot diagrams of second- and third-period atoms and ions in Chapter 3 arise from the eight available sites for electrons in the one s orbital and three p orbitals of the valence shell. The special properties of the transition-metal elements are ascribed to the partial filling of their d orbitals (see Chapter 8 for further discussion of this feature).

FIGURE 5.18 The energy of photoelectrons is determined by measuring the voltage required to deflect the electrons along a semicircular pathway between two charged metallic hemispherical plates in vacuum so they arrive at the detector.

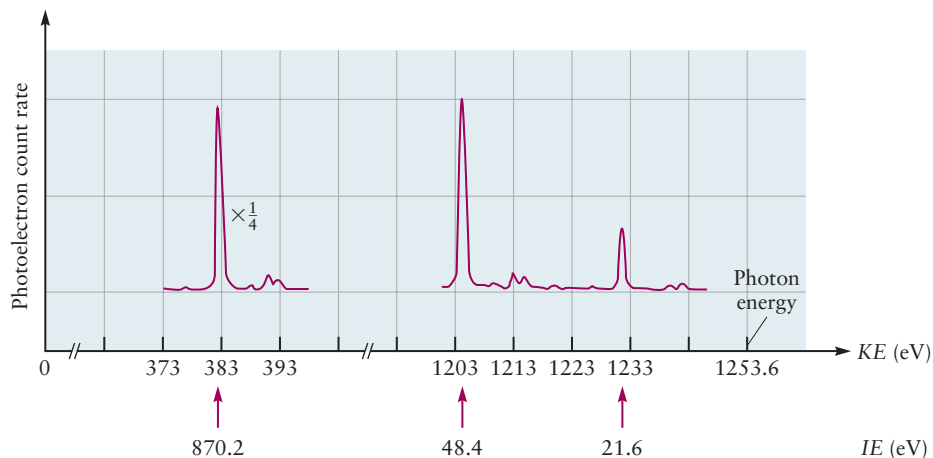


The shell structure is confirmed directly by an important experimental technique called **photoelectron spectroscopy**, or PES. Photoelectron spectroscopy determines the energy level of each orbital by measuring the ionization energy required to remove each electron from the atom. Photoelectron spectroscopy is simply the photoelectric effect of Section 4.4 applied not to metals, but instead to free atoms. If radiation of sufficiently high frequency ν (in the ultraviolet or x-ray region of the spectrum) strikes an atom, an electron will be ejected with kinetic energy $\frac{1}{2}m_e v^2$. The kinetic energy of the ejected electrons is measured by an **energy analyzer**, which records the voltage required to deflect the electrons around a semicircular pathway in vacuum to reach the detector (Fig. 5.18). As the voltage between the hemispherical plates is changed, electrons with different values of kinetic energy will be deflected to the detector, and the spectrum of kinetic energy values can be recorded. Measuring the kinetic energy by deflection is analogous to measuring energy in the photoelectric effect experiments, and the results are conveniently expressed in units of electron volts (eV). Then the ionization energy spectrum, IE , is calculated by the principle of conservation of energy (see Section 4.4),

$$IE = h\nu_{\text{photon}} - \frac{1}{2}m_e v_{\text{electron}}^2 \quad [5.11]$$

Figure 5.19 shows the measured photoelectron spectrum for neon excited by x-rays with wavelength 9.890×10^{-10} m, and Example 5.6 shows how the spectrum is obtained and interpreted. Three peaks appear with kinetic energy values 383.4, 1205.2, and 1232.0 eV. The corresponding ionization energy is shown beneath each peak. (See Example 5.6 for details.) Note that ionization energy increases from right to left in Figure 5.19, opposite to kinetic energy. The peak at

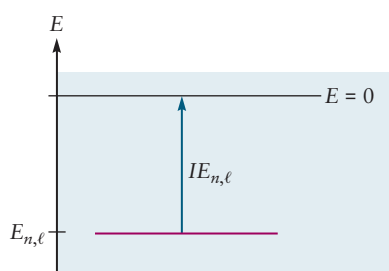
FIGURE 5.19 Photoelectron spectrum of neon. The spectrum shows three peaks, demonstrating that the electrons of neon are organized in three bonding states of distinct energy values. The peak at 383.4 eV has been reduced by a factor of 4 for display on the same scale as the other two.



lowest ionization energy (highest kinetic energy) is produced by the most weakly bound electrons (see Eq. 5.11). This is the minimum amount of energy required to detach an electron from an atom and is the same as the ionization energy IE_1 introduced in Section 3.3. Clearly, there can be no signal in the photoelectron spectrum at ionization energies less than this value. Peaks at higher ionization energies correspond to electrons removed from more strongly bound states. This spectrum demonstrates that the ten electrons of neon are arranged in bonding states that produce three distinct, discrete energy levels.

These results are connected to the shell model by **Koopmans's approximation**, which asserts in a form suitable for our discussion that the ionization energy of an electron is the negative of the energy of the Hartree orbital of the electron:

$$IE_{\alpha} = -\varepsilon_{\alpha} \quad [5.12]$$



The Hartree orbital energies are intrinsically negative because they represent the energy stabilization of an electron bound in an atom relative to the free electron and a positive ion. The ionization energy is positive because it must be supplied to liberate the electron from the atom. Therefore, we should be able to read off the orbital energies directly from the measured spectrum of ionization energies. Koopmans's approximation is not strictly valid because it assumes the orbital energies are the same in the ion as in the parent atom, despite the loss of an electron. This is called the **frozen orbital approximation**. The theorem assumes no energy is lost to *relaxation* of the electronic structure during the ionization process. In fact, relaxation effects are usually no larger than 1 – 3 eV. They can be included with orbital energies calculated by the more advanced Hartree–Fock method. So Koopmans's approximation and PES provide a quantitative test for advanced theoretical models of electronic structure.

These experimental results for neon are consistent with the electron configuration Ne: $1s^2 2s^2 2p^6$ predicted by the aufbau principle. Ionization energies measured in this way are used to construct the energy-level diagram for atoms and to show explicitly the value of the ground-state energy.

EXAMPLE 5.6

Construct the energy-level diagram for neon from the data in Figure 5.19.

SOLUTION

The ionization energy of each level is calculated as $IE = E_{\text{photon}} - \mathcal{T}_{\text{electron}}$. Because the measured kinetic energy values for the photoelectrons are reported in units of electron volts, the most convenient approach is to calculate the photon energy in electron volts and then subtract the kinetic energy values. The energy of the photon is given by

$$E_{\text{photon}} = \frac{hc}{\lambda} = \frac{(6.6261 \times 10^{-34} \text{ J s})(2.9979 \times 10^8 \text{ m s}^{-1})}{(9.890 \times 10^{-10} \text{ m})(1.6022 \times 10^{-19} \text{ J eV}^{-1})} = 1253.6 \text{ eV}$$

The calculated ionization energies for the peaks are summarized as follows:

Kinetic Energy (eV)	Ionization Energy (eV)
383.4	870.2
1205.2	48.4
1232.0	21.6

The energy-level diagram (Fig. 5.20) is drawn by showing the negative of each ionization energy value as the energy of an orbital, in accordance with Equation 5.12 and Koopmans's approximation.

Related Problems: 25, 26, 27, 28, 29, 30

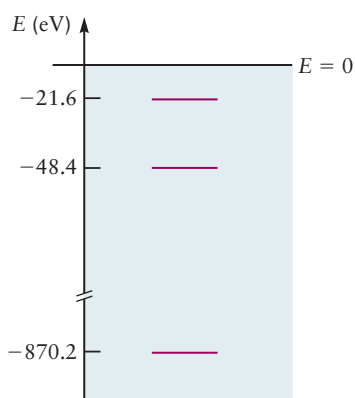


FIGURE 5.20 Energy-level diagram of neon as determined by photoelectron spectroscopy.

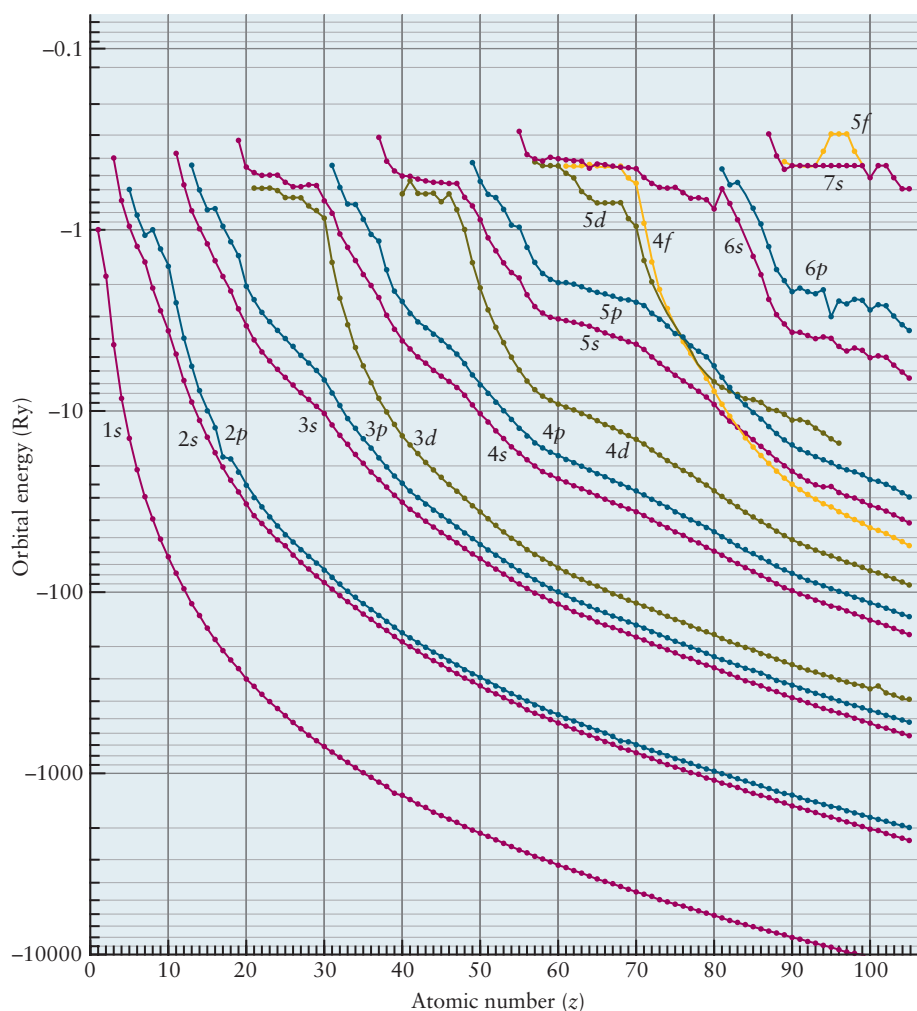


FIGURE 5.21 The energies of different subshells in the first 97 elements, as determined by photoelectron spectroscopy. Negative values on the vertical axis correspond to the bound state orbital energies. Subshells having the same principal quantum number n , such as $2s$ and $2p$, have similar energies and are well separated from orbitals of different n . Significant exceptions do exist, as explained in the text. Note the logarithmic energy scale. One rydberg is 2.18×10^{-18} J.

This method has been used to determine the energy levels for orbitals in most neutral atoms (Fig. 5.21). The energies are reported in units of rydbergs and plotted on a logarithmic scale. These data confirm the existence of subshells, which are grouped into shells having similar energies. However, there are significant exceptions. The $3d$ subshell for elements 21 through 29 (scandium through copper) lies substantially higher than $3s$ and $3p$ and only slightly lower than $4s$. This is consistent with the chemical observation that the $3d$ electrons are valence electrons in these transition metals. As Z goes above 30, the energy of the $3d$ subshell decreases rapidly, so the $3d$ electrons are not valence electrons for zinc and higher elements. The $4d$, $5d$, $4f$, and $5f$ subshells all behave similarly, so electrons in filled d and f subshells are not valence electrons. We can develop an approximate criterion for distinguishing valence and core electrons by examining the noble gases (elements 2, 10, 18, 36, 54, and 86), which participate poorly or not at all in chemical bonding. The highest-energy subshell for each of them lies below -1 rydberg. Therefore, -1 rydberg is a reasonable approximate boundary for the difference between valence and core electrons.

5.5 Periodic Properties and Electronic Structure

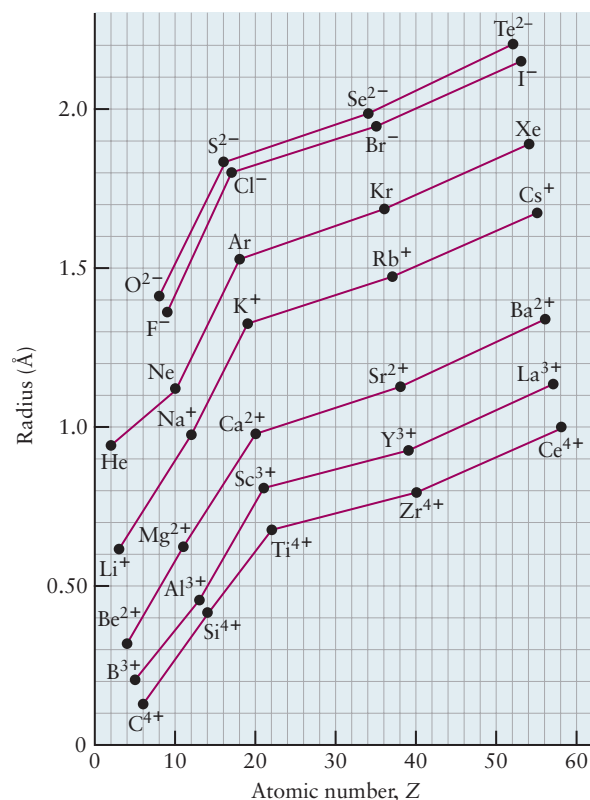
Sizes of Atoms and Ions

The sizes of atoms and ions influence how they interact in chemical compounds. Although atomic radius is not a precisely defined concept, these sizes can be estimated in several ways. If the electron density is known from theory or experiment, a contour surface of fixed electron density can be drawn, as demonstrated in Section 5.1 for one-electron atoms. Alternatively, if the atoms or ions in a crystal are assumed to be in contact with one another, a size can be defined from the measured distances between their centers (this approach is explored in greater detail in Chapter 21). These and other measures of size are reasonably consistent with each other and allow for the tabulation of sets of atomic and ionic radii, many of which are listed in Appendix F.

Certain systematic trends appear in these radii. For a series of elements or ions in the same group (column) of the periodic table, the radius usually increases with increasing atomic number. This occurs mainly because the Pauli exclusion principle effectively excludes added electrons from the region occupied by the core electrons, thus forcing an increase in size as more distant electron shells are occupied. By contrast, Coulomb (electrostatic) forces cause the radii of atoms to *decrease* with increasing atomic number across a period. As the nuclear charge increases steadily, electrons are added to the same valence shell and are ineffective in shielding each other from its attraction. This “incomplete shielding” of the added proton by the added electron as we go from atomic number Z to $Z + 1$ leads to an increase in Z_{eff} across a period.

Superimposed on these broad trends are some subtler effects that have significant consequences in chemistry. One dramatic example is shown in Figure 5.22.

FIGURE 5.22 Ionic and atomic radii plotted versus atomic number. Each line connects a set of atoms or ions that have the same charge; all species have noble-gas configurations.



H 11.4																	He 21.0
Li 13.0	Be 4.85											B 4.39	C 3.42	N 13.5	O 17.4	F 11.2	Ne 13.2
Na 23.8	Mg 14.0											Al 10.0	Si 12.1	P 17.0	S 15.5	Cl 17.4	Ar 22.6
K 45.9	Ca 26.2	Sc 15.0	Ti 10.6	V 8.32	Cr 7.23	Mn 7.35	Fe 7.09	Co 6.67	Ni 6.59	Cu 7.11	Zn 9.16	Ga 11.8	Ge 13.6	As 13.0	Se 16.4	Br 19.8	Kr 28.0
Rb 55.8	Sr 33.9	Y 19.9	Zr 14.0	Nb 10.8	Mo 9.38	Tc 8.63	Ru 8.17	Rh 8.28	Pd 8.56	Ag 10.3	Cd 13.0	In 15.8	Sn 16.3	Sb 18.2	Te 20.5	I 25.7	Xe 35.9
Cs 70.9	Ba 38.2	Lu 17.8	Hf 13.4	Ta 10.9	W 9.47	Re 8.86	Os 8.42	Ir 8.52	Pt 9.09	Au 10.2	Hg 14.1	Tl 17.2	Pb 18.3	Bi 21.3	Po 23.0		Rn 50.5

FIGURE 5.23 The molar volumes (measured in $\text{cm}^3 \text{mol}^{-1}$ of atoms) of some elements in their solid states. Note the large values for the alkali metals.

The radii of several sets of ions and atoms increase with atomic number in a given group (see earlier), but the *rate* of this increase changes considerably when the ions and atoms that contain the same number of electrons as argon are reached (S^{2-} , Cl^- , Ar, K^+ , Ca^{2+} , Sc^{3+} , Ti^{4+}). For example, the change in size from Li^+ to Na^+ to K^+ is substantial, but the subsequent changes, to Rb^+ and Cs^+ , are significantly smaller due to the filling of the *d* orbitals, which begins after K^+ is reached. Because atomic and ionic size decrease from left to right across a series of transition-metal elements (due to the increased effective nuclear charge), the radius of a main-group element is smaller than it would have been had the transition series not intervened. A similar phenomenon, called the **lanthanide contraction**, occurs during the filling of the *4f* orbitals in the lanthanide series. Its effect on the sizes of transition-metal atoms is discussed in Section 8.1.

A different measure of atomic size is the volume occupied by a mole of atoms of the element in the solid phase. Figure 5.23 shows the pronounced periodicity of the molar volume, with maxima occurring for the alkali metals. Two factors affect the experimentally measured molar volume: the “size” of the atoms, and the geometry of the bonding that connects them. The large molar volumes of the alkali metals stem both from the large size of the atoms and the fact that they are organized in a rather open, loosely packed structure in the solid.

EXAMPLE 5.7

Predict which atom or ion in each of the following pairs should be larger: (a) Kr or Rb, (b) Y or Cd, (c) F^- or Br^- .

SOLUTION

- (a) Rb should be larger because it has an extra electron in a *5s* orbital beyond the Kr closed shell.
- (b) Y should be larger because the effective nuclear charge increases through the transition series from Y to Cd.
- (c) Br^- should be larger because the extra outer electrons are excluded from the core.

Related Problems: 31, 32, 33, 34

Periodic Trends in Ionization Energies

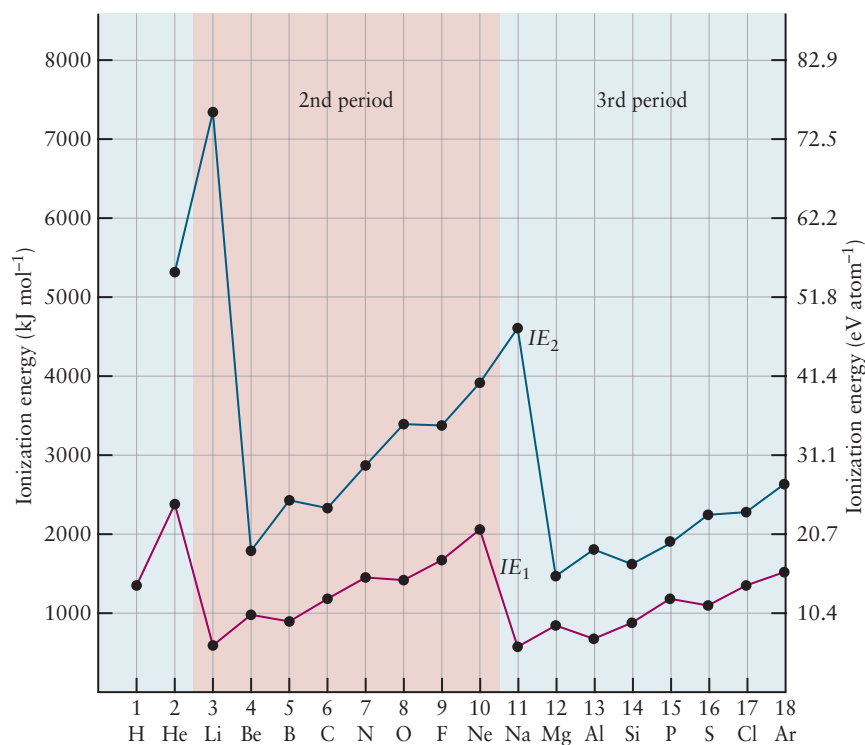
The ionization energy of an atom is defined as the minimum energy necessary to detach an electron from the neutral gaseous atom (see Section 3.3). It can be obtained directly from the photoelectron spectrum of an atomic gas. Appendix F lists measured ionization energies of the elements, and Figure 5.24 shows the periodic trends in first and second ionization energies with increasing atomic number.

Let's use insight from quantum mechanics to examine the periodic trends in the first ionization energy. We obtain deeper understanding of the stabilities of the various electron configurations using this approach than we did in our empirical discovery of shell structure in Section 3.3. There is a large reduction in IE_1 from helium to lithium for two reasons: (1) a $2s$ electron is much farther from the nucleus than a $1s$ electron, and (2) the $1s$ electrons screen the nucleus in lithium so effectively that the $2s$ electron “sees” a net positive charge close to $+1$, rather than the larger charge seen by the electrons in helium. Beryllium shows an increase in IE_1 compared with lithium because the effective nuclear charge has increased, but the electron being removed is still from a $2s$ orbital.

The IE_1 of boron is somewhat less than that of beryllium because the fifth electron is in a higher energy (and therefore less stable) $2p$ orbital. In carbon and nitrogen, the additional electrons go into $2p$ orbitals as the effective nuclear charge increases to hold the outer electrons more tightly; hence, IE_1 increases. The nuclear charge is higher in oxygen than in nitrogen, which would give it a higher ionization energy if this were the only consideration. However, oxygen must accommodate two electrons in the same $2p$ orbital, leading to greater electron–electron repulsion and diminished binding, thus more than compensating for the increased electron–nuclear interaction. Consequently, oxygen has a lower IE_1 than nitrogen. Fluorine and neon have successively higher first ionization energies because of increasing effective nuclear charge. The general trends of increasing ionization energy across a given period, as well as the dips that occur at certain points, can thus be understood through the orbital description of many-electron atoms.

The ionization energy tends to decrease down a group in the periodic table (for example, from lithium to sodium to potassium). As the principal quantum number increases, so does the distance of the outer electrons from the nucleus. There are some exceptions to this trend, however, especially for the heavier

FIGURE 5.24 First and second ionization energies of atoms of the first three periods.



H 73																		He *
Li 60	Be *											B 27	C 122	N *	O 141	F 328		Ne *
Na 53	Mg *											Al 43	Si 134	P 72	S 200	Cl 349		Ar *
K 48	Ca 2	Sc 18	Ti 8	V 51	Cr 64	Mn *	Fe 16	Co 64	Ni 111	Cu 118	Zn *	Ga 29	Ge 116	As 78	Se 195	Br 325		Kr *
Rb 47	Sr 5	Y 30	Zr 41	Nb 86	Mo 72	Tc 53	Ru 99	Rh 110	Pd 52	Ag 126	Cd *	In 29	Sn 116	Sb 103	Te 190	I 295		Xe *
Cs 46	Ba 14	Lu 50	Hf *	Ta 31	W 79	Re 14	Os 106	Ir 151	Pt 214	Au 223	Hg *	Tl 19	Pb 35	Bi 91	Po 183	At 270		Rn *

FIGURE 5.25 Electron affinities (measured in kJ mol^{-1}) of gaseous atoms of the elements. An asterisk means that the element does not have a stable anion in the gas phase.

elements in the middle of the periodic table. For example, the first ionization energy of gold is higher than that of silver or copper. This fact is crucial in making gold a “noble metal”; that is, one that is resistant to attack by oxygen.

Similar trends are observed in the second ionization energies, but they are shifted higher in atomic number by one unit (see Fig. 5.24). Thus, IE_2 is large for lithium (because Li^+ has a filled $1s^2$ shell), but relatively small for beryllium (because Be^+ has a single electron in the outermost $2s$ orbital).

Electron Affinity

The **electron affinity**, EA , of an atom is the energy *released* when an electron is added to it (see Section 3.4). Appendix F lists the electron affinities of the elements.

The periodic trends in electron affinity (Fig. 5.25) parallel those in ionization energy for the most part, except that they are shifted one unit *lower* in atomic number. The reason is clear. Attaching an electron to F gives F^- , with the configuration $1s^2 2s^2 2p^6$, the same as that for neon. Fluorine has a large affinity for electrons because the resulting closed-shell configuration is stable. In contrast, the noble gases do not have well-defined electron affinities because the “extra” electron would reside in a new shell far from the nucleus and be almost totally screened from the nuclear charge.

EXAMPLE 5.8

Consider the elements selenium (Se) and bromine (Br). Which has the higher first ionization energy? Which has the higher electron affinity?

SOLUTION

These two atoms are adjacent to each other in the periodic table. Bromine has one more electron in the $4p$ subshell, and this electron should be more tightly bound than the $4p$ electrons in selenium because of the incomplete shielding and the extra unit of positive charge on the nucleus. Thus, IE_1 should be greater for bromine.

Bromine has a greater electron affinity than selenium. Gaining the extra electron changes the Br atom into Br^- , which has a particularly stable closed-shell electron configuration (the same as that of the noble gas atom krypton [Kr]). No such configuration is created when a Se atom gains an additional electron.

Related Problems: 35, 36, 37, 38

CHAPTER SUMMARY

The planetary model of the atom provides a reliable physical picture of the structure of the atom. This model is based securely on extensive experimental evidence obtained in the period roughly 1890 to 1915, part of an era of great excitement in the development of modern science. Although a great deal of physical insight into the structure and behavior of atoms can be obtained just by analyzing the consequences of the Coulomb force law between the nucleus and the electrons, theoretical explanation of the structure, properties, and behavior of atoms requires quantum mechanics. Quantum mechanics tells us that an atom can have only specific, discrete amounts of energy. Indeed, the very existence of quantum states explains the stability of the atom, which was predicted to collapse according to classical physics. Quantum mechanics also demonstrates that the concept of planetary orbits is simply not applicable on the atomic scale. We cannot know the detailed trajectory of an electron in the intuitive, classical sense familiar to ordinary human perception. Instead, we describe the probability for finding the electron at a particular location in the atom, based on knowing the quantum state of the atom.

For the hydrogen atom, we can solve the Schrödinger equation exactly to obtain the allowed energy levels and the hydrogen atomic orbitals. The sizes and shapes of these orbitals tell us the probability distribution for the electron in each quantum state of the atom. We are led to picture this distribution as a smeared cloud of electron density (probability density) with a shape that is determined by the quantum state.

For all other atoms, we have to generate approximations to solve the Schrödinger equation. The Hartree orbitals describe approximately the amplitude for each electron in the atom, moving under an effective force obtained by averaging over the interactions with all the other electrons. The Hartree orbitals have the same shapes as the hydrogen atomic orbitals—but very different sizes and energy values—and thus guide us to view the probability distribution for each electron as a smeared cloud of electron density.

The Hartree orbitals are the foundation of the quantum explanation of atomic structure. They justify the shell model of the atom, they explain the structure of the periodic table, and they provide the starting point for the quantum explanation of chemical bond formation in the following chapter.

CUMULATIVE EXERCISE

Interstellar Space

The vast stretches of space between the stars are by no means empty. They contain both gases and dust particles at very low concentrations. Interstellar space extends so far that these low-density species significantly affect the electromagnetic radiation arriving from distant stars and other sources, which is detected by telescopes. The gas in interstellar space consists primarily of hydrogen atoms (either neutral or ionized) at a concentration of about one atom per cubic centimeter. The dust (thought to be mostly solid water, methane, or ammonia) is even less concentrated, with typically only a few dust particles (each 10^{-4} to 10^{-5} cm in radius) per cubic kilometer.

- The hydrogen in interstellar space near a star is largely ionized by the high-energy photons from the star. Such regions are called H II regions. Suppose a ground-state hydrogen atom absorbs a photon with a wavelength of 65 nm. Calculate the kinetic energy of the electron ejected. (Note: This is the gas-phase analog of the photoelectric effect for solids.)
- What is the de Broglie wavelength of the electron from part (a)?



J. J. Hester (Arizona State University), and NASA

Clouds of gas surround hot stars in these galactic clusters. The red color arises from hydrogen radiation.

- (c) Free electrons in H II regions can be recaptured by hydrogen nuclei. In such an event, the atom emits a series of photons of increasing energy as the electrons cascade down through the quantum states of the hydrogen atom. The particle densities are so low that extremely high quantum states can be detected in interstellar space. In particular, the transition from the state $n = 110$ to $n = 109$ for the hydrogen atom has been detected. What is the Bohr radius of an electron for hydrogen in the state $n = 110$?
- (d) Calculate the wavelength of light emitted as an electron undergoes a transition from level $n = 110$ to $n = 109$. In what region of the electromagnetic spectrum does this lie?
- (e) H II regions also contain ionized atoms that are heavier than hydrogen. Calculate the longest wavelength of light that will ionize a ground-state helium atom. Use data from Appendix F.
- (f) The regions farther from stars are called H I regions. There, almost all of the hydrogen atoms are neutral rather than ionized and are in the ground state. Will such hydrogen atoms absorb light in the Balmer series emitted by atoms in H II regions?
- (g) We stated in Section 5.1 that the energy of the hydrogen atom depends only on the quantum number n . In fact, this is not quite true. The electron spin (m_s quantum number) couples weakly with the spin of the nucleus, making the ground state split into two states of almost equal energy. The radiation emitted in a transition from the upper to the lower of these levels has a wavelength of 21.2 cm and is of great importance in astronomy because it allows the H I regions to be studied. What is the energy difference between these two levels, both for a single atom and for a mole of atoms?
- (h) The gas and dust particles between a star and the earth scatter the star's light more strongly in the blue region of the spectrum than in the red. As a result, stars appear slightly redder than they actually are. Will an estimate of the temperature of a star based on its apparent color give too high or too low a number?

Answers

- (a) 8.8×10^{-19} J
- (b) $0.52 \text{ nm} = 5.2 \text{ \AA}$
- (c) $6.40 \times 10^{-7} \text{ m} = 6400 \text{ \AA}$
- (d) $5.98 \times 10^{-2} \text{ m} = 5.98 \text{ cm}$, in the microwave region
- (e) 50.4 nm
- (f) No, because the lowest energy absorption for a ground-state hydrogen atom is in the ultraviolet region of the spectrum.
- (g) 9.37×10^{-25} J; 0.564 J mol^{-1}
- (h) Too low, because red corresponds to emitted light of lower energy. Experience with blackbody radiation curves would assign a lower temperature to a star emitting lower energy light.

CHAPTER REVIEW

- The physical structure of the atom, as determined by experiments, is summarized in the planetary model. In an atom with atomic number Z , there are Z electrons moving around a dense nucleus that has positive charge $+Ze$. Coulomb's law describes the forces and potential energy of interaction between each electron and the nucleus and between the electrons in many-electron atoms.

- Quantum mechanics explains the physical stability of the planetary atom, predicts its allowed energy levels, and defines the wave functions (also called atomic orbitals), which determine the probability density for finding the electrons at particular locations in the atom.
- The allowed energy levels for a one-electron atom or ion with atomic number Z are given by the expression $E_n \propto -Z/n^2$, where the quantum number $n = 1, 2, 3, \dots$. These values are negative numbers because they measure the energy of the bound states of the stable atom relative to a separated electron and cation, which is defined to be the zero of the energy scale. The energy of the ground state of the hydrogen atom is -13.6 eV, a number worth remembering.
- The spacing between adjacent energy levels of a one-electron atom becomes narrower as n increases. As $n \rightarrow \infty$, the value of $E_n \rightarrow 0$, which corresponds to a separated electron and cation. Both of these important facts originate in the expression for the energy levels.
- Ionization energy is the amount of energy required to remove an electron from an atom and place it infinitely far away with zero kinetic energy. For any state n of a one-electron atom, the ionization energy IE_n is given by the transition $IE_n = E_\infty - E_n$. Ionization energy is intrinsically positive because the energy of the final state is higher than the energy of the initial state. The ionization energy of the ground state of the hydrogen atom is $+13.6$ eV.
- Because the potential energy in a one-electron atom depends only on r , the wave functions (atomic orbitals) have the product form $\psi_{n\ell m}(r, \theta, \phi) = R_{n\ell}(r)Y_{\ell m}(\theta, \phi)$. The quantum number ℓ describes quantization of the total angular momentum of the electron, and the quantum number m describes quantization of the component of angular momentum along the z -axis. Whereas the quantum number n determines the allowed energy levels, the quantum numbers ℓ and m determine the shapes of the orbitals.
- The Stern–Gerlach experiment demonstrates that the electron has a property called spin, which leads to a magnetic dipole moment. Spin is quantized with only two allowed values described by the quantum number m_s . Complete determination of the quantum state of the electron required values for all four quantum numbers (n, ℓ, m_ℓ, m_s).
- Atoms with many electrons are described by Hartree’s SCF method, in which each electron is assumed to move under the influence of an effective field $V_{\text{eff}}(r)$ due to the average positions of all the other electrons. This method generates a set of one-electron wave functions called the Hartree orbitals $\varphi_\alpha(r)$ with energy values ε_α , where α represents the proper set of quantum numbers. Hartree orbitals bear close relation to the hydrogen atomic orbitals but are not the same objects.
- Energies of the Hartree orbitals are different from those of the corresponding hydrogen atomic orbitals. For an atom with atomic number Z they can be estimated as $\varepsilon_n \propto -Z_{\text{eff}}/n^2$, where the effective nuclear charge experienced by each electron is determined by screening of that electron from the full nuclear charge by other electrons.
- The electron configuration for an atom with atomic number Z is determined by arranging the Hartree orbitals in order of increasing energy, then placing at most two electrons in each orbital in accordance with the Pauli exclusion principle and Hund’s rule until all Z electrons have been placed. The configuration consists of specifying the set of four quantum numbers (n, ℓ, m_ℓ, m_s) for each electron in the atom.
- The Hartree orbitals have the same shapes as the corresponding hydrogen atomic orbitals, but their sizes are quite different.
- The Hartree orbitals and their electron configurations justify the shell model of the atom; that is, the electrons are grouped into shells of 2, 8, or 18 electrons

arranged concentrically around the nucleus at increasing distances from the nucleus. As we move outward from the nucleus, the electrons in each successive shell are bound progressively less strongly to the nucleus. Electrons in the outermost shell, called the valence electrons, are the least strongly bound, and they participate in the formation of chemical bonds.

- The shell model is verified experimentally by the technique of PES, in which ionization energy is measured for electrons in each shell. The results are connected to the shell model by Koopmans's theorem, which asserts that the orbital energy is the negative of the ionization energy.
- The Hartree orbitals and their electron configurations explain the structure of the periodic table.
- The Hartree orbitals and the shell model explain periodic trends in ionization energy, electron affinity, and the radii of atoms and ions. Small changes in these properties within a period are further explained by detailed changes in Z_{eff} within that period.

CONCEPTS & SKILLS

After studying this chapter and working the problems that follow, you should be able to:

1. Give the quantum numbers that characterize one-electron atoms, and discuss the shapes, sizes, and nodal properties of the corresponding orbitals (Section 5.1, Problems 1–6).
2. Prepare an approximate energy-level diagram for an atom using values for Z_{eff} (Section 5.2, Problems 9–14).
3. Use the aufbau principle to predict electron configurations of atoms and ions and to account for the structure of the periodic table (Section 5.3, Problems 15–24).
4. Construct the energy-level diagram for an atom using PES for orbital energies (Section 5.4, Problems 25–30).
5. Discuss the factors that lead to systematic variation of sizes of atoms and ions through the periodic table (Section 5.5, Problems 31–34).
6. Describe the trends in ionization energy and electron affinity across the periodic table and relate them to the electronic structure of atoms (Section 5.5, Problems 35–40).

KEY EQUATIONS

$$E = E_n = -\frac{Z^2 e^4 m_e}{8\epsilon_0^2 n^2 h^2} \quad n = 1, 2, 3, \dots \quad (\text{Section 5.1})$$

$$E_n = -\frac{Z^2}{n^2} \quad (\text{rydberg}) \quad n = 1, 2, 3, \dots \quad (\text{Section 5.1})$$

$$L^2 = \ell(\ell + 1) \frac{h^2}{4\pi^2} \quad \ell = 0, 1, \dots, n - 1 \quad (\text{Section 5.1})$$

$$L_z = m \frac{h}{2\pi} \quad m = -\ell, -\ell + 1, \dots, 0, \dots, \ell - 1, \ell \quad (\text{Section 5.1})$$

$$\psi_{n\ell m}(r, \theta, \phi) = R_{n\ell}(r)Y_{\ell m}(\theta, \phi) \quad (\text{Section 5.1})$$

$$(\psi_{n\ell m})^2 dV = [R_{n\ell}(r)]^2 [Y_{\ell m}(\theta, \phi)]^2 dV \quad (\text{Section 5.1})$$

$$dV = r^2 \sin \theta dr d\theta d\phi \quad (\text{Section 5.1})$$

$$\bar{r}_{n\ell} = \frac{n^2 a_0}{Z} \left\{ 1 + \frac{1}{2} \left[1 - \frac{\ell(\ell+1)}{n^2} \right] \right\} \quad (\text{Section 5.1})$$

$$V_n^{\text{eff}}(r) = -\frac{Z_{\text{eff}}(n)e^2}{r} \quad (\text{Section 5.2})$$

$$\varepsilon_n \approx -\frac{[Z_{\text{eff}}(n)]^2}{n^2} \quad (\text{rydbergs}) \quad (\text{Section 5.2})$$

$$\bar{r}_{n\ell} \approx \frac{n^2 a_0}{Z_{\text{eff}}(n)} \left\{ 1 + \frac{1}{2} \left[1 - \frac{\ell(\ell+1)}{n^2} \right] \right\} \quad (\text{Section 5.2})$$

$$IE = h\nu_{\text{photon}} - \frac{1}{2}m_e v_{\text{electron}}^2 \quad (\text{Section 5.4})$$

$$IE_{\alpha} = -\varepsilon_{\alpha} \quad (\text{Section 5.4})$$

PROBLEMS

Answers to problems whose numbers are boldface appear in Appendix G. Problems that are more challenging are indicated with asterisks.

The Hydrogen Atom

- Which of the following combinations of quantum numbers are allowed for an electron in a one-electron atom? Which are not?
 - $n = 2, \ell = 2, m = 1, m_s = \frac{1}{2}$
 - $n = 3, \ell = 1, m = 0, m_s = -\frac{1}{2}$
 - $n = 5, \ell = 1, m = 2, m_s = \frac{1}{2}$
 - $n = 4, \ell = -1, m = 0, m_s = \frac{1}{2}$
- Which of the following combinations of quantum numbers are allowed for an electron in a one-electron atom? Which are not?
 - $n = 3, \ell = 2, m = 1, m_s = 0$
 - $n = 2, \ell = 0, m = 0, m_s = -\frac{1}{2}$
 - $n = 7, \ell = 2, m = -2, m_s = \frac{1}{2}$
 - $n = 3, \ell = -3, m_s = -\frac{1}{2}$
- Label the orbitals described by each of the following sets of quantum numbers:
 - $n = 4, \ell = 1$
 - $n = 2, \ell = 0$
 - $n = 6, \ell = 3$
- Label the orbitals described by each of the following sets of quantum numbers:
 - $n = 3, \ell = 2$
 - $n = 7, \ell = 4$
 - $n = 5, \ell = 1$
- How many radial nodes and how many angular nodes does each of the orbitals in Problem 3 have?
- How many radial nodes and how many angular nodes does each of the orbitals in Problem 4 have?
- Use the mathematical expression for the $2p_z$ wave function of a one-electron atom (see Table 5.2) to show that the probability of finding an electron in that orbital anywhere in the x - y plane is 0. What are the nodal planes for a d_{xz} orbital and for a $d_{x^2-y^2}$ orbital?

- Use the radial wave function for the $3p$ orbital of a hydrogen atom (see Table 5.2) to calculate the value of r for which a node exists.
- Find the values of r for which nodes exist for the $3s$ wave function of the hydrogen atom.

Shell Model for Many-Electron Atoms

- Calculate the average distance of the electron from the nucleus in a hydrogen atom when the electron is in the $2s$ orbital. Repeat the calculation for an electron in the $2p$ orbital.
- The helium ion He^+ is a one-electron system whose wave functions and energy levels are obtained from those for H by changing the atomic number to $Z = 2$. Calculate the average distance of the electron from the nucleus in the $2s$ orbital and in the $2p$ orbital. Compare your results with those in Problem 9 and explain the difference.
- Spectroscopic studies show that Li can have electrons in its $1s$, $2s$, and $2p$ Hartree orbitals, and that $Z_{\text{eff}}(2s) = 1.26$. Estimate the energy of the $2s$ orbital of Li. Calculate the average distance of the electron from the nucleus in the $2s$ orbital of Li.
- Spectroscopic studies of Li also show that $Z_{\text{eff}}(2p) = 1.02$. Estimate the energy of the $2p$ orbital of Li. Calculate the average distance of the electron from the nucleus in the $2p$ orbital of Li. Comparing your results with those in Problem 11 shows that the energy values differ by about 50%, whereas the average distances are nearly equal. Explain this observation.
- Spectroscopic studies show that Na can have electrons in its $1s$, $2s$, $2p$, and $3s$ Hartree orbitals, and that $Z_{\text{eff}}(3s) = 1.84$. Using data from Problem 11, compare the energies of the Na $3s$ orbital, the Li $2s$ orbital, and the H $1s$ orbital.
- Using data from Problems 11 and 13, calculate the average distance of the electron from the nucleus in the Na $3s$ orbital, the Li $2s$ orbital, and the H $1s$ orbital. Explain the trend in your results.

Aufbau Principle and Electron Configurations

15. Give the ground-state electron configurations of the following elements:

- (a) C (b) Se (c) Fe

16. Give the ground-state electron configurations of the following elements:

- (a) P (b) Tc (c) Ho

17. Write ground-state electron configurations for the ions Be^+ , C^- , Ne^{2+} , Mg^+ , P^{2+} , Cl^- , As^+ , and I^- . Which do you expect will be paramagnetic due to the presence of unpaired electrons?

18. Write ground-state electron configurations for the ions Li^- , B^+ , F^- , Al^{3+} , S^- , Ar^+ , Br^+ , and Te^- . Which do you expect to be paramagnetic due to the presence of unpaired electrons?

19. Identify the atom or ion corresponding to each of the following descriptions:

- (a) an atom with ground-state electron configuration $[\text{Kr}]4d^{10}5s^25p^1$
 (b) an ion with charge -2 and ground-state electron configuration $[\text{Ne}]3s^23p^6$
 (c) an ion with charge $+4$ and ground-state electron configuration $[\text{Ar}]3d^3$

20. Identify the atom or ion corresponding to each of the following descriptions:

- (a) an atom with ground-state electron configuration $[\text{Xe}]4f^{14}5d^66s^2$
 (b) an ion with charge -1 and ground-state electron configuration $[\text{He}]2s^22p^6$
 (c) an ion with charge $+5$ and ground-state electron configuration $[\text{Kr}]4d^6$

21. Predict the atomic number of the (as yet undiscovered) element in the seventh period that is a halogen.

22. (a) Predict the atomic number of the (as yet undiscovered) alkali-metal element in the eighth period.

- (b) Suppose the eighth-period alkali-metal atom turned out to have atomic number 137. What explanation would you give for such a high atomic number (recall that the atomic number of francium is only 87)?

23. Suppose that the spin quantum number did not exist, and therefore only one electron could occupy each orbital of a many-electron atom. Give the atomic numbers of the first three noble-gas atoms in this case.

24. Suppose that the spin quantum number had three allowed values ($m_s = 0, +\frac{1}{2}, -\frac{1}{2}$). Give the atomic numbers of the first three noble-gas atoms in this case.

Shells and the Periodic Table:**Photoelectron Spectroscopy**

25. Photoelectron spectra of mercury (Hg) atoms acquired with radiation from a helium lamp at 584.4 \AA show a peak in which the photoelectrons have kinetic energy of 11.7 eV . Calculate the ionization energy of electrons in that level.

26. Quantum mechanics predicts that the energy of the ground state of the H atom is -13.6 eV . Insight into the magnitude of this quantity is gained by considering several methods by which it can be measured.

(a) Calculate the longest wavelength of light that will ionize H atoms in their ground state.

(b) Assume the atom is ionized by collision with an electron that transfers all its kinetic energy to the atom in the ionization process. Calculate the speed of the electron before the collision. Express your answer in meters per second (m s^{-1}) and miles per hour (miles h^{-1}).

(c) Calculate the temperature required to ionize a H atom in its ground state by thermal excitation. (*Hint:* Recall the criterion for thermal excitation of an oscillator in Planck's theory of blackbody radiation is that $h\nu \approx k_B T$.)

27. Photoelectron spectroscopy studies of sodium atoms excited by x-rays with wavelength $9.890 \times 10^{-10} \text{ m}$ show four peaks in which the electrons have speeds $4.956 \times 10^6 \text{ m s}^{-1}$, $1.277 \times 10^7 \text{ m s}^{-1}$, $1.294 \times 10^7 \text{ m s}^{-1}$, and $1.310 \times 10^7 \text{ m s}^{-1}$. (Recall that $1 \text{ J} = 1 \text{ kg m}^2 \text{ s}^{-2}$.)

(a) Calculate the ionization energy of the electrons in each peak.

(b) Assign each peak to an orbital of the sodium atom.

28. Photoelectron spectroscopy studies of silicon atoms excited by X-rays with wavelength $9.890 \times 10^{-10} \text{ m}$ show four peaks in which the electrons have speeds $1.230 \times 10^7 \text{ m s}^{-1}$, $1.258 \times 10^7 \text{ m s}^{-1}$, $1.306 \times 10^7 \text{ m s}^{-1}$, and $1.308 \times 10^7 \text{ m s}^{-1}$. (Recall that $1 \text{ J} = 1 \text{ kg m}^2 \text{ s}^{-2}$.)

(a) Calculate the ionization energy of the electrons in each peak.

(b) Assign each peak to an orbital of the silicon atom.

29. Photoelectron spectroscopy studies have determined the orbital energies for fluorine atoms to be

1s	-689 eV
2s	-34 eV
2p	-12 eV

Estimate the value of Z_{eff} for F in each of these orbitals.

30. Photoelectron spectroscopy studies have determined the orbital energies for chlorine atoms to be

1s	-2,835 eV
2s	-273 eV
2p	-205 eV
s	-21 eV
3p	-10 eV

Estimate the value of Z_{eff} for Cl in each of these orbitals.

Periodic Properties and Electronic Structure

31. For each of the following pairs of atoms or ions, state which you expect to have the larger radius.

- (a) Na or K (b) Cs or Cs^+
 (c) Rb^+ or Kr (d) K or Ca
 (e) Cl^- or Ar

32. For each of the following pairs of atoms or ions, state which you expect to have the larger radius.

- (a) Sm or Sm^{3+} (b) Mg or Ca
 (c) I^- or Xe (d) Ge or As
 (e) Sr^+ or Rb

33. Predict the larger ion in each of the following pairs. Give reasons for your answers.

- (a) O^- , S^{2-} (b) Co^{2+} , Ti^{2+}
 (c) Mn^{2+} , Mn^{4+} (d) Ca^{2+} , Sr^{2+}

34. Predict the larger ion in each of the following pairs. Give reasons for your answers.
- (a) S^{2-} , Cl^- (b) Tl^+ , Tl^{3+}
 (c) Ce^{3+} , Dy^{3+} (d) S^- , I^-
35. The first ionization energy of helium is 2370 kJ mol^{-1} , the highest for any element.
- (a) Define *ionization energy* and discuss why for helium it should be so high.
 (b) Which element would you expect to have the highest *second* ionization energy? Why?
 (c) Suppose that you wished to ionize some helium by shining electromagnetic radiation on it. What is the maximum wavelength you could use?
36. The energy needed to remove one electron from a gaseous potassium atom is only about two-thirds as much as that needed to remove one electron from a gaseous calcium atom, yet nearly three times as much energy as that needed to remove one electron from K^+ as from Ca^+ . What explanation can you give for this contrast? What do you expect to be the relation between the ionization energy of Ca^+ and that of neutral K?
37. Without consulting any tables, arrange the following substances in order and explain your choice of order:
- (a) Mg^{2+} , Ar, Br^- , Ca^{2+} in order of increasing radius
 (b) Na, Na^+ , O, Ne in order of increasing ionization energy
 (c) H, F, Al, O in order of increasing electronegativity
38. Both the electron affinity and the ionization energy of chlorine are higher than the corresponding quantities for sulfur. Explain why in terms of the electronic structure of the atoms.
39. The cesium atom has the lowest ionization energy, $375.7 \text{ kJ mol}^{-1}$, of all the neutral atoms in the periodic table. What is the longest wavelength of light that could ionize a cesium atom? In which region of the electromagnetic spectrum does this light fall?
40. Until recently, it was thought that Ca^- was unstable, and that the Ca atom therefore had a negative electron affinity. Some new experiments have now measured an electron affinity of $+2.0 \text{ kJ mol}^{-1}$ for calcium. What is the longest wavelength of light that could remove an electron from Ca^- ? In which region of the electromagnetic spectrum does this light fall?

ADDITIONAL PROBLEMS

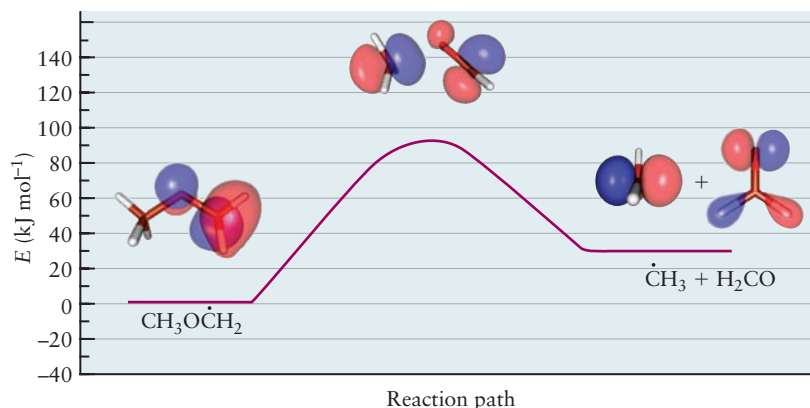
41. In the hydrogen atom, the transition from the $2p$ state to the $1s$ state emits a photon with energy $16.2 \times 10^{-19} \text{ J}$. In an iron atom, the same transition emits x-rays with wavelength 0.193 nm . Calculate the energy difference between these two states in iron. Explain the difference in the $2p$ - $1s$ energy level spacing in these two atoms.
42. The energy needed to ionize an atom of element X when it is in its most stable state is 500 kJ mol^{-1} . However, if an atom of X is in its lowest excited state, only 120 kJ mol^{-1} is needed to ionize it. What is the wavelength of the radiation emitted when an atom of X undergoes a transition from the lowest excited state to the ground state?
43. Suppose an atom in an excited state can return to the ground state in two steps. It first falls to an intermediate state, emitting radiation of wavelength λ_1 , and then to the ground state, emitting radiation of wavelength λ_2 . The same atom can also return to the ground state in one step, with the emission of radiation of wavelength λ . How are λ_1 , λ_2 , and λ related? How are the frequencies of the three radiations related?
44. For the Li atom, the energy difference between the ground state and the first excited state, in which the outermost electron is in a $2p$ orbital, is $2.96 \times 10^{-19} \text{ J}$. In the Li^{2+} ion, the energy difference between the $2s$ and $2p$ levels is less than 0.00002 of this value. Explain this observation.
45. How does the $3d_{xy}$ orbital of an electron in O^{7+} resemble the $3d_{xy}$ orbital of an electron in a hydrogen atom? How does it differ?
- * 46. The wave function of an electron in the lowest (that is, ground) state of the hydrogen atom is
- $$\psi(r) = \left(\frac{1}{\pi a_0^3}\right)^{1/2} \exp\left(-\frac{r}{a_0}\right)$$
- $$a_0 = 0.529 \times 10^{-10} \text{ m}$$
- (a) What is the probability of finding the electron inside a sphere of volume 1.0 pm^3 , centered at the nucleus ($1 \text{ pm} = 10^{-12} \text{ m}$)?
 (b) What is the probability of finding the electron in a volume of 1.0 pm^3 at a distance of 52.9 pm from the nucleus, in a fixed but arbitrary direction?
 (c) What is the probability of finding the electron in a spherical shell of 1.0 pm in thickness, at a distance of 52.9 pm from the nucleus?
47. An atom of sodium has the electron configuration $[Ne]6s^1$. Explain how this is possible.
48. (a) The nitrogen atom has one electron in each of the $2p_x$, $2p_y$, and $2p_z$ orbitals. By using the form of the angular wave functions, show that the total electron density, $\psi^2(2p_x) + \psi^2(2p_y) + \psi^2(2p_z)$, is spherically symmetric (that is, it is independent of the angles θ and ϕ). The neon atom, which has *two* electrons in each $2p$ orbital, is also spherically symmetric.
 (b) The same result as in part (a) applies to d orbitals, thus a filled or half-filled subshell of d orbitals is spherically symmetric. Identify the spherically symmetric atoms or ions among the following: F^- , Na, Si, S^{2-} , Ar^+ , Ni, Cu, Mo, Rh, Sb, W, Au.
49. Chromium(IV) oxide is used in making magnetic recording tapes because it is paramagnetic. It can be described as a solid made up of Cr^{4+} and O^{2-} . Give the electron configuration of Cr^{4+} in CrO_2 , and determine the number of unpaired electrons on each chromium ion.
50. Use the data from Appendix F to graph the variation of atomic radius with atomic number for the rare-earth elements from lanthanum to lutetium.
- (a) What is the general trend in these radii? How do you account for it?
 (b) Which two elements in the series present exceptions to the trend?
51. Arrange the following seven atoms or ions in order of size, from smallest to largest: K, F^+ , Rb, Co^{25+} , Br, F, Rb^- .
52. Which is higher, the third ionization energy of lithium or the energy required to eject a $1s$ electron from a Li atom in a PES experiment? Explain.

53. The outermost electron in an alkali-metal atom is sometimes described as resembling an electron in the corresponding state of a one-electron atom. Compare the first ionization energy of lithium with the binding energy of a $2s$ electron in a one-electron atom that has nuclear charge Z_{eff} , and determine the value of Z_{eff} that is necessary for the two energies to agree. Repeat the calculation for the $3s$ electron of sodium and the $4s$ electron of potassium.
- * 54. In two-photon ionization spectroscopy, the combined energies carried by two different photons are used to remove an electron from an atom or molecule. In such an experiment, a K atom in the gas phase is to be ionized by two different light beams, one of which has a 650-nm wavelength. What is the maximum wavelength for the second beam that will cause two-photon ionization?
55. For the H atom, the transition from the $2p$ state to the $1s$ state is accompanied by the emission of a photon with an energy of 16.2×10^{-19} J. For an Fe atom, the same transition ($2p$ to $1s$) is accompanied by the emission of x-rays of 193-nm wavelengths. What is the energy difference between these states in iron? Comment on the reason for the variation (if any) in the $2p$ - $1s$ energy-level spacing for these two atoms.
56. (a) Give the complete electron configuration ($1s^2 2s^2 2p \dots$) of aluminum in the ground state.
(b) The wavelength of the radiation emitted when the outermost electron of aluminum falls from the $4s$ state to the ground state is about 395 nm. Calculate the energy separation (in joules) between these two states in the Al atom.
(c) When the outermost electron in aluminum falls from the $3d$ state to the ground state, the radiation emitted has a wavelength of about 310 nm. Draw an energy-level diagram of the states and transitions discussed here and in (b). Calculate the separation (in joules) between the $3d$ and $4s$ states in aluminum. Indicate clearly which has higher energy.
57. What experimental evidence does the periodic table provide that an electron in a $5s$ orbital is slightly more stable than an electron in a $4d$ orbital for the elements with 37 and 38 electrons?

This page intentionally left blank

Quantum Mechanics and Molecular Structure

- 6.1 Quantum Picture of the Chemical Bond
 - 6.1.1 The Simplest Molecule: H_2^+
 - 6.1.2 Born–Oppenheimer Approximation
 - 6.1.3 Electronic Wave Functions for H_2^+
 - 6.1.4 Electron Density in H_2^+
 - 6.1.5 Summary: Key Features of the Quantum Picture of Chemical Bonding
 - 6.1.6 **A DEEPER LOOK** *Nature of the Chemical Bond in H_2^+*
- 6.2 De-localized Bonds: Molecular Orbital Theory and the LCAO Approximation
 - 6.2.1 *Linear Combination of Atomic Orbitals Approximation for H_2^+*
 - 6.2.2 *Homonuclear Diatomic Molecules: First-Period Atoms*
 - 6.2.3 *Homonuclear Diatomic Molecules: Second-Period Atoms*
 - 6.2.4 *Heteronuclear Diatomic Molecules*
 - 6.2.5 **A DEEPER LOOK** *Potential Energy and Bond Formation in the LCAO Approximation*
 - 6.2.6 **A DEEPER LOOK** *Small Polyatomic Molecules*
- 6.3 Photoelectron Spectroscopy for Molecules
- 6.4 Localized Bonds: The Valence Bond Model
 - 6.4.1 *Wave Function for Electron-Pair Bonds*
 - 6.4.2 *Orbital Hybridization for Polyatomic Molecules*
- 6.5 Comparison of LCAO and Valence Bond Methods



Potential energy diagram for the decomposition of the methoxymethyl radical, an important intermediate in the combustion of diethyl ether. Highly accurate computational quantum chemistry methods were used to calculate the configurations and the relative energies of the species shown.

Quantum mechanics embraces the experimental fact that matter and energy have a dual nature—part particle and part wave—and from this notion it correctly predicts the sizes, energy levels, and spectra of atoms and ions. This is a substantial achievement. But if quantum mechanics could do no more, the subject would hold little interest for chemists. Chemists seek to understand the atomic interactions that form molecules and extended solid structures, to understand intermolecular interactions, and most importantly, to understand chemical reactivity. Quantum mechanics provides a firm conceptual foundation on which an understanding of all of these phenomena can be built.

The concept of the chemical bond as an agent for holding atoms together in molecules—analogue to the connections between planets in our solar system—was formulated around the middle of the 19th century. In the 1860s, the chemists August Wilhelm Hofmann and Edward Frankland used three-dimensional arrays of colored wooden balls as models for molecular structure in their lectures in Berlin and London. In 1875, the Dutch chemist Jacobus van't Hoff popularized

these developments in a book entitled *Chemistry in Space*, and by 1885, the three-dimensional representation of molecules was universally accepted.

Even today, chemists continue to use “ball-and-stick models,” in which the balls represent atomic nuclei and the sticks represent chemical bonds, to help them think about the structures of molecules (see Fig. 3.17). After J. J. Thomson discovered the electron in 1897, and especially after Ernest Rutherford formulated the planetary model of the atom in 1912, physicists and chemists sought to explain the chemical bond as arrangements of the electrons around the nuclei. For example, G. N. Lewis considered the electrons to be “localized” in pairs to form covalent bonds between the nuclei. Nonetheless, electrons do not appear in the ball-and-stick figures, and they are not explicitly included in the description of molecular structure. The electrons function as the “glue” that holds the molecule together in a structure defined by a particular set of bond lengths and bond angles. How the electrons glue the molecule together can only be explained by using quantum mechanics (see Section 6.2).

How can we reconcile the traditional (and widely used to this day) picture of chemical bonding with the quantum description of atomic structure (see Chapter 5)? We could, in principle, proceed just like we did with the hydrogen (H) atom (see Section 5.1); that is, set up the Schrödinger equation for a molecule and solve it to find molecular wave functions, energy levels, and electron probability densities. If we could perform such a calculation, we would know all that it is possible to know about the molecule: its bond length, dissociation energy, dipole moment, and the energies of all of its excited states, among other characteristics. Unfortunately, this problem is even more difficult than the many-electron atom. Electron–electron repulsion forces must be considered. Worse yet, the solutions would depend on the many nuclear coordinates needed to describe the positions of even small molecules. Progress requires not only approximations but also new insights.

Fortunately, modern quantum chemistry provides good approximate solutions to the Schrödinger equation and also, perhaps more importantly, new qualitative concepts that we can use to represent and understand chemical bonds, molecular structure, and chemical reactivity. The quantum description of the chemical bond is a dramatic advance over the electron dot model, and it forms the basis for all modern studies in structural chemistry.

This chapter begins with a description of the quantum picture of the chemical bond for the simplest possible molecule, H_2^+ , which contains only one electron. The Schrödinger equation for H_2^+ can be solved exactly, and we use its solutions to illustrate the general features of **molecular orbitals (MOs)**, the one-electron wave functions that describe the electronic structure of molecules. Recall that we used the atomic orbitals (AOs) of the hydrogen atom to suggest approximate AOs for complex atoms. Similarly, we let the MOs for H_2^+ guide us to develop approximations for the MOs of more complex molecules.

Two powerful ways exist to construct approximate wave functions from AOs: the **linear combination of atomic orbitals (LCAO)** method and the **valence bond (VB)** method. The LCAO method generates MOs that are *de-localized* over the entire molecule and builds up the electronic configurations of molecules using an aufbau principle just like the one for atoms. In contrast, the VB method describes electron pairs that are *localized* between a pair of atoms, and it provides a quantum mechanical foundation for the valence shell electron-pair repulsion (VSEPR) theory. We apply both these methods to describe structure and bonding in a variety of molecules. We conclude the chapter by comparing the LCAO and VB methods and showing how each is the starting point for developing modern methods for computational quantum chemistry. These are now sufficiently accurate and so easy to use that they are becoming part of every chemist’s set of tools for both research and education.

The central conceptual goal of this chapter is for you to understand how the wave functions of electrons initially localized on different atoms begin to interact

with one another and form new wave functions that represent chemical bonds in molecules.

6.1 Quantum Picture of the Chemical Bond

The hydrogen molecular ion contains a single electron bound to two protons. It is a stable but highly reactive species produced by electrical discharge in H_2 gas. Its bond length is 1.060 Å, and its bond dissociation energy to produce H and H^+ is 2.791 eV. The similarity of these values to those for more familiar molecules (see Chapter 3) suggests that the exact quantum solutions for H_2^+ will provide insights into chemical bonding that can be transferred to more complex molecules. The solutions for H_2^+ introduce essential notation and terminology to guide our approximations for more complex molecules. Therefore, it is important to achieve a good understanding of H_2^+ as the foundation for the quantum explanation of chemical bonding.

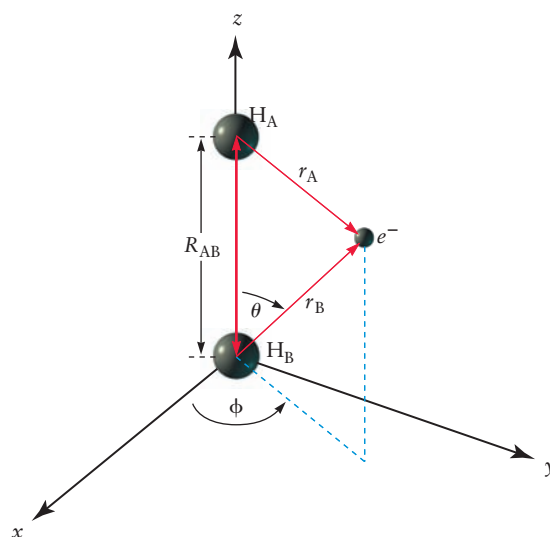
6.1.1 The Simplest Molecule: H_2^+

The hydrogen molecular ion is sketched in Figure 6.1. The two nuclei, for convenience labeled A and B, are separated by the distance R_{AB} along the internuclear axis, chosen by convention to be the z -axis. The electron is located at distance r_A from nucleus A and at distance r_B from nucleus B. The angle ϕ describes rotation about the internuclear axis. For a fixed value of R_{AB} , the position of the electron is more conveniently specified by the values of (r_A, r_B, ϕ) than by (x, y, z) because the former set reflects the natural symmetry of the system. The internal potential energy is given by

$$V = -\frac{e^2}{4\pi\epsilon_0} \left(\frac{1}{r_A} + \frac{1}{r_B} \right) + \frac{e^2}{4\pi\epsilon_0} \left(\frac{1}{R_{AB}} \right) = V_{en} + V_{nn} \quad [6.1]$$

The first two terms in Equation 6.1 represent the attractions between the electron and the two nuclei, and the last term represents the repulsion between the pair of protons. We can write the Schrödinger equation for this system, and we expect a solution of the form $\psi_{\text{mol}}(R_{AB}, r_A, r_B, \phi)$, because the potential energy is a function of all four of these coordinates.

FIGURE 6.1 Coordinates for the H_2^+ molecular ion. The two nuclei are located along the z -axis, separated by the distance R_{AB} . The coordinates r_A and r_B are the distances of the electron from nuclei A and B, respectively; r_A and r_B range from 0 to ∞ . The angle θ is determined from r_A , r_B , and R_{AB} by the law of cosines; it does not appear explicitly in the calculation. The angle ϕ varies from 0 to 2π .



The quantum treatment of this molecule appears to be a straightforward extension of that for the hydrogen atom (see Section 5.1 for the solutions). One more proton has been added, and symmetry of the system has changed from spherical to cylindrical. But this apparently small change has converted the system into the so-called three-body problem, for which there is no general solution, even in classical physics. Fortunately, there is an excellent approximation that treats the nuclear and electronic motions almost as if they were independent. This method allows us to solve the Schrödinger equation exactly for the electron in H_2^+ and provides an approximate solution for the protons as if they were almost independent.

6.1.2 Born–Oppenheimer Approximation

The **Born–Oppenheimer approximation** was developed in 1927 by the physicists Max Born (German) and J. Robert Oppenheimer (American), just one year after Schrödinger presented his quantum treatment of the hydrogen atom. This approximation method is the foundation for all of molecular quantum mechanics, so you should become familiar with it. The basic idea of the Born–Oppenheimer approximation is simple: because the nuclei are so much more massive than the electrons, they can be considered fixed for many periods of electronic motion. Let’s see if this is a reasonable approximation. Using H_2 as a specific example, we estimate the velocity of the electrons to be roughly the same as that of an electron in the ground state ($n = 1$) of the hydrogen atom. From the Bohr formula, $v = e^2/2\epsilon_0 h$, we calculate an electron velocity of $2.2 \times 10^6 \text{ m sec}^{-1}$. We can calculate a typical nuclear velocity from the vibrational spectrum of H_2 (see Section 4.7); the result is $1 \times 10^4 \text{ m sec}^{-1}$. The electrons do indeed move much more rapidly than the nuclei, even for the lightest diatomic molecule, H_2 . So, it is quite reasonable to think of the nuclei as fixed in space for many periods of electronic motion. We simply fix the nuclei in space, solve the Schrödinger equation for the electron with the nuclei fixed at that position, then move the nuclei a bit, and repeat the calculation until we have covered all reasonable values of the nuclear positions. This series of calculations gives $\psi_{\text{el}}(r_A, r_B, \phi; R_{\text{AB}})$, the *electronic wave function* for the electrons around the fixed nuclei. The semicolon inside the parentheses indicates that the nuclear coordinates are held fixed as a *parameter*, whereas the electronic coordinates range over all values as we seek the solution for ψ_{el} . Subsequently, we put in corrections to account for the sluggish motion of the nuclei by solving for the *nuclear wave function*, $\psi_{\text{nuc}}(R_{\text{AB}})$. By solving the electronic and nuclear motions separately, the Born–Oppenheimer approximation obtains the molecular wave function for H_2^+ in the form

$$\psi_{\text{mol}}(R_{\text{AB}}, r_A, r_B, \phi) \approx \psi_{\text{el}}(r_A, r_B, \phi; R_{\text{AB}}) \times \psi_{\text{nuc}}(R_{\text{AB}}) \quad [6.2]$$

The electronic wave function ψ_{el} lies at the heart of chemical bonding because its square gives the probability density for locating the electrons at particular positions around the fixed nuclei. (Probability density is the probability per unit volume. See the discussion preceding Eq. 4.30.) Thus, we concentrate here on obtaining ψ_{el} and later will describe motion of the nuclei using ψ_{nuc} .

To obtain the specific form of ψ_{el} for H_2^+ , we solve the Schrödinger equation for the electron by the same methods we applied to the hydrogen atom in Section 5.1. We enforce general mathematical conditions to ensure we obtain a legitimate wave function. (The solution must be smooth, single-valued, and finite in value in all regions of space.) We also enforce general boundary conditions to guarantee that our solution describes a bound state of the electron (ψ_{el} must approach 0 as $r_A \rightarrow \infty$ and as $r_B \rightarrow \infty$). We find that solutions exist only when the total energy and the component of angular momentum along the internuclear

axis are quantized. The complete set of quantum numbers is more extensive than those for the hydrogen atom. In particular, the allowed energy values for the electron cannot be represented by simple, discrete diagrams as we obtained for atoms in Chapter 5. Rather, we generate an explicit mathematical relation between each allowed value $E_n^{(el)}$ of the electronic energy and the values of R_{AB} . This family of curves shows how the allowed energy values for the electron depend on the internuclear separation for each quantum state. We focus first on describing the electronic wave functions at a fixed internuclear separation, R_{AB} . We then discuss how the energy of the system changes as a function of the internuclear distance.

6.1.3 Electronic Wave Functions for H_2^+

We emphasize that the solutions for ψ_{el} are mathematically exact. Because of their ellipsoidal symmetry, they cannot be written as simple exponential and polynomial functions that are easily manipulated, as were the hydrogen atom solutions. Consequently, we present and interpret these exact solutions in graphical form. The first eight wave functions, starting with the ground state, are shown in Figure 6.2. These are plotted using the same coordinates as in Figure 6.1, where the two protons lie on the z -axis and the value of R_{AB} is the experimental bond length for H_2^+ , which is 1.060 Å. Each wave function is shown in three different representations: (a) an isosurface comprising all those points in three-dimensional space where the wave function has a value equal to 0.1 of its maximum value; (b) a contour plot in a plane containing the internuclear axis with contours shown for ± 0.1 , ± 0.3 , ± 0.5 , ± 0.7 , and ± 0.9 of the maximum amplitude; (c) a plot of the amplitude along the internuclear axis, which amounts to a “line scan” across the contour plot. Each wave function is identified by four labels: an integer, either σ or π , a subscript g or u , and some are labeled with a superscript asterisk. Each of these labels provides insight into the shape and symmetry of the wave function and its corresponding probability density for locating the electron. These labels are discussed in turn in the following paragraphs.

First, the Greek letter identifies the component of the angular momentum for the electron that is directed along the internuclear axis. This tells us how the electron probability density is distributed around the internuclear axis, as viewed in a plane perpendicular to the axis. The Greek letter identifies the value of the angular momentum as follows:

$$\begin{aligned}\sigma &\longrightarrow \text{angular momentum component} = 0 \\ \pi &\longrightarrow \text{angular momentum component} = \pm h/2\pi \\ \delta &\longrightarrow \text{angular momentum component} = \pm 2h/2\pi \\ \varphi &\longrightarrow \text{angular momentum component} = \pm 3h/2\pi\end{aligned}$$

Because the σ wave functions have no angular nodes (just like the s orbitals in an atom), they have finite amplitudes on the internuclear axis, and the probability of finding the electron on that axis is therefore finite. Although not shown in Figure 6.2, the σ wave functions are cylindrically symmetric about the internuclear axis. The π wave functions, in contrast, describe electron motion about the internuclear axis with angular momentum $+h/2\pi$ or $-h/2\pi$. This leads to two wave functions— π_{u2p_x} and π_{u2p_y} —with the same energy, one of which lies mainly along the x -axis and the other of which lies mainly along the y -axis (the internuclear axis is chosen to be the z -axis). Because the π wave functions have nodal planes that include the internuclear axis, there is zero probability of finding the electron anywhere along the z -axis, just as there is zero probability of finding the electron at the nucleus in an atomic p orbital. Viewed perpendicular to the z -axis, the π

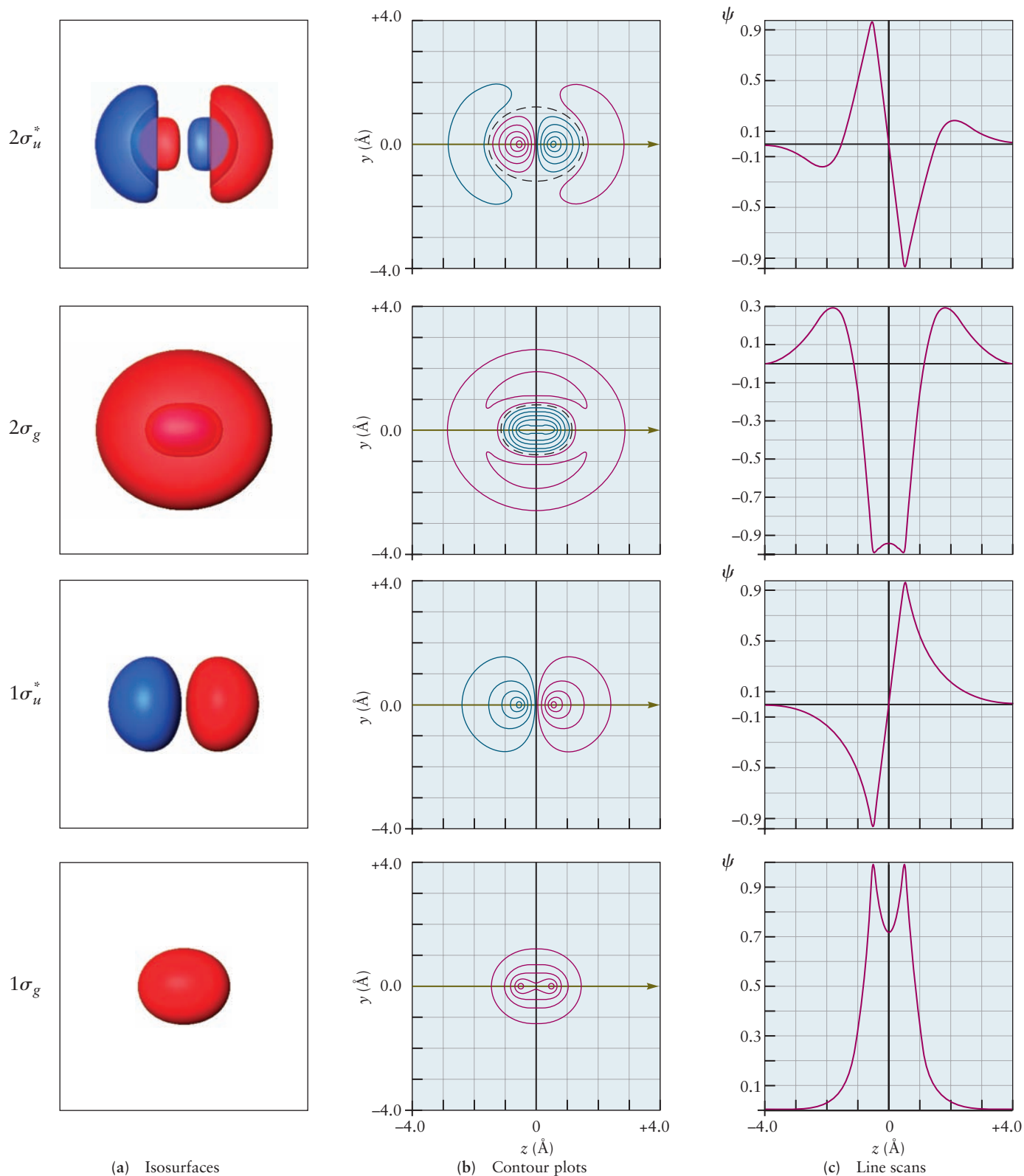


FIGURE 6.2 Wave functions for the first eight energy levels of the H_2^+ molecular ion, calculated exactly by quantum mechanics. The ground-state wave function is at the bottom of the figure; the others are arranged above it in order of increasing energy. The two nuclei lie along the z -axis, which is in the plane of the paper. Regions of positive and negative amplitude are shown in red and blue, respectively. The labels for each orbital are explained in the text. (a) Isosurfaces corresponding to contours at ± 0.1 of the maximum amplitude.

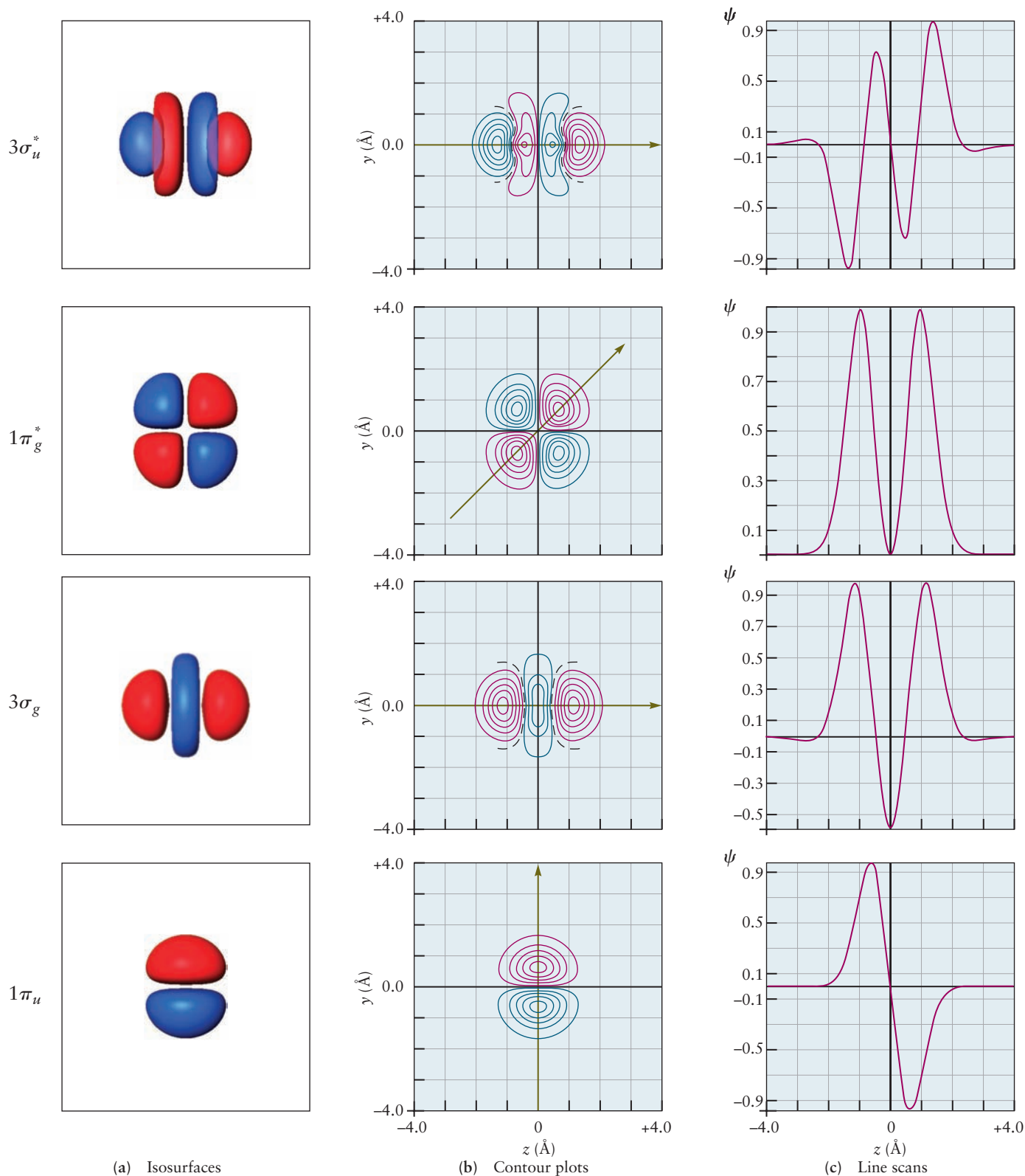


FIGURE 6.2 cont'd (b) Contours of constant amplitude in the $x-z$ plane, at values ± 0.1 , ± 0.3 , ± 0.5 , ± 0.7 , and ± 0.9 of the maximum amplitude. Radial nodes are represented by black dashed lines. (c) The amplitude along the z -axis, obtained as a “line scan” across the contour plot, along the direction indicated by the green arrow in (b).

(Courtesy of Mr. Hatem Helal and Professor William A. Goddard III, California Institute of Technology, and Dr. Kelly P. Gaither, University of Texas at Austin.)

wave functions do not have cylindrical symmetry. These results remind us of the s , p , d , f progression for angular momentum of the electron about the nucleus in the hydrogen atom and the fact that s orbitals have amplitude at the nucleus, whereas p orbitals have nodes at the nucleus.

Second, the subscript g or u describes how the properties of the wave function change as we invert our point of observation through the center of the molecule. More precisely, imagine Cartesian coordinates with their origin at the center of the molecule, and compare the wave function at the point (x, y, z) and at the point $(-x, -y, -z)$. If the sign of the wave function is the same at these two points, it is called symmetric and is labeled g , for the German word *gerade* (meaning “even”). If the sign of the wave function is opposite at these two points, it is called antisymmetric and labeled u , for the German word *ungerade* (meaning “odd”).

Third, the asterisk denotes an antibonding orbital. As discussed later, antibonding orbitals have much less electron density concentrated between the nuclei, and the density goes to zero at a node between the nuclei. In addition, the energy of an electron in an antibonding orbital of H_2^+ is greater than that of the corresponding H and H^+ species, so it is unstable with respect to dissociation.

Fourth, the integer is merely an index to track the relative energies of the wave functions of each symmetry type. For example, $1\sigma_g$ is the first (lowest on the energy scale) of the σ_g wave functions, whereas $2\sigma_u^*$ has the second lowest energy of the σ_u^* wave functions, and $1\pi_u$ has the lowest energy of the π_u wave functions. The energy indexing integer is somewhat analogous to the principal quantum number n for AOs, but unlike n , it does not arise explicitly from quantization of energy.

We call each of these exact one-electron wave functions a molecular orbital (MO), just as we called the exact one-electron wave functions for the hydrogen atom AOs. These exact MOs play a fundamental role in the quantum description of chemical bonding.

6.1.4 Electron Density in H_2^+

Our intuitive understanding of the chemical bond is that the nuclei and electrons arrange themselves in a manner that reduces their total energy to a value lower than the energy of the isolated atoms. Achieving this arrangement requires that new attractive interactions come into play to reduce the total potential energy as the bond is formed. Naively, we expect this to occur when the electrons are arranged so they spend most of their time “between” the nuclei where they would experience maximum attraction to all the nuclei, not just the nucleus of the parent atom. We saw in Section 3.6 that classical electrostatics could not explain this stabilization mechanism, so we relied on the qualitative Lewis model of electron-shared pair bonds. Now we want to see how these ideas are handled by quantum mechanics in the simplest case. We recommend that you review Section 3.6 at this point.

First, let's explore the electron density around the nuclei, which are assumed to be fixed in position. In quantum mechanics, the electron density in a region of space is simply proportional to the probability density for an electron to be in that region. The probability density functions for locating the electron at each point in space are shown in Figure 6.3; they were calculated by squaring each MO wave function shown in Figure 6.2. The probability density functions are shown in three views: (a) isosurfaces comprising all points at which the probability density is 0.01 of its maximum value; (b) contour plots in a plane containing the internuclear axis with contours at 0.05, 0.01, 0.3, 0.5, 0.7, and 0.9 of the maximum value; (c) line scans across the contour plot show the variation in probability density along the internuclear axis. The ground-state wave function $1\sigma_g$ has much greater electron density in the region between the nuclei than at the extremes of the molecule, and so is consistent with our expectations about chemical bonding. But, the

first excited state wave function $1\sigma_u^*$ has a node halfway between the nuclei, and thus appears inconsistent with a chemical bond.

It appears that $1\sigma_g$ supports formation of the bond by increasing electron density between the nuclei, whereas $1\sigma_u^*$ opposes bond formation by reducing electron density between the nuclei, relative to the density between noninteracting atoms. Yet, both functions are part of the exact quantum solution for H_2^+ . To understand the role each of them plays in forming the bond, we need to determine how the energy of these states compares with the energy of the isolated atom and proton. Reducing the energy relative to the separated particles is the key to bond formation.

Solving the Schrödinger equation for H_2^+ within the Born–Oppenheimer approximation gives the electronic energy $E_n^{(el)}(R_{AB})$ as a function of the positions of the nuclei. The results, which we quote without verification, are as follows. At all distances, the energy in the $1\sigma_u^*$ MO is greater than that of the separated atoms and increases as the internuclear distance becomes shorter. This energy represents a repulsive interaction, under which the nuclei would fly apart rather than remain close together. In contrast, the energy in the $1\sigma_g$ MO is lower than that for noninteracting hydrogen atoms, and indeed reaches a minimum between the nuclei. In this orbital, the molecular ion is energetically stable with a bond length that corresponds to the minimum in the potential energy curve.

Considered together, the increased electron density and the lowered energy between the nuclei in the $1\sigma_g$ orbital indicate formation of a chemical bond. Consequently, $1\sigma_g$ is called a **bonding molecular orbital**. By contrast, the $1\sigma_u^*$ orbital shows increased energy and zero electron density between the nuclei and is called an **antibonding molecular orbital**. Similar analysis of the remaining six orbitals in Figure 6.2 shows that all those labeled with superscript asterisk (*) are antibonding, whereas those without the (*) labels are bonding, with increased electron density and decreased potential energy between the nuclei.

6.1.5 Summary: Key Features of the Quantum Picture of Chemical Bonding

In the remainder of this chapter, key features of the quantum picture of the chemical bond and the exact MOs for H_2^+ guide the development of approximate MO methods. These features are:

1. In representing molecular structures, we consider the nuclei to be fixed in specific positions while the electrons move rapidly around them (the Born–Oppenheimer approximation).
2. A molecular orbital is a one-electron wave function whose square describes the distribution of electron density around the nuclei.
3. Bonding orbitals describe arrangements with increased electron density in the region between the nuclei and decreased potential energy relative to that of the separated atoms.
4. Each bonding MO is related to an antibonding MO in which the amplitude is zero at some point corresponding to a node on the internuclear axis between the nuclei and the potential energy is increased relative to that of the separated atoms.
5. Bonding and antibonding MOs of type σ are those for which the electron has no component of angular momentum along the internuclear axis. A σ orbital is cylindrically symmetric about the internuclear axis.
6. Bonding and antibonding MOs of type π are those for which the electron has one unit of angular momentum along the internuclear axis. The internuclear axis lies in the nodal plane of a bonding π orbital. Consequently, the amplitude is concentrated “off the axis” and the orbital is not cylindrically symmetric.

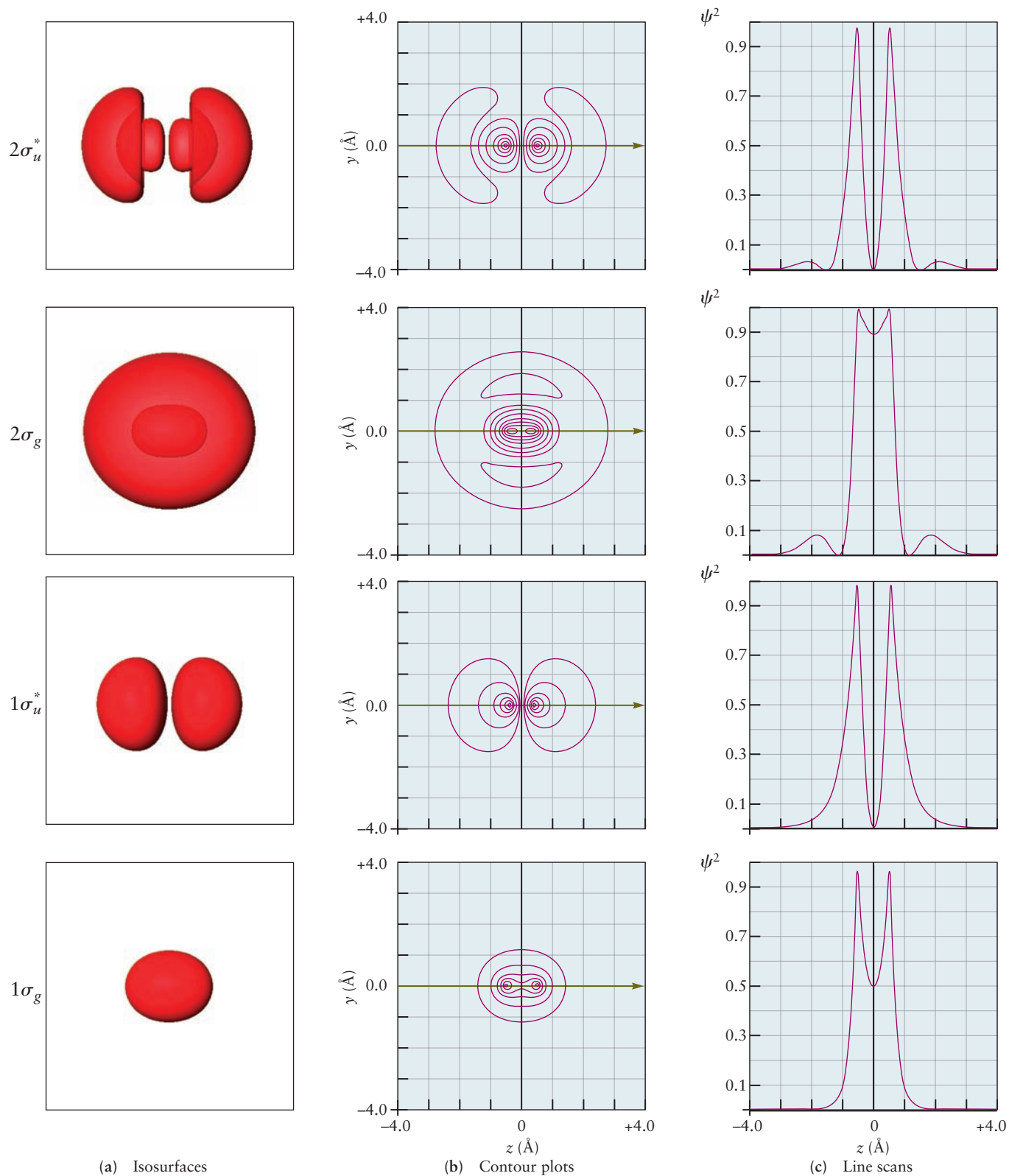


FIGURE 6.3 Probability density distributions for the first eight energy levels of the H_2^+ molecular ion, calculated exactly by quantum mechanics. (a) Isosurfaces comprising all points at which the probability density is 0.1 of its maximum value. (b) Contour plots in the x - z plane with contours at 0.01, 0.1, 0.3, 0.5, 0.7, and 0.9 of the maximum value. (c) Line scans across the contour plot, along the direction indicated by the green arrow in (b), showing the variation in probability density along the internuclear axis.

(Courtesy of Mr. Hatem Helal and Professor William A. Goddard III, California Institute of Technology, and Dr. Kelly P. Gaither, University of Texas at Austin.)

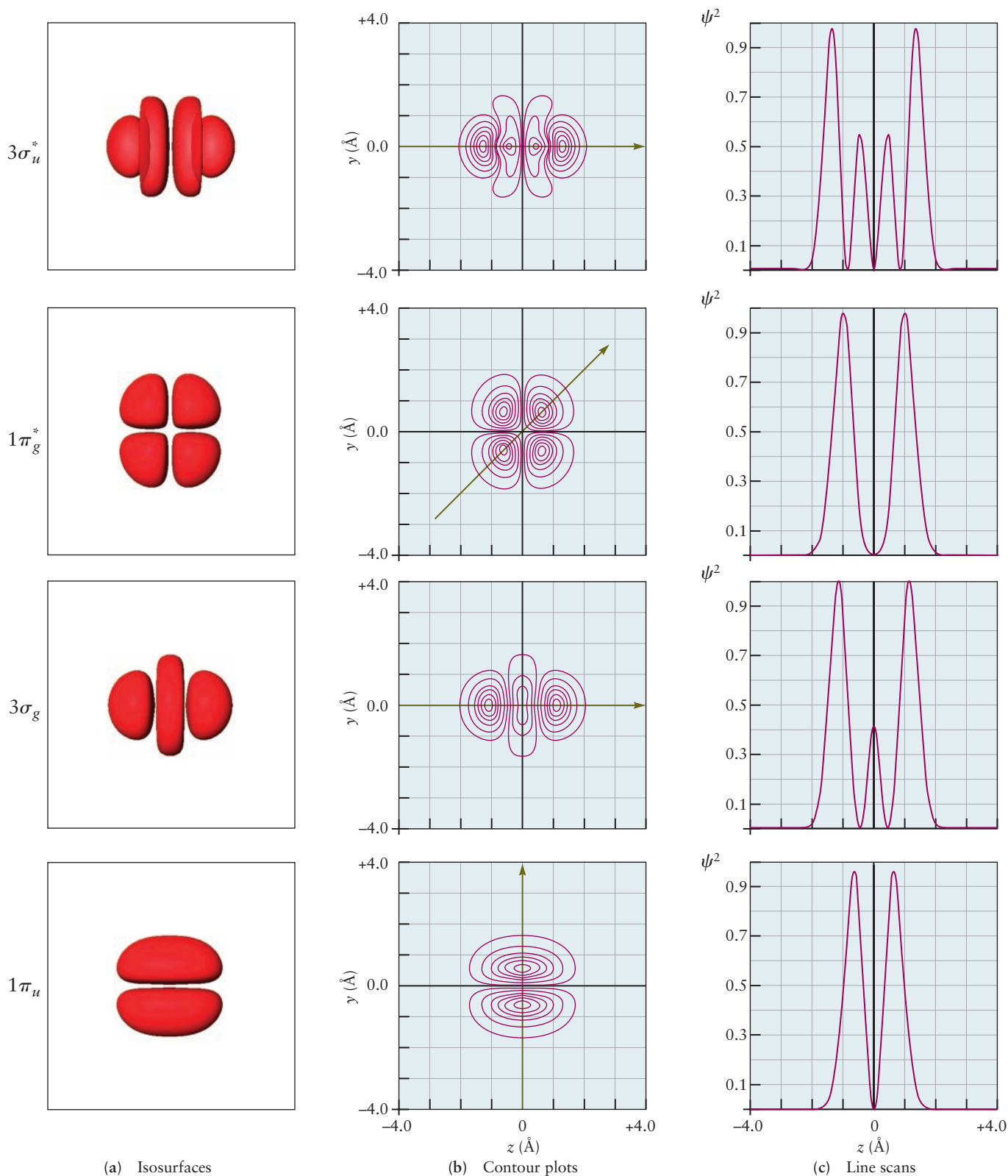


FIGURE 6.3 cont'd Probability density distributions for the first eight energy levels of the H_2^+ molecular ion, calculated exactly by quantum mechanics. (a) Isosurfaces comprising all points at which the probability density is 0.1 of its maximum value. (b) Contour plots in the x - z plane with contours at 0.01, 0.1, 0.3, 0.5, 0.7, and 0.9 of the maximum value. (c) Line scans across the contour plot, along the direction indicated by the green arrow in (b), showing the variation in probability density along the internuclear axis.

(Courtesy of Mr. Hatem Helal and Professor William A. Goddard III, California Institute of Technology, and Dr. Kelly P. Gaither, University of Texas at Austin.)

A DEEPER LOOK

6.1.6 Nature of the Chemical Bond in H_2^+

We can obtain deeper insight into the exact MOs described in Section 6.1.3 by comparing these unfamiliar wave functions with simpler cases that we understand already. As shown in Figure 6.4, let's start with a proton H^+ and a hydrogen atom H

separated at great distance, and then imagine bringing them close together to form H_2^+ . We imagine squeezing the particles even closer together, so the two protons merge to produce the helium ion He^+ . At very large separations and at extremely short separations we understand the wave functions and energy levels completely from the one-electron exact solutions in Section 5.1. Although there is only one electron in H_2^+ it is equally likely to be bound to either proton in the separated atom limit, so we have shown orbitals associated with both protons.

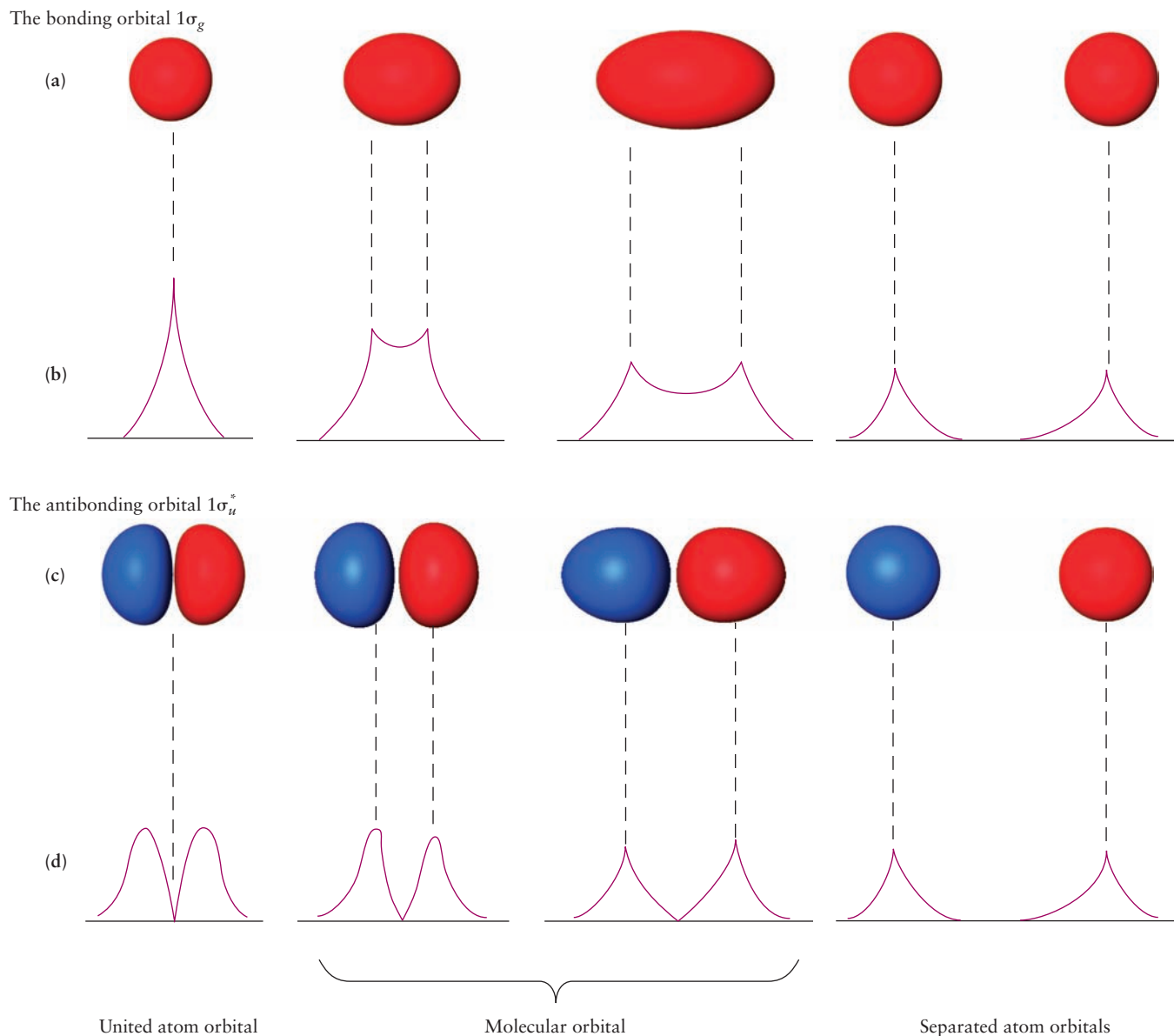


FIGURE 6.4 Evolution of the atomic orbitals on H and H^+ as the separation between them is decreased, eventually resulting in the atomic orbitals of He^+ . The molecular ion H_2^+ appears at intermediate distances between the united atom and the separated atom limits. (a) Isosurfaces representing the changes in shape during the evolution of the bonding MO. (b) Line scans representing the changes in amplitude along the internuclear axis during the evolution of the bonding MO. (c) Isosurfaces representing the changes in shape during the evolution of the antibonding MO. (d) Line scans representing the changes in amplitude along their internuclear axis during the evolution of the antibonding MO.

(Adapted from G. C. Pimentel and R. D. Spratley, *Chemical Bonding Clarified through Quantum Mechanics*. San Francisco: Holden-Day, 1969, Figures 3.5 and 3.4, by permission.)

As the distance is initially decreased in Figure 6.4a, we expect the AOs of the H atom to distort smoothly into the wave functions of H_2^+ , which, in turn, distort smoothly into the AOs of He^+ . The reason is that this mental experiment is just another way of looking at the Born–Oppenheimer approximation. As we move the sluggish nuclei extremely slowly from one position to another, the electron density will adjust its shape to accommodate the changed internuclear distances, but will not be disrupted. In particular, the nodal structure of the wave function cannot change. As we know from solutions for the particle in box models (see Section 4.6) and the hydrogen atom (see Section 5.1), the number of nodes increases only when the system is moved into an excited state by absorbing energy. There is not sufficient energy in the experiment we are describing here to create excited states.

We can track exactly which AOs are involved in these changes by paying careful attention to the nodes in the wave functions. Suppose we start with the electron in the ground state of He^+ and pull that ion apart as the reverse of the process just described. The $\text{He}^+(1s)$ orbital is spherical and has no nodes. As the nuclei are separated, that orbital is distorted first into an elliptical shape, then at large internuclear distance it begins to resemble two separated atom wave functions with the same phase. These must be $1s$ orbitals; any others would require changes in the nodal structure. No new nodes have been created; the nodal pattern has remained constant through the mental experiment. The change in the wave function and the probability density in the experiment are shown in Figures 6.4a and b, respectively.

Now we have some insight into the structure of the ground-state wave function $1\sigma_g$. When the nuclei are infinitely far apart, it correlates with an in-phase or symmetric combination of the AOs, in which the orbitals have the same phase: $\varphi_{1s}^A + \varphi_{1s}^B$. In physical terms, when a proton and a hydrogen atom approach one another, at intermediate distances the electron begins to experience the attraction of both protons, and instead of residing in the orbitals of just one of them, it is now described by a new wave function characteristic of the entire molecule. We can visualize that this new wave function arose from constructive

interference of the two AOs to produce amplitude spread over both nuclei. We have understood qualitatively how its electron density is greater between the nuclei than at the extremes of the molecule (see Fig. 6.3) and recognized that it is crudely approximated at large internuclear separations by the sum $\varphi_{1s}^A + \varphi_{1s}^B$.

The same reasoning provides insight into the first excited state $1\sigma_u^*$. Because it has a node between the two nuclei, at very small separations it must correlate with an orbital of He^+ that also has a nodal plane perpendicular to the z -axis, that is, in the x - y plane. The $2p_z$ orbital (see Fig. 5.8) is the proper choice. Now let's imagine pulling apart the protons in He^+ with its electron in the $\text{He}^+(2p_z)$ orbital. The orbital will distort into an elliptical shape along the z -axis, with a node in its center. At very large distances, this must resemble two separated atom wave functions. The only way to maintain the nodal structure is to correlate with the out-of-phase, antisymmetric combination in which the AOs have opposite phase: $\varphi_{1s}^A - \varphi_{1s}^B$. The change in the wave function and in the probability density are shown in Figures 6.4c and d, respectively. In physical terms, when a proton and a hydrogen atom approach each other at intermediate distances the electron still feels the attractions of both nuclei and is again described by a new MO characteristic of the molecule as a whole. We must also allow for the possibility that the AOs interfere destructively, giving reduced amplitude in the region between the nuclei, with a node at the midpoint of the internuclear separation. Thus, we have explained qualitatively how the MO $1\sigma_u^*$ has less electron density between the nuclei than in the extremes, and we have recognized that it is approximated crudely at large internuclear separation by the difference $\varphi_{1s}^A - \varphi_{1s}^B$.

A similar analysis can be applied to the remaining six exact MOs shown in Figure 6.2. Each of them is intermediate between an AO for He^+ (at very short separations) and the sum or difference of a pair of AOs for H (at very large separations). The results are summarized in Figure 6.5. We recommend that you work through each of these correlations in Figure 6.5 to develop experience and intuition for the exact MOs and their relation to AOs. We rely on Figure 6.5 to generate approximate MOs later in the chapter.

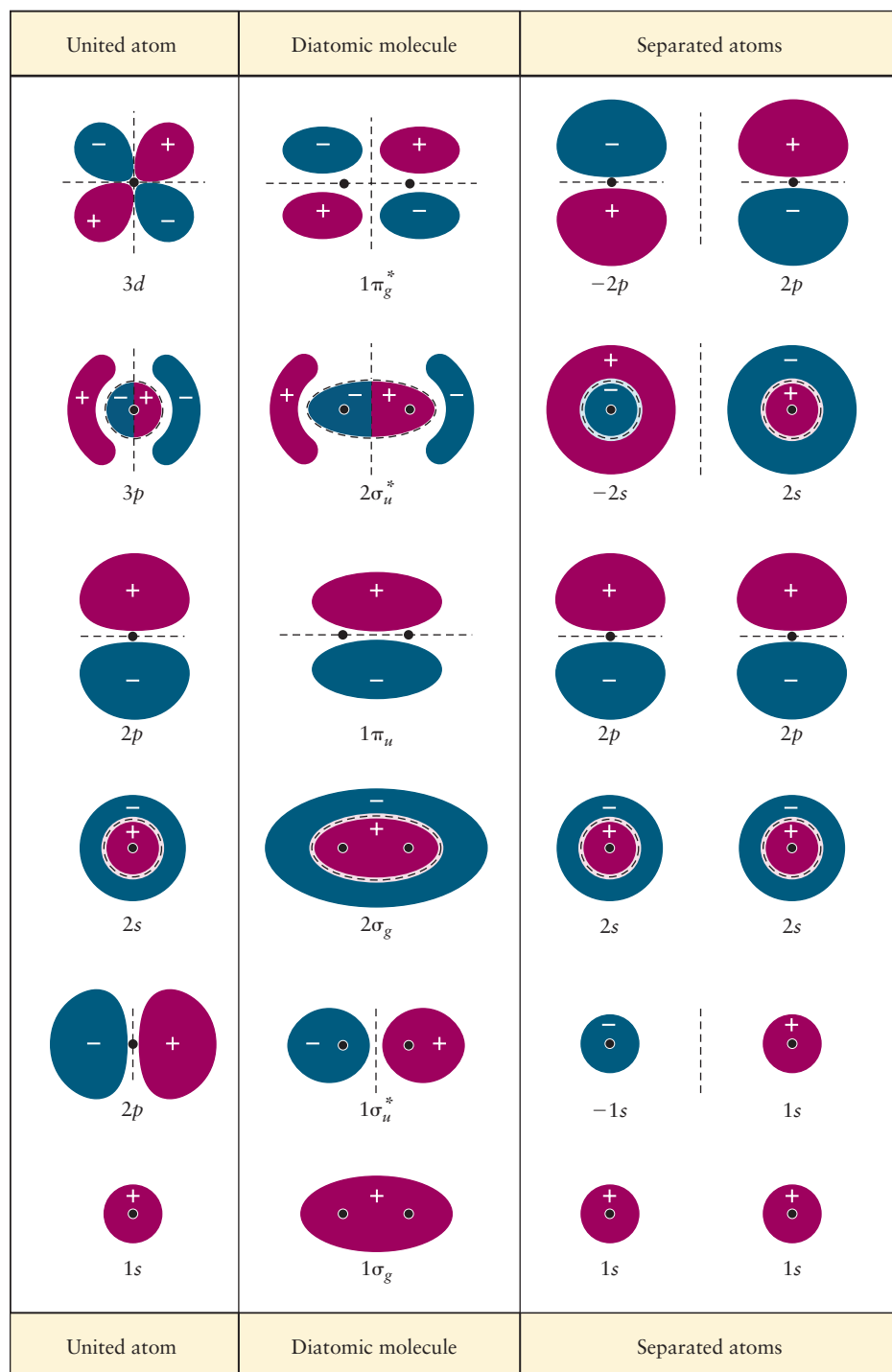
6.2 De-localized Bonds: Molecular Orbital Theory and the Linear Combination of Atomic Orbitals Approximation

The goal of this section is to introduce the first of the two main methods for generating approximate electronic wave functions for molecules. The methods we describe work well in qualitative descriptions of bonding and are used for that purpose in all branches of chemistry. They also serve as the starting point for sophisticated computer calculations of molecular electronic structure with readily available molecular modeling software packages.

The LCAO method extends to molecules the description developed for many-electron atoms in Section 5.2. Just as the wave function for a many-electron atom is written as a product of single-particle AOs, here the electronic wave function for a molecule is written as a product of single-particle MOs. This form is called the **orbital approximation for molecules**. We construct MOs, and we place electrons in them according to the Pauli exclusion principle to assign molecular electron configurations.

FIGURE 6.5 Correlation table showing how six of the exact H_2^+ MOs correlate at large separations to sums or differences of hydrogen atom orbitals and at short separations to the atomic orbitals of He^+ .

(Adapted from R. S. Berry, S. A. Rice, and J. Ross, *Physical Chemistry* (2nd ed), New York: Oxford, 2000, Figure 6.2, by permission.)



What functions shall we use for the single-electron MOs? We could try the exact MOs for H_2^+ shown in Figure 6.2. However, these exact MOs are not described by simple equations, and they are inconvenient for applications. Therefore, we introduce the LCAO method to construct *approximate* MOs directly from the Hartree AOs for the atoms in the molecule, guided by molecular symmetry and chemical intuition. The essential new feature compared with the atomic case is that the (multicenter) approximate MOs are spread around all the nuclei in the molecule, so the electron density is *de-localized* over the entire molecule. The approximate MOs therefore differ considerably from the (single-center) AOs used in Section 5.2. Constructing the approximate MOs and using them in qualitative descriptions of bonding are the core objectives of this section.

Computer calculations of molecular electronic structure use the orbital approximation in exactly the same way. Approximate MOs are initially generated by starting with “trial functions” selected by symmetry and chemical intuition. The electronic wave function for the molecule is written in terms of trial functions, and then optimized through self-consistent field (SCF) calculations to produce the best values of the adjustable parameters in the trial functions. With these best values, the trial functions then become the optimized MOs and are ready for use in subsequent applications. Throughout this chapter, we provide glimpses of how the SCF calculations are carried out and how the optimized results are interpreted and applied.

6.2.1 Linear Combination of Atomic Orbitals

Approximation for H_2^+

The LCAO method is best explained with the help of a specific example, so we start with the hydrogen molecular ion H_2^+ . We can evaluate the success of the method by comparing its results with the exact solution described in Section 6.1, and gain confidence in applying the method to more complex molecules. The LCAO approximation is motivated by the “separated atom” limits of the exact MOs shown in Figure 6.2. Consider the $1\sigma_g$ MO. When the electron is close to nucleus A, it experiences a potential not very different from that in an isolated hydrogen atom. The ground-state wave function for the electron near A should therefore resemble a 1s atomic wave function φ_{1s}^A . Near B, the wave function should resemble φ_{1s}^B . The 1s orbitals at A and B are identical; the labels are attached to emphasize the presence of two nuclei. Note that A and B are labels, not exponents. A simple way to construct a MO with these properties is to approximate the $1\sigma_g$ MO as a sum of the H 1s orbitals with adjustable coefficients. Their values will change as the internuclear distance is reduced, to adjust the limiting form to values appropriate for each internuclear distance. The best value of the coefficients for each value of R_{AB} can be determined by self-consistent numerical calculations. For our purposes, it is adequate to ignore the dependence on R_{AB} when we evaluate the coefficients by normalizing the wave function. Similarly, we can approximate the other exact MOs in Figure 6.2 by forming linear combinations of the AOs to which they correlate in the separated atom limit in Figure 6.5.

The general form for an approximate MO is a linear combination of two AOs, obtained by adding or subtracting the two with coefficients whose values depend on R_{AB} :

$$\psi_{\text{MO}} = C_A \varphi_{1s}^A + C_B \varphi_{1s}^B$$

The coefficients C_A and C_B give the relative weights of the two AOs. If C_A were greater in magnitude than C_B , the φ_{1s}^A orbital would be more heavily weighted and the electron would be more likely to be found near nucleus A, and vice versa. But because the two nuclei in H_2^+ are identical, the electron is just as likely to be found near one nucleus as the other. Therefore, the magnitudes of C_A and C_B must be equal, and either $C_A = C_B$ or $C_A = -C_B$. For both these choices, $(\psi_{\text{MO}})^2$ is symmetric in the two nuclei.

To maintain the distinctions among the various orbitals, we use the following notation in describing the LCAO approximation. Atomic orbitals will be represented by φ and MOs by σ or π . Generic wave functions will be represented by ψ . Occasionally, ψ will represent some special wave function, in which case appropriate subscripts will be attached.

LCAO MOLECULAR ORBITALS FOR H_2^+ Proceeding as described in the preceding paragraphs, we construct approximate MOs for the exact $1\sigma_g$ and $1\sigma_u^*$ MOs in Figure 6.2:

$$1\sigma_g \approx \sigma_{g1s} = C_g(R_{AB})[\varphi_{1s}^A + \varphi_{1s}^B] \quad [6.3a]$$

$$1\sigma_u^* \approx \sigma_{u1s}^* = C_u(R_{AB})[\varphi_{1s}^A - \varphi_{1s}^B] \quad [6.3b]$$

where C_g and C_u are chosen to ensure that the total probability of finding the electron *somewhere* is one. Their values will depend on the choice of R_{AB} at which we have fixed the nuclei. Notice that we have introduced new symbols σ_{g1s} and σ_{u1s}^* for the approximate MOs, not only to distinguish them from the exact MOs but also to indicate explicitly the AOs from which they were constructed. The symbols for the exact and approximate MOs are summarized in Table 6.1. To simplify the notation, henceforth we omit the dependence of σ_{g1s} and σ_{u1s}^* on R_{AB} . The distribution of electron probability density is obtained by squaring each of the approximate MOs:

$$[\sigma_{g1s}]^2 = C_g^2[(\varphi_{1s}^A)^2 + (\varphi_{1s}^B)^2 + 2\varphi_{1s}^A\varphi_{1s}^B] \quad [6.4a]$$

$$[\sigma_{u1s}^*]^2 = C_u^2[(\varphi_{1s}^A)^2 + (\varphi_{1s}^B)^2 - 2\varphi_{1s}^A\varphi_{1s}^B] \quad [6.4b]$$

These probability distributions can be compared with the probability distribution for a noninteracting (n.i.) system (obtained by averaging the probabilities for $H_A + H_B^+$ and $H_A^+ + H_B$), which is

$$\psi_{\text{n.i.}}^2 = C_3^2[(\varphi_{1s}^A)^2 + (\varphi_{1s}^B)^2] \quad [6.5]$$

To describe the noninteracting system as one electron distributed over two possible sites, we set $C_3^2 = 0.5$. The interpretation of these approximate MOs in relation to the noninteracting system is best explained graphically. The plots of these various wave functions (left side) and their squares (right side) are shown in Figure 6.6. Compared with the noninteracting pair of atoms, the system described by the approximate MO σ_{g1s} shows increased electron density with a node between the nuclei. It is therefore a bonding orbital as defined in Section 6.1. By contrast, the approximate MO σ_{u1s}^* shows reduced probability for finding an electron between the nuclei and so is an antibonding orbital. Note in Figure 6.6 that σ_{u1s}^* has a node between the nuclei and is antisymmetric for inversion through the molecular center (see Section 6.1). Comparing Figure 6.6 with Figure 6.2 shows that the LCAO method has reproduced qualitatively the probability density in the first two exact wave functions for H_2^+ .

ENERGY OF H_2^+ IN THE LCAO APPROXIMATION To complete the demonstration that σ_{g1s} and σ_{u1s}^* are bonding and antibonding MOs, respectively, we

TABLE 6.1 Molecular Orbitals for Homonuclear Diatomic Molecules

Exact MO Notation	LCAO MO Notation
$1\sigma_g$	σ_{g1s}
$1\sigma_u^*$	σ_{u1s}^*
$2\sigma_g$	σ_{g2s}
$2\sigma_u^*$	σ_{u2s}^*
$1\pi_u$	π_{u2p_x}, π_{u2p_y}
$3\sigma_g$	σ_{g2p_z}
$1\pi_g^*$	$\pi_{g2p_x}^*, \pi_{g2p_y}^*$
$3\sigma_u^*$	$\sigma_{u2p_z}^*$

FIGURE 6.6 Antibonding and bonding molecular orbitals of H_2^+ along the internuclear axis in the linear combination of atomic orbitals (LCAO) approximation. For comparison, the green lines show the independent atomic orbitals and the electron probability distribution $\psi^2(\text{n.i.})$ for a noninteracting system. Compared with this reference system, the bonding orbital shows *increased* probability density between the nuclei, but the antibonding orbital shows *decreased* probability density in this region.

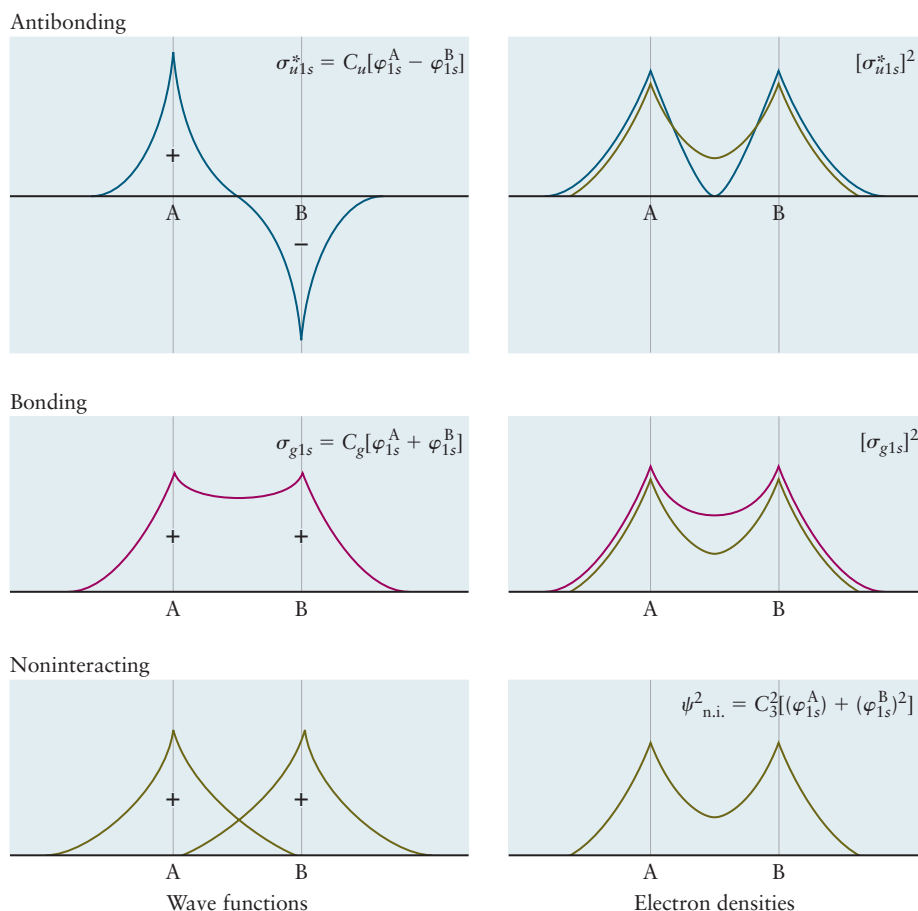
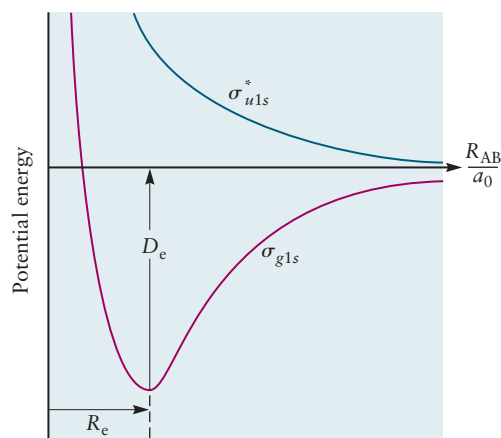


FIGURE 6.7 Potential energy of H_2^+ in a σ_{g1s} (bonding) and σ_{u1s}^* (antibonding) molecular orbital, shown as a function of internuclear separation R_{AB} in the LCAO approximation.



examine the potential energy in each of these approximate MOs. Figure 6.7 shows the potential energy of the H_2^+ ion in the LCAO approximation for the σ_{g1s} and σ_{u1s}^* MOs. The force between the nuclei in the antibonding state is everywhere repulsive, but in the bonding state the nuclei are attracted to each other and form a bound state at the distance corresponding to the lowest potential energy.

The energy minimum of the potential at R_e is called D_e , the **bond dissociation energy**—that is, the energy required to dissociate the molecule into separated atoms. At R_e , where the effective potential has its minimum value, the attractive and repulsive forces between the nuclei balance exactly and hold the internuclear distance at this value. The equilibrium bond length of the molecule is determined by the competition between attractive forces, which originate in electron–nuclear interactions, and repulsive forces, which originate in nuclear–nuclear interactions.

This is the sense in which the electrons function as the “glue” that holds the nuclei to their special positions that define the structure of a molecule.

How well does the LCAO approximation describe the energy values in H_2^+ ? We compare the exact and LCAO results in Figure 6.8, where the zero of energy at infinite separation is again taken to be that of the separated species H and H^+ . The energy in σ_{g1s} has a minimum at $R_{\text{AB}} = 1.32 \text{ \AA}$, and the predicted energy required to dissociate the diatomic molecular ion to H and H^+ is $D_e = 1.76 \text{ eV}$. These results compare reasonably well with the experimentally measured values $R_{\text{AB}} = 1.060 \text{ \AA}$ and $D_e = 2.791 \text{ eV}$, which were also obtained from the exact solution in Section 6.1.

Let's put these results of the LCAO approximation in perspective. The results in Figures 6.6 and 6.7 were obtained by working out the details of the approximation expressed in Equations 6.3a and 6.3b. These LCAO results have captured qualitatively the results of the exact calculation. Therefore, we can apply the LCAO method in other more complex cases and be confident we have included the essential qualitative features of bond formation. Also, we can always improve the results by following up with a self-consistent computer calculation that produces optimized MOs.

The energy-level diagram within the LCAO approximation is given by a **correlation diagram** (Fig. 6.9), which shows that two $1s$ AOs have been combined to give a σ_{g1s} MO with energy lower than the AOs and a σ_{u1s}^* MO with energy higher than the AOs. This diagram is a purely qualitative representation of the same information contained in Figure 6.7. The exact energy level values will depend on the separation between the fixed nuclei (as shown in Fig. 6.7). Even without the results shown in Figure 6.7, we would know that an electron in an antibonding orbital has more energy than one in a bonding orbital because the antibonding orbital has a node. Consequently, in the ground state of H_2^+ , the electron occupies the σ_{g1s} MO. By forming the bond in the molecular ion, the total system of two hydrogen nuclei and one electron becomes more stable than the separated atoms by the energy difference $-\Delta E$ shown in Figure 6.9.

FIGURE 6.8 Comparison of potential energy for the σ_{g1s} and σ_{u1s}^* orbitals of H_2^+ in the LCAO approximation (dashed lines) with the exact results (solid lines). The internuclear separation is plotted in units of the Bohr radius.

(Adapted from R. S. Berry, S. A. Rice, and J. Ross, *Physical Chemistry* (2nd ed), New York: Oxford, 2000, Figure 6.6, by permission.)

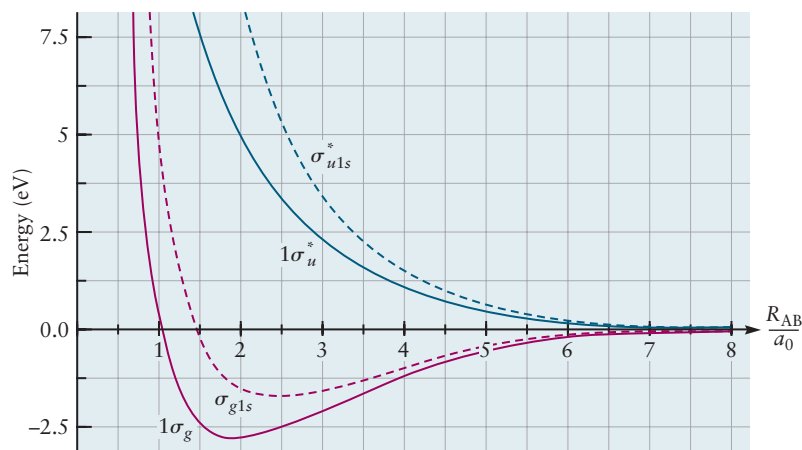
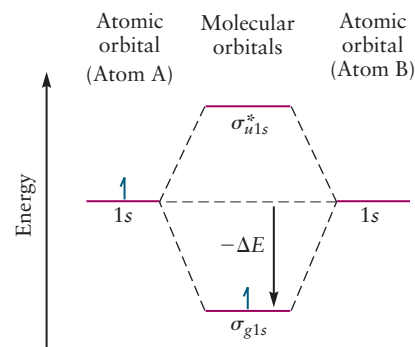


FIGURE 6.9 Correlation diagram for H_2^+ in the linear combination of atomic orbitals (LCAO) approximation. The bonding orbital is stabilized relative to the noninteracting system by the energy difference ΔE .



6.2.2 Homonuclear Diatomic Molecules: First-Period Atoms

We can combine the LCAO method for H_2^+ with an aufbau principle, analogous to that developed for atoms, to describe the electron configuration of more complex molecules. Electrons available from the two atoms are “fed” into the MOs, starting with the MO of lowest energy. At most, two electrons can occupy each MO. The ground-state H_2 molecule, therefore, accommodates two electrons with opposite spins in a σ_{g1s} bonding MO (Fig. 6.10). The diatomic molecule is more stable than the isolated atoms by the energy difference $-2\Delta E$.

The LCAO approximation can be applied in this same way to He_2^+ and He_2 , with one change. The MOs must be generated as linear combinations of $\text{He}(1s)$ AOs, not $\text{H}(1s)$ orbitals. The reason is that when the electrons in He_2^+ and He_2 approach close to one of the nuclei, they experience a potential much closer to that in a helium atom than in a hydrogen atom. Therefore, the equations for the MOs are

$$\sigma_{g1s} = C_g[\varphi_{1s}^A(\text{He}) + \varphi_{1s}^B(\text{He})] \quad [6.6a]$$

$$\sigma_{u1s}^* = C_u[\varphi_{1s}^A(\text{He}) - \varphi_{1s}^B(\text{He})] \quad [6.6b]$$

We rewrite Equation 6.6ab using a simpler notation, which we adopt for the remainder of the text:

$$\sigma_{g1s} = C_g[1s^A + 1s^B] \quad [6.7a]$$

$$\sigma_{u1s}^* = C_u[1s^A - 1s^B] \quad [6.7b]$$

In Equations 6.7a and 6.7b, the symbol for the atomic wave function φ has been dropped and the AOs are identified by their hydrogenic labels $1s$, $2s$, $2p$, and so on. The superscripts A and B are used to identify particular atoms of the same element in bonds formed from the same elements (**homonuclear** diatomics) and will be replaced by the symbols for the elements in bonds formed from different elements (**heteronuclear** diatomics). These helium MOs have the same general shapes and potential energy curves as shown in Figures 6.6 and 6.7 for the MOs constructed from $\text{H}(1s)$, and a correlation diagram similar to Figure 6.10. Quantitative calculations of electron density and energy (these calculations are not performed in this book) would produce different values for the two sets of MOs in Equations 6.3a and 6.3b and Equations 6.7a and 6.7b. Keep in mind that we construct the MOs as combinations of all the AOs required to accommodate the electrons in the ground states of the atoms that form the molecule. This set of AOs is called the **minimum basis set** for that specific molecule. Therefore, quantitative calculations for each molecule are influenced by the detailed properties of the atoms in the molecule.

FIGURE 6.10 Correlation diagram for first-period diatomic molecules. Blue arrows indicate the electron filling for the H_2 molecule. All of the atomic electrons are pooled and used to fill the molecular orbitals using the aufbau principle. In the molecules, electrons are no longer connected to any particular atom.

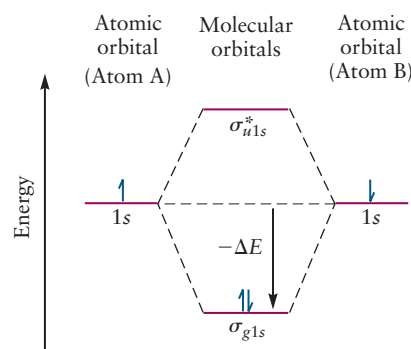
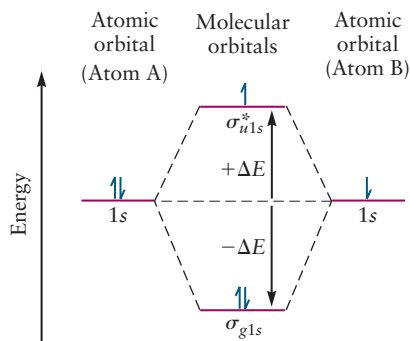


FIGURE 6.11 Correlation diagram for first-period diatomic molecules. Blue arrows indicate the electron filling for the He_2^+ molecule. The aufbau principle fills the bonding orbital with two electrons, so the third electron must go into the antibonding orbital, thus reducing the bond order compared with that in H_2 .



Because He_2^+ and He_2 have more than two electrons, the aufbau principle requires them to have some electrons in the σ_{u^*1s} antibonding orbital. Each of these electrons contributes a destabilization energy in the amount $+\Delta E$ relative to the separated helium atoms (Fig. 6.11). This effect competes with the stabilization energy of $-\Delta E$ per electron in the σ_{g1s} bonding orbital, giving a weak bond in He_2^+ and no stable bond in He_2 .

The general features of covalent bonding in the LCAO picture can be summarized as follows. In *bonding* MOs, bond formation arises from the sharing of electrons (most often electron pairs with opposite spins). The average electron density is greatest between the nuclei and tends to pull them together. Electrons that are shared in an *antibonding* MO tend to force the nuclei apart, reducing the bond strength. This competition is described by the **bond order**, which is defined as follows:

$$\text{Bond order} = \frac{1}{2} (\text{number of electrons in bonding molecular orbitals} - \text{number of electrons in antibonding molecular orbitals})$$

In the LCAO MO description, the H_2 molecule in its ground state has a pair of electrons in a bonding MO, and thus a single bond (that is, its bond order is 1). Later in this chapter, as we describe more complex diatomic molecules in the LCAO approximation, bond orders greater than 1 are discussed. This quantum mechanical definition of bond order generalizes the concept first developed in the Lewis theory of chemical bonding—a shared pair of electrons corresponds to a single bond, two shared pairs to a double bond, and so forth.

EXAMPLE 6.1

Give the ground-state electron configuration and the bond order of the He_2^+ molecular ion.

SOLUTION

He_2^+ has three electrons, which are placed in MOs to give the ground-state configuration $(\sigma_{g1s})^2(\sigma_{u^*1s})^1$, indicating that the ion has a doubly occupied σ_{g1s} orbital (bonding) and a singly occupied σ_{u^*1s} orbital (antibonding). The bond order is

$$\text{bond order} = \frac{1}{2} (2 \text{ electrons in } \sigma_{g1s} - 1 \text{ electron in } \sigma_{u^*1s}) = \frac{1}{2}$$

This should be a weaker bond than that in H_2 .

Related Problems: 9, 10, 11, 12, 13, 14, 15, 16

Table 6.2 lists the MO configurations of homonuclear diatomic molecules and molecular ions made from first-period elements. These configurations are simply the occupied MOs in order of increasing energy, together with the number of electrons in each orbital. Higher bond order corresponds to higher bond energies and shorter bond lengths. The species He_2 has bond order zero and does not form a true chemical bond.

TABLE 6.2 Electron Configurations and Bond Orders for First-Row Diatomic Molecules

Species	Electron Configuration	Bond Order	Bond Energy (kJ mol ⁻¹)	Bond Length (Å)
H ₂ ⁺	(σ _{g1s}) ¹	½	255	1.06
H ₂	(σ _{g1s}) ²	1	431	0.74
He ₂ ⁺	(σ _{g1s}) ² (σ _{u1s} [*]) ¹	½	251	1.08
He ₂	(σ _{g1s}) ² (σ _{u1s} [*]) ²	0	~0	Large

The preceding paragraphs have illustrated the LCAO approximation with specific examples and shown how the character of the chemical bond is determined by the difference in the number of electrons in bonding and antibonding MOs. This subsection concludes with the following summary of the systematic procedure for applying the LCAO approximation to the MOs for any diatomic molecule:

1. Form linear combinations of the minimum basis set of AOs to generate MOs. The total number of MOs formed in this way must equal the number of AOs used.
2. Arrange the MOs in order from lowest to highest energy.
3. Put in electrons (at most two electrons per MO), starting from the orbital of lowest energy. Apply Hund's rules when appropriate.

6.2.3 Homonuclear Diatomic Molecules: Second-Period Atoms

How shall we generate approximate MOs to accommodate electrons from AOs higher than the 1s orbitals? The excited states of H₂⁺ provide a clue, in their limiting behavior at large internuclear separation. Figure 6.5 correlated each of these excited states with sums or differences of the excited states of the hydrogen atom. Using these results, we can propose approximate MOs as linear combinations of the excited states of atoms. Because we must include in the minimum basis set all occupied AOs for the participating atoms, the question naturally arises whether these simple two-term approximate MOs will be sufficient, or whether each MO will require contributions from several AOs. For example, N₂ will require at least 7 approximate MOs to accommodate its 14 electrons. We could generate each of these MOs as a linear combination of the 1s, 2s, and 2p orbitals (the minimum basis set) with proper coefficients. The general form for these MOs is

$$\psi_{\text{MO}} = C_1[1s^{\text{A}} + 1s^{\text{B}}] + C_2[2s^{\text{A}} + 2s^{\text{B}}] + C_3[2p_x^{\text{A}} + 2p_x^{\text{B}}] + C_4[2p_y^{\text{A}} + 2p_y^{\text{B}}] + C_5[2p_z^{\text{A}} + 2p_z^{\text{B}}] \quad [6.8]$$

These MOs would be distinguished from one another by the values of their coefficients. The square of each of these MOs would give the electron density distribution for the electrons in that MO. This distribution function would include many cross terms, each of which represents the interaction between a pair of AOs on the two different atoms. It is difficult to visualize the result as the basis for qualitative arguments.

Two conclusions from more advanced quantum mechanics guide us to a simplified approach for constructing MOs for atoms with more than two electrons.

1. *Two AOs contribute significantly to bond formation only if their atomic energy levels are very close to one another.*

Consequently, we can ignore mixing between the core-shell 1s orbitals and the valence-shell 2s and 2p orbitals. Similarly, we can ignore mixing between the 2s and 2p orbitals, except in special cases to be described later.

2. *Two AOs on different atoms contribute significantly to bond formation only if they overlap significantly.*

Overlap must be defined somewhat precisely to understand the second statement. Two orbitals overlap significantly if they both have appreciable amplitudes over the same region of space. The *net* overlap may be positive or zero, depending on the relative phases of the orbitals involved. Bonding orbitals arise from positive overlap (constructive interference), whereas antibonding orbitals result from zero overlap (destructive interference).

For s orbitals, it is rather easy to guess the degree of overlap; the closer the nuclei, the greater the overlap. If the wave functions have the same phase, the overlap is positive; if they have opposite phases, the overlap is zero. For more complex cases, the overlap between participating AOs depends strongly on both the symmetry of the arrangement of the nuclei and on the phases of the orbitals. If the two orbitals are shaped so that neither has substantial amplitude in the region of interest, then their overlap is negligible. However, if they both have significant amplitude in the region of interest, it is important to know whether regions of positive overlap (where the two orbitals have the same phase) are canceled by regions of negative overlap (where the two orbitals have opposite phases). Such cancellation leads to negligible or zero overlap between the orbitals. Qualitative sketches that illustrate significant or negligible overlap in several common cases are shown in Figure 6.12. In particular, constructive interference and overlap between s and p orbitals is significant only in the case where an s orbital approaches a p orbital “end-on.” The phase of the p orbital lobe pointing toward the s orbital must be the same as that of the s orbital. We recommend reviewing the “sizes and shapes” of hydrogenic orbitals discussed in Section 5.1 and depicted in Figure 5.4. A great deal of qualitative insight into the construction of MOs can be gleaned from these considerations.

The two conclusions stated earlier justify the following simplified LCAO MOs for the second-period homonuclear diatomic molecules. As with the first-period atoms, we use the new labels in Table 6.1 to distinguish the approximate MOs from the exact H_2^+ MOs in Figure 6.2 and to indicate their atomic parentage.

We combine the $2s$ AOs of the two atoms in the same fashion as $1s$ orbitals, giving a σ_{g2s} bonding orbital and a σ_{u2s}^* antibonding orbital:

$$\sigma_{g2s} = C_g[2s^A + 2s^B] \quad [6.9a]$$

$$\sigma_{u2s}^* = C_u[2s^A - 2s^B] \quad [6.9b]$$

The choice of appropriate combinations of the $2p$ orbitals is guided by the overlap arguments and by recalling that the bond axis is the z -axis. The $2p$ orbitals form different MOs depending on whether they are parallel or perpendicular to the internuclear (bond) axis. Consider first the $2p_z$ orbitals, which can be used to form two different kinds of σ orbitals. If the relative phases of the p_z orbitals are such that they interfere constructively in the internuclear region, then a bonding σ_{g2p_z} orbital is formed. If, conversely, lobes of opposite phases overlap, they form an antibonding MO labeled $\sigma_{u2p_z}^*$. These orbitals are shown in Figure 6.13.

$$\sigma_{g2p_z} = C_g[2p_z^A - 2p_z^B] \quad [6.10a]$$

$$\sigma_{u2p_z}^* = C_u[2p_z^A + 2p_z^B] \quad [6.10b]$$

The electron density in the bonding orbital has increased between the nuclei, whereas the antibonding orbital has a node.

$$\pi_{u2p_x} = C_u[2p_x^A + 2p_x^B] \quad [6.11a]$$

$$\pi_{g2p_x}^* = C_g[2p_x^A - 2p_x^B] \quad [6.11b]$$

FIGURE 6.12 Overlap of orbitals in several common combinations. The magnitude of overlap can be estimated qualitatively from the relative size and symmetry of the two orbitals involved. (Note the radial nodes in the $2s$ orbitals, clearly visible in these images.)

(Courtesy of Mr. Hatem Helal and Professor William A. Goddard III, California Institute of Technology, and Dr. Kelly P. Gaither, University of Texas at Austin.)

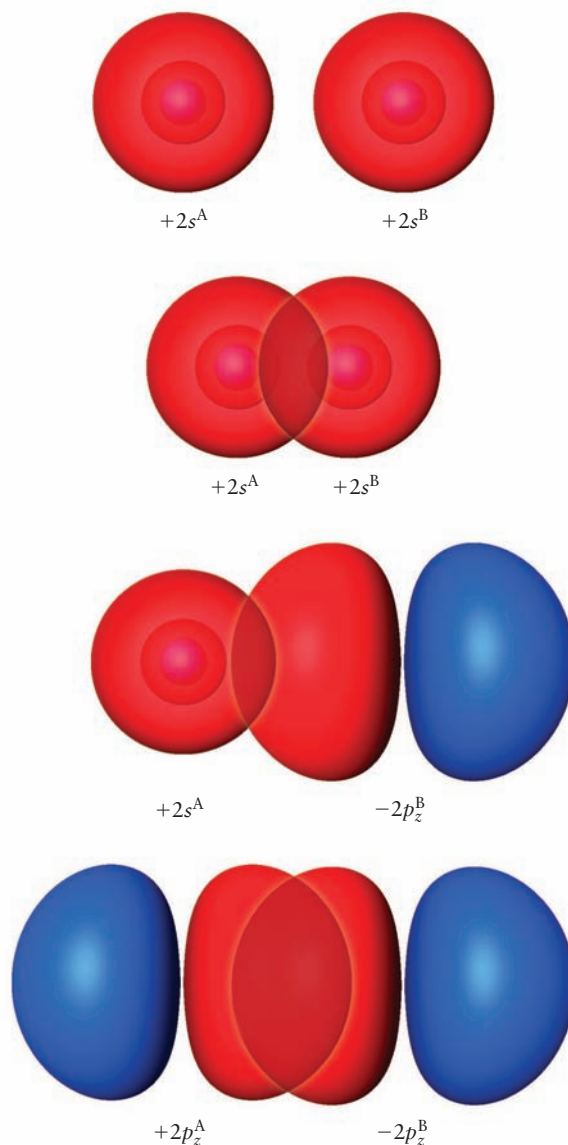


FIGURE 6.13 Formation of (a) σ_{g2p_z} bonding and (b) $\sigma_{u2p_z}^*$ antibonding molecular orbitals from $2p_z$ orbitals on atoms A and B. Regions with positive amplitude are shown in red, and those with negative amplitude are shown in blue.

(Courtesy of Mr. Hatem Helal and Professor William A. Goddard III, California Institute of Technology, and Dr. Kelly P. Gaither, University of Texas at Austin.)

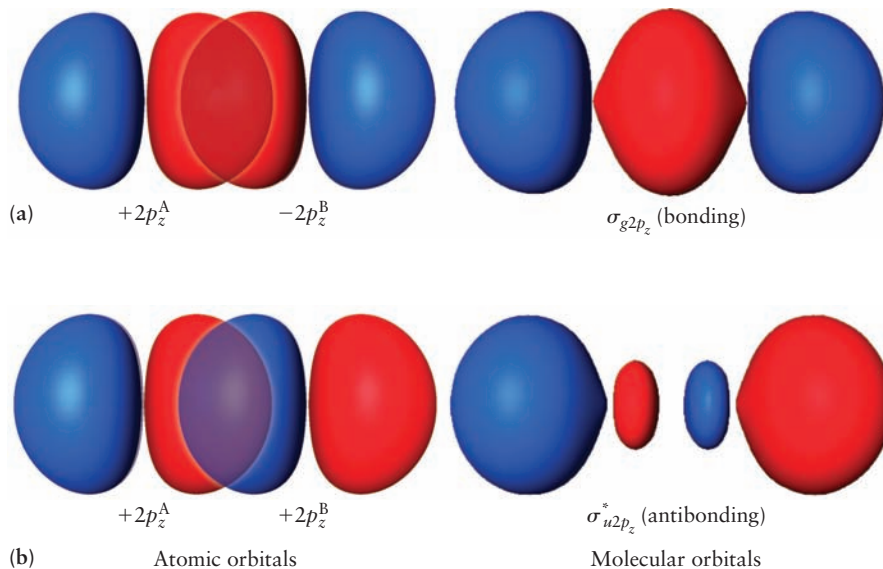
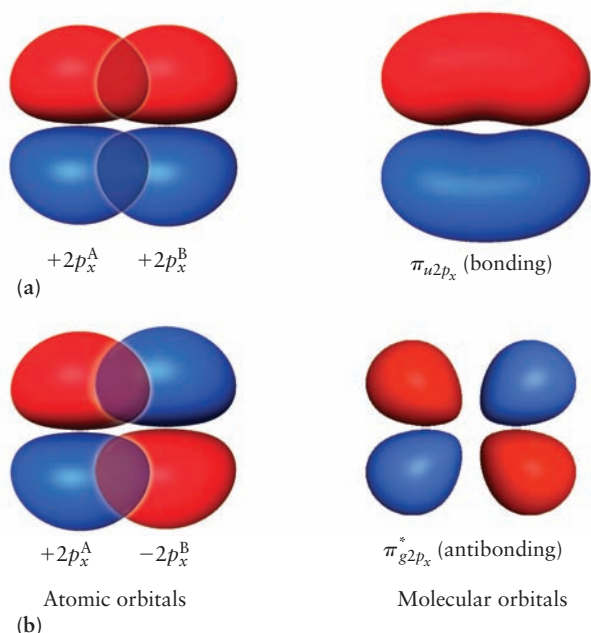


FIGURE 6.14 Formation of (a) π_{u2p_x} bonding and (b) $\pi_{g2p_x}^*$ antibonding molecular orbitals from $2p_x$ orbitals on atoms A and B.

(Courtesy of Mr. Hatem Helal and Professor William A. Goddard III, California Institute of Technology, and Dr. Kelly P. Gaither, University of Texas at Austin.)



These orbitals have a nodal plane that contains the internuclear axis (in this case, the y - z plane) and are designated by π rather than σ . In the same way, π_{u2p_y} and $\pi_{g2p_y}^*$ orbitals can be formed from the $2p_y$ AOs. Their lobes project above and below the x - z nodal plane, which is the plane of the page in Figure 6.14.

$$\pi_{u2p_y} = C_u[2p_y^A + 2p_y^B] \quad [6.12a]$$

$$\pi_{g2p_y}^* = C_g[2p_y^A - 2p_y^B] \quad [6.12b]$$

Like the $2p$ AOs from which they are constructed, the π_{2p} MOs are degenerate: π_{u2p_x} and π_{u2p_y} have the same energy, and $\pi_{g2p_x}^*$ and $\pi_{g2p_y}^*$ have the same energy. We expect π_{u2p_x} and π_{u2p_y} to be less effective than σ_{g2p_z} as bonding orbitals, because the overlap in the π orbitals occurs off the internuclear axis, and therefore has less tendency to increase the electron density between the nuclei and to pull them closer together.

The most important point to understand in constructing MOs and predicting their behavior by the overlap argument is that the relative phases of the two AOs are critical in determining whether the resulting MO is bonding or antibonding. Bonding orbitals form through the overlap of wave functions with the same phase, by constructive interference of “electron waves”; antibonding orbitals form through the overlap of wave functions with opposite phase, by destructive interference of “electron waves.”

The next step is to determine the energy ordering of the MOs. In general, that step requires a calculation, as we did for the first-period diatomics in Figures 6.8 and 6.9. The results for Li_2 through F_2 are shown in Figure 6.15. The electrons for each molecule have been placed in MOs according to the aufbau principle. We show only the MOs formed from the $2s$ and $2p$ orbitals. In second-period diatomic molecules, the $1s$ orbitals of the two atoms barely overlap. Because the σ_{g1s} bonding and σ_{u1s}^* antibonding orbitals are both doubly occupied, they have little net effect on bonding properties and need not be considered. There are two different energy ordering schemes for diatomic molecules formed from second-period elements. The first ordering (Fig. 6.16a) applies to the molecules with atoms Li

FIGURE 6.15 Energy levels for the homonuclear diatomics Li_2 through F_2 . Notice how the highest occupied level changes with the number of valence electrons. Notice especially the change between N_2 and O_2 .



through N (that is, the first part of the period) and their positive and negative ions. The second (see Fig. 6.16b) applies to the later elements, O, F, and Ne, and their positive and negative ions. The relative ordering of the σ_{g2p_z} and the π_{u2p_x} , π_{u2p_y} changes as we move across the periodic table. The energy of the π orbital remains essentially constant, whereas the energy of the σ orbital falls rapidly, dropping below that of the π orbital at O_2 . This effect is largely caused by the increased nuclear charge felt by the electrons in the σ orbital in the heavier elements.

An important prediction comes from the correlation diagrams in Figure 6.15. Hund's rules require that, in the ground state, the electrons occupy different orbitals and have parallel spins; thus, B_2 and O_2 are predicted to be paramagnetic. This paramagnetism is exactly what is found experimentally (Fig. 6.17). In contrast, in the Lewis electron dot diagram for O_2 ,



all the electrons appear to be paired. Moreover, the extremely reactive nature of molecular oxygen can be rationalized as resulting from the readiness of the two π^* electrons, unpaired and in different regions of space, to find additional bonding partners in other molecules.

The electron configurations in Figure 6.15 allow us to calculate the bond order for each molecule and correlate it with other properties of the molecules.

EXAMPLE 6.2

Determine the ground-state electron configuration and bond order of the F_2 molecule.

SOLUTION

Each atom of fluorine has 7 valence electrons, so 14 electrons are placed in the MOs to represent bonding in the F_2 molecule. The correlation diagram of Figure 6.15 gives the following electron configuration:

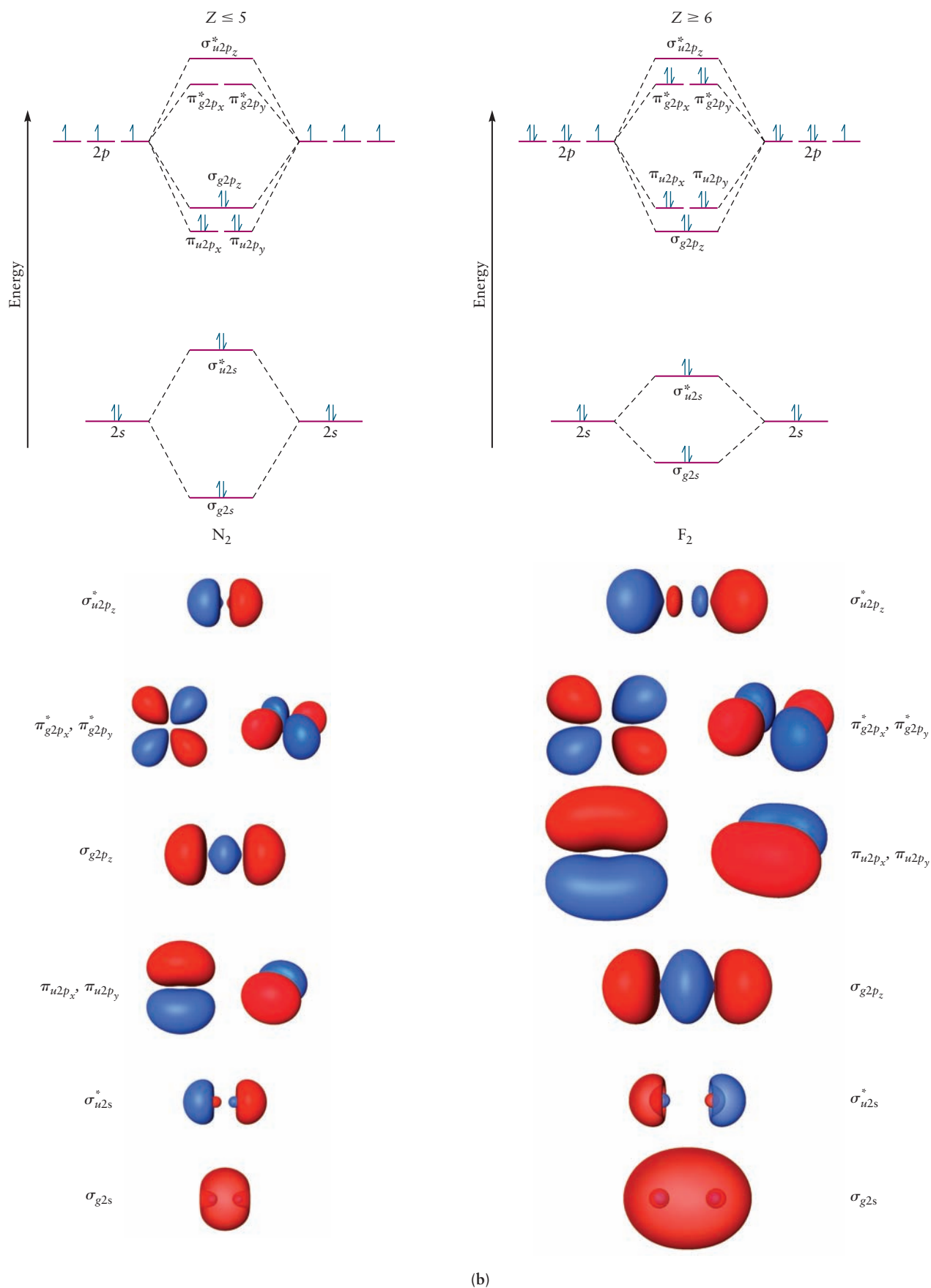
$$(\sigma_{g2s})^2(\sigma_{u2s}^*)^2(\sigma_{g2p_z})^2(\pi_{u2p_x}, \pi_{u2p_y})^4(\pi_{g2p_x}^*, \pi_{g2p_y}^*)^4$$

Because there are eight valence electrons in bonding orbitals and six in antibonding orbitals, the bond order is

$$\text{Bond order} = \frac{1}{2}(8 - 6) = 1$$

and the F_2 molecule has a single bond.

Related Problems: 17, 18, 19, 20, 21, 22, 23, 24



(a) (b)
FIGURE 6.16 Correlation diagrams for second-period diatomic molecules. (a) Correlation diagram and molecular orbitals calculated for N_2 . (b) Correlation diagram and molecular orbitals calculated for F_2 .
 (Courtesy of Mr. Hatem Helal and Professor William A. Goddard III, California Institute of Technology, and Dr. Kelly P. Gaither, University of Texas at Austin.)

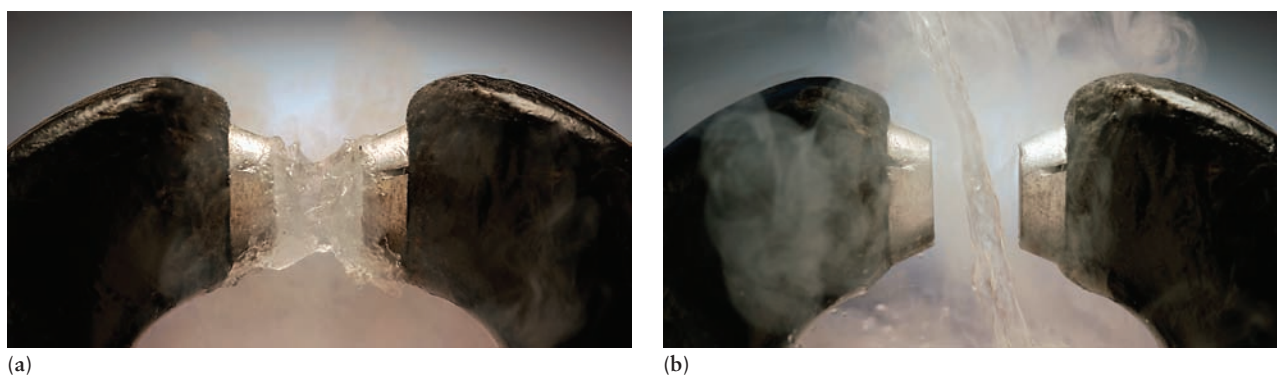


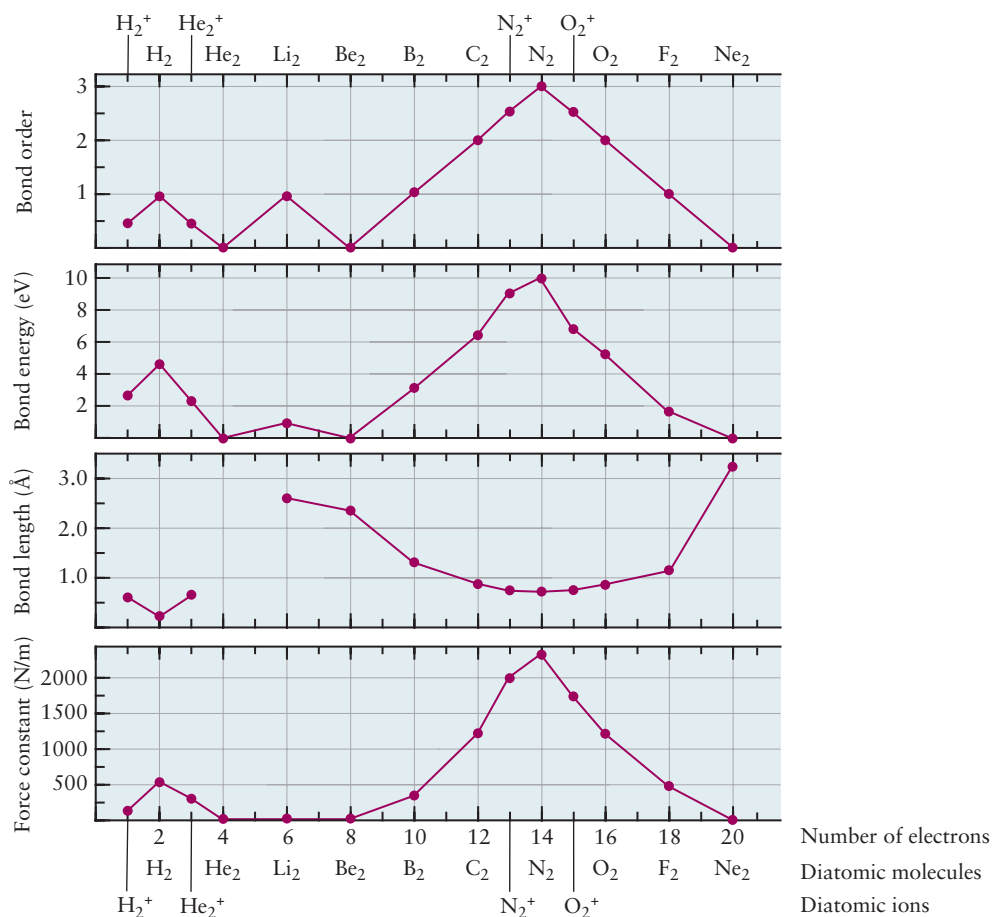
FIGURE 6.17 (a) Oxygen is paramagnetic; liquid oxygen (O_2) poured between the pole faces of a magnet is attracted and held there. (b) When the experiment is repeated with liquid nitrogen (N_2), which is diamagnetic, the liquid pours straight through. (Courtesy Larry Cameron.)

Table 6.3 summarizes the properties of second-period homonuclear diatomic molecules. Note the close relationship among bond order, bond length, and bond energy, and that the bond orders calculated from the MOs agree completely with the results of the Lewis electron dot model. How these properties depend on the number of electrons in the molecules is shown in Figure 6.18. The bond orders simply follow the filling of MOs in a given subshell, rising from 0 to 1, and then falling back to 0 for the first-period diatomics and also for Li_2 , Be_2 and their ions. The bond orders move in half-integral steps if the molecular ions are included; they increase as the σ orbitals are filled and decrease as the σ^* orbitals begin to fill. These MOs are all constructed from s orbitals, so there is no possibility for multiple bonds. Moving from Be_2 through Ne_2 , the bond orders move again in half-integer increments from 0 to 3 and back to 0 as the π orbitals and then the π^* orbitals are filled. Both bond energies and force constants are correlated directly with the bond order, whereas the bond length varies in the opposite direction. This makes perfect sense; multiple bonds between atoms should be stronger and shorter than single bonds. In summary, the simple LCAO method provides a great deal of insight into the nature of chemical bonding in homonuclear diatomic molecules and the trends in the properties that result. It is consistent with the predictions of simpler theories, such as that of G. N. Lewis, but clearly more powerful and more easily generalized to problems of greater complexity.

TABLE 6.3 Molecular Orbitals of Homonuclear Diatomic Molecules

Species	Number of Valence Electrons	Valence Electron Configuration	Bond Order	Bond Length (Å)	Bond Energy (kJ mol^{-1})
H_2	2	$(\sigma_{g1s})^2$	1	0.74	431
He_2	4	$(\sigma_{g1s})^2(\sigma_{u1s}^*)^2$	0		
Li_2	2	$(\sigma_{g2s})^2$	1	2.67	105
Be_2	4	$(\sigma_{g2s})^2(\sigma_{u2s}^*)^2$	0	2.45	9
B_2	6	$(\sigma_{g2s})^2(\sigma_{u2s}^*)^2(\pi_{u2p})^2$	1	1.59	289
C_2	8	$(\sigma_{g2s})^2(\sigma_{u2s}^*)^2(\pi_{u2p})^4$	2	1.24	599
N_2	10	$(\sigma_{g2s})^2(\sigma_{u2s}^*)^2(\pi_{u2p})^4(\sigma_{g2p_z})^2$	3	1.10	942
O_2	12	$(\sigma_{g2s})^2(\sigma_{u2s}^*)^2(\sigma_{g2p_z})^2(\pi_{u2p})^4(\pi_{g2p_z}^*)^2$	2	1.21	494
F_2	14	$(\sigma_{g2s})^2(\sigma_{u2s}^*)^2(\sigma_{g2p_z})^2(\pi_{u2p})^4(\pi_{g2p_z}^*)^4$	1	1.41	154
Ne_2	16	$(\sigma_{g2s})^2(\sigma_{u2s}^*)^2(\sigma_{g2p_z})^2(\pi_{u2p})^4(\pi_{g2p_z}^*)^4(\sigma_{u2p_z}^*)^2$	0		

FIGURE 6.18 Trends in bond order, bond length, bond energy, and force constant with the number of valence electrons in the second-row diatomic molecules.



6.2.4 Heteronuclear Diatomic Molecules

Diatomic molecules such as CO and NO, formed from atoms of two different elements, are called heteronuclear. We construct MOs for such molecules by following the procedure described earlier, with two changes. First, we use a different set of labels because heteronuclear diatomic molecules lack the inversion symmetry of homonuclear diatomic molecules. We therefore drop the *g* and *u* subscripts on the MO labels. Second, we recognize that the AOs on the participating atoms now correspond to different energies. For example, we combine the 2*s* AO of carbon and the 2*s* AO of oxygen to produce a bonding MO (without a node),

$$\sigma_{2s} = C_A 2s^A + C_B 2s^B \quad [6.13a]$$

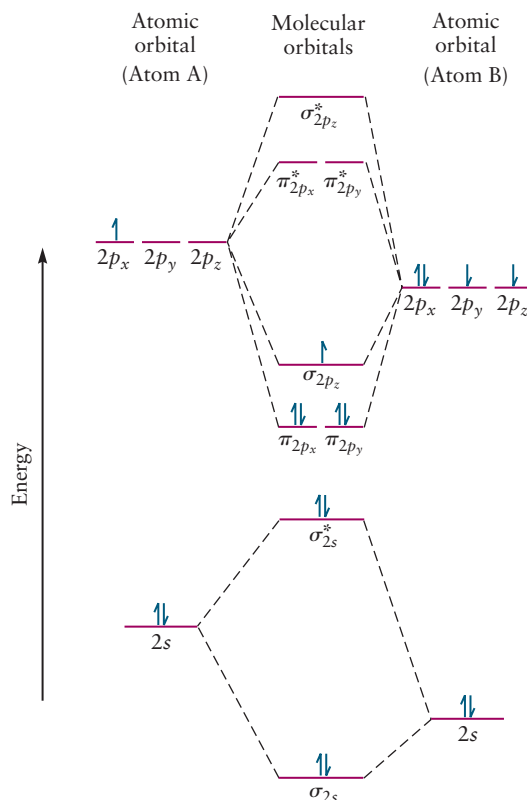
and an antibonding MO (with a node),

$$\sigma_{2s}^* = C'_A 2s^A - C'_B 2s^B \quad [6.13b]$$

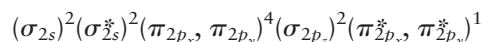
where A and B refer to the two different atoms in the molecule. In the homonuclear case, we argued that $C_A = C_B$ and $C'_A = C'_B$ because the electron must have equal probability of being near each nucleus, as required by symmetry. When the two nuclei are different, this reasoning does not apply. If atom B is more electronegative than atom A, then $C_B > C_A$ for the bonding σ MO (and the electron spends more time on the electronegative atom); $C'_A > C'_B$ for the higher energy σ^* MO, and it will more closely resemble a $2s^A$ AO.

Molecular orbital correlation diagrams for heteronuclear diatomics start with the energy levels of the more electronegative atom displaced *downward*, because

FIGURE 6.19 Correlation diagram for heteronuclear diatomic molecules, AB. The atomic orbitals for the more electronegative atom (B) are displaced downward because they have lower energies than those for A. The orbital filling shown is that for (boron monoxide) BO.

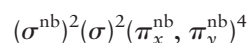


that atom attracts valence electrons more strongly than does the less electronegative atom. Figure 6.19 shows the diagram appropriate for many heteronuclear diatomic molecules of second-period elements (where the electronegativity difference is not too great). This diagram has been filled with the valence electrons for the ground state of the molecule BO. Another example, NO, with 11 valence electrons (5 from N, 6 from O), has the following ground-state configuration:



With eight electrons in bonding orbitals and three in antibonding orbitals, the bond order of NO is $\frac{1}{2}(8 - 3) = 2\frac{1}{2}$ and it is paramagnetic. The bond energy of NO should be smaller than that of CO, which has one fewer electron but a bond order of 3; experiment agrees with this prediction.

We explained earlier that, in homonuclear diatomics, AOs mix significantly to form MOs only if they are fairly close in energy and have similar symmetries. The same reasoning is helpful in constructing MOs for heteronuclear diatomics. For example, in the HF molecule, both the 1s and 2s orbitals of the F atom are far too low in energy to mix with the H 1s orbital. Moreover, the overlap between the H 1s and F 2s is negligible (Fig. 6.20a). The net overlap of the H 1s orbital with the $2p_x$ or $2p_y$ F orbital is zero (see Fig. 6.20c) because the regions of positive and negative overlap sum to zero. This leaves only the $2p_z$ orbital of F to mix with the H 1s orbital to give both σ bonding and σ^* antibonding orbitals (see Figs. 6.20b, d). The correlation diagram for HF is shown in Figure 6.21. The $2s$, $2p_x$, and $2p_y$ orbitals of fluorine do not mix with the 1s of hydrogen, and therefore remain as atomic (nonbonding) states denoted σ^{nb} and π^{nb} . Electrons in these orbitals do not contribute significantly to the chemical bonding. Because fluorine is more electronegative than hydrogen, its $2p$ orbitals lie below the 1s hydrogen orbital in energy. The σ orbital then contains more fluorine $2p_z$ character, and the σ^* orbital more closely resembles a hydrogen 1s AO. When the eight valence electrons are put in for HF, the result is the MO configuration:



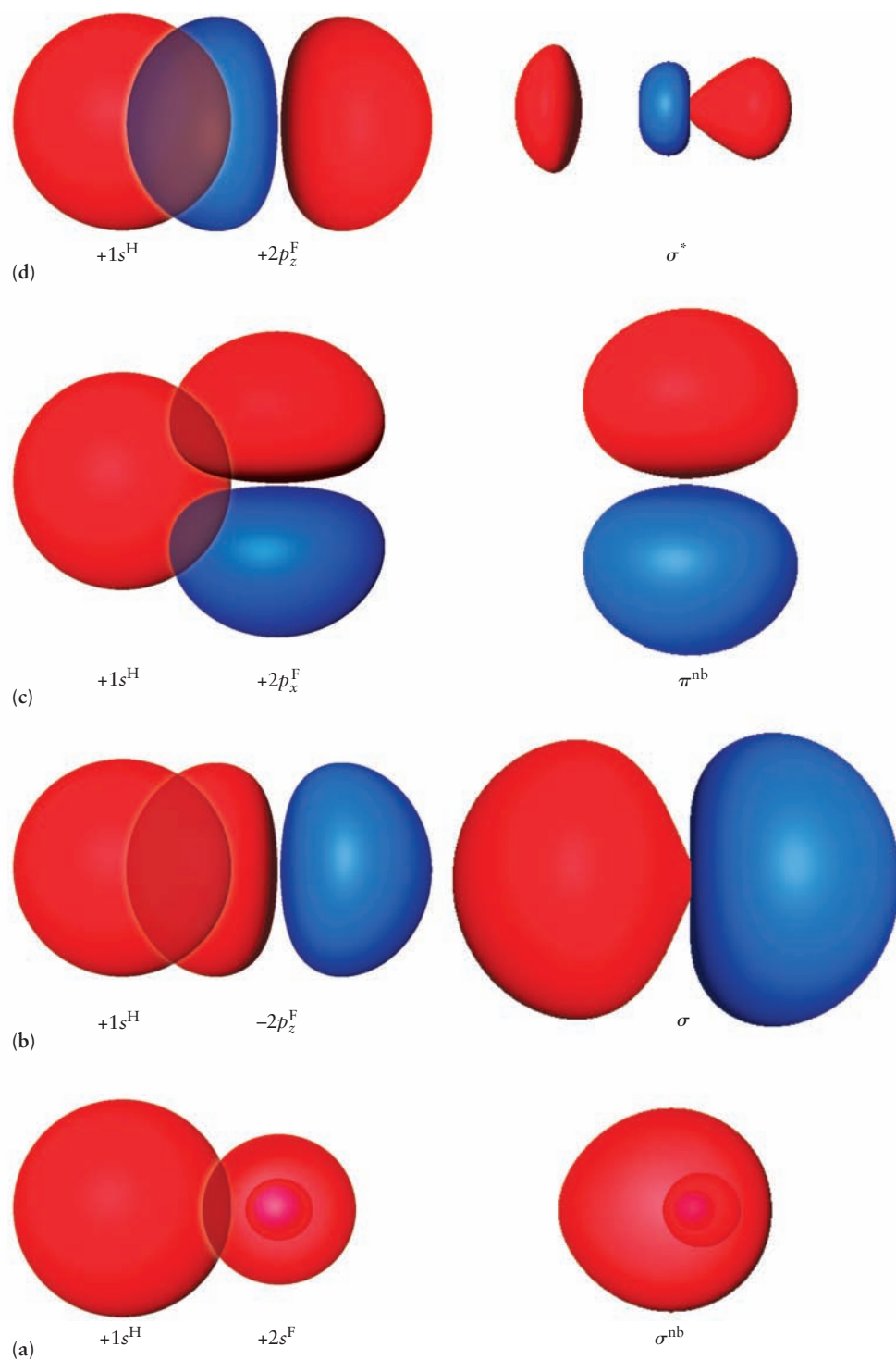
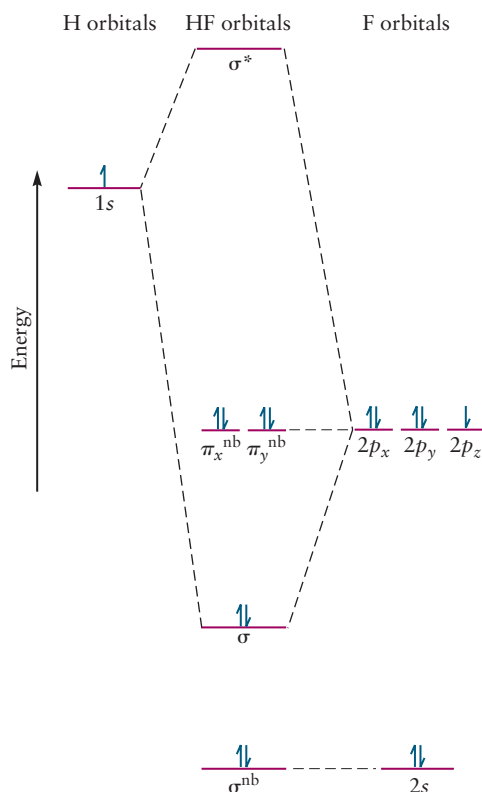


FIGURE 6.20 Overlap of atomic orbitals in HF.

(Courtesy of Mr. Hatem Helal and Professor William A. Goddard III, California Institute of Technology, and Dr. Kelly P. Gaither, University of Texas at Austin.)

FIGURE 6.21 Correlation diagram for HF. The $2s$, $2p_x$ and $2p_y$ atomic orbitals of fluorine do not mix with the $1s$ atomic orbital of hydrogen, and therefore remain nonbonding.



The net bond order is 1, because electrons in **nonbonding** AOs do not affect bond order. The electrons in the 1σ orbital are more likely to be found near the fluorine atom than near the hydrogen atom; thus, HF has the dipole moment $\text{H}^{\delta+}\text{F}^{\delta-}$.

If a more electropositive atom (such as Na or K) is substituted for H, the energy of its outermost s orbital will be higher than that of the H atom, because its ionization energy is lower. In this case, the σ orbital will resemble a fluorine $2p_z$ orbital even more (that is, the coefficient C_F of the fluorine wave function will be close to 1, and C_A for the alkali atom will be very small). In this limit, the molecule can be described as having the valence electron configuration $(\sigma^{\text{nb}})^2(\pi_x^{\text{nb}}, \pi_y^{\text{nb}}, \pi_z^{\text{nb}})^6$, which corresponds to the ionic species Na^+F^- or K^+F^- . The magnitudes of the coefficients in the MO wave function are thus closely related to the ionic-covalent character of the bonding and to the dipole moment.

Summary Comments for the Linear Combination of Atomic Orbitals Method and Diatomic Molecules

The qualitative LCAO method can rationalize trends in bond length and bond energy in a group of molecules by relating both these properties to bond order, but it cannot predict bond energy or molecular geometry. Both of these properties require calculation of the electron energy as a function of the positions of the nuclei, as shown in Figure 6.7 for H_2^+ . The equilibrium bond length is then identified as the minimum of this potential energy curve. The LCAO method can be extended to quantitative calculations of molecular properties using modern computer programs to calculate this potential energy curve, once the basis set of AOs has been chosen. Through a variety of software packages, such calculations are now routinely available to chemists engaged in both fundamental and applied work.

A DEEPER LOOK

6.2.5 Potential Energy and Bond Formation in the LCAO Approximation

The potential energy curves shown in Figure 6.7 are among the most important concepts in the quantum picture of the chemical bond and molecular structure. It is important to see how these curves arise from the electron–nucleus attractions and the nuclear–nuclear repulsions in the molecule and how the chemical bond is formed.

Although beyond the scope of this textbook, it is straightforward in quantum mechanics to calculate the energy of the electron in σ_{g1s} and σ_{u1s}^* when the nuclei are fixed at R_{AB} , and to include the value of the nuclear repulsion at R_{AB} . We will represent these values as E_{1g} and E_{1u} , respectively. The results are

$$E_{1g}(R_{AB}) = E_H(1s) + \frac{J + K}{1 + S_{AB}} + \frac{e^2}{4\pi\epsilon_0 R_{AB}} \quad [6.14a]$$

$$E_{1u}(R_{AB}) = E_H(1s) + \frac{J - K}{1 - S_{AB}} + \frac{e^2}{4\pi\epsilon_0 R_{AB}} \quad [6.14b]$$

where J , K , and S_{AB} represent collections of terms that depend on R_{AB} through the dimensionless variable $\rho = R_{AB}/a_0$:

$$S_{AB} = e^{-\rho} \left(1 + \rho - \frac{\rho^2}{3} \right)$$

$$J = -\frac{e^2}{4\pi a_0} \left[\frac{1}{\rho} - e^{-2\rho} \left(1 + \frac{1}{\rho} \right) \right]$$

$$K = -\frac{e^2}{4\pi a_0} e^{-\rho} (1 + \rho)$$

We will see that each term in Equations 6.14a and 6.14b has a straightforward interpretation and is easily understood in graphical form.

The first term in each equation is the energy of the H(1s) state, which is independent of R_{AB} . Therefore, it is just a constant added to the other terms.

As R_{AB} becomes large, approaching infinity, the second and third terms are negligible, so both E_{1g} and E_{1u} approach the value $E_H(1s)$. This is the correct energy for a hydrogen atom and a proton separated by a large distance. This result shows that both E_{1g} and E_{1u} have the simple limiting behavior that we expect.

The second term in each equation is the energy contribution arising from the interaction of the electron with both of the protons; note that this term differs in the two orbitals. We call this the *electronic bonding energy* of the electron in each orbital and denote it by $E_{1g}^{(el)}$ or $E_{1u}^{(el)}$.

The final term in each equation is the nuclear repulsion energy at R_{AB} . This term goes to zero at large values of R_{AB} , when the protons are very far apart. This term becomes large and positive at small values of R_{AB} , as the protons get very close together.

Now, let's put these pieces together to understand the overall behavior, first for the MO σ_{g1s} . In Figure 6.22a, we plot $E_{1g}^{(el)}$ as the lighter red curve and the nuclear repulsive term as the black

curve. The electronic bonding energy represents the strength with which the electron is held by the two protons. Conversely, it also represents the effect of the electron in holding the two protons close together. Therefore, it is conventional in molecular quantum mechanics to interpret the electronic bonding energy of the electron as the *attractive* portion of the potential energy of interaction between the two protons. With this insight, we account for all the potential energy of interaction between the protons—both attractive and repulsive—and define the effective potential energy between the protons by adding the proton–proton repulsion to the electronic bonding energy at each point along the internuclear axis,

$$V_{1g}^{(eff)}(R_{AB}) = E_{1g}^{(el)}(R_{AB}) + V_{nn}(R_{AB}) \quad [6.15]$$

The heavy red curve in Figure 6.22a shows $V_{1g}^{(eff)}(R_{AB})$. By omitting $E_H(1s)$ from this plot, we are setting the zero of the effective potential energy as the energy of a proton and a hydrogen atom when they are infinitely far apart. The effective potential energy in the σ_{g1s} MO decreases as the proton and hydrogen atom begin to interact, reaching a minimum at the position $R_{AB} = R_e$ before rising again because of the strong repulsive forces between the nuclei. Considered together, the increased electron density and the lowered potential energy between the nuclei demonstrate that σ_{g1s} is a bonding MO.

Now let's see how the effective potential energy curve behaves in the σ_{u1s}^* MO. Proceeding exactly as before, we show the electron electronic bonding energy $E_{1u}^{(el)}$ as the light blue curve and the nuclear repulsive term as the black curve in Figure 6.22b. We combine these to obtain $V_{1u}^{(eff)}(R_{AB})$ (shown by the heavy blue curve in Fig. 6.22b). The effective potential energy in the σ_{u1s}^* state is positive at all distances, increasing as the internuclear distance becomes shorter. This potential generates a repulsive force that pushes the nuclei apart, so the system remains a separated proton and hydrogen atom. In contrast with σ_{g1s} , the σ_{u1s}^* MO shows potential energy higher than the energy of the separated proton and hydrogen atom and zero electron density at the midpoint between the nuclei. So, σ_{u1s}^* is an antibonding MO.

The effective potential energy $V(R_{AB})$ for a diatomic molecule has the general shape shown on the next page where D_e is the bond dissociation energy and R_e is the equilibrium bond length. How do we connect the effective potential energy curve to the total energy of the molecule, which must decrease during bond formation? Each point on this curve represents the potential energy stored in the molecule, by virtue of the interactions of the protons with the electron and with each other, as a function of the internuclear separation R_{AB} . We must now include the kinetic energy of the nuclei. The molecule displays translational kinetic energy as it flies through space, rotational kinetic energy as it rotates about its center of mass, and vibrational kinetic energy as the bond is stretched. Let's focus attention to the vibrational kinetic energy because it relates directly to the changes in the internuclear separation R_{AB} . Suppose the molecule contains a total amount of internal energy E_{tot} , which consists of the effective potential energy and the vibrational kinetic energy. At each value of R_{AB} the vibrational kinetic energy of the nuclei is given by $\mathcal{T} = E_{tot} - V_{eff}$. The kinetic energy goes to

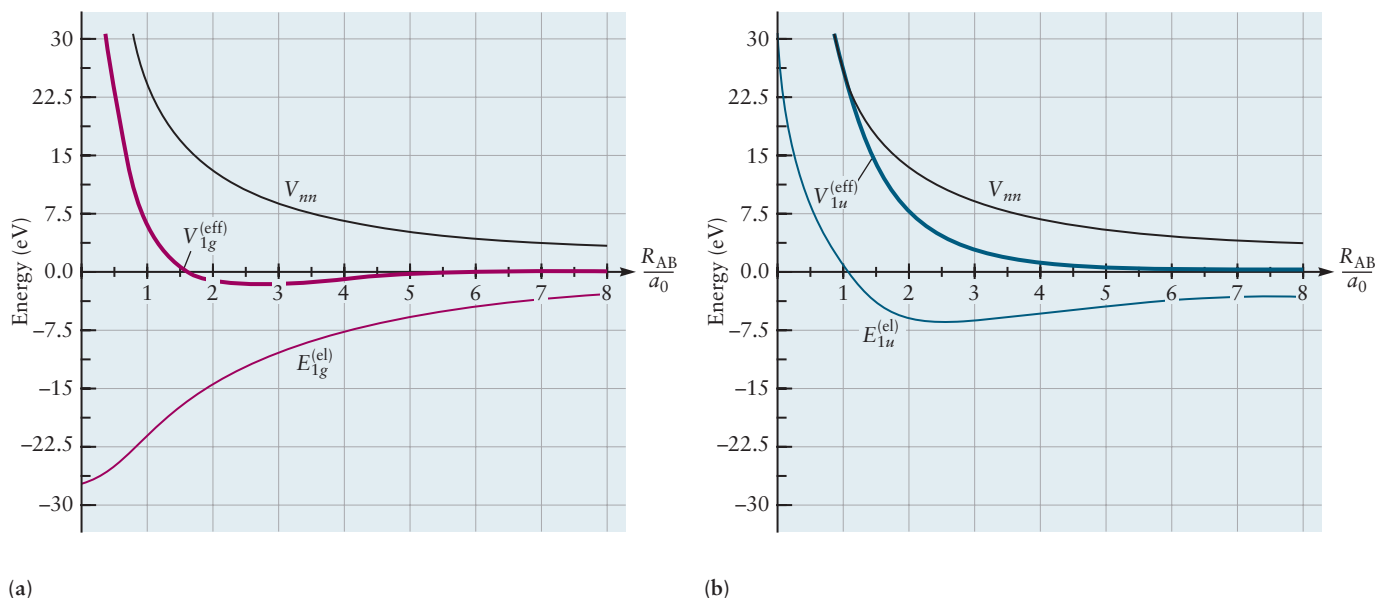
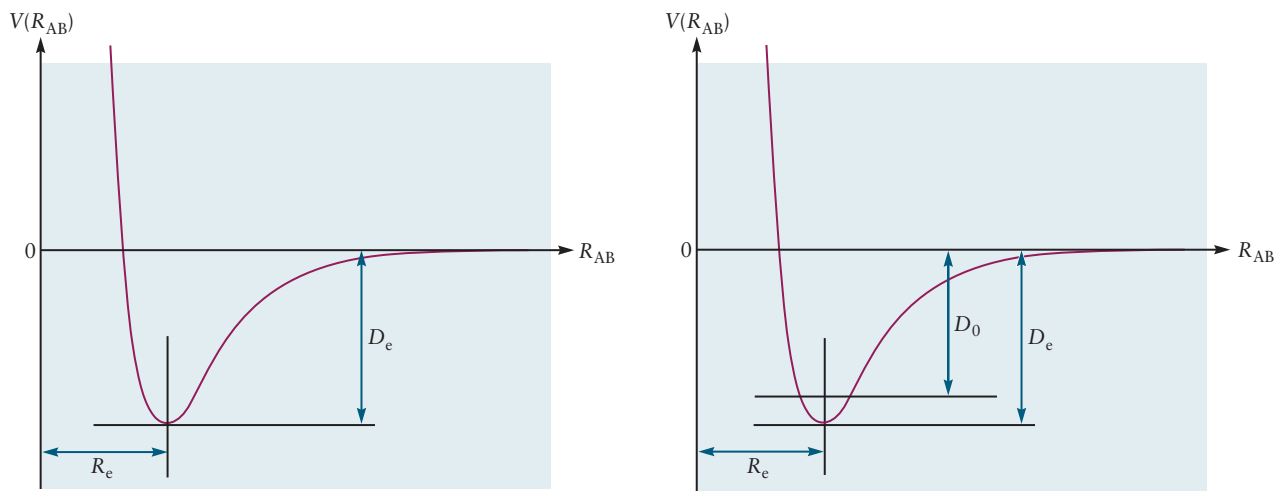


FIGURE 6.22 Dependence on internuclear distance of the contributions to the effective potential energy of the nuclei in H_2^+ . (a) The effective potential energy in the σ_{g1s} MO. The electronic bonding energy for the electron is the lighter red curve, the internuclear repulsion between the protons is the black curve, and their sum is the heavier red curve. (b) The effective potential energy in the σ_{u1s} MO. The electronic bonding energy for the electron is the lighter blue curve, the internuclear repulsion between the protons is the black curve, and their sum is the heavier blue curve. The behavior of the effective potential energy shows that the σ_{g1s} MO is bonding and that the σ_{u1s} MO is antibonding.

(Adapted from R. S. Berry, S. A. Rice, and J. Ross, *Physical Chemistry* (2nd ed), New York: Oxford, 2000, Figure 6.5ab, by permission.)



zero at the *classical turning points* where $E_{\text{tot}} = V_{\text{eff}}$, and the motion of the nuclei reverses direction. (See the discussion of vibrational motion in Appendix B2, especially Figure B.1.)

The total internal energy of the molecule is quantized, so we can visualize a set of energy levels superposed on the effective potential energy curve. Just as shown for the particle-in-a-box model (see Sec. 4.6), the uncertainty principle requires that there is a **zero-point energy** for the molecule (see Sec. 4.7). This is the lowest allowed value of the total internal energy, and is represented by the line D_0 . Because the zero-point energy can never be removed from the molecule, it provides a reference point for the additional amount of energy required to dissociate the molecule. Relative to the zero-point energy, the dissociation energy is defined as D_0 . Although both D_0 and D_e are called dissociation energies, only the former is measurable experimentally as the energy needed to dissociate the molecule. D_e is useful as a

parameter to construct model potentials and optimize geometry in calculations.

In summary then, the structure and energetics of a diatomic molecule are defined by the parameters R_e , D_e , and D_0 on the effective potential energy curve for the molecule, all of which can be calculated within the Born–Oppenheimer approximation (see the figure above). In Chapter 20 we show how R_e and D_0 can be determined experimentally by molecular spectroscopy.

The idea of an effective potential function between the nuclei in a molecule can be formulated empirically (as we have done in Section 3.5 and Fig. 3.9), but it can be defined precisely and related to molecular parameters R_e , D_e , and D_0 only through quantum mechanics. The fundamental significance of the Born–Oppenheimer approximation is its separation of electronic and nuclear motions, which leads directly to the effective potential function.

MECHANISM OF BOND FORMATION Let's inquire a bit more deeply into the energy changes involved in formation of the bond. Recall from Section 3.6 that spontaneous formation of a bond requires the collection of nuclei and electrons to give up some portion of their total energy to the surroundings. Recall also that the virial theorem guarantees this reduction in the average total energy, $\Delta\bar{E}$, is accompanied by a decrease in the average potential energy, $\Delta\bar{V}$, and an increase in the average kinetic energy, $\Delta\bar{\mathcal{T}}$. Moreover, the reduction in potential energy must be twice as large as the gain in kinetic energy: $\Delta\bar{V} = -2\Delta\bar{\mathcal{T}}$.

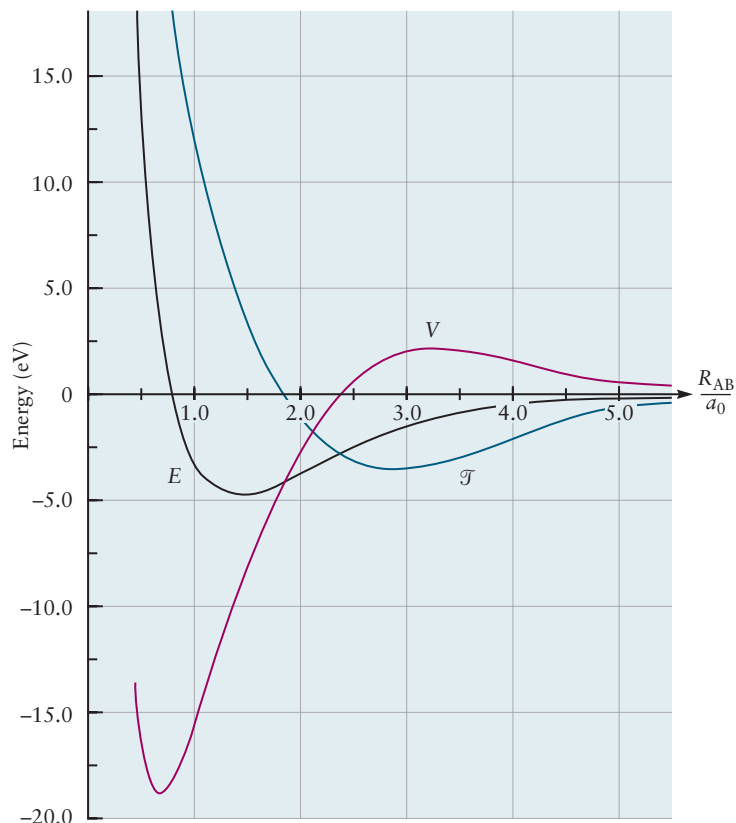
How are these conditions satisfied during bond formation? It is helpful to think about a hydrogen atom and a proton approaching together to form H_2^+ in one dimension, along the bond axis. When the atoms are far apart, they are completely independent, and the electron is confined to one of the protons. As the proton and the hydrogen atom approach one another, the electron of the hydrogen atom begins to be attracted to the proton. This attraction reduces the Coulomb attraction between the electron and the proton to which it was originally bound, thus increasing its potential energy. Because the electron is now interacting with two protons, it can occupy a greater region of space than when it was part of an isolated hydrogen atom. So, its kinetic energy decreases as it becomes less confined (recall that the energies of the particle in a box decrease as the size of the box increases). The rapid decrease in kinetic energy more than offsets the initial increase in potential energy, so it is responsible for initiating bond formation.

As bond formation continues, the distance between the protons decreases. Then, the simultaneous electrostatic attraction of the electron to *two* protons decreases the potential energy, and the confinement of the electron to the now smaller internuclear region increases its kinetic energy. The equilibrium bond length is determined by these opposing forces.

In more advanced work, it is possible to calculate separately the average kinetic and potential energy, as well as the average total energy, at various stages of bond formation. The results are shown as a function of R_{AB} in Figure 6.23. Notice that the average total energy decreases steadily, as required for bond formation, until it begins to increase at very short internuclear distances due to nuclear–nuclear repulsion. As the internuclear separation decreases, at each step the change in average kinetic energy and the change in average potential energy can be compared through the virial theorem to see which provides the dominant contribution to the decrease in total energy. As shown in Figure 6.23, decreasing the kinetic energy in the early stages of bond formation is essential to overcome the increase in potential energy as the electron leaves “its” nucleus. Then, the kinetic energy rapidly increases again at short distances to balance the strong Coulomb attraction of the electron to the protons.

Most introductory accounts of chemical bonding attribute the stability of the covalent bond solely to a reduction in the electrostatic potential energy, relative to that of the isolated atoms. But that is only one part of the story. The interplay between kinetic and potential energy at each stage of bond formation determines the ultimate stability. The driving force for bond formation in an ionic bond is readily explained by the reduction in the potential energy alone, because the bonding in this case is well described by the *electrostatic* interaction between two charged ions. But in the covalent bond the charge distribution is *dynamic* and cannot be described by classical electrostatics alone. The energetics of covalent bond formation must be described by quantum mechanics. The virial theorem provides a conceptual guide for analyzing the subtle transfer of energy that occurs during the formation of a covalent chemical bond.

FIGURE 6.23 Average values of the total, kinetic, and potential energies of H_2 as functions of the internuclear distance.



A DEEPER LOOK

6.2.6 Small Polyatomic Molecules

In this section, we extend the LCAO treatment to the linear triatomics BeH_2 and CO_2 not only to illustrate its generality but also to compare the results with the predictions of VSEPR theory and (later) VB theory for these molecules.

 BeH_2

Recall from the assertions made in Section 6.2.4 that AOs only make significant contributions to a MO if: (1) their atomic energy levels are close together, and (2) they overlap significantly. Consequently, we need to consider only the $2s$ and $2p_z$ orbitals on beryllium (Be) and the $1s$ orbitals on hydrogen. Formation of the bonding MOs is illustrated in Figure 6.24. Note the direction of the positive z -axis because it defines our sign convention. We form two bonding orbitals by taking linear combinations of either the beryllium $2s$ or $2p_z$ orbital with the hydrogen $1s$ orbitals, choosing the relative phases to concentrate the amplitude (and thus the electron density) between each pair of atoms. We use the simplified notation introduced in Equations 6.9a and 6.9b, but adopt the convention that the first AO

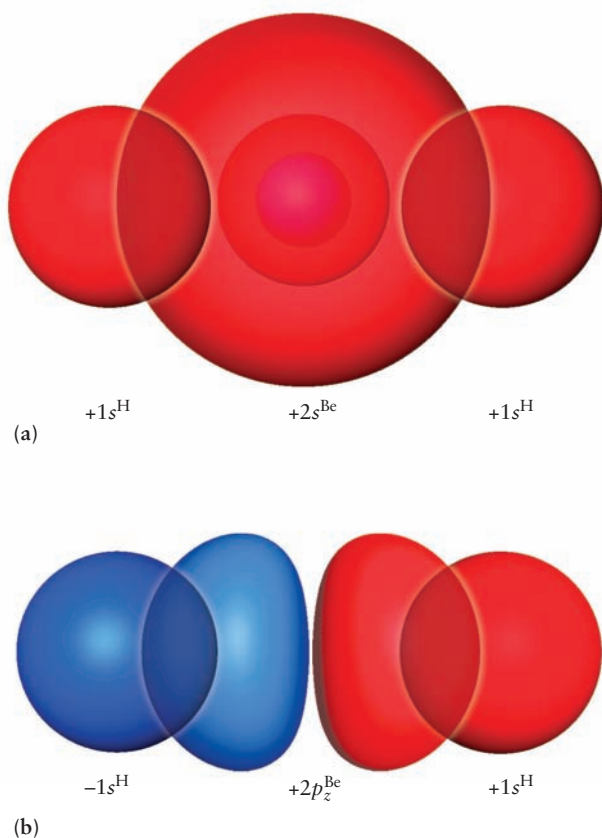


FIGURE 6.24 Overlap of atomic orbitals to form bonding molecular orbitals in BeH_2 . (a) Overlap of H $1s$ orbitals with Be $2s$. (b) Overlap of H $1s$ orbitals with Be $2p_z$.

(Courtesy of Mr. Hatem Helal and Professor William A. Goddard III, California Institute of Technology, and Dr. Kelly P. Gaither, University of Texas at Austin.)

belongs to beryllium and the second pair of orbitals belongs to hydrogen. Because the beryllium $2s$ orbital is spherically symmetric, it is clear that we form the bonding MO by adding the hydrogen orbitals in phase with the beryllium $2s$ orbital. Adding the hydrogen orbitals out of phase with the beryllium $2s$ orbital generates the antibonding MO. The results are

$$\sigma_s = C_1 2s + C_2(1s^{\text{A}} + 1s^{\text{B}}) \quad [6.16\text{a}]$$

$$\sigma_s^* = C_3 2s - C_4(1s^{\text{A}} + 1s^{\text{B}}) \quad [6.16\text{b}]$$

In these equations for small polyatomic molecules, the first AO belongs to the central atom, and the second set of equivalent starting orbitals from the surrounding atoms are identified by the labels A, B, C, D. In this case, A and B identify the left and right hydrogen atoms shown in Figure 6.24. Constructing σ orbitals from the beryllium $2p_z$ orbital, in contrast, requires a different choice of phases because it has a node at the nucleus. We must add the hydrogen orbitals with opposite phases to ensure constructive interference with each lobe of the beryllium $2p_z$ orbital to form a bonding MO; the opposite choice leads to the antibonding MO. Therefore, the resulting MOs are

$$\sigma_p = C_5 2p_z + C_6(1s^{\text{A}} - 1s^{\text{B}}) \quad [6.17\text{a}]$$

$$\sigma_p^* = C_7 2p_z - C_8(1s^{\text{A}} - 1s^{\text{B}}) \quad [6.17\text{b}]$$

The $2p_x$ and $2p_y$ beryllium orbitals do not participate in bonding because they would form π orbitals, but hydrogen does not have any p orbitals in its valence shell that can be used to form π bonds. So, they are labeled π_x^{nb} and π_y^{nb} .

Further progress in understanding these MOs requires values for the coefficients $C_1 - C_8$. We used an iterative, self-consistent computer calculation to identify the best values. The resulting MOs are shown in Figure 6.25.

The MO energy-level diagram for BeH_2 is shown in Figure 6.26. The relative displacements of the AOs are determined from the ionization energies of the respective atoms. The energy levels of the four MOs just constructed are shown in the center of the diagram and are linked to their parent AOs by the dashed lines. Note the energy levels of the two nonbonding orbitals arising from the beryllium p_x and p_y orbitals; they remain the same as in the beryllium atom. The ground-state electron configuration for BeH_2 is obtained in the usual way by applying the aufbau principle. Beryllium contributes two electrons, and each hydrogen atom contributes one electron; thus, the resulting electron configuration for the ground state is $(\sigma_s)^2(\sigma_p)^2$. Each bond is a single bond.

 CO_2

CO_2 is a linear triatomic molecule whose MOs and energy-level structure are slightly more complex than those of BeH_2 due to the existence of π bonds. As for the diatomics, we separate the σ bonds from the π bonds based on their symmetry. The carbon $2s$ and $2p_z$ orbitals have the proper (cylindrical) symmetry to participate in the formation of σ bonds, as do the oxygen $2s$ and $2p_z$ orbitals. Including the oxygen $2s$ orbitals would certainly improve the accuracy of the approximation but would greatly complicate the development of the argument without adding any

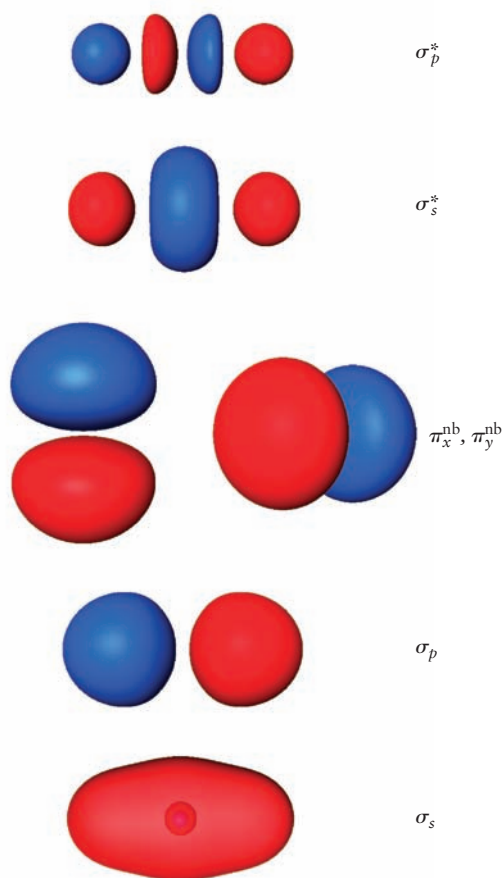


FIGURE 6.25 The isosurfaces shown are those for which the amplitude of the wave function is ± 0.2 of the maximum amplitude.

(Courtesy of Mr. Hatem Helal and Professor William A. Goddard III, California Institute of Technology, and Dr. Kelly P. Gaither, University of Texas at Austin.)

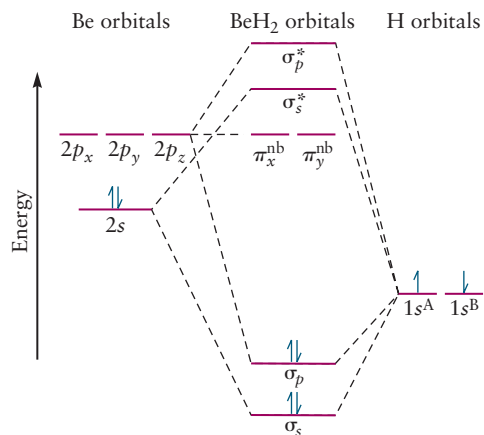


FIGURE 6.26 Energy-level diagram for BeH_2 .

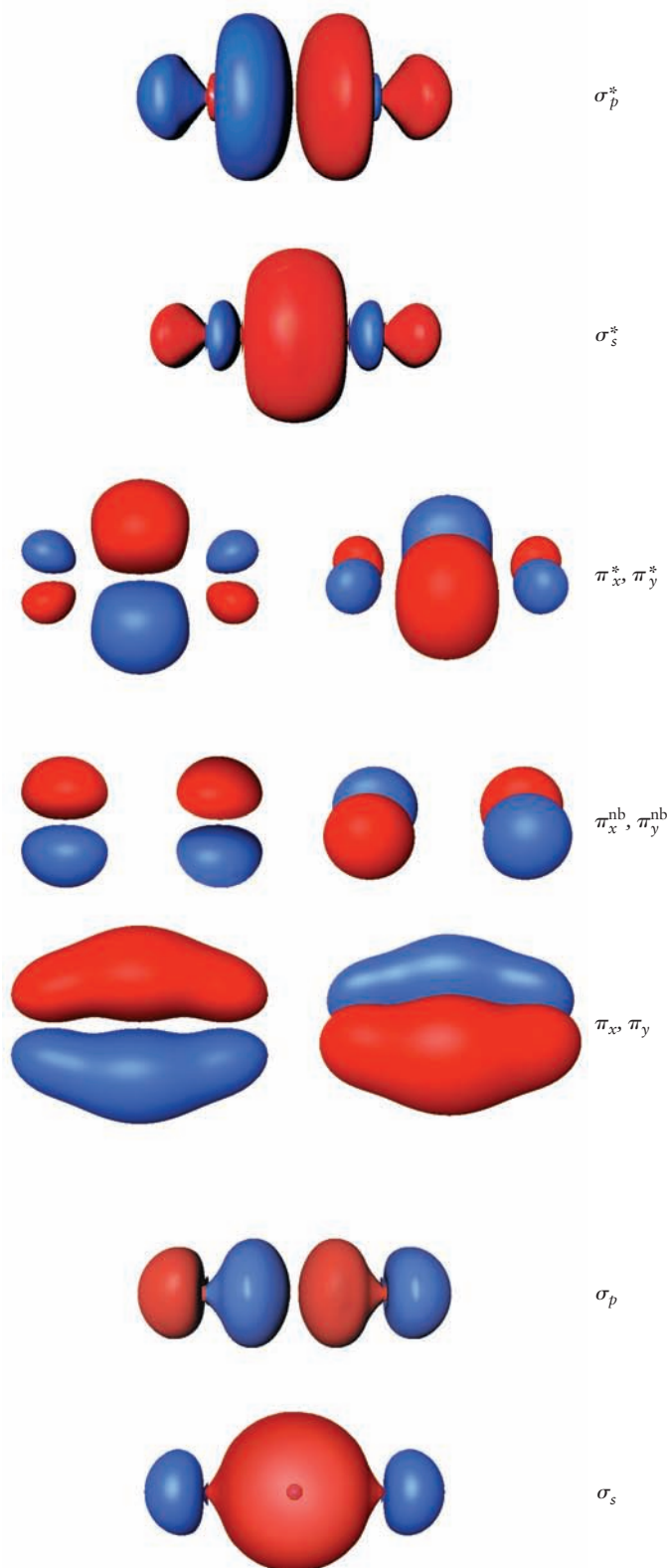
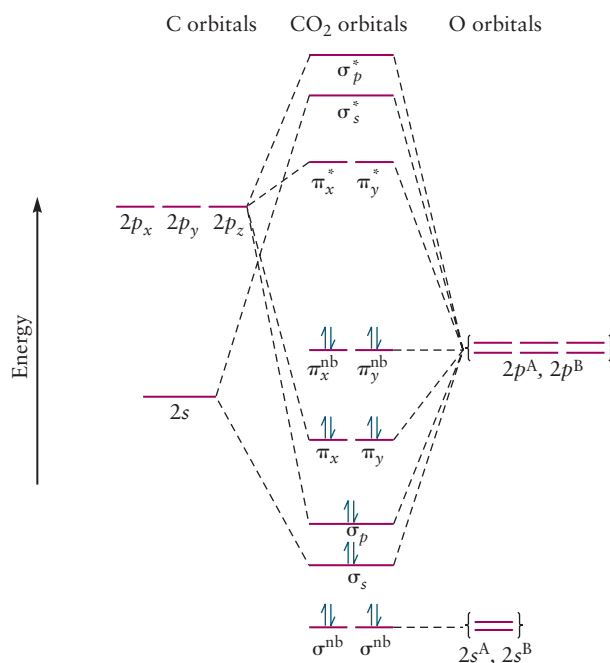


FIGURE 6.27 The isosurfaces shown are those for which the amplitude of the wave function is ± 0.2 of the maximum amplitude.

(Courtesy of Mr. Hatem Helal and Professor William A. Goddard III, California Institute of Technology, and Dr. Kelly P. Gaither, University of Texas at Austin.)

FIGURE 6.28 Energy-level diagram for CO₂.



new insights, so we omit them here for simplicity. The resulting bonding and antibonding MOs are

$$\sigma_s = C_1 2s + C_2 (2p_z^A + 2p_z^B) \quad [6.18a]$$

$$\sigma_s^* = C_3 2s - C_4 (2p_z^A + 2p_z^B) \quad [6.18b]$$

$$\sigma_p = C_5 2p_z + C_6 (2p_z^A - 2p_z^B) \quad [6.19a]$$

$$\sigma_p^* = C_7 2p_z - C_8 (2p_z^A - 2p_z^B) \quad [6.19b]$$

$$\pi_x = C_9 2p_x + C_{10} (2p_x^A + 2p_x^B) \quad [6.20a]$$

$$\pi_x^* = C_{11} 2p_x - C_{12} (2p_x^A + 2p_x^B) \quad [6.20b]$$

$$\pi_y = C_{13} 2p_y + C_{14} (2p_y^A + 2p_y^B) \quad [6.21a]$$

$$\pi_y^* = C_{15} 2p_y - C_{16} (2p_y^A + 2p_y^B) \quad [6.21b]$$

where, as for BeH₂, A and B are used to label the outer atoms, in this case, the oxygen atoms. In addition to the bonding and antibonding MOs, there is a pair of nonbonding MOs that result from no *net* overlap with the central carbon 2p_x or 2p_y orbitals.

$$\pi_x^{\text{nb}} = C_{17} (2p_x^A - 2p_x^B) \quad [6.22a]$$

$$\pi_y^{\text{nb}} = C_{18} (2p_y^A - 2p_y^B) \quad [6.22b]$$

We determined the optimum values for the coefficients by an iterative, self-consistent computer calculation. The resulting MOs for CO₂ are shown in Figure 6.27.

The energy-level structure of CO₂ is shown in Figure 6.28. With 16 valence electrons, the ground-state configuration of CO₂ is $(\sigma^{\text{nb}})^2 (\sigma^{\text{nb}})^2 (\sigma_s)^2 (\sigma_p)^2 (\pi_x, \pi_y)^4 (\pi_x^{\text{nb}}, \pi_y^{\text{nb}})^4$. The bond order for each CO bond is 2 because there is a σ bond and a π bond between each pair of atoms.

6.3 Photoelectron Spectroscopy for Molecules

In photoelectron spectroscopy (PES), we illuminate a sample with high-frequency radiation (ultraviolet or x-ray) and measure the kinetic energy of the photoelectrons emitted from the sample (see Fig. 5.18.) We show the results as a graph or spectrum of the count rate (number of photoelectrons emitted per second) plotted against the kinetic energy (see Fig. 5.19). We used PES in Section 5.4 to confirm the shell structure of the atom predicted by quantum mechanics (see Fig. 5.21). For molecules, PES confirms the MO description of bonding and measures the energy, ϵ , for individual MOs. The bridge between PES results and MO theory is Koopmans's theorem (stated in Section 5.4). These three tools are used together to study the electronic structure of molecules in all branches of chemistry. You should master each of them and become expert in using them together.

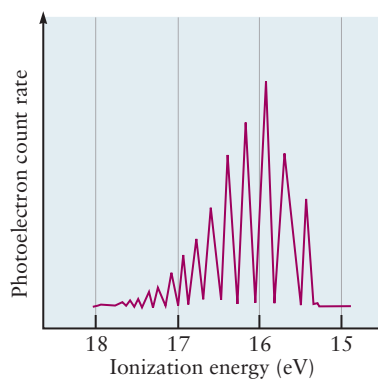


FIGURE 6.29 The photoelectron spectrum of H_2 shows a series of peaks corresponding to vibrational excitation of H_2^+ .

As a concrete example, suppose we illuminate a diatomic gaseous sample with He(I) radiation, which has energy of 21.22 eV and a wavelength of 58.43 nm. The energy of the photon is specified, and we measure the kinetic energy of the emitted photoelectrons with an energy analyzer. The resulting PES spectrum shows a series of peaks, each of which we label with an index i . We subtract the measured kinetic energy from the photon energy, which is fixed in our experiment. Thus, by conservation of energy, we are measuring the *ionization energy*, IE_i , required to liberate those electrons that contribute to peak i . Koopmans's theorem states that the measured ionization energy is the negative of the energy of the orbital from which the photoelectrons were emitted: $IE_i = -\varepsilon_i$. (Recall that IE_i is positive because it must be provided to the system, and that ε_i is negative because it measures the amount by which the orbital is stabilized relative to free atoms.) Koopmans's theorem is only an approximation, because it assumes that the ion produced during photoemission has the same orbital energies as the parent neutral molecule. In addition to the relaxation of the resulting ion as observed for atoms (see discussion in Section 5.4), some of the energy provided by the photon can be used to excite vibrational states in the molecular ion, which requires an amount of energy, $E_i^{(\text{vib})}$. Now the energy conservation equation is

$$h\nu_{\text{photon}} - \frac{1}{2} m_e v^2 = -\varepsilon_i + E_i^{(\text{vib})} = IE_i \quad [6.23]$$

We know from Section 4.7 that the vibrational energy is quantized, and we treat it as a simple harmonic oscillator: $E_i^{(\text{vib})} = nh\nu_{\text{vib}}$, where $n = 0, 1, 2, 3, \dots$ is the vibrational quantum number. As a result of the vibrational excitation, the peak i in the spectrum is actually a series of narrower peaks; the separation between adjacent peaks depends on the vibrational frequency of the diatomic ion:

$$h\nu_{\text{photon}} - \frac{1}{2} m_e v^2 = -\varepsilon_i + nh\nu_{\text{vib}} \quad n = 0, 1, 2, 3, \dots \quad [6.24]$$

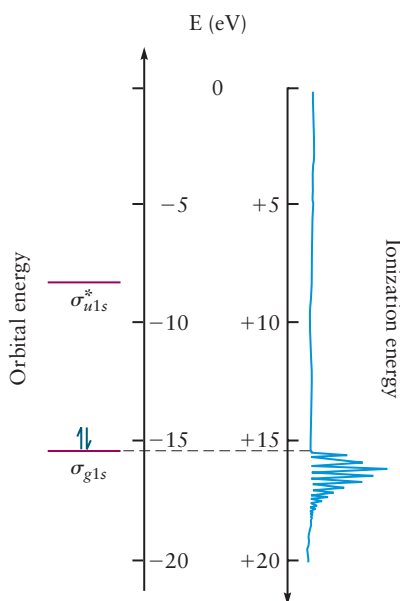


FIGURE 6.30 The photoelectron spectrum of H_2 measures the ionization energy of the σ_{g1s} molecular orbital. The procedures for obtaining orbital energies from measured ionization energies are described in the text. Photoelectron spectroscopy gives no information about the unoccupied σ_{u1s}^* orbital.

This pattern is illustrated in Figure 6.29, which shows the PES of hydrogen. Just as in Figure 5.19, the ionization energy of the electrons is plotted increasing to the left, whereas their kinetic energy (not shown in Fig. 6.29) increases to the right in the figure. The peak near 15.5 eV corresponds to $n = 0$ and represents the ionization energy for removing electrons with no vibrational excitation of the resulting molecular ion. As the energy increases along the axis toward 18 eV, the amount of vibrational excitation of the H_2^+ ion increases, and the spacing between vibrational levels becomes smaller. H_2^+ is approaching its dissociation limit.

We have just described the PES peaks for the σ_{g1s} MO of H_2 ; the correlation diagram is shown in Figure 6.10. The experimental results and the correlation diagram are displayed together in Figure 6.30 to show how PES measures the energies of MOs with the aid of Koopmans's theorem. The orbital energy becomes more negative (larger in magnitude) in the downward direction below zero along the axis. The ionization energy is positive and increases upward above the zero of energy. Purely for ease of interpreting the results, it is conventional in PES to flip the ionization energy axis to the opposite direction, so in Figure 6.30 ionization energy becomes larger and more positive in the *downward* direction along the black arrow. This procedure makes it easy to connect measured ionization energy values with the orbital energies. Note that the experimental peak with $n = 0$ is aligned with the energy of the MO, because this peak measures the energy of the orbital without vibrational excitation. In the other experimental peaks, some of the energy of the photon has been used to excite molecular vibrations and is not available to the outgoing photoelectron; therefore, these peaks appear to have orbital energies that are too large by the amount of their vibrational excitation.

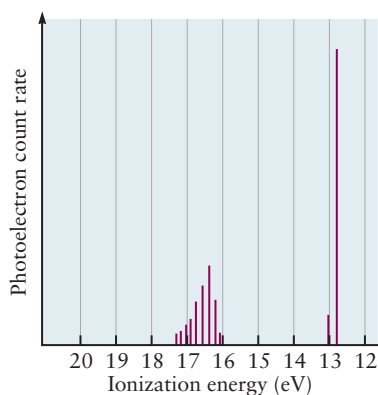


FIGURE 6.31 Peaks in the photoelectron spectrum of HCl measured with He(I) photons at 21.2 eV.

These vibrational “fine-structure” peaks on the PES data at first appear to be a nuisance, but in fact, they greatly aid in relating experimental data to particular MOs. The connection is made through the concept of bond order introduced in Section 6.2. We illustrate the procedure for three separate cases.

Case A

If the photoelectron is removed from a bonding orbital, the bond order of the positive ion will be smaller than the bond order of the parent molecule. Consequently, the bond in the molecular ion will be less stiff, and its vibrational frequency (determined directly from the PES fine structure) will be lower than that of the parent molecule (determined by vibrational spectroscopy). For example, in Figure 6.29, the vibrational frequency for H_2^+ is $6.78 \times 10^{13} \text{ s}^{-1}$, compared with $12.84 \times 10^{13} \text{ s}^{-1}$ for the parent molecule.

Case B

If the photoelectron is emitted from an antibonding orbital, the bond order of the positive ion will be larger than the bond order of the parent molecule. The bond in the diatomic molecular ion will be stiffer and will show a higher vibrational frequency.

Case C

If the photoelectron is emitted from a nonbonding orbital, there is no change in the bond order, and consequently little or no change in the vibrational frequency. The PES spectrum for the orbital will show few vibrational peaks, because the disturbance to the bond during photoemission is quite small. By contrast, the spectrum in Case A will show several vibrational fine structure peaks because removal of a bonding electron is a major disturbance that starts many vibrations of the bond. Case B is intermediate, with fewer vibrational subpeaks, because removing an antibonding electron disturbs the bond, but less so than in Case A.

We summarize these results in Table 6.4 and use them to interpret PES data for several additional molecules.

The PES data for gaseous hydrogen chloride (HCl) acquired with He(I) radiation are shown in Figure 6.31. The portion of the spectrum just below 13 eV shows few vibrational components, which suggests that it originates in a nonbonding orbital. The vibrational spacing in these components corresponds to a vibrational frequency of $7.98 \times 10^{13} \text{ s}^{-1}$. The sequence of peaks starting at 16.25 eV shows numerous vibrational contributions, suggesting they originate in a bonding orbital; the vibrational separation is $4.83 \times 10^{13} \text{ s}^{-1}$. The fundamental vibrational frequency for the parent HCl molecule is $8.66 \times 10^{13} \text{ s}^{-1}$. The changes in vibrational energy are consistent with the peak assignments based on number of vibrational peaks. Now, which orbitals of this heteronuclear diatomic are actually

TABLE 6.4 Identification of Molecular Orbitals in Photoelectron Spectra of Diatomic Molecules

Vibrational Frequency of Ion Relative to Parent Molecule	Number of Vibrational Lines in Peak	Molecular Orbital from Which Electron Is Emitted
Much smaller	Many	Bonding
Similar	Few	Nonbonding
Similar to slightly larger	Intermediate	Antibonding

involved? Figure 6.23 shows the correlation diagram for HF, where the σ bonding orbital is formed by overlap of the $1s$ AO of hydrogen with the $2p_z$ AO of fluorine; the $2p_x$ and $2p_y$ AOs of fluorine are nonbonding. The correlation diagram for HCl would show a σ bonding orbital formed by overlap of the $1s$ AO of hydrogen with the $3p_z$ AO of chlorine (Cl); the $3p_x$ and $3p_y$ AOs of chlorine would be nonbonding. Figure 6.32 shows the schematic photoelectron spectrum and the correlation diagram for HCl, with the orbital energies becoming more negative in the downward direction along the axis and the ionization energies becoming more positive in the downward direction along the black axis. (See the discussion of Figure 6.30 for the reasons behind these choices.) We assign the sequence of peaks starting at 16.25 eV to the σ bonding orbital and the pair of peaks near 12.73 eV to the $3p_x$ and $3p_y$ AOs of Cl. So far, we have explained the spectrum without involving the $3s$ electrons of Cl. In Figure 6.32 we show the $3s$ level for Cl, which appears at a lower orbital energy characteristic of pure chlorine. This suggests that the $3s$ electrons are not involved in formation of the H—Cl bond. The corresponding peak does not appear in Figure 6.31 because this deeper energy level is not accessible to the ultraviolet lines from helium and requires higher energy photons for photoionization.

The photoelectron spectra for N_2 and O_2 are shown in Figures 6.33 and 6.34, respectively. The experimental peaks have been assigned to orbitals by slightly more complex versions of the arguments used previously. Note that for N_2 , the energy for the σ_{g2p_z} MO is lower than that for the π_{u2p_x} and π_{u2p_y} , whereas the order is switched for O_2 , as indicated in Figure 6.15, Table 6.3, and the related text. This switch is due to interaction between the $2s$ and $2p$ AOs.

The photoelectron spectrum for NO is shown in Figure 6.35. The orbital assignments are based on the arguments summarized in Table 6.4. Note that the $1s$ core levels for both N and O appear at the same orbital energies as they do in their respective elemental gases, N_2 in Figure 6.33 and O_2 in Figure 6.34. This experimental result demonstrates clearly that the core levels do not participate in chemical bond formation and can be neglected in the MO analysis of bond formation.

These examples show that photoelectron spectroscopy is useful in testing theoretical models for bonding because it directly measures ionization energies that can be correlated with theoretical orbital energies through Koopmans's theorem. These methods are readily extended to polyatomic molecules.

FIGURE 6.32 The photoelectron spectrum and the molecular orbital energy-level diagram for HCl. The peaks with ionization energies lower than 20 eV originate in the σ bonding molecular orbital and in the Cl_{3p} nonbonding orbitals. Photoionization of the Cl $3s$ electrons requires higher energy photons.

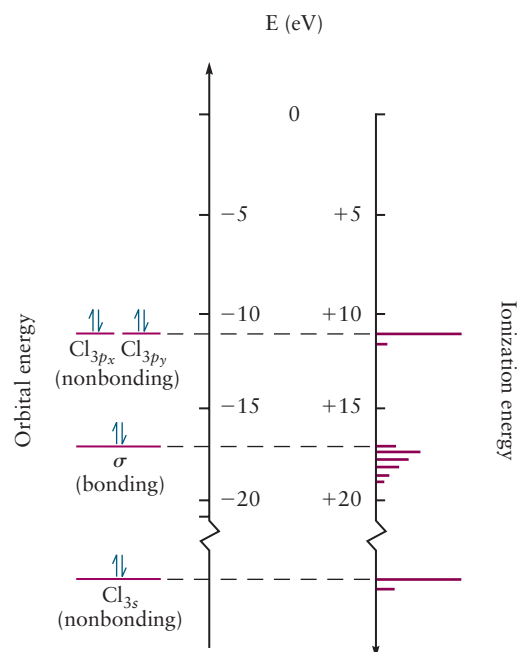


FIGURE 6.33 The photoelectron spectrum for N_2 shows the valence electrons in the occupied molecular orbitals and the $N(1s)$ core electrons.

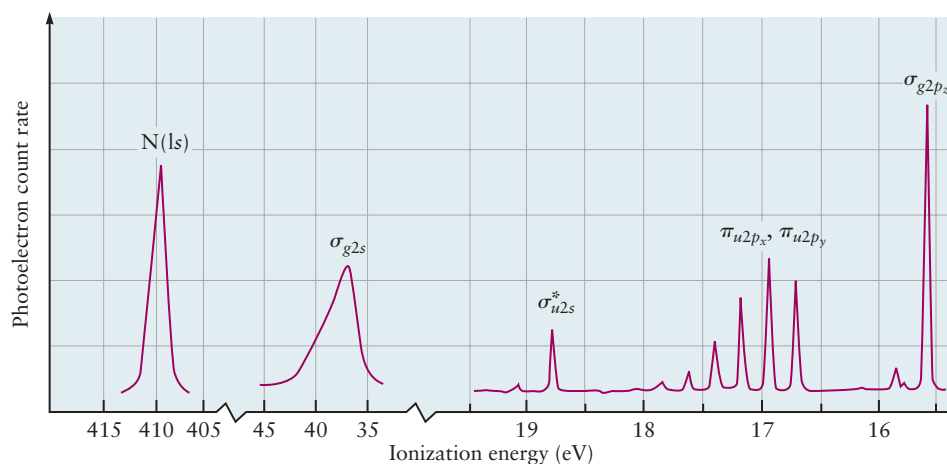


FIGURE 6.34 The photoelectron spectrum for O_2 shows valence electrons in the occupied molecular orbitals and the $O(1s)$ core electrons. Note that the order of the σ_{g2p_z} and π_{u2p_x}, π_{u2p_y} orbitals has switched between N_2 and O_2 . More advanced theory is required to explain why σ_{g2p_z} is split into two groups.

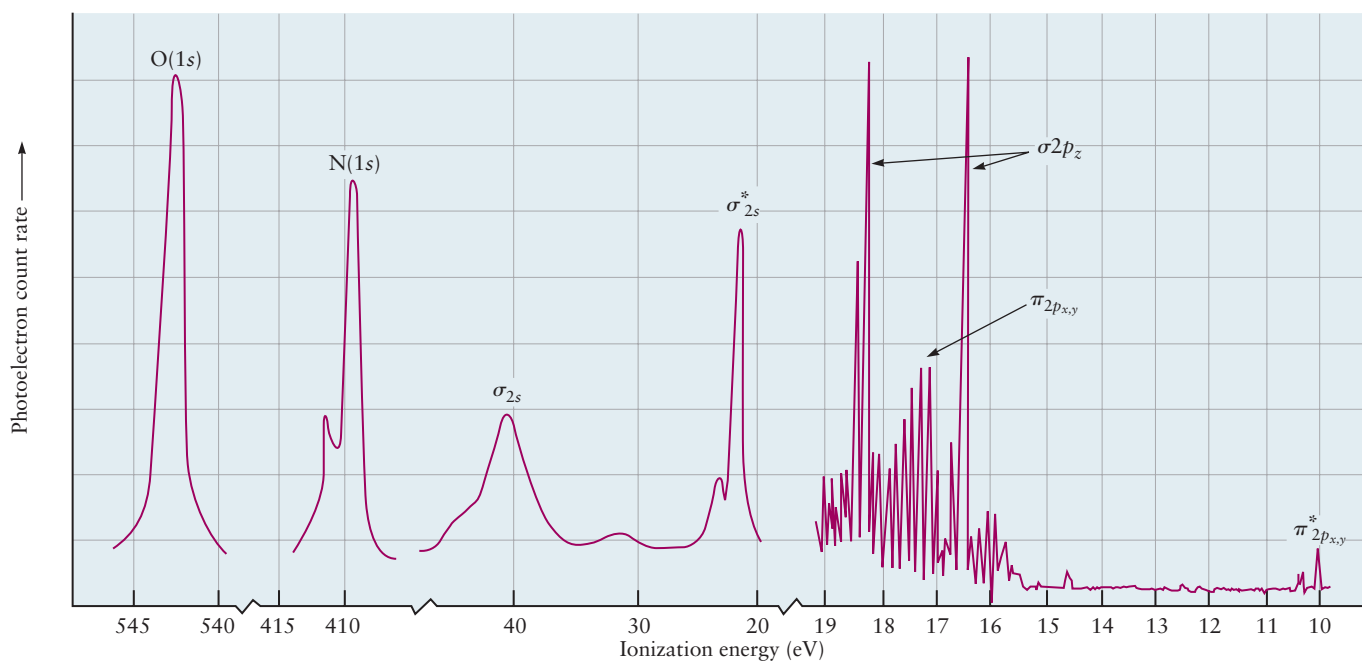
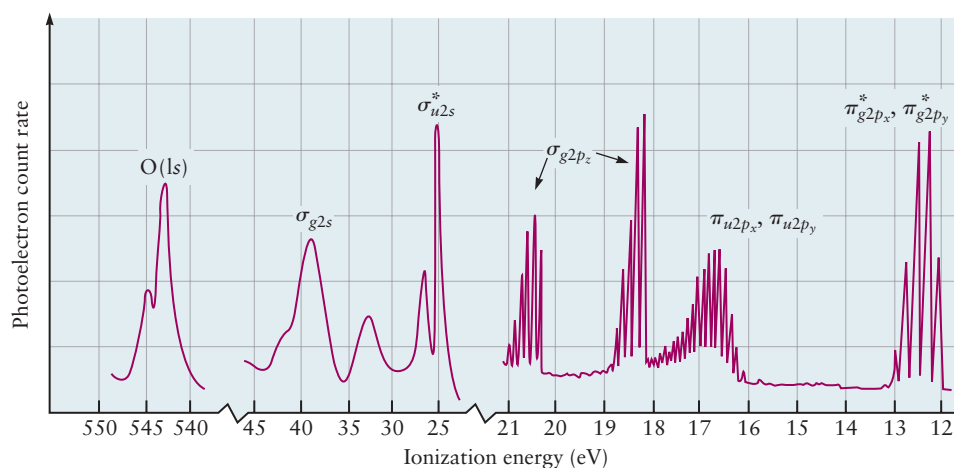


FIGURE 6.35 The photoelectron spectrum for NO . Note that the $O(1s)$ and $N(1s)$ orbitals remain at the same energies as in O_2 and N_2 ; these core electrons do not participate significantly in formation of the $N-O$ bond. More advanced theory is required to explain why σ_{2p_z} is split into two groups.

6.4 Localized Bonds: The Valence Bond Model

The characteristics of most chemical bonds (bond length, bond energy, polarity, and so forth) do not differ significantly from molecule to molecule (see Section 3.7). If the bonding electrons are spread out over the entire molecule, as described by the LCAO model, then why should the properties of a bond be nearly independent of the nature of the rest of the molecule? Would some other model be more suitable to describe chemical bonds?

The **valence bond (VB) model** grew out of the qualitative Lewis electron-pair model in which the chemical bond is described as a pair of electrons that is localized between two atoms. The VB model constructs a wave function for the bond by assuming that each atom arrives with at least one unpaired electron in an AO. The resulting wave function is a *product* of two one-electron wave functions, each describing an electron localized on one of the arriving atoms. The spins of the electrons must be paired to satisfy the Pauli exclusion principle.

The VB description for H_2 was developed by the German physicists Walter Heitler and Fritz London in 1927, just one year after Schrödinger introduced wave mechanics to explain the structure of the hydrogen atom. The American physicist John C. Slater also made important contributions to developing the VB method. Establishing the VB model as one of the cornerstones of modern structural chemistry awaited the pioneering work of the American chemist Linus Pauling, who used it to describe structure and bonding in polyatomic molecules, starting in 1931.

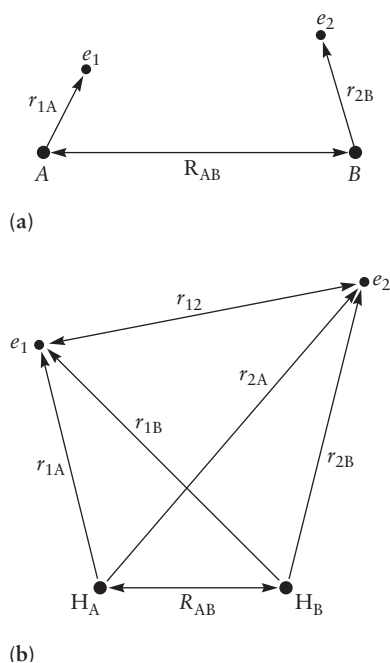


FIGURE 6.36 Two hydrogen atoms approach one another. The protons are separated by the distance R_{AB} . (a) At large values of R_{AB} each electron interacts only with the proton to which it is bound. (b) As the atoms approach closer, both electrons interact with both protons. The distance of electron 1 from nuclei A and B is given by r_{1A} , r_{1B} ; the distance of electron 2 from nuclei A and B is given by r_{2A} , r_{2B} ; the distance between the electrons is given by r_{12} .

6.4.1 Wave Function for Electron-Pair Bonds

SINGLE BONDS Consider that the hydrogen molecule, described by the Lewis structure $H:H$, is formed by combining two hydrogen atoms each with the electron configuration $H:(1s)^1$. The two atoms approach one another (Fig. 6.36), and the protons are separated by the distance R_{AB} . At very large separation, each electron is bound to its own proton and is located by coordinate r_{1A} or r_{2B} . At very large distances, the atoms are independent, and the wave function that describes the pair of them is $\varphi^A(r_{1A})\varphi^B(r_{2B})$. As the atoms approach closer together so that bond formation is a possibility, it is reasonable to guess that the molecular wave function would take the form

$$\psi^{\text{el}}(r_{1A}, r_{2B}; R_{AB}) = C(R_{AB})\varphi^A(r_{1A})\varphi^B(r_{2B}) \quad [6.25]$$

As the atoms begin to interact strongly, we cannot determine whether electron 1 arrived with proton A and electron 2 with proton B, or vice versa. (The electrons are indistinguishable.) Therefore, the wave function must allow for both possibilities:

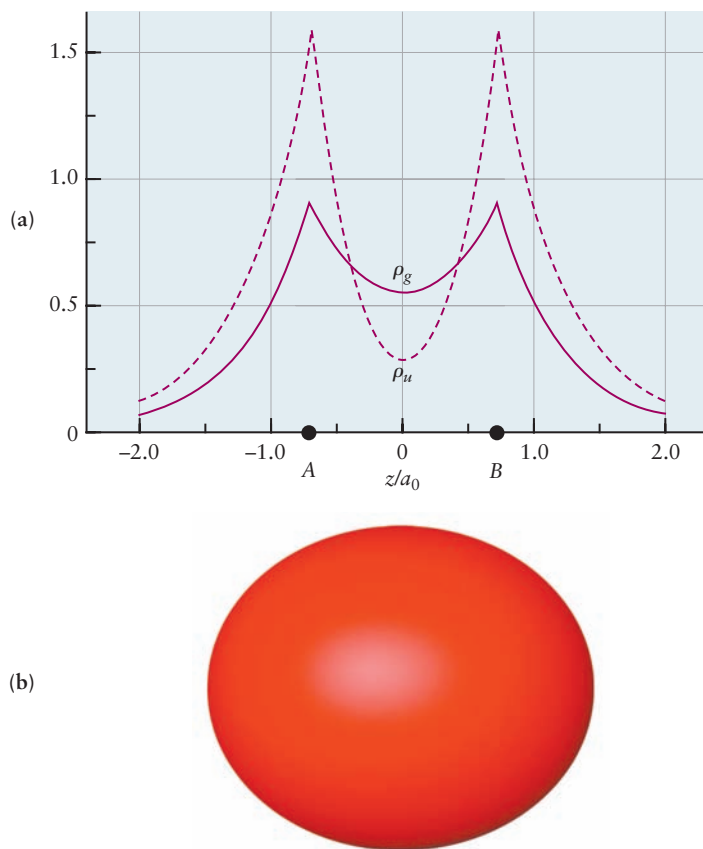
$$\psi^{\text{el}}(r_{1A}, r_{2B}; R_{AB}) = C_1(R_{AB})\varphi^A(r_{1A})\varphi^B(r_{2B}) + C_2(R_{AB})\varphi^A(r_{2A})\varphi^B(r_{1B}) \quad [6.26]$$

Symmetry requires that $c_1 = c_2$ and $c_1 = -c_2$ are equally valid choices. We label these combinations *gerade* (*g*) and *ungerade* (*u*), respectively, to show how each behaves under inversion symmetry (see Sections 6.1 and 6.2). We must check both cases to determine whether they describe bond formation, using our familiar criteria of increased electron density between the nuclei and energy reduced below that of the separated atoms.

It requires some care to calculate the electron density for ψ_g^{el} and ψ_u^{el} . Unlike the wave functions we have seen earlier, these are *two-electron functions*, and their squares give the probability density for finding electron 1 at r_1 and electron 2 at r_2 . To calculate the probability density of finding electron 1 at r_1 , no matter where

FIGURE 6.37 The electron density for the ψ_g^{el} and ψ_u^{el} wave functions in the simple valence bond model for H_2 . (a) The electron density ρ_g for ψ_g^{el} and ρ_u for ψ_u^{el} , calculated analytically as described in the text. (b) Three-dimensional isosurface of the electron density for the ψ_g^{el} wave function, as calculated numerically by Generalized Valence Bond Theory (GVB).

(Courtesy of Mr. Hatem Helal and Professor William A. Goddard III, California Institute of Technology, and Dr. Kelly P. Gaither, University of Texas at Austin.)



electron 2 is located, we must square the function and then average over all possible locations for electron 2. Similarly, we calculate the probability density for finding electron 2 at r_2 , regardless of the location of electron 1. Adding these results together gives the total electron density at each point in space, as a function of the internuclear distance R_{AB} . The results for ψ_g^{el} and ψ_u^{el} are shown in Figure 6.37a. The combination ψ_g^{el} results in increased electron density between the nuclei, whereas the combination ψ_u^{el} results in reduced electron density between the nuclei. It is more convenient to obtain the electron density from computer calculations using a newer version of the VB method called Generalized Valence Bond Theory (GVB), which will be described later. Figure 6.37b shows the electron density for ψ_g^{el} obtained in a GVB calculation for H_2 .

It is a straightforward exercise in quantum mechanics—although beyond the scope of this textbook—to calculate the total energy of the molecule as a function of R_{AB} for ψ_g^{el} and for ψ_u^{el} . The results give the potential energy of interaction between the protons for each value of R_{AB} . (Recall the discussion of potential energy in Section 6.2.1. See the discussion in Section 6.2.5 for a deeper analysis.) The two calculated potential energy curves (not shown) are qualitatively similar to those in Figure 6.7. They show that ψ_g^{el} describes a state with lower energy than that of the separated atoms, whereas ψ_u^{el} describes a state whose energy is higher than that of the separated atoms for all values of R_{AB} .

Taken together, the reduced potential energy and increased electron density between the nuclei demonstrate that ψ_g^{el} describes a stable chemical bond, whereas ψ_u^{el} describes a state that is strictly repulsive everywhere and does not lead to bond formation. Therefore, we take the proper VB electronic wave function for a pair bond to be

$$\psi_g^{\text{el}} = C_1[1s^{\text{A}}(1)1s^{\text{B}}(2) + 1s^{\text{A}}(2)1s^{\text{B}}(1)] \quad [6.27]$$

In this and the following equations we have switched to the simplified notation for orbitals introduced earlier in our discussion of the LCAO approximation in Section 6.2. In addition, we use “1” and “2” as shorthand notation for the coordinates locating electrons 1 and 2, and C_1 is a normalization constant.

Now let's consider the formation of F_2 , represented by its Lewis diagram from two fluorine atoms each with electron configuration $F: (1s)^2(2s)^2(2p_x)^2(2p_y)^2(2p_z)^1$. Suppose the two atoms labeled A and B approach each other along the z -axis so that the lobes of their $2p_z$ orbitals with the same phase point toward each other. As the atoms draw close, these two orbitals can overlap to form a single bond with two electrons. Reasoning as we did earlier for H_2 , we write the VB wave function for the bonding pair in F_2 as

$$\psi_g^{\text{bond}} = C_1[2p_z^A(1)2p_z^B(2) + 2p_z^A(2)2p_z^B(1)] \quad [6.28]$$



The electron density associated with this two-electron wave function, obtained from a GVB calculation for F_2 at the experimentally measured bond length for R_{AB} , is shown in Figure 6.38. This wave function gives no information on the eight pairs of electrons remaining in their AOs on atoms A and B, six pairs of which are shown as unshared pairs in the Lewis diagram for F_2 .

The VB model also describes bond formation in heteronuclear diatomics. We can combine the features of the two preceding examples to describe the bonding in HF, with one shared pair in a single bond produced by overlap of $H(1s)$ and $F(2p_z)$. We suggest that you work through the details to show that the wave function for the bonding pair is

$$\psi^{\text{bond}} = C_1[2p_z^F(1)1s^H(2)] + C_2[2p_z^F(2)1s^H(1)] \quad [6.29]$$

The electron density in this bond, obtained from a GVB calculation for HF, is shown in Figure 6.39. Remember that the *gerade* and *ungerade* labels no longer apply, and $c_1 \neq c_2$, because HF is a heteronuclear diatomic molecule.

The bond-pair wave functions in Equations 6.27, 6.28, and 6.29 were specially constructed to describe two electrons localized between two atoms as a single chemical bond between the atoms. These wave functions should not be called MOs, because they are not single-electron functions and they are not de-localized over the entire molecule. The corresponding single bonds (see Figs. 6.37, 6.38, and 6.39) are called σ **bonds**, because their electron density is cylindrically symmetric about the bond axis. There is no simple correlation between this symmetry

FIGURE 6.38 Isosurface representation of the electron density in the F_2 σ bond formed from a pair of electrons initially localized in a $2p_z$ orbital on each F atom.

(Courtesy of Mr. Hatem Helal and Professor William A. Goddard III, California Institute of Technology, and Dr. Kelly P. Gaither, University of Texas at Austin.)

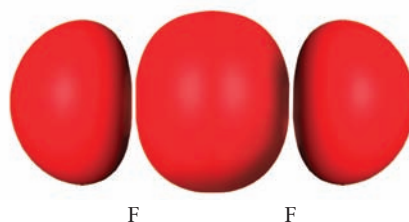
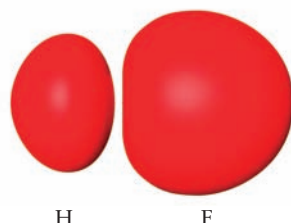
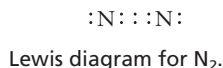


FIGURE 6.39 Isosurface representation of the electron density in the HF σ bond formed from a pair of electrons initially localized in a $2s$ orbital on H and in a $2p_z$ orbital on F.

(Courtesy of Mr. Hatem Helal and Professor William A. Goddard III, California Institute of Technology, and Dr. Kelly P. Gaither, University of Texas at Austin.)



and the angular momentum of electrons about the bond axis. Finally, electrons are not placed in these bonds by the aufbau principle. Rather, each bond is formed by overlap of two AOs, each of which is already half filled with one electron. The electrons in the two participating AOs must have opposite spin; thus, the bond corresponds to an electron pair with opposite, or “paired,” spins.



MULTIPLE BONDS To see how the VB method describes multiple bonds, let's examine N₂. Suppose two nitrogen atoms with electron configuration N: (1s)²(2s)²(2p_x)¹(2p_y)¹(2p_z)¹ approach one another along the z-axis. The two 2p_z orbitals can overlap and form a σ bond, the wave function of which is

$$\psi_{\sigma}^{\text{bond}} = C_1[2p_z^{\text{A}}(1)2p_z^{\text{B}}(2) + 2p_z^{\text{A}}(2)2p_z^{\text{B}}(1)] \quad [6.30]$$

The 2p_x and 2p_y orbitals from the two atoms do not approach head-on in this configuration, but rather side by side. Therefore, the positive lobes of the 2p_x orbitals can overlap laterally, as can the negative lobes. Together, they form a π bond, which has a node through the plane containing the bond axis with electron density concentrated above and below the plane. The wave function for the bond pair is

$$\psi_{\pi_x}^{\text{bond}}(1, 2; R_{\text{AB}}) = C_1(R_{\text{AB}})[2p_x^{\text{A}}(1)2p_x^{\text{B}}(2)] + C_1(R_{\text{AB}})[2p_x^{\text{A}}(2)2p_x^{\text{B}}(1)] \quad [6.31]$$

Similarly, the 2p_y orbitals on the two atoms can overlap to form a second π bond. Altogether, N₂ has a triple bond, for which the wave function is

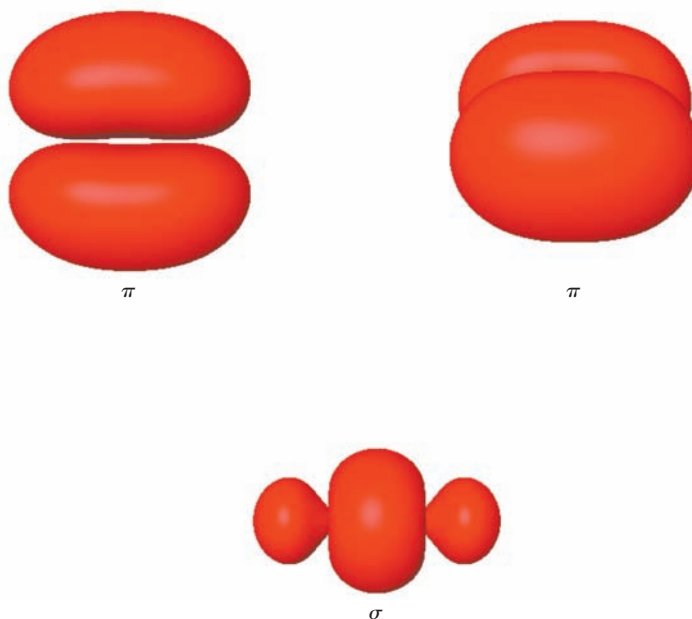
$$\begin{aligned} \psi_{\sigma\pi\pi}^{\text{bond}}(1, 2, 3, 4, 5, 6; R_{\text{AB}}) = & C_1(R_{\text{AB}})[2p_z^{\text{A}}(1)2p_z^{\text{B}}(2)][2p_x^{\text{A}}(3)2p_x^{\text{B}}(4)][2p_y^{\text{A}}(5)2p_y^{\text{B}}(6)] + \\ & C_1(R_{\text{AB}})[2p_z^{\text{A}}(2)2p_z^{\text{B}}(1)][2p_x^{\text{A}}(4)2p_x^{\text{B}}(3)][2p_y^{\text{A}}(6)2p_y^{\text{B}}(5)] \quad [6.32] \end{aligned}$$

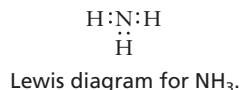
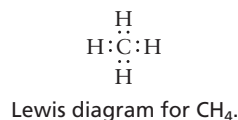
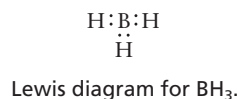
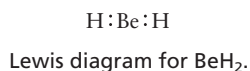
The electron densities in each bond contributing to the triple bond in N₂, as determined from a GVB calculation, are shown in Figure 6.40.

POLYATOMIC MOLECULES Specifying the three-dimensional structure of polyatomic molecules requires that we include bond angles and bond lengths. Any successful theory of bonding must explain and predict these structures. Let's test the VB approximation on the second-period hydrides, the structures of which we have already examined in Chapter 3 using VSEPR theory.

FIGURE 6.40 Isosurface representation of the electron densities in the σ bond and the two π bonds calculated by Generalized Valence Bond Theory (GVB).

(Courtesy of Mr. Hatem Helal and Professor William A. Goddard III, California Institute of Technology, and Dr. Kelly P. Gaither, University of Texas at Austin.)





Beryllium hydride, BeH_2 , has four valence electrons, two from beryllium and one each from the two hydrogen atoms, all of which appear in its Lewis diagram. In VSEPR theory, the steric number is 2, so the molecule is predicted to be linear, and this prediction is verified by experiment. The electron configuration of the central atom is $\text{Be}:(1s)^2(2s)^2$. There are no unpaired electrons to overlap with $\text{H}(1s)$ orbitals, so the VB model fails to predict the formation of BeH_2 .

Boron hydride, BH_3 , has six valence electrons corresponding to steric number 3 and a trigonal planar structure. With the electron configuration $\text{B}:(1s)^2(2s)^2(2p)^1$ on the central atom, the VB model cannot account for the formation of BH_3 and, in fact, predicts that BH is the stable molecule, which does not agree with experimental results.

Methane, CH_4 , has steric number 4, and VSEPR predicts a tetrahedral structure, which is confirmed by experimental results. Starting with the electron configuration $\text{C}:(1s)^2(2s)^2(2p)^2$, the VB model cannot account for the formation of CH_4 and predicts that CH_2 would be the stable hydride, which is again contrary to the experimental results.

Ammonia, NH_3 , has steric number 4 with three shared pairs and one unshared pair on the nitrogen atom. VSEPR predicts a trigonal pyramid structure, as a subcase of tetrahedral structure, with bond angles slightly less than 109° due to repulsion between the unshared pair and the three bonding pairs. Experiment verifies this structure with bond angles of 107° . The electron configuration $\text{N}:(1s)^2(2s)^2(2p_x)^1(2p_y)^1(2p_z)^1$ would permit the formation of three σ bonds by overlap of $\text{H}(1s)$ orbitals with each of the $2p$ orbitals on nitrogen. Because these $2p$ orbitals are all mutually perpendicular, the VB model predicts a trigonal pyramidal structure, but one with bond angles of 90° .

Finally, water, H_2O , has steric number 4 with two shared pairs and two unshared pairs on the oxygen atom. VSEPR theory predicts a bent structure, as a subcase of tetrahedral structure, with angles significantly less than the tetrahedral value of 109° due to repulsion between the two unshared pairs and the bonding pairs. Experimentally determined bond angles of 104° verify this prediction.

The VB model does not accurately describe bonding in the second-period hydrides. It predicts the wrong valence for atoms in Groups IIA through IVA and the wrong structure for atoms in Groups VA and VIA. Clearly, the model had to be improved. Linus Pauling gave the answer in 1931 by introducing the concepts of promotion and hybridization.

Atoms such as Be, B, and C can have the correct valence for bonding by **promotion** of valence electrons from the ground state to excited states at higher energy. For example, $\text{Be}:(1s)^2(2s)^2 \rightarrow \text{Be}:(1s)^2(2s)^1(2p)^1$ and $\text{C}:(1s)^2(2s)^2(2p)^2 \rightarrow \text{C}:(1s)^2(2s)^1(2p_x)^1(2p_y)^1(2p_z)^1$ are ready to form BeH_2 and CH_4 , respectively. These excited states are known from spectroscopy. The excited state of carbon lies about 8.26 eV (190 kJ mol^{-1}) above the ground state, and energy is clearly required for promotion. Pauling argued that this investment would be repaid by the energy released when the C—H bonds of methane form (about 100 kJ mol^{-1} for each bond).

Even though the valence would be correct after promotion, the structure still would be wrong. Beryllium hydride would have two different kinds of bonds, and methane would have three identical bonds formed by overlap of $\text{H}(1s)$ with the $\text{C}(2p)$ orbitals and a different bond formed by $\text{H}(1s)$ and $\text{C}(2s)$. Pauling proposed that new orbitals with the proper symmetry for bond formation could be formed by **hybridization** of $2s$ and $2p$ orbitals after promotion. The $\text{Be}(2s)$ and $\text{Be}(2p_z)$ orbitals would combine to form two equivalent hybrid orbitals oriented 180° apart. The $\text{C}(2s)$ would hybridize with the three $\text{C}(2p)$ orbitals to give four equivalent new orbitals in a tetrahedral arrangement around the carbon atom.

Pauling's achievements made it possible to describe polyatomic molecules by VB theory, and hybridization has provided the vocabulary and structural concepts for much of the fields of inorganic chemistry, organic chemistry, and biochemistry.

6.4.2 Orbital Hybridization for Polyatomic Molecules

Pauling developed the concept of hybrid orbitals to describe the bonding in molecules containing second-period atoms with steric numbers 2, 3, and 4. Let's discuss these hybridization schemes in sequence, starting with BeH_2 . We will use the lowercase Greek letter *chi*, χ , to represent hybrid orbitals.

The BeH_2 molecule is known to be linear. Let's define the z -axis of the coordinate system to lie along the $\text{H}-\text{Be}-\text{H}$ bonds, and place the beryllium nucleus at the origin. We mix the $2s$ and $2p_z$ orbitals of beryllium to form two new orbitals on the beryllium atom:

$$\chi_1(r) = \frac{1}{\sqrt{2}} [2s + 2p_z] \quad [6.33a]$$

$$\chi_2(r) = \frac{1}{\sqrt{2}} [2s - 2p_z] \quad [6.33b]$$

The coefficient $1/\sqrt{2}$ is a normalization constant. We call these ***sp* hybrid atomic orbitals** because they are formed as the sum or difference of one s orbital and one p orbital. Like the familiar s and p orbitals, a hybrid AO is a one-electron wave function whose amplitude is defined at every point in space. Its amplitude at each point is the sum or difference of the other orbitals in the equation that defines the hybrid. Its square at each point gives the probability density for finding the electron at that point, when the electron is in the hybrid orbital.

The formation and the shapes of the sp hybrid orbitals and their participation in chemical bonds are shown in Figure 6.41. The first column shows the non-hybridized orbitals on the Be atom, and the second column shows the hybrid orbitals. The amplitude for each hybrid at any point r from the beryllium nucleus is easily visualized as the result of constructive and destructive interference of the $2s$ and $2p$ wave functions at that point. Because the sign of the $2s$ orbital is always positive, whereas that of the $2p_z$ orbital is different in the $+$ and $-z$ directions, the amplitude of χ_1 is greatest along $+z$, and that of χ_2 is greatest along $-z$. Because the probabilities are the squares of the amplitudes, an electron in χ_2 is much more likely to be found on the left side of the nucleus than on the right; the opposite is

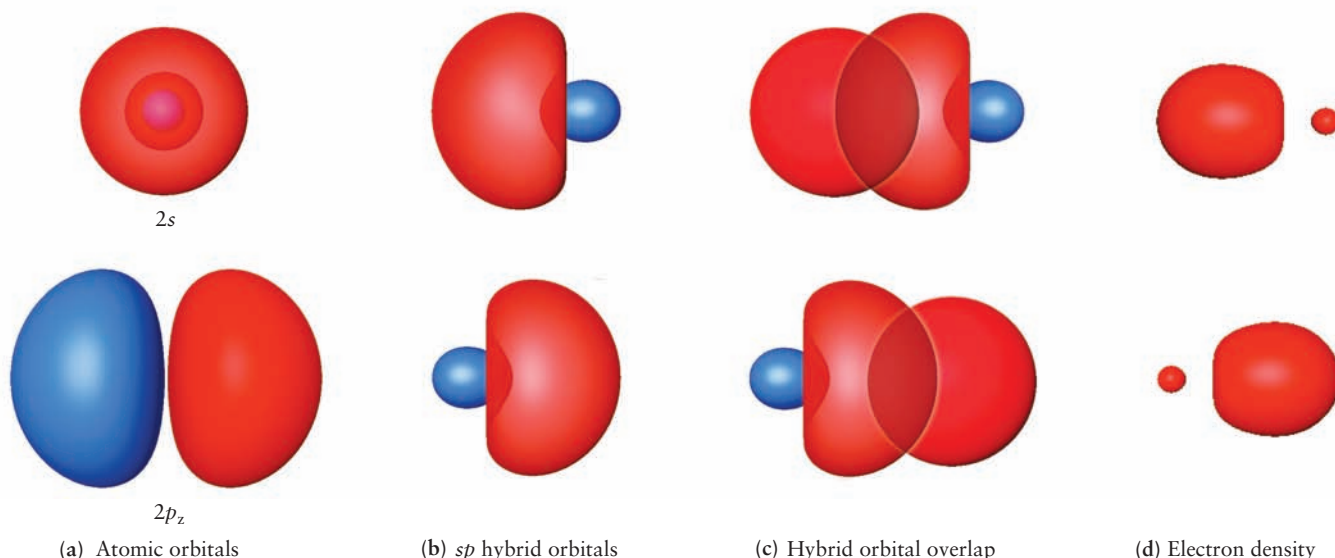


FIGURE 6.41 Formation, shapes, and bonding of the sp hybrid orbitals in the BeH_2 molecule. (a) The $2s$ and $2p$ orbitals of the Be atom. (b) The two sp hybrid orbitals formed from the $2s$ and $2p_z$ orbitals on the beryllium atom. (c) The two σ bonds that form from the overlap of the sp hybrid orbitals with the hydrogen $1s$ orbitals, making two single bonds in the BeH_2 molecule. (d) Electron density in the two σ bonds as calculated by Generalized Valence Bond (GVB) theory.

(Courtesy of Mr. Hatem Helal and Professor William A. Goddard III, California Institute of Technology, and Dr. Kelly P. Gaither, University of Texas at Austin.)

true for an electron in χ_1 . Once the hybrid AOs form on the central atom, its electron configuration becomes $\text{Be}:(1s)^2(\chi_1)^1(\chi_2)^1$. As the two hydrogen atoms approach, each shares its electron with the corresponding hybrid orbital to form two localized single σ bonds (see Fig. 6.41). The wave functions for the two bonding pairs are

$$\psi_{\sigma_1}^{\text{bond}}(1,2) = c_+[\chi_1(1)1s^{\text{H}}(2) + \chi_1(2)1s^{\text{H}}(1)] \quad [6.34a]$$

$$\psi_{\sigma_2}^{\text{bond}}(3,4) = c_-[\chi_2(3)1s^{\text{H}}(4) + \chi_2(4)1s^{\text{H}}(3)] \quad [6.34b]$$

The third column in Figure 6.41 illustrates these σ bonds by locating Be and H atoms a distance apart equal to the experimental bond length of BeH_2 , placing an sp hybrid on the Be atom and a $1s$ AO on the H atom and coloring the region where these orbitals overlap. Chemists have used such qualitative sketches since the advent of the VB method but have been hindered from more detailed representations by the mathematical complexity of obtaining the electron density from Equations 6.34a and 6.34b. This barrier has been overcome by GVB theory. The fourth column in Figure 6.41 shows the electron density in the σ bonds of BeH_2 , as calculated by GVB.

The BH_3 molecule is known to have a trigonal planar structure with three equivalent bonds. Let's choose coordinates so that the structure lies in the

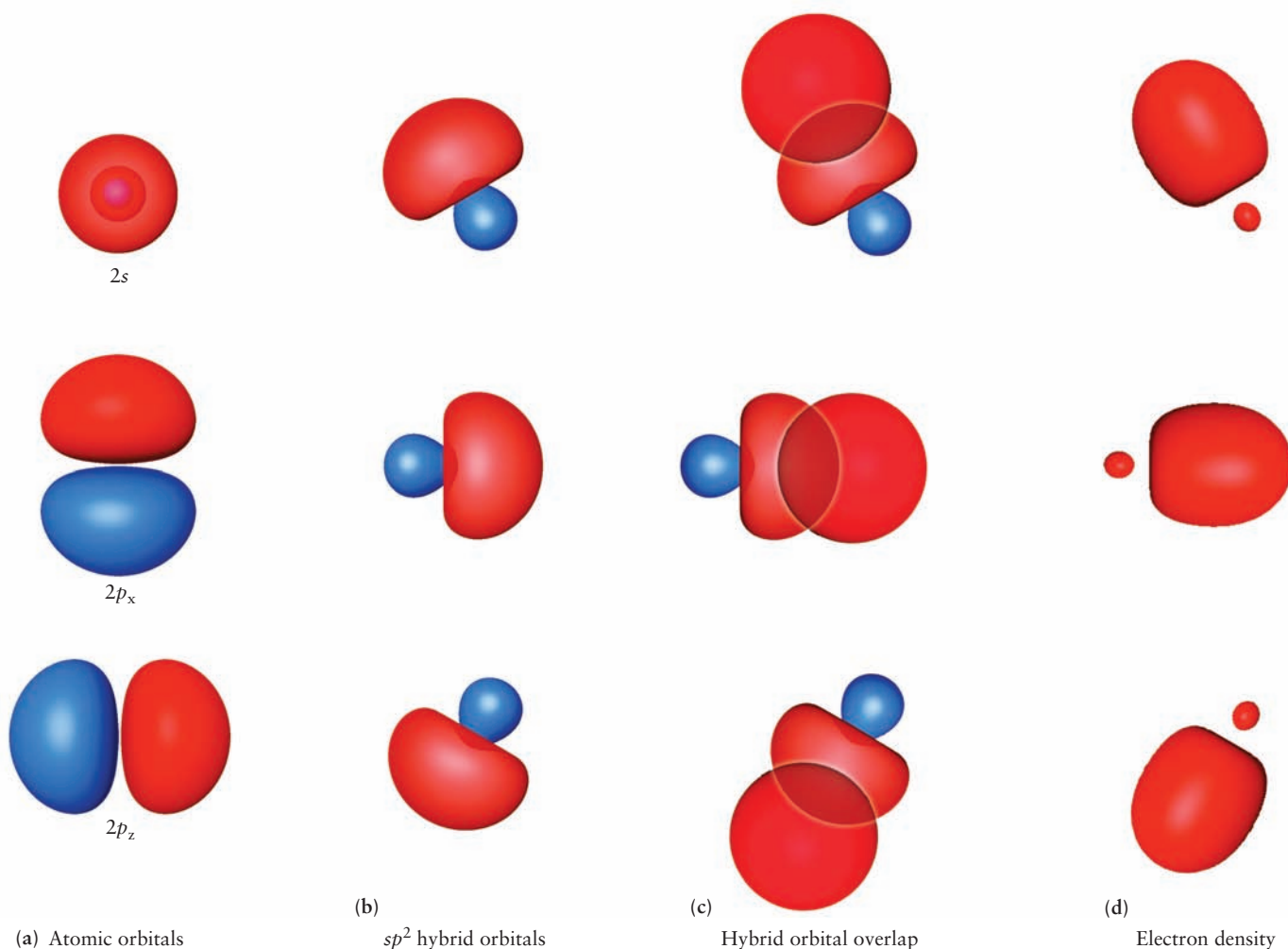


FIGURE 6.42 Formation, shapes, relative orientation, and bonding of the three sp^2 hybrid orbitals in the BH_3 molecule. (a) The $2s$, $2p_x$ and $2p_y$ atomic orbitals on a boron atom. (b) The three sp^2 hybrid orbitals on a boron atom. (c) Overlap of the sp^2 hybrid orbitals with hydrogen $1s$ orbitals to form three σ bonds in BH_3 . (d) Electron density in the three σ bonds as calculated by Generalized Valence Bond (GVB) theory.

(Courtesy of Mr. Hatem Helal and Professor William A. Goddard III, California Institute of Technology, and Dr. Kelly P. Gaither, University of Texas at Austin.)

x - y plane with the beryllium atom at the origin. Promotion of one of the $2s$ electrons creates the excited-state configuration $\text{Be}: 2s^1 2p_x^1 2p_y^1$, and these three AOs can be mixed to form the three equivalent new orbitals:

$$\chi_1(r) = 2s + \left(\frac{1}{2}\right)^{1/2} 2p_y \quad [6.35a]$$

$$\chi_2(r) = 2s + \left(\frac{3}{2}\right)^{1/2} 2p_x - \left(\frac{1}{2}\right)^{1/2} 2p_y \quad [6.35b]$$

$$\chi_3(r) = 2s - \left(\frac{3}{2}\right)^{1/2} 2p_x - \left(\frac{1}{2}\right)^{1/2} 2p_y \quad [6.35c]$$

These are called **sp^2 hybrid atomic orbitals** because they are formed from one s and two p orbitals. The formation, shape, and orientation of the sp^2 hybrids are shown in Figure 6.42. They lie in the x - y plane with an angle of 120° between them. After hybridization, the electron configuration of the atom is $\text{B}: (1s)^2 (\chi_1)^1 (\chi_2)^1 (\chi_3)^1$. Each of the sp^2 hybrids can overlap with a $\text{H}(1s)$ orbital to produce a σ bond. The wave functions for all bonding pairs would be the same, and they will have the same form as those in Equations 6.34a and 6.34b. The third column of Figure 6.42 shows the traditional qualitative sketches of the orbital overlap leading to σ bonds in BH_3 , and the fourth column shows the electron density in these bonds as calculated by GVB. Experimentally, BH_3 molecules turn out to be unstable and react rapidly to form B_2H_6 or other higher compounds called “boranes.” However, the closely related BF_3 molecule has the trigonal planar geometry characteristic of sp^2 hybridization. It forms three σ bonds by overlap of a boron sp^2 hybrid with a $\text{F}(2p_z)$.

To describe the known structure for CH_4 , we combine the $2s$ and three $2p$ orbitals of the central carbon atom to form four equivalent **sp^3 hybrid atomic orbitals**, which point toward the vertices of a tetrahedron:

$$\chi_1(r) = \frac{1}{2} [2s + 2p_x + 2p_y + 2p_z] \quad [6.36a]$$

$$\chi_2(r) = \frac{1}{2} [2s - 2p_x - 2p_y + 2p_z] \quad [6.36b]$$

$$\chi_3(r) = \frac{1}{2} [2s + 2p_x - 2p_y - 2p_z] \quad [6.36c]$$

$$\chi_4(r) = \frac{1}{2} [2s - 2p_x + 2p_y - 2p_z] \quad [6.36d]$$

Figure 6.43 shows the shape and orientation of these four orbitals, pointing toward the vertices of a tetrahedron, which has the carbon atom at its center. The bottom image in Figure 6.43 shows an “exploded view” in which the orbitals have been displaced from one another to show the tetrahedral geometry. Each hybrid orbital can overlap a $1s$ orbital of one of the hydrogen atoms to give an overall tetrahedral structure for CH_4 .

Because of their widespread use in chemistry, it is important to have a good sense of the sizes and shapes of the hybrid orbitals. The shapes of the sp hybrid orbitals in Figure 6.41 are quantitatively correct and properly scaled in size relative to the other orbitals shown. Chemists tend to sketch these orbitals by hand like those in Figure 6.44, which gives the misleading impression that the hybrids are thin, cigarlike shapes with highly directional electron density concentrated right along the direction of the bonds. A contour map of χ_1 (from Eq. 6.33a) shows that the orbital is rather diffuse and broadly spread out, despite its directional concentration (see Fig. 6.44). Because this plot is symmetric about the z -axis, each of these contours can be rotated about the z -axis to produce a three-dimensional isosurface at a specified fraction of the maximum amplitude; the isosurfaces in Figure 6.41 were generated in just that way. Visualizing these isosurfaces helps us see the real effect of sp hybridization: The amplitudes of the

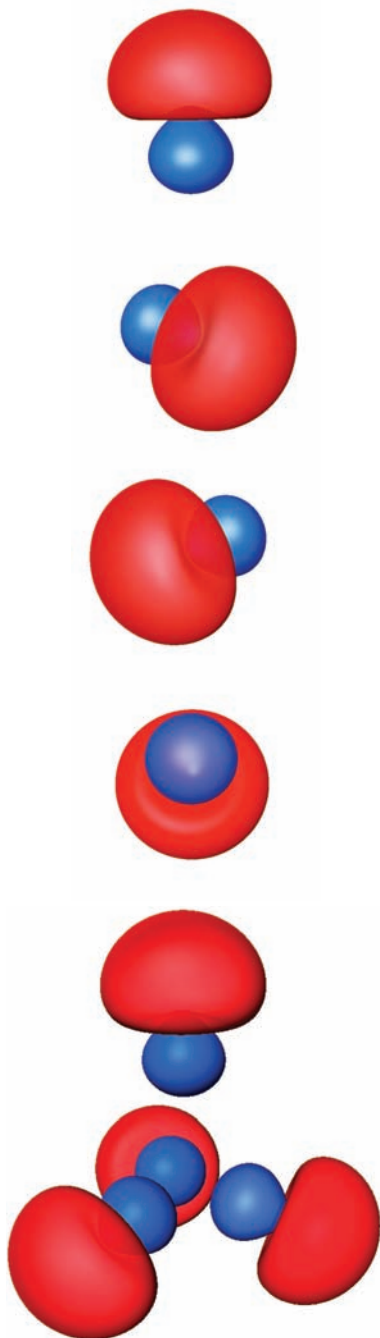


FIGURE 6.43 Shapes and relative orientations of the four sp^3 hybrid orbitals in CH_4 pointing at the corners of a tetrahedron with the carbon atom at its center. The “exploded view” at the bottom shows the tetrahedral geometry.

(Courtesy of Mr. Hatem Helal and Professor William A. Goddard III, California Institute of Technology, and Dr. Kelly P. Gaither, University of Texas at Austin.)

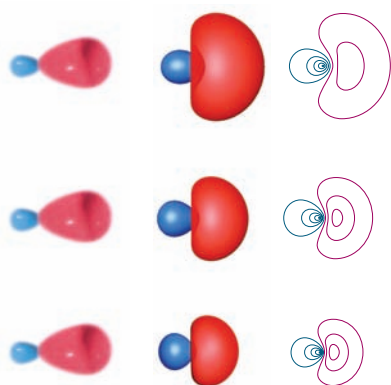


FIGURE 6.44 Exact and approximate representations of the hybrid orbital shapes. For each type of hybrid orbital shown the left column shows typical chemist's sketches, the center column shows isosurfaces, and the right column shows contour plots. The top row are the sp hybrid orbitals, the middle row are the sp^2 hybrid orbitals, and the bottom row are the sp^3 hybrid orbitals.

(Courtesy of Mr. Hatem Helal and Professor William A. Goddard III, California Institute of Technology, and Dr. Kelly P. Gaither, University of Texas at Austin.)

beryllium atom orbitals are now “pooched out” a bit in the $+z$ and $-z$ directions, but it has not been squeezed down into a thin tube. The $2p_x$ and $2p_y$ orbitals remain unchanged, oriented perpendicular to each other and to the sp hybrid orbitals

The chemist's sketches, which are typically drawn to emphasize directionality of the sp^2 hybrid orbitals, and a contour plot of the actual shape, are shown in Figure 6.44. Each of these contours can be rotated about the x - y plane to produce a three-dimensional isosurface whose amplitude is chosen to be a specific fraction of the maximum amplitude of the wave function. These isosurfaces demonstrate that sp^2 hybridization causes the amplitude of the boron atom to be “pooched out” at three equally spaced locations around the “equator” of the atom (see Fig. 6.42). The $2p_z$ orbital is not involved and remains perpendicular to the plane of the sp^2 hybrids. The standard chemist's sketches of the sp^3 hybrid orbitals and a contour plot that displays the exact shape and directionality of each orbital are shown in Figure 6.44. The isosurfaces shown in Figure 6.43 were generated from these contour plots.

Lone-pair electrons, as well as bonding pairs, can occupy hybrid orbitals. The nitrogen atom in NH_3 also has steric number 4, and its bonding can be described in terms of sp^3 hybridization. Of the eight valence electrons in NH_3 , six are involved in σ bonds between nitrogen and hydrogen; the other two occupy the fourth sp^3 hybrid orbital as a lone pair (Fig. 6.45a). Oxygen in H_2O likewise has steric number 4 and can be described with sp^3 hybridization, with two lone pairs in sp^3 orbitals (see Fig. 6.45b). Placing the unshared pairs in sp^3 hybrid orbitals predicts bond angles of 109.5° , which are reasonably close to the measured values of 107° for NH_3 and 104° for H_2O .

There is a close relationship between the VSEPR theory discussed in Section 3.9 and the hybrid orbital approach, with steric numbers of 2, 3, and 4 corresponding to sp , sp^2 , and sp^3 hybridization, respectively. The method can be extended to more complex structures; d^2sp^3 hybridization (see Sec. 8.7), which gives six equivalent hybrid orbitals pointing toward the vertices of a regular octahedron, is applicable to molecules with steric number 6. Both theories are based on minimizing the energy by reducing electron–electron repulsion.

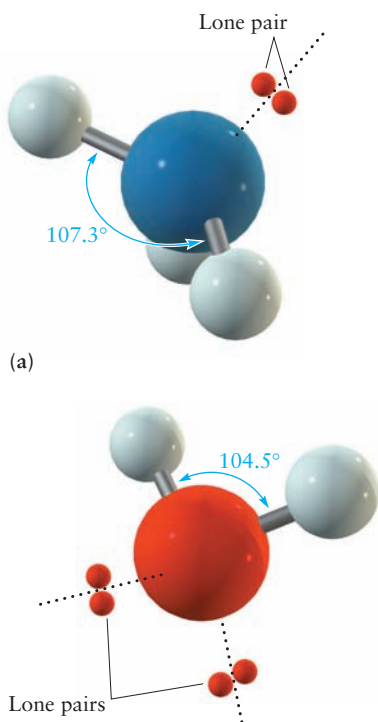


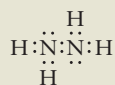
FIGURE 6.45 (a) Ammonia (NH_3) has a pyramidal structure in which the bond angles are less than 109.5° . (b) Water (H_2O) has a bent structure, with a bond angle less than 109.5° and smaller than that of NH_3 .

EXAMPLE 6.3

Predict the structure of hydrazine (H_2NNH_2) by writing down its Lewis diagram and using the VSEPR theory. What is the hybridization of the two nitrogen atoms?

SOLUTION

The Lewis diagram is



Lewis diagram for hydrazine, N_2H_4 .

Both nitrogen atoms have steric number 4 and are sp^3 hybridized, with $\text{H}-\text{N}-\text{H}$ and $\text{H}-\text{N}-\text{N}$ angles of approximately 109.5° . The extent of rotation about the $\text{N}-\text{N}$ bond cannot be predicted from the VSEPR theory or the hybrid orbital model. The full three-dimensional structure of hydrazine is shown in Figure 6.46.

Related Problems: 49, 50, 51, 52

The concept of orbital hybridization deserves a few summary comments. The method is used throughout basic and applied chemistry to give quick and convenient representations of molecular structure. The method provides a sound quantum mechanical basis for *organizing and correlating* vast amounts of experimental data for molecular structure. The simple examples discussed earlier all involved

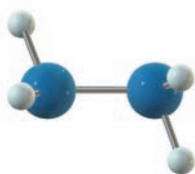


FIGURE 6.46 The structure of hydrazine, N_2H_4 .

symmetric molecules with identical ligands, and we simply “placed” lone pairs in hybrid orbitals when necessary. Constructing the hybrids for non-symmetrical molecules, bonding with different ligands, and giving explicit attention to lone pairs all involve considerable difficulty. The resulting models provide concrete images for visualizing and testing chemical reaction pathways by comparing the electron density at different possible “reactive sites” on a molecule. You will use hybridization extensively for these purposes in your subsequent chemistry classes, especially organic chemistry.

Hybridization is less successful as a tool for *predicting* molecular structure. The bond angle is usually known or assumed at the beginning. If the bond angle is not known in advance, various semiempirical schemes must be used to estimate the *s* and *p* character and search for the optimum value of bond angle. The calculations involved are less well suited to computer analysis than those done using the LCAO method; thus, extensive predictions of molecular geometry are quite difficult. In recent years, a newer version of the VB method called **Generalized Valence Bond Theory** has been developed by the American chemist William A. Goddard III as a powerful tool for large-scale practical calculations for localized orbitals.

Finally, orbital hybridization has inspired a great deal of discussion, some of it impassioned, on the meaning and significance of “promotion” and “return of the energy investment.” Where does the energy input for promotion come from? How is the bond formed? How does the energy released on bond formation compensate for promotion? Do these concerns cast doubt on the validity and usefulness of the hybrid orbital representations of the chemical bond? These may be legitimate concerns if one is trying to describe the dynamical events by which the bond is actually formed. However, these concerns are largely side issues for our main question: Is hybridization a useful way to describe the *structure* of a chemical bond after it has been formed? Quantum mechanics provides a fundamental explanation of atomic structure for the allowed values of energy and angular momentum. One set of values is appropriate for describing free carbon atoms in the gas phase, and another set is appropriate for describing carbon atoms involved in tetravalent chemical bonds. Equations 6.36a–d provide the connections between these two sets. Pauling provided the following description: “If quantum theory had been developed by the chemist rather than the spectroscopist it is probable that the tetrahedral orbitals described above would play the fundamental role in the theory, in place of the *s* and *p* orbitals.”¹

6.5 Comparison of Linear Combination of Atomic Orbitals and Valence Bond Methods

The LCAO and VB methods start with different quantum mechanical approaches to the description of chemical bonding. The former constructs MOs that are delocalized over the entire molecule by taking linear combinations of the AOs. In contrast, the VB model provides a quantum mechanical description of the localized chemical bond between two atoms in the spirit of the Lewis dot model. The two methods look different at the beginning, and their results look quite different. Are the two methods equally valid? Are they equally applicable to a broad range of molecules? The accuracy of any particular quantum chemical method is ultimately judged by the degree to which its predictions agree with experimental results. The electronic wave function for the molecule is the key construct used for calculating the values of molecular properties that we can measure. Therefore, the best way to compare the LCAO and VB methods is to compare the electronic wave functions for the molecule generated by each.

¹L. Pauling, *The Nature of the Chemical Bond*, 3rd ed. Ithaca, NY: Cornell University Press, 1960, p. 113.

Comparison for H₂

This comparison of LCAO with VB methods is most easily seen by explicitly writing out the electronic wave functions for the specific case of H₂ constructed using both methods.

In the LCAO method for H₂, a σ bonding orbital is constructed as a linear combination of H 1s orbitals centered on the two hydrogen atoms. This MO is de-localized over the entire molecule. The bonding orbital is given by the following equation:

$$\sigma_{g1s} = C_g(R_{AB})[\varphi_{1s}^A + \varphi_{1s}^B] \quad [6.37]$$

Neglecting the normalization constant and using the simplified notation from Section 6.2 give the following form:

$$\sigma_{g1s} = [1s^A + 1s^B] \quad [6.38]$$

Both electrons occupy this bonding orbital, satisfying the condition of indistinguishability and the Pauli principle. Recall from Section 6.2 that the electronic wave function for the entire molecule in the LCAO approximation is the *product* of all of the occupied MOs, just as an atomic wave function is the product of all occupied Hartree orbitals of an atom. Thus, we get

$$\psi_{\text{MO}}^{\text{el}} = \sigma_{g1s}(1)\sigma_{g1s}(2) = [1s^A(1) + 1s^B(1)][1s^A(2) + 1s^B(2)] \quad [6.39]$$

The VB model, in contrast, starts with the notion that a good approximation to the molecular electronic wave function for H₂ is the product of an H(1s) orbital centered on atom A, occupied by electron 1, and another H(1s) orbital centered on atom B, occupied by electron 2. As discussed in Section 6.4, the equation for this molecular electronic wave function is

$$\psi_{\text{VB}}^{\text{el}}(r_{1A}, r_{2B}; R_{AB}) = C_1(R_{AB})\varphi_A(r_{1A})\varphi_B(r_{2B}) + C_2(R_{AB})\varphi_A(r_{2A})\varphi_B(r_{1B}) \quad [6.40]$$

which on dropping the normalization factors and using the simplified notation introduced in Section 6.4 becomes

$$\psi_{\text{VB}}^{\text{el}} = 1s^A(1)1s^B(2) + 1s^A(2)1s^B(1) \quad [6.41]$$

Now we can compare the LCAO and VB versions of the electronic wave functions for the molecule directly by multiplying out $\psi_{\text{MO}}^{\text{el}}$ and rearranging terms to obtain

$$\psi_{\text{MO}}^{\text{el}} = [1s^A(1)1s^B(2) + 1s^A(2)1s^B(1)] + [1s^A(1)1s^A(2) + 1s^B(1)1s^B(2)] \quad [6.42]$$

The first term in $\psi_{\text{MO}}^{\text{el}}$ is identical to $\psi_{\text{VB}}^{\text{el}}$. The second term may be labeled ψ_{ionic} because it is a mixture of the ionic states H_A^-H_B^+ and H_A^+H_B^- , respectively. This can be seen by looking at the two terms in the second set of brackets; the first term puts both electrons on nucleus A (making it H^-), and the second term puts both electrons on nucleus B (making it H^-).

Our comparison shows that the LCAO method includes an ionic contribution to the bond, but the VB method does not. In fact, the simple MO approach suggests that the bond in H₂ is 50% covalent and 50% ionic, which is contrary both to experience and intuition. Because the electronegativities of the two atoms in a homonuclear diatomic molecule are the same, there is no reason to expect any ionic contribution to the bond, much less such a large one. The complete absence of ionic contributions in the VB wave function suggests this method is not well suited for polar molecules such as HF. Thus, the truth in describing the chemical bond and molecular structure appears to lie somewhere between the LCAO and

VB methods. It is also informative to compare these methods for describing chemical reactivity, which requires bonds to be broken. We already know that the VB wave function for H_2 correctly describes the long-distance limit as two separate hydrogen atoms. But, the LCAO wave function predicts that, in the long-distance limit H_2 , dissociates into ionic species, as well as hydrogen atoms. Ionic products are not usually produced by dissociation under ordinary thermal conditions. Again, the best description must lie between the extremes provided by the simple LCAO and VB methods.

Improving the Linear Combination of Atomic Orbitals and Valence Bond Methods

The simple form of LCAO and VB methods, as presented in this chapter, must be refined to provide more accurate wave functions for molecules and solids from which measurable properties can be calculated. Both methods have been improved on significantly in a number of ways. We illustrate one approach, starting with ψ_{VB} , not only because it is easier to understand than methods for refining ψ_{MO} , but also because the method is generally applicable in many areas of quantum chemistry. The accuracy of the simple VB wave function can be improved by adding in (mixing) some ionic character. We write

$$\psi_{\text{improved}} = \psi_{VB} + \lambda\psi_{\text{ionic}} \quad [6.43]$$

and then choose λ on the basis of some criterion. The most common way to do this is to adjust λ to minimize the energy of the orbital. One simply calculates the energy, using the methods developed in Chapter 5, with λ as a parameter, and then differentiates the result with respect to λ to find that value of λ that minimizes the energy, as is done in ordinary calculus. Using that special value of λ in Equation 6.43 gives a wave function that is a better approximation to the true wave function than the simple VB wave function. Moreover, the energy calculated for the ground state of the system using the “improved” wave function is guaranteed never to be lower than the true ground-state energy. These results are consequences of the **variational principle** in quantum mechanics, which gives an exceptionally powerful criterion for improving the accuracy of various approximations; lower energy is always better. Refinements of both approaches have led to highly accurate methods of modern computational quantum chemistry in which the distinction between the two starting points has completely disappeared.

Using the Linear Combination of Atomic Orbitals and Valence Bond Methods

The LCAO and VB approaches are both good starting points for describing bonding and reactivity. You can apply either one to set up a purely qualitative description of the problem of interest, confident that you can move on to a high-level quantitative calculation as your needs demand. Which method you choose at the beginning depends primarily on the area of chemistry in which you are working and the broad class of problems you are investigating. LCAO theory is most often used to describe the electronic states of molecules in contexts that require knowledge of energy levels. Examples include molecular spectroscopy, photochemistry, and phenomena that involve ionization (such as electron-induced reactions and PES). VB theory is more widely used to describe molecular structure, especially in pictorial ways.

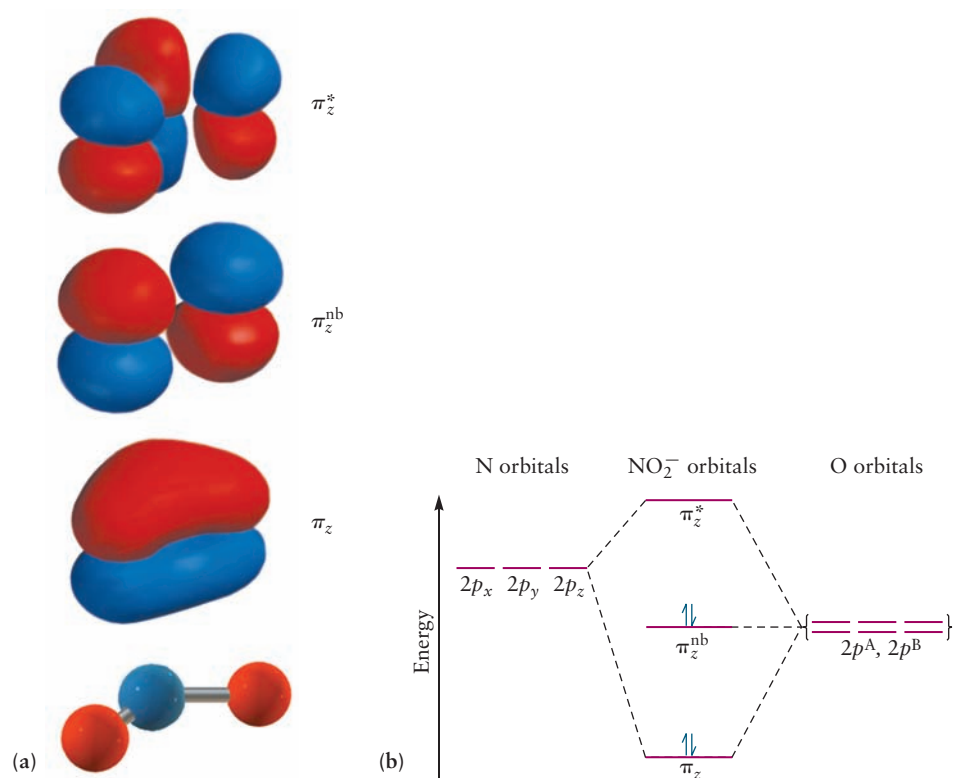
Many chemists use a mixture of the two, where localized VB σ bonds describe the network holding the molecule together and de-localized LCAO π bonds

describe the spread of electron density over the molecule. We illustrate this combination here for the case of bent triatomic molecules, and also much more extensively in Chapter 7 for organic molecules.

Nonlinear triatomic molecules can be described through sp^2 hybridization of the central atom. If the molecule lies in the x - y plane, then the s , p_x , and p_y orbitals of the central atom can be combined to form three sp^2 hybrid orbitals with an angle close to 120° between each pair. One of these orbitals holds a lone pair of electrons, and the other two take part in σ bonds with the outer atoms. The fourth orbital, a p_z orbital, takes part in de-localized π bonding (Fig. 6.47a). On the outer atoms, the p orbital pointing toward the central atom takes part in a localized σ bond, and the p_z orbital takes part in π bonding; the third p orbital and the s orbital are AOs that do not participate in bonding. The three p_z AOs can be combined into bonding, nonbonding, and antibonding π orbitals much as in the linear molecule case (see Fig. 6.47b). Here, there is only one of each type of orbital (π , π^{nb} , π^*) rather than two as for linear molecules.

Consider a specific example, NO_2^- , with 18 electrons. Two electrons are placed in each oxygen atom $2s$ orbital and 2 more in each nonbonding oxygen atom $2p$ orbital, so that a total of 8 electrons are localized on oxygen atoms. Two electrons also are placed as a lone pair in the third sp^2 orbital of the nitrogen atom. Of the remaining 8 electrons, 4 are involved in the 2 σ bonds between nitrogen and the oxygen atoms. The last 4 are placed into the π electron system: 2 into the bonding π orbital and 2 into the nonbonding π^{nb} orbital. Because a total of 6 electrons are in bonding orbitals and none are in antibonding orbitals, the net bond order for the molecule is 3, or $1\frac{1}{2}$ per bond. In the Lewis model, 2 resonance forms are needed to represent NO_2^- . The awkwardness of the resonance model is avoided by treating the electrons in the bonding π MO as de-localized over the 3 atoms in the molecule.

FIGURE 6.47 (a) Ball-and-stick model (bottom) and molecular orbitals for bent triatomic molecules. The central atom has three sp^2 hybrid orbitals (not shown) that would lie in the plane of the molecule. From the three p_z orbitals perpendicular to this plane, three π orbitals can be constructed. (b) Correlation diagram for the π orbitals.



Epilogue

At this point you might wonder why we presented such an extensive discussion of various approximate quantum mechanical approaches to describe chemical bonding when accurate, high-level calculational methods are widely available and relatively easy to use. The answer is that most of our understanding of chemical bonding, structure, and reactivity is based on the simple approaches to MO and VB theory presented in this chapter. They provide the foundation on which our chemical intuition has been built. The concepts we have introduced are central to all areas of modern chemistry. You will likely begin to use modern computational chemistry methods in your advanced chemistry courses. You will certainly use them in your career, if you pursue an advanced degree in the chemical sciences, molecular biology, or materials science and engineering. We believe it is essential for you to understand these fundamentals so you can maximize the benefits of the powerful tools of modern computational quantum chemistry.

CHAPTER SUMMARY

Modern methods of computational quantum chemistry are now sufficiently accurate and easy to use that they are indispensable tools in chemical research and education. Our goal has been to give you a comprehensive introduction to molecular quantum mechanics so you can easily read more advanced treatments and begin to use commercially available software with intelligence and confidence.

The Born–Oppenheimer approximation is the starting point for all of molecular quantum mechanics. The fact that electrons move so much faster than nuclei allows us to treat electronic motion independently of nuclear motion by solving an electronic Schrödinger equation for each value of the internuclear separation. The resulting MOs provide all of the information of interest, the probability density distributions and the electronic energies being the most important. The electronic bonding energy and the nuclear repulsion together define the effective potential energy function for the motion of the nuclei in the molecule.

The MOs for the simplest molecule, H_2^+ , can be calculated exactly within the Born–Oppenheimer approximation. The results illustrate the general features of molecular quantum mechanics that form the basis for our understanding of structure and bonding in more complicated molecules. The orbitals are characterized by their symmetry, the number and nature of their nodes, and their energies. Orbitals in which the electron density increases between the nuclei lead to energies lower than that of separated H and H^+ ; these are called bonding MOs. Orbitals in which there is a node in the wave function and the electron density goes to zero midway between the nuclei are called antibonding orbitals. States of H_2^+ in which the electron resides in an antibonding orbital are unstable with respect to dissociation to H and H^+ .

Additional approximations must be made to calculate the MOs for many-electron molecules. The most important approximation procedures are the LCAO method and the VB model. The LCAO method constructs de-localized one-electron MOs by taking linear combinations of AOs centered on different atoms and generates electron configurations by placing electrons in these MOs using an aufbau principle and invoking Hund's rules for the ground-state configuration. The VB model constructs a wave function for a localized pair bond starting with an “occupied” AO on each of the two atoms that form the bond. These two procedures provide the conceptual foundation and vocabulary for qualitative and even semiquantitative understanding of chemical bonding and molecular structure in contemporary chemistry. A variety of sophisticated computational methods have been developed using these procedures as starting points, and the results of these calculations are now sufficiently accurate to have both analytical and predictive value.



Charles D. Winters

Iodine sublimes from the bottom of the beaker and condenses on the bottom of the chilled round-bottom flask.

CUMULATIVE EXERCISE

Iodine

The shiny purple-black crystals of elemental iodine were first prepared in 1811 from the ashes of seaweed. Several species of seaweed concentrate the iodine that is present in low proportions in seawater, and for many years, seaweed was the major practical source of this element. Most iodine is now produced from natural brines via oxidation of iodide ion with chlorine.

- Iodine is an essential trace element in the human diet, and iodine deficiency causes goiter, the enlargement of the thyroid gland. Much of the salt intended for human consumption is “iodized” by the addition of small quantities of sodium iodide to prevent goiter. Calculate the electronegativity difference between sodium and iodine. Is sodium iodide an ionic or a covalent compound? What is its chemical formula?
- Iodine is an important reagent in synthetic organic chemistry because bonds between carbon and iodine form readily. Use electronegativities to determine whether the C—I bond is ionic, purely covalent, or polar covalent in character.
- Give the steric numbers for the iodine atom and identify the geometries of the following ions containing iodine and oxygen: IO_3^- , IO_6^{5-} , and IO_4^- .
- What is the ground-state electron configuration of the valence electrons of iodine molecules (I_2)? Is iodine paramagnetic or diamagnetic?
- What is the electron configuration of the I_2^+ molecular ion? Is its bond stronger or weaker than that in I_2 ? What is its bond order?

Answers

- The electronegativity difference is 1.73; thus, the compound is largely ionic, with formula NaI.
- The electronegativity difference is 0.11; thus, the C—I bond is largely covalent, with nearly equal sharing of electrons between the atoms.
- IO_3^- : $SN = 4$, structure is pyramidal; IO_6^{5-} : $SN = 6$, structure is octahedral; IO_4^- : $SN = 4$, structure is tetrahedral.
- $(\sigma_{g5s})^2(\sigma_{u5s}^*)^2(\sigma_{g5p_z})^2(\pi_{u5p_x} \pi_{u5p_y})^4(\pi_{g5p_x}^* \pi_{g5p_y}^*)^4$; iodine is diamagnetic.
- $(\sigma_{g5s})^2(\sigma_{u5s}^*)^2(\sigma_{g5p_z})^2(\pi_{u5p_x} \pi_{u5p_y})^4(\pi_{g5p_x}^* \pi_{g5p_y}^*)^3$; the bond is stronger; bond order is $3/2$ versus 1.

CHAPTER REVIEW

The Born–Oppenheimer Approximation

- Nuclei are so much heavier than electrons that they may be considered fixed in space while the electrons move rapidly around them.
- The Born–Oppenheimer approximation allows us to solve the electronic Schrödinger equation for H_2^+ for a fixed internuclear separation R_{AB} . The result is a one-electron MO, which is analogous to the one-electron hydrogen AO.
- We calculate the electronic bonding energies for every value of R_{AB} and add to that the nuclear–nuclear repulsion energy to generate the effective potential energy function $V_{\text{eff}}(R_{AB})$ that governs the nuclear motion.
- We find the kinetic energy of the nuclei and add it to the potential energy described above to find the quantized ground-state energy of the molecule. The nuclei vibrate about the equilibrium bond length—this is the *zero point motion* required by the uncertainty principle. The energy required to dissociate the molecular ion from the ground state into a separated proton and hydrogen atom is the bond dissociation energy.

Exact Solutions for Molecular Orbitals: H_2^+

- We illustrate graphically the first eight MOs for H_2^+ to show their shapes and to characterize them by their energies and symmetry, just as we characterized the atomic orbitals for the hydrogen atom. The MOs are characterized by the component of the angular momentum along the internuclear axis: by analogy to the hydrogen atom, these are called σ for $L_Z = 0$, π for $L_Z = 1$, δ for $L_Z = 2$, and ϕ for $L_Z = 3$.

Linear Combination of Atomic Orbitals Approximation

- A good approximation to the one-electron MOs for a diatomic molecule is the sum or difference of AOs of the atoms of the molecule. The *sum* linear combination leads to increased electron density between the nuclei and bonding; the *difference* linear combination leads to a node between the nuclei and decreased electron density, and it is antibonding.
- Correlation diagrams show how pairs of AOs lead to bonding and antibonding pairs of MOs. An aufbau principle is used to build up electron configurations, just like for atoms. Hund's rules predict the lowest energy electron configurations and either paramagnetic or diamagnetic behavior.
- The bond order is found by counting the number of electrons in bonding orbitals, subtracting the number in antibonding orbitals, and dividing the result by two. Electrons in antibonding orbitals effectively cancel the bonding capacity of those in bonding orbitals. This scheme explains the trends in bond length, bond stiffness, and bond energy of the first- and second-row diatomic molecules.
- The energy sequence of the MOs is slightly more complicated in second-row homonuclear diatomic molecules, because the p orbitals can overlap in two different ways. Moving from left to right across the row, the energy-level ordering changes at N_2 because the energy of the π orbital remains nearly constant, whereas that of the σ orbital drops rapidly (see Fig. 6.15). Therefore two energy-level diagrams are required to explain the bonding in the second-period diatomic molecules.
- The MOs for heteronuclear diatomic molecules are obtained by the same approach, with the AO energies of the more electronegative element placed lower (more stable) than those of the other element. If the difference in AO energies is small, the MO energy sequence is given in Figure 6.19; for larger energy AO energy differences the MOs are described by Figure 6.21.
- The LCAO approximation can also be used to generate MOs for small polyatomic molecules, which are often also treated using the VB model. For small polyatomics the proper combinations of AOs for each MO can be identified by symmetry arguments, but iterative computer calculations are necessary to find the optimum value of the coefficients for the AOs.

Photoelectron Spectroscopy for Molecules

- Photoelectron spectroscopy confirms the validity of the orbital approximation by measuring the ionization energies of the MOs directly. The ionization energy of the orbital is obtained as the difference in the energy of the photon used to ionize the molecule and the measured kinetic energy of the emitted electrons. Koopmans's approximation states that the orbital energy ϵ in the LCAO method is the negative of the ionization energy.
- In addition to the orbital energies, PES provides a great deal of information about the nature of the orbital (bonding, nonbonding, or antibonding) from the vibrational fine structure observed in the spectra.

Valence Bond Model

- The VB model constructs wave functions to describe localized electron-pair bonds. The model describes bonding in diatomic molecules, including the

formation of multiple (σ and π) bonds. It is most frequently applied to organize and correlate data on molecular structures, especially for molecules of the type AB_x , the geometries of which are described by VSEPR theory.

- The simple VB model is augmented with the concept of orbital hybridization to account for the valence of second-row atoms and the structures of their compounds. Hybrid orbitals are constructed by adding s and p orbitals with different coefficients (weights or percentage contributions) and phases. The number of hybrid orbitals produced equals the number of starting AOs; there are two sp hybrid orbitals, three sp^2 hybrid orbitals, and four sp^3 hybrid orbitals.

Comparison of Linear Combination of Atomic Orbitals and Valence Bond Methods

- Comparing the LCAO and VB treatments for the hydrogen molecule at the level of the *electronic wave function for the molecule* gives considerable insight into the differences between the methods and also suggests ways to improve each. The VB wave function predicts a purely covalent bond, whereas the LCAO wave function predicts a bond with an equal mixture of covalent and ionic character. Neither of these is the best representation of bonding in H_2 , so refinements of both approaches are necessary to produce results that are in better agreement with experiment.
- Many methods have been developed to improve both the simple LCAO and VB models; it is easiest to illustrate one approach for improving the VB model. Let $\psi_{\text{improved}} = \psi_{\text{VB}} + \lambda\psi_{\text{MO}}$, where λ is chosen so that the energy of the orbital is in better agreement with experiment. The variational principle ensures that the true energy is always lower than the energy calculated using an approximate wave function. This provides a well-defined criterion to judge improvement—lower energy is always better.
- Many chemists combine the LCAO and VB methods to describe bonding in polyatomic molecules. They use the VB model to describe the localized σ bonds that provide “connectivity” for the molecule structure and use the LCAO method to describe the de-localized π bonds that distribute electrons over the entire structure.

CONCEPTS & SKILLS

After studying this chapter and working the problems that follow, you should be able to:

1. Give a general description of the quantum picture of the chemical bond and how it differs from the classical picture. Describe the key features of the quantum picture, including the nature of bonding and anti-bonding MOs, symmetry of MOs, and the energy sequence of MOs (Section 6.1, Problems 1–8).
2. Show how MOs can be constructed from the AOs of two atoms that form a chemical bond, and explain how the electron density between the atoms is related to the MO (Section 6.2, Problems 9–12).
3. Construct correlation diagrams for diatomic molecules formed from second- and third-period main-group elements. From these diagrams, give the electron configurations, work out the bond orders, and comment on their magnetic properties (Section 6.2, Problems 17–30).
4. Construct qualitative potential energy curves for diatomic molecules and relate trends in well depth (bond dissociation energies) and location of the

potential minimum (equilibrium bond length) with trends in bond order predicted by the LCAO method (Section 6.2, Problems 13–16).

5. Use symmetry arguments to find the proper combinations of AOs to construct MOs for small polyatomic molecules (Section 6.2, Problems 31–34).
6. Relate photoelectron spectra to correlation diagrams for MOs (Section 6.3, Problems 35–40).
7. Use the VB method to construct wave functions for localized electron pair bonds, including multiple bonds, and predict the molecular geometry from these bonds (Section 6.4, Problems 41–48).
8. Describe the hybrid/AO basis for representing the structures of molecules and the geometry predicted by each hybridization class (Section 6.4, Problems 49–56).
9. Compare the LCAO and VB approaches, and combine them to describe the molecular network and delocalized bonds in certain classes of molecules (Section 6.5, Problems 57–62).

KEY EQUATIONS

$$1\sigma_g \approx \sigma_{g1s} = C_g(R_{AB})[\varphi_{1s}^A + \varphi_{1s}^B] \quad (\text{Section 6.2.1})$$

$$1\sigma_u^* \approx \sigma_{u1s}^* = C_u(R_{AB})[\varphi_{1s}^A - \varphi_{1s}^B] \quad (\text{Section 6.2.1})$$

$$[\sigma_{g1s}]^2 = C_g^2[(\varphi_{1s}^A)^2 + (\varphi_{1s}^B)^2 + 2\varphi_{1s}^A\varphi_{1s}^B] \quad (\text{Section 6.2.1})$$

$$[\sigma_{u1s}^*]^2 = C_u^2[(\varphi_{1s}^A)^2 + (\varphi_{1s}^B)^2 - 2\varphi_{1s}^A\varphi_{1s}^B] \quad (\text{Section 6.2.1})$$

$$\psi_{n.i.}^2 = C_3^2[(\varphi_{1s}^A)^2 + (\varphi_{1s}^B)^2] \quad (\text{Section 6.2.1})$$

$$\sigma_{g1s} = C_g[1s^A + 1s^B] \quad (\text{Section 6.2.2})$$

$$\sigma_{g1s}^* = C_g[1s^A - 1s^B] \quad (\text{Section 6.2.2})$$

$$\sigma_{g2s} = C_g[2s^A + 2s^B] \quad (\text{Section 6.2.4})$$

$$\sigma_{u2s}^* = C_u[2s^A - 2s^B] \quad (\text{Section 6.2.4})$$

$$\sigma_{g2p_z} = C_g[2p_z^A - 2p_z^B] \quad (\text{Section 6.2.4})$$

$$\sigma_{u2p_x}^* = C_u[2p_x^A + 2p_x^B] \quad (\text{Section 6.2.4})$$

$$\pi_{u2p_x} = C_u[2p_x^A + 2p_x^B] \quad (\text{Section 6.2.4})$$

$$\pi_{g2p_x}^* = C_g[2p_x^A - 2p_x^B] \quad (\text{Section 6.2.4})$$

$$\pi_{u2p_y} = C_u[2p_y^A + 2p_y^B] \quad (\text{Section 6.2.4})$$

$$\pi_{g2p_y}^* = C_g[2p_y^A - 2p_y^B] \quad (\text{Section 6.2.4})$$

$$\sigma_{2s} = C_A 2s^A + C_B 2s^B \quad (\text{Section 6.2.4})$$

$$\sigma_{2s}^* = C_A' 2s^A - C_B' 2s^B \quad (\text{Section 6.2.4})$$

$$V_{1g}^{(\text{eff})}(R_{AB}) = E_{1g}^{(\text{cl})}(R_{AB}) + V_m(R_{AB}) \quad (\text{Section 6.2.5})$$

$$h\nu_{\text{photon}} - \frac{1}{2} m_e v^2 = -\varepsilon_i + E_i^{(\text{vib})} = IE_i \quad (\text{Section 6.3})$$

$$h\nu_{\text{photon}} - \frac{1}{2} m_e v^2 = -\varepsilon_i + nh\nu_{\text{vib}} \quad n = 0, 1, 2, 3, \dots \quad (\text{Section 6.3})$$

$$\psi^{\text{cl}}(r_{1A}, r_{2B}; R_{AB}) = C_1(R_{AB})\varphi^A(r_{1A})\varphi^B(r_{2B}) + C_2(R_{AB})\varphi^A(r_{2A})\varphi^B(r_{1B}) \quad (\text{Section 6.4.1})$$

$$\psi_g^{\text{cl}} = C_1[1s^A(1)1s^B(2) + 1s^A(2)1s^B(1)] \quad (\text{Section 6.4.1})$$

$$\psi_g^{\text{bond}} = C_1[2p_z^A(1)2p_z^B(2) + 2p_z^A(2)2p_z^B(1)] \quad (\text{Section 6.4.1})$$

$$\psi_{\pi_x}^{\text{bond}}(1, 2; R_{AB}) = C_1(R_{AB})[2p_x^A(1)2p_x^B(2)] + C_1(R_{AB})[2p_x^A(2)2p_x^B(1)] \quad (\text{Section 6.4.1})$$

$$\psi_{\text{MO}}^{\text{el}} = \sigma_{g1s}(1)\sigma_{g1s}(2) = [1s^A(1) + 1s^B(1)][1s^A(2) + 1s^B(2)] \quad (\text{Section 6.5})$$

$$\psi_{\text{MO}}^{\text{el}} = [1s^A(1)1s^B(2) + 1s^A(2)1s^B(1)] + [1s^A(1)1s^A(2) + 1s^B(1)1s^B(2)] \quad (\text{Section 6.5})$$

$$\psi_{\text{improved}} = \psi_{\text{VB}} + \lambda\psi_{\text{ionic}} \quad (\text{Section 6.5})$$

PROBLEMS

Answers to problems whose numbers are boldface appear in Appendix G. Problems that are more challenging are indicated with asterisks.

Quantum Picture of the Chemical Bond

- Determine the number of nodes along the internuclear axis for each of the σ molecular orbitals for H_2^+ shown in Figure 6.2.
- Determine the number of nodes along the internuclear axis and the number of nodal planes for each of the π molecular orbitals for H_2^+ shown in Figure 6.2.
- Sketch the shape of each of the σ molecular orbitals for H_2^+ shown in Figure 6.2 in a plane perpendicular to the internuclear axis located at the midpoint between the two nuclei. Repeat the sketches for a plane perpendicular to the internuclear axis located at a point one quarter of the distance between the two nuclei.
- Sketch the shape of each of the π molecular orbitals for H_2^+ shown in Figure 6.2 in a plane perpendicular to the internuclear axis located at the midpoint between the two nuclei. Repeat the sketches for a plane perpendicular to the internuclear axis located at a point one quarter of the distance between the two nuclei.
- Compare the electron density in the $1\sigma_g$ and $1\sigma_u^*$ molecular orbitals for H_2^+ shown in Figure 6.3 with the classical model for bonding for H_2^+ summarized in Figures 3.11 and 3.12. Which of these molecular orbitals describes the bond in H_2^+ ?
- Explain why $1\sigma_g$ is the ground state for H_2^+ . By combining your answer with the answer to Problem 5, what conclusions can you draw about the molecular orbital description of the bond in H_2^+ ?
- The discussion summarized in Figure 6.4 explained how, at large internuclear separations, the $1\sigma_g$ molecular orbital for H_2^+ approaches the sum of two hydrogen atomic orbitals, and the $1\sigma_u^*$ molecular orbital approaches the difference of two hydrogen atomic orbitals. As illustrated in Figure 6.5, the 3σ molecular orbitals behave differently: $3\sigma_g$ approaches the *difference* of two hydrogen atomic orbitals, and $3\sigma_u^*$ approaches the *sum* of two hydrogen atomic orbitals. Explain this different behavior in the two sets of σ molecular orbitals.
- The discussion summarized in Figure 6.4 explained how, at large internuclear separations, the $1\sigma_g$ molecular orbital for H_2^+ approaches the sum of two hydrogen atomic orbitals, and the $1\sigma_u^*$ molecular orbital approaches the difference of two hydrogen atomic orbitals. As illustrated in Figure 6.5, the 1π molecular orbitals behave differently:

$1\pi_g^*$ approaches the *difference* of two hydrogen atomic orbitals, and $1\pi_u$ approaches the *sum* of two hydrogen atomic orbitals. Explain this different behavior in the two sets of molecular orbitals.

De-localized Bonds: Molecular Orbital Theory and the Linear Combination of Atomic Orbitals Approximation

- Without consulting tables of data, predict which species has the higher bond energy, H_2 or He_2^+ .
- Without consulting tables of data, predict which species has the higher bond energy, H_2^+ or H_2 .
- Without consulting tables of data, predict which species has the greater bond length, H_2 or He_2^+ .
- Without consulting tables of data, predict which species has the greater bond length, H_2^+ or H_2 .
- Without consulting tables of data, on the same graph sketch the effective potential energy curves for H_2 and He_2^+ .
- Without consulting tables of data, on the same graph sketch the effective potential energy curves for H_2^+ and H_2 .
- Suppose we supply enough energy to H_2 to remove one of its electrons. Is the bond energy of the resulting ion larger or smaller than that of H_2 ? Is the bond length of the resulting ion larger or smaller than that of H_2 ?
- Suppose we supply enough energy to He_2^+ to remove its most weakly bound electron. Is the bond energy of the resulting ion larger or smaller than that of He_2^+ ? Is the bond length of the resulting ion larger or smaller than that of He_2^+ ?
- If an electron is removed from a fluorine molecule, an F_2^+ molecular ion forms.
 - Give the molecular electron configurations for F_2 and F_2^+ .
 - Give the bond order of each species.
 - Predict which species should be paramagnetic.
 - Predict which species has the greater bond dissociation energy.
- When one electron is added to an oxygen molecule, a superoxide ion (O_2^-) is formed. The addition of two electrons gives a peroxide ion (O_2^{2-}). Removal of an electron from O_2 leads to O_2^+ .
 - Construct the correlation diagram for O_2^- .
 - Give the molecular electron configuration for each of the following species: O_2^+ , O_2 , O_2^- , O_2^{2-} .
 - Give the bond order of each species.
 - Predict which species are paramagnetic.
 - Predict the order of increasing bond dissociation energy among the species.

19. Predict the valence electron configuration and the total bond order for the molecule S_2 , which forms in the gas phase when sulfur is heated to a high temperature. Will S_2 be paramagnetic or diamagnetic?
20. Predict the valence electron configuration and the total bond order for the molecule I_2 . Will I_2 be paramagnetic or diamagnetic?
21. For each of the following valence electron configurations of a homonuclear diatomic molecule or molecular ion, identify the element X, Q, or Z and determine the total bond order.
- (a) $X_2: (\sigma_{g2s})^2 (\sigma_{u2s}^*)^2 (\sigma_{g2p_z})^2 (\pi_{u2p})^4 (\pi_{g2p}^*)^4$
 (b) $Q_2^+: (\sigma_{g2s})^2 (\sigma_{u2s}^*)^2 (\pi_{u2p})^4 (\sigma_{g2p_z}^*)^1$
 (c) $Z_2^-: (\sigma_{g2s})^2 (\sigma_{u2s}^*)^2 (\sigma_{g2p_z})^2 (\pi_{u2p})^4 (\pi_{g2p}^*)^3$
22. For each of the following valence electron configurations of a homonuclear diatomic molecule or molecular ion, identify the element X, Q, or Z and determine the total bond order.
- (a) $X_2: (\sigma_{g2s})^2 (\sigma_{u2s}^*)^2 (\sigma_{g2p_z})^2 (\pi_{u2p})^4 (\pi_{g2p}^*)^2$
 (b) $Q_2^-: (\sigma_{g2s})^2 (\sigma_{u2s}^*)^2 (\pi_{u2p})^3$
 (c) $Z_2^{2+}: (\sigma_{g2s})^2 (\sigma_{u2s}^*)^2 (\sigma_{g2p_z})^2 (\pi_{u2p})^4 (\pi_{g2p}^*)^2$
23. For each of the electron configurations in Problem 21, determine whether the molecule or molecular ion is paramagnetic or diamagnetic.
24. For each of the electron configurations in Problem 22, determine whether the molecule or molecular ion is paramagnetic or diamagnetic.
25. Following the pattern of Figure 6.19, work out the correlation diagram for the CN molecule, showing the relative energy levels of the atoms and the bonding and antibonding orbitals of the molecule. Indicate the occupation of the MOs with arrows. State the order of the bond and comment on the magnetic properties of CN.
26. Following the pattern of Figure 6.19, work out the correlation diagram for the BeN molecule, showing the relative energy levels of the atoms and the bonding and antibonding orbitals of the molecule. Indicate the occupation of the MOs with arrows. State the order of the bond and comment on the magnetic properties of BeN.
27. The bond length of the transient diatomic molecule CF is 1.291 Å; that of the molecular ion CF^+ is 1.173 Å. Explain why the CF bond shortens with the loss of an electron. Refer to the proper MO correlation diagram.
28. The compound nitrogen oxide (NO) forms when the nitrogen and oxygen in air are heated. Predict whether the nitrosyl ion (NO^+) will have a shorter or a longer bond than the NO molecule. Will NO^+ be paramagnetic like NO or diamagnetic?
29. What would be the electron configuration for a HeH^- molecular ion? What bond order would you predict? How stable should such a species be?
30. The molecular ion HeH^+ has an equilibrium bond length of 0.774 Å. Draw an electron correlation diagram for this ion, indicating the occupied MOs. Is HeH^+ paramagnetic? When HeH^+ dissociates, is a lower energy state reached by forming $He + H^+$ or $He^+ + H$?
31. Suppose we supply enough energy to BeH_2 to remove one of its electrons. Is the dissociation energy of the resulting ion larger or smaller than that of BeH_2 ? Explain your answer.

32. Suppose we supply enough energy to BeH_2 to remove one of its electrons. Is the length of the Be—H bonds in the resulting ion larger or smaller than those in BeH_2 ? Will both Be—H bonds change in the same way? Explain your answers.
33. Suppose we remove an electron from the highest energy occupied molecular orbital in CO_2 . Is the dissociation energy of the resulting ion larger or smaller than that of CO_2 ? How will the C—O bonds change? Explain your answers.
34. Suppose we remove three electrons from CO_2 to create the ion CO_2^{3+} . Is the dissociation energy of the resulting ion larger or smaller than that of CO_2 ? How will the C—O bonds change? Explain your answers.

Photoelectron Spectroscopy for Molecules

35. Photoelectron spectra were acquired from a sample of gaseous N_2 using He(I) light with energy 21.22 eV as the ionization source. Photoelectrons were detected with kinetic energy values 5.63 eV and also with 4.53 eV. Calculate the ionization energy for each group of electrons. Identify the MOs that were most likely the sources of these two groups of electrons.
36. Photoelectron spectra were acquired from a sample of gaseous O_2 using x-ray radiation with wavelength 0.99 nm and energy 1253.6 eV. The spectrum contained a large peak for photoelectrons with speed of 1.57×10^7 m s^{-1} . Calculate the ionization energy of these electrons. Identify the orbital from which they were most likely emitted.
37. From the $n = 0$ peaks in the photoelectron spectrum for N_2 shown in Figure 6.33, prepare a quantitative energy level diagram for the molecular orbitals of N_2 .
38. From the $n = 0$ peaks in the photoelectron spectrum for O_2 shown in Figure 6.34, prepare a quantitative energy level diagram for the molecular orbitals of O_2 .
39. The photoelectron spectrum of HBr has two main groups of peaks. The first has ionization energy 11.88 eV. The next peak has ionization energy 15.2 eV, and it is followed by a long progression of peaks with higher ionization energies. Identify the molecular orbitals corresponding to these two groups of peaks.
40. The photoelectron spectrum of CO has four major peaks with ionization energies of 14.5, 17.2, 20.1, and 38.3 eV. Assign these peaks of molecular orbitals of CO, and prepare a quantitative energy level correlation diagram for CO. The ionization energy of carbon atoms is 11.26 eV, and the ionization energy of oxygen atoms is 13.62 eV.

Localized Bonds: The Valence Bond Model

41. Write simple valence bond wave functions for the diatomic molecules Li_2 and C_2 . State the bond order predicted by the simple VB model and compare with the LCAO predictions in Table 6.3
42. Write simple valence bond wave functions for the diatomic molecules B_2 and O_2 . State the bond order predicted by the simple VB model and compare with the LCAO predictions in Table 6.3
43. Both the simple VB model and the LCAO method predict that the bond order of Be_2 is 0. Explain how each arrives at that conclusion.

44. Both the simple VB model and the LCAO method predict that the bond order of Ne_2 is 0. Explain how each arrives at that conclusion.
45. Write simple valence bond wave functions for formation of bonds between B atoms and H atoms. What B–H compound does the VB model predict? What geometry does it predict for the molecules?
46. Write simple valence bond wave functions for formation of bonds between C and H atoms. What C–H compound does the VB model predict? What geometry does it predict for the molecules?
47. Write simple valence bond wave functions for the bonds in NH_3 . What geometry does the VB model predict for NH_3 ?
48. Write simple valence bond wave functions for the bonds in H_2O . What geometry does the VB model predict for H_2O ?
49. Formulate a localized bond picture for the amide ion (NH_2^-). What hybridization do you expect the central nitrogen atom to have, and what geometry do you predict for the molecular ion?
50. Formulate a localized bond picture for the hydronium ion (H_3O^+). What hybridization do you expect the central oxygen atom to have, and what geometry do you predict for the molecular ion?
51. Draw a Lewis electron dot diagram for each of the following molecules and ions. Formulate the hybridization for the central atom in each case and give the molecular geometry.
- CCl_4
 - CO_2
 - OF_2
 - CH_3^-
 - BeH_2
52. Draw a Lewis electron dot diagram for each of the following molecules and ions. Formulate the hybridization for the central atom in each case and give the molecular geometry.
- BF_3
 - BH_4^-
 - PH_3
 - CS_2
 - CH_3^+
53. Describe the hybrid orbitals on the chlorine atom in the ClO_3^+ and ClO_2^+ molecular ions. Sketch the expected geometries of these ions.
54. Describe the hybrid orbitals on the chlorine atom in the ClO_4^- and ClO_3^- molecular ions. Sketch the expected geometries of these ions.
55. The sodium salt of the unfamiliar orthonitrate ion (NO_4^{3-}) has been prepared. What hybridization is expected on the nitrogen atom at the center of this ion? Predict the geometry of the NO_4^{3-} ion.
56. Describe the hybrid orbitals used by the carbon atom in $\text{N}\equiv\text{C}-\text{Cl}$. Predict the geometry of the molecule.
58. Describe the bonding in the bent molecule OF_2 . Predict its energy level diagram and electron configuration.
59. The azide ion (N_3^-) is a weakly bound molecular ion. Formulate its MO structure for localized σ bonds and de-localized π bonds. Do you expect N_3 and N_3^+ to be bound as well? Which of the three species do you expect to be paramagnetic?
60. Formulate the MO structure of (NO_2^+) for localized π bonds and de-localized π bonds. Is it linear or nonlinear? Do you expect it to be paramagnetic? Repeat the analysis for NO_2 and for NO_2^- .
61. Discuss the nature of the bonding in the nitrite ion (NO_2^-). Draw the possible Lewis resonance diagrams for this ion. Use the VSEPR theory to determine the steric number, the hybridization of the central nitrogen atom, and the geometry of the ion. Show how the use of resonance structures can be avoided by introducing a de-localized π MO. What bond order does the MO model predict for the N–O bonds in the nitrite ion?
62. Discuss the nature of the bonding in the nitrate ion (NO_3^-). Draw the possible Lewis resonance diagrams for this ion. Use the VSEPR theory to determine the steric number, the hybridization of the central N atom, and the geometry of the ion. Show how the use of resonance structures can be avoided by introducing a de-localized π MO. What bond order is predicted by the MO model for the N–O bonds in the nitrate ion?

ADDITIONAL PROBLEMS

63. (a) Sketch the occupied MOs of the valence shell for the N_2 molecule. Label the orbitals as σ or π orbitals, and specify which are bonding and which are antibonding.
 (b) If one electron is removed from the highest occupied orbital of N_2 , will the equilibrium N–N distance become longer or shorter? Explain briefly.
64. Calcium carbide (CaC_2) is an intermediate in the manufacturing of acetylene (C_2H_2). It is the calcium salt of the carbide (also called acetylide) ion (C_2^{2-}). What is the electron configuration of this molecular ion? What is its bond order?
65. Show how that the B_2 molecule is paramagnetic indicates that the energy ordering of the orbitals in this molecule is given by Figure 6.16a rather than 6.16b.
66. The Be_2 molecule has been detected experimentally. It has a bond length of 2.45 Å and a bond dissociation energy of 9.46 kJ mol⁻¹. Write the ground-state electron configuration of Be_2 and predict its bond order using the theory developed in the text. Compare the experimental bonding data on Be_2 with those recorded for B_2 , C_2 , N_2 , and O_2 in Table 6.3. Is the prediction that stems from the simple theory significantly incorrect?
- * 67. (a) The ionization energy of molecular hydrogen (H_2) is *greater* than that of atomic hydrogen (H), but that of molecular oxygen (O_2) is *lower* than that of atomic oxygen (O). Explain. (*Hint*: Think about the stability of the molecular ion that forms in relation to bonding and antibonding electrons.)
 (b) What prediction would you make for the relative ionization energies of atomic and molecular fluorine (F and F_2)?

Comparison of Linear Combination of Atomic Orbitals and Valence Bond Methods

57. Describe the bonding in the bent molecule NF_2 . Predict its energy level diagram and electron configuration.

68. The molecular ion HeH^+ has an equilibrium bond length of 0.774 Å. Draw an electron correlation diagram for this molecule, indicating the occupied MOs. If the lowest energy MO has the form $C_1\psi_{1s}^{\text{H}} + C_2\psi_{1s}^{\text{He}}$, do you expect C_2 to be larger or smaller than C_1 ?

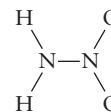
* 69. The MO of the ground state of a heteronuclear diatomic molecule AB is

$$\psi_{\text{mol}} = C_A\varphi^{\text{A}} + C_B\varphi^{\text{B}}$$

If a bonding electron spends 90% of its time in an orbital φ^{A} on atom A and 10% of its time in φ^{B} on atom B, what are the values of C_A and C_B ? (Neglect the overlap of the two orbitals.)

70. The stable molecular ion H_3^+ is triangular, with H—H distances of 0.87 Å. Sketch the molecule and indicate the region of greatest electron density of the lowest energy MO.

* 71. According to recent spectroscopic results, nitramide



is a nonplanar molecule. It was previously thought to be planar.

(a) Predict the bond order of the N—N bond in the nonplanar structure.

(b) If the molecule really were planar after all, what would be the bond order of the N—N bond?

72. *trans*-Tetrazene (N_4H_4) consists of a chain of four nitrogen atoms with each of the two end atoms bonded to two hydrogen atoms. Use the concepts of steric number and hybridization to predict the overall geometry of the molecule. Give the expected structure of *cis*-tetrazene.

This page intentionally left blank

Bonding in Organic Molecules

- 7.1 Petroleum Refining and the Hydrocarbons
- 7.2 The Alkanes
- 7.3 The Alkenes and Alkynes
- 7.4 Aromatic Hydrocarbons
- 7.5 Fullerenes
- 7.6 Functional Groups and Organic Reactions
- 7.7 Pesticides and Pharmaceuticals



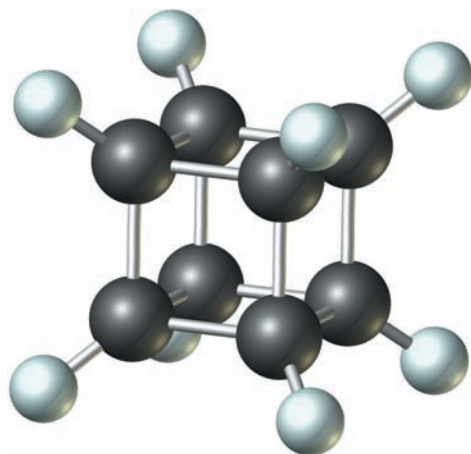
© Royalty-free/CORBIS

A petroleum refining tower.

Carbon (C) is unique among the elements in the large number of compounds it forms and in the variety of their structures. In combination with hydrogen (H), it forms molecules with single, double, and triple bonds; chains; rings; branched structures; and cages. There are thousands of stable hydrocarbons in sharp contrast to the mere two stable compounds between oxygen and hydrogen (water and hydrogen peroxide). Even the rather versatile elements nitrogen and oxygen form only six nitrogen oxides.

The unique properties of carbon relate to its position in the periodic table. As a second-period element, carbon atoms are relatively small. Therefore, it can easily form the double and triple bonds that are rare in the compounds of related elements, such as silicon. As a Group IV element, carbon can form four bonds, which is more than the other second-period elements; this characteristic gives it wide

One simple and unusual hydrocarbon is cubane (C_8H_8), in which the eight carbon atoms are arranged at the corners of a cube. Recently, a derivative was made in which all eight hydrogen atoms were replaced by $-NO_2$ groups.



scope for structural elaboration. Finally, as an element of intermediate electronegativity, carbon forms covalent compounds both with relatively electronegative elements, such as oxygen, nitrogen, and the halogens, and with relatively electropositive elements, such as hydrogen and the heavy metals mercury and lead.

The study of the compounds of carbon is the discipline traditionally called **organic chemistry**, although the chemistry of carbon is intimately bound up with that of inorganic elements and with biochemistry. This chapter builds on the general principles of covalent bonding in carbon compounds presented in Sections 6.2, 6.4, and 6.5. The relation between molecular structure and properties of organic substances is illustrated by examining the composition, refining, and chemical processing of petroleum, the primary starting material for the production of hydrocarbons and their derivatives. This chapter continues with an introduction to the types of compounds that result when elements such as chlorine, oxygen, and nitrogen combine with carbon and hydrogen. The chapter concludes with a brief introduction to some organic molecules important to agriculture and to medicine.

7.1 Petroleum Refining and the Hydrocarbons

When the first oil well was drilled in 1859 near Titusville, Pennsylvania, the future effects of the exploitation of petroleum on everyday life could not have been anticipated. Today, the petroleum and petrochemical industries span the world and influence nearly every aspect of our daily lives. In the early years of the 20th century, the development of the automobile, fueled by low-cost gasoline derived from petroleum, dramatically changed many people's lifestyles. The subsequent use of gasoline and oil to power trains and planes, tractors and harvesters, and pumps and coolers transformed travel, agriculture, and industry. Natural gas and heating oil warm most homes in the United States. Finally, the spectacular growth of the petrochemical industry since 1945 has led to the introduction of innumerable new products, ranging from pharmaceuticals to plastics and synthetic fibers. More than half of the chemical compounds produced in greatest volumes are synthesized from petroleum feedstocks.

In the 21st century the prospects for the continued availability of cheap petroleum and petrochemicals are clouded. Many wells have been drained, and the remaining petroleum is relatively difficult and costly to extract. Petroleum is not easy to make. It originated from the deposition and decay of organic matter (of animal or vegetable origin) in oxygen-poor marine sediments. Subsequently, petroleum migrated to the porous sandstone rocks from which it is extracted today. Over the past 100 years, we have consumed a significant fraction of the petroleum

accumulated in the earth over many millions of years. The imperative for the future is to save the remaining reserves for uses for which few substitutes are available (such as the manufacture of specialty chemicals) while finding other sources of heat and energy.

Although crude petroleum contains small amounts of oxygen, nitrogen, and sulfur, its major constituents are **hydrocarbons**—compounds of carbon and hydrogen. Isolating individual hydrocarbon substances from petroleum mixtures is an industrial process of central importance. Moreover, it provides a fascinating story that illustrates how the structures of molecules determines the properties of substances and the behavior of those substances in particular processes. The next three sections present a brief introduction to this story, emphasizing the structure–property correlations.

7.2 The Alkanes

Normal Alkanes

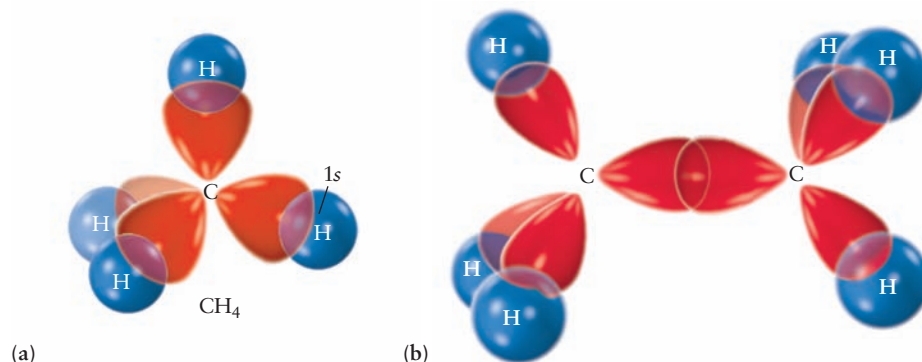
The most prevalent hydrocarbons in petroleum are the **straight-chain alkanes** (also called normal alkanes, or *n*-alkanes), which consist of chains of carbon atoms bonded to one another by single bonds, with enough hydrogen atoms on each carbon atom to bring it to the maximum bonding capacity of four. These alkanes have the generic formula C_nH_{2n+2} ; Table 7.1 lists the names and formulas of the first few alkanes. The ends of the molecules are methyl ($-CH_3$) groups, with methylene ($-CH_2-$) groups between them. We could write pentane (C_5H_{12}) as $CH_3CH_2CH_2CH_2CH_3$ to indicate the structure more explicitly or, in abbreviated fashion, as $CH_3(CH_2)_3CH_3$.

Bonding in the normal alkanes is explained by the valence bond (VB) model with orbital hybridization described in Section 6.4. The carbon atom in methane has four sp^3 hybridized orbitals, which overlap with hydrogen 1s orbitals to form four σ bonds pointing toward the vertices of a tetrahedron with the carbon atom at its center. These orbitals are represented in Figures 6.43 and 6.44; the methane molecule is shown in Figure 7.1a. The bonds in ethane are also described sp^3 hybridization. One hybrid orbital on each carbon atom overlaps another hybrid orbital to form the C–C σ bond. The remaining three hybrids on each carbon overlap with hydrogen 1s orbitals to form σ bonds. The ethane molecule is shown in Figure 7.1b.

The same bonding scheme applies to the larger straight-chain alkanes. Two of the sp^3 hybrid orbitals on each carbon atom overlap those of adjacent atoms to form the backbone of the chain, and the remaining two bond to hydrogen atoms. Although bond *lengths* change little through vibration, rotation about a C–C single bond occurs quite easily (Fig. 7.2). Thus, a hydrocarbon molecule in a gas or

Name	Formula
Methane	CH_4
Ethane	C_2H_6
Propane	C_3H_8
Butane	C_4H_{10}
Pentane	C_5H_{12}
Hexane	C_6H_{14}
Heptane	C_7H_{16}
Octane	C_8H_{18}
Nonane	C_9H_{20}
Decane	$C_{10}H_{22}$
Undecane	$C_{11}H_{24}$
Dodecane	$C_{12}H_{26}$
Tridecane	$C_{13}H_{28}$
Tetradecane	$C_{14}H_{30}$
Pentadecane	$C_{15}H_{32}$
·	·
·	·
·	·
·	·
Triacontane	$C_{30}H_{62}$

FIGURE 7.1 Bonding in the alkanes involves sp^3 hybridized orbitals on carbon. (a) Methane. (b) Ethane. The orbitals shown here are typical sketches used by organic chemists to describe bonding in organic molecules. Figure 6.44 compares these shapes to the actual shapes of the hybrid orbitals.



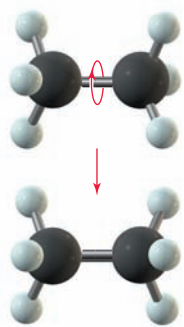


FIGURE 7.2 The two $-\text{CH}_3$ groups in ethane rotate easily about the bond that joins them.

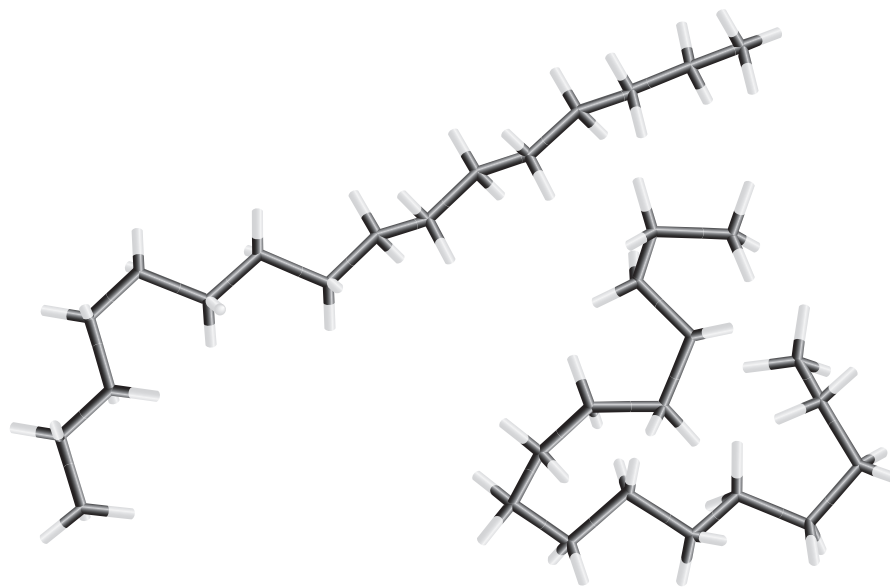
liquid constantly changes its conformation, and through free rotation can become quite “balled up” in normal motions. The term *straight chain* refers only to the bonding pattern in which each carbon atom is bonded to the next one in a sequence; it does not mean that the carbon atoms are positioned along a straight line. An alkane molecule with 10 to 20 carbon atoms looks quite different when “balled up” than when its bonds are extended to give a “stretched” molecule (Fig. 7.3). These two extreme conformations and many others interconvert rapidly at room temperature.

Figure 7.4 shows the melting and boiling points of the straight-chain alkanes; both increase with the number of carbon atoms, and thus with molecular mass. This is a consequence of the increasing strength of *dispersion forces* between heavier molecules (see discussion in Section 10.2). Methane, ethane, propane, and butane are all gases at room temperature, but the hydrocarbons that follow them in the alkane series are liquids. Alkanes beyond about $\text{C}_{17}\text{H}_{36}$ are waxy solids at 20°C , whose melting points increase with the number of carbon atoms present. Paraffin wax, a low-melting solid, is a mixture of alkanes with 20 to 30 carbon atoms per molecule. Petrolatum (petroleum jelly, or Vaseline) is a different mixture that is semisolid at room temperature.

A mixture of hydrocarbons such as petroleum does not boil at a single, sharply defined temperature. Instead, as such a mixture is heated, the compounds with lower boiling points (the most volatile) boil off first, and as the temperature increases, more and more of the material vaporizes. The existence of a boiling-point range permits components of a mixture to be separated by distillation (see discussion in Section 11.6). The earliest petroleum distillation was a simple batch process: The crude oil was heated in a still, the volatile fractions were removed at the top and condensed to gasoline, and the still was cleaned for another batch. Modern petroleum refineries use much more sophisticated and efficient distillation methods, in which crude oil is added continuously and fractions of different volatility are tapped off at various points up and down the distillation column (Fig. 7.5). To save on energy costs, heat exchangers capture the heat liberated from condensation of the liquid products.

Distillation allows hydrocarbons to be separated by boiling point, and thus by molecular mass. A mixture of gases emerges from the top of the column, resembling the natural gas that collects in rock cavities above petroleum deposits. These gas mixtures contain ethane, propane, and butane, which can be separated further by redissolving them in a liquid solvent such as hexane. The methane-rich mixture of gases that remains is used for chemical synthesis or is shipped by pipeline to

FIGURE 7.3 Two of the many possible conformations of the alkane $\text{C}_{16}\text{H}_{34}$. The carbon atoms are not shown explicitly, but they lie at the black intersections. Hydrogen atoms are at the white ends. Eliminating the spheres representing atoms in these tube (or Dreiding) models reveals the conformations more clearly.



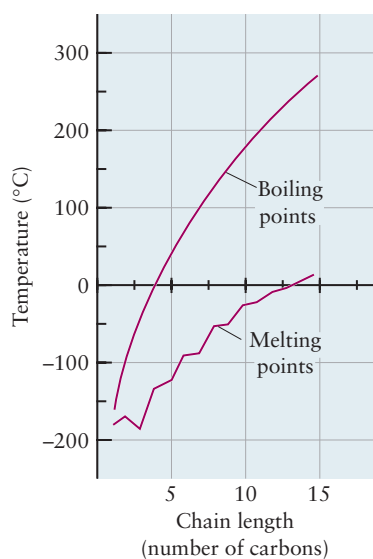


FIGURE 7.4 The melting and boiling points of the straight-chain alkanes increase with chain length n . Note the alternation in the melting points: Alkanes with n odd tend to have lower melting points because they are more difficult to pack into a crystal lattice.

heat homes. The gases dissolved in hexane can be separated by redistilling, after which they can be used as starting materials in chemical processes. Propane and butane are also bottled under pressure and sold as liquefied petroleum gas, which is used for fuel in areas where natural gas is not available from pipelines. After the gases, the next fraction to emerge from the petroleum distillation column is **naphtha**, which is used primarily in the manufacture of gasoline. Subsequent fractions of successively higher molecular mass are used for jet and diesel fuel, heating oil, and machine lubricating oil. The heavy, involatile sludge that remains at the bottom of the distillation unit is pitch or asphalt, which is used for roofing and paving.

Cyclic Alkanes

In addition to the straight-chain alkanes, the cyclic alkanes also appear in petroleum. A **cycloalkane** consists of at least one chain of carbon atoms attached at the ends to form a closed loop. In the formation of this additional C—C bond, two hydrogen atoms must be eliminated; thus, the general formula for cycloalkanes having one ring is C_nH_{2n} (Fig. 7.6). The cycloalkanes are named by adding the prefix *cyclo-* to the name of the straight-chain alkane that has the same number of carbon atoms as the ring compound. Bonding in the cycloalkanes involves sp^3 hybridization of the carbon atoms, just as in the straight-chain alkanes. But, coupling the tetrahedral angle of 109.5 degrees with the restriction of a cyclic structure leads to two new interesting structural features that introduce **strain energy** in the cycloalkanes and influence the stability of their conformations.

It is easy to see from inspection of molecular models that two distinct conformations of cyclohexane can be formed when the tetrahedral angle is maintained at each carbon atom. These are called the **boat** and **chair conformations** because of their resemblance to these objects (Fig. 7.7). The chair conformation has four carbon atoms in a plane with one above and one below that plane, located on opposite sides of the molecule. The boat conformation also has four carbon atoms in a plane, but both of the remaining atoms are located above this plane. Both conformations exist and appear to interconvert rapidly at room temperature through a sequence of rotations about single bonds (see Fig. 7.2). The chair conformation is significantly more stable than the boat, because the hydrogen atoms can become

FIGURE 7.5 In the distillation of petroleum, the lighter, more volatile hydrocarbon fractions are removed from higher up the column and the heavier fractions from lower down.

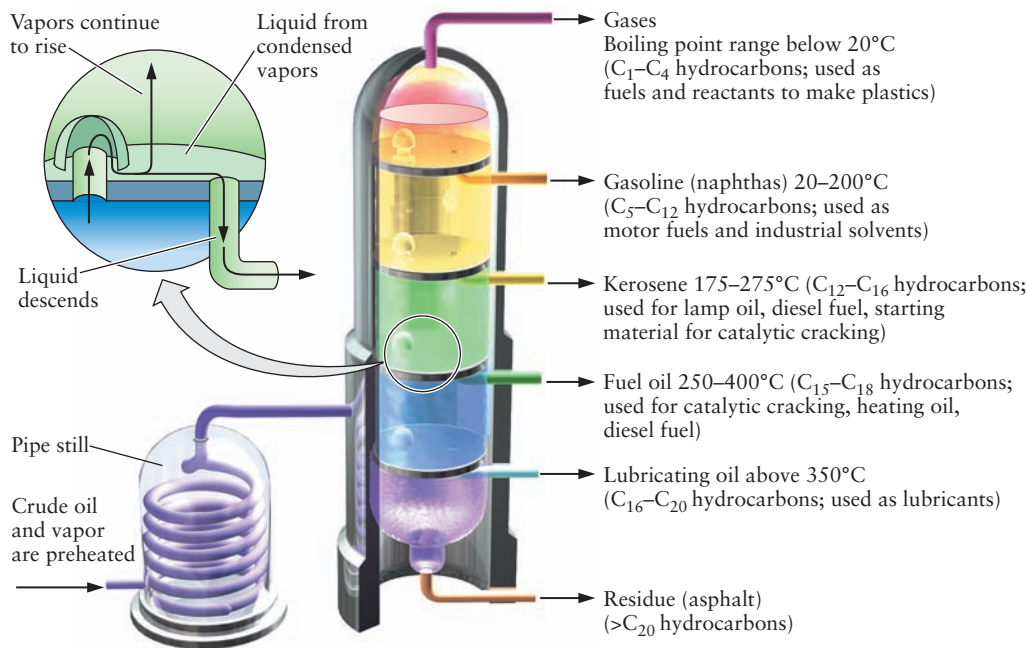


FIGURE 7.6 Three cyclic hydrocarbons. (a) Cyclopropane, C_3H_6 . (b) Cyclobutane, C_4H_8 . (c) Cyclohexane, C_6H_{12} .

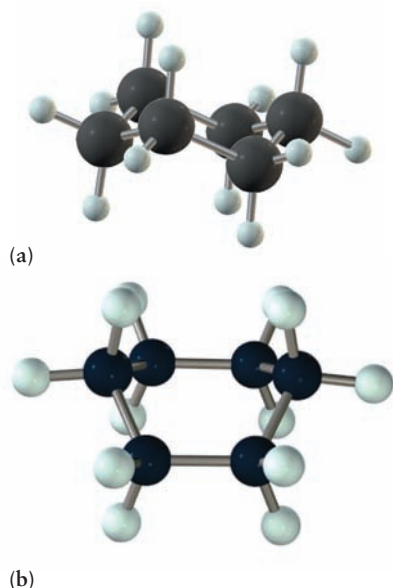
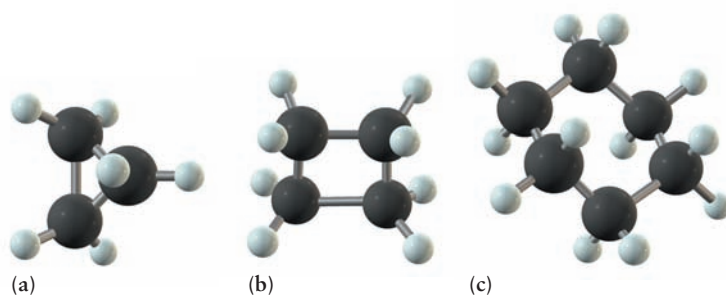


FIGURE 7.7 The conformations of cyclohexane. (a) Chair. (b) Boat.

quite close and interfere with one another in the boat conformation. When atoms that are not bonded to each other come sufficiently close in space to experience a repulsive interaction, this increase in potential energy reduces the stability of the molecule. Such interactions are called **steric strain**, and they play a significant role in determining the structure of polyatomic molecules. When the hydrogen atoms on cyclohexane are replaced with larger substituents, these effects can prevent interconversion between the boat and chair conformations. This effect is seen in many large molecules of biological significance, where the cyclohexane ring is an important structural unit, locked into one of its conformations.

Consider the possibility that cyclohexane could have a planar hexagonal structure. Then each C—C—C bond angle would be 120 degrees resulting in angle strain of 10.5 degrees. This distortion of the bond angle from the tetrahedral value increases the potential energy of the bond above its stable equilibrium value, and the resulting **angle strain** energy reduces the stability of the molecule. Cyclohexane minimizes this effect through rotation about single bonds. The smallest cycloalkanes, namely, cyclopropane and cyclobutane, have much less freedom to rotate about single bonds. Consequently, they are strained compounds because the C—C—C bond angle is 60 (in C_3H_6) or 90 degrees (in C_4H_8), which is far less than the normal tetrahedral angle of 109.5 degrees. As a result, these compounds are more reactive than the heavier cycloalkanes or their straight-chain analogs, propane and butane.

Branched-Chain Alkanes

Branched-chain alkanes are hydrocarbons that contain only C—C and C—H single bonds, but in which the carbon atoms are no longer arranged in a straight chain. One or more carbon atoms in each molecule is bonded to three or four other carbon atoms, rather than to only one or two as in the normal alkanes or cycloalkanes. The simplest branched-chain molecule (Fig. 7.8) is 2-methylpropane, sometimes referred to as isobutane. This molecule has the same molecular formula as butane (C_4H_{10}) but a different bonding structure in which the central carbon atom is bonded to three $-CH_3$ groups and only one hydrogen atom. The compounds butane and 2-methylpropane are called **geometrical isomers**. Their molecules have the same formula but different three-dimensional structures that could be interconverted only by breaking and re-forming chemical bonds.

The number of possible isomers increases rapidly with increasing numbers of carbon atoms in the hydrocarbon molecule. Butane and 2-methylpropane are the only two isomers of chemical formula C_4H_{10} , but there are three isomers of C_5H_{12} , five of C_6H_{14} , nine of C_7H_{16} , and millions of $C_{30}H_{62}$. A systematic procedure for naming these isomers has been codified by the International Union of Pure and Applied Chemistry (IUPAC). The following set of rules is a part of that procedure:

1. Find the longest continuous chain of carbon atoms in the molecule. The molecule is named as a derivative of this alkane. In Figure 7.8b, a chain of three carbon atoms can be found; thus, the molecule is a derivative of propane.

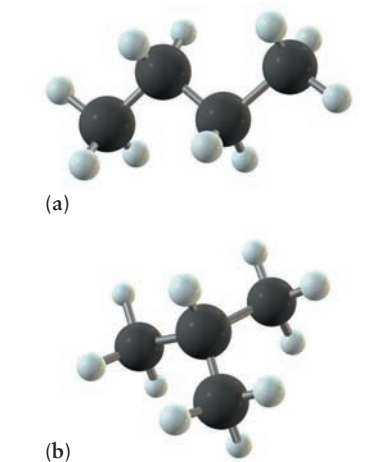


FIGURE 7.8 Two isomeric hydrocarbons with the molecular formula C_4H_{10} . (a) Butane. (b) 2-Methylpropane.

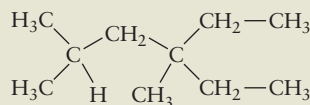
TABLE 7.2 Alkyl Side Groups

Name	Formula
Methyl	—CH ₃
Ethyl	—CH ₂ CH ₃
Propyl	—CH ₂ CH ₂ CH ₃
Isopropyl	—CH(CH ₃) ₂
Butyl	—CH ₂ CH ₂ CH ₂ CH ₃

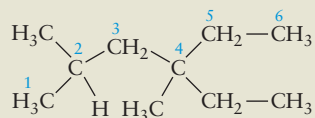
- The hydrocarbon groups attached to the chain are called alkyl groups. Their names are obtained by dropping the ending *-ane* from the corresponding alkane and replacing it with *-yl* (Table 7.2). The methyl group, CH₃, is derived from methane (CH₄), for example. Note also the isopropyl group, which attaches by its middle carbon atom.
- Number the carbon atoms along the chain identified in rule 1. Identify each alkyl group by the number of the carbon atom at which it is attached to the chain. The methyl group in the molecule in Figure 7.8b is attached to the second of the three carbon atoms in the propane chain; therefore, the molecule is called 2-methylpropane. The carbon chain is numbered from the end that gives the lowest number for the position of the first attached group.
- If more than one alkyl group of the same type is attached to the chain, use the prefixes *di-* (two), *tri-* (three), *tetra-* (four), *penta-* (five), and so forth to specify the total number of such attached groups in the molecule. Thus, 2,2,3-trimethylbutane has two methyl groups attached to the second carbon atom and one to the third carbon atom of the four-atom butane chain. It is an isomer of heptane (C₇H₁₆).
- If several types of alkyl groups appear, name them in alphabetical order. Ethyl is listed before methyl, which appears before propyl.

EXAMPLE 7.1

Name the following branched-chain alkane:

**SOLUTION**

The longest continuous chain of carbon atoms is six, so this is a derivative of hexane. Number the carbon atoms starting from the left.

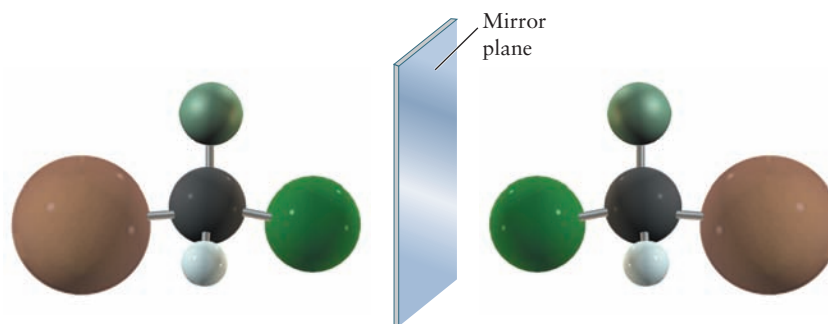


Methyl groups are attached to carbon atoms 2 and 4, and an ethyl group is attached to atom 4. The name is thus 4-ethyl-2,4-dimethylhexane. Note that if we had started numbering from the right, the higher number 3 would have appeared for the position of the first methyl group; therefore, the numbering from the left is preferred.

Related Problems: 7, 8, 9, 10, 11, 12

A second type of isomerism characteristic of organic molecules is **optical isomerism**, or **chirality**. A carbon atom that forms single bonds to four different atoms or groups of atoms can exist in two forms that are mirror images of each other but that cannot be interconverted without breaking and re-forming bonds (Fig. 7.9). If a mixture of the two forms is resolved into its optical isomers, the two forms rotate the plane of polarized light in different directions; therefore, such molecules are said to be “optically active.” Although paired optical isomers have identical physical properties, their chemical properties can differ when they interact with other optically active molecules. As discussed in Section 23.4, proteins and other biomolecules are optically active. One goal of pharmaceutical research is to prepare

FIGURE 7.9 A molecule such as CHBrClF , which has four different atoms or groups of atoms bonded to a single carbon atom, exists in two mirror-image forms that cannot be superimposed by rotation. Such pairs of molecules are optical isomers; the carbon atom is called a chiral center.



particular optical isomers of carbon compounds for medicinal use. In many cases, one optical isomer is beneficial and the other is useless or even harmful.

The fraction of branched-chain alkanes in gasoline affects how it burns in an engine. Gasoline consisting entirely of straight-chain alkanes burns unevenly, causing “knocking” that can damage the engine. Blends that are richer in branched-chain and cyclic alkanes burn with much less knocking. Smoothness of combustion is rated quantitatively via the **octane number** of the gasoline, which was defined in 1927 by selecting as references one compound that causes large amounts of knocking and another that causes little to no knocking. Pure 2,2,4-trimethylpentane (commonly known as isooctane) burns smoothly and was assigned an octane number of 100. Of the compounds examined at the time, pure heptane caused the most knocking and was assigned octane number 0. Mixtures of heptane and isooctane cause intermediate amounts of knocking. Standard mixtures of these two compounds define a scale for evaluating the knocking caused by real gasolines, which are complex mixtures of branched- and straight-chain hydrocarbons. If a gasoline sample produces the same amount of knocking in a test engine as a mixture of 90% (by volume) 2,2,4-trimethylpentane and 10% heptane, it is assigned the octane number 90.

Certain additives increase the octane rating of gasoline. The least expensive of these is tetraethyllead, $\text{Pb}(\text{C}_2\text{H}_5)_4$, a compound that has weak bonds between the central lead atom and the ethyl carbon atoms. It readily releases ethyl radicals ($\cdot\text{C}_2\text{H}_5$) into the gasoline during combustion; these reactive species speed and smooth the combustion process, reducing knocking and giving better fuel performance. The lead released into the atmosphere is a long-term health hazard. Lead poisons catalytic converters (Section 18.7) rendering them ineffective. The use of lead in gasoline has been phased out and other low-cost additives have been developed to increase octane numbers. Chemical processing to make branched-chain compounds from straight-chain compounds is also used to control the octane number of gasoline.

7.3 The Alkenes and Alkynes

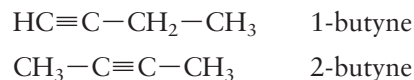
The hydrocarbons discussed so far in this chapter are referred to as **saturated**, because all the carbon–carbon bonds are single bonds. Hydrocarbons that have double and triple carbon–carbon bonds are referred to as **unsaturated** (Fig. 7.10). Ethylene (C_2H_4) has a double bond between its carbon atoms and is called an **alkene**. The simplest **alkyne** is acetylene (C_2H_2), which has a triple bond between its carbon atoms. In naming these compounds, the *-ane* ending of the corresponding alkane is replaced by *-ene* when a double bond is present and by *-yne* when a triple bond is present. Ethene is thus the systematic name for ethylene, and ethyne for acetylene, although we will continue to use their more common names. For any compound with a carbon backbone of four or more carbon atoms, it is necessary to specify the location of the double or triple bond. This is

FIGURE 7.10 One way to distinguish alkanes from alkenes is by their reactions with aqueous KMnO_4 . This strong oxidizing agent undergoes no reaction with hexane and retains its purple color (left). But, when KMnO_4 is placed in contact with 1-hexene, a redox reaction occurs in which the brown solid MnO_2 forms (right) and $-\text{OH}$ groups are added to both sides of the double bond in the 1-hexene, giving a compound with the formula $\text{CH}_3(\text{CH}_2)_3\text{CH}(\text{OH})\text{CH}_2\text{OH}$.



© Thomson Learning/Charles Steele

done by numbering the carbon-carbon bonds and putting the number of the lower numbered carbon involved in the multiple bond before the name of the alkene or alkyne. Thus, the two different isomeric alkynes with the formula C_4H_6 are



Bonding in alkenes is described by the VB method with sp^2 hybrid orbitals on each carbon atom. (This method is described in Section 6.4 and shown in Figures 6.42 and 6.44. You should review that material before proceeding.) Figure 7.11a shows three sp^2 hybrid orbitals and Figure 7.11b shows the remaining nonhybridized $2p_z$ orbital with the sp^2 hybrid orbitals represented as shadows in the x - y plane. In ethylene, a σ orbital is formed between the two sp^2 hybrid orbitals on the carbon atoms (Fig. 7.12a) and the remaining four sp^2 hybrid orbitals are used to form bonds with four hydrogen atoms. The nonhybridized $2p_z$ orbitals on the two carbon atoms are parallel to each other and overlap to form a π bond (see example in Fig. 6.16). The result is a double bond between the two carbon atoms (see Fig. 7.12b).

FIGURE 7.11 Sketches of sp^2 hybridized orbitals on carbon. (a) The three sp^2 hybridized orbitals are oriented in a plane with their axes at angles of 120 degrees. (b) The nonhybridized $2p$ orbital is perpendicular to the plane containing the three sp^2 hybrid orbitals.

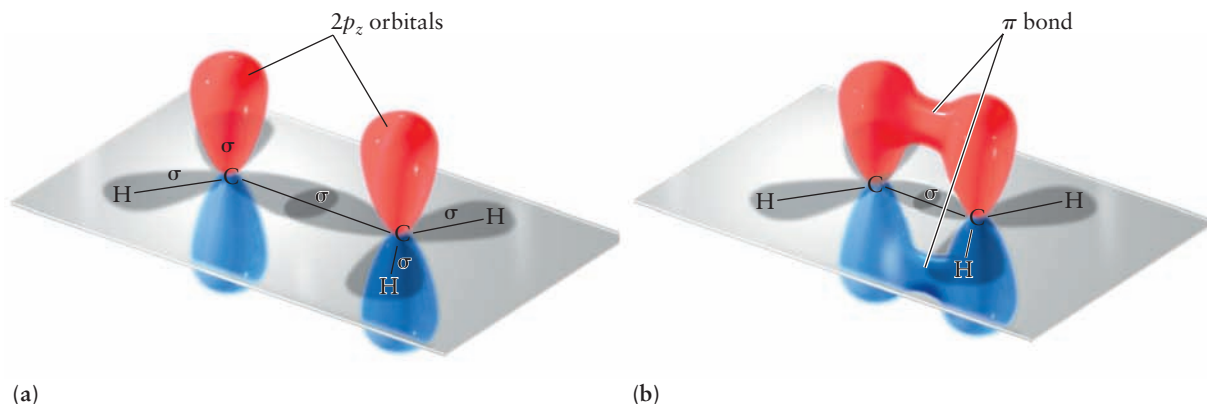
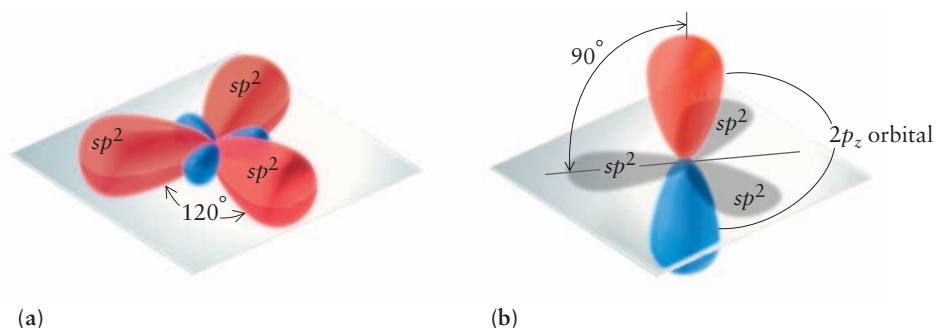


FIGURE 7.12 Bond formation in ethylene. (a) Overlap of sp^2 hybrid orbitals forms a σ bond between the carbon atoms. (b) Overlap of parallel $2p$ orbitals forms a π bond.

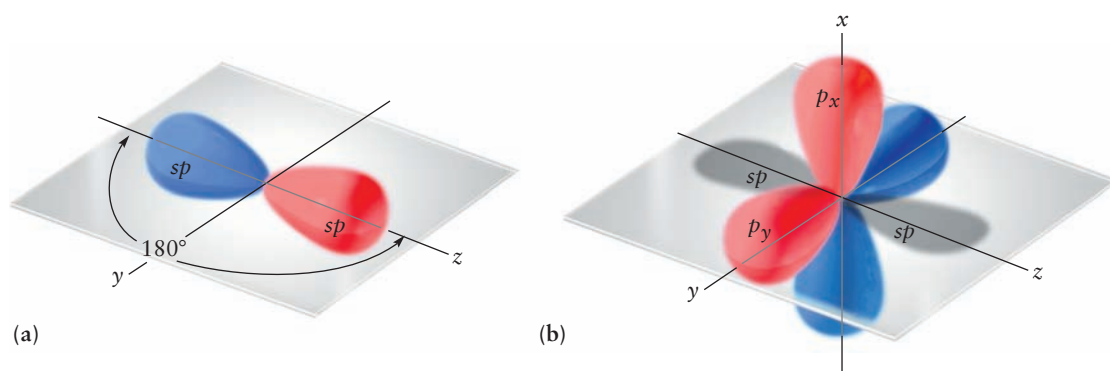
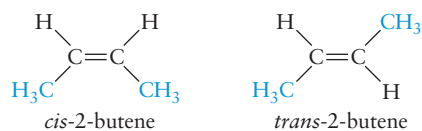


FIGURE 7.13 Sketches of sp hybridized orbitals on carbon. (a) The two sp hybridized orbitals are oriented in a plane with their axes at angles of 180 degrees. (b) Two nonhybridized $2p$ orbitals are oriented perpendicular to the axes of the two sp hybrid orbitals.

Bonding in alkynes is explained by sp hybridization (see description in Section 6.4 and illustrations in Figs. 6.41 and 6.44). Figure 7.13a sketches the formation of the sp hybrid orbitals, and Figure 7.13b shows these together with the $2p_x$ and $2p_y$ nonhybridized atomic orbitals. Bond formation in acetylene is shown in Figures 7.14a and b. A σ bond between the two carbon atoms is formed by overlap of sp hybrids on each carbon, and each carbon forms a σ bond with one hydrogen atom using its other sp hybrid. The $2p_x$ and $2p_y$ nonhybridized atomic orbitals are parallel pairs on the two adjacent carbon atoms. Each pair overlaps to form a π bond (see Fig. 6.16). The result is a triple bond in acetylene, analogous to the triple bond in N_2 shown in Figure 6.40.

As explained later in this chapter, bond rotation does not occur readily about a carbon–carbon double bond. Many alkenes therefore exist in contrasting isomeric forms, depending on whether bonding groups are on the same (*cis*) or opposite sides (*trans*) of the double bond. There is only a single isomer of 1-butene but two of 2-butene, distinguished by the two possible placements for the outer CH_3 groups relative to the double bond:



These compounds differ in melting and boiling points, density, and other physical and chemical properties.

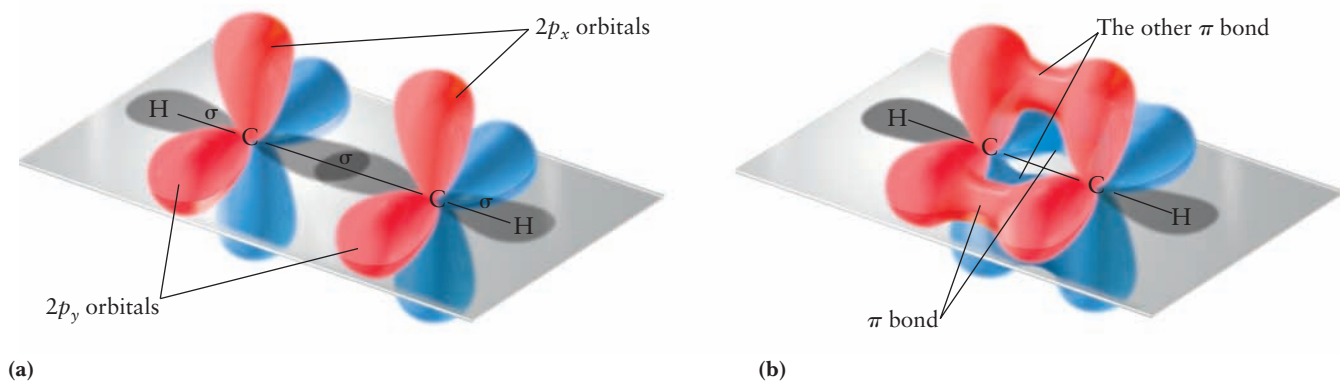
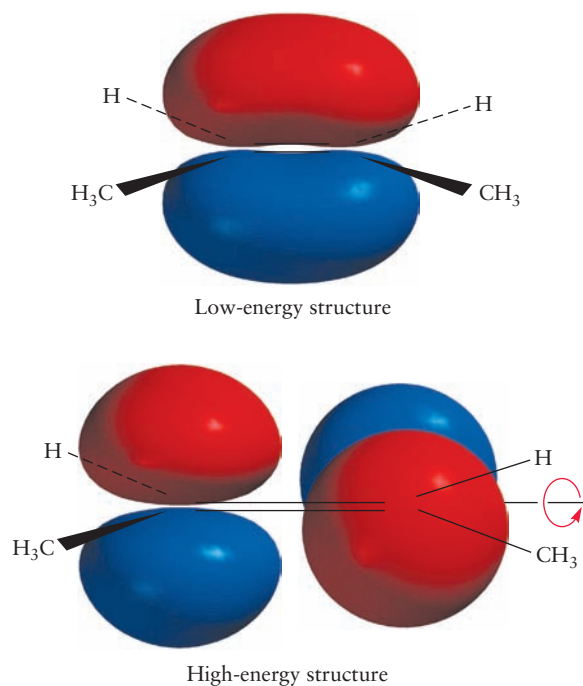
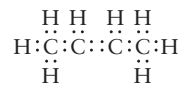


FIGURE 7.14 Bond formation in acetylene. (a) The σ bond framework and the two nonhybridized $2p$ orbitals on each carbon. (b) Overlap of two sets of parallel $2p$ orbitals forms two π bonds.

FIGURE 7.15 As the 2-butene molecule is twisted about the C=C bond, the overlap of the two p orbitals decreases, giving a higher energy.



The structures and bonding in substituted alkenes and alkynes can be described through the combined molecular orbital (MO) and VB picture presented in Section 6.5, which uses localized VB bonds to describe the molecular framework and delocalized MOs to describe the π electrons. Let's apply this method to 2-butene ($\text{CH}_3\text{CHCHCH}_3$) and gain deeper understanding of the isomers discussed earlier. The Lewis diagram for 2-butene is



From the valence shell electron-pair repulsion (VSEPR) theory, the steric number of the two outer carbon atoms is 4 (so they are sp^3 hybridized), and that of the two central carbon atoms is 3 (sp^2 hybridized). The bonding around the outer carbon atoms is tetrahedral, and that about the central ones is trigonal planar. Each localized σ bond uses two electrons, resulting in a single bond between each pair of bonding atoms. In the case of 2-butene, these placements use 22 of the 24 available valence electrons, forming a total of 11 single bonds.

Next, the remaining p orbitals that were not involved in hybridization are combined to form π MOs. The p_z orbitals from the two central carbon atoms can be mixed to form a π (bonding) MO and a π^* (antibonding) MO. The remaining two valence electrons are placed into the π orbital, resulting in a double bond between the central carbon atoms. If the p_z orbital of one of these atoms is rotated about the central C—C axis, its overlap with the p_z orbital of the other carbon atom changes (Fig. 7.15). The overlap is greatest and the energy lowest when the two p_z orbitals are parallel to each other. In the most stable molecular geometry, the hydrogen atoms on the central carbon atoms lie in the same plane as the C—C—C—C carbon skeleton. This prediction is verified by experiment.

Figure 7.16 shows the structures of the isomers *cis*-2-butene and *trans*-2-butene. Converting one form to the other requires breaking the central π bond (by rotating the two p_z orbitals 180 degrees with respect to each other as in Fig. 7.15), then re-forming it in the other configuration. Because breaking a π bond costs a significant amount of energy, both *cis* and *trans* forms are stable at room temperature, and interconversion between the two is slow. The change in molecular structure from *trans* to *cis* can be accomplished by photochemistry

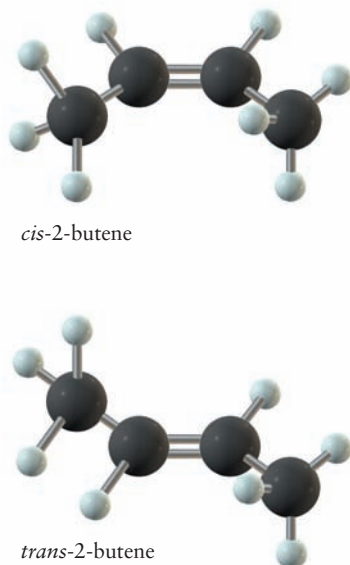
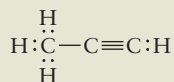


FIGURE 7.16 The two *cis-trans* isomers of 2-butene.

without complete breaking of bonds (see later). Molecules such as *trans*-2-butene can absorb ultraviolet light, which excites an electron from a π to a π^* MO. In the excited electronic state of *trans*-2-butene, the carbon–carbon double bond is effectively reduced to a single bond, and one CH_3 group can rotate relative to the other to form *cis*-2-butene.

EXAMPLE 7.2

The Lewis diagram for propyne (CH_3CCH) is



Discuss its bonding and predict its geometry.

SOLUTION

The leftmost carbon atom in the structure is sp^3 hybridized, and the other two carbon atoms are sp hybridized. The atoms in the molecule are located on a single straight line, with the exception of the three hydrogen atoms on the leftmost carbon atom, which point outward toward three of the vertices of a tetrahedron. There is a σ bond between each pair of bonded atoms. The p_x and p_y orbitals on carbon atoms 2 and 3 combine to form two π orbitals and two π^* orbitals; only the former are occupied in the ground-state electron configuration.

Related Problems: 27, 28

Compounds with two double bonds are called *dienes*, those with three are called *trienes*, and so forth. The compound 1,3-pentadiene, for example, is a derivative of pentane with two double bonds:



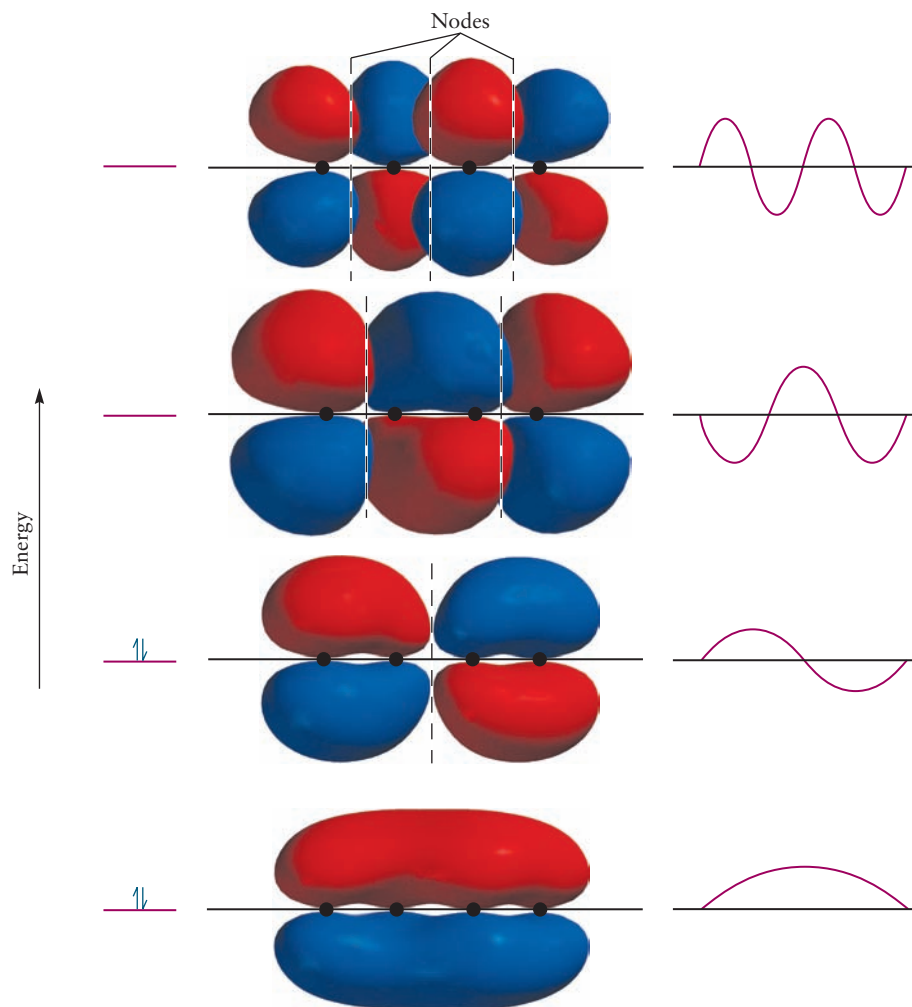
In such **polyenes**, each double bond may lead to *cis* and *trans* conformations, depending on its neighboring groups; therefore, several isomers may have the same bonding patterns but different molecular geometries and physical properties.

When two or more double or triple bonds occur close to each other in a molecule, a delocalized MO picture of the bonding should be used. As an example, let's examine 1,3-butadiene ($\text{CH}_2\text{CHCHCH}_2$), which has the following Lewis diagram

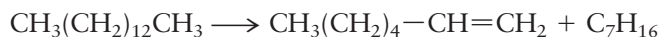


All four carbon atoms have steric number 3, so all are sp^2 hybridized. The remaining p_z orbitals have maximum overlap when the four carbon atoms lie in the same plane, so this molecule is predicted to be planar. From these four p_z atomic orbitals, four MOs can be constructed by combining their phases, as shown in Figure 7.17. The four electrons that remain after the σ orbitals are filled are placed in the two lowest π orbitals. The first of these is bonding among all four carbon atoms; the second is bonding between the outer carbon atom pairs, but antibonding between the central pair. Therefore, 1,3-butadiene has stronger and shorter bonds between the outer carbon pairs than between the two central carbon atoms. It is an example of a **conjugated π electron system**, in which two or more double or triple bonds alternate with single bonds. Such conjugated systems have lower energies than would be predicted from localized bond models and are best described with delocalized MOs extending over the entire π electron system.

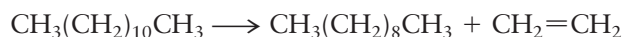
FIGURE 7.17 The four π molecular orbitals formed from four $2p_z$ atomic orbitals in 1,3-butadiene, viewed from the side. The dashed white lines represent nodes between the carbon atoms in the y - z plane. The horizontal black line represents the x - y nodal plane across which the p orbitals change sign. Note the similarity in the y - z nodal patterns to those of the first four modes of a vibrating string or the first four wave functions of the one-dimensional particle in a box (right). Only the lowest two orbitals are occupied in the ground state of 1,3-butadiene.



Alkenes are not present to a significant extent in crude petroleum. They are essential starting compounds for the synthesis of organic chemicals and polymers, so their production from alkanes is of great importance. One way to produce alkenes is by **cracking** the petroleum by heat or with catalysts. In **catalytic cracking**, the heavier fractions from the distillation column (compounds of C_{12} or higher) are passed over a silica–alumina catalyst at temperatures of 450°C to 550°C . Reactions such as



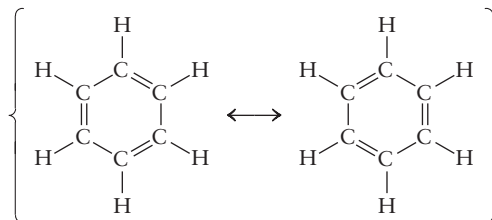
occur to break the long chain into fragments. This type of reaction accomplishes two purposes. First, the shorter chain hydrocarbons have lower boiling points and can be added to gasoline. Second, the alkenes that result have higher octane numbers than the corresponding alkanes and perform better in the engine. Moreover, these alkenes can react with alkanes to give the more highly branched alkanes that are desirable in gasoline. **Thermal cracking** uses higher temperatures of 850°C to 900°C and no catalyst. It produces shorter chain alkenes, such as ethylene and propylene, through reactions such as



The short-chain alkenes are too volatile to be good components of gasoline, but they are among the most important starting materials for chemical synthesis.

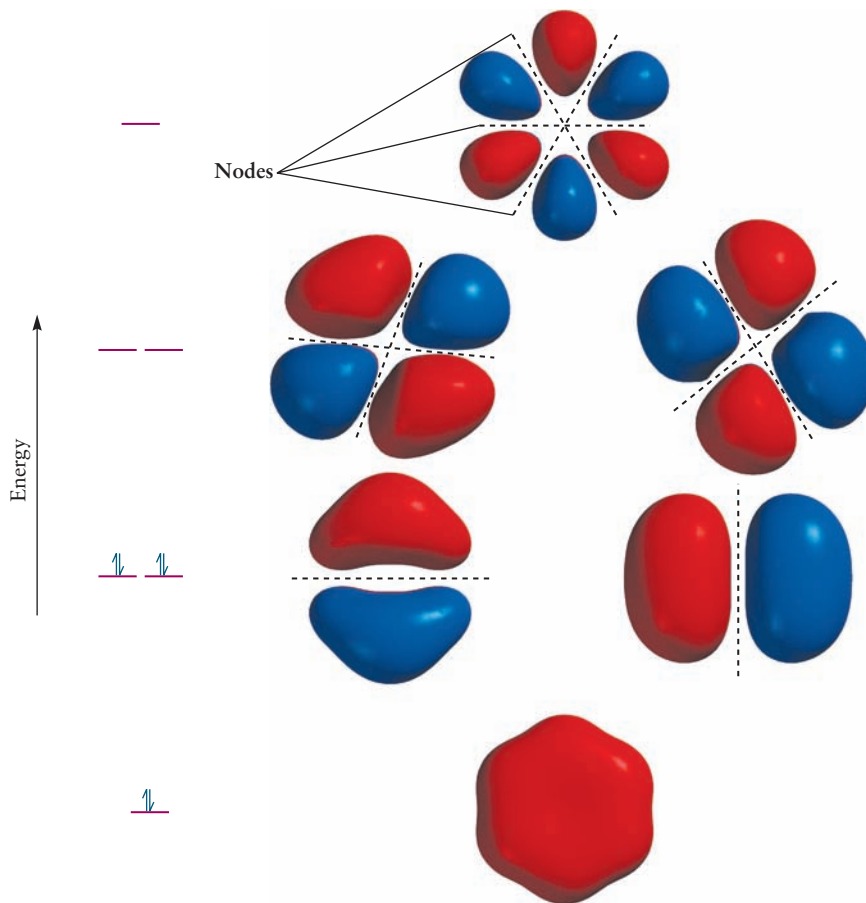
7.4 Aromatic Hydrocarbons

One last group of hydrocarbons found in crude petroleum is the **aromatic hydrocarbons**, of which benzene is the simplest example. Benzene is a cyclic molecule with the formula C_6H_6 . In the language of Chapter 3, benzene is represented as a resonance hybrid of two Lewis diagrams:



The modern view of resonant structures is that the molecule does not jump between two structures, but rather has a single, time-independent electron distribution in which the π bonding is described by delocalized MOs. Each carbon atom is sp^2 hybridized, and the remaining six p_z orbitals combine to give six MOs delocalized over the entire molecule. Figure 7.18 shows the π orbitals and their energy-level diagram. The lowest energy π orbital has no nodes, the next two have two nodes, the next two have four nodes, and the highest energy orbital has six nodes. The C_6H_6 molecule has 30 valence electrons, of which 24 occupy sp^2 hybrid orbitals and form σ bonds. When the six remaining valence electrons are placed in the three lowest energy π orbitals, the resulting electron distribution is the same in all six carbon-carbon bonds. As a result, benzene has six carbon-carbon bonds of equal length with properties intermediate between those of single and double bonds.

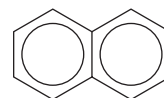
FIGURE 7.18 The six π molecular orbitals for benzene, viewed from the top, formed from the six $2p_z$ atomic orbitals lying perpendicular to the plane of the molecule. Note the similarity in nodal properties to the standing waves on a loop shown in Figure 4.18. Only the three lowest energy orbitals are occupied in molecules of benzene in the ground state.



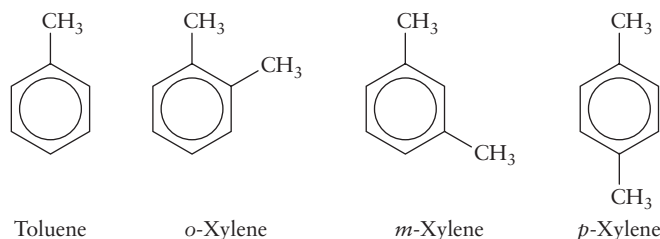
Benzene is sometimes represented by its chemical formula C_6H_6 and sometimes (to show structure) by a hexagon with a circle inside it:



The six points of the hexagon represent the six carbon atoms, with the hydrogen atoms omitted for simplicity. The circle represents the de-localized π electrons, which are spread out evenly over the ring. The molecules of other aromatic compounds contain benzene rings with various side groups or two (or more) benzene rings linked by alkyl chains or fused side by side, as in naphthalene ($C_{10}H_8$):

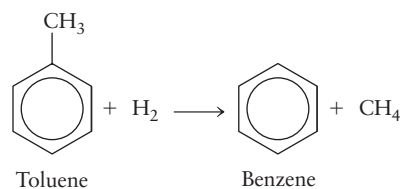


Besides benzene, the most prevalent aromatic compounds in petroleum are toluene, in which one hydrogen atom on the benzene ring is replaced by a methyl group, and the xylenes, in which two such replacements are made:



This set of compounds is referred to as BTX (for *benzene-toluene-xylene*). The BTX in petroleum is important to polymer synthesis (see Section 23.1). These components also significantly increase octane number and are used to make high-performance fuels with octane numbers above 100, as are required in modern aviation.

A major advance in petroleum refining has been the development of **reforming reactions**, which produce BTX aromatics from straight-chain alkanes that contain the same numbers of carbon atoms. A fairly narrow distillation fraction that contains only C_6 to C_8 alkanes is taken as the starting material. The reactions use high temperatures and transition-metal catalysts such as platinum or rhenium on alumina supports, and their detailed mechanisms are not fully understood. Apparently, a normal alkane such as hexane is cyclized and dehydrogenated to give benzene as the primary product (Fig. 7.19). Heptane yields mostly toluene, and octane yields a mixture of xylenes. Toluene is replacing benzene as a solvent in industrial applications because tests on laboratory animals show it to be far less carcinogenic (cancer-causing) than benzene. Benzene is more important for chemical synthesis; so a large fraction of the toluene produced is converted to benzene by **hydrodealkylation**:



This reaction is conducted at high temperatures (550–650°C) and pressures of 40 to 80 atm.

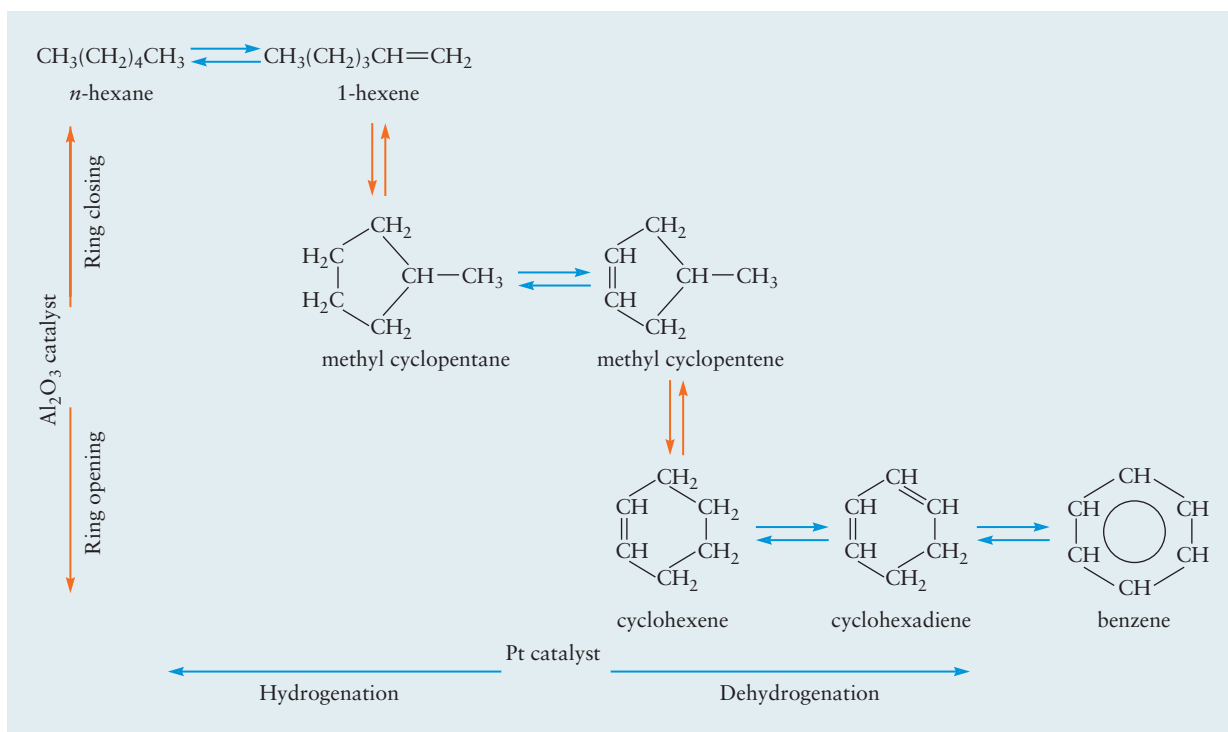


FIGURE 7.19 The reforming reaction that produces benzene from hexane uses a catalyst of platinum on alumina. The platinum facilitates the removal of hydrogen, and the alumina (Al_2O_3) facilitates the opening and closing of rings. One typical multistep sequence is shown; other intermediates can form as well.

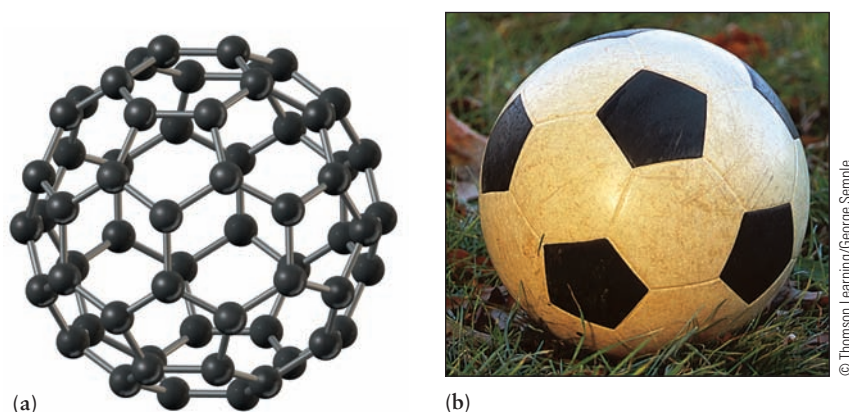
7.5 Fullerenes

Among the most interesting conjugated π electron systems is a molecule discovered in 1985: buckminsterfullerene, C_{60} . Previously, only two forms of carbon (diamond and graphite) were known. In 1985, Harold Kroto, Robert Curl, and Richard Smalley were studying certain long-chain carbon molecules that had been discovered in the vicinity of red giant stars by radioastronomers using spectroscopy. They sought to duplicate the conditions near those stars by vaporizing a graphite target with a laser beam. Analysis of the products by mass spectrometry demonstrated not only the hoped-for molecules but a large proportion of molecules of molar mass 720 g mol^{-1} , which corresponds to the molecular formula C_{60} . Although the amounts of C_{60} present were far too small to isolate for direct determination of molecular structure, Kroto, Curl, and Smalley correctly suggested the cage structure shown in Figure 7.20a and named the molecule *buckminsterfullerene* after the architect Buckminster Fuller, the inventor of the geodesic dome, which the molecular structure of C_{60} resembles.

Molecules of C_{60} have a highly symmetric structure: 60 carbon atoms are arranged in a closed net with 20 hexagonal faces and 12 pentagonal faces. The pattern is exactly the design on the surface of a soccer ball (see Fig. 7.20b). Every carbon atom has a steric number of 3; all 60 atoms are sp^2 hybridized accordingly, although 1 of the 3 bond angles at each carbon atom must be distorted from the usual 120-degree sp^2 bond angle down to 108 degrees. The π electrons of the double bonds are de-localized: The 60 p orbitals (1 from each carbon atom) mix to give 60 MOs with amplitude spread over both the inner and outer surfaces of the molecule. The lowest 30 of these MOs are occupied by the 60 π electrons.

In 1990, scientists succeeded in synthesizing C_{60} in gram quantities by striking an electric arc between two carbon rods held under an inert atmosphere. The

FIGURE 7.20 (a) The structure of C_{60} , buckminsterfullerene. Note the pattern of hexagons and pentagons. (b) The design on the surface of a soccer ball has the same pattern as the structure of C_{60} .

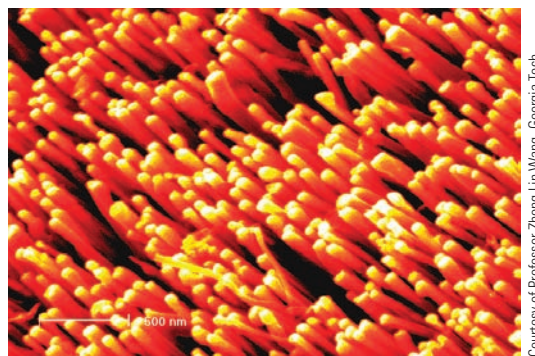


carbon vapors condensed to form soot, which was extracted with an organic solvent. Using chromatography, the scientists could separate the C_{60} —first as a solution of a delicate magenta hue (Fig. 7.21) and, finally, as a crystalline solid—from the various impurities in the growth batch. Since 1990, C_{60} has since been found in soot-forming flames when hydrocarbons are burned. Thus, the newest form of carbon has been (in the words of one of its discoverers) “under our noses since time immemorial.” In 1994, the first buckminsterfullerene molecules were brought back from outer space in the form of the impact crater from a tiny meteorite colliding with an orbiting spacecraft.

Buckminsterfullerene is not the only new form of carbon to emerge from the chaos of carbon vapor condensing at high temperature. Synthesis of C_{60} simultaneously produces a whole family of closed-cage carbon molecules called **fullerenes**. All the fullerenes have even numbers of atoms, with formulas ranging up to C_{400} and higher. These materials offer exciting prospects for technical applications. For example, because C_{60} readily accepts and donates electrons to or from its π MOs, it has possible applications in batteries. It forms compounds (such as Rb_3C_{60}) that are superconducting (have zero resistance to the passage of an electric current) up to 30 K. Fullerenes also can encapsulate foreign atoms present during its synthesis. If a graphite disk is soaked with a solution of $LaCl_3$, dried, and used as a laser target, the substance $La@C_{60}$ forms, where the symbol @ means that the lanthanum atom is trapped within the 60-atom carbon cage.

Condensation of the carbon vapor under certain conditions favors the formation of *nanotubes*, which consist of seamless, cylindrical shells of thousands of sp^2 hybridized carbon atoms arranged in hexagons. The ends of the tubes are capped by pentagons inserted into the hexagonal network. These structures all have a delocalized π -electron system that covers the inner and outer surfaces of the cage or cylinder. Nanotubes also offer exciting prospects for material science and technological applications. For example, the mechanical properties of nanotubes suggest applications as high-strength fibers (Fig. 7.22).

FIGURE 7.22 A bundle of carbon nanotubes, each about 1.4 nm in diameter. The bundle is 10 to 20 nm in thickness. Note that the tubes are packed in a triangular arrangement (or, alternatively, six tubes are arranged hexagonally around a central tube.)

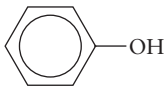
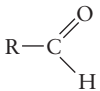
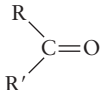
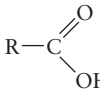
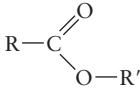
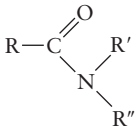


7.6 Functional Groups and Organic Reactions

Section 7.1 describes the diverse compounds formed from the two elements carbon and hydrogen and the recovery of these compounds from petroleum. We now consider the structures, properties, and reactions of molecules formed by adding substituent atoms such as oxygen, nitrogen, and the halogens to the hydrocarbon backbone. In doing so, we shift our attention from the structures of entire molecules to the properties of **functional groups**, which consist of the noncarbon atoms plus the portions of the molecule immediately adjacent to them. Functional groups tend to be the reactive sites in organic molecules, and their chemical properties depend only rather weakly on the natures of the hydrocarbons to which they are attached. This fact permits us to regard an organic molecule as a hydrocarbon frame, which mainly governs size and shape, to which are attached functional groups that mainly determine the chemistry of the molecule. Table 7.3 shows some of the most important functional groups.

Industrial processes for the high-volume organic chemicals produced today require starting materials with appropriate functional groups. A small number of hydrocarbon building blocks from petroleum and natural gas (methane, ethylene, propylene, benzene, and xylene) are the starting points for the synthesis of most of these starting materials. This section introduces the common functional groups, describes their bonding, and illustrates typical reactions in their synthesis or applications.

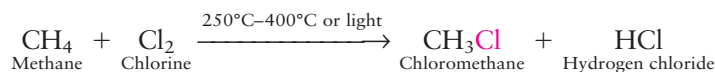
TABLE 7.3 Common Functional Groups

Functional Group†	Type of Compound	Examples
$R-F, -Cl, -Br, -I$	Alkyl or aryl halide	CH_3CH_2Br (bromoethane)
$R-OH$	Alcohol	CH_3CH_2OH (ethanol)
	Phenol	 (phenol)
$R-O-R'$	Ether	$H_3C-O-CH_3$ (dimethyl ether)
	Aldehyde	$CH_3CH_2CH_2-C(=O)H$ (butyraldehyde, or butanal)
	Ketone	$H_3C-C(=O)CH_3$ (propanone, or acetone)
	Carboxylic acid	CH_3COOH (acetic acid, or ethanoic acid)
	Ester	$H_3C-C(=O)O-CH_3$ (methyl acetate)
$R-NH_2$	Amine	CH_3NH_2 (methylamine)
	Amide	$H_3C-C(=O)NH_2$ (acetamide)

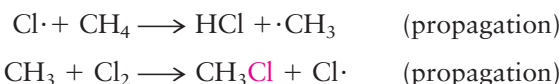
†The symbols R, R', and R'' stand for hydrocarbon radicals. In some cases, they may represent hydrogen.

Halides

One of the simplest functional groups consists of a single halogen atom, which we take to be chlorine for illustrative purposes. The chlorine atom forms a σ bond to a carbon atom by overlap of its $3p_z$ orbital with a hybridized orbital on the carbon. The hybridized orbital may be sp^3 , sp^2 , or sp depending on the bonding in the hydrocarbon frame. **Alkyl halides** form when mixtures of alkanes and halogens (except iodine) are heated or exposed to light.

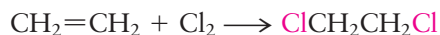


The mechanism is a chain reaction (see description in Section 18.4). Ultraviolet light initiates the reaction by dissociating a small number of chlorine molecules into highly reactive atoms. These atoms take part in linked reactions of the following form:

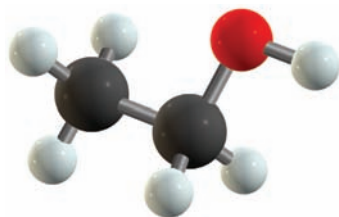


The chlorine atoms and the methyl species are called free radicals, and are denoted by the dots next to the chemical symbols. A **free radical** is a chemical species that contains an odd (unpaired) electron; it is usually formed by breaking a covalent bond to form a pair of such species. Radicals are often highly reactive and often appear as intermediates in reactions. Chloromethane (also called methyl chloride) is used in synthesis to add methyl groups to organic molecules. If sufficient chlorine is present, more highly chlorinated methanes form, providing a route for the industrial synthesis of dichloromethane (CH_2Cl_2 , also called methylene chloride), trichloromethane (CHCl_3 , chloroform), and tetrachloromethane (CCl_4 , carbon tetrachloride). All three chloromethanes are used as solvents and have vapors with anesthetic or narcotic effects; environmental and health concerns about toxicity have reduced the use of these compounds in everyday life.

Adding chlorine to $\text{C}=\text{C}$ bonds is a more important industrial route to alkyl halides than the free-radical reactions just described. Billions of kilograms of 1,2-dichloroethane (commonly called ethylene dichloride) are manufactured each year, making this compound the largest volume derived organic chemical. It is made by adding chlorine to ethylene over an iron(III) oxide catalyst at moderate temperatures ($40\text{--}50^\circ\text{C}$), either in the vapor phase or in a solution of 1,2-dibromoethane:



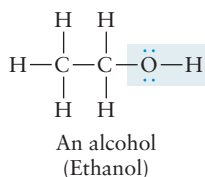
Almost all of the 1,2-dichloroethane produced is used to make chloroethylene (vinyl chloride, $\text{CH}_2=\text{CHCl}$). This is accomplished by heating the 1,2-dichloroethane to 500°C over a charcoal catalyst to abstract HCl:



The HCl can be recovered and converted to Cl_2 for further production of 1,2-dichloroethane from ethylene. Vinyl chloride has a much lower boiling point than 1,2-dichloroethane (-13°C compared with 84°C), so the two are easily separated by fractional distillation. Vinyl chloride is used in the production of polyvinyl chloride plastic (see Section 23.1).

Alcohols and Phenols

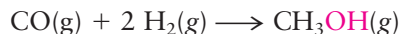
Alcohols have the $-\text{OH}$ functional group attached to a tetrahedral carbon atom, that is, a carbon atom with single bonds to four other atoms. The carbon atom in the functional group is sp^3 hybridized. The oxygen atom is likewise sp^3 hybridized; two of the hybrid orbitals form σ bonds, whereas the other two hold lone pairs of electrons.



The simplest alcohol is methanol (CH₃OH), which is made from methane in a two-step process. The first is the **reforming reaction**



conducted at high temperatures (750–1000°C) with a nickel catalyst. The gas mixture that results, called **synthesis gas**, reacts directly to form methanol at 300°C.

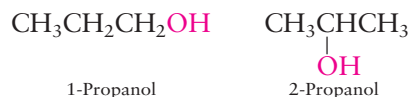


The next higher alcohol, ethanol (CH₃CH₂OH), can be produced from the fermentation of sugars. Although fermentation is the major source of ethanol for alcoholic beverages and for “gasohol” (automobile fuel made up of 90% gasoline and 10% ethanol), it is not significant for industrial production, which relies on the direct hydration of ethylene:

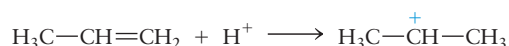


Temperatures of 300°C to 400°C and pressures of 60 to 70 atm are used with a phosphoric acid catalyst. Both methanol and ethanol are used widely as solvents and as intermediates for further chemical synthesis.

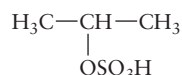
Two three-carbon alcohols exist, depending on whether the —OH group is attached to a terminal carbon atom or the central carbon atom. They are 1-propanol and 2-propanol:



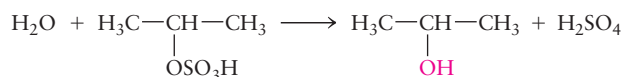
1-Propanol and 2-propanol are commonly referred to as *n*-propyl alcohol and isopropyl alcohol, respectively. The systematic names of alcohols are obtained by replacing the *-ane* ending of the corresponding alkane with *-anol* and using a numeric prefix, when necessary, to identify the carbon atom to which the —OH group is attached.¹ Isopropyl alcohol is made from propylene by means of an interesting hydration reaction that is catalyzed by sulfuric acid. The first step is addition of H⁺ to the double bond,



producing a transient charged species in which the positive charge is centered on the central carbon atom. Attack by negative HSO₄[−] occurs at this positive site and leads to a neutral intermediate that can be isolated:



Further reaction with water then causes the replacement of the —OSO₃H group with an —OH group and the regeneration of the sulfuric acid:

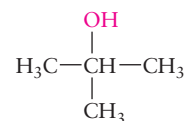


This mechanism explains why only 2-propanol forms, with no 1-propanol.

The compound 1-propanol is a **primary alcohol**: The carbon atom to which the —OH group is bonded has exactly one other carbon atom attached to it. The isomeric compound 2-propanol is a **secondary alcohol** because the carbon atom to which the —OH group is attached has two carbon atoms (in the two methyl

¹Contrast the names of alcohols with the corresponding names of alkyl halides. If the —OH group were replaced by a chlorine atom, the names of these compounds would be 1-chloropropane and 2-chloropropane.

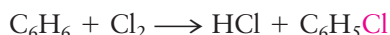
groups) attached to it. The simplest **tertiary alcohol** (in which the carbon atom attached to the —OH group is also bonded to three other carbon atoms) is 2-methyl-2-propanol:



Primary, secondary, and tertiary alcohols differ in chemical properties.

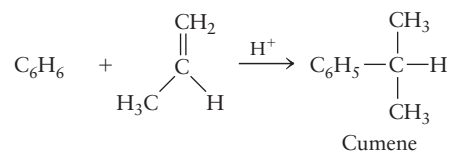
Phenols are compounds in which an —OH group is attached directly to an aromatic ring. The simplest example is phenol itself ($\text{C}_6\text{H}_5\text{OH}$). As in the alcohols, the oxygen atom is sp^3 hybridized with two unshared pairs. The carbon atom, which is part of the aromatic ring, is sp^2 hybridized (see Section 7.4).

The manufacture of phenols uses quite different types of reactions from those used to make alcohols. One method, introduced in 1924 and still used to a small extent today, involves the chlorination of the benzene ring followed by reaction with sodium hydroxide:

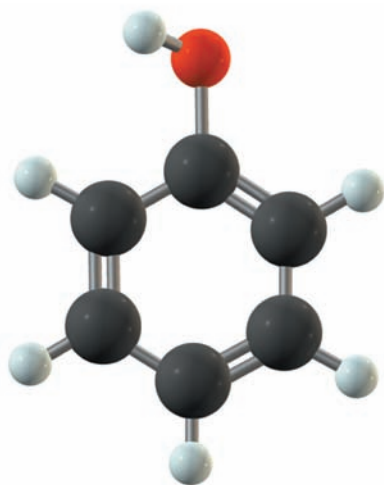


This approach illustrates a characteristic difference between the reactions of aromatics and alkenes. When chlorine reacts with an alkene, it *adds* across the double bond (as shown in the production of 1,2-dichloroethane). When an aromatic ring is involved, substitution of chlorine for hydrogen occurs instead and the aromatic π -bonding structure is preserved.

A different approach is used to make almost all phenol today. It involves, first, the acid-catalyzed reaction of benzene with propylene to give cumene, or isopropyl benzene:



As in the production of 2-propanol, the first step is the addition of H^+ to propylene to give $\text{CH}_3\text{—CH}^+\text{—CH}_3$ (see page 294). This ion then attaches to the benzene ring through its central carbon atom to give the cumene and regenerate H^+ . Subsequent reaction of cumene with oxygen (Fig. 7.23) gives phenol and acetone, an important compound that is discussed later in this section. The main use of phenol is in the manufacturing of polymers and aspirin.



The structure of phenol, $\text{C}_6\text{H}_5\text{OH}$.

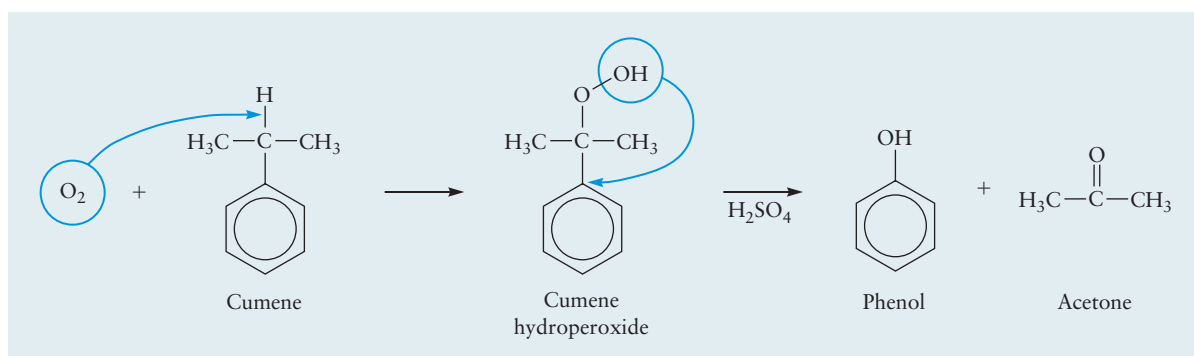


FIGURE 7.23 The production of phenol and acetone from cumene is a two-step process that involves insertion of O_2 to make a peroxide, followed by acid-catalyzed migration of the —OH group to form the products.

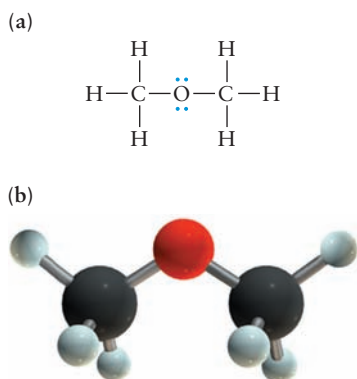


FIGURE 7.24 Structure of dimethyl ether. (a) Lewis diagram. (b) Ball-and-stick model.

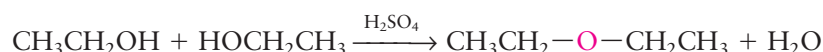
Ethers

Ethers are characterized by the —O— functional group, in which an oxygen atom provides a link between two separate alkyl or aromatic groups. Figure 7.24 shows the simplest ether, dimethyl ether. The oxygen atom is sp^3 hybridized. Two of these hybrid orbitals form σ bonds to the carbon atoms, whereas each of the other two holds an unshared pair. The C—O—C bond angle is 110.3 degrees, which is close to the tetrahedral value 109.5 degrees predicted by sp^3 hybridization.

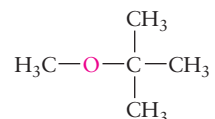
One important ether is diethyl ether, often called simply ether, in which two ethyl groups are linked to the same oxygen atom:



Diethyl ether is a useful solvent for organic reactions, and was formerly used as an anesthetic. It can be produced by a **condensation reaction** (a reaction in which a small molecule such as water is split out) between two molecules of ethanol in the presence of concentrated sulfuric acid as a dehydrating agent:

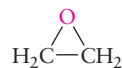


Another ether of considerable importance is methyl *t*-butyl ether (MTBE):

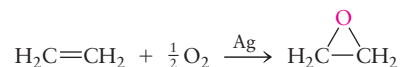


This compound appeared to be a successful replacement for tetraethyllead as an additive to gasolines to increase their octane ratings. The bond between the oxygen and the *t*-butyl group is weak, and it breaks to form radicals that assist the smooth combustion of gasoline. MTBE is readily soluble in water, and has appeared in drinking water supplies through leaks from underground storage tanks for gasoline. Concern over possible health risks has caused MTBE to be phased out in various regions of the United States.

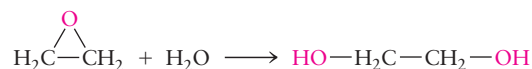
In a cyclic ether, oxygen forms part of a ring with carbon atoms, as in the common solvent tetrahydrofuran (Fig. 7.25). The smallest such ring has two carbon atoms bonded to each other and to the oxygen atom; it occurs in ethylene oxide,



which is made by direct oxidation of ethylene over a silver catalyst:



Such ethers with three-membered rings are called **epoxides**. The major use of ethylene oxide is in the preparation of ethylene glycol:



This reaction is conducted either at 195°C under pressure or at lower temperatures (50–70°C) with sulfuric acid as a catalyst. Ethylene glycol is a dialcohol, or **diol**, in which two —OH groups are attached to adjacent carbon atoms. Its primary use is as antifreeze to decrease the freezing point of water in automobile radiators.

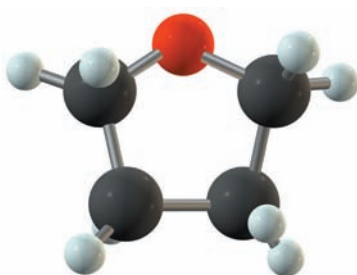
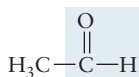
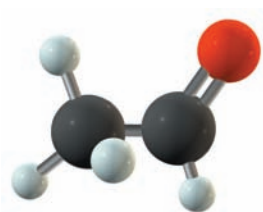


FIGURE 7.25 The structure of tetrahydrofuran, $\text{C}_4\text{H}_8\text{O}$.

Aldehydes and Ketones

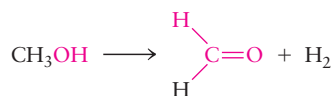
An **aldehyde** contains the characteristic $\text{—}\overset{\text{O}}{\parallel}{\text{C}}\text{—H}$ functional group in its molecules. Figure 7.26 shows the bonding in formaldehyde, which is the simplest organic



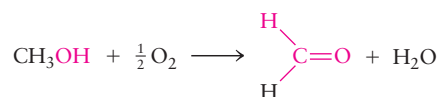
Acetaldehyde
(an aldehyde)

molecule with a double bond between carbon and oxygen. The carbon is sp^2 hybridized and forms σ bonds to two hydrogen atoms. The oxygen is also sp^2 hybridized. Carbon and oxygen form one σ bond by overlap of sp^2 orbitals and one π bond by overlap of parallel nonhybridized $2p$ orbitals. This is the same bonding model used to describe $\text{C}=\text{C}$ double bonds in Figure 7.12.

Aldehydes can be prepared by the dehydrogenation of a primary alcohol. Formaldehyde results from the dehydrogenation of methanol at high temperatures with an iron oxide–molybdenum oxide catalyst:



Another reaction that gives the same primary product is the oxidation reaction



Formaldehyde is readily soluble in water, and a 40% aqueous solution called *formalin* is used to preserve biological specimens. It is a component of wood smoke and helps to preserve smoked meat and fish, probably by reacting with nitrogen-containing groups in the proteins of attacking bacteria. Its major use is in making polymer adhesives and insulating foam.

The next aldehyde in the series is acetaldehyde, the structure of which is shown above. Industrially, acetaldehyde is produced not from ethanol but by the oxidation of ethylene, using a PdCl_2 catalyst.

Ketones have the $\overset{\text{O}}{\parallel}{\text{C}}$ functional group in which a carbon atom forms a double bond to an oxygen atom and single bonds to two separate alkyl or aromatic groups. The simplest ketone is acetone, in which two methyl groups are bonded to the central carbon. The bonding scheme is the same as that in Figure 7.26, with alkyl or aromatic groups replacing hydrogen in the two single bonds. Such compounds can be prepared by dehydrogenation or oxidation of secondary alcohols, just as aldehydes come from primary alcohols. Acetone is made by the dehydrogenation of 2-propanol over a copper oxide or zinc oxide catalyst at 500°C :

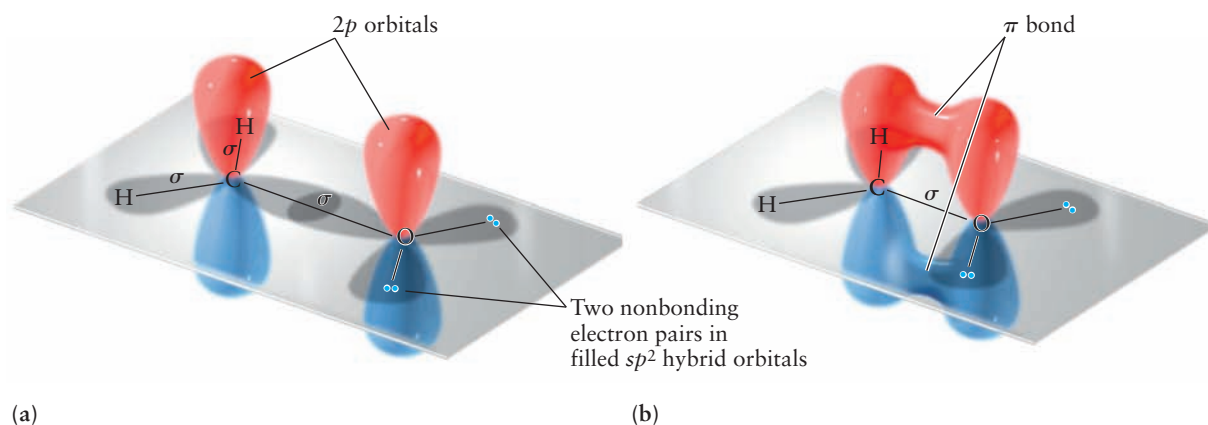
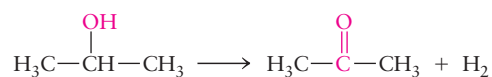
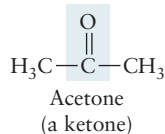
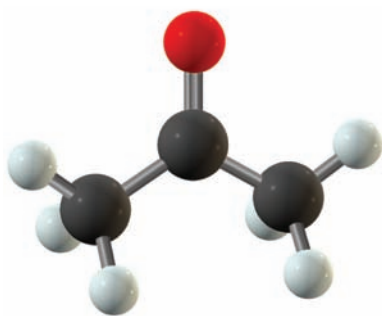


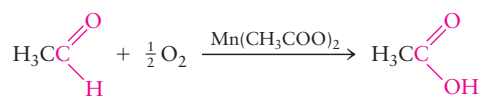
FIGURE 7.26 Bond formation in formaldehyde involves sp^2 hybridization of the carbon (C) and oxygen (O) atoms. (a) The σ bond framework and the parallel nonhybridized $2p$ orbitals on C and O. (b) Overlap of the parallel $2p$ orbitals to form a π bond.



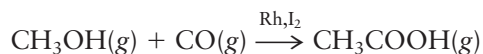
Acetone is also produced (in greater volume) as the coproduct with phenol of the oxidation of cumene (see earlier). It is a widely used solvent and is the starting material for the synthesis of a number of polymers.

Carboxylic Acids and Esters

Carboxylic acids contain the $\text{—}\overset{\text{O}}{\parallel}{\text{C}}\text{—OH}$ functional group (also written as —COOH). The bonding scheme is a variation of that in Figure 7.26, in which the doubly bonded oxygen atom is sp^2 hybridized and the singly bonded oxygen is sp^3 hybridized with unshared pairs in two of the hybrid orbitals. Carboxylic acids are the products of the oxidation of aldehydes, just as aldehydes are the products of the oxidation of primary alcohols. (The turning of wine to vinegar is a two-step oxidation leading from ethanol through acetaldehyde to acetic acid.) Industrially, acetic acid can be produced by the air oxidation of acetaldehyde over a manganese acetate catalyst at 55°C to 80°C :



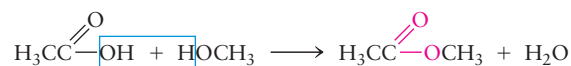
The reaction now preferred on economic grounds for acetic acid production is the combination of methanol with carbon monoxide (both derived from natural gas) over a catalyst that contains rhodium and iodine. The overall reaction is



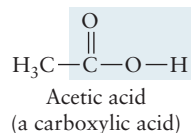
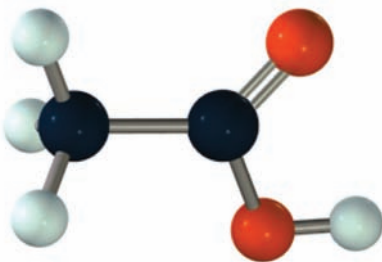
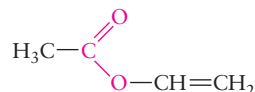
and can be described as a **carbonylation**, or the insertion of CO into the methanol C—O bond.

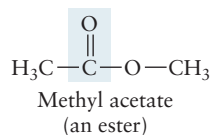
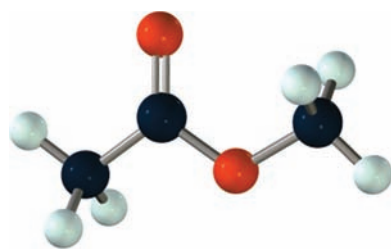
Acetic acid is a member of a series of carboxylic acids with formulas $\text{H}-(\text{CH}_2)_n-\text{COOH}$. Before acetic acid (with $n = 1$) comes the simplest of these carboxylic acids, formic acid (HCOOH), in which $n = 0$. This compound was first isolated from extracts of the crushed bodies of ants, and its name stems from the Latin word *formica*, meaning “ant.” Formic acid is the strongest acid of the series, and acid strength decreases with increasing length of the hydrocarbon chain. (See Section 15.9.) The longer chain carboxylic acids are called fatty acids. Sodium stearate, the sodium salt of stearic acid, $\text{CH}_3(\text{CH}_2)_{16}\text{COOH}$, is a typical component of soap. It cuts grime by simultaneously interacting with grease particles at its hydrocarbon tail and with water at its carboxylate ion end group to make the grease soluble in water.

Carboxylic acids react with alcohols or phenols to give **esters**, forming water as the coproduct. The bonding scheme in esters is a variation of that shown in Figure 7.26, in which the doubly bonded oxygen atom is sp^2 hybridized and the singly bonded oxygen is sp^3 hybridized with unshared pairs in two of the hybrid orbitals. An example is the condensation of acetic acid with methanol to give methyl acetate:

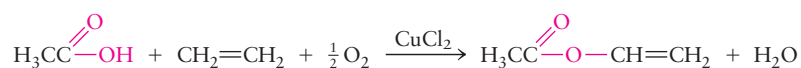


Esters are named by stating the name of the alkyl group of the alcohol (the methyl group in this case), followed by the name of the carboxylic acid with the ending *-ate* (acetate). One of the most important esters in commercial production is vinyl acetate, with the structure



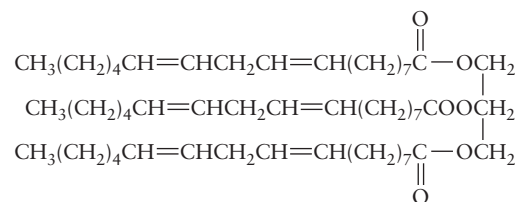


Despite its name, it is not prepared by the reaction of acetic acid with an alcohol but rather with ethylene and oxygen over a catalyst such as CuCl_2 and PdCl_2 :



Esters are colorless, volatile liquids that often have pleasant odors. Many occur naturally in flowers and fruits. Isoamyl acetate (Fig. 7.27a) is generated in apples as they ripen and contributes to the flavor and odor of the fruit. Benzyl acetate, the ester formed from acetic acid and benzyl alcohol (see Fig. 7.27b), is a major component of oil of jasmine and is used in the preparation of perfumes.

Animal fats and vegetable oils are triesters of long-chain carboxylic acids with glycerol, $\text{HOCH}_2\text{CH}(\text{OH})\text{CH}_2\text{OH}$, a trialcohol; they are referred to as **triglycerides**. These are energy-storage molecules of biological origin. A large proportion of sunflower oil is an oily liquid composed of molecules with the structural formula



This is a **polyunsaturated oil** because there are six $\text{C}=\text{C}$ bonds per molecule. Butter is a mixture of triglycerides, many of which are **saturated** because their hydrocarbon chains contain no double bonds. Hydrogen is used in food processing to convert unsaturated liquid vegetable oils to saturated solids. **Hydrogenation** of sunflower oil with 6 mol H_2 in the presence of a catalyst saturates it, and the product has a high enough melting point to make it a solid at room conditions. The use of solid fats (or solidified oils) has advantages in food processing and preservation; therefore, “hydrogenated vegetable oil” is an ingredient in many foodstuffs. Heavy consumption of saturated fats has been linked to diseases of the heart and circulatory system, and the presence of *unhydrogenated* (polyunsaturated) oils in foods is now extensively advertised. *Trans* fats, which have only one double bond with hydrocarbon chains in the *trans* configuration, have recently been shown to be as harmful as saturated fats, and a ban on their use in food preparation is under consideration. When a triglyceride is hydrolyzed through addition of sodium hydroxide, the ester bonds are broken and glycerol and sodium salts of long-chain carboxylic acids are produced. This reaction is the basis for traditional soap making through the addition of lye (sodium hydroxide) to animal fats.

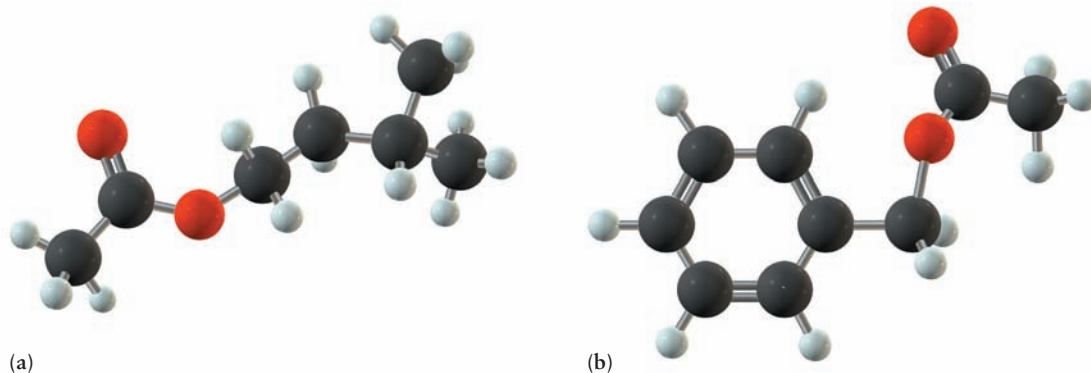
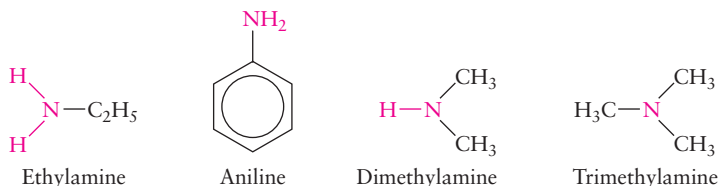


FIGURE 7.27 The structures of (a) isoamyl acetate, $\text{CH}_3\text{COO}(\text{CH}_2)_2\text{CH}(\text{CH}_3)_2$, and (b) benzyl acetate, $\text{CH}_3\text{COOCH}_2\text{C}_6\text{H}_5$.

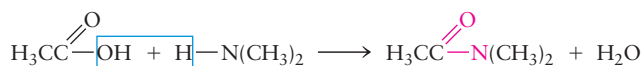
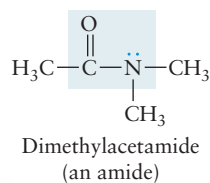
Amines and Amides

The **amines** are derivatives of ammonia with the general formula R_3N , where R can represent a hydrocarbon group or hydrogen. If only one hydrogen atom of ammonia is replaced by a hydrocarbon group, the result is a **primary amine**. Examples are ethylamine and aniline:



If two hydrocarbon groups replace hydrogen atoms in the ammonia molecule, the compound is a **secondary amine** (such as dimethylamine), and three replacements make a **tertiary amine** (trimethylamine). You should draw Lewis dot diagrams for several amines and recognize that the nitrogen is sp^3 hybridized and forms three σ bonds with one unshared pair in a hybridized orbital. Amines are bases because the lone electron pair on the nitrogen can accept a hydrogen ion in the same way that the lone pair on the nitrogen in ammonia does (see Chapter 15).

A primary or secondary amine (or ammonia itself) can react with a carboxylic acid to form an **amide**. This is another example of a condensation reaction and is analogous to the formation of an ester from reaction of an alcohol with a carboxylic acid. An example of amide formation is



If ammonia is the reactant, an $-NH_2$ group replaces the $-OH$ group in the carboxylic acid as the amide is formed:

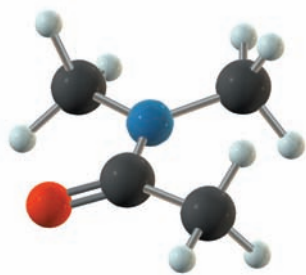
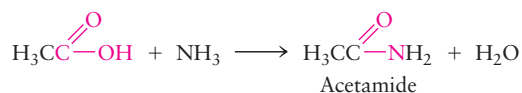


FIGURE 7.28 Bonding in dimethyl acetamide, an amide. The amide linkage is planar.

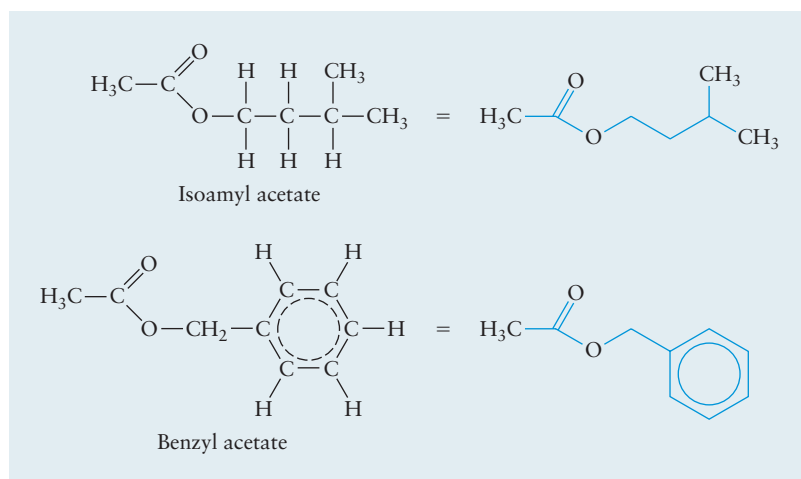
Amide linkages are present in the backbone of every protein molecule and are very important in biochemistry, where the structure of the molecule strongly influences its function (see Section 23.4). The bonding scheme in amides is a variation of that in Figure 7.26, in which the doubly bonded carbon and oxygen atoms are sp^2 hybridized and the singly bonded nitrogen atom is sp^3 hybridized with an unshared pair in one of the hybrid orbitals. As shown by the ball-and-stick model in Figure 7.28, the amide group is planar.

7.7 Pesticides and Pharmaceuticals

Most of the organic compounds discussed so far in this chapter have relatively small molecules and are produced in large volume. Molecules like these are starting materials for synthesis of numerous structurally more complex organic compounds with applications in agriculture, medicine, and consumer products. This section discusses a selection of these compounds, all of which are used in agriculture or as pharmaceuticals. Some of the structures and syntheses of these compounds are intricate; do not try to memorize them. Your goals instead, should be to note the hydrocarbon frames of the molecules, to recognize functional groups, and to begin to appreciate the extremely diverse structures and properties of organic compounds in relation to the chemical bonds in the frameworks and the functional groups.

Chemists have developed a shorthand notation to represent the structures of complex organic molecules. This notation, which focuses attention to the most

FIGURE 7.29 In the shorthand notation for the structures of organic compounds illustrated on the right side of this figure, carbon atoms are assumed to lie where the lines indicating bonds intersect. Furthermore, enough hydrogen atoms are assumed to be bonded to each carbon atom to give it a total valence of four. Terminal carbon atoms (those at the ends of chains) and their associated hydrogen atoms are shown explicitly, however.



important aspects of structure, is illustrated in Figure 7.29. In this notation, the symbol “C” for a carbon atom is omitted, and only the C—C bonds are shown. A carbon atom is assumed to lie at each end of the line segments that represent bonds. In addition, symbols for the hydrogen atoms attached to carbon are omitted. Terminal carbon atoms (those at the end of chains) and their associated hydrogen atoms are shown explicitly. To generate the full structure (and the molecular formula) from such a shorthand formula, carbon atoms must be inserted at the end of each bond, and enough hydrogen atoms must be attached to each carbon atom to satisfy its valence of four.

Insecticides

The chemical control of insect pests dates back thousands of years. The earliest insecticides were inorganic compounds of copper, lead, and arsenic, as well as some naturally occurring organic compounds such as nicotine (Fig. 7.30a). Few of these “first-generation” insecticides are in use today because of their adverse side effects on plants, animals, and humans.

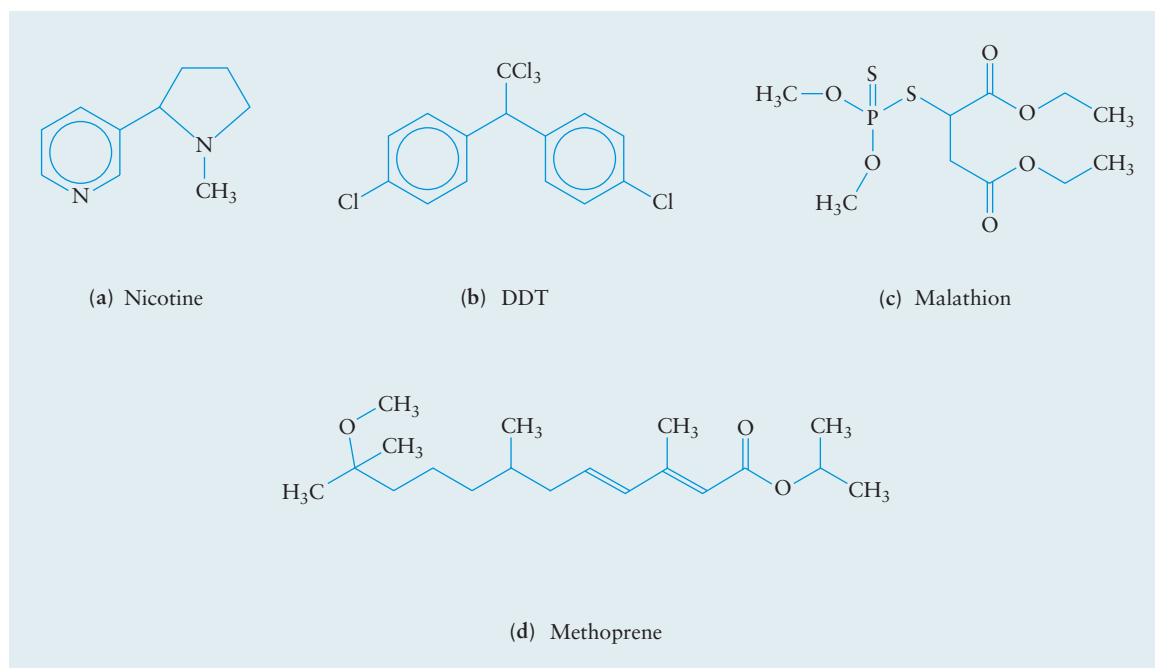


FIGURE 7.30 Structures of several insecticides: (a) nicotine; (b) dichlorodiphenyltrichloroethane (DDT); (c) malathion; and (d) methoprene.

After World War II, controlled organic syntheses gave rise to a second generation of insecticides. The success of these agents led to rapid growth in the use of chemicals for insect control. The leading insecticide of the 1950s and 1960s was DDT (an abbreviation for dichlorodiphenyltrichloroethane; see Fig. 7.30b). DDT was extremely important worldwide in slowing the spread of typhus (transmitted by body lice) and malaria (transmitted by mosquitoes). But, mosquitoes developed strong resistance to DDT, and its use was banned in the United States in 1972 because of its adverse effects on birds, fish, and other life-forms that can accumulate DDT to high concentrations. Many other chlorine-substituted hydrocarbons are no longer used as insecticides for the same reason. Today, organophosphorus compounds are used widely instead. The structure of the insecticide malathion, in which phosphorus appears with organic functional groups, is given in Figure 7.30c. Note the two ester groups, the two kinds of sulfur, and the “expanded octet” on the central phosphorus atom that lets it form five bonds.

Unless applied at the right times and in properly controlled doses, second-generation insecticides frequently kill beneficent insects together with the pests. Third-generation insecticides are more subtle. Many are based on sex attractants (to collect insects together in one place before exterminating them or to lead them to mate with sterile partners) or juvenile hormones (to prevent insects from maturing and reproducing). These compounds have the advantages of being specific against the pests and doing little or no harm to other organisms. Moreover, they can be used in small quantities, and they degrade rapidly in the environment. An example is the juvenile hormone methoprene (see Fig. 7.30d), which is used in controlling mosquitoes. It consists of a branched dialkene chain with a methyl ether (methoxy) and an isopropyl-ester functional group.

Herbicides

Chemical control of weeds, together with use of fertilizers, has contributed to the “green revolution” that began in the 1940s and during which agricultural productivity has increased dramatically throughout the world. The first herbicide of major importance, introduced in 1945 and still in use today, was 2,4-D (2,4-dichlorophenoxyacetic acid; Fig. 7.31a), a derivative of phenol with chlorine and carboxylic acid functional groups. 2,4-D kills broadleaf weeds in wheat, corn, and cotton without unduly persisting in the environment, as the chlorinated insecticides discussed earlier do. A related compound is 2,4,5-T (2,4,5-trichlorophenoxyacetic acid), in which a hydrogen atom in 2,4-D is replaced by a chlorine atom. In recent years, much attention has been given to TCDD (“dioxin,” or 2,3,7,8-tetrachlorodibenzo-*p*-dioxin; see Fig. 7.31b), which occurs as a trace impurity (10–20 ppb by mass) in 2,4,5-T and which, in animal tests, is the most toxic compound of low-to-moderate molar mass currently known. The use of 2,4,5-T as a

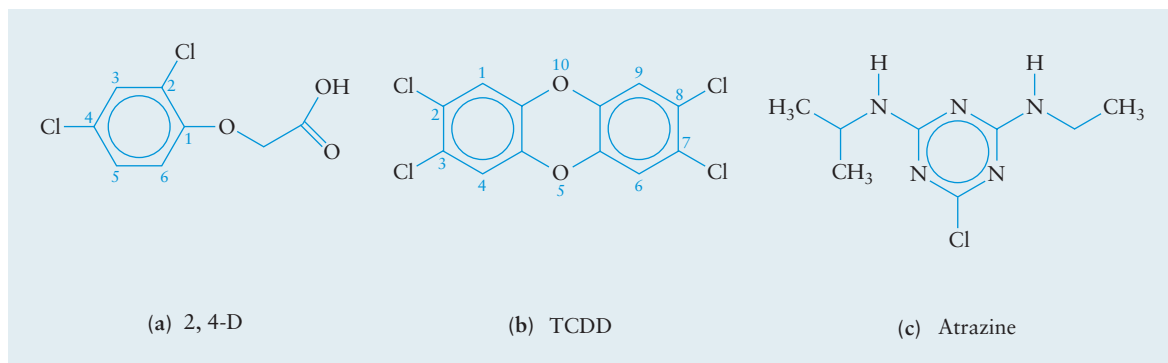


FIGURE 7.31 Structures of some herbicides. (a) 2,4-D (2,4-dichlorophenoxyacetic acid); (b) TCDD (“dioxin,” or 2,3,7,8-tetrachlorodibenzo-*p*-dioxin); and (c) atrazine.

Crystals of 4-acetaminophen (Tylenol) viewed under polarized light.



© Michael W. Davidson/Photo Researchers, Inc.

defoliant (Agent Orange) during the Vietnam War led to a lawsuit by veterans who claimed that health problems arose from contact with the traces of TCDD present in the 2,4,5-T. Although such a direct connection has never been proved, the use of chlorinated phenoxy herbicides has decreased, and that of other herbicides, such as atrazine (see Fig. 7.31c), has grown.

Analgesics

Drugs that relieve pain are called **analgesics**. The oldest and most widely used analgesic is aspirin, which has the chemical name acetylsalicylic acid (Fig. 7.32a). More than 15 million kg of aspirin is synthesized each year. Aspirin acts to reduce fevers and to relieve pain. Some recent studies have suggested that regular moderate consumption may reduce the chances of heart disease. As an acid, aspirin can irritate the stomach lining, a side effect that can be reduced by combining it in a buffer with a weak base such as sodium hydrogen carbonate. Another important pain reliever is 4-acetaminophen, or acetaminophen (see Fig. 7.32b). This compound is sold under many trademarks, most prominently Tylenol. Both acetylsalicylic acid and 4-acetaminophen are derivatives of phenol. During synthesis, the former is converted to an acetic acid ester with an additional carboxylic acid functional group, and the latter with an amide functional group.

A much more powerful pain reliever, which is available only by prescription because of its addictive properties, is morphine (see Fig. 7.32c). Morphine acts on

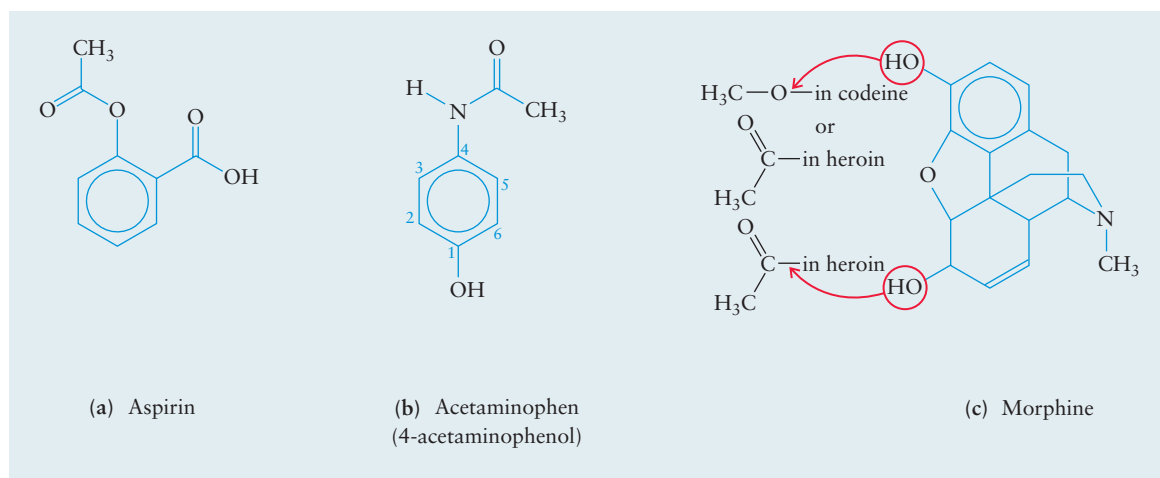
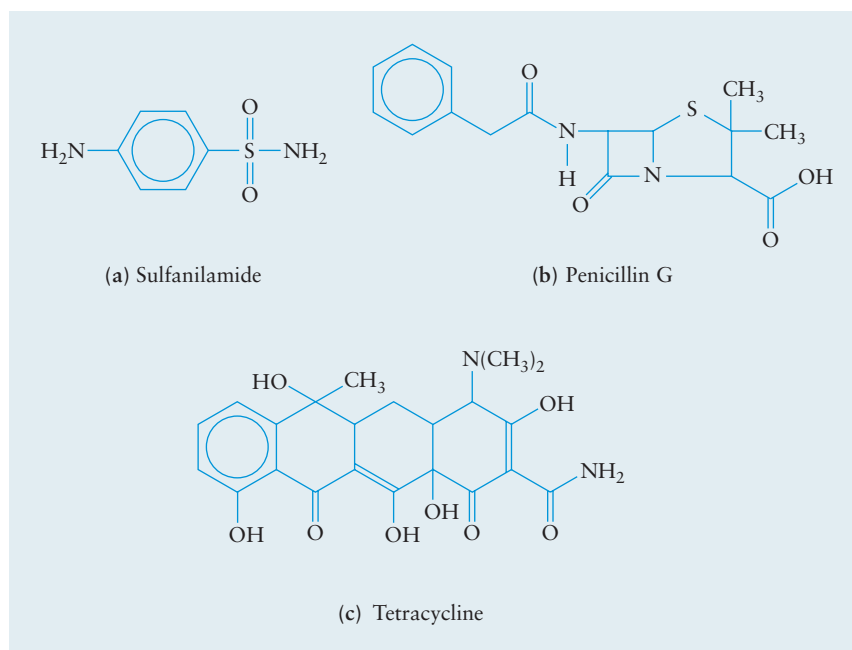


FIGURE 7.32 The molecular structures of some analgesics: (a) aspirin; (b) acetaminophen; and (c) morphine. Note how slight the differences are among morphine, codeine, and heroin.

FIGURE 7.33 Molecular structures of some antibiotics: (a) sulfanilamide; (b) penicillin G; and (c) tetracycline.



the central nervous system, apparently because its shape fits a receptor site on the nerve cell, and blocks the transmission of pain signals to the brain. Its structure contains five interconnected rings. A small change (the replacement of one $-\text{OH}$ group by an $-\text{OCH}_3$ group, giving a methyl ether) converts morphine into codeine, a prescription drug used as a cough suppressant. Replacing *both* $-\text{OH}$ groups by acetyl groups ($-\text{COCH}_3$) generates the notoriously addictive substance heroin.

Antibacterial Agents

The advent of antibacterial agents changed the treatment of bacterial diseases such as tuberculosis and pneumonia dramatically beginning in the 1930s. The first “wonder drug” was sulfanilamide (Fig. 7.33a), a derivative of aniline. Other “sulfa drugs” are obtained by replacing one of the hydrogen atoms on the sulfonamide group by other functional groups. Bacteria mistake sulfanilamide for *p*-aminobenzoic acid, a molecule with a very similar shape but a carboxylic acid ($-\text{COOH}$) group in place of the $-\text{SO}_2\text{NH}_2$ group. The drug then interferes with the bacterium’s synthesis of folic acid, an essential biochemical, so the organism dies. Mammals do not synthesize folic acid (they obtain it from their diet), so they are not affected by sulfanilamide.

The penicillin molecule (see Fig. 7.33b) contains an amide linkage that connects a substituted double ring (including sulfur and nitrogen atoms) to a benzyl (phenylmethyl) group. It is a natural product formed by certain molds. Although the total synthesis of penicillin was achieved in 1957, that chemical route is not competitive economically with biosynthesis via fermentation. The mold grows for several days in tanks that may hold up to 100,000 L of a fermentation broth (Fig. 7.34). The penicillin is later separated by solvent extraction. Penicillin functions by deactivating enzymes responsible for building cell walls in the bacteria. Derivatives of natural penicillin have been developed and are commercially available.

Finally we mention the tetracyclines, which are derivatives of the four-ring aromatic compound represented in Figure 7.33c. These drugs have the broadest spectrum of antibacterial activity found to date.



© Maximilian Stock Ltd./Photo Researchers, Inc.

FIGURE 7.34 Fermentation tanks used in modern penicillin production.

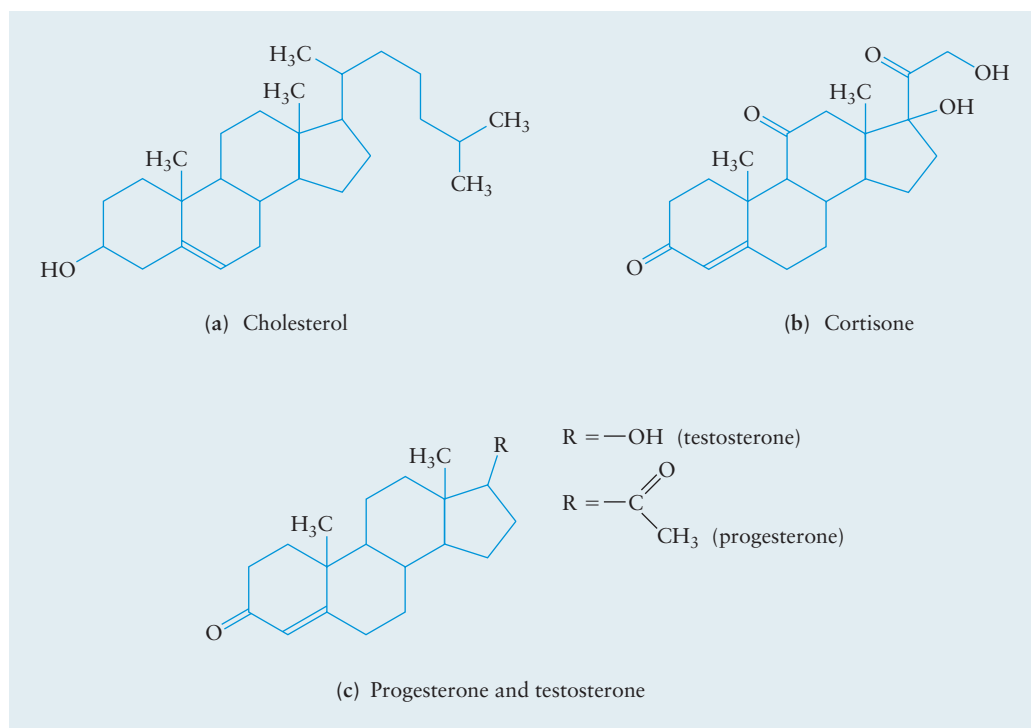


FIGURE 7.35 Molecular structures of some steroids: (a) cholesterol; (b) cortisone; and (c) progesterone and testosterone.

Steroids

The **steroids** are a family of naturally occurring compounds with a wide variety of functions. Most of them are synthesized from cholesterol. The structure of cholesterol (Fig. 7.35a) contains a group of four fused hydrocarbon rings (3 six-atom rings and 1 five-atom ring). All steroids possess this “steroid nucleus.” Cholesterol itself is present in all tissues of the human body. When present in excess in the bloodstream, it can accumulate in the arteries, restricting the flow of blood and leading to heart attacks. Its derivatives have widely different functions. The hormone cortisone (see Fig. 7.35b), which is secreted by the adrenal glands, regulates the metabolism of sugars, fats, and proteins in all body cells. As a drug, cortisone reduces inflammation and moderates allergic responses. It often is prescribed to combat arthritic inflammation of the joints.

The human sex hormones are also derivatives of cholesterol. Here the resourcefulness of nature for building compounds with quite different functions from the same starting material is particularly evident. The female sex hormone progesterone (see Fig. 7.35c) differs from the male sex hormone testosterone only by replacing an acetyl (—COCH_3) group by a hydroxyl (—OH) group. Oral contraceptives are synthetic compounds with structures that are closely related to progesterone.

CHAPTER SUMMARY

The element carbon has a rich and varied chemistry because of its location in the periodic table. As a Group IV element, each carbon atom forms four covalent bonds, more than any other second-period element. In consequence of its intermediate value of electronegativity, carbon can bond with more electronegative

elements such as oxygen, nitrogen, and the halogens, and also with more electropositive elements such as hydrogen and some of the heavy metals. Carbon also bonds with carbon, forming single, double, and triple bonds.

The hydrocarbons—molecules that contain only carbon and hydrogen—are fundamental to organic chemistry because they provide the archetypes for models of bond formation and the starting point for synthesis of other organic molecules. The hydrocarbons fall naturally into three families, based on their chemical properties and types of bonds.

The alkanes, also called saturated hydrocarbons, have only single bonds. The bonds are described by sp^3 hybridization of the carbon atoms. When the carbon atoms are not bonded in a linear sequence, cases can occur in which two molecules with the same formula can have different structures, called geometrical isomers, with quite distinct properties.

Unsaturated hydrocarbons have double or triple bonds between carbon atoms. The alkenes have C—C double bonds, described by sp^2 hybridization of the carbon atoms. The alkynes have C—C triple bonds, described by sp hybridization of the carbon atoms. Because bond rotation does not occur readily about a carbon–carbon double bond, many alkenes exist in contrasting isomeric forms, depending on whether bonding groups are on the same (*cis*) or opposite sides (*trans*) of the double bond. When two or more double or triple bonds are separated by one single bond, the p orbitals form a conjugated system, in which the de-localized π orbitals are best described by MO theory.

The aromatic hydrocarbons are conjugated cyclic structures in which the π bonding is described through de-localized MOs formed at carbon atoms that have sp^2 hybridization.

The fullerenes, which contain only carbon, are an allotropic form of carbon discovered in 1985. All the fullerenes have even numbers of atoms, with formulas ranging up to C_{400} and higher. Their π bonds are conjugated π electron systems.

Functional groups are sites of specific, heightened reactivity caused by insertion of noncarbon atoms into hydrocarbon structures or the attachment of noncarbon atoms to a hydrocarbon chain. Thus, organic molecules are conveniently viewed as carbon skeletal templates on which these highly reactive sites are located. Because of their reactivity, functional groups are key elements in strategies for synthesizing more complex organic structures.

The hydrocarbons recovered from petroleum, and their derivatives containing functional groups, are relatively small molecules with simple structures. Substances such as these provide starting materials for the synthesis of numerous structurally more complex organic compounds with applications in agriculture, medicine, and consumer products. These compounds include insecticides and herbicides for pest control and analgesics for controlling pain in the human body. Antibacterial agents fight disease. Steroids are naturally occurring compounds that derive from cholesterol. Hormones, including the human sex hormones, are derivatives of cholesterol. The bonding in these more elaborate structures is explained in the same way as the hydrocarbon skeletons and functional groups that comprise the structures.

CHAPTER REVIEW

- The alkanes, also called saturated hydrocarbons, have only single bonds, described by sp^3 hybridization of the carbon atoms.
- Carbon–carbon σ bonds form by overlap of sp^3 orbitals on adjacent atoms, and carbon–hydrogen σ bonds form by overlap of sp^3 orbitals with hydrogen 1s orbitals.
- In the straight-chain alkanes (general formula C_nH_{2n+2}), the carbon atoms are bonded in a linear sequence, and the molecules may take up numerous detailed

molecular conformations because of the ease of rotation about C—C single bonds.

- In cycloalkanes (general formula C_nH_{2n}), the carbon atoms at the end of a chain are attached together to form a closed loop. This connectivity reduces the ease with which the molecule changes conformations by rotation about single bonds and introduces both steric and angle strain into the total energy of the molecule. Consequently, cycloalkanes have particular preferred conformations such as boat and chair, and the molecule must absorb energy to move between them.
- In the branched-chain alkanes (general formula C_nH_{2n+2}), the carbon atoms are no longer arranged in a linear sequence, but instead can be bonded to three or four other carbon atoms. This possibility leads to a rich elaboration of structure in which two molecules with the same formula can have different structures, called geometrical isomers, and therefore quite distinct properties.
- Unsaturated hydrocarbons have double or triple bonds between carbon atoms.
- The alkenes have C—C double bonds, described by sp^2 hybridization of the carbon atoms. A σ bond forms by overlap of sp^2 orbitals on adjacent carbon atoms. The parallel nonhybridized $2p$ orbitals on adjacent carbon atoms overlap to form a C—C π bond.
- The alkynes have C—C triple bonds, described by sp hybridization of the carbon atoms. A σ bond forms by overlap of sp orbitals on adjacent carbon atoms. The two pairs of parallel nonhybridized $2p$ orbitals on adjacent carbon atoms overlap to form two C—C π bonds.
- Because bond rotation does not occur readily about a carbon–carbon double bond, many alkenes exist in contrasting isomeric forms, depending on whether bonding groups are on the same (*cis*) or opposite sides (*trans*) of the double bond.
- The structures and bonding in substituted alkenes and alkynes can be described by the combined MO-VB picture presented in Section 6.5, in which localized VB bonds describe the molecular framework and delocalized MOs describe the π electrons.
- When two or more double or triple bonds are separated by a single bond in a molecule, a conjugated system is formed, and a delocalized MO picture of the bonding should be used.
- The aromatic hydrocarbons are conjugated cyclic structures in which the π bonding is described by delocalized MOs. Each carbon atom has sp^2 hybrid orbitals that overlap to form C—C σ bonds that define the molecular framework. The remaining nonhybridized p_z orbitals combine to give π MOs delocalized over the entire molecule.
- The fullerenes, which contain only carbon, are an allotropic form of carbon discovered in 1985. All the fullerenes have even numbers of atoms, with formulas ranging up to C_{400} and higher. Their π bonds are conjugated π electron systems.
- Functional groups are sites of specific, heightened reactivity caused by insertion of noncarbon atoms into hydrocarbon structures or the attachment of noncarbon atoms to a hydrocarbon chain. The structures, shapes, and chemical reactivity of functional groups are largely independent of their location in organic molecules. Thus, organic molecules are conveniently viewed as carbon skeletal templates on which the highly reactive sites are located. Because of their specific reactivity, functional groups are key elements in strategies for synthesizing more complex organic structures.
- Replacing a hydrogen atom by a halogen atom creates an alkyl halide. Replacing a hydrogen atom by an —OH group produces an alcohol. If the —OH group is attached to an aromatic hydrocarbon ring, the resulting structure is called a phenol.

- Ethers are characterized by the —O— functional group, where the oxygen atom links either alkyl or aromatic groups. Cyclic ethers, with various ring sizes, are called epoxides.
- An aldehyde has the functional group $\text{—}\overset{\text{O}}{\parallel}\text{C—H}$ derived from dehydrogenation of an alcohol.
- A ketone has the functional group $\text{—}\overset{\text{O}}{\parallel}\text{C—}$.
- Carboxylic acids contain the functional group $\text{—}\overset{\text{O}}{\parallel}\text{C—OH}$ and react with alcohols to produce esters.
- The C—O double bonds in all these structures are described by sp^2 hybrid orbitals on both atoms for the σ bonds and nonhybridized $2p$ orbitals for the π bonds.
- The amines are organic derivatives of NH_3 in which one, two, or three hydrogens have been replaced by hydrocarbon groups to give primary, secondary, or tertiary amines, respectively. Primary or secondary amines react with carboxylic acids to give amides. The bonds in all these are described by sp^3 hybridization of the nitrogen atom.
- Controlled chemical syntheses have produced organic compounds that are used as pesticides and others to fight pain and disease in the human body.

CONCEPTS & SKILLS

After studying this chapter and working the problems that follow, you should be able to:

1. Identify important hydrocarbons in crude petroleum and describe their behavior in combustion (Sections 7.1–7.4, Problems 1–4).
2. Write names and structural formulas for hydrocarbons (Sections 7.2–7.4, Problems 5–12).
3. Describe the hybrid–atomic–orbital basis for representing the bonding and structure of organic molecules (Sections 7.2–7.4, Problems 13–14).
4. Discuss the delocalization of π electrons in organic molecules and fullerenes (Sections 7.3–7.5, Problems 12–16).
5. Identify important functional groups and outline chemical processes by which important chemical compounds are synthesized (Section 7.6, Problems 17–26).
6. Describe the bonding in important functional groups using the hybrid orbitals approach (Section 7.6, Problems 27–30).
7. Recognize and describe the shapes and functional groups for molecules used as pesticides and pharmaceuticals (Section 7.7, Problems 31–36).

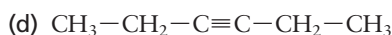
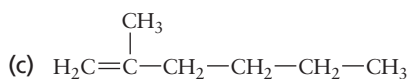
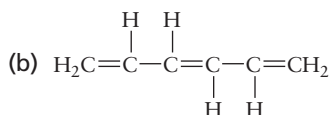
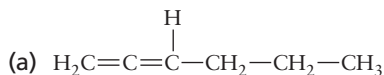
PROBLEMS

Answers to problems whose numbers are boldface appear in Appendix G. Problems that are more challenging are indicated with asterisks.

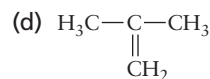
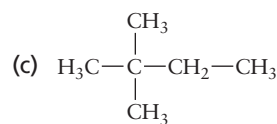
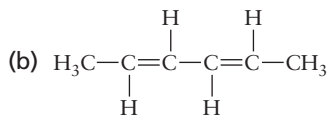
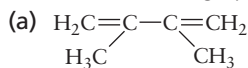
Petroleum Refining and the Hydrocarbons

1. Is it possible for a gasoline to have an octane number exceeding 100? Explain.
2. Is it possible for a motor fuel to have a negative octane rating? Explain.
3. A gaseous alkane is burned completely in oxygen. The volume of the carbon dioxide that forms equals twice the volume of the alkane burned (the volumes are measured at the same temperature and pressure). Name the alkane and write a balanced equation for its combustion.

4. A gaseous alkyne is burned completely in oxygen. The volume of the water vapor that forms equals the volume of the alkyne burned (the volumes are measured at the same temperature and pressure). Name the alkyne and write a balanced equation for its combustion.
5. (a) Write a chemical equation involving structural formulas for the catalytic cracking of decane into an alkane and an alkene that contain equal numbers of carbon atoms. Assume that both products have straight chains of carbon atoms.
(b) Draw and name one other isomer of the alkene.
6. (a) Write an equation involving structural formulas for the catalytic cracking of 2,2,3,4,5,5-hexamethylhexane. Assume that the cracking occurs between carbon atoms 3 and 4.
(b) Draw and name one other isomer of the alkene.
7. Write structural formulas for the following:
(a) 2,3-Dimethylpentane
(b) 3-Ethyl-2-pentene
(c) Methylcyclopropane
(d) 2,2-Dimethylbutane
(e) 3-Propyl-2-hexene
(f) 3-Methyl-1-hexene
(g) 4-Ethyl-2-methylheptane
(h) 4-Ethyl-2-heptyne
8. Write structural formulas for the following:
(a) 2,3-Dimethyl-1-cyclobutene
(b) 2-Methyl-2-butene
(c) 2-Methyl-1,3-butadiene
(d) 2,3-Dimethyl-3-ethylhexane
(e) 4,5-Diethyloctane
(f) Cyclooctene
(g) Propadiene
(h) 2-pentyne
9. Write structural formulas for *trans*-3-heptene and *cis*-3-heptene.
10. Write structural formulas for *cis*-4-octene and *trans*-4-octene.
11. Name the following hydrocarbons:



12. Name the following hydrocarbons:



13. State the hybridization of each of the carbon atoms in the hydrocarbon structures in Problem 11.
14. State the hybridization of each of the carbon atoms in the hydrocarbon structures in Problem 12.

Fullerenes

15. To satisfy the octet rule, fullerenes must have double bonds. How many? Give a simple rule for one way of placing them in the structure shown in Figure 7.20a.
16. It has been suggested that a compound of formula $\text{C}_{12}\text{B}_{24}\text{N}_{24}$ might exist and have a structure similar to that of C_{60} (buckminsterfullerene).
(a) Explain the logic of this suggestion by comparing the number of valence electrons in C_{60} and $\text{C}_{12}\text{B}_{24}\text{N}_{24}$.
(b) Propose the most symmetric pattern of carbon, boron, and nitrogen atoms in $\text{C}_{12}\text{B}_{24}\text{N}_{24}$ to occupy the 60 atom sites in the buckminsterfullerene structure. Where could the double bonds be placed in such a structure?

Functional Groups and Organic Reactions

17. In a recent year, the United States produced 6.26×10^9 kg ethylene dichloride (1,2-dichloroethane) and 15.87×10^9 kg ethylene. Assuming that all significant quantities of ethylene dichloride were produced from ethylene, what fraction of the ethylene production went into making ethylene dichloride? What mass of chlorine was required for this conversion?
18. In a recent year, the United States produced 6.26×10^9 kg ethylene dichloride (1,2-dichloroethane) and 3.73×10^9 kg vinyl chloride. Assuming that all significant quantities of vinyl chloride were produced from ethylene dichloride, what fraction of the ethylene dichloride production went into making vinyl chloride? What mass of hydrogen chloride was generated as a by-product?
19. Write balanced equations for the following reactions. Use structural formulas to represent the organic compounds.
(a) The production of butyl acetate from butanol and acetic acid
(b) The conversion of ammonium acetate to acetamide and water
(c) The dehydrogenation of 1-propanol
(d) The complete combustion (to CO_2 and H_2O) of heptane
20. Write balanced equations for the following reactions. Use structural formulas to represent the organic compounds.
(a) The complete combustion (to CO_2 and H_2O) of cyclopropanol
(b) The reaction of isopropyl acetate with water to give acetic acid and isopropanol
(c) The dehydration of ethanol to give ethylene
(d) The reaction of 1-iodobutane with water to give 1-butanol

21. Outline, using chemical equations, the synthesis of the following from easily available petrochemicals and inorganic starting materials.
- Vinyl bromide ($\text{CH}_2=\text{CHBr}$)
 - 2-Butanol
 - Acetone (CH_3COCH_3)
22. Outline, using chemical equations, the synthesis of the following from easily available petrochemicals and inorganic starting materials.
- Vinyl acetate ($\text{CH}_3\text{COOCH}=\text{CH}_2$)
 - Formamide (HCONH_2)
 - 1,2-Difluoroethane
23. Write a general equation (using R to represent a general alkyl group) for the formation of an ester by the condensation of a tertiary alcohol with a carboxylic acid.
24. Explain why it is impossible to form an amide by the condensation of a tertiary amine with a carboxylic acid.
25. Calculate the volume of hydrogen at 0°C and 1.00 atm that is required to convert 500.0 g linoleic acid ($\text{C}_{18}\text{H}_{32}\text{O}_2$) to stearic acid ($\text{C}_{18}\text{H}_{36}\text{O}_2$).
26. A chemist determines that 4.20 L hydrogen at 298 K and a pressure of 1.00 atm is required to completely hydrogenate 48.5 g of the unsaturated compound oleic acid to stearic acid ($\text{C}_{18}\text{H}_{36}\text{O}_2$). How many units of unsaturation (where a unit of unsaturation is one double bond) are in a molecule of oleic acid?
27. Acetic acid can be made by the oxidation of acetaldehyde (CH_3CHO). Molecules of acetaldehyde have a $-\text{CH}_3$ group, an oxygen atom, and a hydrogen atom attached to a carbon atom. Draw the Lewis diagram for this molecule, give the hybridization of each carbon atom, and describe the π orbitals and the number of electrons that occupy each one. Draw the three-dimensional structure of the molecule, showing all angles.
28. Acrylic fibers are polymers made from a starting material called acrylonitrile, $\text{H}_2\text{C}(\text{CH})\text{CN}$. In acrylonitrile, a $-\text{C}\equiv\text{N}$ group replaces a hydrogen atom on ethylene. Draw the Lewis diagram for this molecule, give the hybridization of each carbon atom, and describe the π orbitals and the number of electrons that occupy each one. Draw the three-dimensional structure of the molecule, showing all angles.
29. Compare the bonding in formic acid (HCOOH) with that in its conjugate base formate ion (HCOO^-). Each molecule has a central carbon atom bonded to the two oxygen atoms and to a hydrogen atom. Draw Lewis diagrams, determine the steric numbers and hybridization of the central carbon atom, and give the molecular geometries. How do the π orbitals differ in formic acid and the formate molecular ion? The bond lengths of the $\text{C}-\text{O}$ bonds in HCOOH are 1.23 (for the bond to the lone oxygen) and 1.36 \AA (for the bond to the oxygen with a hydrogen atom attached). In what range of lengths do you predict the $\text{C}-\text{O}$ bond length in the formate ion to lie?
30. Section 7.3 shows that the compound 2-butene exists in two isomeric forms, which can be interconverted only by breaking a bond (in that case, the central double bond). How many possible isomers correspond to each of the following chemical formulas? Remember that a simple rotation of an entire molecule does not give a different isomer. Each molecule contains a central $\text{C}=\text{C}$ bond.

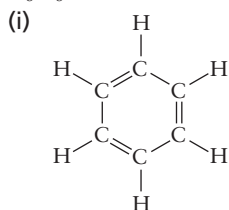
- $\text{C}_2\text{H}_2\text{Br}_2$
- $\text{C}_2\text{H}_2\text{BrCl}$
- C_2HBrClF

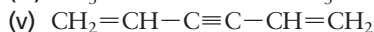
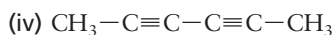
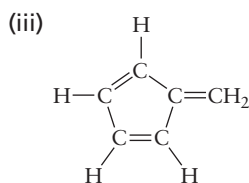
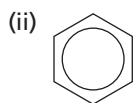
Pesticides and Pharmaceuticals

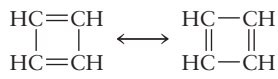
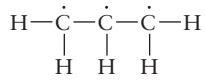
31. (a) The insecticide methoprene (see Fig. 7.30d) is an ester. Write the structural formulas for the alcohol and the carboxylic acid that react to form it. Name the alcohol.
- (b) Suppose that the carboxylic acid from part (a) is changed chemically so that the OCH_3 group is replaced by a hydrogen atom and the COOH group is replaced by a CH_3 group. Name the hydrocarbon that would result.
32. (a) The herbicide 2,4-D (see Fig. 7.31a) is an ether. Write the structural formulas of the two alcohol or phenol compounds that, on condensation, would form this ether. (The usual method of synthesis does not follow this plan.)
- (b) Suppose that hydrogen atoms replace the chlorine atoms and a $-\text{CH}_3$ group replaces the carboxylic acid group in the two compounds in part (a). Name the resulting compounds.
33. (a) Write the molecular formula of acetylsalicylic acid (see Fig. 7.32a).
- (b) An aspirin tablet contains 325 mg acetylsalicylic acid. Calculate the number of moles of that compound in the tablet.
34. (a) Write the molecular formula of acetaminophen (see Fig. 7.32b).
- (b) A tablet of Extra Strength Tylenol contains 500 mg acetaminophen. Calculate the chemical amount (in moles) of that compound in the tablet.
35. Describe the changes in hydrocarbon structure and functional groups that are needed to make cortisone from cholesterol (see Fig. 7.35).
36. Describe the changes in hydrocarbon structure and functional groups that are needed to make testosterone from cortisone (see Fig. 7.35).

ADDITIONAL PROBLEMS

37. *trans*-Cyclodecene boils at 193°C , but *cis*-cyclodecene boils at 195.6°C . Write structural formulas for these two compounds.
38. A compound $\text{C}_4\text{H}_{11}\text{N}$ is known from its reactivity and spectroscopic properties to have no hydrogen atoms attached directly to the nitrogen atom. Write all structural formulas consistent with this information.
39. A compound $\text{C}_3\text{H}_6\text{O}$ has a hydroxyl group but no double bonds. Write a structural formula consistent with this information.
40. Consider the following proposed structures for benzene, each of which is consistent with the molecular formula C_6H_6 .





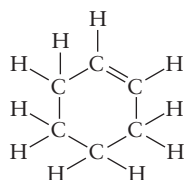
- (a) When benzene reacts with chlorine to give $\text{C}_6\text{H}_5\text{Cl}$, only one isomer of that compound forms. Which of the five proposed structures for benzene are consistent with this observation?
- (b) When $\text{C}_6\text{H}_5\text{Cl}$ reacts further with chlorine to give $\text{C}_6\text{H}_4\text{Cl}_2$, exactly three isomers of the latter compound form. Which of the five proposed structures for benzene are consistent with this observation?
41. Acetyl chloride, CH_3COCl , reacts with the hydroxyl groups of alcohols to form ester groups with the elimination of HCl . When an unknown compound X with formula $\text{C}_4\text{H}_8\text{O}_3$ reacted with acetyl chloride, a new compound Y with formula $\text{C}_8\text{H}_{12}\text{O}_5$ was formed.
- (a) How many hydroxyl groups were there in X?
- (b) Assume that X is an aldehyde. Write a possible structure for X and a possible structure for Y consistent with your structure for X.
42. When an ester forms from an alcohol and a carboxylic acid, an oxygen atom links the two parts of each ester molecule. This atom could have come originally from the alcohol, from the carboxylic acid, or randomly from either. Propose an experiment using isotopes to determine which is the case.
43. Hydrogen can be added to a certain unsaturated hydrocarbon in the presence of a platinum catalyst to form hexane. When the same hydrocarbon is oxidized with KMnO_4 , it yields acetic acid and butanoic acid. Identify the hydrocarbon and write balanced chemical equations for the reactions.
44. (a) It is reported that ethylene is released when pure ethanol is passed over alumina (Al_2O_3) that is heated to 400°C , but diethyl ether is obtained at a temperature of 230°C . Write balanced equations for both of these dehydration reactions.
- (b) If the temperature is increased well above 400°C , an aldehyde forms. Write a chemical equation for this reaction.
- * 45. The pyridine molecule ($\text{C}_5\text{H}_5\text{N}$) is obtained by replacing one C—H group in benzene with a nitrogen atom. Because nitrogen is more electronegative than the C—H group, orbitals with electron density on nitrogen are lower in energy. How do you expect the π MOs and energy levels of pyridine to differ from those of benzene?
- * 46. For each of the following molecules, construct the π MOs from the $2p_z$ atomic orbitals perpendicular to the plane of the carbon atoms.
- (a) Cyclobutadiene 
- (b) Allyl radical 

Indicate which, if any, of these orbitals have identical energies from symmetry considerations. Show the number of electrons occupying each π MO in the ground state, and indicate whether either or both of the molecules are paramagnetic. (*Hint*: Refer to Figs. 7.17 and 7.18.)

47. In what ways do the systematic developments of pesticides and of pharmaceuticals resemble each other, and in what ways do they differ? Consider such aspects as “deceptor” molecules, which are mistaken by living organisms for other molecules; side effects; and the relative advantages of a broad versus a narrow spectrum of activity.
48. The steroid stanolone is an androgenic steroid (a steroid that develops or maintains certain male sexual characteristics). It is derived from testosterone by adding a molecule of hydrogen across the $\text{C}=\text{C}$ bond in testosterone.
- (a) Using Figure 7.35c as a guide, draw the molecular structure of stanolone.
- (b) What is the molecular formula of stanolone?

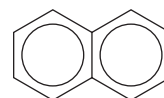
CUMULATIVE PROBLEMS

49. The structure of the molecule cyclohexene is



Does the absorption of ultraviolet light by cyclohexene occur at longer or at shorter wavelengths than the absorption by benzene? Explain.

50. The naphthalene molecule has a structure that corresponds to two benzene molecules fused together:



The π electrons in this molecule are delocalized over the entire molecule. The wavelength of maximum absorption in benzene is 255 nm. Will the corresponding wavelength in naphthalene be shorter or longer than 255 nm?

This page intentionally left blank

Bonding in Transition Metal Compounds and Coordination Complexes

- 8.1 Chemistry of the Transition Metals
- 8.2 Bonding in Simple Molecules That Contain Transition Metals
- 8.3 Introduction to Coordination Chemistry
- 8.4 Structures of Coordination Complexes
- 8.5 Crystal Field Theory: Optical and Magnetic Properties
- 8.6 Optical Properties and the Spectrochemical Series
- 8.7 Bonding in Coordination Complexes



© Mark A. Schneider/Photo Researchers, Inc.

The colors of gemstones originate with transition-metal ions. Emerald is the mineral beryl (beryllium aluminum silicate $3\text{BeO}\cdot\text{Al}_2\text{O}_3\cdot 6\text{SiO}_2$), in which some of the Al^{3+} ions have been replaced by Cr^{3+} ions. This structural environment splits the $3d$ orbitals to give a new energy separation that absorbs yellow and blue-violet light and transmits green light. The green color of emerald is the result.

The partially filled d -electron shells of the transition-metal elements are responsible for a range of physical properties and chemical reactions quite different from those of the main-group elements. The presence of unpaired electrons in the transition-metal elements and their compounds, the availability of low-energy unoccupied orbitals, and the facility with which transition-metal oxidation states change are important factors that determine their rich and fascinating chemistry. Transition-metal complexes are characterized by a wide variety of geometric structures, variable and striking colors, and magnetic properties that depend on subtle details of their structure and bonding. This chapter begins with a descriptive overview of the systematic trends in the properties of these metals, and then presents a comprehensive introduction to the classical and quantum mechanical models that describe bond formation in their compounds.

8.1 Chemistry of the Transition Metals

Let's begin by surveying some of the key physical and chemical properties of the transition-metal elements and interpreting trends in those properties using the quantum theory of atomic structure developed in Chapter 5. We focus initially on the fourth-period elements, also called the first transition series (those from scandium through zinc in which the $3d$ shell is progressively filled). Then we discuss the periodic trends in the melting points and atomic radii of the second and third transition series elements.

Physical Properties

Table 8.1 lists some key physical properties of the elements of the first transition series, taken mostly from Appendix F. The general trends in all of these properties can be understood by recalling that nuclear charge also increases across a period as electrons are being added to the same subshell, in this case, the d shell. The first and second ionization energies tend to increase across the period, but not smoothly. The energies of the $4s$ and $3d$ orbitals are so close to one another that the electron configurations of the neutral atoms and their ions are not easily predicted from the simplest model of atomic structure.

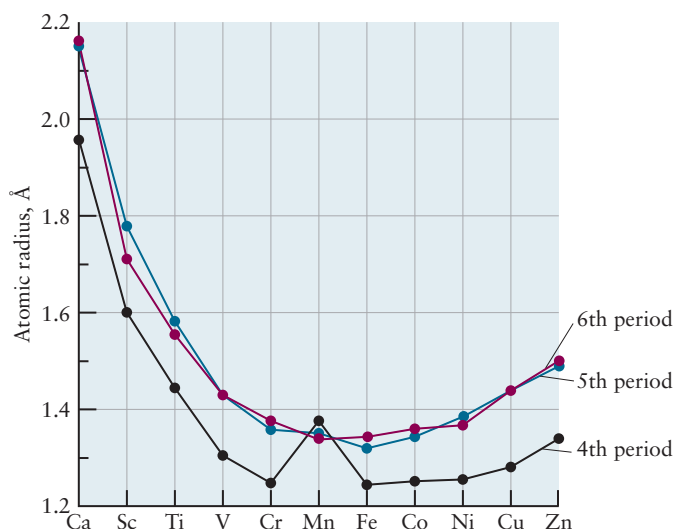
Electron-nuclear attraction increases as Z increases; thus, atomic and ionic radii generally decrease across each period as shown in Table 8.1 and Figure 8.1. But near the end of each period, repulsion between the electrons in the nearly filled d shell increases faster than the electron-nuclear attraction; thus, both the atomic and ionic radii begin to increase. Atoms of the second transition series (from yttrium to cadmium) are larger than those of the first transition series, as expected from the fact that the $4d$ orbitals are larger than the $3d$ orbitals. However, the atomic radii of the third transition series are not that much different from those of the second (see Fig. 8.1). This experimental fact is explained by the **lanthanide contraction**. The first and second transition series are separated by 18 elements, whereas the second and third are separated by 32 elements. The lanthanides have intervened, but their presence is not so obvious from the modern periodic table. Both the nuclear charge and electron count have increased between second- and third-period elements of the same group, but the f orbitals are much more diffuse than the d orbitals and much less effective in screening the nuclear charge. Elements in the third transition series experience a much greater effective nuclear charge than otherwise expected and thus are smaller. The atomic and ionic radii of hafnium, in the sixth period, are essentially the same as those of zirconium, in the fifth period. Because these elements are similar in both valence configuration and size, their properties are quite similar and they are difficult to separate from

TABLE 8.1 Properties of the Fourth-Period Transition Elements

Element	Sc	Ti	V	Cr	Mn	Fe	Co	Ni	Cu	Zn
I_1 (kJ mol ⁻¹)	631	658	650	653	717	759	758	737	745	906
I_2 (kJ mol ⁻¹)	1235	1310	1414	1592	1509	1562	1648	1753	1958	1733
Boiling point (°C)	2831	3287	3380	2672	1962	2750	2870	2732	2567	907
Melting point (°C)	1541	1660	1890	1857	1244	1535	1495	1453	1083	420
Atomic radius (Å)	1.61	1.45	1.31	1.25	1.37	1.24	1.25	1.25	1.28	1.34
M ²⁺ ionic radius (Å)	0.81	0.68	0.88	0.89	0.80	0.72	0.72	0.69	0.72	0.74
M ²⁺ configuration	d^1	d^2	d^3	d^4	d^5	d^6	d^7	d^8	d^9	d^{10}
$\Delta H_{\text{hyd}}(\text{M}^{2+})^\dagger$ (kJ mol ⁻¹)				-2799	-2740	-2839	-2902	-2985	-2989	-2937

[†]Defined as $\Delta H_f^\circ(\text{M}^{2+}(\text{aq})) - \Delta H_f^\circ(\text{M}^{2+}(\text{g}))$. Because aqueous species are defined relative to $\Delta H_f^\circ(\text{H}^+(\text{aq})) = 0$, this is not an absolute enthalpy of hydration.

FIGURE 8.1 Variation of atomic radii through the fourth-, fifth-, and sixth-period transition-metal elements. Symbols shown are for the fourth-period elements.

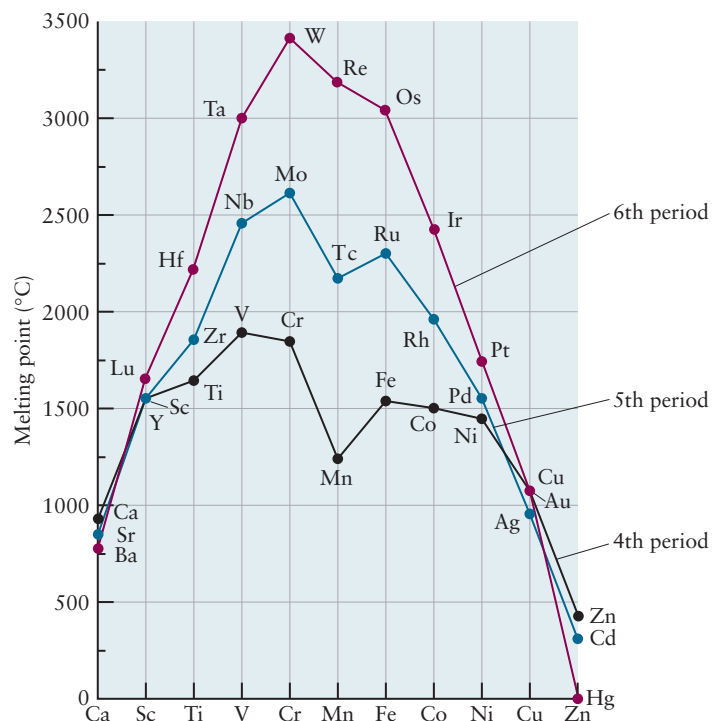


one another. (A parallel effect, shown in Fig. 5.41 and discussed in Section 5.5 for main-group atoms and ions, arises from the filling of the $3d$ shell.)

The term *lanthanide contraction* is also used for another trend—the decrease in the atomic and ionic radii of the lanthanides from left to right along the sixth period. This trend has the same physical origin as that discussed previously in Chapter 5 for the second- and third-period elements and repeated earlier here: Nuclear charge is increasing while electrons are being added to the same subshell, in this case, the f shell. Using the same term for two different phenomena can cause confusion; therefore, we suggest you pay careful attention to the context when you see the term *lanthanide contraction*.

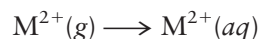
Metal-metal bond strengths first increase and then decrease going across each transition series, reaching a maximum in the middle. Evidence supporting this conclusion comes from the periodic variation in the melting and boiling points of the fourth-period elements shown in Table 8.1 and the corresponding trends in melting points for the three transition series shown in Figure 8.2. The melting and

FIGURE 8.2 Variation of melting points through the three periods of transition-metal elements.



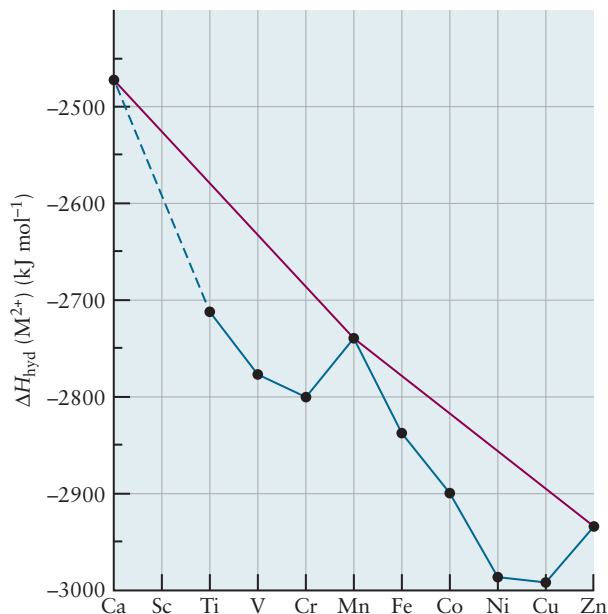
boiling points are functions of the bond strengths between the atoms or ions in solids. Both of these properties correlate roughly with the number of unpaired electrons in the elements involved, which reaches a maximum in the middle of the corresponding series. We can rationalize this correlation by thinking about the number of covalent bonds a given metal atom can form with its neighbors; the larger the number of unpaired electrons available for bonding, the greater the number of potential bonds. Another way to understand this trend is to think about bonding in terms of the formation of molecular orbitals delocalized over the entire solid. These molecular orbitals are constructed from the outermost d orbitals on the metal atoms, and each of them can accommodate two electrons. Lower energy orbitals in the solid are primarily bonding. As they are progressively filled through the first half of each transition series, the overall metal-metal bond strength increases. In the second half of each transition series, the higher energy antibonding orbitals become filled, and the bond strength decreases. Tungsten, near the middle of the sixth period, has a very high melting point (3410°C), which makes it useful in lightbulb filaments; mercury, at the end of the same period, has a melting point well below room temperature (-39°C).

Historically, most reactions of transition-metal ions have been carried out in aqueous solution; thus, it is important to understand the energy change that occurs when a metal ion is hydrated. These reactions are studied in solution under constant pressure. Under these conditions, the energy change is related to changes in the thermodynamic function *enthalpy*, denoted by H . Section 12.6 gives a proper discussion of enthalpies of reaction; for the present purpose, the enthalpy change can be treated simply as the energy change associated with the hydration of the gaseous ion



Energies of hydration for the M^{2+} ions of the first transition series show an interesting trend (see Table 8.1 and Fig. 8.3). Although we have not yet discussed how ions interact with water in aqueous solutions (see Section 10.2), we might expect the strength of the interactions to increase as the ionic radii decrease, allowing the water molecules to approach the ions more closely. A linear trend that might be expected using this reasoning is shown as the red line in Figure 8.3. The experimental results shown as the black points connected by the blue line follow the same general trend, but clear deviations from linearity suggest that factors other than ionic radii are important. In particular, the experimental results show no

FIGURE 8.3 Enthalpies of hydration of M^{2+} ions, defined as $\Delta H_{\text{f}}^{\circ}(\text{M}^{2+}(\text{aq})) - \Delta H_{\text{f}}^{\circ}(\text{M}^{2+}(\text{g}))$. The crystal field stabilization energy (discussed in Section 8.5) preferentially stabilizes certain ions, lowering ΔH_{hyd} from a line representing a linear change with increasing atomic number (red line) to the experimental (blue) line.



deviations for ions with filled shells (Ca^{2+} , Zn^{2+} with d^{10} configurations) or a shell that is exactly half filled (Mn^{2+} with a d^5 configuration). In Section 8.5, we connect this behavior to the way in which the shells are filled. Similar anomalies in the periodic trends in atomic radii and melting points occur for manganese (see Figs. 8.1 and 8.2); they are also related to the fact that manganese has a half-filled d shell.

Oxidation States of the Transition-Metal Elements

Figure 8.4 shows the characteristic oxidation states of the transition metals, which you should compare with those of the main-group elements shown in Figure 3.24. The maximum oxidation states of the early members of each period result from the participation of all the outer s and d electrons in ionic or covalent bonding. Thus, the maximum oxidation state for elements in the scandium group is +3, whereas manganese has a maximum oxidation state of +7, as do the other elements in its group. They form compounds such as HReO_4 and the dark red liquid Mn_2O_7 . Higher oxidation states are more common in compounds of the heavier transition metals of a given group. The chemistry of iron is dominated by the +2 and +3 oxidation states, as in the common oxides FeO and Fe_2O_3 , but the +8 state, which is nonexistent for iron, is important for the later members of the iron group, ruthenium and osmium. The oxide OsO_4 , for example, is a volatile yellow solid that melts at 41°C and boils at 131°C . It selectively oxidizes $\text{C}=\text{C}$ double bonds to *cis* diols, which makes it useful in organic synthesis (see Fig. 7.10) and as a biological stain, where it precipitates out easily seen black osmium metal. The chemistry of nickel is almost entirely that of the +2 oxidation state, but the higher oxidation states of the heavier elements in the nickel group, palladium and platinum, are commonly observed.

Compounds with transition metals in high oxidation states tend to be relatively covalent, whereas those with lower oxidation states are more ionic. Oxides are a good example: Mn_2O_7 is a covalent compound that is a liquid at room temperature (crystallizing only at 6°C), but Mn_3O_4 is an ionic compound, containing both Mn(II) and Mn(III), that melts at 1564°C . We can rationalize this important generalization by recalling that bonding configurations that have the smallest degree of charge separation tend to be the most stable. We used this principle (often called Pauling's principle of **electroneutrality**) as one way to choose among various possible Lewis dot diagrams (see Section 3.8).

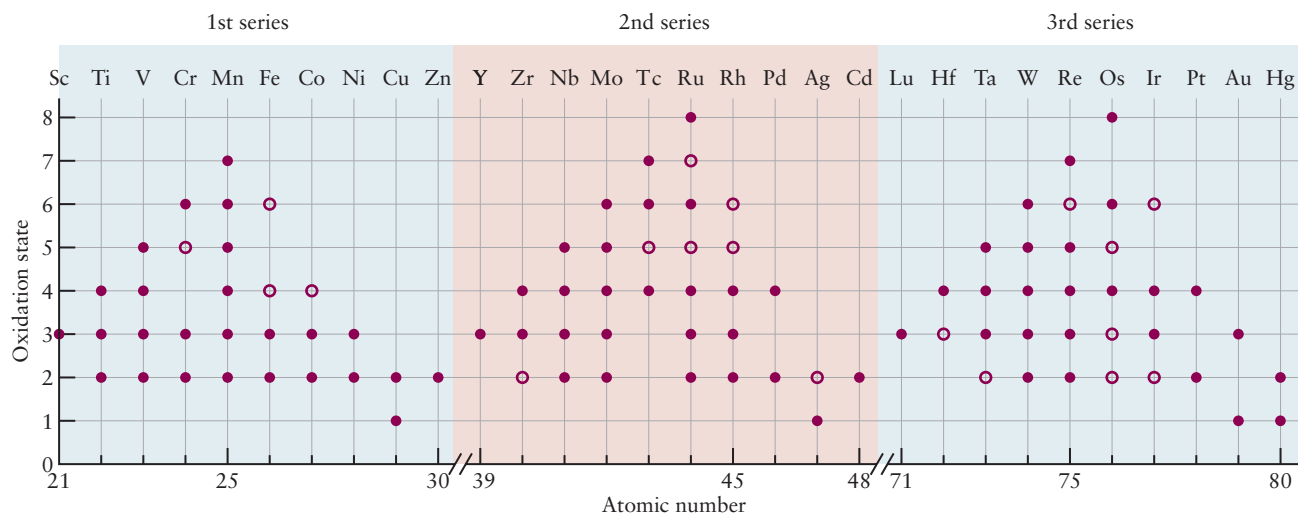


FIGURE 8.4 Some of the oxidation states found in compounds of the transition-metal elements. The more common oxidation states are represented by solid circles, and the less common ones are represented by open circles.

Transition metals exist in such a wide range of oxidation states because their partially filled d orbitals can either accept or donate electrons to form chemical bonds. For this same reason, many of their compounds are effective catalysts, substances that increase the rates of chemical reactions without undergoing permanent chemical changes themselves (see Chapter 18). Because an element such as iron can exist as Fe^{2+} or Fe^{3+} in solution, it can facilitate electron transfer reactions by shuttling back and forth between its oxidized and reduced forms without leaving solution. Elements like the alkali metal ions (K^+ , for example) that have only one stable oxidation state in solution do not offer this possibility. Examples of catalysis by transition metal compounds include ammonia synthesis from elemental nitrogen and hydrogen catalyzed by iron oxides and the oxidation of SO_2 to SO_3 catalyzed by V_2O_5 . The active sites of many enzymes (biological catalysts, see Section 18.7) are transition metal complexes that also facilitate electron transfer reactions by the mechanism just described.

Inorganic chemists use oxidation states to systematically organize patterns of structure and reactivity among the elements. Quantum chemical descriptions of the chemical bond (see Chapter 6) focus on the electron configurations of molecules. We can connect the two approaches by noting that metals in high oxidation states have relatively few d electrons, whereas those in low oxidation states are relatively rich in d electrons. Although this connection does not explain all of the patterns of bonding and reactivity in inorganic chemistry—it overlooks differences in the nuclear charge and energy levels of specific metals, for example—it does provide a useful way to organize our thinking about bonding in inorganic chemistry. Whether you focus on electron configurations or on oxidation states is a matter of choice for you (or your instructor). Either way, we suggest that you be mindful of the connection as we develop the molecular orbital theory of bonding in transition-metal compounds and coordination complexes

8.2 Bonding in Simple Molecules That Contain Transition Metals¹

Homonuclear Diatomic Molecules

The elemental transition metals are all solids at normal temperatures and pressures, but many of them form stable homonuclear diatomic molecules at high temperatures in the gas phase. These include all of the elements in the first transition series and many from the second and third transition series. We can use molecular orbital theory to understand bonding in these molecules just as we did for the first- and second-period homonuclear diatomics in Section 6.2. The situation is slightly more complicated for molecules that contain metal atoms because of the availability of the d electrons for bonding. Two important issues should be kept in mind when constructing molecular orbitals that include atomic d orbitals. First, the energies of the nd and the $(n + 1)s$ orbitals are close to one another, and the relative ordering of these levels changes as we move across a row in the periodic table. We know from photoelectron spectroscopy that the energy level order is $\epsilon_{4s} \cong \epsilon_{3d} < \epsilon_{4p}$ for the elements of the left side of the first transition series, changing to $\epsilon_{3d} < \epsilon_{4s} < \epsilon_{4p}$ as we move to the right side. Similar changes occur in the second and third transition series. To simplify this discussion, we adopt the energy level order $\epsilon_{3d} < \epsilon_{4s} < \epsilon_{4p}$ for most examples that follow. Second, the metal $3d_{z^2}$ and $4s$ orbitals can mix prior to forming molecular orbitals because they have the same symmetry and lie close to one another in energy. This mixing can result in an

¹The discussion in this section follows closely the arguments developed in *Chemical Structure and Bonding*, Roger L. DeKock and Harry B. Gray, University Science Books, Sausalito, 1989, and was adapted with permission.

energy level structure that is quite different from one predicted without considering such mixing. We ignore s - d mixing as we develop our molecular orbital treatment of bonding in transition-metal compounds, but we do point out its consequences as they arise in examples. These approximations allow us to develop a simple conceptual framework that captures the essential features of bonding in these molecules; refinements can be added in more advanced work.

We construct molecular orbitals for the homonuclear diatomic metal molecules following exactly the same procedure developed in Chapter 6 for the main-group diatomic molecules. The relevant atomic orbitals for the first transition series are the valence orbitals $3d$, $4s$, and $4p$. The $4s$ and $4p_z$ orbitals each generate a pair of bonding and antibonding σ and σ^* molecular orbitals, and the $4p_x$ and $4p_y$ orbitals each form a pair of bonding and antibonding π and π^* molecular orbitals, just as in the main-group diatomic molecules. The d orbitals can form six kinds of molecular orbitals (Fig. 8.5). The d_{z^2} orbitals are oriented along the

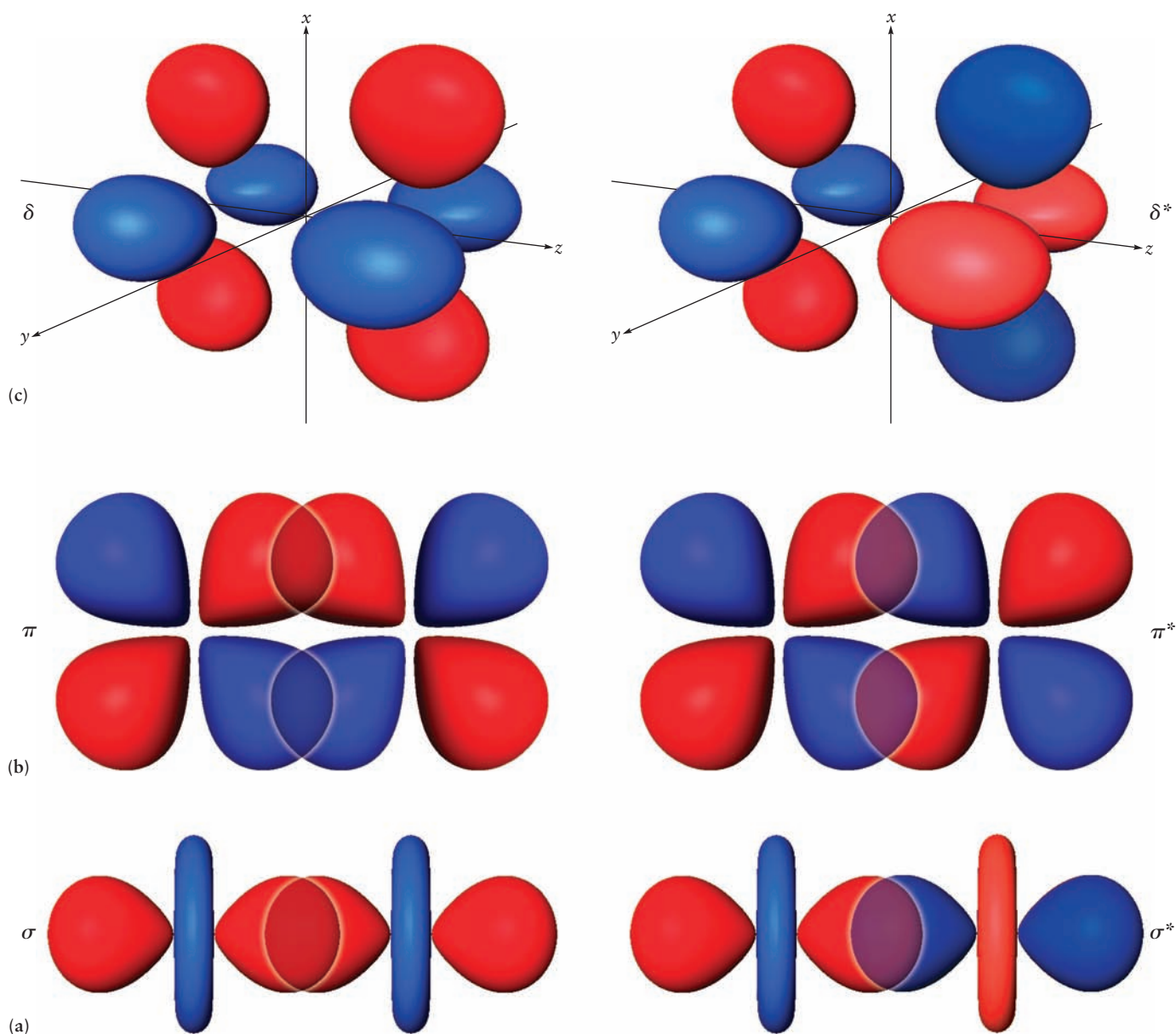


FIGURE 8.5 Bonding and antibonding molecular orbitals (MOs) formed from d -orbital overlap. (a) σ and σ^* orbitals formed by end-to-end overlap of d_{z^2} orbitals along the internuclear axis. (b) π and π^* MOs formed from side-by-side overlap of d_{xz} orbitals in the x - z plane (there is a corresponding pair of MOs formed from side-by-side overlap of d_{yz} orbitals in the y - z plane). (c) δ and δ^* orbitals from the face-to-face overlap of a pair of $d_{x^2-y^2}$ MOs (there is a corresponding pair of MOs constructed from the d_{xy} orbitals, which are rotated 45° from the set shown here).

internuclear axis (conventionally chosen to be the z -axis) and can overlap to form a pair of bonding and antibonding σ and σ^* molecular orbitals. Two pairs of bonding and antibonding π and π^* molecular orbitals can be formed from the side-by-side overlap of a pair of d_{xz} orbitals or a pair of d_{yz} orbitals. Finally, two molecular orbitals of a type we have not encountered earlier can be formed from the face-to-face overlap of a pair $d_{x^2-y^2}$ orbitals or a pair of d_{xy} orbitals. These δ orbitals have two units that contain the internuclear axis, and they have two units of angular momentum along that axis. The bonding δ orbital does not have a nodal plane perpendicular to the internuclear axis but the antibonding δ^* orbital does. Recall (see Section 6.1) that molecular orbitals are labeled according to the angular momentum component along the internuclear axis. They follow the Greek sequence σ , π , δ by analogy to s , p , d for atoms.

A typical energy-level diagram for homonuclear diatomic molecules of the first transition series is shown in Figure 8.6. The relative energy ordering for the molecular orbitals derived from the d orbitals is determined by precisely the same energy level proximity and overlap arguments presented in Section 6.2: Orbitals mix strongly only if they are close in energy and if their spatial overlap is significant. The d orbitals all have the same energy for both atoms of a homonuclear diatomic molecule; thus, the energy level ordering of the molecular orbitals is determined only by overlap considerations. Consequently, the energy separation between the bonding and antibonding σ orbitals derived from the end-to-end overlap of a pair of d_{z^2} orbitals is the largest, with σ being the most stable bonding molecular orbital (and σ^* the least stable), the separation between the bonding and antibonding π orbitals formed from the side-by-side overlap of a pair of d_{xz} orbitals or a pair of d_{yz} orbitals is the next largest (π lies at higher energy than σ , and π^* at lower energy than σ^*), and finally, the separation between the bonding and antibonding δ and δ^* orbitals formed from the face-to-face overlap of a pair of $d_{x^2-y^2}$ orbitals or a pair of d_{xy} orbitals is the smallest.

To make these energy-level diagrams broadly applicable, we introduce a simplified notation that will accommodate elements from all three transition series. Rather than specifying the atomic orbitals from which a particular molecular orbital is constructed, we simply label all of the molecular orbitals of a given symmetry in order of increasing energy. The set of atomic orbitals from which they are constructed is clearly shown in the correlation diagram in Figure 8.6, and the specific atomic orbitals leading to a particular molecular orbital are shown in Figure 8.5. The lowest energy σ orbital is labeled 1σ and it is derived from the metal $3d_{z^2}$ atomic orbitals. The lowest energy π and δ orbitals are labeled 1π and 1δ and they are derived from the metal d_{xz} , d_{yz} and $d_{xy^2-y^2}$, d_{xy} orbital pairs, respectively. The second highest energy σ orbital is derived from the metal $4s$ orbitals and is labeled 2σ . The energy of the 2σ orbital relative to the set of molecular orbitals derived from the d orbitals varies depending on the relative energies of the atomic orbitals of the elements involved. The energy level order shown in Figure 8.6 has been determined by experiment and it is typical for the first transition period

FIGURE 8.6 Orbital correlation diagram for homonuclear diatomic molecules of the transition metals
(Adapted from R. L. DeKock and H. B. Gray, *Chemical Bonding and Structure*, Sausalito: University Science Books, 1989, Figure 4-26, by permission).

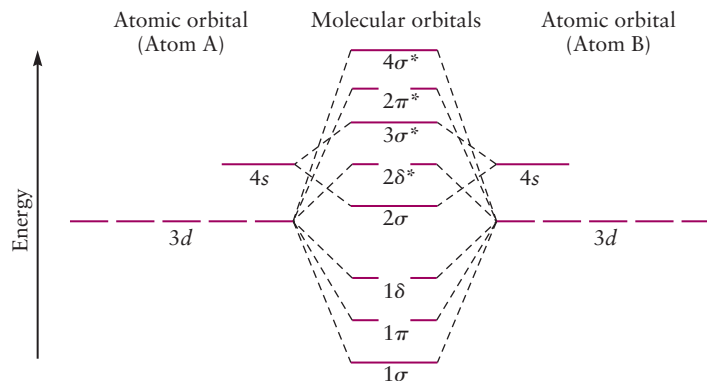


TABLE 8.2 Properties of Some Homonuclear Diatomic Transition Metals

Molecule	Bond Length (Å)	Bond Energy (kJ mol ⁻¹)
Ag ₂	—	38.7 ± 2.2
As ₂	2.288	91.3
Cu ₂	2.220	47.3 ± 2.2
K ₂	3.923	11.8
Li ₂	2.672	26.3
Na ₂	3.078	17.3
Pb ₂	—	23
Rb ₂	—	11.3
Sb ₂	2.21	71.3
Se ₂	2.166	77.6
Sn ₂	—	46
Te ₂	2.557	62.3

Note: The bond energy is the energy required to dissociate the gas-phase diatomic molecule into its constituent atoms. Bond energies for the second-period homonuclear diatomic molecules are given in Table 6.3.

homonuclear diatomic molecules. We identify antibonding orbitals with an asterisk. Because other authors may use a different label for antibonding orbitals, you should be sure to check the definitions when reading other sources.

The diatomic molecule Cu₂, which is easily prepared and stable in the gas phase, provides a good illustration of this molecular orbital description of bonding in transition-metal homonuclear diatomic molecules without *s-d* mixing. The electronic configuration for Cu is [Ar]3*d*¹⁰4*s*¹, so there are 22 electrons available for bonding. The highest filled molecular orbitals are the 2*π** pair and the only unfilled molecular orbital is the 4*σ**. Because every bonding and antibonding orbital derived from the *d* orbitals is filled, they effectively cancel each other out and do not contribute to the bonding in Cu₂. Two electrons occupy the bonding 2*σ* orbital, which is derived from the atomic 4*s* orbitals. Thus, Cu₂ has a single bond just like those in the alkali metal dimers Li₂ and K₂. Although the details of the bonding in transition-metal diatomic molecules can be considerably more complicated than in the first and second rows of main-group elements, the concepts and approaches are exactly the same. Molecular orbital theory satisfactorily accounts for the general features of bonding, and modern computational quantum chemistry is now widely used to calculate all properties of interest with great accuracy. The bond lengths and dissociation energies of a few homonuclear transition-metal diatomic molecules are presented in Table 8.2.

Heteronuclear Diatomic Molecules

The method presented earlier is easily extended to describe the bonding and properties of heteronuclear diatomic molecules comprising either two transition metals (e.g., YCo, YNi, ZrCo) or a transition-metal and a main-group element. We illustrate the method for a general transition-metal monoxide denoted MO. The results are easily applied to related compounds such as hydrides and halides (see Table 8.3). This example also gives us the chance to introduce some specialized language used by inorganic chemists to describe several important types of orbital interactions and to connect this language to the description of bonding in Chapter 6.

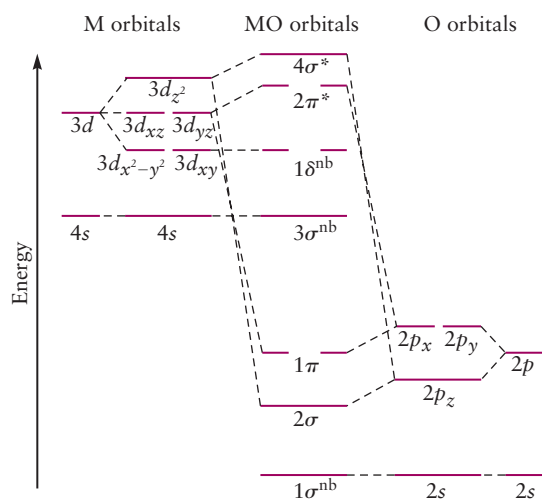
Figure 8.7 shows the energy-level correlation diagram for a general transition-metal monoxide constructed from atomic energy levels located by photoelectron spectra. Because the 4*s* and 3*d* orbitals are nearly degenerate we place the 4*s* at slightly lower energy than the 3*d* to simplify the resulting MO diagram. We also ignore mixing that would complicate the discussion, in this case the mixing of the 4*s* and 3*d*_{z²} orbitals. We construct molecular orbitals using our standard criteria:

TABLE 8.3 Properties of Selected Transition Metal Hydrides, Oxides, and Halides

Molecule	Bond Length (Å)	Bond Energy (kJ mol ⁻¹)
CrH	1.656	—
MnH	1.722	—
CoH	1.542	—
NiH	1.475	—
PtH	1.528	—
CuH	1.463	63.0 ± 1.5
AgH	1.618	53.2 ± 1.5
AuH	1.524	74.3 ± 3.0
ScO	1.668	161.0
YO	1.790	168.5
LaO	1.825	192.5
TiO	1.620	167.38 ± 2.30
ZrO	1.711	181 ± 5
HfO	1.724	182.6 ± 6
VO	1.589	147.5 ± 4.5
NbO	1.691	180.0 ± 2.5
TaO	1.687	197 ± 12
CuO	—	62.7 ± 3
ScF	1.788	—
YF	1.925	—
LaF	2.026	—
CuF	1.749	88 ± 10
CuCl	2.050	88 ± 10
CuBr	—	79 ± 6
CuI	2.337	<75
AgF	—	—
AgCl	2.281	78
AgBr	2.392	73
AgI	2.544	60
AuCl	—	—

FIGURE 8.7 Orbital correlation diagram for a typical transition metal monoxide. The metal 3d and 4s atomic orbitals are nearly degenerate, and we have located $\epsilon_{4s} < \epsilon_{3d}$ to simplify the resulting MO level diagram. We also assume no 4s-3d_{z²} mixing. The energies of the set of 3d states and those of the 2p states have also been separated a bit in this correlation diagram to make it easier to see which atomic orbitals mix to form which molecular orbitals.

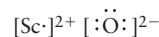
(Adapted from R. L. DeKock and H. B. Gray, *Chemical Bonding and Structure*, Sausalito: University Science Books, 1989, Figure 4-43, by permission).



Atomic orbitals interact strongly if they are close to one another in energy, have the appropriate symmetry, and overlap significantly in space. We have separated the energy levels of the degenerate set of $3d$ orbitals, as well as those of the degenerate set of $2p$ orbitals, to more clearly show which atomic orbitals mix to form specific MOs. Beginning at the bottom of the figure, we see no metal orbitals close in energy to the O $2s$ orbital. Thus, the lowest energy MO is essentially a nonbonding atomic $2s$ orbital localized on the oxygen (O) atom, just as the lowest energy MO in HF was essentially a nonbonding F $2s$ orbital (see Figure 6.20). Continuing upward, we see two kinds of bonds that can be formed from linear combinations of the metal d orbitals and the oxygen p orbitals. σ bonds result from overlap of the $3d_{z^2}$ and $2p_z$ orbitals, both of which point along the internuclear axis. π bonds are formed by overlap of the $3d_{xz}$ orbital with $2p_x$ and from overlap of $3d_{yz}$ with $2p_y$. Because there are no oxygen orbitals with the correct symmetry to mix with the metal $d_{x^2-y^2}$ or d_{xy} orbitals, they remain nonbonding atomic orbitals, which we label δ^{nb} . Recall that BeH_2 has a pair of nonbonding π orbitals that are essentially F $2p_x$ and $2p_y$ atomic orbitals (see Fig. 6.25). We labeled them π^{nb} orbitals to emphasize that they are still molecular orbitals with one unit of angular momentum quantized along the internuclear axis. Here, we choose the δ^{nb} notation for the same reasons. The nonbonding δ orbital has two units of angular momentum along the z -axis.

Let's use Figure 8.7 to obtain the ground-state electron configuration for a specific example, ScO, using the aufbau principle. ScO has nine valence electrons, three from $\text{Sc}(4s^23d^1)$ and six from $\text{O}(2s^22p^4)$. Using the aufbau principle, we expect the ground-state electronic configuration to be $(1\sigma^{\text{nb}})^2(2\sigma)^2(1\pi)^4(3\sigma^{\text{nb}})^1$. With two electrons occupying the bonding 2σ orbital and four electrons occupying the pair of bonding π orbitals, this simple MO picture predicts that the bond order is three and that ScO has a triple bond just like that in N_2 . This prediction is confirmed by experiment, demonstrating the power of simple MO theory in describing bonding in molecules containing transition metal atoms.

We can examine the formation of the ScO bond from a different starting point in order to introduce specialized language used by inorganic chemists to describe bonding interactions in transition metal compounds and to connect that language to the language of molecular orbital theory developed earlier. Let's begin with a pair of widely separated Sc^{2+} and O^{2-} ions and see what happens as they come together to form an ScO molecule. At large distances the electron configurations of Sc^{2+} and O^{2-} are $3d^1$ and $2s^22p^6$, respectively, and the atomic orbitals do not overlap significantly. We can consider any bonding at large distances to be purely ionic and represent the molecule by the following Lewis dot diagram.

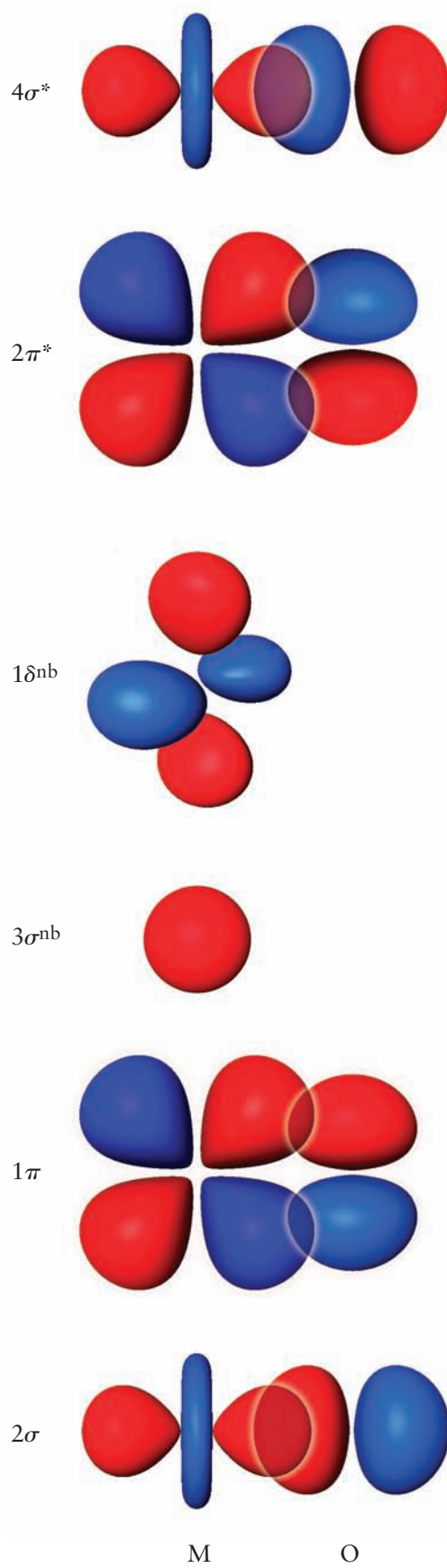


As the ions approach one another their atomic orbitals begin to overlap, forming molecular orbitals. We imagine that the molecular orbitals are formed and filled sequentially purely for illustrative purposes. The O $2s$ orbital becomes the ScO $1\sigma^{\text{nb}}$ molecular orbital, which is nonbonding because it lies too low in energy to interact with any of the metal orbitals; it is filled by the O $2s$ electrons. Mixing of the O $2p_z$ orbital with the Sc $3d_{z^2}$ orbital produces the bonding 2σ and antibonding $4\sigma^*$ molecular orbitals. The 2σ orbital is mostly O $2p_z$ in character and lies at lower energy than the O $2p_z$ from which it was derived. Electrons will flow from the filled O $2p_z$ orbital to the empty, newly created 2σ molecular orbital in a process inorganic chemists call **ligand-to-metal (L→M) σ donation**. A bond that results from the transfer of a pair of electrons from one bonding partner to another is called a **dative bond**. This electron transfer introduces some covalent character into the ScO bond, which may now be represented by the following Lewis dot diagram:



FIGURE 8.8 Orbital overlaps between metal and oxygen atom orbitals to form bonding, nonbonding, and antibonding molecular orbitals.

(Adapted from R. L. DeKock and H. B. Gray, *Chemical Bonding and Structure*, Sausalito: University Science Books, 1989, Figure 4-44, by permission.)



The formal charge on Sc has been reduced from +2 to +1 and that on O from -2 to -1 . (Recall from Section 3.8 that we assume the electrons in a bond are shared equally between the atoms when calculating formal charges.)

Continuing our thought experiment, we next imagine the formation of bonding and antibonding π molecular orbitals constructed from the O $2p$ and Sc $3d$ orbitals. Overlap between the O $2p_y$ and Sc $3d_{yz}$ orbitals leads to the formation of a bonding 1π and an antibonding $2\pi^*$ molecular orbital, which are shown in Figure 8.8. (A second set of orbitals constructed from the O $2p_x$ and Sc $3d_{xz}$ orbitals is oriented in the y - z plane and is not shown in the figure.) In our thought experiment, electrons will flow from the occupied O $2p$ orbitals to the newly created, initially empty, bonding 1π orbitals because they lie at lower energy than the O atomic orbitals. This interaction is called **ligand-to-metal (L \rightarrow M) π donation**. O^{2-} can donate all six of its p electrons to Sc^{2+} to form a σ bond and a pair of π bonds resulting in a triple bond overall, in agreement with experiment. This bonding scheme is represented by the following Lewis dot diagram in which the formal charge on Sc is -1 and that on O is $+1$.

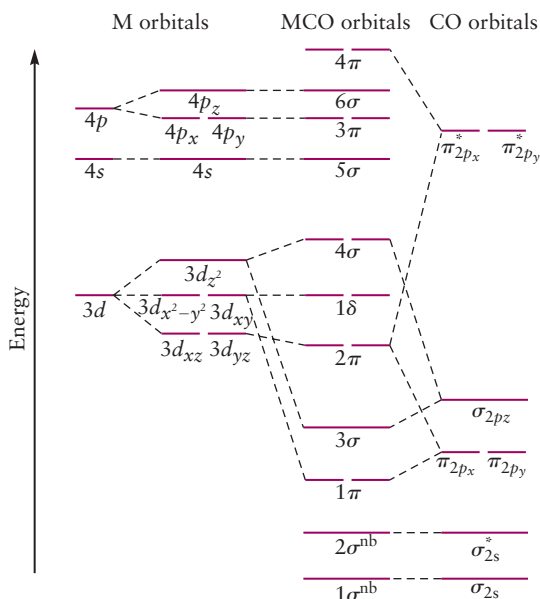


Bonding between a Transition-Metal Atom and an Unsaturated Ligand

A **ligand** is any atom or chemical fragment bonded to a transition-metal atom. An unsaturated ligand, like an unsaturated organic molecule, is not bonded to the maximum number of atoms allowed by its valence. Alternatively, an unsaturated ligand can be defined as one that can accept additional electrons without breaking any bonds in the ligand. The carbonyl (CO) ligand, which is extremely important in inorganic and coordination chemistry, can accept up to four additional electrons in its π^* orbitals, reducing the bond order from three to one, but not to zero. Many stable metal carbonyls exist ($\text{Cr}(\text{CO})_6$, $\text{Mn}_2(\text{CO})_{10}$, $\text{Ni}(\text{CO})_4$, for example). For simplicity, we consider the bonding in a simple metal monocarbonyl, MCO, a number of which can be prepared and stabilized at very low temperatures.

The energy-level diagram for MCO is shown in Figure 8.9. The relative energies of the metal atomic orbitals and the CO molecular orbitals were determined by photoelectron spectroscopy. Recalling that significant interactions occur only

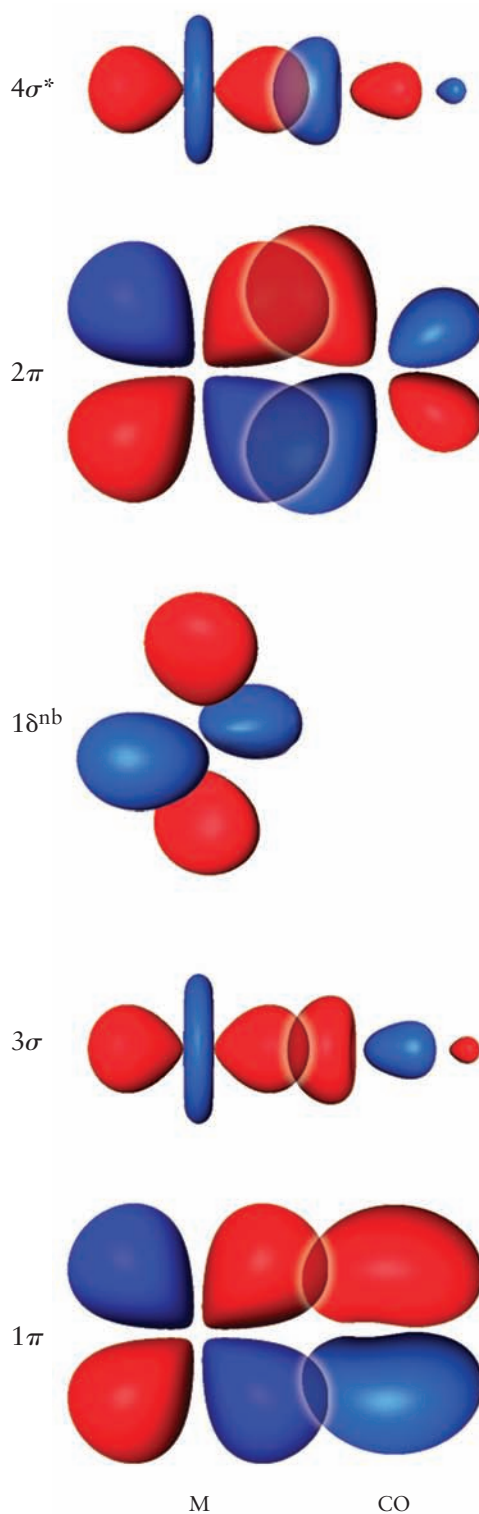
FIGURE 8.9 Orbital correlation diagram for a metal monocarbonyl.



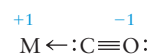
between orbitals that are close in energy, we see that the dominant interactions between the metal atom and CO involve the metal d - electrons and the π_{2p_x} and π_{2p_y} , σ_{2p_z} , and $\pi_{2p_x}^*$ and $\pi_{2p_y}^*$ molecular orbitals of CO.

The orbital overlaps leading to the formation of the MCO molecular orbitals are shown in Figure 8.10. The 1σ and 2σ orbitals have been omitted because they are essentially unperturbed CO molecular orbitals at energies too low to interact with the atomic orbitals of the metal. Similar situations arise in heteronuclear diatomic molecules (ScO, earlier and HF in Fig. 6.20). Starting at the bottom of the diagram we see that a 1π orbital is formed by the overlap of a metal d_{yz}

FIGURE 8.10 Overlaps between metal atomic orbitals and molecular orbitals (MOs) of CO leading to bonding, nonbonding and antibonding MOs.

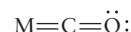


orbital with the bonding CO π_{2p_y} orbital that is located in the y - z plane. A second 1π orbital, oriented in the plane perpendicular to the first, is formed from metal d_{xz} and the other CO π_{2p_y} orbital that is located in the x - z plane. For metal carbonyls in which the metal has few d electrons, electrons will flow from the occupied CO π orbitals to the empty metal d orbitals in the process characterized as ligand-to-metal (L→M) π donation, which was discussed earlier for ScO. The 3σ MCO molecular orbital is formed by the overlap of the $3\sigma_{2p_z}$ CO orbital with a metal orbital of the appropriate symmetry, which could be a $4s$, $4p_z$, or $3d_{z^2}$ orbital. Energy considerations favor the participation of the $3d_{z^2}$ orbital, which is illustrated in the figure. L→M σ donation transfers electron density from the filled $3\pi_{2p_z}$ CO orbital to the empty metal orbital. The following Lewis dot diagram represents the “ionic” structure M^+CO^- resulting from complete transfer of an electron pair from CO to the metal. The formal charge on the metal is -1 and that on the CO ligand is $+1$.



Continuing higher in energy, the next orbitals we encounter are a pair of δ^{nb} non-binding orbitals derived from the metal $3d_{x^2-y^2}$ and $3d_{xy}$ orbitals. So far the bonding interactions are quite similar to those described earlier for metal oxides like ScO.

In addition to the lone pair of electrons on the carbon atom and the filled π orbitals, CO has empty π^* orbitals that can also participate in bonding. The energy of these orbitals is close to the energy of metal orbitals with the same symmetry so they can be expected to mix to form molecular orbitals. Figure 8.10 shows the formation of a molecular orbital that results from the overlap of the CO $\pi_{2p_y}^*$ orbital with the metal $3d_{yz}$ orbital. This molecular orbital is quite interesting in that it is bonding between M and O but antibonding between C and O. If the metal orbital is initially occupied and the CO $\pi_{2p_y}^*$ orbital is initially empty, electron density will flow from the metal to the ligand in a process called **metal-to-ligand (M→L) π donation**. M→L π donation transfers electron density from occupied metal atomic orbitals to unoccupied ligand molecular orbitals, in this case, from the metal $3d_{xz}$ and $3d_{yz}$ orbitals to the CO $\pi_{2p_x}^*$ and $\pi_{2p_y}^*$ orbitals, respectively, partially offsetting the effects of L→M σ donation described earlier. M→L π donation strengthens the M–C bond, weakens the C–O bond, and restores electron density on the O atom. L→M σ and M→L π bonding are synergistic; they strengthen the M–C bond and reduce excess negative charge on the metal (the electroneutrality principle again). Because M→L π bonding transfers charge density back to the ligand, it is generally referred to as **backbonding**. The Lewis dot diagram that results from both L→M σ donation and M→L π donation is shown below.



Both the M–C and C–O bonds are now double bonds and the formal charges on both the metal and the ligand are now zero. These conclusions are supported by infrared spectroscopy (see Section 20.2), which shows that the CO bond does indeed weaken when coordinated to a metal atom. The experimental metal-carbon bond length observed is also consistent with a M–C double bond.

L→M π donation is certainly possible for complexes with ligands that have empty π^* orbitals because they also have filled π orbitals that can donate electron density to empty metal orbitals. The experimental evidence cited earlier suggests that L→M π donation is less important than M→L π donation for metal carbonyls. As a general rule, L→M π donation is more important for metals with few d electrons (high oxidation states), and M→L π backbonding is more important for metals with largely occupied d orbitals (low oxidation states).

Inorganic chemists have put their own special twist on the molecular orbital description of bonding developed in Chapter 6. Instead of first developing molecular orbitals from all the atomic orbitals in the molecule, and then putting in all the electrons by the aufbau principle to arrive at the ground-state configuration, they

start by considering charge transfer between the metal atom and its ligands to form dative bonds. Because the energy of an electron pair initially localized in an atomic orbital decreases as the electrons become more delocalized on charge transfer, they reason that increased charge transfer by σ and π donation stabilizes the bonding molecular orbital and de-stabilizes the antibonding molecular orbital. (Recall our virial theorem arguments for the stabilizing effect of de-localization in Section 6.2.) Even so, when inorganic chemists refer to ligand-to-metal σ and π donation and metal-to-ligand π donation, they are implicitly considering two issues. First, formation of the molecular orbitals is governed by our familiar consideration of energy proximity and orbital overlap. Strong overlap of orbitals close in energy results in stable bonding molecular orbitals and unstable antibonding molecular orbitals. Weaker interactions lead to less stabilization of the bonding molecular orbitals and less destabilization of the antibonding molecular orbitals. The second issue is the source of the electrons: Instead of building up the ground state for the complete molecule, inorganic chemists obtain a great deal of qualitative insight into structure and bonding from assessing the relative energies and orbital occupancies of the atoms involved and the ability of each to donate or accept charge. The interactions in the molecule are always the same, but they can be described either in the language of basic molecular orbital theory or the language of inorganic chemistry. Choosing which one to use is a matter of convenience. In Section 8.6, we examine how the viewpoint of inorganic chemists effectively describes the bonding and energy levels in coordination complexes.

8.3 Introduction to Coordination Chemistry

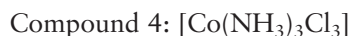
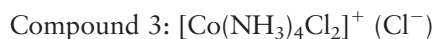
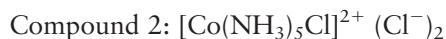
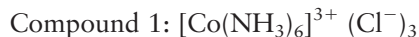
Formation of Coordination Complexes

The Alsatian-Swiss chemist Alfred Werner pioneered the field of coordination chemistry in the late nineteenth century. At that time, a number of compounds of cobalt(III) chloride with ammonia were known. They had the following chemical formulas and colors:

Compound 1: $\text{CoCl}_3 \cdot 6\text{NH}_3$	Orange-yellow
Compound 2: $\text{CoCl}_3 \cdot 5\text{NH}_3$	Purple
Compound 3: $\text{CoCl}_3 \cdot 4\text{NH}_3$	Green
Compound 4: $\text{CoCl}_3 \cdot 3\text{NH}_3$	Green

Treatment of these compounds with aqueous hydrochloric acid did not remove the ammonia, which suggested that the ammonia was somehow closely bound with the cobalt ions. Treatment with aqueous silver nitrate at 0°C , however, gave interesting results. With compound 1, all of the chloride present precipitated as solid AgCl . With compound 2, only two thirds of the chloride precipitated, and with compound 3, only one third precipitated. Compound 4 did not react at all with the silver nitrate. These results suggested that there were two different kinds of species associated with the cobalt ions, which Werner called *valences* (recall that the electron, the key player in the formation of the chemical bond, was just being characterized by J.J. Thomson). The primary, or ionizable, valences were anions like Cl^- in simple salts such as CoCl_3 , whereas the secondary valences could be either simple anions or neutral molecules such as NH_3 . Werner assumed that the primary valences were nondirectional, whereas the secondary valences were oriented along well-defined directions in space. The picture that emerged was that of a metal atom coordinated to the secondary valences (ligands) in the **inner coordination sphere** surrounded by the primary valences and solvent in the **outer coordination sphere**. The primary valences neutralize the charge on the complex ion. Werner accounted for experimental results described earlier by positing the existence of **coordination**

complexes with six ligands (either chloride ions or ammonia molecules) attached to each Co^{3+} ion. Specifically, he wrote the formulas for compounds 1 through 4 as



with the charge on each complex ion being balanced by an equal number of Cl^- ions in the outer coordination sphere. Only these chloride ions, which were *not* bonded directly to cobalt, could react with the silver ions in cold aqueous silver nitrate to form the AgCl precipitate.

Werner realized that he could test his hypothesis by measuring the electrical conductivity of aqueous solutions of the salts of these complex ions. Ions are the electrical conductors in aqueous solutions, and the conductivity is proportional to the ion concentration. If Werner's proposal was correct, then an aqueous solution of Compound 1, for example, should have a molar conductivity close to that of an aqueous solution of $\text{Al}(\text{NO}_3)_3$, which also forms four ions per formula unit on complete dissociation in water (one $3+$ ion and three $1-$ ions). His experiments confirmed that the conductivities of these two solutions were, indeed, similar. Furthermore the conductivity of aqueous solutions of compound 2 was close to those of $\text{Mg}(\text{NO}_3)_2$, and solutions of compound 3 conducted electricity about as well as those containing NaNO_3 . Compound 4, in contrast, did not dissociate into ions when dissolved in water, producing a solution of very low electrical conductivity.

Werner and other chemists studied a variety of other coordination complexes, using both physical and chemical techniques. Their research has shown that the most common coordination number by far is 6, as in the cobalt complexes discussed earlier. Coordination numbers ranging from 1 to 16 are commonly observed, however. Examples include coordination numbers 2 (as in $[\text{Ag}(\text{NH}_2)_2]^+$), 4 (as in $[\text{PtCl}_4]^{2-}$), and 5 (as in $[\text{Ni}(\text{CN})_5]^{3-}$).

A second example illustrates the ability of transition metals to form complexes with small molecules and ions. Copper metal and hot concentrated sulfuric acid ("oil of vitriol") react to form solid copper(II) sulfate, commonly called "blue vitriol" by virtue of its deep blue color. There is more to this compound than copper and sulfate, however; it contains water as well. When the water is driven away by heating, the blue color vanishes, leaving greenish white anhydrous copper(II) sulfate (Fig. 8.11). The blue color of blue vitriol comes from a

FIGURE 8.11 Hydrated copper(II) sulfate, $\text{CuSO}_4 \cdot 5\text{H}_2\text{O}$, is blue (left), but the anhydrous compound, CuSO_4 , is greenish white (right). A structural study of the solid compound demonstrates that four of the water molecules are closely associated with the copper and the fifth is not. Thus, a better representation of the hydrated compound is $[\text{Cu}(\text{H}_2\text{O})_4]\text{SO}_4 \cdot \text{H}_2\text{O}$.



TABLE 8.4 Common Ligands and Their Names

Ligand [†]	Name
:NO ₂ ⁻	Nitro
:OCO ₂ ²⁻	Carbonato
:ONO ⁻	Nitrito
:CN ⁻	Cyano
:SCN ⁻	Thiocyanato
:NCS ⁻	Isothiocyanato
:OH ⁻	Hydroxo
:OH ₂	Aqua
:NH ₃	Ammine
:CO	Carbonyl
:NO ⁺	Nitrosyl

[†]The ligating atom is indicated by a pair of dots (:) to show a lone pair of electrons. In the CO₃²⁻ ligand, either one or both of the O atoms can donate a lone pair to a metal.

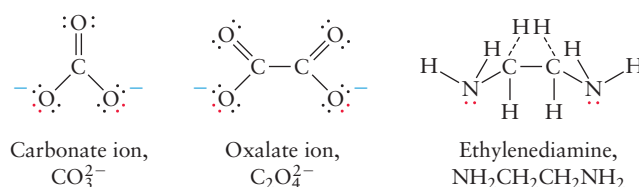
coordination complex in which H₂O molecules bond directly to Cu²⁺ ions to form coordination complexes with the formula [Cu(H₂O)₄]²⁺. Bonding in this complex ion can be described qualitatively using the Lewis theory of acids and bases (see Section 15.1). A Lewis acid is an electron-pair donor and a Lewis base is an electron-pair acceptor; thus, the transfer of a pair of electrons from water to Cu²⁺ to form a dative bond can be thought of as an acid–base reaction. As a Lewis acid, the Cu²⁺ ion *coordinates* four water molecules into a group by accepting electron density from a lone pair on each. By acting as electron-pair donors and sharing electron density with the Cu²⁺ ion, the four water molecules are the ligands, occupying the inner coordination sphere of the ion. The chemical formula of blue vitriol is [Cu(H₂O)₄]SO₄·H₂O; the fifth water molecule is not coordinated directly to copper.

The positive ions of every metal in the periodic table accept electron density to some degree and can therefore coordinate surrounding electron donors, even if only weakly. The solvation of Na⁺ by H₂O molecules in aqueous solution (see Fig. 10.6) is an example of weak coordination. The ability to make fairly strong, *directional* bonds by accepting electron pairs from neighboring molecules or ions is characteristic of the transition-metal elements. Coordination occupies a middle place energetically between the weak intermolecular attractions in solids (see Chapter 10) and the stronger covalent and ionic bonding (see Chapters 3 and 6). Thus, heating blue vitriol disrupts the Cu–H₂O bonds at temperatures well below those required to break the covalent bonds in the SO₄²⁻ group. The energy (more precisely, the enthalpy) required to break a M²⁺–H₂O bond in a transition metal coordination complex falls in the range between 170 and 210 kJ mol⁻¹. This bond dissociation energy is far less than the bond energies of the strongest chemical bonds (e.g., 942 kJ mol⁻¹ for N₂), but it is by no means small. Trivalent metal cations (+3 charge) make still stronger coordinate bonds with water.

A wide variety of molecules and ions bond to metals as ligands; common ones include the halide ions (F⁻, Cl⁻, Br⁻, I⁻), ammonia (NH₃), carbon monoxide (CO), water, and a few other simple ligands listed in Table 8.4. Ligands that bond to a metal atom through a single point of attachment are called *monodentate* (derived from Latin *mono*, meaning “one,” plus *dens*, meaning “tooth,” indicating that they bind at only one point). More complex ligands can bond through two or more attachment points; they are referred to as *bidentate*, *tridentate*, and so forth. Ethylenediamine (NH₂CH₂CH₂NH₂), in which two NH₂ groups are held together by a carbon backbone, is a particularly important bidentate ligand. Both N atoms in ethylenediamine have lone electron pairs to share. If all the nitrogen donors of three ethylenediamine molecules bind to a single Co³⁺ ion, then that ion has a coordination number of 6 and the formula of the resulting complex is [Co(en)₃]³⁺ (where “en” is the abbreviation for ethylenediamine). Complexes in which a ligand coordinates via two or more donors to the same central atom are called **chelates** (derived from Greek *chele*, meaning “claw,” because the ligand grabs onto the central atom like a pincers). Figure 8.12 shows the structures of some important chelating ligands.

In the modern version of Werner’s notation, brackets are used in writing cations or anions, but the net charges of the ions are not shown. In the formula [Pt(NH₃)₆]Cl₄, the portion in brackets represents a positively charged coordination complex in which Pt coordinates six NH₃ ligands. The brackets emphasize

FIGURE 8.12 These three ligands are bidentate; each is capable of donating two pairs of electrons.



that a complex is a distinct chemical entity with its own properties. Within the brackets, the symbol of the central atom comes first. The electric charge on a coordination complex is the sum of the oxidation number of the metal ion and the charges of the ligands that surround it. Thus, the complex of copper(II) (Cu^{2+}) with four Br^- ions is an anion with a -2 charge, $[\text{CuBr}_4]^{2-}$.

EXAMPLE 8.1

Determine the oxidation state of the coordinated metal atom in each of the following compounds:

(a) $\text{K}[\text{Co}(\text{NH}_3)_2(\text{CN})_4]$; (b) $\text{Os}(\text{CO})_5$; (c) $\text{Na}[\text{Co}(\text{H}_2\text{O})_3(\text{OH})_3]$.

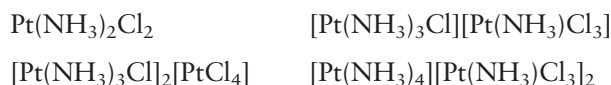
SOLUTION

- (a) The oxidation state of K is known to be $+1$, so the complex in brackets is an anion with a -1 charge, $[\text{Co}(\text{NH}_3)_2(\text{CN})_4]^-$. The charge on the two NH_3 ligands is 0 , and the charge on each of the four CN^- ligands is -1 . The oxidation state of the Co must then be $+3$, because 4×-1 (for the CN^-) $+ 2 \times 0$ (for the NH_3) $+ 3$ (for Co) equals the required -1 .
- (b) The ligand CO has zero charge, and the complex has zero charge as well. Therefore, the oxidation state of the osmium is 0 .
- (c) There are three neutral ligands (the water molecules) and three ligands with -1 charges (the hydroxide ions). The Na^+ ion contributes only $+1$; thus, the oxidation state of the cobalt must be $+2$.

Related Problems: 9, 10

Coordination modifies the chemical and physical properties of both the central atom and the ligands. Consider the chemistry of aqueous cyanide (CN^-) and iron(II) (Fe^{2+}) ions. The CN^- ion reacts immediately with acid to generate gaseous HCN, a deadly poison, and Fe^{2+} , when mixed with aqueous base, instantly precipitates a gelatinous hydroxide. The reaction between Fe^{2+} and CN^- produces the complex ion $[\text{Fe}(\text{CN})_6]^{4-}$ (*aq*), which undergoes neither of the two reactions just described nor any others considered characteristic of CN^- or Fe^{2+} . Ions or molecules may be present in multiple forms in the same compound. The two Cl^- ions in $[\text{Pt}(\text{NH}_3)_3\text{Cl}]\text{Cl}$ are chemically different, because one is coordinated and the other is not. Treatment of an aqueous solution of this substance with Ag^+ immediately precipitates the uncoordinated Cl^- as $\text{AgCl}(s)$, but *not* the coordinated Cl^- just as it did for Werner's complexes discussed earlier.

Ionic coordination complexes of opposite charges can combine with each other—just as any positive ion can combine with a negative ion—to form a salt. For example, the cation $[\text{Pt}(\text{NH}_3)_4]^{2+}$ and the anion $[\text{PtCl}_4]^{2-}$ form a doubly complex ionic compound of formula $[\text{Pt}(\text{NH}_3)_4][\text{PtCl}_4]$. This compound and the following four compounds



all contain Pt, NH_3 , and Cl in the ratio of $1:2:2$; that is, they have the same percentage composition. Two pairs even have the same molar mass. Yet, the five compounds differ in structure and in physical and chemical properties. The concept of coordination organizes an immense number of chemical compositions and patterns of reactivity by considering combinations of ligands linked in varied ratios with central metal atoms or ions.

Naming Coordination Compounds

So far, we have identified coordination compounds only by their chemical formulas, but names are also useful for many purposes. Some substances were named before their structures were known. Thus, $K_3[Fe(CN)_6]$ was called potassium ferricyanide, and $K_4[Fe(CN)_6]$ was potassium ferrocyanide [these are complexes of Fe^{3+} (ferric) and Fe^{2+} (ferrous) ions, respectively]. These older names are still used conversationally but systematic names are preferred to avoid ambiguity. The definitive source for the naming of inorganic compounds is *Nomenclature of Inorganic Chemistry-IUPAC Recommendations 2005* (N. G. Connelly and T. Damhus, Sr., Eds. Royal Society of Chemistry, 2005).

1. The name of a coordination complex is written as a single word built from the names of the ligands, a prefix before each ligand to indicate how many ligands of that kind are present in the complex, and a name for the central metal.
2. Compounds containing coordination complexes are named following the same rules as those for simple ionic compounds: The positive ion is named first, followed (after a space) by the name of the negative ion.
3. Anionic ligands are named by replacing the usual ending with the suffix *-o*. The names of neutral ligands are unchanged. Exceptions to the latter rule are aqua (for water), ammine (for NH_3), and carbonyl (for CO) (see Table 8.4).
4. Greek prefixes (*di-*, *tri-*, *tetra-*, *penta-*, *hexa-*) are used to specify the number of ligands of a given type attached to the central ion, if there is more than one. The prefix *mono-* (for one) is not used. If the name of the ligand itself contains a term such as *mono-* or *di-* (as in ethylenediamine), then the name of the ligand is placed in parentheses and the prefixes *bis-*, *tris-*, and *tetrakis-* are used instead of *di-*, *tri-*, and *tetra-*.
5. The ligands are listed in alphabetical order, without regard for the prefixes that tell how often each type of ligand occurs in the coordination sphere.
6. A Roman numeral, enclosed in parentheses placed immediately after the name of the metal, specifies the oxidation state of the central metal atom. If the complex ion has a net negative charge, the ending *-ate* is added to the stem of the name of the metal.

Examples of complexes and their systematic names follow.

Complex	Systematic Name
$K_3[Fe(CN)_6]$	Potassium hexacyanoferrate(III)
$K_4[Fe(CN)_6]$	Potassium hexacyanoferrate(II)
$Fe(CO)_5$	Pentacarbonyliron(0)
$[Co(NH_3)_5CO_3]Cl$	Penta-amminecarbonatocobalt(III) chloride
$K_3[Co(NO_2)_6]$	Potassium hexanitrocobaltate(III)
$[Cr(H_2O)_4Cl_2]Cl$	Tetra-aquadichlorochromium(III) chloride
$[Pt(NH_2CH_2CH_2NH_2)_3]Br_4$	Tris(ethylenediamine)platinum(IV) bromide
$K_2[CuCl_4]$	Potassium tetrachlorocuprate(II)

EXAMPLE 8.2

Interpret the names and write the formulas of these coordination compounds:

- (a) sodium tricarbonatocobaltate(III)
- (b) diamminediaquadichloroplatinum(IV) bromide
- (c) sodium tetranitratoborate(III)

SOLUTION

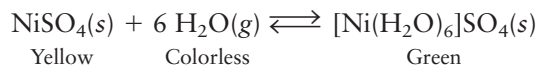
- (a) In the anion, three carbonate ligands (with -2 charges) are coordinated to a cobalt atom in the $+3$ oxidation state. Because the complex ion thus has an overall charge of -3 , three sodium cations are required, and the correct formula is $\text{Na}_3[\text{Co}(\text{CO}_3)_3]$.
- (b) The ligands coordinated to a Pt(IV) include two ammonia molecules, two water molecules, and two chloride ions. Ammonia and water are electrically neutral, but the two chloride ions contribute a total charge of $2 \times (-1) = -2$ that sums with the $+4$ of the platinum and gives the complex ion a $+2$ charge. Two bromide anions are required to balance this; thus, the formula is $[\text{Pt}(\text{NH}_3)_2(\text{H}_2\text{O})_2\text{Cl}_2]\text{Br}_2$.
- (c) The complex anion has four -1 nitrate ligands coordinated to a central boron(III). This gives a net charge of -1 on the complex ion and requires one sodium ion in the formula $\text{Na}[\text{B}(\text{NO}_3)_4]$.

Related Problems: 11, 12

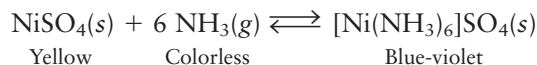
Ligand Substitution Reactions

We discuss a few ligand substitution reactions to give you a feel for the properties and reactions of coordination complexes. These simple reactions are aptly named; one or more ligands are simply substituted for one another. We have already discussed one example of a series of ligand substitution reactions: the exchange of NH_3 and Cl^- in Werner's cobalt complexes.

If the yellow crystalline solid nickel(II) sulfate is exposed to moist air at room temperature, it takes up six water molecules per formula unit. These water molecules coordinate the nickel ions to form a bright green complex:



Heating the green hexa-aquanickel(II) sulfate to temperatures well above the boiling point of water drives off the water and regenerates the yellow NiSO_4 in the reverse reaction. A different coordination complex forms when yellow $\text{NiSO}_4(s)$ is exposed to gaseous ammonia, $\text{NH}_3(g)$. This time, the product is a blue-violet complex:



Heating the blue-violet product drives off ammonia, and the color of the solid returns to yellow. Given these facts, it is not difficult to explain the observation that a green $[\text{Ni}(\text{H}_2\text{O})_6]^{2+}(aq)$ solution turns blue-violet when treated with $\text{NH}_3(aq)$ (Fig. 8.13). NH_3 must have displaced the H_2O ligands from the coordination sphere forming the blue-violet $[\text{Ni}(\text{NH}_3)_6]^{2+}$ complex.

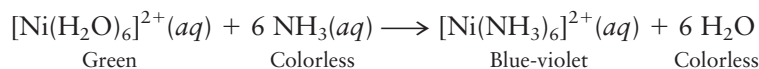
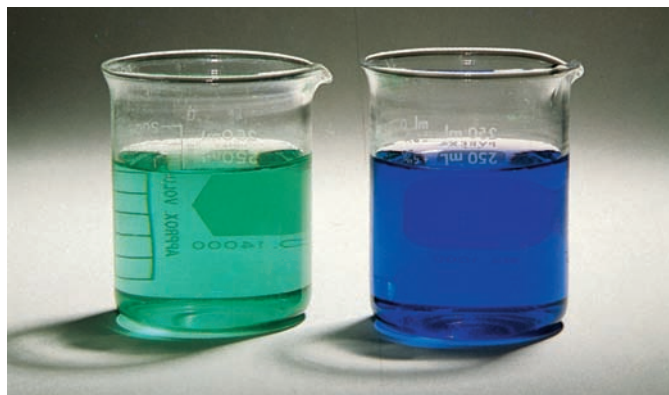
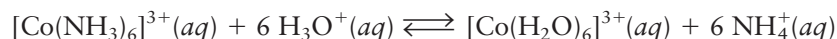


FIGURE 8.13 When ammonia is added to the green solution of nickel(II) sulfate on the left (which contains $[\text{Ni}(\text{H}_2\text{O})_6]^{2+}$ ions), ligand substitution occurs to give the blue-violet solution on the right (which contains $[\text{Ni}(\text{NH}_3)_6]^{2+}$ ions).



© Thomson Learning/Leon Levandowski

Labile complexes are those for which ligand substitution reactions proceed rapidly. Those in which substitution proceeds slowly or not at all are **inert**. These terms are used to describe the different kinetics (rates) of the reactions (see Chapter 18) that are thermodynamically allowed (see Chapter 13). Large activation energy barriers for ligand substitution reactions of inert complexes make those reactions slow even though there may be a thermodynamic tendency to proceed. In the substitution reaction



the products are favored thermodynamically by an enormous amount, yet the inert $[\text{Co}(\text{NH}_3)_6]^{3+}$ complex ion lasts for weeks in acidic solution because there is no low-energy pathway for the reaction. The cobalt(III) ion, $[\text{Co}(\text{NH}_3)_6]^{3+}$, is thermodynamically unstable relative to $[\text{Co}(\text{H}_2\text{O})_6]^{3+}$, but kinetically stable (inert). The closely related cobalt(II) complex, $[\text{Co}(\text{NH}_3)_6]^{2+}$, reacts with water in a matter of seconds:



The hexa-aminocobalt(II) complex is thermodynamically unstable and also kinetically labile.

Ligand substitution reactions proceed in stages and they can usually be stopped at intermediate stages by controlling the reaction conditions. The following series of stable complexes represents all possible four-coordinate compositions of Pt(II) with the two ligands NH_3 and Cl^- .



Such mixed-ligand complexes are wonderful examples of the variety and richness of coordination chemistry.

8.4 Structures of Coordination Complexes

Octahedral Geometries

What is the geometric structure of the complex $[\text{Co}(\text{NH}_3)_6]^{3+}$? This question naturally occurred to Werner, who suggested that the arrangement should be the simplest and most symmetric possible, with the ligands positioned at the six vertices of a regular octahedron (Fig. 8.14). Modern methods of x-ray diffraction (see Section 21.1) enable us to make precise determinations of atomic positions in crystals and have confirmed Werner's proposed octahedral structure for this complex. X-ray diffraction techniques were not available in the late 19th century, however, so Werner turned to a study of the properties of substituted complexes to test his hypothesis. Having a set of molecular ball-and-stick models at hand as you read this section will make it much easier for you to visualize the structures and transformations described.

Replacing one ammonia ligand by a chloride ion results in a complex with the formula $[\text{Co}(\text{NH}_3)_5\text{Cl}]^{2+}$, in which one vertex of the octahedron is occupied by Cl^- and the other five by NH_3 . Only one structure of this type is possible, because all six vertices of a regular octahedron are equivalent and the various singly substituted complexes $[\text{MA}_5\text{B}]$ (where $\text{A} = \text{NH}_3$, $\text{B} = \text{Cl}^-$, $\text{M} = \text{Co}^{3+}$, for example) can be superimposed on one another. Now, suppose a second NH_3 ligand is replaced by Cl^- . The second Cl^- can lie in one of the four equivalent positions closest to the first Cl^- (in the horizontal plane; see Fig. 8.15a) or in position labeled 3, on the opposite side of the central metal atom (see Fig. 8.15b). The first of these **geometric isomers**, in which the two Cl^- ligands are closer to each other, is called *cis*- $[\text{Co}(\text{NH}_3)_4\text{Cl}_2]^+$, and the second, with the two Cl^- ligands farther apart, is called *trans*- $[\text{Co}(\text{NH}_3)_4\text{Cl}_2]^+$. The octahedral structure model predicts that there can be only two different ions with the chemical formula $[\text{Co}(\text{NH}_3)_4\text{Cl}_2]^+$. You

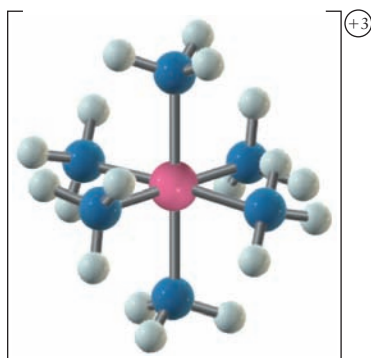


FIGURE 8.14 Octahedral structure of the $[\text{Co}(\text{NH}_3)_6]^{3+}$ ion. All six corners of the octahedron are equivalent.

FIGURE 8.15 (a) The cis - $[\text{Co}(\text{NH}_3)_4\text{Cl}_2]^+$ and (b) $trans$ - $[\text{Co}(\text{NH}_3)_4\text{Cl}_2]^+$ ions. The cis complex is purple in solution, but the $trans$ complex is green.

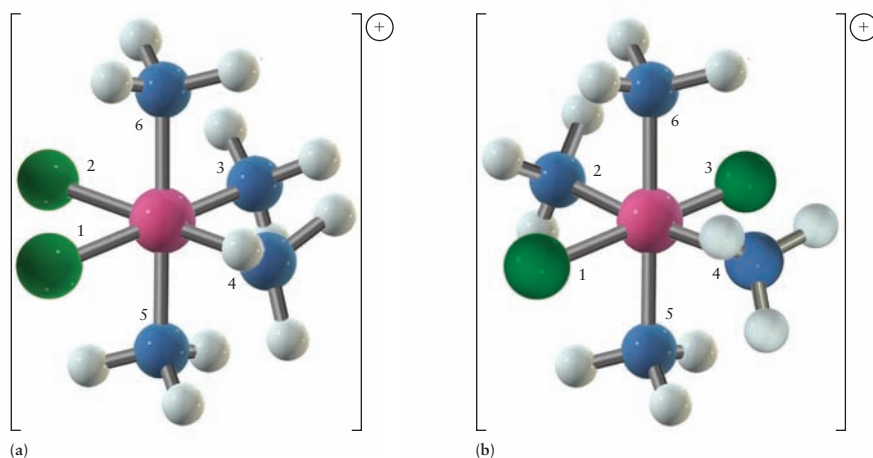
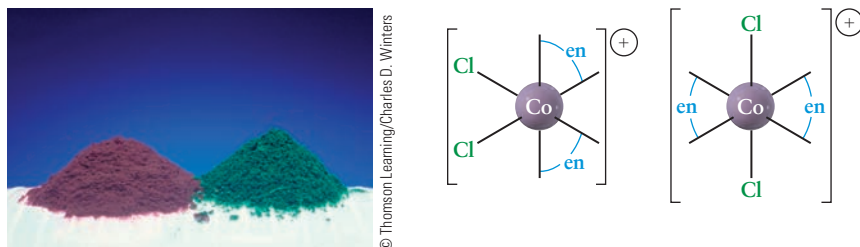


FIGURE 8.16 The complex ion $[\text{CoCl}_2(\text{en})_2]^+$ is an octahedral complex that has cis and $trans$ isomers, according to the relative positions of the two Cl^- ligands. Salts of the cis isomers are purple, and salts of the $trans$ isomers are green.



may have already encountered geometric isomers in Chapter 7. When Werner began his work, only the green $trans$ (across) form was known, but by 1907, he had prepared the cis (near) isomer and shown that it differed from the $trans$ isomer in color (it was violet rather than green) and other physical properties. The isolation of two, and only two, geometric isomers of this ion was good (although not conclusive) evidence that the octahedral structure was correct. Similar isomerism is displayed by the complex ion $[\text{CoCl}_2(\text{en})_2]^+$, which also exists in a purple cis form and a green $trans$ form (Fig. 8.16).

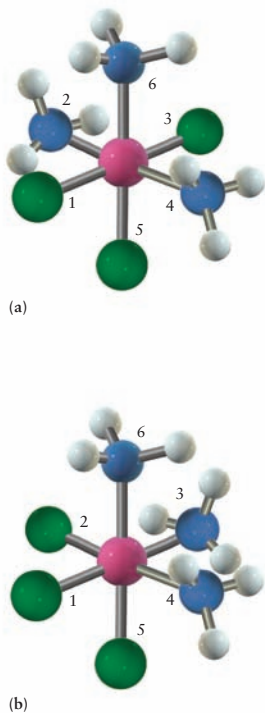


FIGURE 8.17 Two structural isomers of the coordination compound $\text{Co}(\text{NH}_3)_3\text{Cl}_3$.

EXAMPLE 8.3

How many geometric isomers does the octahedral coordination compound $[\text{Co}(\text{NH}_3)_3\text{Cl}_3]$ have?

SOLUTION

We begin with the two isomers of $[\text{Co}(\text{NH}_3)_4\text{Cl}_2]^+$ shown in Figure 8.15 and see how many different structures can be made by replacing one of the ammonia ligands with Cl^- .

Starting with the $trans$ form (see Fig. 8.15b), it is clear that replacement of any of the four NH_3 ligands at site 2, 4, 5, or 6 gives a set of equivalent structures that can be superimposed on one another by rotation of the starting structure. Figure 8.17a shows the structure that results from substitution at the position 5. What isomers can be made from the cis form shown in Figure 8.17a? If either the ammonia ligand at site 3 or the one at site 4 (i.e., one of the two that are $trans$ to existing Cl^- ligands) is replaced, the result is simply a rotated version of Figure 8.17a; therefore, these replacements do *not* give another isomer. Replacement of the ligand at site 5 or 6, however, gives a different structure (see Fig. 8.17b). (Note that Cl^- occupying sites 1, 2, 5 and 1, 2, 6 results in equivalent structures.)

We conclude that there are two, and only two, possible isomers of the octahedral complex structure MA_3B_3 . In fact, only one form of $[\text{Co}(\text{NH}_3)_3\text{Cl}_3]$ has been prepared to date, presumably because the two isomers interconvert rapidly. However, two isomers are known for the closely related coordination complex $[\text{Cr}(\text{NH}_3)_3(\text{NO}_2)_3]$.

Related Problems: 17, 18

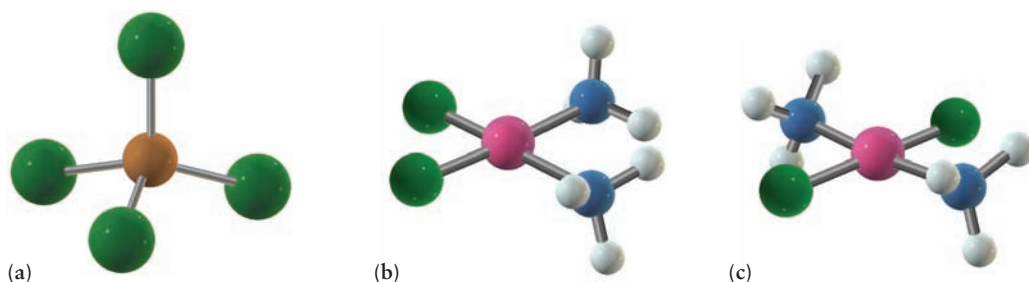


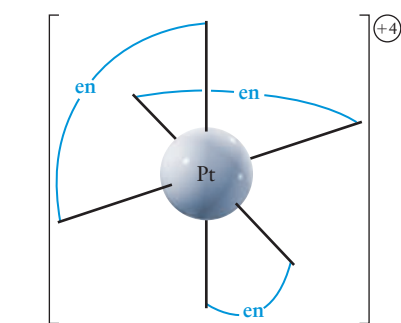
FIGURE 8.18 Four-coordinate complexes. (a) Tetrahedral, $[\text{FeCl}_4]^-$. (b, c) Square planar, illustrating (b) the *cis* and (c) the *trans* forms of $[\text{Pt}(\text{NH}_3)_2\text{Cl}_2]$.

Square-Planar, Tetrahedral, and Linear Geometries

Complexes with coordination numbers of 4 are typically either tetrahedral or square planar. The tetrahedral geometry (Fig. 8.18a) predominates for four-coordinate complexes of the early transition metals (those toward the left side of the *d* block of elements in the periodic table). Geometric isomerism is not possible for tetrahedral complexes of the general form MA_2B_2 , because all four tetrahedral sites are completely equivalent.

The square-planar geometry (see Figs. 8.18b,c) is common for four-coordinate complexes of Au^{3+} , Ir^+ , Rh^+ , and especially common for ions with the d^8 valence electron configurations: Ni^{2+} , Pd^{2+} , and Pt^{2+} , for example. The Ni^{2+} ion forms a few tetrahedral complexes, but four-coordinate Pd^{2+} and Pt^{2+} are nearly always square planar. Square-planar complexes of the type MA_2B_2 can have isomers, as illustrated in Figures 8.18b and c for *cis*- and *trans*- $[\text{Pt}(\text{NH}_3)_2\text{Cl}_2]$. The *cis* form of this compound is a potent and widely used anticancer drug called cisplatin, but the *trans* form has no therapeutic properties.

Finally, linear complexes with coordination numbers of 2 are known, especially for ions with d^{10} configurations such as Cu^+ , Ag^+ , Au^+ , and Hg^{2+} . The central Ag atom in a complex such as $[\text{Ag}(\text{NH}_3)_2]^+$ in aqueous solution strongly attracts several water molecules as well, however, so its actual coordination number under these circumstances may be greater than 2.



Mirror plane

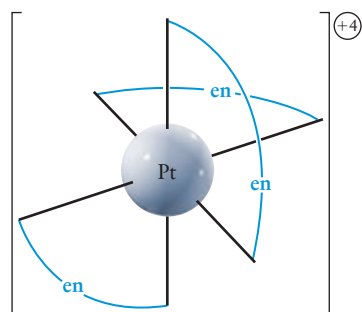


FIGURE 8.19 Enantiomers of the $[\text{Pt}(\text{en})_3]^{4+}$ ion. Reflection through the mirror plane transforms one enantiomer into the other. The two cannot be superimposed by simple rotation.

Chiral Structures

Molecules that rotate plane polarized light in opposite directions are called optical isomers (see Section 7.1, Fig. 7.9). They typically have chiral structures that cannot be superimposed on their mirror images by rotation. The two structures shown in Figure 8.19 for the complex ion $[\text{Pt}(\text{en})_3]^{4+}$ are examples of such a mirror-image pair.

EXAMPLE 8.4

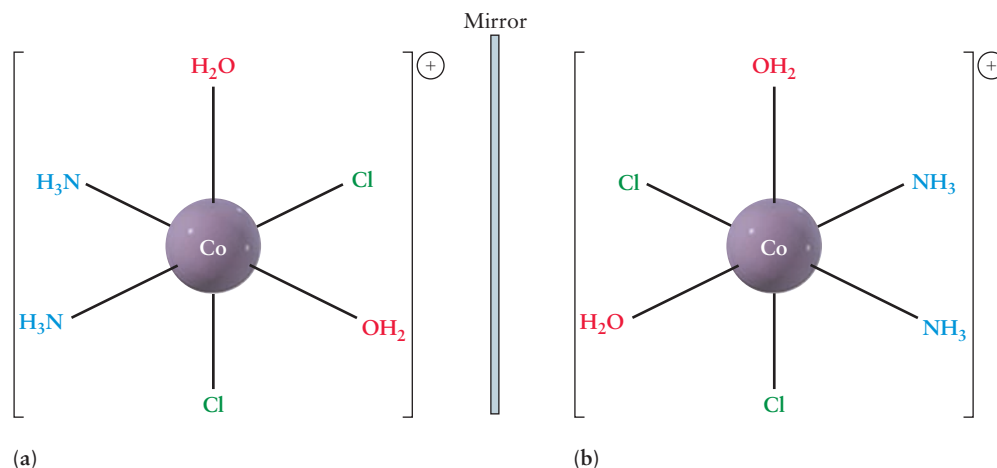
Suppose that the complex ion $[\text{Co}(\text{NH}_3)_2(\text{H}_2\text{O})_2\text{Cl}_2]^+$ is synthesized with the two ammine ligands *cis* to each other, the two aqua ligands *cis* to each other, and the two chloro ligands *cis* to each other (Fig. 8.20a). Is this complex optically active?

SOLUTION

We represent a mirror by a shaded line and create the mirror image by making each point in the image lie at the same distance from the shaded line as the corresponding point in the original structure (see Fig. 8.20). Comparing the original (see Fig. 8.20a) with the mirror image (see Fig. 8.20b) shows that *cis, cis*- $[\text{Co}(\text{NH}_3)_2(\text{H}_2\text{O})_2\text{Cl}_2]^+$ is chiral, because the two structures cannot be superimposed even after they are turned. Although many chiral complexes contain chelating ligands, this example proves that nonchelates can be chiral.

Related Problems: 19, 20

FIGURE 8.20 The structure of (a) the all-*cis* $[\text{Co}(\text{NH}_3)_2(\text{H}_2\text{O})_2\text{Cl}_2]^+$ complex ion, together with (b) its mirror image.



The hexadentate ligand EDTA (ethylenediaminetetra-acetate ion) forms chiral complexes. Figure 8.21 shows the structure of this chelating ligand coordinated to a Co^{3+} ion. The central metal ion is literally “enveloped” by the ligand forming six coordinate covalent bonds with two nitrogen atoms and four oxygen anions. A chelating agent like EDTA has a strong affinity for certain metal ions and can **sequester** them effectively in solution. EDTA solubilizes the scummy precipitates that Ca^{2+} ion forms with anionic constituents of soap by forming a stable complex with Ca^{2+} . In so doing it breaks up the main contributor to bathtub rings and it is a “miracle ingredient” in some bathtub cleaners. EDTA is also used to recover trace contaminants from water (some metal ions, especially heavy ones, are toxic). It has been used as an antidote for lead poisoning because of its great affinity for Pb^{2+} ions. Iron complexes of EDTA in plant foods permit a slow release of iron to the plant. EDTA also sequesters copper and nickel ions in edible fats and oils. Because these metal ions catalyze the oxidation reactions that turn oils rancid, EDTA preserves freshness.

Coordination Complexes in Biology

Coordination complexes, particularly chelates, play fundamental roles in the biochemistry of both plants and animals. Trace amounts of at least nine transition elements are essential to life—vanadium, chromium, manganese, iron, cobalt, nickel, copper, zinc, and molybdenum.

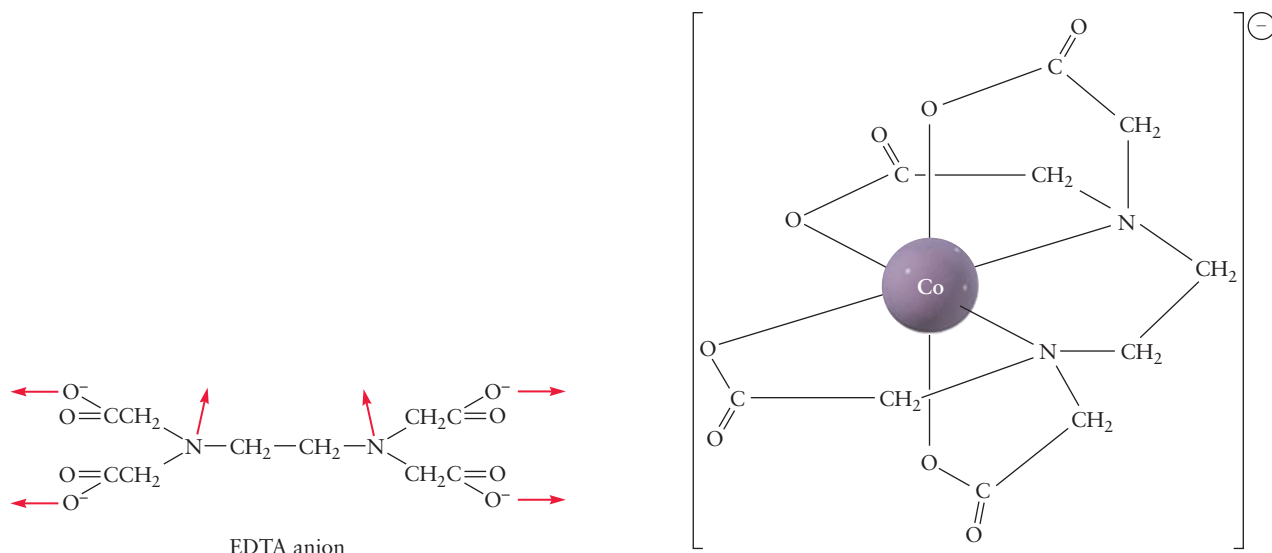


FIGURE 8.21 The chelation complex of EDTA with cobalt(III). Each EDTA ion has six donor sites at which it can bind (by donating lone-pair electrons) to the central metal ion.

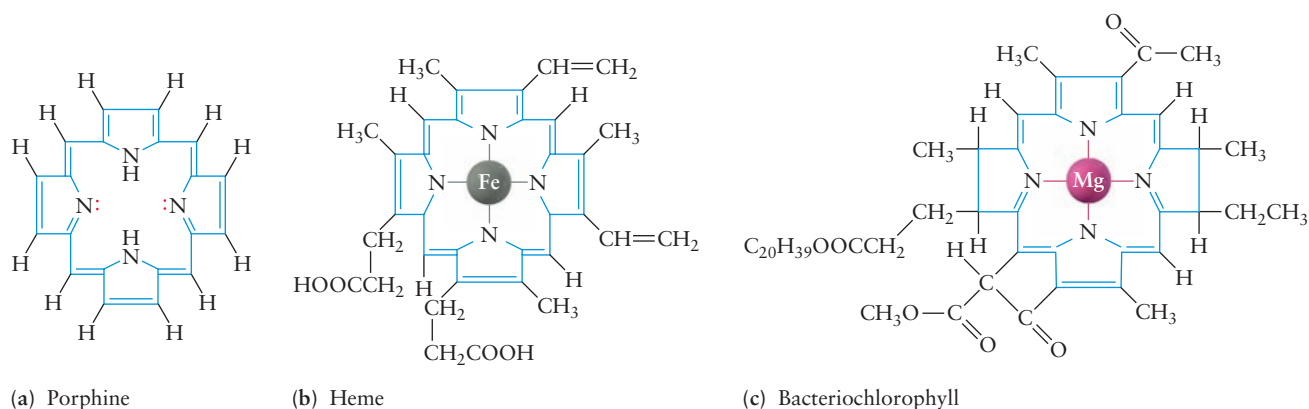
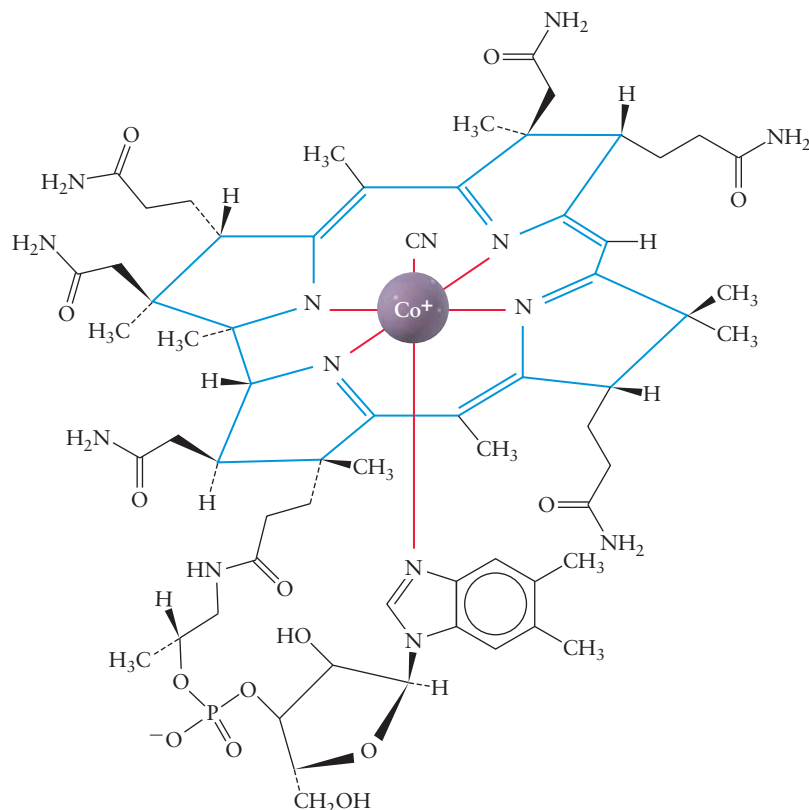


FIGURE 8.22 Structures of (a) porphine, (b) heme, and (c) bacteriochlorophyll. The porphine ring common to the three structures is highlighted in blue.

Several of the most important complexes are based on *porphine*, a compound of carbon, nitrogen, and hydrogen whose structure is shown in Figure 8.22a. Removal of two central H ions leaves four N atoms that can bind to a metal ion M^{2+} and form a tetradentate chelate structure. Such a structure, modified by the addition of several side groups, gives a complex with Fe^{2+} ions called *heme* (see Fig. 8.22b). *Hemoglobin*, the compound that transports oxygen in the blood, contains four such heme groups. The fifth coordination site of each iron(II) ion binds *globin* (a high-molar-mass protein) via N atoms on that protein, and the sixth site is occupied by water or molecular oxygen. Oxygen is a strong-field ligand that makes the d^6 Fe^{2+} diamagnetic and is responsible for the short-wavelength absorption (See Section 8.5) that leads to the red color of blood in the arteries. After the oxygen is delivered to the cells, it is replaced by water, a weaker field ligand, and a paramagnetic complex forms that absorbs at longer wavelengths, producing the bluish tint of blood in the veins. In cases of carbon monoxide (CO) poisoning,

FIGURE 8.23 Structure of vitamin B_{12} .



CO molecules occupy the sixth coordination site and block the binding and transport of oxygen; the equilibrium constant for CO binding is 200 times greater than that for O₂ binding (see Chapter 14).

Figure 8.22c shows the structure of a related compound, bacteriochlorophyll, which is part of the photosynthetic apparatus of photosynthetic bacteria. Section 20.6 describes the key role such structures play in photosynthesis, the process by which green plants, algae, and certain bacteria capture light and transform it into energy for use in chemical reactions.

Vitamin B₁₂ is useful in the treatment of pernicious anemia and other diseases. Its structure (Fig. 8.23) has certain similarities to that of heme. Again, a metal ion is coordinated by a planar tetradentate ligand, with two other donors completing the coordination octahedron by occupying *trans* positions. In vitamin B₁₂, the metal ion is cobalt and the planar ring is *corrin*, which is somewhat similar to porphine. In the human body, enzymes derived from vitamin B₁₂ accelerate a range of important reactions, including those involved in producing red blood cells.

8.5 Crystal Field Theory: Optical and Magnetic Properties

What is the nature of the bonding in coordination complexes of the transition metals that leads to their special properties? Why does Pt(IV) form only octahedral complexes, whereas Pt(II) forms square-planar ones, and under what circumstances does Ni(II) form octahedral, square-planar, and tetrahedral complexes? Can trends in the length and strength of metal–ligand bonds be understood? To answer these questions, we need a theoretical description of bonding in coordination complexes.

Crystal Field Theory

Crystal field theory, which is based on an ionic description of metal–ligand bonding, provides a simple and useful model for understanding the electronic structure, optical properties, and magnetic properties of coordination complexes. Crystal field theory was originally developed to explain these properties of ions in solids, for example, the red color of ruby, which arises from Cr³⁺ ions in an Al₂O₃ lattice. It was quickly applied to the related problem of understanding the bonding, structures, and other properties of coordination complexes. The theory treats the complex as a central metal ion perturbed by the approach of negatively charged ligands. In an octahedral complex, the six ligands are treated as negative point charges that are brought up along the $\pm x$, $\pm y$, and $\pm z$ coordinate axes toward a metal atom or ion at the origin. The energy of an electron in free space is the same in any of the five *d* orbitals in an atom or ion of a transition metal. When external charges are present, however (Fig. 8.24), the energies of electrons in the various *d* orbitals change by different amounts because of the Coulomb repulsion between the external charges and the electrons in the *d* orbitals. The magnitude of the Coulomb repulsion depends inversely on the separation between the charges, which differs for the different orbitals. An electron in a $d_{x^2-y^2}$ or d_{z^2} orbital on the central metal atom is most likely to be found along the coordinate axes, where it experiences a strong repulsive interaction with the electrons from the ligand, raising the energy of the orbital. In contrast, an electron in a d_{xy} , d_{yz} , or d_{xz} orbital of the metal is most likely to be found *between* the coordinate axes, and therefore experiences less repulsion from an octahedral array of approaching charges; the energy of these orbitals is also raised but not by as much as that of the $d_{x^2-y^2}$ and d_{z^2} orbitals. In the octahedral field of the ions, the *d* orbital energy

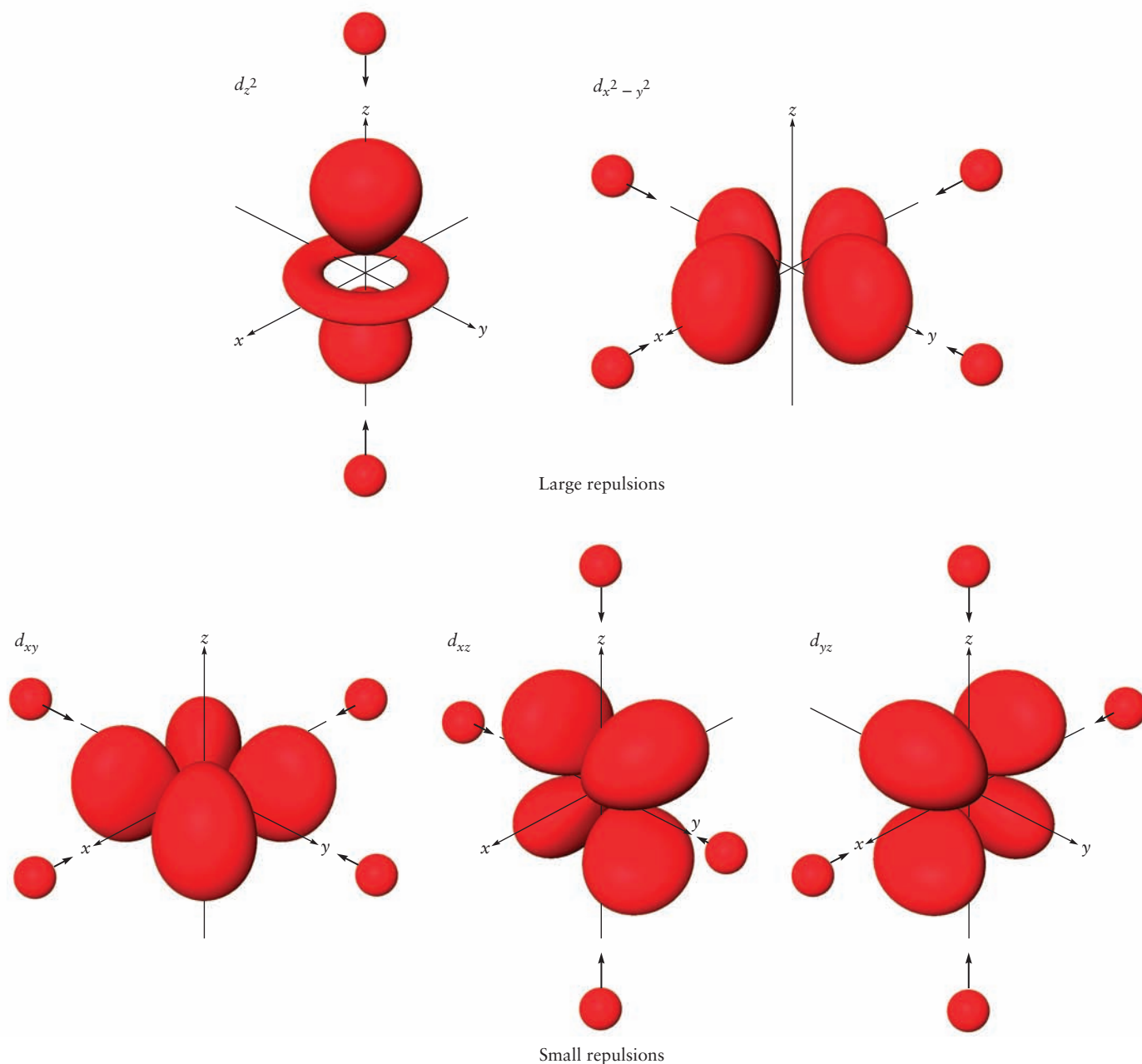
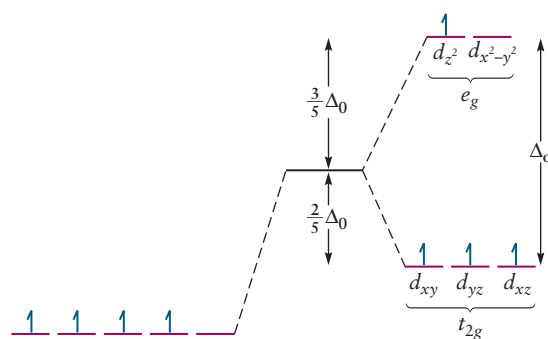


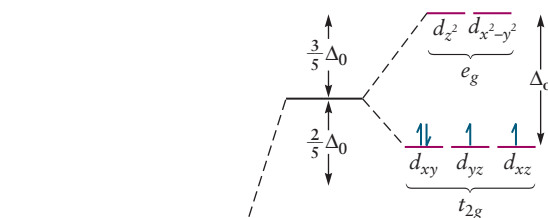
FIGURE 8.24 The basis for octahedral crystal field splitting of $3d$ -orbital energies by ligands. As the external charges approach the five $3d$ orbitals, the largest repulsions arise in the d_{z^2} and $d_{x^2-y^2}$ orbitals, which point directly at two or four of the approaching charges. External charges that have negligible interactions with the d electrons are not shown.

levels split into two groups (Fig. 8.25). The three lower energy orbitals, called t_{2g} orbitals, correspond to the d_{xy} , d_{yz} , and d_{xz} orbitals of the transition-metal atom; the two higher energy orbitals, called e_g orbitals, correspond to the $d_{x^2-y^2}$ and d_{z^2} orbitals. The labels t_{2g} and e_g specify the symmetry and degeneracy (number of orbitals with the same energy) of each set of orbitals. t orbitals are threefold (triply) degenerate, whereas e orbitals are twofold (doubly) degenerate. The subscript g has its usual meaning; g orbitals are symmetric with respect to inversion of the coordinates (see Section 6.1). The energy difference between the two sets of levels is Δ_o , the **crystal field splitting energy** for the octahedral complex that has formed.

FIGURE 8.25 An octahedral field increases the energies of all five d orbitals, but the increase is greater for the d_{z^2} and $d_{x^2-y^2}$ orbitals. As a result, the orbitals are split into two sets that differ by the energy Δ_o . The orbital occupancy shown is for (a) the high-spin (small Δ_o) and (b) the low-spin (large Δ_o) complexes of Mn(III).



(a) $[\text{Mn}(\text{H}_2\text{O})_6]^{3+}$ (high spin)



(b) $[\text{Mn}(\text{CN})_6]^{3-}$ (low spin)

Let's consider the electron configuration expected for a transition-metal ion in the presence of such a crystal field. The Cr^{3+} ion, for example, has three d electrons. According to Hund's rules (see Section 5.3), the lowest energy configuration is one in which the three electrons occupy different t_{2g} levels with parallel spins, so complexes of Cr^{3+} are predicted to be paramagnetic. In an ion such as Mn^{3+} , which has a fourth d electron, two ground-state electron configurations are possible. The fourth electron can occupy either a t_{2g} level, with its spin opposite that of the electron already in that level (see Fig. 8.25a), or an e_g level, with its spin parallel to those of the three t_{2g} electrons (see Fig. 8.25b). The former configuration is the lower energy configuration when the splitting Δ_o is large, because it costs energy to promote the electron to the e_g level. More precisely, the cost of promoting the electron to the e_g orbital is greater than the electrostatic repulsion energy between two electrons occupying the same orbital. If the splitting is small, however, the e_g orbital will be preferentially occupied; the cost of promoting the electron to the higher energy orbital is less than the electrostatic repulsion energy.

In central metal atoms or ions with four to seven d electrons, two types of electron configurations are possible. When Δ_o is large, **low-spin complexes** are the most stable. Electrons are paired in the lower energy t_{2g} orbital, and the e_g orbitals are not occupied until the t_{2g} levels are filled. When Δ_o is small, **high-spin complexes** are the most stable. Electrons are placed one at a time, with parallel spins, in each of the three t_{2g} orbitals and then in each of the e_g orbitals. The terms *low spin* and *high spin* refer to the total number of unpaired electrons; configurations with a large number of unpaired electrons are called **high-spin configurations** and those with a small number of unpaired electrons are called **low-spin configurations**. Because low-spin configurations occur for large values of the crystal field Δ_o they are also called **strong field configurations**, and the ligands that produce such fields are called **strong field ligands**. **Weak field ligands** generate small crystal field splittings, resulting in **high-spin configurations**. These terms are used interchangeably (weak field \leftrightarrow high spin; strong field \leftrightarrow low spin); therefore, you should be alert when reading inorganic texts or the literature.

TABLE 8.5 Electron Configurations and Crystal Field Stabilization Energies for High- and Low-Spin Octahedral Complexes

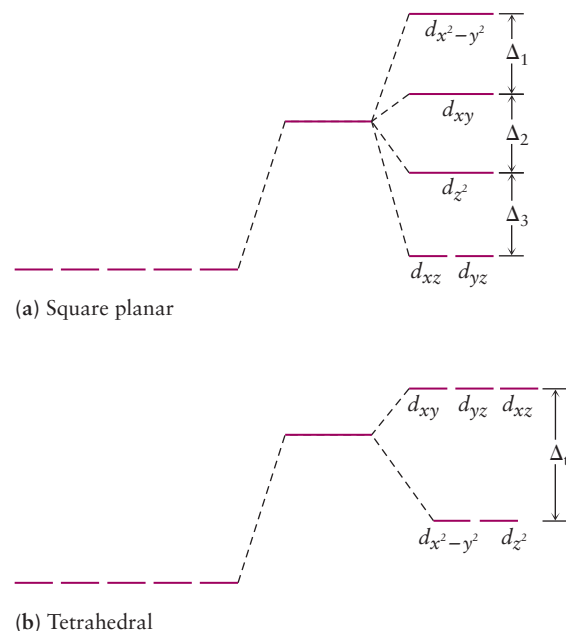
Configuration	d^1	d^2	d^3	d^4	d^5	d^6	d^7	d^8	d^9	d^{10}
Examples	Ti^{3+}	Ti^{2+}, V^{3+}	V^{2+}, Cr^{3+}	Mn^{3+}, Re^{3+}	Mn^{2+}, Fe^{3+}	Fe^{2+}, Pd^{4+}	Co^{2+}, Rh^{2+}	Ni^{2+}, Pt^{2+}	Cu^{2+}	Zn^{2+}, Ag^+
HIGH SPIN	e_g	— —	— —	— —	↑ —	↑ ↑	↑ ↑	↑ ↑	↑ ↓	↑ ↓
	t_{2g}	↑ — —	↑ ↑ —	↑ ↑ ↑	↑ ↑ ↑	↑ ↑ ↑	↑ ↓ ↑	↑ ↓ ↑	↑ ↓ ↓	↑ ↓ ↓
	CFSE	$-\frac{2}{5}\Delta_o$	$-\frac{4}{5}\Delta_o$	$-\frac{6}{5}\Delta_o$	$-\frac{3}{5}\Delta_o$	0	$-\frac{2}{5}\Delta_o$	$-\frac{4}{5}\Delta_o$	$-\frac{6}{5}\Delta_o$	$-\frac{3}{5}\Delta_o$
LOW SPIN	e_g				— —	— —	— —	— —		
	t_{2g}				↑ ↓ ↑	↑ ↓ ↑	↑ ↓ ↓	↑ ↓ ↓		
	CFSE	Same as high spin			$-\frac{8}{5}\Delta_o$	$-\frac{10}{5}\Delta_o$	$-\frac{12}{5}\Delta_o$	$-\frac{9}{5}\Delta_o$	Same as high spin	

CFSE, Crystal field stabilization energies.

Table 8.5 summarizes the electron configurations possible for 10 electrons in an octahedral crystal field, provides specific examples of transition metals with these configurations, and tabulates the **crystal field stabilization energies (CFSE)** of their complexes. The CFSE is the energy difference between electrons in an octahedral crystal field and those in a hypothetical spherical crystal field. In an octahedral field, the energy of the three t_{2g} orbitals is lowered by $\frac{2}{5}\Delta_o$, and that of the two e_g orbitals is raised by $\frac{3}{5}\Delta_o$ relative to the spherical field (see Fig. 8.25). If these five orbitals are fully occupied or half occupied (as in d^{10} or high-spin d^5 complexes), then the energy of the ion is the same as in a spherical field: the CFSE is zero. If the lower energy levels are preferentially occupied, however, the configuration is stabilized. For example, in a low-spin d^4 complex, the energy of each of the four electrons in the t_{2g} orbitals is lowered by $\frac{2}{5}\Delta_o$, resulting in a total CFSE of $-\frac{8}{5}\Delta_o$.

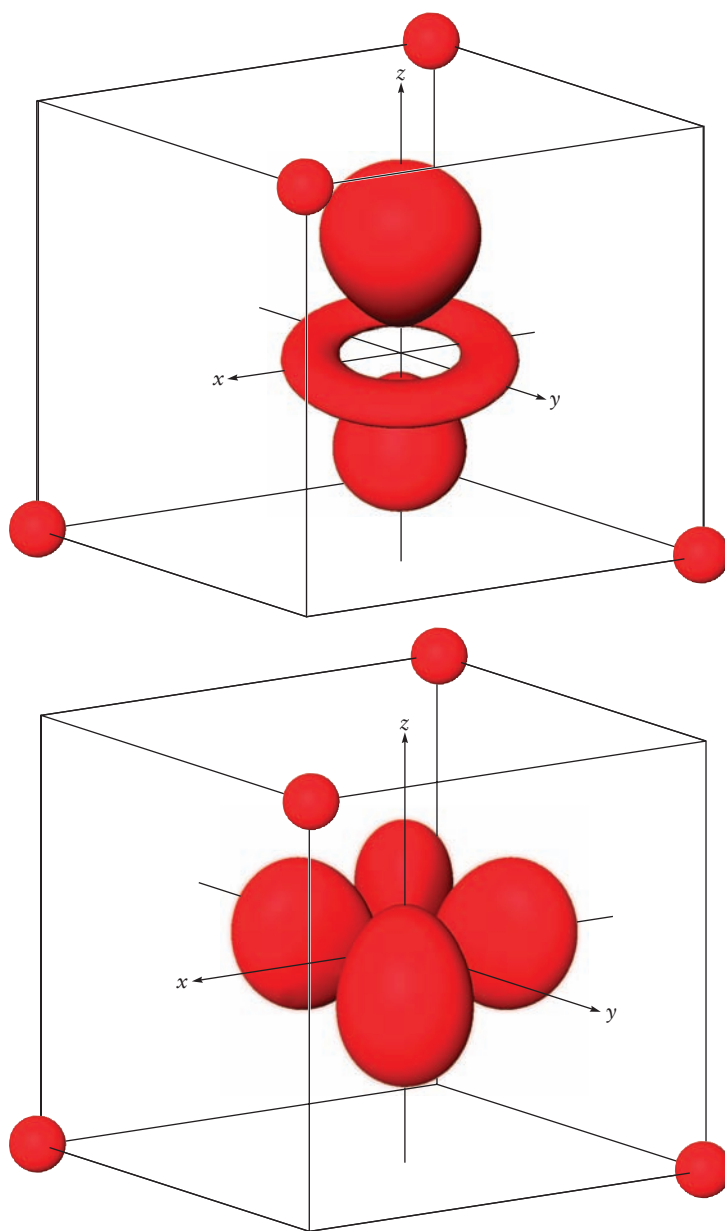
The CFSE helps to explain the trends in the enthalpies of hydration of ions in the first transition series shown in Figure 8.3. If each measured value (blue curve) is adjusted by correcting for the CFSE of that complex ion, results quite close to the straight red lines are obtained. The relatively small magnitude of the enthalpy of hydration for Mn^{2+} arises from the high-spin d^5 configuration of Mn^{2+} , which results in a CFSE of zero. On either side of this ion, the negative CFSE lowers the enthalpy of hydration.

FIGURE 8.26 Energy-level structures of the 3d orbitals in square-planar and tetrahedral crystal fields.



Square-Planar and Tetrahedral Complexes

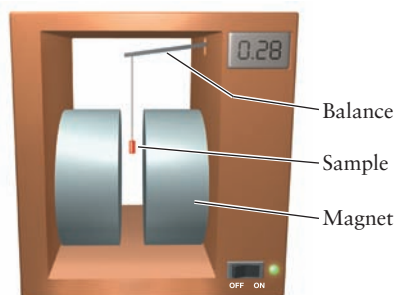
Crystal field theory applies to square-planar and tetrahedral complexes, as well as to octahedral complexes. Let's consider a square-planar complex in which four negative charges are brought toward the metal ion along the $\pm x$ - and $\pm y$ -axes. The relative d -orbital energy level ordering in a square-planar crystal field can be predicted using the same reasoning we applied to the octahedral case. The magnitude of the repulsive interaction between an electron in a given orbital and the electrons of the ligand depends on the degree to which the electron density is concentrated along the x - and y - axes. An electron in the $d_{x^2-y^2}$ orbital, which is oriented along these axes, experiences the greatest repulsion and lies at the highest energy. The energy of the d_{xy} orbital is lower than that of the $d_{x^2-y^2}$ orbital because the lobes of this orbital are oriented at 45 degrees to the axes. The d_z^2 orbital energy level is lower still because its electron density is concentrated along the z -axis, with a small component in the x - y plane. Finally, the d_{xz} and d_{yz} orbitals experience the least repulsion. These orbitals are the most stable in a square-planar crystal field because they have nodes in the x - y plane. Figure 8.26a shows the resulting energy level diagram.



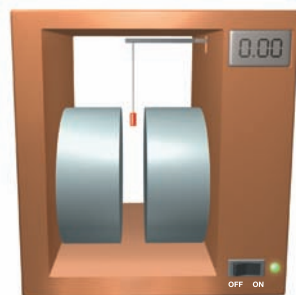
Another way to think of the square-planar crystal field splittings is to consider what happens to the octahedral energy levels shown in Figure 8.25 as the two ligands on the $\pm z$ axis move away from the metal. Let's consider each of the two degenerate levels separately. As the ligands retreat, the energy of the d_{z^2} orbital falls because of the decreased repulsion; the energy of the $d_{x^2-y^2}$ orbital must increase to conserve the total energy of the e_g level. Similarly, the energies of the d_{xz} and d_{yz} orbitals of the t_{2g} level are stabilized as the ligands are pulled away and the energy of the d_{xy} orbital increases. So the octahedral crystal field energy levels distort smoothly into the square planar levels as the z axis ligands are pulled away. Some coordination complexes are described as having distorted octahedral structures, with the two z -axis ligands moved outward but not removed completely. The level splittings observed in these cases are intermediate between the octahedral and the square-planar patterns.

Tetrahedral complexes result from bringing up ligands to four of the eight corners of an imaginary cube with the metal ion at its center. The $d_{x^2-y^2}$ and d_{z^2} orbitals point toward the centers of the cube faces, but the other three orbitals point toward the centers of the cube edges, which are closer to the corners occupied by the ligands. Electrons in the latter orbitals are therefore more strongly repelled than those in the former (see figures on page 343). Figure 8.25b shows the result; the energy level ordering is the reverse of that found for octahedral complexes. In addition, the magnitude of the splitting Δ_t is about half that of Δ_o .

Octahedral complexes are the most common because the formation of six bonds to ligands, rather than four, confers greater stability. Square-planar arrangements are important primarily for complexes of d^8 ions with strong field ligands. The low-spin configuration that leaves the high-energy $d_{x^2-y^2}$ orbital vacant is the most stable. The low-spin configuration of a square planar d^8 complex is more stable than the corresponding configuration of an octahedral complex because the energy of the highest occupied orbitals in the square planar complex is lower than those in the octahedral complex. Finally, tetrahedral complexes are less stable than either octahedral or square planar complexes for two reasons. First, the crystal field splitting is smaller so the lower set of energy levels is stabilized less than in the other geometries. Second, because the lower-energy set of levels is only doubly degenerate, electrons must be placed into the upper level at an earlier stage in the filling process.



(a)



(b)

FIGURE 8.27 (a) If a sample of a paramagnetic substance is dipped into a magnetic field, it is drawn down into the field and weighs more than it does in the absence of the field. (b) If a diamagnetic substance is dipped into the field in the same way, it is buoyed up and weighs less than it would in the absence of the field.

Magnetic Properties

The existence of high- and low-spin configurations accounts for the magnetic properties of many different coordination compounds. As discussed in Section 6.2, substances are classified as paramagnetic or diamagnetic according to whether they are attracted into a magnetic field. Figure 8.27 shows a schematic of an experiment that demonstrates the universal *susceptibility* of substances to the influence of magnetic fields. A cylindrical sample is suspended between the poles of a powerful magnet. It is weighed accurately in the absence of a magnetic field and then again in the presence of the field. (There are several ways to do this; either the sample or the magnet may be moved, or the magnet may be switched off and then on.) The net force on the sample (apparent weight) is found to be different in the presence of the magnetic field. Substances that are repelled by a magnetic field weigh less when dipped into one and they are called *diamagnetic*; substances that are attracted by a magnetic field weigh more and they are called *paramagnetic* (see Section 6.2). The measurements just described provide not only qualitative characterization of a sample's magnetic properties, but also a quantitative value for its **magnetic susceptibility**, that is, the strength of its interaction with a magnetic field. The susceptibility of a diamagnet is negative and small, whereas that of a paramagnet is positive and can be quite large.

As explained in Section 6.2, paramagnetism is associated with atoms, ions, or molecules that contain one or more electrons with unpaired spins. Diamagnetic

substances have the spins of all of their electrons paired. Thus, measurements of magnetic susceptibility show which substances have unpaired electron spins and which have completely paired electron spins. The number of unpaired electrons per molecule in a paramagnet can even be counted on the basis of the magnitude of the magnetic susceptibility of the sample. On a molar basis, a substance with two unpaired electrons per molecule is pulled into a magnetic field more strongly than a substance with only one unpaired electron per molecule.

These facts emerge in connection with coordination complexes, because paramagnetism is prevalent among transition-metal complexes, whereas most other chemical substances are diamagnetic. Among complexes of a given metal ion, the number of unpaired electrons, as observed by magnetic susceptibility, varies with the identities of the ligands. Both $[\text{Co}(\text{NH}_3)_6]^{3+}$ and $[\text{CoF}_6]^{3-}$ have six ligands surrounding a central Co^{3+} ion; yet, the former is diamagnetic (because it is a strong-field, low-spin complex), and the latter is paramagnetic to the extent of four unpaired electrons (because it is a weak-field, high-spin complex). Similarly, $[\text{Fe}(\text{CN})_6]^{4-}$ is diamagnetic, but $[\text{Fe}(\text{H}_2\text{O})_6]^{2+}$ has four unpaired electrons; these complexes also correspond to the two d^6 configurations shown in Table 8.4.

EXAMPLE 8.5

The octahedral complex ions $[\text{FeCl}_6]^{3-}$ and $[\text{Fe}(\text{CN})_6]^{3-}$ are both paramagnetic, but the former is high spin and the latter is low spin. Identify the d -electron configurations in these two octahedral complex ions. In which is the octahedral field splitting greater? How does the CFSE differ between the complexes?

SOLUTION

The Fe^{3+} ion has five d electrons. A high-spin complex such as $[\text{FeCl}_6]^{3-}$ has five unpaired spins ($t_{2g}^3 e_g^2$); a low-spin complex such as $[\text{Fe}(\text{CN})_6]^{3-}$ has one unpaired spin (t_{2g}^5). The splitting Δ_o must be greater for cyanide than for chloride ion ligands. The CFSE for the $[\text{FeCl}_6]^{3-}$ complex is zero, whereas that for the $[\text{Fe}(\text{CN})_6]^{3-}$ complex is $-2\Delta_o$.

Related Problems: 27, 28

8.6 Optical Properties and the Spectrochemical Series



FIGURE 8.28 Several colored coordination compounds. (clockwise from top left) They are $\text{Cr}(\text{CO})_6$ (white), $\text{K}_3[\text{Fe}(\text{C}_2\text{O}_4)_3]$ (green), $[\text{Co}(\text{en})_3]^{3+}$ (orange), $[\text{Co}(\text{NH}_3)_5(\text{H}_2\text{O})]\text{Cl}_3$ (red), and $\text{K}_3[\text{Fe}(\text{CN})_6]$ (red-orange).

Transition-metal complexes are characterized by their rich colors, which are often deep, vibrant, and saturated (Fig. 8.28). The colors depend on the oxidation state of the metal ion, the number and nature of the ligands, and the geometry of the complex. Earlier figures have shown the color changes that accompany dehydration and ligand substitution reactions and also the different colors of a pair of geometric isomers. The following series of $\text{Co}(\text{III})$ complexes shows how the colors of coordination complexes of the same ion can vary with different ligands:

$[\text{Co}(\text{NH}_3)_6]^{3+}$	Orange
$[\text{Co}(\text{NH}_3)_4\text{Cl}_2]^+$	A green form and a violet form
$[\text{Co}(\text{NH}_3)_5(\text{H}_2\text{O})]^{3+}$	Purple

Coordination complexes appear colored when they absorb visible light. Recall that atoms absorb light when the energy of an incident photon exactly matches the energy difference between two atomic energy levels (see Fig. 4.9). The missing wavelengths appear as dark lines against the spectral rainbow. The transmitted light still appears quite white to our eyes, however, because atomic absorption

lines are so narrow. Only a small fraction of the visible light has been absorbed. Coordination complexes, on the other hand, absorb light over significant regions of the visible spectrum. What we see is the color that is *complementary* to the color that is most strongly absorbed (see Section 20.3). The $[\text{Co}(\text{NH}_3)_5\text{Cl}]^{2+}$ ion, for example, absorbs greenish yellow light, with the strongest absorption occurring near 530 nm. Only the red and blue components of white light are transmitted through an aqueous solution of this ion, which appears purple to us. Materials that absorb all visible wavelengths appear gray or black, and those that absorb visible light weakly or not at all appear colorless.

Crystal field theory was developed, in part, to explain the colors of transition-metal complexes. It was not completely successful, however. Its failure to predict trends in the optical absorption of a series of related compounds stimulated the development of ligand field and molecular orbital theories and their application in coordination chemistry. The colors of coordination complexes are due to the excitation of the d electrons from filled to empty d orbitals ($d-d$ transitions). In octahedral complexes, the electrons are excited from occupied t_{2g} levels to empty e_g levels. The crystal field splitting Δ_o is measured directly from the optical absorption spectrum of the complex. The wavelength of the strongest absorption is called λ_{max} and it is related to Δ_o as follows. $E = h\nu$, so $\Delta_o = h\nu = hc/\lambda_{\text{max}}$. Because energy is inversely proportional to wavelength, compounds with small crystal field splittings absorb light with longer wavelengths, toward the red end of the visible spectrum, and those with large crystal field splitting absorb light with shorter wavelengths, toward the blue end of the spectrum.

In $[\text{Co}(\text{NH}_3)_6]^{3+}$, an orange compound that absorbs most strongly in the violet region of the spectrum, the crystal field splitting Δ_o is larger than in $[\text{Co}(\text{NH}_3)_5\text{Cl}]^{2+}$, a violet compound that absorbs most strongly at lower frequencies (longer wavelengths) in the yellow–green region of the spectrum. d^{10} complexes (like those of Zn^{2+} or Cd^{2+}) are colorless because all of the d levels (both t_{2g} and e_g) are filled. Because there are no empty orbitals available to accept an excited electron, the transition is not allowed, which means that the absorption is weak or nonexistent. High-spin d^5 complexes such as $[\text{Mn}(\text{H}_2\text{O})_6]^{2+}$ and $[\text{Fe}(\text{H}_2\text{O})_6]^{3+}$ also show only weak absorption because promotion from a filled t_{2g} level to an empty e_g level would require a spin flip to satisfy the Pauli principle. (Recall that all of the spins are parallel to one another in high-spin complexes.) Light absorption rarely reverses the spin of an electron, so the optical absorption of these compounds is weak, as shown by the pale pink color of the hexa-aqua Mn^{2+} complex in Figure 8.29. Table 8.6 lists the crystal field splittings and absorption wavelengths for a number of coordination complexes to give you a feel for their diversity.

Experimental measurements of the optical absorption spectra and magnetic properties of transition-metal complexes provide a critical test of the validity of crystal field theory. The theory makes specific predictions about the strengths of crystal fields produced by different ligands. Charged ligands such as the halides

FIGURE 8.29 The colors of the hexa-aqua complexes of metal ions (from left) Mn^{2+} , Fe^{3+} , Co^{2+} , Ni^{2+} , Cu^{2+} , and Zn^{2+} , prepared from their nitrate salts. Note that the d^{10} Zn^{2+} complex is colorless. The green color of the Ni^{2+} is due to absorption of both red and blue light that passes through the solution. The yellow color of the solution containing $\text{Fe}(\text{H}_2\text{O})_6^{3+}$ is caused by hydrolysis of that ion to form $\text{Fe}(\text{OH})(\text{H}_2\text{O})_5^{2+}$; if this reaction is suppressed, the solution is pale violet.

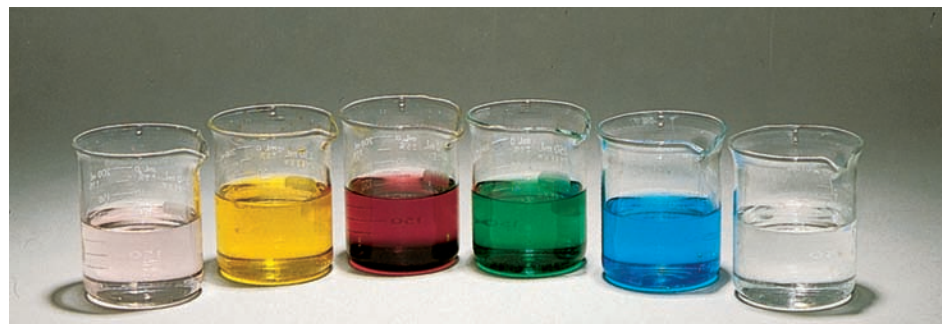
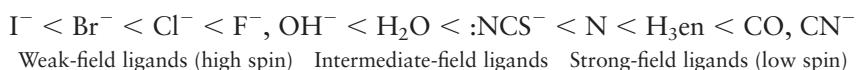


TABLE 8.6 Absorption Wavelengths for Selected Octahedral Transition-Metal Complexes

Octahedral Complexes	λ_{\max} (nm)	Octahedral Complexes	λ_{\max} (nm)
$[\text{TiF}_6]^{3-}$	588	$[\text{Co}(\text{NH}_3)_6]^{3+}$	437
$[\text{Ti}(\text{H}_2\text{O})_6]^{3+}$	492	$[\text{Co}(\text{CN})_6]^{3-}$	290
$[\text{V}(\text{H}_2\text{O})_6]^{3+}$	560	$[\text{Co}(\text{H}_2\text{O})_6]^{2+}$	1075
$[\text{V}(\text{H}_2\text{O})_6]^{2+}$	806	$[\text{Ni}(\text{H}_2\text{O})_6]^{2+}$	1176
$[\text{Cr}(\text{H}_2\text{O})_6]^{3+}$	575	$[\text{Ni}(\text{NH}_3)_6]^{2+}$	926
$[\text{Cr}(\text{NH}_3)_6]^{3+}$	463	$[\text{RhBr}_6]^{3-}$	463
$[\text{Cr}(\text{CN})_6]^{3-}$	376	$[\text{RhCl}_6]^{3-}$	439
$\text{Cr}(\text{CO})_6$	311	$[\text{Rh}(\text{NH}_3)_6]^{3+}$	293
$[\text{Fe}(\text{CN})_6]^{3-}$	310	$[\text{Rh}(\text{CN})_6]^{3-}$	227
$[\text{Fe}(\text{CN})_6]^{4-}$	296	$[\text{IrCl}_6]^{3-}$	362
$[\text{Co}(\text{H}_2\text{O})_6]^{3+}$	549	$[\text{Ir}(\text{NH}_3)_6]^{3+}$	250

should produce much stronger crystal fields than neutral ligands. The interaction between the halides and a metal ion should increase with decreasing ionic radius. The smaller halide ions can approach the metal ion more closely, resulting in greater electrostatic repulsion. Crystal field theory predicts splittings that increase in the order $\text{I}^- < \text{Br}^- < \text{Cl}^- < \text{F}^-$. A systematic ranking of the strength of various ligands was obtained by comparing the optical absorption spectra of a series of complexes with the general formula $[\text{Co}(\text{III})(\text{NH}_3)_5\text{X}]^{n+}$. The strength of the interaction between a single ligand X and the Co^{3+} ion could be measured directly because all other interactions and the geometry of the complex remained constant. Ligands were ranked from weakest to strongest in the **spectrochemical series** as follows:



Although this order is not followed for all metal ions, it is a useful generalization. More importantly, it illustrates the failure of crystal field theory to provide a satisfactory account of the factors that govern crystal field splitting. Neutral ligands with lone pairs, such as water and ammonia, produce larger splittings than any of the halides, and ligands with low-lying antibonding π molecular orbitals produce the largest splittings of all. A more comprehensive theory is clearly required to explain the spectrochemical series. Section 8.7 examines how molecular orbital theory correctly accounts for the trend observed in the spectrochemical series.

EXAMPLE 8.6

Predict which of the following octahedral complexes has the shortest λ_{\max} : $[\text{FeF}_6]^{3-}$, $[\text{Fe}(\text{CN})_6]^{3-}$, $[\text{Fe}(\text{H}_2\text{O})_6]^{3+}$.

SOLUTION

$[\text{Fe}(\text{CN})_6]^{3-}$ has the strongest field ligands of the three complexes; thus, its energy levels are split by the greatest amount. The frequency of the light absorbed should be greatest, and λ_{\max} should be the shortest for this ion.

$[\text{Fe}(\text{CN})_6]^{3-}$ solutions are red, which means that they absorb blue and violet light. Solutions of $[\text{Fe}(\text{H}_2\text{O})_6]^{3+}$ are a pale violet due to the weak absorption of red light, and $[\text{FeF}_6]^{3-}$ solutions are colorless, indicating that the absorption lies beyond the long wavelength limit of the visible spectrum.

Related Problems: 37, 38, 39, 40

8.7 Bonding in Coordination Complexes

Valence Bond Theory

Valence bond (VB) theory is used widely in contemporary chemistry to describe structure and bonding in transition-metal compounds, especially coordination complexes. The VB model is intuitively appealing for this purpose for several reasons. Because transition-metal compounds, particularly coordination complexes, often comprise a central atom surrounded by ligands in a symmetric arrangement, forming hybrid orbitals on the central atom with the appropriate symmetry to bond to these ligands is a natural approach to the problem. Often, little interaction occurs among metal–ligand bonds, so the local description is reasonable. Participation of the d electrons enables a much more varied set of structures and hybrid orbitals than can be formed from only s and p orbitals. This section describes two sets of hybrid orbitals used to describe bonding in transition-metal compounds and complexes, and provides examples of each.

Hybridization is justified here for precisely the same reasons we laid out in Section 6.4. The lobes of the hybrid orbitals point toward the ligands and overlap the ligand orbitals more strongly than the standard atomic orbitals. The energy cost of promoting electrons from lower energy atomic orbitals (e.g., $3d$ and $4s$) to the highest energy orbital ($4p$) to form a hybrid orbital is more than offset by the energy gained in forming a stronger bond with the ligand.

We construct the first set of hybrid orbitals from one s atomic orbital, the three p atomic orbitals and the d_{z^2} atomic orbital; they are called dsp^3 hybrid orbitals. The principal quantum numbers of the participating atomic orbitals depend on the particular metal atom under consideration; for Co, they would be the $3d$, $4s$, and $4p$ atomic orbitals. The dsp^3 hybrid orbitals in the most general case are written out as

$$\chi_1 = \sqrt{\frac{1}{3}} [s + \sqrt{2} (p_x)]$$

$$\chi_2 = \sqrt{\frac{1}{3}} \left[s - \sqrt{\frac{1}{2}} (p_x) + \sqrt{\frac{3}{2}} (p_y) \right]$$

$$\chi_3 = \sqrt{\frac{1}{3}} \left[s - \sqrt{\frac{1}{2}} (p_x) - \sqrt{\frac{3}{2}} (p_y) \right]$$

$$\chi_4 = \sqrt{\frac{1}{2}} [p_z + d_{z^2}]$$

$$\chi_5 = \sqrt{\frac{1}{2}} [p_z - d_{z^2}]$$

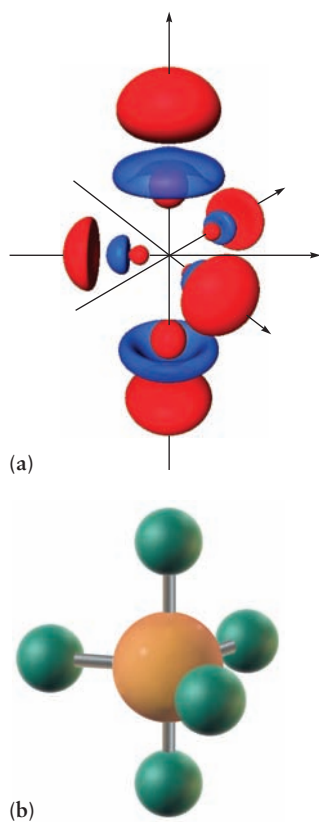


FIGURE 8.30 (a) Hybrid orbitals formed from linear combinations of d_{z^2} , s , p_x , p_y , and p_z orbitals. The pair of orbitals that point along the positive and negative z -axes are the same except for their orientation in space; they are called *axial* orbitals. The set of three orbitals in the x - y plane are equivalent to one another and are called *equatorial* orbitals. (b) This set of hybrid orbitals can be used to describe the bonding in PF_5 , for example.

As shown in Figure 8.30a, these orbitals point to the vertices of a trigonal bipyramid; there are three equivalent equatorial hybrids and two equivalent axial hybrids. Examples of molecules whose shapes are described by dsp^3 hybridization include PF_5 , which you have seen in Section 3.9, and CuCl_3^{3-} . PF_5 is shown in Figure 8.30b for comparison with the set of dsp^3 hybrid orbitals.

The second set of hybrid orbitals we construct are the d^2sp^3 hybrids; these are six equivalent orbitals directed toward the vertices of an octahedron (Fig. 8.31a). They describe the structures and bonding in all of the octahedral coordination complexes discussed in Section 8.6, as well as that in SF_6 , which we show in Figure 8.31b.

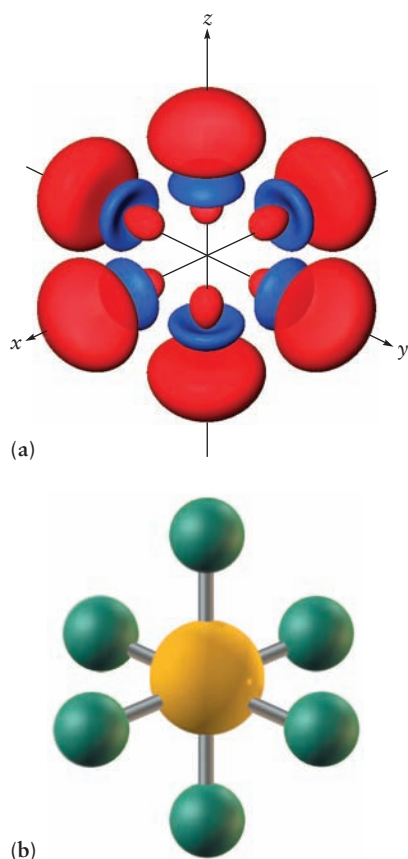


FIGURE 8.31 (a) Hybrid orbitals formed from linear combinations of d_{z^2} , $d_{x^2-y^2}$, p_x , p_y , and p_z orbitals. All six orbitals are equivalent except for their orientation in space. (b) This set of hybrid orbitals can be used to describe the bonding in SF_6 , for example.

$$\begin{aligned}\chi_1 &= \sqrt{\frac{1}{6}} [s + \sqrt{3} (p_z) + \sqrt{2} (d_{z^2})] \\ \chi_2 &= \sqrt{\frac{1}{6}} \left[s + \sqrt{3} (p_z) - \sqrt{\frac{1}{2}} (d_{z^2}) + \sqrt{\frac{3}{2}} (d_{x^2-y^2}) \right] \\ \chi_3 &= \sqrt{\frac{1}{6}} \left[s + \sqrt{3} (p_z) - \sqrt{\frac{1}{2}} (d_{z^2}) - \sqrt{\frac{3}{2}} (d_{x^2-y^2}) \right] \\ \chi_4 &= \sqrt{\frac{1}{6}} \left[s - \sqrt{3} (p_z) - \sqrt{\frac{1}{2}} (d_{z^2}) + \sqrt{\frac{3}{2}} (d_{x^2-y^2}) \right] \\ \chi_5 &= \sqrt{\frac{1}{6}} \left[s - \sqrt{3} (p_z) - \sqrt{\frac{1}{2}} (d_{z^2}) - \sqrt{\frac{3}{2}} (d_{x^2-y^2}) \right] \\ \chi_6 &= \sqrt{\frac{1}{6}} [s - \sqrt{3} (p_z) + \sqrt{2} (d_{z^2})]\end{aligned}$$

Table 8.7 shows the variety of hybrid orbitals that can be constructed from various combinations of s , p , and d orbitals, the shapes of the molecules that result, and selected examples.

VB theory with hybrid orbitals is widely used to rationalize the structures of coordination complexes. It complements classical valence shell electron-pair repulsion (VSEPR) theory by using methods of quantum mechanics to describe the geometry of coordination complexes. As with main-group elements, VB theory is better suited to rationalize structure and bonding after the fact than to predict structure. And by treating the bonds as local and equivalent, it fails completely to account for the colors and magnetic properties of coordination complexes. These shortcomings motivate the application of molecular orbital theory to describe structure and bonding in coordination chemistry.

Molecular Orbital Theory

The failure of crystal field theory and VB theory to explain the spectrochemical series stimulated the development of **ligand field theory**, which applies qualitative methods of molecular orbital theory to describe the bonding and structure of coordination complexes. The terms *ligand field theory* and *molecular orbital theory* are often used interchangeably in inorganic chemistry today.

We apply molecular orbital theory to octahedral coordination complexes just as we did for the simple metal carbonyl in Section 8.2. We begin by constructing the σ MOs from the valence d , s , and p orbitals of the central metal atom and the six ligand orbitals that point along the metal–ligand bond directions in an octahedral complex. In the case of the Cr^{3+} complexes we use as examples, the relevant

TABLE 8.7 Examples of Hybrid Orbitals and Bonding in Complexes

Coordination Number	Hybrid Orbital	Configuration	Examples
2	sp	Linear	$[\text{Ag}(\text{NH}_3)_2]^+$
3	sp^2	Trigonal planar	BF_3 , NO_3^- , $[\text{Ag}(\text{R}_3\text{P})_3]^+$
4	sp^3	Tetrahedral	$\text{Ni}(\text{CO})_4$, $[\text{MnO}_4]^-$, $[\text{Zn}(\text{NH}_3)_4]^{2+}$
4	dsp^2	Planar	$[\text{Ni}(\text{CN})_4]^{2-}$, $[\text{Pt}(\text{NH}_3)_4]^{2+}$
5	dsp^3	Trigonal bipyramid	TaF_5 , $[\text{CuCl}_5]^{3-}$, $[\text{Ni}(\text{PET}_3)_2\text{Br}_3]$
6	d^2sp^3	Octahedral	$[\text{Co}(\text{NH}_3)_6]^{3+}$, $[\text{PtCl}_6]^{2-}$

From G.E. Kimball, Directed valence. *J. Chem. Phys.* 1940, 8, 188.

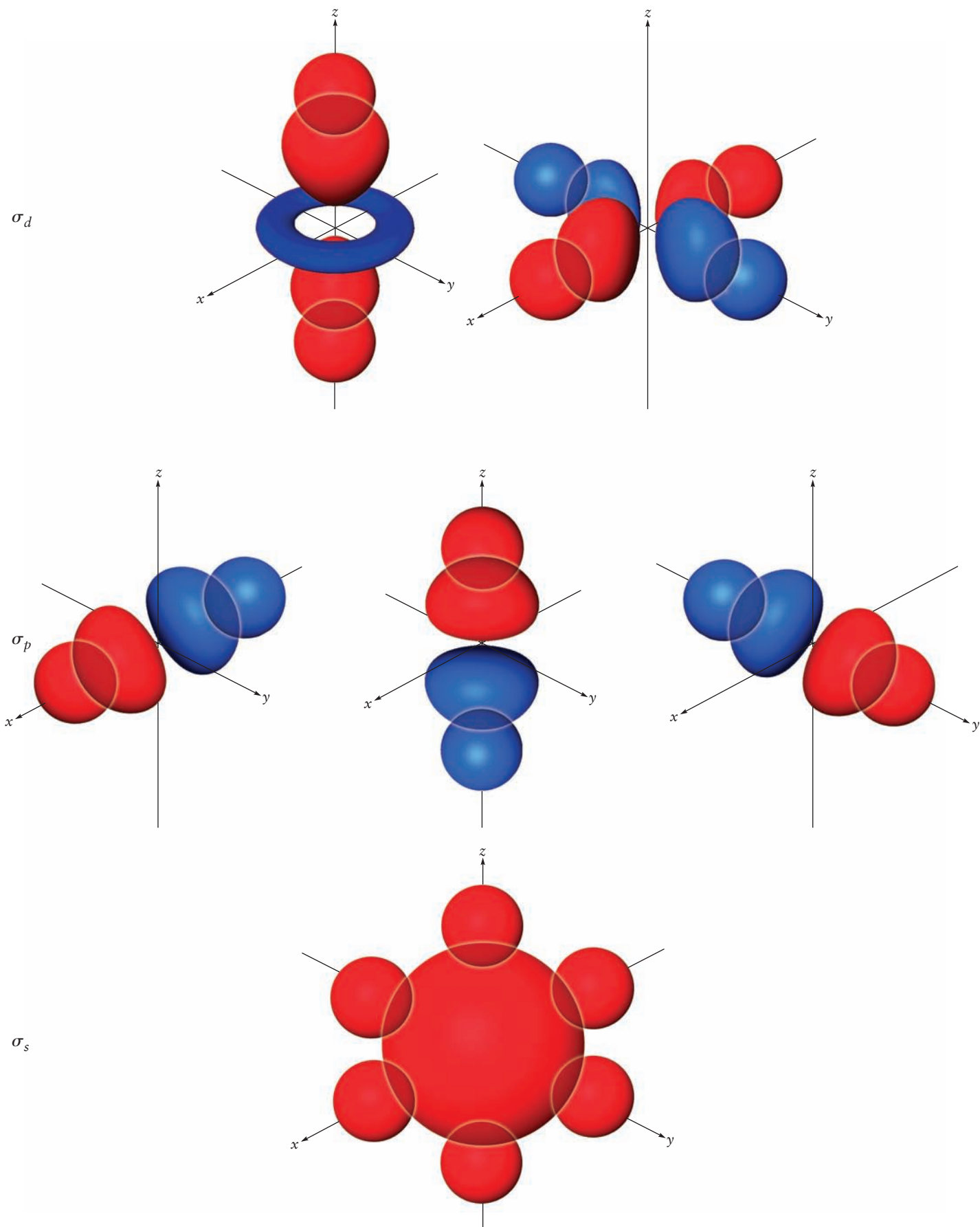
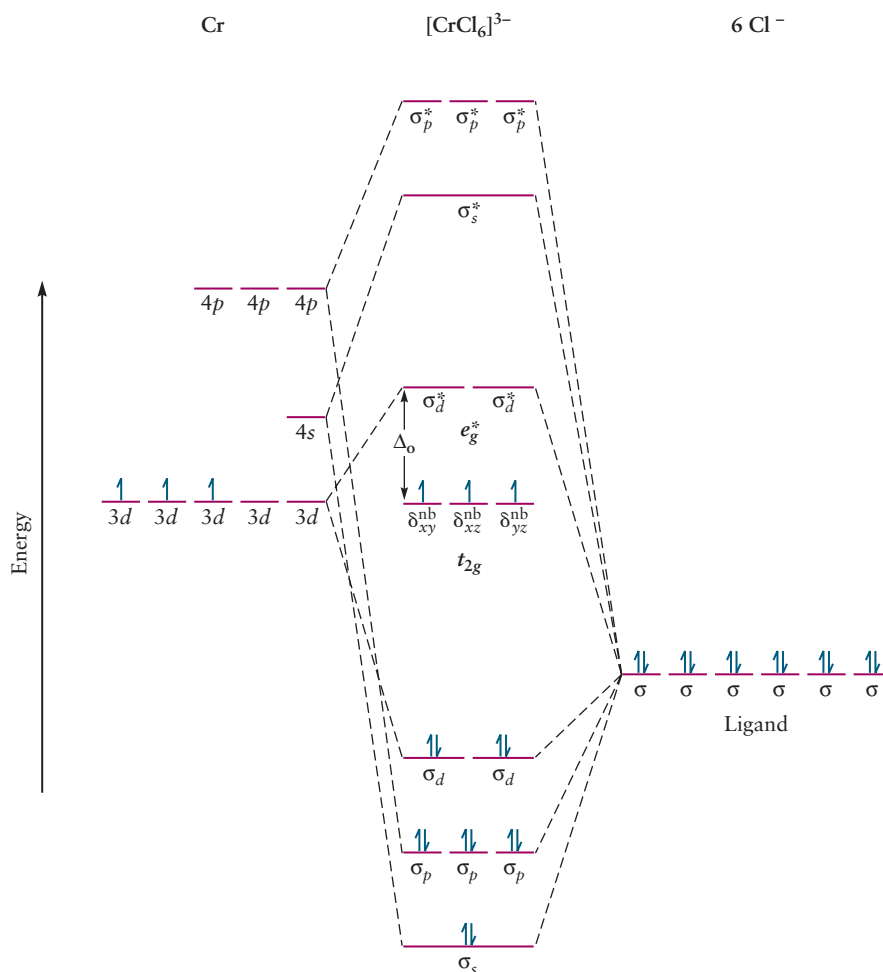


FIGURE 8.32 Overlap of metal orbitals with ligand orbitals to form σ bonds. The ligand orbitals can be either p or hybrid orbitals (e.g., sp^3 for water), and thus they are represented only schematically.

metal orbitals are the $3d$, $4s$, and $4p$ orbitals. The ligand orbitals could be sp^3 orbitals containing a lone pair in H_2O , or the p orbitals from F^- ions directed toward the metal ion. As shown in Figure 8.32, the $4s$ metal orbital can overlap with six ligand orbitals of the same phase to form a bonding σ molecular orbital. Overlap with six ligand orbitals of the opposite phase forms the corresponding antibonding σ^* molecular orbital (not shown). We label these orbitals σ_s and σ_s^* , respectively. In a similar fashion, we generate three bonding and three antibonding combinations using the metal p orbitals, which we label σ_p and σ_p^* , respectively. Only the d_{z^2} and $d_{x^2-y^2}$ orbitals are oriented to overlap with the ligand orbitals, and this overlap generates a pair of bonding and antibonding molecular orbitals, σ_d and σ_d^* . The d_{xy} , d_{yz} , and d_{zx} orbitals, whose lobes are oriented at 45 degrees to the bond axes, do not overlap with the ligand orbitals and are nonbonding. Thus, from our set of 9 metal orbitals and 6 ligand orbitals we have constructed 15 molecular orbitals, as required. Figure 8.33 is the resulting orbital correlation diagram.

Focusing on the set of three nonbonding δ_{xy}^{nb} , δ_{xz}^{nb} , and δ_{yz}^{nb} orbitals (t_{2g}) and the pair of antibonding σ^* (e_g) orbitals, we see that the energy level diagram is exactly the same as that predicted using crystal field theory (see Fig. 8.25). All of the results of that theory remain valid if we consider only σ bonding. The electron configuration of a coordination complex is built up by filling orbitals in order of increasing energy, just as for any other molecule that is characterized using molecular orbital theory. Using the complex ion $[\text{CrCl}_6]^{3-}$ as a specific example, there are 12 electrons available from the 6 ligands and 3 electrons from the metal, for a total of 15 electrons. 12 of these electrons fill the 6 bonding σ orbitals and the remaining 3 electrons are placed in the nonbonding δ_{xy} , δ_{xz} , and δ_{yz} orbitals (t_{2g}). In contrast to the VB treatment, which generates six localized bonding orbitals from

FIGURE 8.33 Orbital correlation diagram for an octahedral ligand field, showing the energy-level filling for a $[\text{CrCl}_6]^{3-}$ ion.

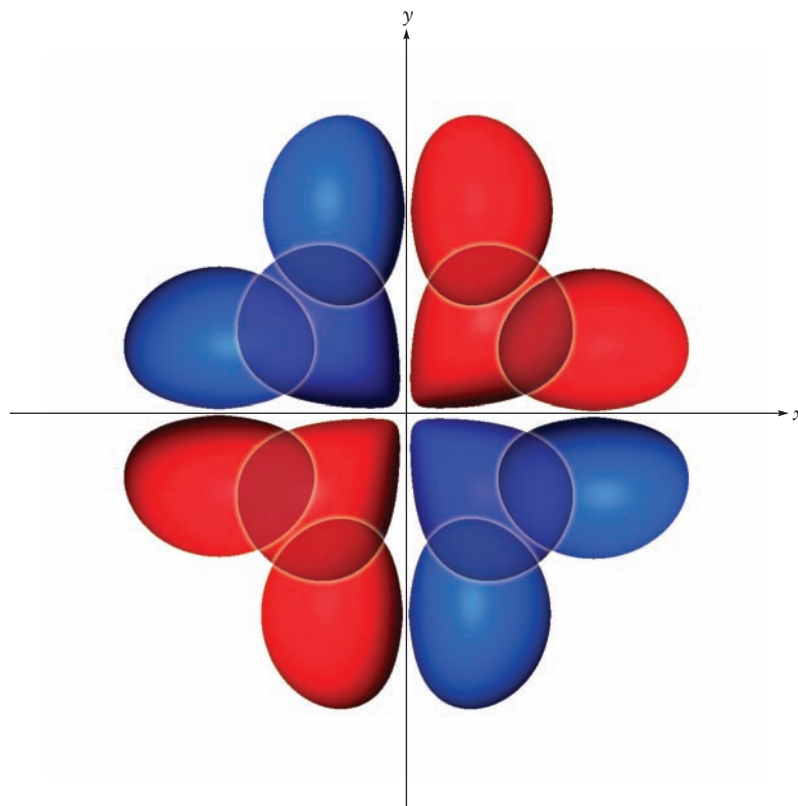


six hybrid orbitals on the metal and six ligand orbitals, the molecular orbital treatment produces six bonding molecular orbitals with different degrees of delocalization and with different spatial orientations. The σ_s orbital is delocalized over the entire complex. The three σ_p orbitals are each delocalized along one of the Cartesian axes. The σ_d orbital derived from the metal d_{z^2} orbital is delocalized along the z -axis whereas the σ_d orbital derived from the metal $d_{x^2-y^2}$ orbital is delocalized over the x - y plane.

There are important differences between crystal field theory and molecular orbital theory, even before we consider the important role of π bonding. The physical origin of the energy-level splitting is quite different in the two cases. Crystal field theory is essentially classical, and it attributes the splitting to the electrostatic repulsion between the electrons of the metal ion and the ionic charges of the ligands. Molecular orbital theory attributes the splitting to the mixing of the metal and ligand wave functions to form bonding, nonbonding, and antibonding molecular orbitals. The splitting Δ_o in molecular orbital theory is the energy difference between the nonbonding t_{2g} metal orbitals and the antibonding σ^* molecular orbitals that lie above them. We see immediately how this description explains the decrease in Δ_o as the strength of the metal–ligand interaction increases. Strong interactions, *whether ionic or covalent*, decrease the energy of (stabilize) the bonding σ_d orbital but increase the energy of (de-stabilize) the σ_d^* orbital.

The dramatically different strengths of ligands such as the halides and those containing unfilled antibonding π orbitals like CO and CN^- cannot be explained considering σ bonding alone. π bonding in octahedral coordination complexes may be treated by extending the arguments we presented in Section 8.2 for metal carbonyls. The only difference is that we must take into account the relative phases of the ligand orbitals as they overlap with the metal orbitals. The most important molecular orbitals for π bonding are constructed from the metal d_{xy} , d_{yz} , and d_{xz} orbitals and the ligand p orbitals that are oriented to overlap the metal orbitals as shown in Figure 8.34. Three degenerate bonding orbitals and a corresponding set

FIGURE 8.34 π bonding between a metal d_{xy} orbital and four ligand π orbitals with phases chosen for maximum constructive overlap.



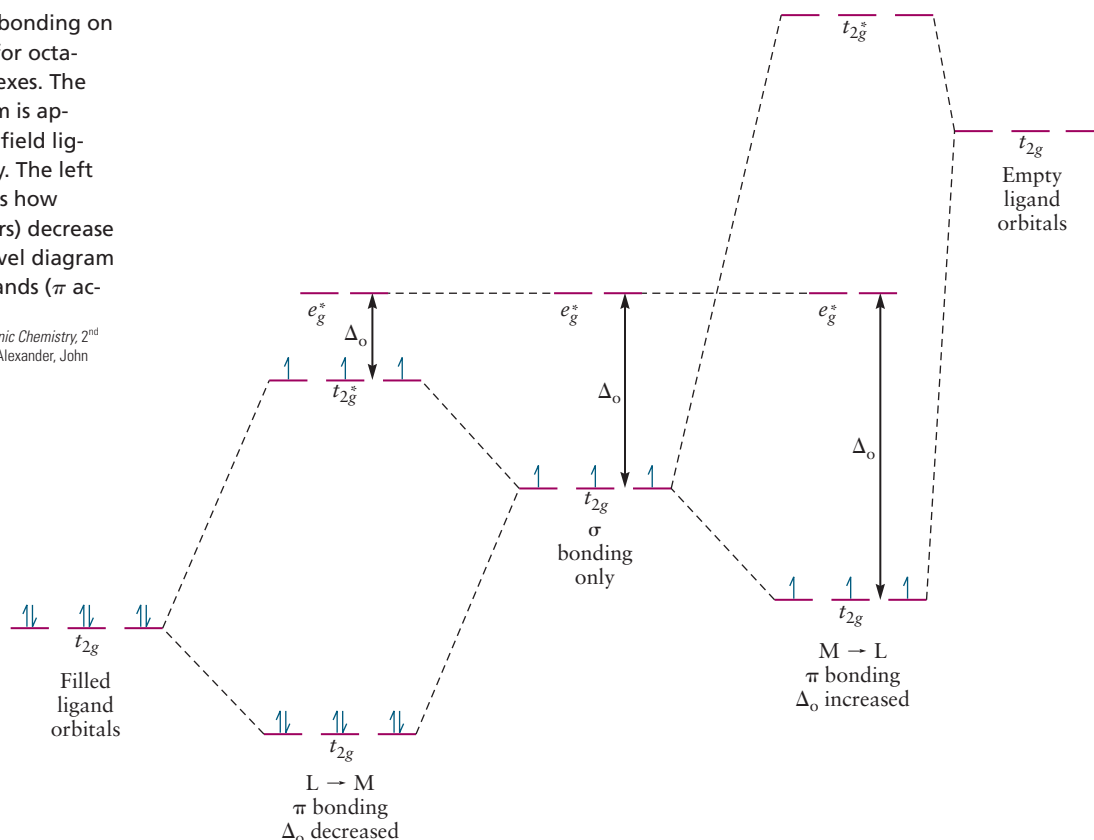
of antibonding orbitals are formed in this way. They are located in the x - y , y - z , and x - z planes, respectively. Because each set of molecular orbitals is triply degenerate and each orbital has g symmetry, they are labeled t_{2g} and t_{2g}^* , respectively. The orbital overlap shown in Figure 8.34 explains both $L \rightarrow M$ π donation and $M \rightarrow L$ π backbonding. The former is important for metals in high oxidation states (with few d electrons and empty d orbitals) and ligands with filled orbitals whose energies lie close to those of the empty d orbitals (the halides, water, OH^- and ammonia). The latter interaction is important for metals in low oxidation states (many d electrons and few unfilled d orbitals) and for ligands with empty orbitals whose energies lie close to those of the filled d orbitals (d orbitals of P or S, or π^* orbitals in ligands such as CO and CN^-).

Figure 8.35 summarizes the molecular orbital picture of bonding in octahedral coordination complexes, identifies the interactions that determine the splitting energy Δ_o , and provides guidance for predicting the bonding and energy-level structure for any coordination compound of interest, based on the oxidation state of the metal (number of d electrons) and the nature and occupancy of the ligand orbitals. The center portion of the figure shows the orbital splitting predicted using the simple molecular orbital picture that includes only σ bonding; the three d electrons shown could be found in complexes of V^{2+} , Cr^{3+} , or Mn^{4+} , for example. Crystal field theory would make the same prediction for the energy-level structure of $[\text{CrCl}_6]^{3-}$, and it can be considered a limiting case of molecular orbital theory.

The left side of Figure 8.35 could represent the bonding interactions and energy-level structure for $[\text{CrCl}_6]^{3-}$ in which a set of filled ligand orbitals (in this case, Cl $2p$ orbitals) donate electrons to a set of empty (or only partially filled) metal d orbitals ($L \rightarrow M$ π donation). The ligand orbitals are assumed to lie lower in energy than the metal orbitals, so the resulting t_{2g} molecular orbital is mostly ligand in character and lies at a relatively low energy. There is a corresponding t_{2g}^* orbital, which is mostly metal-like, at higher energy. This antibonding orbital is

FIGURE 8.35 Effect of π bonding on the energy-level structure for octahedral coordination complexes. The center energy-level diagram is appropriate for intermediate field ligands that are σ donors only. The left energy-level diagram shows how weak field ligands (π donors) decrease Δ_o , and the right energy-level diagram shows how strong field ligands (π acceptors) increase Δ_o .

(Adapted from *Concepts and Models of Inorganic Chemistry*, 2nd edition, B. Douglas, D. H. McDaniel, and J. J. Alexander, John Wiley and Sons, New York, 1983, p. 293.)



the highest occupied molecular orbital in this example; six of the nine available electrons go into the bonding t_{2g} orbital, leaving three to occupy the t_{2g}^* orbital. There are two important differences between this picture and the one in the center of Figure 8.35. First, the t_{2g} orbitals that were nonbonding metal d orbitals in the absence of π bonding have now become antibonding MOs by virtue of L→M π donation. Second, the energy-level splitting, Δ_o , has been reduced from its value without π bonding interactions. So, we now have an explanation for the mechanism by which weak field ligands lead to the smallest field splittings and a criterion with which to classify them. Weak field ligands have filled low-energy p orbitals that can donate electron density to empty metal d orbitals to produce an occupied antibonding molecular orbital at higher energy than the nonbonding metal d orbitals. All of the weak field ligands identified empirically in the spectrochemical series (the halides) fall into this class.

The right side of Figure 8.35 illustrates the case in which the metal d orbitals are nearly filled and the ligand has empty π^* orbitals at higher energies. This situation leads to a bonding and antibonding pair of MOs as before, but in this case, the energy of the t_{2g}^* orbital is too high for it to be occupied. The highest occupied molecular orbital is the bonding t_{2g} orbital, and Δ_o is now the difference in energy between this orbital and the antibonding e_g^* orbital. In the language of inorganic chemistry, the t_{2g} orbital has been stabilized because of M→L π donation. These interactions are important for metals with filled or nearly filled t_{2g} orbitals (such as Fe, Co, and Ni) and ligands with empty, low-lying orbitals such as the d orbitals of P or S or the π^* orbitals of CO, CN⁻, or NO⁺. These ligands, as well as OH⁻, en, and NH₃ are strong field ligands because they can accept electron density from the occupied d orbitals of the metal.

Molecular orbital theory provides a simple yet comprehensive way to understand and predict bonding patterns and energy levels in coordination complexes. Although we have worked out only the octahedral geometry in detail, the same considerations apply for all of the other geometries. Ligands classified empirically by the strengths of their interactions as revealed by the spectrochemical series can now be classified by the bonding interactions responsible. Weak field ligands are **π donors**, intermediate field ligands are **σ donors** with little to no π interactions at all, and strong field ligands are **π acceptors**. These classifications enable us to determine the nature of the ligand by simply looking for these characteristic features and to understand the bonding in coordination complexes by combining this knowledge with the oxidation state of the metal ion of interest.

CHAPTER SUMMARY

Transition-metal compounds and coordination complexes display a much wider variety of physical and chemical properties than the main-group elements in large part because of the participation of the d electrons in bonding and chemical reactions. Because the cost of transferring electrons to and from the d orbitals is low, these elements have several stable oxidation states and can make several kinds of chemical bonds. The ease with which electrons can be transferred to and from transition-metal compounds also makes them excellent catalysts by providing electron transfer reactions as alternate pathways for chemical reactions. Bonding in transition-metal compounds and coordination complexes is well described by molecular orbital theory. A type of bond formed by face-to-face overlap of a pair of $d_{x^2-y^2}$ or d_{xy} orbitals, the δ bond, plays a key role in the bonding of molecules and complexes that contain metal–metal bonds. The overlap of the d orbitals of the metal with the σ and π orbitals of ligands forms bonding and antibonding molecular orbitals; these interactions are often described as ligand-to-metal (L→M) σ and π donation and metal-to-ligand (M→L) π donation, respectively.

Coordination complexes are molecules or ions in which a central metal atom is bound to one or more ligands in a symmetric arrangement. Linear, tetrahedral, square-planar, trigonal bipyramidal, and octahedral arrangements are all known; the octahedral geometry is by far the most common. Crystal field theory accounts for the colors and magnetic properties of coordination complexes by considering the strengths of the repulsive interactions between the electrons in the various d orbitals and the ligands, represented as point charges located along the Cartesian axes. For octahedral geometries, the degenerate set of d orbitals splits into two levels, one set of three at lower energy and a set of two at higher energy. The colors of coordination complexes, as well as their magnetic properties, are rationalized using this model. Large energy differences between the two sets of levels result in the absorption of light in the blue or ultraviolet portion of the spectrum, and the complexes appear red in color. These strong fields also favor electron configurations in which the electrons preferentially occupy the lower levels in pairs, the low-spin configuration. Weak fields lead to optical absorption in the red or yellow regions of the spectrum, and the compounds appear blue. The electrons occupy both sets of orbitals with their spins parallel, the high-spin configuration.

Crystal field theory is only partially successful in explaining the optical and magnetic properties of the coordination complexes; it cannot explain the relative strengths of the ligands in the spectrochemical series. Molecular orbital theory (an earlier version of which is called ligand field theory) provides a more complete and quantitative description of bonding, optical, and magnetic properties by allowing for the formation of both σ and π bonds between the central metal ion and the ligands. Molecular orbital theory provides qualitative insight by classifying ligands by their bonding types and by considering the oxidation states of the metal ion.

CUMULATIVE EXERCISE

Platinum

The precious metal platinum was first used by South American Indians, who found impure, native samples of it in the gold mines of what is now Ecuador and used the samples to make small items of jewelry. Platinum's high melting point (1772°C) makes it harder to work than gold (1064°C) and silver (962°C), but this same property and a high resistance to chemical attack make platinum suitable as a material for high-temperature crucibles. Although platinum is a noble metal, in the +4 and +2 oxidation states it forms a variety of compounds, many of which are coordination complexes. Its coordinating abilities make it an important catalyst for organic and inorganic reactions.

- (a) The anticancer drug cisplatin, $cis\text{-}[\text{Pt}(\text{NH}_3)_2\text{Cl}_2]$ (see Fig. 8.18b), can be prepared from K_2PtCl_6 via reduction with N_2H_4 (hydrazine), giving K_2PtCl_4 , followed by replacement of two chloride ion ligands with ammonia. Give systematic names to the three platinum complexes referred to in this statement.
- (b) The coordination compound diamminetetracyanoplatinum(IV) has been prepared, but salts of the hexacyanoplatinate(IV) ion have not. Write the chemical formulas of these two species.
- (c) Platinum forms organometallic complexes quite readily. In one of the simplest of these, Pt(II) is coordinated to two chloride ions and two molecules of ethylene (C_2H_4) to give an unstable yellow crystalline solid. Can this complex have more than one isomer? If so, describe the possible isomers.

- (d) Platinum(IV) is readily complexed by ethylenediamine. Draw the structures of both enantiomers of the complex ion $cis-[Pt(Cl)_2(en)_2]^{2+}$. In this compound, the Cl^- ligands are *cis* to one another.
- (e) In platinum(IV) complexes, the octahedral crystal field splitting Δ_o is relatively large. Is K_2PtCl_6 diamagnetic or paramagnetic? What is its *d* electron configuration?
- (f) Is cisplatin diamagnetic or paramagnetic?
- (g) The salt $K_2[PtCl_4]$ is red, but $[Pt(NH_3)_4]Cl_2 \cdot H_2O$ is colorless. In what regions of the spectrum do the dominant absorptions for these compounds lie?
- (h) When the two salts from part (g) are dissolved in water and the solutions mixed, a green precipitate called Magnus's green salt forms. Propose a chemical formula for this salt and assign the corresponding systematic name.

Answers

- (a) *cis*-Diamminedichloroplatinum(II), potassium hexachloroplatinate(IV), and potassium tetrachloroplatinate(II)
- (b) $[Pt(NH_3)_2(CN)_4]$ and $[Pt(CN)_6]^{2-}$
- (c) Pt(II) forms square-planar complexes. There are two possible forms, arising from *cis* and *trans* placement of the ethylene molecules. These are analogous to the two isomers shown in Figures 8.18b and c.
- (d) The structures are the *cis* form shown in Figure 8.16 and its mirror image.
- (e) The six *d* electrons in Pt(IV) are all in the lower t_{2g} level in a low-spin, large- Δ_o complex. All are paired; thus, the compound is diamagnetic.
- (f) Diamagnetic, with the bottom four levels in the square-planar configuration (all but $d_{x^2-y^2}$) occupied
- (g) Red transmission corresponds to absorption of green light by $K_2[PtCl_4]$. A colorless solution has absorptions at either higher or lower frequency than visible. Because Cl^- is a weaker field ligand than NH_3 , the absorption frequency should be higher for the $[Pt(NH_3)_4]^{2+}$ complex, putting it in the ultraviolet region of the spectrum.
- (h) $[Pt(NH_3)_4][PtCl_4]$, tetra-ammineplatinum(II) tetrachloroplatinate(II)

CHAPTER REVIEW

- The properties of transition metal compounds and coordination complexes are determined, in large part, by the participation of *d* electrons in bonding and chemical reactions.
- Most transition metals have a number of stable oxidation states that lead to different kinds of chemical bonds and facilitate electron transfer reactions.
- Molecular orbital theory satisfactorily describes bonding in transition metal compounds and coordination complexes.
 - δ bonds, formed by face-to-face overlap of metal $d_{x^2-y^2}$ or d_{xy} orbitals, are significantly more important in the chemistry of the transition metals than that of the main group elements.
 - $L \rightarrow M$ σ donation, $L \rightarrow M$ π donation and $M \rightarrow L$ π donation are terms used by inorganic chemists to describe the formation and filling of molecular orbitals derived from the overlap of metal and ligand orbitals.
- Coordination complexes comprise a central metal atom or ion coordinated by dative bonds to a number of ligands in a symmetrical arrangement. Linear,

tetrahedral, square planar, trigonal bipyramidal, and octahedral geometries are all known, with octahedral being by far the most common.

- Crystal field theory accounts for the optical and magnetic properties of coordination complexes by considering the electrostatic repulsion between the metal d electrons and the charges on ionic ligands.

For octahedral complexes, the degenerate d orbitals split into two levels, a set of three lower energy t_{2g} orbitals and a pair of higher energy e_g orbitals. The energy difference between the two levels is called the crystal field splitting energy Δ_o .

Crystal field splitting is also observed for square-planar and tetrahedral geometries, but the energy level structure and the magnitudes of the splittings are different.

The optical properties arise from electronic transitions between levels split by the crystal field. Electronic absorption spectra measure Δ_o directly.

The magnetic properties depend on Δ_o . Large values of Δ_o (high field) lead to configurations in which electrons preferentially occupy the lower levels with paired spins (low spin). Small values of Δ_o lead to configurations in which electrons singly occupy the upper levels (with spins parallel to those in the lower levels) before doubly occupying any lower level.

- Crystal field theory does not account for the strengths of ligands revealed by the spectrochemical series.
- Molecular orbital theory that considers only σ bonding produces results similar to crystal field theory but with a different physical interpretation for the origin of the splitting.
- Including π bonding in molecular orbital theory is essential to understand the nature of bonding in coordination complexes and to account for the trends observed in the spectrochemical series.

CONCEPTS & SKILLS

After studying this chapter and working the problems that follow, you should be able to:

1. Discuss the systematic variation of physical and chemical properties of the transition elements through the periodic table (Section 8.1, Problems 1–6).
2. Define the terms *coordination compound*, *coordination number*, *ligand*, and *chelation* (Sections 8.3 and 8.5).
3. Name coordination compounds, given their molecular formulas (Section 8.3, Problems 11–14).
4. Draw geometric isomers of octahedral, tetrahedral, and square-planar complexes (Section 8.4, Problems 17–20).
5. Describe several coordination complexes that have roles in biology (Section 8.4).
6. Use crystal field theory to interpret the magnetic properties of coordination compounds in terms of the electron configurations of their central ions (Section 8.4, Problems 21–25).
7. Relate the colors of coordination compounds to their crystal field splitting energies and CFSE (Section 8.5, Problems 27–36).
8. Use ligand field theory to order the energy levels in coordination compounds and to account for the spectrochemical series (Section 8.7).

PROBLEMS

Answers to problems whose numbers are boldface appear in Appendix G. Problems that are more challenging are indicated with asterisks.

Chemistry of the Transition Metals

- Of the compounds PtF_4 and PtF_6 , predict (a) which is more soluble in water and (b) which is more volatile.
- The melting point of TiCl_4 (-24°C) lies below those of TiF_4 (284°C) and TiBr_4 (38°C). Explain why by considering the covalent-ionic nature of these compounds and the intermolecular forces in each case.
- The decavanadate ion is a complex species with chemical formula $\text{V}_{10}\text{O}_{28}^{6-}$. It reacts with an excess of acid to form the dioxovanadium ion, VO_2^+ , and water. Write a balanced chemical equation for this reaction. In what oxidation state is vanadium before and after this reaction? What vanadium oxide has the same oxidation state?
- What is the chemical formula of vanadium(III) oxide? Do you predict this compound to be more basic or more acidic than the vanadium oxide of Problem 3? Write a balanced chemical equation for the reaction of vanadium(III) oxide with a strong acid.
- Titanium(III) oxide is prepared by reaction of titanium(IV) oxide with hydrogen at high temperature. Write a balanced chemical equation for this reaction. Which oxide do you expect to have stronger basic properties?
- Treatment of cobalt(II) oxide with oxygen at high temperatures gives Co_3O_4 . Write a balanced chemical equation for this reaction. What is the oxidation state of cobalt in Co_3O_4 ?

Introduction to Coordination Chemistry

- Will methylamine (CH_3NH_2) be a monodentate or a bidentate ligand? With which of its atoms will it bind to a metal ion?
- Show how the glycinate ion ($\text{H}_2\text{N}-\text{CH}_2-\text{COO}^-$) can act as a bidentate ligand. (Draw a Lewis diagram if necessary.) Which atoms in the glycinate ion will bind to a metal ion?
- Determine the oxidation state of the metal in each of the following coordination complexes: $[\text{V}(\text{NH}_3)_4\text{Cl}_2]$, $[\text{Mo}_2\text{Cl}_8]^{4-}$, $[\text{Co}(\text{H}_2\text{O})_2(\text{NH}_3)\text{Cl}_3]^-$, $[\text{Ni}(\text{CO})_4]$.
- Determine the oxidation state of the metal in each of the following coordination complexes: $\text{Mn}_2(\text{CO})_{10}$, $[\text{Re}_3\text{Br}_{12}]^{3-}$, $[\text{Fe}(\text{H}_2\text{O})_4(\text{OH})_2]^+$, $[\text{Co}(\text{NH}_3)_4\text{Cl}_2]^+$.
- Give the chemical formula that corresponds to each of the following compounds:
 - Sodium tetrahydroxozincate(II)
 - Dichlorobis(ethylenediamine)cobalt(III) nitrate
 - Triaquabromoplatinum(II) chloride
 - Tetra-amminedinitroplatinum(IV) bromide
- Give the chemical formula of each of the following compounds:
 - Silver hexacyanoferrate(II)
 - Potassium tetrakisothiocyanatocobaltate(II)
 - Sodium hexafluorovanadate(III)
 - Potassium trioxalatochromate(III)

- Assign a systematic name to each of the following chemical compounds:
 - $\text{NH}_4[\text{Cr}(\text{NH}_3)_2(\text{NCS})_4]$
 - $[\text{Tc}(\text{CO})_5]\text{I}$
 - $\text{K}[\text{Mn}(\text{CN})_5]$
 - $[\text{Co}(\text{NH}_3)_4(\text{H}_2\text{O})\text{Cl}]\text{Br}_2$
- Give the systematic name for each of the following chemical compounds:
 - $[\text{Ni}(\text{H}_2\text{O})_4(\text{OH})_2]$
 - $[\text{HgClI}]$
 - $\text{K}_4[\text{Os}(\text{CN})_6]$
 - $[\text{FeBrCl}(\text{en})_2]\text{Cl}$

Structures of Coordination Complexes

- Suppose 0.010 mol of each of the following compounds is dissolved (separately) in 1.0 L water: KNO_3 , $[\text{Co}(\text{NH}_3)_6]\text{Cl}_3$, $\text{Na}_2[\text{PtCl}_6]$, $[\text{Cu}(\text{NH}_3)_2\text{Cl}_2]$. Rank the resulting four solutions in order of conductivity, from lowest to highest.
- Suppose 0.010 mol of each of the following compounds is dissolved (separately) in 1.0 L water: BaCl_2 , $\text{K}_4[\text{Fe}(\text{CN})_6]$, $[\text{Cr}(\text{NH}_3)_4\text{Cl}_2]\text{Cl}$, $[\text{Fe}(\text{NH}_3)_3\text{Cl}_3]$. Rank the resulting four solutions in order of conductivity, from lowest to highest.
- Draw the structures of all possible isomers for the following complexes. Indicate which isomers are enantiomer pairs.
 - Diamminebromochloroplatinum(II) (square-planar)
 - Diaquachlorotricyanocobaltate(III) ion (octahedral)
 - Trioxalatovanadate(III) ion (octahedral)
- Draw the structures of all possible isomers for the following complexes. Indicate which isomers are enantiomer pairs.
 - Bromochloro(ethylenediamine)platinum(II) (square-planar)
 - Tetra-amminedichloroiron(III) ion (octahedral)
 - Amminechlorobis(ethylenediamine)iron(III) ion (octahedral)
- Iron(III) forms octahedral complexes. Sketch the structures of all the distinct isomers of $[\text{Fe}(\text{en})_2\text{Cl}_2]^+$, indicating which pairs of structures are mirror images of each other.
- Platinum(IV) forms octahedral complexes. Sketch the structures of all the distinct isomers of $[\text{Pt}(\text{NH}_3)_2\text{Cl}_2\text{F}_2]$, indicating which pairs of structures are mirror images of each other.

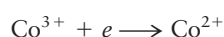
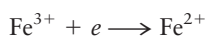
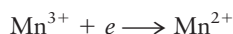
Crystal Field Theory: Optical and Magnetic Properties

- For each of the following ions, draw diagrams like those in Figure 8.25 to show orbital occupancies in both weak and strong octahedral fields. Indicate the total number of unpaired electrons in each case.

(a) Mn^{2+}	(c) Cr^{3+}	(e) Fe^{2+}
(b) Zn^{2+}	(d) Mn^{3+}	
- Repeat the work of the preceding problem for the following ions:

(a) Cr^{2+}	(c) Ni^{2+}	(e) Co^{2+}
(b) V^{3+}	(d) Pt^{4+}	
- Experiments can measure not only whether a compound is paramagnetic, but also the number of unpaired electrons. It is found that the octahedral complex ion $[\text{Fe}(\text{CN})_6]^{3-}$ has

- fewer unpaired electrons than the octahedral complex ion $[\text{Fe}(\text{H}_2\text{O})_6]^{3+}$. How many unpaired electrons are present in each species? Explain. In each case, express the CFSE in terms of Δ_o .
24. The octahedral complex ion $[\text{MnCl}_6]^{3-}$ has more unpaired spins than the octahedral complex ion $[\text{Mn}(\text{CN})_6]^{3-}$. How many unpaired electrons are present in each species? Explain. In each case, express the CFSE in terms of Δ_o .
25. Explain why octahedral coordination complexes with three and eight d electrons on the central metal atom are particularly stable. Under what circumstances would you expect complexes with five or six d electrons on the central metal atom to be particularly stable?
26. Mn, Fe, and Co in the +2 and +3 oxidation states all form hexaqua complexes in acidic aqueous solution. The reduction reactions of the three species are represented schematically below, where the water ligands are not shown for simplicity. It is an experimental fact from electrochemistry that Mn^{2+} and Co^{2+} are more easily reduced than Fe^{3+} ; that is, they will more readily accept an electron. Based on the electron configurations of the ions involved, explain why Fe^{3+} is harder to reduce than Mn^{2+} and Co^{2+} .



Optical Properties and the Spectrochemical Series

27. An aqueous solution of zinc nitrate contains the $[\text{Zn}(\text{H}_2\text{O})_6]^{2+}$ ion and is colorless. What conclusions can be drawn about the absorption spectrum of the $[\text{Zn}(\text{H}_2\text{O})_6]^{2+}$ complex ion?
28. An aqueous solution of sodium hexaiodoplatinate(IV) is black. What conclusions can be drawn about the absorption spectrum of the $[\text{PtI}_6]^{2-}$ complex ion?
29. Estimate the wavelength of maximum absorption for the octahedral ion hexacyanoferrate(III) from the fact that light transmitted by a solution of it is red. Estimate the crystal field splitting energy Δ_o (in kJ mol^{-1}).
30. Estimate the wavelength of maximum absorption for the octahedral ion hexa-aquanickel(II) from the fact that its solutions are colored green by transmitted light. Estimate the crystal field splitting energy Δ_o (in kJ mol^{-1}).
31. Estimate the CFSE for the complex in Problem 29. (Note: This is a high-field (low-spin) complex.)
32. Estimate the CFSE for the complex in Problem 30.
33. The chromium(III) ion in aqueous solution is blue-violet.
- What is the complementary color to blue-violet?
 - Estimate the wavelength of maximum absorption for a $\text{Cr}(\text{NO}_3)_3$ solution.
 - Will the wavelength of maximum absorption increase or decrease if cyano ligands are substituted for the coordinated water? Explain.
34. An aqueous solution containing the hexa-amminecobalt(III) ion is yellow.
- What is the complementary color to yellow?
 - Estimate this solution's wavelength of maximum absorption in the visible spectrum.
35. (a) An aqueous solution of $\text{Fe}(\text{NO}_3)_3$ has only a pale color, but an aqueous solution of $\text{K}_3[\text{Fe}(\text{CN})_6]$ is bright red. Do you expect a solution of $\text{K}_3[\text{FeF}_6]$ to be brightly colored or pale? Explain your reasoning.
- (b) Would you predict a solution of $\text{K}_2[\text{HgI}_4]$ to be colored or colorless? Explain.
36. (a) An aqueous solution of $\text{Mn}(\text{NO}_3)_2$ is very pale pink, but an aqueous solution of $\text{K}_4[\text{Mn}(\text{CN})_6]$ is deep blue. Explain why the two differ so much in the intensities of their colors.
- (b) Predict which of the following compounds would be colorless in aqueous solution: $\text{K}_2[\text{Co}(\text{NCS})_4]$, $\text{Zn}(\text{NO}_3)_2$, $[\text{Cu}(\text{NH}_3)_4]\text{Cl}_2$, CdSO_4 , AgClO_3 , $\text{Cr}(\text{NO}_3)_2$.

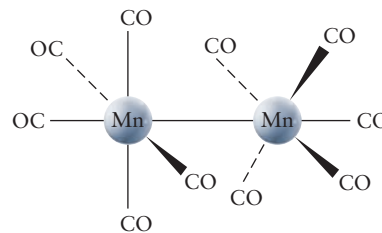
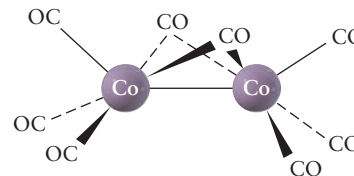
ADDITIONAL PROBLEMS

37. Of the ten fourth-period transition metal elements in Table 8.1, which one has particularly low melting and boiling points? How can you explain this in terms of the electronic configuration of this element?
- * 38. Although copper lies between nickel and zinc in the periodic table, the reduction potential of Cu^{2+} is above that for both Ni^{2+} and Zn^{2+} (see Table 8.1). Use other data from Table 8.1 to account for this observation. (Hint: Think of a multi-step process to convert a metal atom in the solid to a metal ion in solution. For each step, compare the relevant energy or enthalpy changes for Cu with those for Ni or Zn.)
39. A reference book lists five different values for the electronegativity of molybdenum, a different value for each oxidation state from +2 through +6. Predict which electronegativity is highest and which is lowest.
40. If *trans*- $[\text{Cr}(\text{en})_2(\text{NCS})_2]\text{SCN}$ is heated, it forms gaseous ethylenediamine and solid $[\text{Cr}(\text{en})_2(\text{NCS})_2][\text{Cr}(\text{en})(\text{NCS})_4]$. Write a balanced chemical equation for this reaction. What are the oxidation states of the Cr ions in the reactant and in the two complex ions in the product?
41. A coordination complex has the molecular formula $[\text{Ru}_2(\text{NH}_3)_6\text{Br}_3](\text{ClO}_4)_2$. Determine the oxidation state of ruthenium in this complex.
42. Heating 2.0 mol of a coordination compound gives 1.0 mol NH_3 , 2.0 mol H_2O , 1.0 mol HCl , and 1.0 mol $(\text{NH}_4)_3[\text{Ir}_2\text{Cl}_9]$. Write the formula of the original (six-coordinate) coordination compound and name it.
43. Explain why ligands are usually negative or neutral in charge and only rarely positive.
44. Match each compound in the group on the left with the compound on the right that is most likely to have the same electrical conductivity per mole in aqueous solution.
- | | |
|---|------------------------------|
| (a) $[\text{Fe}(\text{H}_2\text{O})_5\text{Cl}]\text{CO}_3$ | HCN |
| (b) $[\text{Mn}(\text{H}_2\text{O})_6]\text{Cl}_3$ | $\text{Fe}_2(\text{SO}_4)_3$ |
| (c) $[\text{Zn}(\text{H}_2\text{O})_3(\text{OH})]\text{Cl}$ | NaCl |
| (d) $[\text{Fe}(\text{NH}_3)_6]_2(\text{CO}_3)_3$ | MgSO_4 |
| (e) $[\text{Cr}(\text{NH}_3)_3\text{Br}_3]$ | Na_3PO_4 |
| (f) $\text{K}_3[\text{Fe}(\text{CN})_6]$ | GaCl_3 |
45. Three different compounds are known to have the empirical formula $\text{CrCl}_3 \cdot 6\text{H}_2\text{O}$. When exposed to a dehydrating agent, compound 1 (which is dark green) loses 2 mol water per mole of compound, compound 2 (light green) loses 1 mol water, and compound 3 (violet) loses no water. What are the probable structures of these compounds? If an

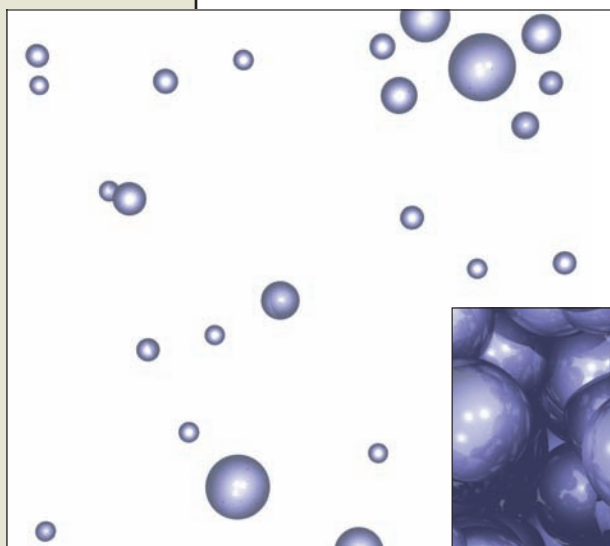
- excess of silver nitrate solution is added to 100.0 g of each of these compounds, what mass of silver chloride will precipitate in each case?
- The octahedral structure is not the only possible six-coordinate structure. Other possibilities include a planar hexagonal structure and a triangular prism structure. In the latter, the ligands are arranged in two parallel triangles, one lying above the metal atom and the other below the metal atom with its corners directly in line with the corners of the first triangle. Show that the existence of two and only two isomers of $[\text{Co}(\text{NH}_3)_4\text{Cl}_2]^+$ is evidence against both of these possible structures.
 - Cobalt(II) forms more tetrahedral complexes than any other ion except zinc(II). Draw the structure(s) of the tetrahedral complex $[\text{CoCl}_2(\text{en})]$. Could this complex exhibit geometric or optical isomerism? If one of the Cl^- ligands is replaced by Br^- , what kinds of isomerism, if any, are possible in the resulting compound?
 - Is the coordination compound $[\text{Co}(\text{NH}_3)_6]\text{Cl}_2$ diamagnetic or paramagnetic?
 - A coordination compound has the empirical formula $\text{PtBr}(\text{en})(\text{SCN})_2$ and is diamagnetic.
 - Examine the d -electron configurations on the metal atoms, and explain why the formulation $[\text{Pt}(\text{en})_2(\text{SCN})_2]$ $[\text{PtBr}_2(\text{SCN})_2]$ is preferred for this substance.
 - Name this compound.
 - We used crystal field theory to order the energy-level splittings induced in the five d orbitals. The same procedure could be applied to p orbitals. Predict the level splittings (if any) induced in the three p orbitals by octahedral and square-planar crystal fields.
 - The three complex ions $[\text{Mn}(\text{CN})_6]^{5-}$, $[\text{Mn}(\text{CN})_6]^{4-}$, and $[\text{Mn}(\text{CN})_6]^{3-}$ have all been synthesized and all are low-spin octahedral complexes. For each complex, determine the oxidation number of Mn, the configuration of the d electrons (how many t_{2g} and how many e_g), and the number of unpaired electrons present.
 - On the basis of the examples presented in Problem 51, can you tell whether $\text{Mn}^{2+}(\text{aq})$ is more easily oxidized or more easily reduced? What can you conclude about the stability of $\text{Mn}^{2+}(\text{aq})$?
 - The following ionic radii (in angstroms) are estimated for the +2 ions of selected elements of the first transition-metal series, based on the structures of their oxides: Ca^{2+} (0.99), Ti^{2+} (0.71), V^{2+} (0.64), Mn^{2+} (0.80), Fe^{2+} (0.75), Co^{2+} (0.72), Ni^{2+} (0.69), Cu^{2+} (0.71), Zn^{2+} (0.74). Draw a graph of ionic radius versus atomic number in this series, and account for its shape. The oxides take the rock salt structure. Are these solids better described as high- or low-spin transition-metal complexes?
 - The coordination geometries of $[\text{Mn}(\text{NCS})_4]^{2-}$ and $[\text{Mn}(\text{NCS})_6]^{4-}$ are tetrahedral and octahedral, respectively. Explain why the two have the same room-temperature molar magnetic susceptibility.
 - The complex ion CoCl_4^{2-} has a tetrahedral structure. How many d electrons are on the Co? What is its electronic configuration? Why is the tetrahedral structure stable in this case?
 - In the coordination compound $(\text{NH}_4)_2[\text{Fe}(\text{H}_2\text{O})\text{F}_5]$, the Fe is octahedrally coordinated.
 - Based on the fact that F^- is a weak-field ligand, predict whether this compound is diamagnetic or paramagnetic. If it is paramagnetic, tell how many unpaired electrons it has.
 - By comparison with other complexes reviewed in this chapter, discuss the likely color of this compound.
 - Determine the d -electron configuration of the iron in this compound.
 - Name this compound.
 - The compound $\text{Cs}_2[\text{CuF}_6]$ is bright orange and paramagnetic. Determine the oxidation number of copper in this compound, the most likely geometry of the coordination around the copper, and the possible configurations of the d electrons of the copper.
 - In what directions do you expect the bond length and vibrational frequency of a free CO molecule to change when it becomes a CO ligand in a $\text{Ni}(\text{CO})_4$ molecule? Explain your reasoning.
 - Give the number of valence electrons surrounding the central transition-metal ion in each of the following known organometallic compounds or complex ions: $[\text{Co}(\text{C}_5\text{H}_5)_2]^+$, $[\text{Fe}(\text{C}_5\text{H}_5)(\text{CO})_2\text{Cl}]$, $[\text{Mo}(\text{C}_5\text{H}_5)_2\text{Cl}_2]$, $[\text{Mn}(\text{C}_5\text{H}_5)(\text{C}_6\text{H}_6)]$.
 - Molecular nitrogen (N_2) can act as a ligand in certain coordination complexes. Predict the structure of $[\text{V}(\text{N}_2)_6]$, which is isolated by condensing V with N_2 at 25 K. Is this compound diamagnetic or paramagnetic? What is the formula of the carbonyl compound of vanadium that has the same number of electrons?
 - What energy levels are occupied in a complex such as hexacarbonylchromium(0)? Are any electrons placed into antibonding orbitals that are derived from the chromium d orbitals?
 - * The compound $\text{WH}_2(\text{C}_5\text{H}_5)_2$ acts as a base, but $\text{TaH}_3(\text{C}_5\text{H}_5)_2$ does not. Explain.
 - Discuss the role of transition-metal complexes in biology. Consider such aspects as their absorption of light, the existence of many different structures, and the possibility of multiple oxidation states.

CUMULATIVE PROBLEMS

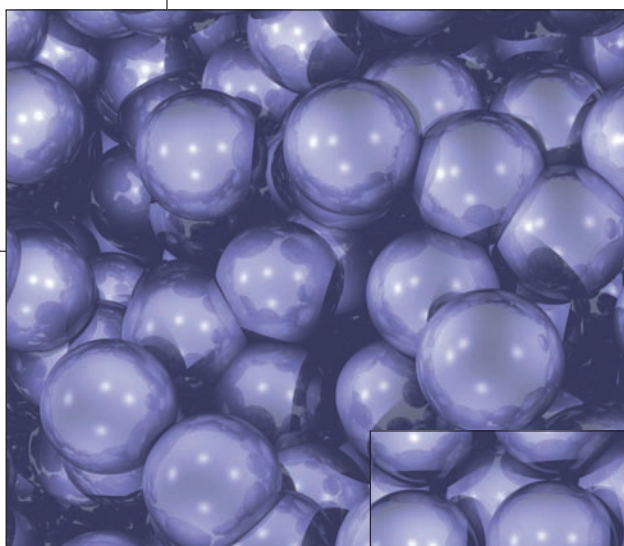
64. Predict the volume of hydrogen generated at 1.00 atm and 25°C by the reaction of 4.53 g scandium with excess aqueous hydrochloric acid.
- * 65. Mendeleev's early periodic table placed manganese and chlorine in the same group. Discuss the chemical evidence for these placements, focusing on the oxides of the two elements and their acid–base and redox properties. Is there a connection between the electronic structures of their atoms? In what ways are the elements different?
66. An orange–yellow osmium carbonyl compound is heated to release CO and leave elemental osmium behind. Treatment of 6.79 g of the compound releases 1.18 L CO(g) at 25°C and 2.00 atm pressure. What is the empirical formula of this compound? Propose a possible structure for it by comparing with the metal carbonyls shown on the right.

(a) $\text{Mn}_2(\text{CO})_{10}$ (b) $\text{Co}_2(\text{CO})_8$

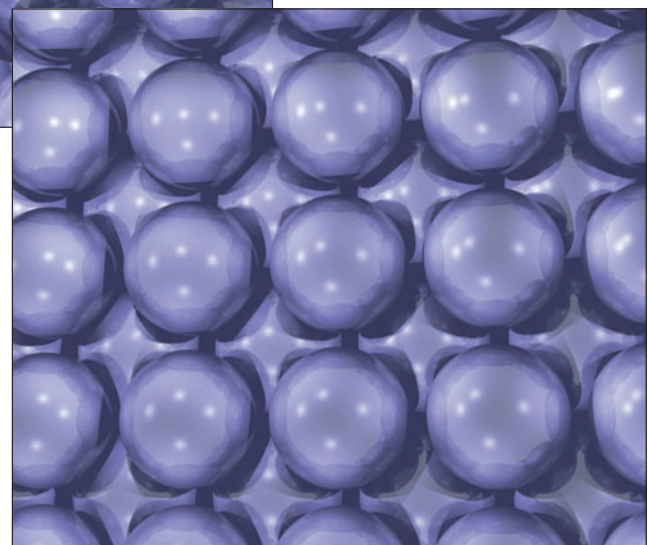
Kinetic Molecular Description of the States of Matter



(a)



(b)



(c)

Spatial arrangement of molecules in a gas (a), a liquid (b), and a solid (c). Because the molecules in a solid or a liquid are in close contact with one another, the volume per molecule of the substance is nearly equal to the volume of the molecule itself. The molecules in a gas are much farther apart, with considerable open space between them.

(Courtesy Dr. Stuart C. Watson and Professor Emily A. Carter/UCLA)

We recognize gases, liquids, and solids quite easily because we are surrounded by important examples of each: air, water, and earth. Gases and liquids are fluid, but solids are rigid. A gas expands to fill any container it occupies. A liquid has a fixed volume but flows to conform to the shape of its container. A solid has a fixed volume *and* a fixed shape, both of which resist deformation. These characteristics originate in the arrangements and motions of molecules, which are determined by the forces between the molecules. In a solid or liquid, molecules (shown as spheres in the images on the previous page) are in very close contact. At these distances, molecules experience strong mutual forces of attraction. In a liquid, molecules can slide past one another, whereas in a solid, molecules remain attached to their home positions. In a gas, the molecules are much farther apart, and the forces between them are strong only during collisions. The molecules in a gas can roam freely throughout the container, unlike those in solids and liquids.

UNIT CHAPTERS

CHAPTER 9

The Gaseous State

CHAPTER 10

Solids, Liquids, and Phase Transitions

CHAPTER 11

Solutions

UNIT GOALS

- To define the essential properties of solids, liquids, and gases
- To relate the magnitudes of these properties to the motions of molecules and to the forces between molecules
- To define the properties of solutions and relate their magnitudes to composition of the solutions

The Gaseous State

- 9.1 The Chemistry of Gases
- 9.2 Pressure and Temperature of Gases
- 9.3 The Ideal Gas Law
- 9.4 Mixtures of Gases
- 9.5 The Kinetic Theory of Gases
- 9.6 **A DEEPER LOOK** *Distribution of Energy among Molecules*
- 9.7 Real Gases: Intermolecular Forces
- 9.8 **A DEEPER LOOK** *Molecular Collisions and Rate Processes*



© Thomson Learning/Charles D. Winters

Gaseous nitrogen dioxide is generated by the reaction of copper with nitric acid.

The *kinetic molecular theory of matter* asserts that the macroscopic properties of matter are determined by the structures of its constituent molecules and the interactions between them. Starting in the latter half of the 19th century, scientists have developed a magnificent theoretical structure called **statistical mechanics** to explain the connection between microscopic structure and macroscopic properties. Statistical mechanics provides this bridge for all types of matter, ranging from biological materials to solid-state integrated circuits. Today, every student of science must be familiar with the concepts that make this connection. We give a qualitative introduction to these concepts, and apply them to numerous cases in the next four chapters.

We start the discussion with gases, because gases provide the simplest opportunity for relating macroscopic properties to the structures and interactions of molecules. This is possible because gases are much less dense than solids or liquids. On the macroscopic level, gases are distinguished from liquids and solids by their much smaller values of *mass density* (conveniently measured in grams per cubic centimeter). On the microscopic level, the *number density* (number of molecules in 1 cm³ of the sample) is smaller—and the distances between molecules are much greater—than in liquids and solids. Molecules with no net electrical charge exert significant forces on each other only when they are close. Consequently, in the study of gases it is a legitimate simplification to ignore interactions between molecules until they collide and then to consider collisions between only two molecules at a time.

In this chapter we develop two themes that are key to relating macroscopic behavior to molecular structure. First, we show how to define and measure the macroscopic properties of gases as temperature, pressure, and volume are changed. This discussion leads us to develop and apply the ideal gas law, which—as verified by experiment—accurately represents the bulk properties of gases at low density. Second, we interpret and explain the ideal gas law in terms of the structures and motions of individual molecules. We obtain refinements to the ideal gas law by analyzing the consequences of collisions between pairs of molecules. The results and insights we obtain are essential background for later study of the rate and extent of chemical reactions since chemical reactions occur through molecular collisions.

9.1 The Chemistry of Gases

The ancient Greeks considered air to be one of the four fundamental elements in nature. European scientists began to study the properties of air (such as its resistance to compression) as early as the 17th century. The chemical composition of air (Table 9.1) was unknown until late in the 18th century, when Lavoisier, Priestley, and others showed that it consists primarily of two substances: oxygen and nitrogen. Oxygen was characterized by its ability to support life. Once the oxygen in a volume of air had been used up (by burning a candle in a closed container, for example), the nitrogen that remained could no longer keep animals alive. More

TABLE 9.1 Composition of Air

Constituent	Formula	Fraction by Volume
Nitrogen	N ₂	0.78110
Oxygen	O ₂	0.20953
Argon	Ar	0.00934
Carbon dioxide	CO ₂	0.00038
Neon	Ne	1.82×10^{-5}
Helium	He	5.2×10^{-6}
Methane	CH ₄	1.5×10^{-6}
Krypton	Kr	1.1×10^{-6}
Hydrogen	H ₂	5×10^{-7}
Dinitrogen oxide	N ₂ O	3×10^{-7}
Xenon	Xe	8.7×10^{-8}

Air also contains other constituents, the abundances of which are quite variable in the atmosphere. Examples are water (H₂O), 0–0.07; ozone (O₃), $0\text{--}7 \times 10^{-8}$; carbon monoxide (CO), $0\text{--}2 \times 10^{-8}$; nitrogen dioxide (NO₂), $0\text{--}2 \times 10^{-8}$; and sulfur dioxide (SO₂), $0\text{--}1 \times 10^{-6}$.